NUREG/CR-7269

U.S.NRC
United States Nuclear Regulatory Commission
Protecting People and the Environment

Enhancing Guidance for Evacuation Time Estimate Studies

Office of Nuclear Regulatory Research

AVAILABILITY OF REFERENCE MATERIALS IN NRC PUBLICATIONS

NRC Reference Material

As of November 1999, you may electronically access NUREG-series publications and other NRC records at the NRC's Public Electronic Reading Room at http://www.nrc.gov/reading-rm.html. Publicly released records include, to name a few, NUREG-series publications; *Federal Register* notices; applicant, licensee, and vendor documents and correspondence; NRC correspondence and internal memoranda; bulletins and information notices; inspection and investigative reports; licensee event reports; and Commission papers and their attachments.

NRC publications in the NUREG series, NRC regulations, and Title 10, "Energy," in the *Code of Federal Regulations* may also be purchased from one of these two sources.

1. **The Superintendent of Documents**
   U.S. Government Publishing Office
   Washington, DC 20402-0001
   Internet: http://bookstore.gpo.gov
   Telephone: 1-866-512-1800
   Fax: (202) 512-2104

2. **The National Technical Information Service**
   5301 Shawnee Road
   Alexandria, VA 22161-0002
   http://www.ntis.gov
   1-800-553-6847 or, locally, (703) 605-6000

A single copy of each NRC draft report for comment is available free, to the extent of supply, upon written request as follows:

U.S. Nuclear Regulatory Commission
Office of Administration
Multimedia, Graphics and Storage & Distribution Branch
Washington, DC 20555-0001
E-mail: distribution.resource@nrc.gov
Facsimile: (301) 415-2289

Some publications in the NUREG series that are posted at the NRC's Web site address http://www.nrc.gov/reading-rm/doc-collections/nuregs are updated periodically and may differ from the last printed version. Although references to material found on a Web site bear the date the material was accessed, the material available on the date cited may subsequently be removed from the site.

Non-NRC Reference Material

Documents available from public and special technical libraries include all open literature items, such as books, journal articles, transactions, *Federal Register* notices, Federal and State legislation, and congressional reports. Such documents as theses, dissertations, foreign reports and translations, and non-NRC conference proceedings may be purchased from their sponsoring organization.

Copies of industry codes and standards used in a substantive manner in the NRC regulatory process are maintained at—

The NRC Technical Library
Two White Flint North
11545 Rockville Pike
Rockville, MD 20852-2738

These standards are available in the library for reference use by the public. Codes and standards are usually copyrighted and may be purchased from the originating organization or, if they are American National Standards, from—

American National Standards Institute
11 West 42nd Street
New York, NY 10036-8002
http://www.ansi.org
(212) 642-4900

Legally binding regulatory requirements are stated only in laws; NRC regulations; licenses, including technical specifications; or orders, not in NUREG-series publications. The views expressed in contractor-prepared publications in this series are not necessarily those of the NRC.

The NUREG series comprises (1) technical and administrative reports and books prepared by the staff (NUREG-XXXX) or agency contractors (NUREG/CR-XXXX), (2) proceedings of conferences (NUREG/CP-XXXX), (3) reports resulting from international agreements (NUREG/IA-XXXX), (4) brochures (NUREG/BR-XXXX), and (5) compilations of legal decisions and orders of the Commission and Atomic and Safety Licensing Boards and of Directors' decisions under Section 2.206 of NRC's regulations (NUREG-0750).

NUREG/CR-7269

U.S.NRC
United States Nuclear Regulatory Commission
Protecting People and the Environment

Enhancing Guidance for Evacuation Time Estimate Studies

Manuscript Completed: October 2019
2019 Date Published: March 2020

Prepared by:
B. Wolshon[1], N. Herrera[1], E. Tuncer[1], J. Jones[1]
S. Parr[2]
T. Smith[3]

Louisiana State University[1]
Baton Rouge, LA 70803

Embry-Riddle Aeronautical University[2]
Daytona Beach, FL 32114

U.S. Nuclear Regulatory Commission[3]
Washington DC, 20555

Todd Smith, NRC Technical Monitor
Sergio Gonzalez, NRC Project Manager
Lindsey Cooke, NRC Project Manager

Office of Nuclear Regulatory Research

ABSTRACT

Evacuation time estimates (ETEs) are an analysis of the time required to evacuate various sectors and distances within the plume exposure pathway emergency planning zone (EPZ) for permanent and transient populations. All nuclear power plant licensees are required to submit an updated ETE study after each decennial census. The objective of this study was to develop a technical basis for revision of NUREG/CR-7002, “Criteria for Development of Evacuation Time Estimate Studies,” in support of the next required ETE update. This applied research examines various aspects of ETE studies. Evacuation models were built for representative small, medium, and large population EPZs. Parametric analyses were conducted to examine modeling of traffic movement during evacuations, including: the impact of shadow evacuations; the effect of model extent; effectiveness of manual traffic control; and significance of parameter values. This report describes the model development and summarizes insights and observations to inform NRC staff efforts to enhance ETE guidance.

TABLE OF CONTENTS

ABSTRACT ..... **iii**

LIST OF FIGURES ..... **ix**

LIST OF TABLES ..... **xv**

EXECUTIVE SUMMARY ..... **xix**

ACKNOWLEDGEMENTS ..... **xxiii**

ABBREVIATIONS AND ACRONYMS ..... **xxv**

1 INTRODUCTION **1-1**
1.1 Objectives 1-2
1.2 Scope 1-2
1.2.1 Task 1: Shadow Evacuation Analysis 1-2
1.2.2 Task 2: Analysis of Distance of Travel 1-3
1.2.3 Task 3: Analysis of Manual Traffic Control 1-3
1.2.4 Task 4: Analysis of Parameters Important to ETE Calculations 1-4
1.3 Background 1-4

2 APPROACH **2-1**
2.1 Representative Sites and EPZ Characteristics 2-2
2.2 Scenario Selection 2-3
2.3 Model Data 2-4
2.4 Base Model Development 2-4
2.5 Parametric Analysis 2-5
2.6 Analysis of Results 2-5

3 MODEL DEVELOPMENT **3-1**
3.1 Model Development Assumptions 3-3
3.2 Base Model Summary 3-3
3.2.1 Summary of Model Characteristics 3-4
3.2.2 Boundary Conditions 3-4
3.3 Demand Estimation 3-5
3.3.1 Site Populations 3-5
3.3.2 Pass-Through and Background Traffic 3-6
3.3.3 Vehicle Volumes 3-8
3.4 Roadway Capacity 3-10
3.4.1 Roadway Types 3-10
3.4.2 Roadway Geometry 3-11
3.4.3 Roadway Grade 3-11
3.4.4 Intersections 3-12
3.5 Vehicle Routing 3-14
3.6 Driver Behavior 3-19
3.6.1 Car Following Models 3-20
3.6.2 Lane Change Parameters 3-22
3.6.3 Vehicle Speed 3-23

3.6.4 Base Model Loading 3-23
3.7 Simulation Coding 3-25
3.7.1 Time Step 3-25
3.7.2 Number of Runs 3-25
3.7.3 Validation and Model Adjustments 3-26
3.8 Base Model Data Collection and Analysis 3-27
3.8.1 Data Collector Locations 3-27
3.8.2 Data Quantity and Data Representation 3-27
3.8.3 Other Performance Indicators 3-29
3.8.4 Base Model MOE Results 3-29

4 TASK 1 SHADOW EVACUATION ANALYSIS 4-1
4.1 Background 4-1
4.1.1 Shadow Evacuation Literature Review 4-2
4.1.2 Shadow Evacuation Assumptions 4-3
4.1.3 Shadow Evacuation Contribution 4-4
4.1.4 Analysis of Shadow Participation 4-5
4.2 Shadow Participation Rate Analysis 4-5
4.2.1 Analysis Scenarios 4-5
4.2.2 Data Collection and Measures of Effectiveness 4-6
4.2.3 Shadow Participation Rate Results 4-6
4.2.4 Average Travel Speed Results 4-12
4.2.5 EPZ Exit Volume Results 4-17
4.3 Site Characteristics that Exacerbate the Impact of a Shadow Evacuation 4-20
4.3.1 Demand-Related Site Characteristics 4-20
4.3.2 Supply-Related Site Characteristics 4-21
4.4 Review of Current Shadow Evacuation Guidance 4-21

5 TASK 2 DISTANCE OF EVACUATION TRAVEL 5-1
5.1 Background 5-1
5.1.1 Queue Spillbacks 5-2
5.1.2 Spatial Boundary Limits for Traffic Simulation Studies 5-2
5.1.3 Spatial Boundary Limits for Hurricane Evacuation Studies 5-3
5.2 Task 2 Analysis 5-5
5.2.1 Model Truncation 5-6
5.2.2 Analysis Results 5-7
5.2.3 Analysis Findings 5-30
5.3 Conclusion 5-31

6 TASK 3 MANUAL TRAFFIC CONTROL STUDY 6-1
6.1 Background 6-2
6.2 Research Task 6-4
6.3 Literature Review 6-5
6.3.1 Manual of Uniform Traffic Control Devices (MUTCD) 6-5
6.3.2 Police Training For Traffic Control 6-6
6.3.3 Special Event and Emergency Planning 6-9
6.3.4 Manual Traffic Control and Empirical Studies 6-11
6.3.5 Summary of Literature Review Findings 6-13
6.4 Video Data Collection and Processing 6-14
6.4.1 General Observations 6-15
6.5 Variables Influencing MTC 6-16

6.5.1 Variable Selection....6-17
6.5.2 Logit Model Coefficients....6-18
6.5.3 Goodness-Of-Fit....6-23
6.5.4 Model Transfer and Validation....6-24
6.5.5 Summary of Logit Model Findings....6-26
6.6 MTC Model Development and Comparisons of Performance....6-27
6.6.1 Geometric Design and Demand Modeling....6-27
6.6.2 Logit Model Programing....6-27
6.6.3 Comparisons of Performance....6-28
6.6.4 Summary of Findings....6-38
6.7 NPP Representative Site Analysis....6-39
6.7.1 Modeling MTC for the ETE Study....6-39
6.7.2 Impact of MTC....6-43
6.7.3 Sensitivity to the Number of MTC Intersections....6-63
6.8 Conclusion....6-73
6.8.1 Summary of Results....6-74

7 TASK 4 PARAMETERS OF IMPORTANCE....7-1
7.1 Background....7-1
7.1.1 Parameters of Importance....7-1
7.2 Description of Scenarios....7-20
7.2.1 Population....7-20
7.2.2 Mobilization Time....7-23
7.2.3 Background Traffic....7-28
7.2.4 Heavy Vehicles....7-29
7.2.5 Free-Flow Speed....7-30
7.2.6 Adverse Weather....7-32
7.2.7 Roadway Impact....7-33
7.2.8 Processing Time Step....7-36
7.2.9 Uncertainty Analysis....7-37
7.3 Task 4 Results....7-37
7.3.1 Population Parameter Results....7-38
7.3.2 Mobilization Time Results....7-54
7.3.3 Background Traffic Parameter Results....7-65
7.3.4 Heavy Vehicle Parameter Results....7-71
7.3.5 Free-Flow Speed Parameter Results....7-78
7.3.6 Adverse Weather Parameter Results....7-90
7.3.7 Roadway Impact Parameter Results....7-97
7.3.8 Processing Time Step Parameter Results....7-110
7.3.9 Random Seed Uncertainty Analysis Parameter Results....7-116
7.4 Conclusion....7-118
7.4.1 Population....7-118
7.4.2 Mobilization Time....7-118
7.4.3 Background Traffic....7-118
7.4.4 Heavy Vehicles....7-119
7.4.5 Free-flow Speed....7-119
7.4.6 Adverse Weather....7-119
7.4.7 Roadway Impact....7-119
7.4.8 Processing Time Step....7-119
7.4.9 Random Number Seeding....7-120
7.4.10 Overall Findings....7-120

8 CONCLUSIONS 8-1
8.1 Base Model Development Observations and Insights 8-1
8.1.1 Model Selection 8-2
8.1.2 Static Models and Dynamic Traffic Assignment 8-2
8.1.3 Signalized Intersections 8-2
8.1.4 Boundary Conditions 8-3
8.1.5 Background Traffic 8-3
8.1.6 Vehicle Loading 8-3
8.1.7 Roadway Grade 8-3
8.1.8 Number of Model Runs 8-4
8.1.9 Traffic Simulation Model Output 8-4
8.2 Supply and Demand 8-4

9 GLOSSARY 9-1

10 REFERENCES 10-1

APPENDIX A LITERATURE REVIEW A-1

APPENDIX B INPUT PARAMETERS B-1

APPENDIX C SELECTION OF REPRESENTATIVE SITES C-1

LIST OF FIGURES

Figure 2-1 Generic EPZ with ERPAs 2-1
Figure 2-2 Typical S-curve Representing Evacuation Response 2-3
Figure 3-1 Destination Zones for the Medium Population Site Model 3-16
Figure 3-2 Destination Zones for the Large Population Site Model 3-17
Figure 3-3 Illustration of Destination Assignments in the Large Population Site Model 3-18
Figure 3-4 Illustration of Pitch-Fork Modeling Approach for Destination Zones 3-19
Figure 3-5 Data Collector Points for the Small Population Site Model 3-28
Figure 3-6 ETE Curves for the Small Population Site Base Model 3-30
Figure 3-7 ETE Curves for the Medium Population Site Base Model 3-31
Figure 3-8 ETE Curves for the Large Population Site Base Model 3-32
Figure 3-9 EPZ Average Exit Speeds (mph) for the Small Population Site Base Model at Various Times in the Evacuation 3-34
Figure 3-10 EPZ Average Exit Speeds (mph) for the Medium Population Site Base Model at Various Times in the Evacuation 3-35
Figure 3-11 EPZ Average Exit Speeds (mph) for the Large Population Site Base Model at Various Times in the Evacuation 3-36
Figure 4-1 Ten Mile ETE Curves, Small Population Site Shadow Analysis 4-7
Figure 4-2 Ten Mile ETE Curves, Medium Population Site Analysis 4-9
Figure 4-3 Ten Mile ETE Curves, Large Population Site Shadow Analysis 4-11
Figure 4-4 Average Exit Speeds at 0:15, Small Population Site Shadow Analysis 4-13
Figure 4-5 Average Exit Speeds at 1:45, Small Population Site Shadow Analysis 4-13
Figure 4-6 Average Exit Speeds at 2:30, Medium Population Site Shadow Analysis 4-14
Figure 4-7 Average Exit Speeds at 3:30, Medium Population Site Shadow Analysis 4-14
Figure 4-8 Average Exit Speeds at 4:30, Medium Population Site Shadow Analysis 4-15
Figure 4-9 Average Exit Speeds at 2:30, Large Population Site Shadow Analysis 4-16
Figure 4-10 Average Exit Speeds at 3:30, Large Population Site Shadow Analysis 4-16
Figure 4-11 Average Exit Speeds at 4:30, Large Population Site Shadow Analysis 4-17
Figure 4-12 EPZ Exit Volumes, Small Population Site Shadow Analysis 4-18
Figure 4-13 EPZ Exit Volumes, Medium Population Site Shadow Analysis 4-19
Figure 4-14 EPZ Exit Volumes, Large Population Site Shadow Analysis 4-20
Figure 5-1 Small Population Site Model Population Beyond the Shadow Region 5-8
Figure 5-2 Ten Mile ETE Curves, Small Population Site Travel Distance Analysis 5-9
Figure 5-3 Ten Mile 90 Percent ETE by Sector, Medium Population Site Travel Distance Analysis 5-10
Figure 5-4 Ten Mile 100 Percent ETE by Sector, Medium Population Site Travel Distance Analysis 5-10
Figure 5-5 Medium Population Site Model Population Beyond the Shadow Region 5-11
Figure 5-6 Two Mile ETE Curves, Medium Population Site Travel Distance Analysis 5-12
Figure 5-7 Five Mile ETE Curves, Medium Population Site Travel Distance Analysis 5-13
Figure 5-8 Ten Mile ETE Curves, Medium Population Site Travel Distance Analysis 5-13
Figure 5-9 Ten Mile 90 Percent ETE by Sector, Large Population Site Travel Distance Analysis 5-15
Figure 5-10 Ten Mile 100 Percent ETE by Sector, Large Population Site Travel Distance Analysis 5-15
Figure 5-11 Large Population Site Model Population Beyond the Shadow Region 5-16
Figure 5-12 Two Mile ETE Curves, Large Population Site Travel Distance Analysis 5-17
Figure 5-13 Five Mile ETE Curves, Large Population Site Travel Distance Analysis 5-17
Figure 5-14 Ten Mile ETE Curves, Large Population Site Travel Distance Analysis 5-18

Figure 5-15 Average Speeds at 0:15, Small Population Site Travel Distance Analysis 5-19
Figure 5-16 Average Speeds at 1:45, Small Population Site Travel Distance Analysis 5-19
Figure 5-17 Average Speeds at 2:30, Medium Population Site Travel Distance Analysis 5-20
Figure 5-18 Average Speeds at 3:30, Medium Population Site Travel Distance Analysis 5-21
Figure 5-19 Average Speeds at 4:30, Medium Population Site Travel Distance Analysis 5-21
Figure 5-20 Average Speeds at 2:30, Large Population Site Travel Distance Analysis 5-22
Figure 5-21 Average Speeds at 3:30, Large Population Site Travel Distance Analysis 5-23
Figure 5-22 Average Speeds at 4:30, Large Population Site Travel Distance Analysis 5-23
Figure 5-23 EPZ Exit Volumes, Small Population Site Travel Distance Analysis 5-24
Figure 5-24 EPZ Exit Volumes, Medium Population Site Travel Distance Analysis 5-25
Figure 5-25 EPZ Exit Volumes, Large Population Site Travel Distance Analysis 5-26
Figure 6-1 Saturation Flow Rate and Lost Time Diagram 6-38
Figure 6-2 Small Population Site Model MTC Intersections in the 10-Mile EPZ 6-40
Figure 6-3 Medium Population Site Model MTC Intersections in the 10-Mile EPZ 6-41
Figure 6-4 Large Population Site Model MTC Intersections in the 10-Mile EPZ 6-42
Figure 6-5 Two Mile ETE Curves, Small Population Site Manual Traffic Control Analysis 6-45
Figure 6-6 Five Mile ETE Curves, Small Population Site Manual Traffic Control Analysis 6-45
Figure 6-7 Ten Mile ETE Curves, Small Population Site Manual Traffic Control Analysis 6-46
Figure 6-8 Two Mile ETE Curves, Medium Population Site Manual Traffic Control Analysis 6-48
Figure 6-9 Five Mile ETE Curves, Medium Population Site Manual Traffic Control Analysis 6-48
Figure 6-10 Ten Mile ETE Curves, Medium Population Site Manual Traffic Control Analysis 6-49
Figure 6-11 Two Mile ETE Curves, Large Population Site Manual Traffic Control Analysis 6-51
Figure 6-12 Five Mile ETE Curves, Large Population Site Manual Traffic Control Analysis 6-51
Figure 6-13 Ten Mile ETE Curves, Large Population Site Manual Traffic Control Analysis 6-52
Figure 6-14 Average Speeds at 1:45, Small Population Site Manual Traffic Control Analysis 6-53
Figure 6-15 Average Speeds at 2:30, Medium Population Site Manual Traffic Control Analysis 6-54
Figure 6-16 Average Speeds at 3:30, Medium Population Site Manual Traffic Control Analysis 6-54
Figure 6-17 Average Speeds at 4:30, Medium Population Site Manual Traffic Control Analysis 6-55
Figure 6-18 Average Speeds at 2:30, Large Population Site Manual Traffic Control Analysis 6-55
Figure 6-19 Average Speeds at 3:30, Large Population Site Manual Traffic Control Analysis 6-56
Figure 6-20 Average Speeds at 4:30, Large Population Site Manual Traffic Control Analysis 6-56
Figure 6-21 EPZ Exit Volumes, Small Population Site Manual Traffic Control Analysis 6-58
Figure 6-22 Two Mile Exit Volumes, Medium Population Site Manual Traffic Control Analysis 6-59
Figure 6-23 Five Mile Exit Volumes, Medium Population Site Manual Traffic Control Analysis 6-59
Figure 6-24 Ten Mile Exit Volumes, Medium Population Site Manual Traffic Control Analysis 6-60
Figure 6-25 Two Mile Exit Volumes, Large Population Site Manual Traffic Control Analysis 6-61
Figure 6-26 Five Mile Exit Volumes, Large Population Site Manual Traffic Control Analysis 6-61
Figure 6-27 Ten Mile Exit Volumes, Large Population Site Manual Traffic Control Analysis 6-62
Figure 6-28 Ten Mile ETE Curves, Small Population Site Varying MTC Intersections 6-65
Figure 6-29 Two Mile ETE Curves, Medium Population Site Varying MTC Intersections 6-66
Figure 6-30 Five Mile ETE Curves, Medium Population Site Varying MTC Intersections 6-67
Figure 6-31 Ten Mile ETE Curves, Medium Population Site Varying MTC Intersections 6-67
Figure 6-32 Two Mile ETE Curves, Large Population Site Varying MTC Intersections 6-69
Figure 6-33 Five Mile ETE Curves, Large Population Site Varying MTC Intersections 6-69
Figure 6-34 Ten Mile ETE Curves, Large Population Site Varying MTC Intersections 6-70
Figure 6-35 EPZ Exit Volumes, Small Population Site Varying MTC Intersections 6-71
Figure 6-36 EPZ Exit Volumes, Medium Population Site Varying MTC Intersections 6-72
Figure 6-37 EPZ Exit Volumes, Large Population Site Varying MTC Intersections 6-72
Figure 7-1 Theoretical Relationship Between Population and ETEs 7-5
Figure 7-2 Adverse Weather Impact on Macroscopic Traffic Flow 7-11

Figure 7-3 Relationship Between Saturation Flow Rate and the Multiplicative Part of the Safety Distance ($\boldsymbol{BXmult}$) in the Wiedemann 74 Car Following Model 7-14
Figure 7-4 Relationship Between Desired Average Safety Distance and Wiedemann 99 Car Following Parameters Headway Time (CC1) and Standstill Distance (CC0) 7-15
Figure 7-5 Relationship Between Saturation Flow Rate in veh/h/lane and Wiedemann 99 CC1 Car Following Parameter (Headway Time) 7-15
Figure 7-6 Relationship Between (a) Saturation Flow Rate and (b) Start-up Delay to the Multiplicative Part ($\boldsymbol{BXmult}$) and Additive Part ($\boldsymbol{BXadd}$) of the Safety Distance in the Wiedemann 74 Car Following Model. Black Line Indicates Combined Parameters ($\boldsymbol{BXmult}$ and $\boldsymbol{BXadd}$) 7-16
Figure 7-7 Spatial Population Breakdown in the Medium Population Site Model 7-21
Figure 7-8 Faster Mobilization Time Curves and Base Scenario Loading Curves 7-27
Figure 7-9 Slower Mobilization Time Curves and Base Scenario Loading Curves 7-28
Figure 7-10 Desired Speed Distribution in VISSIM 7-31
Figure 7-11 Small Population Site Model Roadway Impact Location 7-34
Figure 7-12 Medium Population Site Model Roadway Impact Locations 7-35
Figure 7-13 Large Population Site Model Roadway Impact Locations 7-36
Figure 7-14 Two Mile ETE Curves, Small Population Site Population Analysis 7-40
Figure 7-15 Ten Mile ETE Curves, Small Population Site Population Analysis 7-40
Figure 7-16 Two Mile ETE Curves, Medium–South Population Site Population Analysis 7-42
Figure 7-17 Ten Mile ETE Curves, Medium–South Population Site Population Analysis 7-42
Figure 7-18 Five Mile ETE Curves, Medium–North Population Site Population Analysis 7-44
Figure 7-19 Ten Mile ETE Curves, Medium–North Population Site Population Analysis 7-44
Figure 7-20 Two Mile ETE Curves, Large Population Site Model, Population Analysis 7-46
Figure 7-21 Ten Mile ETE Curves, Large Population Site Model, Population Analysis 7-46
Figure 7-22 Ten Mile 100 percent ETEs, Small and Medium-South Site Population Analyses 7-48
Figure 7-23 Ten Mile 90 percent ETEs, Small and Medium-South Site Population Analyses 7-48
Figure 7-24 Ten Mile 100 percent ETEs, Medium-North and Large Site Population Analysis 7-49
Figure 7-25 Ten Mile 90 Percent ETEs, Medium-North and Large Site Population Analysis 7-49
Figure 7-26 EPZ Exit Volumes, Small Population Site Population Analysis 7-50
Figure 7-27 EPZ Exit Volumes, Medium-South Population Site Population Analysis 7-51
Figure 7-28 EPZ Exit Volumes, Medium-North Population Site Population Analysis 7-52
Figure 7-29 Five Mile Exit Volumes, Medium-North Population Site Population Analysis 7-52
Figure 7-30 EPZ Exit Volumes, Large Population Site Population Analysis 7-53
Figure 7-31 Ten Mile ETE Curves, Small Population Site Faster Mobilization Times 7-56
Figure 7-32 Ten Mile ETE Curves, Small Population Site Slower Mobilization Times 7-56
Figure 7-33 Ten Mile ETE Curves, Medium Population Site Faster Mobilization Times 7-58
Figure 7-34 Ten Mile ETE Curves, Medium Population Site Slower Mobilization Times 7-58
Figure 7-35 Ten Mile ETE Curves, Large Population Site Faster Mobilization Times 7-60
Figure 7-36 Ten Mile ETE Curves, Large Population Site Slower Mobilization Times 7-60
Figure 7-37 Ten Mile 100 Percent ETEs, Small, Medium, and Large Population Site Mobilization Time Analysis 7-62
Figure 7-38 EPZ Exit Volumes, Small Population Site Mobilization Time Analysis 7-63
Figure 7-39 EPZ Exit Volumes, Medium Population Site Mobilization Time Analysis 7-63
Figure 7-40 EPZ Exit Volumes, Large Population Site Mobilization Time Analysis 7-64
Figure 7-41 Ten Mile ETE Curves, Small Population Site Background Traffic Analysis 7-66
Figure 7-42 Ten Mile ETE Curves, Medium Population Site Background Traffic Analysis 7-67
Figure 7-43 Ten Mile ETE Curves, Large Population Site Background Traffic Analysis 7-69
Figure 7-44 EPZ Exit Volumes, Small Population Site Background Traffic Analysis 7-69
Figure 7-45 EPZ Exit Volumes, Medium Population Site Background Traffic Analysis 7-70

Figure 7-46 EPZ Exit Volumes, Large Population Site Background Traffic Analysis 7-70
Figure 7-47 Ten Mile ETE Curves, Small Population Site Heavy Vehicle Analysis.....7-72
Figure 7-48 Five Mile ETE Curves, Medium Population Site Heavy Vehicle Analysis.....7-73
Figure 7-49 Ten Mile ETE Curves, Medium Population Site Heavy Vehicle Analysis.....7-74
Figure 7-50 Five Mile ETE Curves, Large Population Site Heavy Vehicle Analysis.....7-75
Figure 7-51 Ten Mile ETE Curves, Large Population Site Heavy Vehicle Analysis 7-75
Figure 7-52 EPZ Exit Volumes, Small Population Site Heavy Vehicle Analysis.....7-76
Figure 7-53 EPZ Exit Volumes, Medium Population Site Heavy Vehicle Analysis.....7-77
Figure 7-54 EPZ Exit Volumes, Large Population Site Heavy Vehicle Analysis.....7-77
Figure 7-55 Ten Mile ETE Curves, Small Population Site Free-flow Speed Analysis 7-79
Figure 7-56 Five Mile ETE Curves, Medium Population Site Free-flow Speed Analysis.....7-80
Figure 7-57 Ten Mile ETE Curves, Medium Population Site Free-flow Speed Analysis 7-81
Figure 7-58 Ten Mile ETE Curves, Large Population Site Free-flow Speed Aanalysis.....7-82
Figure 7-59 Average Exit Speeds at 0:15, Small Population Site Free-flow Speed Analysis.....7-83
Figure 7-60 Average Exit Speeds at 1:45, Small Population Site Free-flow Speed Analysis.....7-83
Figure 7-61 Average Exit Speeds at 2:30, Medium Population Site Free-flow Speed Analysis.....7-84
Figure 7-62 Average Exit Speeds at 3:30, Medium Population Site Free-flow Speed Analysis.....7-85
Figure 7-63 Average Exit Speeds at 4:30, Medium Population Site Free-flow Speed Analysis.....7-85
Figure 7-64 Average Exit Speeds at 2:30, Large Population Site Free-flow Speed Analysis 7-86
Figure 7-65 Average Exit Speeds at 3:30, Large Population Site Free-flow Speed Analysis 7-87
Figure 7-66 Average Exit Speeds at 4:30, Large Population Site Free-flow Speed Analysis 7-87
Figure 7-67 EPZ Exit Volumes, Small Population Site Free-flow Speed Analysis 7-88
Figure 7-68 EPZ Exit Volumes, Medium Population Site Free-flow Speed Analysis 7-89
Figure 7-69 EPZ Exit Volumes, Large Population Site Free-flow Speed Analysis 7-89
Figure 7-70 Ten Mile ETE Curves, Small Population Site Adverse Weather Analysis.....7-91
Figure 7-71 Ten Mile ETE Curves, Medium Population Site Adverse Weather Analysis.....7-93
Figure 7-72 Ten Mile ETE Curves, Large Population Site Model Adverse Weather Analysis.....7-94
Figure 7-73 EPZ Exit Volumes, Small Population Site Model Adverse Weather Analysis.....7-95
Figure 7-74 EPZ Exit Volumes, Medium Population Site Model Adverse Weather Analysis 7-95
Figure 7-75 EPZ Exit Volumes, Large Population Site Adverse Weather Analysis.....7-96
Figure 7-76 Ten Mile ETE Curves, Small Population Site Roadway Impact Analysis.....7-98
Figure 7-77 Five Mile ETE Curves, Medium Population Site Roadway Impact Analysis 7-99
Figure 7-78 Ten Mile ETE Curves, Medium Population Site Roadway Impact Analysis.....7-100
Figure 7-79 Two Mile ETE Curves, Large Population Site Roadway Impact Analysis.....7-101
Figure 7-80 Five Mile ETE Curves, Large Population Site Roadway Impact Anaysis.....7-102
Figure 7-81 Ten Mile ETE Curves, Large Population Site Roadway Impact Analysis 7-102
Figure 7-82 Segment (Link 647) Travel Times, Small Population Site Roadway Impact Analysis.....7-103
Figure 7-83 Segment (Link 133) Travel Times, Medium Population Site Roadway Impact Analysis.....7-104
Figure 7-84 Segment (Link 222) Travel Times, Medium Population Site Roadway Impact Analysis.....7-105
Figure 7-85 Average Queue Length, Medium Population Site Roadway Impact Analysis 7-105
Figure 7-86 Segment (Link 150) Travel Times, Large Population Site Roadway Impact Analysis.....7-106
Figure 7-87 Segment (Link 32909) Travel Times, Large Population Site Roadway Impact Analysis.....7-107
Figure 7-88 Average Queue Length, Large Population Site Roadway Impact Analysis 7-107
Figure 7-89 EPZ Exit Volumes, Small Population Site Roadway Impact Analysis.....7-108
Figure 7-90 EPZ Exit Volumes, Medium Population Site Roadway Impact Analysis.....7-109
Figure 7-91 EPZ Exit Volumes, Large Population Site Roadway Impact Analysis.....7-109

Figure 7-92 Ten Mile ETE Curves, Small Population Site Processing Time Step Analysis 7-111
Figure 7-93 Two Mile ETE Curves, Medium Population Site Processing Time Step Analysis.....7-112
Figure 7-94 Five Mile ETE Curves, Medium Population Site Processing Time Step Analysis.....7-113
Figure 7-95 Ten Mile ETE Curves, Medium Population Site Processing Time Step Analysis 7-113
Figure 7-96 Two Mile ETE Curves, Large Population Site Processing Time Step Analysis ...7-114
Figure 7-97 Five Mile ETE Curves, Large Population Site Processing Time Step Analysis ...7-115
Figure 7-98 Ten Mile ETE Curves, Large Population Site Processing Time Step Analysis....7-115
Figure B-1 Population and Road Network in the Small Population Site Base Model B-6
Figure B-2 Population and Road Network in the Medium Population Site Base Model B-7
Figure B-3 Population and Road Network in the Large Population Site Base Model B-8
Figure B-4 Speed Distribution Profile with Posted Speed at 85th Percentile B-10
Figure B-5 Small Population Site Model Data Collection Points..... B-11
Figure B-6 Medium Population Site Model Data Collection Points..... B-12
Figure B-7 Large Population Site Model Data Collection Points B-13
Figure B-8 Radial Distances Used in the Base Models B-14
Figure C-1 Relationship Between Resident Population and 90 Percent ETE for the EPZ C-2
Figure C-2 Road Network Topology in the 10-mile Region Around 63 Nuclear Plant Sites..... C-3
Figure C-3 Comparison of Road Network Fractal Dimensions Using MATLAB and Fractalyse Box-counting Methods C-4
Figure C-4 Road Network Fractal Dimension vs. Resident Population in the 10-mile EPZ..... C-5
Figure C-5 Example Fractal Dimension Curve of Scaling Behavior for a Site with $d_f = 1.6$ C-5
Figure C-6 Neural Network Classification of Road Networks: Rural, Coastal, Urban C-6
Figure C-7 Road Network Classification vs. Resident Population C-7
Figure C-8 Medium Population Site Road Network C-8

LIST OF TABLES

Table 3-1 Base Model Characteristics 3-4
Table 3-2 Summary of Modeled Populations 3-6
Table 3-3 Summary of Modeled Vehicle Contribution Inputs 3-8
Table 3-4 General Roadway Characteristics 3-11
Table 3-5 Summary of Signalized Intersections 3-13
Table 3-6 Dynamic Traffic Assignment Cost Functions 3-19
Table 3-7 Driver Behavior Parameters for Non-Freeways (Wiedemann 74) 3-20
Table 3-8 Driver Behavior Parameters for Freeways (Wiedemann 99) 3-21
Table 3-9 VISSIM Lane Change Parameters 3-22
Table 3-10 Modeled Speed Values 3-23
Table 3-11 Traffic Simulation Loading Curves for Representative Models 3-24
Table 3-12 Base Model Average ETEs and Clearance Times 3-29
Table 3-13 ETEs and Clearance Times by Quadrant 3-32
Table 3-14 Low, Mean, and High ETE and Clearance Time Results 3-33
Table 3-15 Summary of EPZ and Shadow Evacuation Vehicle Inputs and Exits 3-38
Table 3-16 Model Output Summary Metrics 3-39
Table 4-1 Scenarios for Shadow Analysis 4-6
Table 4-2 Average ETEs, Small Population Site Shadow Analysis 4-7
Table 4-3 Ten Mile ETEs by Quadrant, Small Population Site Shadow Analysis 4-8
Table 4-4 Average ETEs, Medium Population Site Shadow Analysis 4-8
Table 4-5 Ten Mile ETEs by Quadrant, Medium Population Site Analysis 4-10
Table 4-6 Average ETEs, Large Population Site Shadow Analysis 4-10
Table 4-7 Ten Mile ETEs by Quadrant, Large Population Site Shadow Analysis 4-11
Table 5-1 Small Population Site Average ETEs for Models of Varying Distance 5-8
Table 5-2 Medium Population Site Average ETEs for Models of Varying Distance 5-9
Table 5-3 Large Population Site Average ETEs for Models of Varying Distance 5-14
Table 5-4 Small Population Site Travel Times, Major Route in West-Southwest Sector 5-27
Table 5-5 Small Population Site Travel Times, Major Route in East-Southeast Sector 5-27
Table 5-6 Medium Population Site Travel Times, Major Route in East-Southeast Sector 5-28
Table 5-7 Medium Population Site Travel Times, Major Route in North-Northwest Sector 5-28
Table 5-8 Large Population Site Travel Times, Major Route in South-East Sector 5-29
Table 5-9 Large Population Site Travel Times, Major Route in West-Northwest Sector 5-29
Table 6-1 Observed MTC Signal Timing 6-15
Table 6-2 Constant Variable for MTC Logit Model 6-18
Table 6-3 Statistical Testing for the MTC Constant Variable 6-19
Table 6-4 Primary Direction Variables 6-20
Table 6-5 Statistical Testing of the Primary Direction Variables 6-20
Table 6-6 Secondary Direction Variables 6-21
Table 6-7 Statistical Testing of the Secondary Direction Variables 6-21
Table 6-8 Tertiary Direction Variables 6-22
Table 6-9 Statistical Testing of the Tertiary Direction Variables 6-22
Table 6-10 Quaternary Direction Variables 6-23
Table 6-11 Statistical Testing of the Quaternary Direction Variables 6-23
Table 6-12 Logit Model Goodness-of-Fit 6-24
Table 6-13 MTC Calibration and Validation Datasets 6-24
Table 6-14 Nicholson and Roosevelt Combined Logit Model Parameters 6-25
Table 6-15 Logit Mode Validation Results 6-26
Table 6-16 Simulated MTC Vehicle Counts vs. Observed and Statistical Evaluation 6-30

Table 6-17 Simulated MTC Signal Timing vs. Observed MTC and Statistical Evaluation 6-30
Table 6-18 Simulated MTC Signal Timing vs. Observed Within Alternative Study Area.....6-33
Table 6-19 Intersection Throughput: Observed, Actuated Control, and Simulated MTC.....6-34
Table 6-20 Simulated MTC Signal Timing vs. Simulated Actuated Control.....6-35
Table 6-21 Simulated MTC Network Performance vs. Simulated Actuated Control 6-36
Table 6-22 Traffic Control Point Statistics and Number Modeled in Representative Sites.....6-39
Table 6-23 Representative Actuated Signal Control Timing Four-Phase EB-WB Dominate.....6-43
Table 6-24 Small Population Site Average ETEs for Varying Traffic Control 6-44
Table 6-25 Small Population Site Average ETEs by Quadrant for Varying Traffic Control 6-44
Table 6-26 Medium Population Site Average ETEs for Varying Traffic Control 6-47
Table 6-27 Medium Population Site Average ETEs by Quadrant for Varying Traffic Control.....6-47
Table 6-28 Large Population Site Average ETEs for Varying Traffic Control 6-50
Table 6-29 Large Population Site Average ETEs by Quadrant for Varying Traffic Control.....6-50
Table 6-30 Increments of MTC Intersection Scenarios 6-63
Table 6-31 Small Population Site ETEs for Varying MTC Intersections 6-64
Table 6-32 Small Population Site ETEs by Quadrant for Varying MTC Intersections.....6-64
Table 6-33 Medium Population Site ETEs for Varying MTC Intersections 6-65
Table 6-34 Medium Population Site ETEs by Quadrant for Varying MTC Intersections.....6-66
Table 6-35 Large Population Site ETEs for Varying MTC Intersections.....6-68
Table 6-36 Large Population Site ETEs by Quadrant for Varying MTC Intersections.....6-68
Table 7-1 Traffic Demand Parameters Description and Range 7-2
Table 7-2 Network Supply Parameters Description and Range 7-3
Table 7-3 Simulation Process Parameters Description and Range.....7-3
Table 7-4 Inclement Weather Impacts on Traffic Flow.....7-11
Table 7-5 Small Population Site Model Population Parameters 7-20
Table 7-6 Medium-North Population Site Model Population Parameters 7-22
Table 7-7 Medium-South Population Site Model Population Parameters 7-22
Table 7-8 Large Population Site Model Population Parameters.....7-22
Table 7-9 Mobilization Time Scenarios.....7-23
Table 7-10 Traffic Simulation Loading Curves for Small Population Site Model 7-24
Table 7-11 Traffic Simulation Loading Curves for Medium Population Site Model 7-25
Table 7-12 Traffic Simulation Loading Curves for Large Population Site Model 7-26
Table 7-13 Background Traffic Scenarios 7-29
Table 7-14 Heavy Vehicle Scenarios.....7-30
Table 7-15 Free-flow Speed Scenarios 7-31
Table 7-16 Adverse Weather Scenarios.....7-33
Table 7-17 Roadway Impact Scenarios.....7-34
Table 7-18 Processing Time Step Scenarios 7-37
Table 7-19 Small Population Site Population Analysis.....7-39
Table 7-20 Medium-South Population Site Population Analysis.....7-41
Table 7-21 Medium-North Population Site Population Analysis.....7-43
Table 7-22 Large Population Site Population Analysis 7-45
Table 7-23 Small Population Site Mobilization Time Analysis 7-55
Table 7-24 Medium Population Site Mobilization Time Analysis.....7-57
Table 7-25 Large Population Site Mobilization Time Analysis 7-59
Table 7-26 Small Population Site Background Traffic Analysis 7-66
Table 7-27 Medium Population Site Background Traffic Analysis 7-67
Table 7-28 Large Population Site Background Traffic Analysis 7-68
Table 7-29 Small Population Site Heavy Vehicle Analysis.....7-72
Table 7-30 Medium Population Site Heavy Vehicle Analysis.....7-73
Table 7-31 Large Population Site Heavy Vehicle Analysis 7-74

Table 7-32 Small Population Site Free-flow Speed Analysis 7-79
Table 7-33 Medium Population Site Free-flow Speed Analysis 7-80
Table 7-34 Large Population Site Free-flow Speed Analysis 7-82
Table 7-35 Small Population Site Adverse Weather Analysis 7-91
Table 7-36 Medium Population Site Adverse Weather Analysis 7-92
Table 7-37 Large Population Site Adverse Weather Analysis 7-94
Table 7-38 Small Population Site Roadway Impact Analysis 7-98
Table 7-39 Medium Population Site Roadway Impact Analysis 7-99
Table 7-40 Large Population Site Roadway Impact Analysis 7-100
Table 7-41 Small Population Site Processing Time Step Analysis 7-111
Table 7-42 Medium Population Site Processing Time Step Analysis 7-112
Table 7-43 Large Population Site Processing Time Step Analysis 7-114
Table 7-44 Small Population Site Random Seed Sensitivity Analysis 7-117
Table 7-45 Medium Population Site Random Seed Sensitivity Analysis 7-117
Table 7-46 Large Population Site Random Seed Sensitivity Analysis 7-117
Table 8-1 Base Model ETEs and Clearance Times for Each Site 8-2
Table B-1 Driver Behavior Parameters for Non-Freeways (Wiedemann 74) B-1
Table B-2 Driver Behavior Parameters for Freeways (Wiedemann 99) B-2
Table B-3 Lane Changing Parameters B-3
Table B-4 Small Population Site Population Distribution B-4
Table B-5 Medium Population Site Population Distribution B-5
Table B-6 Large Population Site Population Distribution B-5
Table B-7 Loading Curve B-9

EXECUTIVE SUMMARY

The evacuation time estimate (ETE) is a calculation of the time to evacuate areas within the plume exposure pathway emergency planning zone (EPZ). Nuclear power plant (NPP) licensees are required to submit an updated ETE study after each decennial census. The objective of this project is to provide a technical basis for the revision of NUREG/CR-7002, "Criteria for Development of Evacuation Time Estimate Studies," [4] to support the next required updates to ETE studies.

This applied research study provides information of interest and importance to the United States Nuclear Regulatory Commission (NRC) in its mission to protect public health and safety. The research summarized in this report focused on aspects of evacuation planning and modeling within the context of NPP emergency planning. However, it is also clear that the results gained from this study have application beyond radiological emergency planning. A series of four separate, but closely related, project tasks were carried out to provide a technical basis for potential revisions to current guidance related to development of ETE studies. These tasks are:

- Task 1: Shadow Evacuation Analysis
- Task 2: Distance of Evacuation Travel
- Task 3: Manual Traffic Control Study
- Task 4: Parameters of Importance

The objectives, methods, assumptions, and results from this research are discussed in the various sections of this report and summarized at a broad level in this Executive Summary.

Task Objectives

The objective of Task 1 was to enhance the current understanding of the potential impacts of shadow evacuations. Shadow evacuations occur when persons not under an evacuation order evacuate based on perceived danger. The scope of Task 1 included a determination of the adequacy of the current NRC guidance that ETE studies incorporate 20 percent of the resident population within the area 10 to 15 miles from a nuclear power plant (NPP) site [4]. Task 2 focused on assessing the geographic extent to which a roadway network should be modeled beyond the 10-mile emergency planning zone (EPZ). This was done to understand how population, roadway network, and geographic conditions outside of the EPZ might impact the ETE and to provide a quantitative understanding of travel times to the distances at which care centers may be established by offsite emergency planning agencies. The focus of Task 3 was to quantify the benefits and disadvantages of manual traffic control at intersections during an evacuation. The results of this task can also be used to inform the development of traffic management plans for evacuation. Finally, Task 4 sought to determine the impact and importance of various assumptions and key modeling parameter inputs. Decades of ETE study using traffic simulation modeling has suggested that evacuation traffic simulations can be influenced by the representation of physical processes and simulation modeling assumptions. In this task, a wide range of parameters (and their associated values) were evaluated to determine their potential influence on ETE computation.

The study approach followed the same general process recommended in NUREG/CR-7002 for the development of ETE studies. This process incorporates: 1) developing traffic simulation models, 2) acquiring data to populate the models, and 3) conducting parametric analyses to

compare the resulting model output. The application of traffic simulation models to produce evacuation times reflects the current state of the practice. As a part of this effort, existing ETE studies were reviewed to support development of the model parameters. Current ETE guidance was reviewed to understand how the modeling approaches and criteria are applied in ETE studies. This review supported both development of the traffic simulation models used in this study and was also used to identify the inputs and outputs that are typically provided in an ETE report to assess whether enhancements in guidance could reduce some of the current data requests.

This applied research was designed to produce results that are applicable across NPP sites nationwide. This was accomplished by creating three generic traffic simulation "base" models that are intended to broadly represent key aspects of all small, medium and large population EPZs across the United States. The selection of a simulation modeling tool was also a key part of this research. There are a wide variety of commercial off-the-shelf systems available to model and simulate traffic processes. The VISSIM microscopic simulation program was used to create the traffic simulation models for the three representative sites.

Representative population demographics, infrastructure and other EPZ characteristics were used to code the three base models. While the roadway networks for the base models were based on real NPP sites, it is important to note that the ETEs produced in this study are representative of theoretical conditions and cannot directly be compared to any site-specific ETEs. Numerous changes in the representative site models (such as the evacuation population, spatial distribution, origin and destination locations) were made to facilitate the research objectives. In many instances, the base model assumptions also required modifications of road network topology, connectivity, and utilization to represent reasonable travel decision making.

The level of effort used to develop the base microsimulation models for this study was necessary to provide insights into the ETE process from a research context, and some of these efforts would not be necessary in an NPP ETE study. Throughout the project, models were run, reviewed, modified, and re-run to test, validate and ensure each base model reasonably represented the intended evacuation network. Model outputs were captured using several different measures of effectiveness (MOEs) including: 1) ETEs for the EPZs; 2) clearance times for areas beyond the EPZ; 3) average vehicle speeds at specific times and locations in the network; 4) vehicle volumes at these same times and locations; and 5) average vehicle delay times.

The methodology used in this study required the establishment of a "baseline" from which the effect of testing could be compared. This baseline, in effect, represented average conditions and assumptions required under current NRC guidance. The baseline models were used for comparison of performance across tasks. When changes in the MOEs between the base and task models were noted, they were investigated in detail to gain a better understanding of the impacts and, if possible, the causes for the performance differences.

Task Results

In Task 1, shadow evacuation rates ranged from 0 to 100 percent in the small population site and from 0 to 40 percent in both the large and medium population models. Overall, the results showed that increasing the participation to 100 percent of the resident population in the small population site had no effect on the ETEs. The analyses also showed no significant increase in ETEs at the medium population site. As expected, a significant increase (more than 30 minutes) in the 10-mile 90 percent ETE was observed in the large population site model when the

shadow contribution was increased to 40 percent. However, the increase did not affect the 2-mile and 5-mile ETEs. Based on the results, it was concluded that the current NRC regulatory guidance of a 20 percent shadow evacuation participation in the 10 to 15-mile ring is adequate. Although the current guidance reasonably represents a potential level of shadow participation, the results showed that there is generally no effect on ETEs at small population sites. At medium and large population sites, the impact to the ETE is only significant when shadow participation rates are increased to near a maximum level.

The findings of Task 2 suggested that there are several important considerations related to the model extent and application of traffic modeling for evacuations. From a computational perspective, the results showed that the size of the simulation network—beyond the shadow region—can, under some conditions, play a significant role in influencing the travel and route choice behavior of simulated evacuees within the EPZ, particularly when under the influence of a dynamic traffic assignment (DTA) algorithm. It was found that the inclusion or exclusion of major population generators and capacity restrictions beyond the shadow region may significantly impact the ETE when DTA algorithms are used for determining evacuation routes in a simulation. In some instances, evacuee travel times beyond the EPZ were shown to increase in a non-linear manner when additional population generators or capacity restrictions were included.

The results of Task 3 suggested that the use of an algorithm to represent police manual intersection control within an ETE traffic simulation tended to increase the 90 percent or 100 percent ETEs. Although some benefits, particularly in terms of increased exit flow rates, were observed at traffic control points (TCPs), these gains were ultimately lost when vehicles rejoined queues downstream of MTC intersections where traffic was slowed and stopped because of a downstream flow restriction. These findings were true for both signalized and unsignalized intersections, areas where lane reductions were present, and in areas where volume increased from the introduction of demand from downstream generators. Based on these results, it was concluded that existing methods used to represent MTC using actuated signals appear to be adequate. This was because the results of testing here showed that they yield sufficiently similar results to those of more detailed and sophisticated logit models developed through state-of-the-art research and observations of actual traffic enforcement police actions in the field. This is a positive development because it obviates the need to include sophisticated algorithms to simulate the impact of MTC.

The focus of Task 4 was on how parameter value selection and assumption making in model input and execution can impact results. A total of nine simulation input parameters were selected for study. These input parameters can be classified into three main categories of: traffic demand, traffic supply, and simulation process parameters. The traffic demand parameters that were investigated in this study included the size of the evacuating population, its mobilization time, the level of non-evacuation or “background” traffic in the network, and the number of “heavy” vehicles in the system. Traffic supply parameters included the free-flow speed of vehicles, the occurrence of roadway disruptions, and the effect of adverse weather. Finally, the simulation parameters included computation processing time step duration, and random seed uncertainty.

Overall, Task 4 results revealed several key facets related to ETE development and simulation modeling. The most fundamental of these was the basic relationship between network capacity and travel demand. The parameters, assumptions tested, and conclusions revealed their relative importance in ETE studies.

ACKNOWLEDGEMENTS

This applied research and analysis activity required technical expertise across a range of fields. The project was conceived by Randy Sullivan, Todd Smith provided NRC technical oversight and Tanya Oxenberg, Lindsey Cooke, and Sergio Gonzalez provided the NRC project management oversight. NRC Branch Managers Robert Kahler and Patricia Santiago ensured the technical staff and resources were available to complete the effort. Scott Parr and Brian Wolshon served as the project manager and principal investigator, respectively, for the Louisiana State University (LSU) team. Laurence Lambert and Brin Ferlito developed the traffic simulation models with support from LSU graduate students Nelida Herrera, and Efe Tuncer. Joe Jones provided expert technical consulting and support for the base model document.

ABBREVIATIONS AND ACRONYMS

ACP	Access Control Point
ANOVA	Analysis Of Variance
ANS	Alert and Notification System
ASCE	American Society of Civil Engineers
ATC	Actuated Traffic Control
CC	Calibration Component
CFR	Code of Federal Regulations
CORSIM	CORridor SIMulation
DHS	Department of Homeland Security
DOT	Department of Transportation
DTA	Dynamic Traffic Assignment
EAS	Emergency Alert System
EBT	Eastbound Through
EBL	Eastbound Left
EMO	Evacuation Management Operations
EPZ	Emergency Planning Zone
ERPA	Emergency Response Planning Area
ESF	Emergency Support Function
ESP	Early Site Permit
ETE	Evacuation Time Estimate
FBI	Federal Bureau of Investigation
FEMA	Federal Emergency Management Agency
FFS	Free-flow Speed
FHWA	Federal Highway Administration
GAO	Government Accountability Office
GPS	Geographical Positioning System
HCM	Highway Capacity Manual
HGV	Heavy Goods Vehicles (VISSIM term for trucks)
IACP	International Association of Chiefs of Police
I-DYNEV	Interactive DYnamic EVacuation
LOS	Level of Service
LSU	Louisiana State University
MOE	Measure of Effectiveness
mph	Miles per hour
MTC	Manual Traffic Control
MUTCD	Manual of Uniform Traffic Control Devices
NRF	National Response Framework
NBL	Northbound Left
NBT	Northbound Through

NCHRP	National Cooperative Highway Research Program
NCSHS	National Conference on Street and Highway Safety
NETVAC	NETwork emergency eVACuation
NHTSA	National Highway Traffic Safety Administration
NPP	Nuclear Power Plant
NUMARC	Nuclear Management and Resource Council
NUTI	Northwestern University Traffic Institute
O-D	Origin-Destination
OMB	Office of Management and Budget
ORNL	Oak Ridge National Laboratory
ORO	Offsite Response Organization
PAD	Protective Action Decision
PAR	Protective Action Recommendation
PCE	Passenger Car Equivalent
RV	Recreational Vehicles
ROC	Receiver Operator Curve
SAE	Site Area Emergency
SBL	Southbound Left
SBT	Southbound Through
STD	Standard Deviation
TCP	Traffic Control Point
TMI	Three Mile Island
TRB	Transportation Research Board
v/c	Volume to capacity ratio
VHT	Vehicle Hours of Travel
VMT	Vehicle Miles Traveled
vph	Vehicles per hour
WBL	Westbound Left
WBT	Westbound Through

1 INTRODUCTION

The evacuation time estimate (ETE) is a calculation of the time to evacuate areas within the plume exposure pathway emergency planning zone (EPZ). The EPZ is a defined area around a nuclear power plant (NPP) within which planning is carried out to assure that prompt and effective protective actions can be taken in the event of a radiological emergency [1]. The ETE study informs emergency planning, evacuation planning and protective action strategy development [2] [3]. Licensees and applicants develop ETEs following the guidance provided in NUREG/CR-7002, "Criteria for Development of Evacuation Time Estimate Studies," [4]. ETE development requires gathering site-specific demographic data, modeling the transportation network, gathering data on special facilities and identifying transit-dependent residents. The ETE must address the transportation of the latter two population cohorts usually via ambulances, wheelchair vans and buses. Schools are typically the special facility with the largest population and evacuation must be planned in detail [4].

Section IV of Appendix E to 10 CFR Part 50 requires nuclear power reactor licensees[1] to develop an ETE using United States Census Bureau decennial data [1]. Licensees are required to submit the ETE to the NRC before using it to form protective action recommendations (PARs) and before providing it to State and local governmental authorities for use in developing offsite protective action strategies. During the years between decennial censuses, Section IV of Appendix E to 10 CFR Part 50 also requires licensees to estimate EPZ permanent resident population changes once a year. If at any time during the decennial period the EPZ permanent resident population increases, such that it exceeds specified criteria, the licensee is required to update the ETE analysis to reflect the impact of that population increase.

In preparation for the decennial update of ETEs, the NRC has undertaken this applied research study to review current ETE guidance and determine if updates or enhancements may be appropriate. The objective of this activity was to develop a technical basis for revision of current ETE guidance provided in NUREG/CR-7002. Original guidance in Appendix 4 of NUREG-0654/FEMA-REP-1, Rev.1 [5], established the concepts of population groups, trip generation times, and combination of distributions for various evacuation time components. Subsequent guidance added detail regarding development of trip generation times, evacuation times for special facilities, use of the ETEs in Early Site Permits (ESPs), use of traffic simulation models, and assessment of shadow evacuations [2] [3]. While previous guidance updates were based on research related to ETE demographics, public response, and other contributing factors, this project includes the entire process of developing traffic simulation models, selecting input parameters, testing the models, and performing technical analyses. The methodology implemented in developing these models and conducting the analyses produced insights, observations, and conclusions, that can form the technical basis for updating NRC ETE guidance. In general, the findings of this study are non-hazard specific and could be applied in the development of evacuation simulations for other short-notice events.

The application of traffic simulation models to produce evacuation times reflects the current state of practice for ETE development. All current licensee ETEs have been developed using traffic simulation models. Furthermore, current ETE studies typically employ dynamic modeling features (e.g., dynamic traffic assignment) which allow the modeled vehicles to change direction during the evacuation based on the perceived best path. The current state of practice and consistent application of these models in the development of ETEs provides the impetus for

[1] The term "licensees" refers to licensees of NPPs under 10 CFR Parts 50 and 52.

studying model development and the associated input parameters. As such, a detailed description of the traffic simulation modeling process is included in this report.

To conduct the specific task analyses, traffic simulation models were created to represent generic small, medium, and large population EPZs. Base models were created for three representative sites and were populated with default model input values and representative evacuation response characteristics. The base models contain many assumptions to facilitate the research and are not replications of any site-specific ETE study. Using the base models, parametric analyses were conducted wherein a single parameter was modified, and all remaining model parameters and characteristics remained unchanged. The results of the analyses conducted with the modified parameters were then compared to the base model results.

1.1 Objectives

The overall project objective was to develop insights, observations, and conclusions sufficient to provide a technical basis for revision of NRC ETE guidance. The insights, observations, and conclusions were identified through the development of the traffic simulation models, acquisition of data for the models, and results of various parametric analyses. In addition to the overall project objective, each of the four project tasks had a specific objective. The Task 1 objective was to develop an understanding of the potential impacts of shadow evacuations to support a determination of the adequacy of the guidance provided in NUREG/CR-7002. The Task 2 objective was to determine the extent a network should be modeled beyond the EPZ to provide a realistic estimate of ETEs. The Task 3 objective was to quantify the impact of manual traffic control (MTC). The Task 4 objective was to determine the sensitivity of ETEs to a selected set of input parameters.

1.2 Scope

The project scope was to conduct an applied research study to examine, through modeling and simulation, technical subjects associated with ETE studies of the plume exposure pathway EPZ. Implementation of this multi-task, broad-based, applied research included developing evacuation models that are representative of small, medium, and large population EPZs. The timing implemented in the modeling was based on evacuation of the entire EPZ upon receipt of the alert and notification. Simultaneous evacuation of the entire 10-mile EPZ was assumed for research purposes only and is not intended to represent a preferred evacuation strategy. For similar considerations, staged evacuation was not included in the scope of the project.

1.2.1 Task 1: Shadow Evacuation Analysis

The Task 1 scope included conducting an in-depth study of the impact of shadow evacuations to understand and quantify potential impacts to the ETE. Task 1 included identifying three representative sites in terms of site characteristics and ETEs. Additional Task 1 activities included:

- Determining the size of a shadow evacuation that would be necessary to increase clearance times significantly (generally an increase of 30 minutes or more).
- Determining site characteristics that exacerbate the effect of shadow evacuations.
- Reviewing the current 20 percent shadow evacuation guidance in NUREG/CR-7002 against the study results to determine adequacy.

1.2.2 Task 2: Analysis of Distance of Travel

The Task 2 scope included a review of the travel distance assumed in the current guidance to determine whether it is appropriate for realistic ETEs. A sensitivity analysis was performed in order to determine the impact the model extent has on EPZ evacuation times. This was accomplished by truncating the base model at various distances and rerunning the analyses. Results were compared to the base models to identify differences. An analysis of the travel times beyond the EPZ boundary was also conducted to determine the value of such analysis for ETE reports.

1.2.3 Task 3: Analysis of Manual Traffic Control

The Task 3 scope is to quantify the benefit or detriment of manual traffic control (MTC). Guidance in NUREG/CR-7002 describes how the ETE may be used in emergency planning to assist in the development of traffic management plans and contains guidance for modeling manned traffic control intersections as an actuated signal. The scope for Task 3 includes:

1. Determining the value of implementing MTC to enhance traffic flow and quantifying the value to enhance assumptions used to develop ETEs, if a benefit is found to exist.

2. Developing guidelines which may be used to enhance evacuation planning for consideration by offsite response organizations (OROs).

3. Reviewing MTC documentation of practices and training for police officers during emergencies and major events to develop an understanding of the expected resources and timing required to implement MTC in evacuation plans. This review included relevant materials related to manual intersection control, focused on technical and training manuals developed for or by police agencies.

4. Identifying and reviewing available video observation of MTC for use in quantifying the allocation of right-of-way by police officers at oversaturated intersections during major events and emergencies. Also, determining the cycle length and vehicle volume to assess the rate at which vehicles flow through intersections and the conditions under which changes to the right-of-way occur.

5. Developing a quantitative analysis on the stimulus-response relationship between the traffic stream and officer decisions while directing traffic. Traffic stream variables with strong and weak correlation to observed officer actions will be determined and fit to a model to predict police officer action (change of right-of-way).

6. Benchmarking the developed model of MTC for simulated test intersections. The benefit-detriment (in terms of ETE) relationship between MTC and automatic traffic control will be evaluated. Four comparisons of performance will be made, including:

    a. Simulated MTC to Observed MTC (validation)
    b. Simulated MTC to automatic Actuated Control
    c. Simulated MTC to Observed MTC of alternative study area (validation for general application)
    d. Sensitivity to the number of simulated MTC intersections

7. Using the results of the analyses to determine the characteristics of ETEs or intersections that warrant consideration for use of MTC. Identifying other information appropriate for use as guidance.

1.2.4 Task 4: Analysis of Parameters Important to ETE Calculations

The Task 4 scope is a parametric study to develop an understanding of parameter importance. Specifically, the Task 4 scope includes:

1. Developing a detailed list of input parameters used in ETE modeling. These parameters will be investigated for the set of representative sites. The identification and selection of these parameters will be based on several sources including those found in a review of relevant literature, ETE studies, and NUREG/CR-7002. Key parameters identified in current guidance, such as population, vehicles, adverse weather factors, headway discharge, and lane capacities, will be included.

2. Creating a list of the typical values for each parameter listed, including upper and lower bounds and identifying the technical basis for these bounds, if practicable.

3. Identifying input parameters that are most likely to significantly influence the calculation of ETEs and warrant further study.

4. Performing sensitivity analyses for the selected parameters.

5. Assessing MOEs to identify parameter importance and any dependency between variables that may mask true importance.

6. Quantifying the results and creating a list of important parameters and identifying any limitations of the study.

1.3 Background

In 2011, the NRC updated the regulatory requirements of Appendix E to 10 CFR Part 50 regarding development of ETEs and other emergency planning requirements [1]. Licensees are required by regulation to submit an updated ETE based upon the latest decennial census. Updates are also submitted if specific criteria, identified in Appendix E are met. By the end of 2012, all sites had submitted ETEs using data from the 2010 census.

Prior to the 2011 rule, updates to ETEs were not routine. Variation of ETEs had been observed in terms of vintage, quality, content, and assumptions. Original guidance in Appendix 4 of NUREG-0654/FEMA-REP-1, Rev.15, established the concepts of population groups, trip generation times, and probabilistic analyses based on combining distributions for various evacuation time components. In 1992, the NRC published NUREG/CR-4831, “State of the Art in Evacuation Time Estimate Studies for Nuclear Power Plants,” [2] which expanded upon the original guidance, discussed the use of traffic models in the development of ETEs, provided additional detail in developing trip generation times, and described in greater detail the data necessary for estimating evacuation times for special facilities and special needs residents. Guidance was updated again in NUREG/CR-6863, “Development of Evacuation Time Estimate Studies for Nuclear Power Plants,” [3] which included guidance on the use of the ETE in early site permit (ESP) applications and expanded guidance on the use of traffic simulation models and an assessment of shadow evacuations.

The most recent ETE guidance in NUREG/CR-7002, provides criteria for assessing the impact of a shadow evacuation, and expands upon the data necessary for estimating evacuation times for special facilities and special needs residents. Current guidance also addresses selection of traffic simulation models, characteristics of models that should be described in the ETE study, model inputs, and specific model outputs to provide the MOEs used in the review of ETEs.

Historically, the impetus for updating ETE guidance was typically to describe the current state of practice with regard to obtaining demographic data, developing response timing elements, and calculating ETEs, or to provide guidance on specific regulatory applications, such as the use of the ETE in early site permit (ESP) applications [3]. Generally, updates to guidance were based on information that had been gathered through evacuation research [6] [7] [8] and information gained through review of ETEs submitted by licensees as updates or as part of license applications or renewals. Such reviews followed criteria established in NUREG-0800, “Standard Review Plan for the Review of Safety Analysis Reports for Nuclear Power Plants,” [9]. The NUREG-0800 review process includes NRC requests for additional information (RAIs), which are submitted to the licensee. RAIs are developed when criteria are not met, or when additional information is needed to ensure criteria has been met. Information gained from this process has supported identification of enhancements and technical insights, some of which were included in the NUREG/CR-7002 guidance.

The NRC has studied evacuations [6] [7] and identified that large-scale evacuations were found to occur in the United States about once every 2 to 3 weeks. These evacuations occur for a wide variety of emergency conditions, such as wildfires, flash floods, and chemical spills. The rate was found to be consistent over a period of more than 20 years; this includes the periods from 1980 to 1987 in a study sponsored by the Nuclear Management and Resource Council (NUMARC) [10] and in the NRC study of evacuations covering the period of January 1990 through June of 2003 [6]. It has also been observed for more than 30 years that the public response may include a shadow evacuation of some residents who live beyond the declared evacuation area [11].

The NRC also studied the likely response of EPZ residents to an incident [8]. A telephone survey approved by the Office of Management and Budget (OMB) was conducted nationally to residents of EPZs. From the telephone survey and focus groups, extensive knowledge was gained regarding the expected response of EPZ residents. It was through this research, that a shadow evacuation estimate of 20 percent of the resident population in the area out to five miles beyond the EPZ was identified for use in development of ETE studies [4].

Use of traffic simulation modeling is not required to develop an ETE; however, all current licensee ETEs submitted to the NRC have been developed through the application of computer modeling. The NRC does not specify model parameter values but provides, via guidance, that the licensee identify the basis for input parameter values selected. NUREG/CR-7002 guidance provides that specific attributes of the model be described and MOEs be included in the study. It was observed through review of ETE studies that choices of model parameters can vary among the types of models employed in the analysis and among the different EPZs for which they are applied. The importance of individual parameters was first investigated in a benchmark study of the I-DYNEV model, which was developed for the Federal Emergency Management Agency (FEMA) to aid in evaluation of ETEs [12]. I-DYNEV and NETVAC (NETwork emergency eVACuation) were among the first traffic simulation models used in NRC ETE analyses. In the benchmark study of I-DYNEV, the mean queue discharge headway, which is the time spacing between vehicles, was identified as one of the most critical input parameters for the model [12]. Because the discharge headway was the means of setting roadway capacity in the I-DYNEV

model, the value used for this parameter had a significant impact on the simulation output. This supports the hypothesis that capacity is likely the single most significant factor when investigating an ETE. A corresponding document, NUREG/CR-4874, "The Sensitivity of Evacuation Time Estimates to Changes in Input Parameters for the I-DYNEV Computer Code," also identified vehicle population, network capacity, and loading time as some of the important factors in ETE development [13].

2 APPROACH

The general approach for this study was to implement the guidance provided in NUREG/CR-7002 in development of three representative ETE models. To achieve the overall objective of developing a technical basis to support the update of ETE guidance, results of analyses needed to be applicable across the fleet of operating nuclear power plant sites. Certain task analyses necessitated developing the model networks to distances well beyond the EPZ boundary. The three traffic simulation models were built to 20 miles from the NPP to accommodate all the calculations needed to complete the project objectives.

Figure 2-1 is an illustration of a generic EPZ (not from an actual NPP site). The figure illustrates key EPZ elements, including emergency response planning areas (ERPAs). As indicated in the figure, ERPAs are bounded by geographical or political boundaries and do not necessarily end at a 10-mile radius from an NPP. For purposes of this study, all distances are radial and the generic EPZs end at precisely 10 miles from the plant. All the analyses conducted with the models were of the evacuation of the entire EPZ.

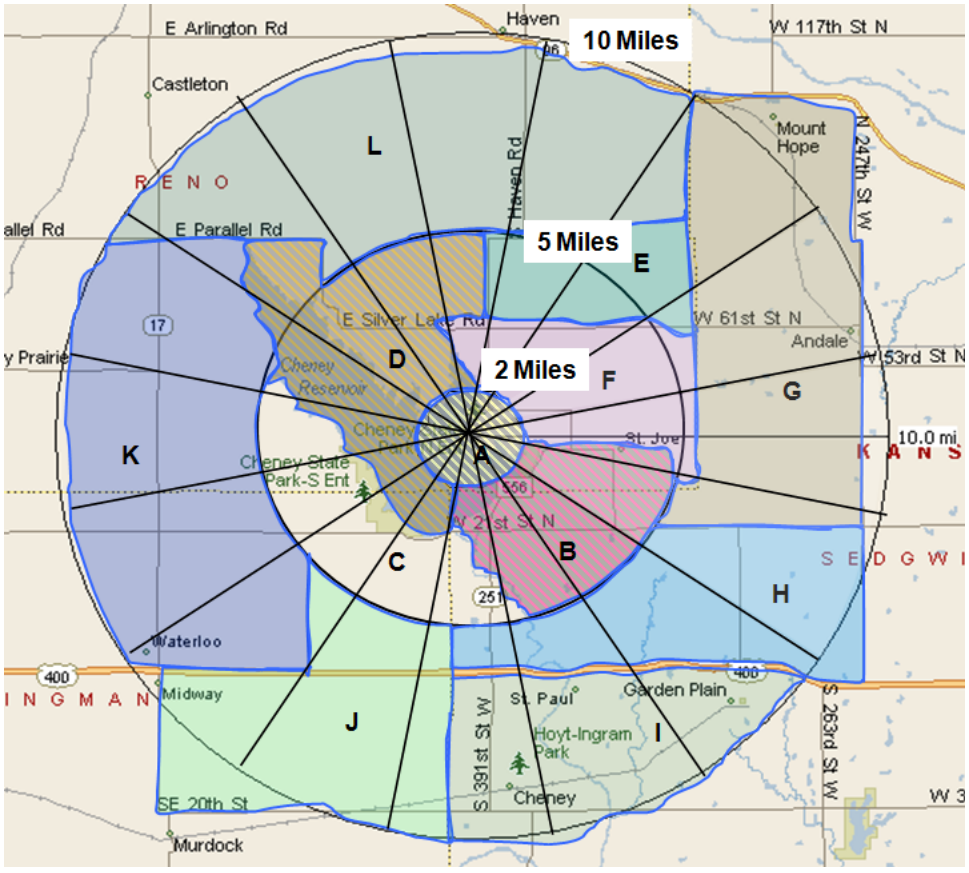

Figure 2-1 Generic EPZ with ERPAs

To build the traffic simulation models for each of the representative sites a number of individual tasks were performed. These included the coding of key assumptions associated with the behavioral responses of evacuees and relevant aspects of the transportation network. Together, these and other steps (described later in this report), formed the basis of each model and, more

critically, the bases upon which to vary specific parameters of interest in each task of the study. The general process of model development used for each model included completion of each of the following activities:

- Establish representative sites and EPZ characteristics
- Select a scenario for modeling
- Obtain data for use in the models
- Identify MOEs appropriate for the analyses
- Develop and run base models
- Conduct parametric analyses for each of the specific tasks
- Analyze results

As part of this effort, many existing ETE studies were reviewed and used to support some of the developed parameters. Additionally, the current guidance was studied to understand the approach and criteria for developing ETE studies. This was necessary not only to support development of the base model, but also to evaluate the inputs and outputs that are typically provided in an ETE study and determine whether enhancements in guidance could reduce some of the current data requests.

2.1 Representative Sites and EPZ Characteristics

With more than 60 NPP sites located throughout the United States, conducting analyses that would be applicable across the fleet necessitated a generalized approach. A full discussion on the selection of representative sites is provided in Appendix C. ETE studies were obtained from the NRC ADAMS website and reviewed to identify common characteristics that would facilitate grouping of small, medium, and large population sites. The review identified that demographics and infrastructure within EPZs are as diverse as the regions of the country in which they are located. Plume exposure pathway EPZ boundaries are typically demarcated by geographic or political boundaries to support emergency response and seldom conform to a precise 10-mile radius from the NPP.

A primary EPZ characteristic used in identifying the representative sites was population. This included consideration of the population in the shadow evacuation areas. However, population alone does not assure representativeness. For example, EPZs that are coastal, whether on a great lake or an ocean, often have only half of the land area of a non-coastal EPZ. A coastal EPZ may quantitatively have a small or medium population, but the infrastructure may be more reflective of a medium or large population site. Similar condensed demographic distributions were observed in non-coastal EPZs, where large portions of the EPZ areas were encumbered by national, state, or local parks or large lakes and rivers. In the application of this project, small, medium, and large population sites were defined as an EPZ population of 0 – 50,000; 50,000 – 200,000; and > 200,000, respectively. For most of the analyses conducted herein, the use of representative sites presented a reasonable approach. However, site-specific conditions often contribute to important elements in ETEs. Thus, although grouping EPZs into three site categories was appropriate for this study, there are elements that may not be directly applicable to all sites.

Review of ETE studies identified that the transportation infrastructure within EPZs was generally proportional to the population. High population EPZs generally have more freeway miles within the EPZ than small population EPZs. However, the relationship was not consistent enough to provide hard criteria. Some high population sites have no access to a freeway within the EPZ,

while some small population sites have access to multiple freeways within the EPZ. EPZ geographic representation also varies among NPPs, with some EPZ boundaries extending 5 miles or more beyond the 10-mile radius. EPZs with little or no population in some sectors sometimes end the EPZ boundary at distances slightly less than 10 miles from the NPP.

One of the more important characteristics of an ETE is the response of the public. Research has shown that once alerted, the public generally mobilizes and evacuates following the characteristic S-shaped evacuation response curve illustrated in Figure 2-2 [14] [15] [16]. In the figure, the alert and notification (e.g., siren and emergency alert system (EAS) message) occurs at time zero. The curve flattens at the top, illustrating the evacuation tail, which represents a small percentage of people who take longer to evacuate. An estimate of 10 percent of the evacuating population contributes to the evacuation tail [4] [16].

For this study, the initial response of the public is assumed to begin when the sirens sound; however, that does not mean evacuees enter the roadway network immediately. As discussed later with the trip generation times, it takes time for the public to receive the warning, understand what is necessary, and prepare to respond. Some state and local governments include early precautionary actions, such as the dismissal of schools at a site area emergency (SAE), in the site-specific radiological and emergency preparedness plans. Early precautionary actions are not considered in this study.

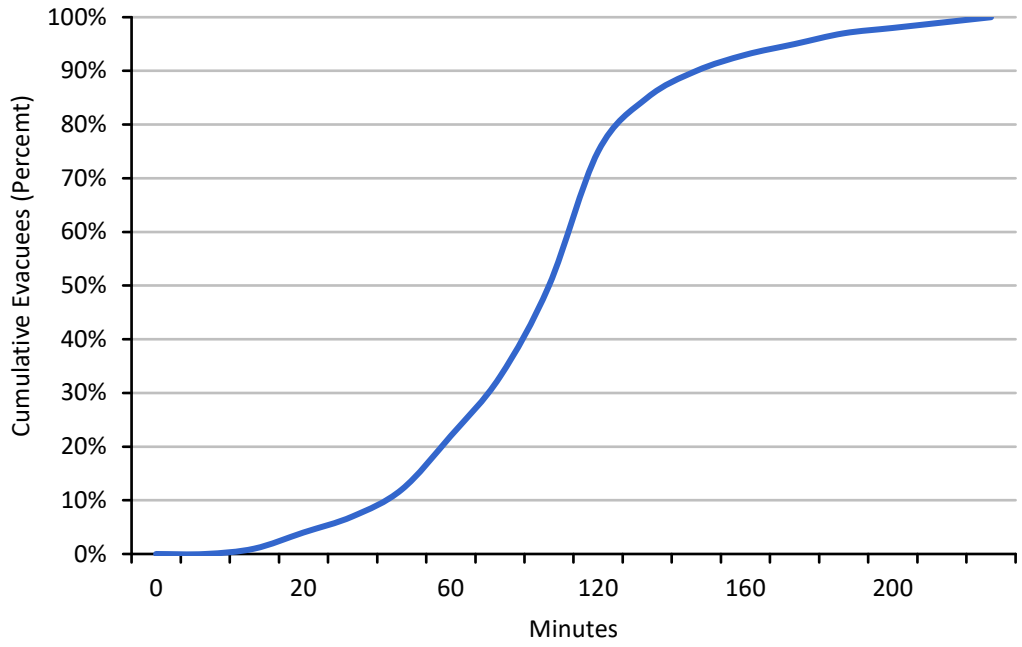

Figure 2-2 Typical S-curve Representing Evacuation Response

2.2 Scenario Selection

The ETE response scenario defines the specific conditions assumed for the analysis being conducted. Guidance is provided in NUREG/CR-7002 to assist analysts in identifying combinations of variables and events to be considered. Typically, 10 or more scenarios are developed in a site-specific ETE study. Only one scenario was used in the base model development and variations occurred within the task analyses.

The baseline scenario is a weekday, daytime, normal weather event, with normal background traffic on the roadway. This scenario was selected because of its general applicability. The consensus within ETE studies has been to develop a weekday, daytime, normal weather scenario as a de facto “base case” and then make modification to this scenario to represent various other situations. Specific consideration of trip generation times for schools, special facilities, and transit-dependent residents were not included. However, the populations used in the analysis are sufficient to account for the vehicles from each of these population groups. Consistent with guidance in NUREG/CR-7002, the scenario was developed with an assumption that evacuation is ordered promptly, coincident with sounding of the sirens and broadcast of an EAS message. Use of this planning basis allows the ETE to be consistently calculated beginning with the initial notification to the public [4].

2.3 Model Data

The evacuees within the EPZ were modeled as a single population group representative of a total evacuation contribution in the analysis. The population was spatially distributed within 16 sectors (22.5-degree sectors) at one-mile distances, creating model grid elements. Background traffic, pass-through traffic, and shadow evacuees were also contributing populations in the model development. The roadway infrastructure implemented in the models is generally representative of small, medium, and large population EPZs. This assured that roadway types, intersection designs, roadway segments, and other infrastructure features were realistic. Default model parameter values for driver behavior and vehicle characteristics were typically implemented.

2.4 Base Model Development

The PTV VISSIM software package was used to create the traffic simulation models. Base models were populated with VISSIM default model values and with generic parameter values for evacuation response characteristics. The models developed are representative of EPZs of similar population and traffic infrastructure and contain many assumptions necessary to facilitate the task analyses. As such, the models are not replications of any site-specific ETE study. Throughout the project, models were run, reviewed, modified, and rerun to test, verify, and ensure each model reasonably represented the intended evacuation network. After multiple preliminary iterations, corrections of errors and model adjustments, the base model for each site was established. The base models were run, and results were produced for comparison to the parametric analyses conducted for each specific task.

The generic EPZ models were built considering the above characteristics and demographics and are not reflective of any actual NPP EPZ. Specifically, characteristics that make these models generic include the following:

- The modeled EPZs end precisely at 10 miles from the NPP.
- A single population group was modeled representing populations of the general public transients, schools, special facilities, and employees.
- All roadways are assumed to be flat (e.g., level terrain) for the analysis.
- Traffic signals use pre-timed (fixed) signal timing.
- Default model parameter values in VISSIM were applied where appropriate.
- Evacuee response curves were developed by averaging ETE response curves for similar population EPZs.

2.5 Parametric Analysis

Upon completion of the base model runs, the models were used to conduct parametric analyses related to shadow evacuations, distance of travel, use of MTC, and parameter importance. For the parametric analyses, a single parameter was modified, and all remaining model parameters and characteristics remained unchanged. Task 3 required that intersection control be modified, which involved more than a single parameter, but was limited to the intersection control elements. The results produced with each analysis were compared to the base model results. Additional metrics were evaluated specific to each parameter or condition being assessed as needed.

2.6 Analysis of Results

Results produced from the base models established values for comparison to the parametric analyses conducted for each task. To conduct all the required analyses, the three models were built to 20 miles from the NPP. VISSIM requires the user to identify where data is to be collected and to specify the metrics to be captured at each specified location. Data was collected at roadway crossings at the 2, 5, 10, 15, and 20-mile rings.

Data from all collection points was tabulated and reviewed to understand the network performance and the distribution of MOEs. The MOEs also provided indication regarding when to investigate the data in greater detail to understand why a specific collector point had larger or smaller values than an adjacent or similar collector point. Depending on the parameter being investigated, additional output was also reviewed to assist in interpreting the results. The differences in the MOEs provided the general impact observed from adjusting the specific parameter.

3 MODEL DEVELOPMENT

At the most fundamental level, evacuation processes can be described within a construct of supply and demand relationships. In simple terms, evacuation travel “demand” is the number of vehicles that will access the road network during an evacuation. And evacuation “supply” can be thought of as the ability of a network or system to serve the demand placed upon it. Supply in an evacuation context can be described a number of ways, but essentially, it is the outflow capacity of a system. The ability of highway routes to move outbound traffic from threat areas is a common metric used to evaluate the outflow capacity of the network.

In an evacuation, sources of traffic generation within an EPZ come from different population cohorts, each having varying sizes, spatial distributions, access to information, levels of mobility, and support needs. Travel demand generation can also include non-evacuee sources such as traffic passing through an evacuation region, commonly referred to as “pass-through” traffic, and traffic moving within the evacuation area for daily work, shopping, or recreational purposes. In traffic modeling, this latter category is known as “background” traffic.

Determining the amount and availability of transportation network capacity can be equally as diverse and complex to quantify. The ability to move evacuees is not just a function of the number of outbound lanes. It may also be effected by the arrangement of roadways within a system (known as network topology); the location and orientation of these roads with respect to the populations they serve; the geometric configuration of the roadway and geographic characteristics of the evacuation area; traffic controls (signals, lane regulations, etc.); the occurrence of incidents (vehicle crashes, breakdowns, etc.); the driving behaviors of the evacuees, and the mix of vehicles within the traffic stream (trucks, buses, RVs, passenger cars, etc.) among others.

Neither the demand nor supply variables remain static during most evacuations. Both often change frequently and are influenced by other spatial and temporal conditions during emergencies. For example, flow bottlenecks, flooded roads, and incidents can decrease the outflow capacity of a network, while use of contraflow can increase it. Likewise, dynamic threat conditions, phased evacuation orders, and other factors can change demand by influencing evacuee departure time, location, and loading into a system.

The application of traffic simulation models to produce evacuation times reflects the current state of practice for ETE development. All current licensee ETEs have been developed using such models. Furthermore, all the ETE studies employed models that included dynamic modeling features (e.g., dynamic traffic assignment (DTA)) which allow the modeled vehicles to change direction during the evacuation based on the perceived best path. Current guidance in NUREG/CR-7002 addresses this state of practice, describing model inputs, outputs, and MOEs to be provided in ETE studies.

Neither regulation nor guidance prescribe the specific method in which an ETE is to be calculated. The licensee may choose whatever is most appropriate for the EPZ, although all current ETE studies make use of traffic simulation software. A wide variety of traffic simulation models capable of calculating ETEs are available. Characteristics of many of these models are described in the U.S. Department of Transportation (DOT) sponsored “Evacuation Management Operations (EMO) Modeling Assessment: Transportation Modeling Inventory,” [17]. Additionally, the Federal Highway Administration (FHWA) prepared a toolbox that includes comprehensive

guidance on development of traffic simulation models [18] [19] [20]. These documents are useful in assisting analysts in determining the most appropriate model for the specific site.

Traffic simulation models are categorized as microscopic, mesoscopic, and macroscopic [18], all of which may be appropriate for use in calculating evacuation times. As the descriptions of the model types indicate, they reflect different fidelities in both the inputs and outputs. Although the models differ in complexity, much of the fundamental data (e.g., roadway network, number of vehicles, etc.) used to develop inputs is applicable to each model type. Microscopic models simulate the movement of individual vehicles based on car-following and lane changing theories and provide the ability to model signalized intersections and associated queuing in detail. However, to produce realistic results using a microscopic model, a significant amount of field data and accurate representation of driver behavior characteristics are needed. Macroscopic models employ deterministic relationships of speed, capacity, and density of the traffic stream, such as those contained in the Highway Capacity Manual (HCM) [22]. The vehicle simulations in macroscopic models are grouped and are governed by the average speed on a link, rather than based on individual vehicles. Mesoscopic models implement properties of both microscopic and macroscopic by analyzing small, homogenous groups of vehicles. Mesoscopic models facilitate analyses that are more detailed than macroscopic and less detailed than microscopic. All three model types can be run with dynamic traffic assignment (DTA) applications. The DTA model implements time-dependent origin and destination (O-D) trips which are assigned based on traffic conditions.

The VISSIM microscopic simulator [21] was used to create the traffic simulation base models as it provides a level of detail needed for the analysis. VISSIM is a time-step and behavior-based model. It can be applied to analyze traffic operations that are influenced by roadway geometry, lane configuration, traffic composition, traffic signals, pedestrians, and other network characteristics. In VISSIM, driver behavior is coded with the Wiedemann functions, which address car following distances, sight distances, wait times to change lanes, changes in speed, and other driver characteristics. As with any microscopic model, to achieve realistic results, the inputs need to be adjusted for the scenario to be analyzed. The importance of these adjustments is emphasized in Volume III of the FHWA toolbox [20]. For the base models, default values, which are based on empirical data, were used.

The experience of developing the small, medium, and large population site models for this project identified that the level of effort for each of the models was increasingly complex. The increase in effort was not linear, and the small population site required much less effort than the medium or large. This finding was consistent with conclusions of the FHWA study, “Guidance on the Level of Effort Required to Conduct Traffic Analysis Using Microsimulation,” [26] which compared level of effort required to model regions of various sizes with microscopic traffic simulation. The FHWA study identified a factor of five increase in development of a large population site compared to a small population site. In general, the study concluded that the level of effort in development of large models was disproportionately greater than the development of small models [26].

The additional effort to code the microscopic model, select and adjust site-specific input parameters, and validate the performance against field conditions to ensure reasonable baseline results, makes microscopic models challenging for developing ETE studies, particularly when macroscopic simulation models have been shown to produce ETEs within a few percent of the microscopic simulation models [23] [28]. However, for testing and analysis of specific inputs, which was a focus of this study, microscopic modelling provided the extra level of detail

intended to support the analyses. The base models were generally populated with VISSIM default values and with generic inputs to represent evacuation response characteristics.

Replicating driver behavior in simulation models presents one of the challenges in creating a realistic model. For example, many drivers have geographical positioning system (GPS) travel assistants that perform real-time calculations to recommend the fastest route to a destination but sometimes suggest unrealistic routing. Such a route may take an individual off a freeway and onto a frontage road, only to recommend getting back on the freeway at the next on-ramp. The GPS calculation estimates a small-time savings, but the action is not something rational drivers would implement, and traffic controls during an evacuation may not allow such action in any case. Less sophisticated systems always suggest a freeway route, regardless of congestion. Traffic simulation models operate with similar algorithms, sometimes routing vehicles along obscure paths that may not be reasonable. Models must be reviewed in detail to identify these situations and implement rules to avoid unreasonable actions.

3.1 Model Development Assumptions

The following assumptions were implemented in the base models developed for the three generic EPZs. These assumptions are specific to this study and are not necessarily intended to represent assumptions that would be used in a site-specific ETE study.

- Small, medium and large population EPZs were used to represent NPP sites nation-wide.
- The model scenario is a midday, midweek evacuation that is ordered promptly, coincident with sounding of the sirens and broadcast of an EAS message.
- Evacuee populations within each model were considered as a single cohort.
- Population movement within each model was represented by a single loading curve specific for that model.
- Consistent with guidance [4], pass-through traffic ceases to enter the EPZ two hours after the initial notification.
- All modeled roadways are paved and flat, representing a level terrain.
- Traffic signals use pre-timed (fixed) signal timing.
- Default VISSIM values for model parameters were used.

Throughout this report, whenever ETE and other time data are reported without units, it should be understood to be in hours and minutes (h:mm); e.g., 2:15 is two hours and 15 minutes.

3.2 Base Model Summary

Implementation of this multi-task, broad-based, applied research required developing base models beyond the range typically included in an ETE study. The models were built to a 20-mile radius from the NPP. The 10-mile EPZ is represented as a radial distance from the NPP. Current guidance provides the shadow evacuation be evaluated to 5 miles beyond the EPZ [4]; as such, most ETE studies end the analysis at or near this distance. However, congregate care centers and relocation centers may be established well beyond this distance. To assess travel times to hypothetical locations of congregate care centers, the roadway networks were built to 20 miles from the NPP.

3.2.1 Summary of Model Characteristics

As described earlier, microsimulation requires substantial input to simulate the movement of individual vehicles. Table 3-1 lists model characteristics for the 0-20 mile network and the 10-mile EPZ

Table 3-1 Base Model Characteristics

0-20 Mile Network			
Characteristic	**Small**	**Medium**	**Large**
Total number of origin points	65	413	457
Total number of destination points	42	27	58
Total number of links	376	2,645	10,605
Total number of connectors	863	3,846	14,719
Total lane-miles of roadway modeled	1,348	2,259	4,487
Total number of signalized intersections	9	320	535
Total number of stop signs	165	129	439
Traffic signals	Pre-timed	Pre-timed	Pre-timed
0-10 Mile EPZ			
Characteristic	**Small**	**Medium**	**Large**
Total number of origin points within the EPZ	28	159	183
Average number of vehicles loaded at EPZ origin point	134	629	888
Maximum number of vehicles loaded at an EPZ origin point	1,150	1,463	3,860
Minimum number of vehicles loaded at an EPZ origin point	25	7	15
Total number of evacuee vehicles loaded for the EPZ	3,750	100,000	162,500
Total lane-miles of freeway within EPZ	0	64	80
Total lane-miles of non-freeway within EPZ	277	566	1,147
Total number of signalized intersections within EPZ	0	144	191
Total number of stop signs within EPZ	22	31	211

3.2.2 Boundary Conditions

Boundary conditions define the extent of the network that is to be modeled. Important changes in infrastructure beyond the limits of the ETE analysis area can potentially impact the ETE. Review of ETE studies as a part of this project found that in many instances the modeled network was extended beyond the limits of the shadow region to capture these important infrastructure conditions in order to include the effects of such conditions in the calculation.

When building a traffic simulation model, boundary conditions should be established early. For ETEs, boundary conditions describe the arrangement by which the modeled network will terminate. The arrangement of the infrastructure beyond an EPZ study area has often been found to change within a short distance. For example, roadways may have a reduction in the number of lanes, or a constraining intersection may be located a short distance from the boundary. An indiscriminate discharge of the modeled vehicles at predetermined radii might miss these important changes in infrastructure. Such conditions can impact the ETE, particularly for medium and large population sites.

Impediments and constraints near the limit of the traffic simulation network should be included in the analysis to capture the impacts and support realistic results. The distance to which the network should be extended is case-by-case. If it is determined a roadway should be extended in one direction in the model to capture a lane reduction, this would not suggest a need to extend the entire network to the same distance. Only the affected roadway would need to be extended. Furthermore, an impediment that exists on a route with little evacuation traffic may not need to be included in the analysis. The distances to which the calculations were performed for this study were predefined to support specific analyses with regard to model extent making identification of boundary conditions unnecessary for this effort.

3.3 Demand Estimation

The process for developing an estimate of the number of people to be evacuated is called demand estimation. All persons located within the EPZ are included in the demand estimation. NRC guidance in NUREG/CR-7002 further defines population groups, as follows:

1. Permanent residents and transients (e.g., tourists, shoppers, employees, etc., who visit but do not reside in the area)
2. Transit-dependent permanent residents
3. Special facility residents
4. Schools

For the purpose of this project, the total populations modeled for each site included the contribution from the above categories; however, specific attributes (e.g., individual trip generation times, specialized vehicles, etc.) of these population groups were not considered. After the population values were established, they were converted into vehicles for the analysis.

3.3.1 Site Populations

Evacuee and shadow populations were selected for the representative sites based on U.S. census information and a review of EPZs. Total evacuees for the generic EPZs were 7,500, 200,000, and 325,000 for the small, medium, and large population sites, respectively. These values represent the general public, transients, schools, special facilities, and employees within the EPZ at the time of the emergency. In addition, pass-through traffic and background traffic are also on the roadway when the evacuation order is issued.

Shadow evacuee populations for the 5-mile area beyond the generic EPZs were 3,000, 30,000, and 60,000 for the small, medium, and large population sites, respectively. These values reflect a 20 percent contribution of the public from the 5-mile area beyond each generic EPZ. Table 3-2 provides a summary of the site populations considered in the analysis. Detailed population data by sector is provided in Appendix B. A percent of the resident populations within the area from 10 to 20 miles from the NPP were also included in the models. This data was used to populate the roadway networks beyond the EPZ with background traffic, such that when the EPZ evacuees and shadow evacuees travel in these areas, the interaction with background traffic is considered. While average EPZ populations center around 80,000 residents based on current ETE studies, it was necessary to set the population in the medium site model large enough to observe meaningful changes to the MOEs in the task analyses. For similar reasons, after the completion of Task 1, the shadow population for the small site model was increased to 10850 shadow evacuees (72 % shadow participation rate) in order to stress the network outside of the EPZ and observe measurable impacts in the task analyses.

Table 3-2 Summary of Modeled Populations

Population Site Model	EPZ Population	Shadow Evacuees
Small	7,500	3,000[1]
Medium	200,000	30,000
Large	325,000	60,000

[1] Small population site base model includes 10850 shadow evacuees (5425 vehicles) after Task 1.

3.3.2 Pass-Through and Background Traffic

Each model simulation begins with an empty roadway network. Therefore, the first step in loading a traffic simulation model (microscopic or macroscopic) is to seed the network for a predetermined time period. This may be referred to as seed time, fill time, model equilibration, or other terminology, depending on the model used. Model seeding is the process of populating a reasonable number of vehicles on the modeled roadway network to represent the scenario being evaluated. For evacuation models, the initial conditions are those of the roadway immediately prior to the start of the evacuation.

Pass-through traffic and background traffic contribute to the demand estimation because these vehicles are on the roadway network when the evacuation commences [4]. Pass-through traffic is defined as vehicles that enter the EPZ roadway network and 'pass through' prior to the establishment of access control points (ACPs) at the EPZ boundary. Pass-through vehicles would typically be expected to travel freeways and major arterials within an EPZ because these are the roadways that would facilitate the 'pass through' activity. Site-specific traffic control plans generally stipulate that ACPs will be established within 2 hours, to prohibit this traffic flow. ETE guidance utilizes this assumption [4]. A fixed number of pass-through vehicles, representative of the quantities of pass-through traffic that would be expected for the medium and large population sites, were added to the demand estimation. Because most small population sites are predominantly rural with few major arterials and typically no freeways, pass through vehicles were not included in the small population site.

Background traffic refers to vehicles in the network that are initially not part of the active evacuation [31]. These vehicles consist of residents and transients within the EPZ and outside of the EPZ. Estimates of the amount of background traffic on the roadway may vary for the specific scenario, as nighttime scenarios would have a lower volume of background traffic than a daytime scenario. Some background traffic can be attributed to intermediate trips [31], which are trips that are undertaken by evacuees but are not the final departure out of the hazard area. Murray-Tuite and Mahmassani [32] [33] suggest this behavior be incorporated into evacuation modeling for no-notice events. Incorporating such behavior in terms of an ETE analysis could increase the trip generation time slightly.

Background traffic was loaded onto collectors, arterials, and highways. These roadways represent the evacuation routes that were also used in loading the general public vehicles. Background traffic was loaded at a specified percent of total vehicles over 15-minute periods. The loading of background traffic within the EPZ included two 15-minute background traffic seeding periods prior to the siren. During this 30-minute period, background traffic was loaded onto empty roadway networks with O-D matrices that direct the background traffic out of the EPZ. Because the small population site used a static route choice model, it did not require an O-D matrix. Instead, background traffic was loaded onto the network and followed the same routes as evacuation vehicles. To prevent all the background traffic from exiting the area before

evacuees begin travel, the background traffic continues to be loaded during the first 15-minute interval when evacuating vehicles are also loaded onto the network. Background traffic outside of the EPZ was continuously loaded throughout the entire evacuation process. Based on the loading curves established for this study, the small population site begins evacuating when the siren sounds, the medium population site begins 15 minutes after the siren, and the large population site begins 30 minutes after the siren. The background traffic was loaded as follows:

- Small population site model: Within the EPZ, background traffic was loaded as 20 percent of the total EPZ vehicles (or 5 percent every 15 minutes) over each of two 15-minute seeding periods prior to the siren and an additional 5 percent loaded over the first two 15-minute evacuation periods coincident with evacuees beginning to enter the network. Thus, within the EPZ, background loading was implemented over four 15-minute periods. In the 10 to 20-mile network area, background traffic was loaded at 2.5 percent of the total 10 to 20-mile resident vehicles for each of 10 loading periods of 15 minutes each.

  With the static model, fixed turning percentages were assigned for the background traffic during the seeding period. During this period, turning movements of 20 percent left turns and 30 percent right turns were assigned with the remaining 50 percent continuing straight through the intersection. This was done to seed the model with traffic before the start of the evacuation event to ensure evacuees did not enter an empty network. These movements were not intended to represent actual trips but were used to randomly spread traffic throughout the network before the start of the evacuation. The fixed turning movements cease after the three 15-minute seed periods at which time turning percentages were manually assigned at all intersections. Assignment of turning percentages was not necessary for the larger sites where DTA was implemented.

- Medium population site model: Within the EPZ, background traffic was loaded at a rate of one percent of the total EPZ vehicles over each of two 15-minute seeding periods, prior to the siren. An additional one percent was loaded over the first 15-minute period after the siren, prior to evacuees beginning to load the network. An additional one percent was loaded over the next 15-minute evacuation period coincident with evacuees beginning to enter the network. Thus, within the EPZ, background loading was implemented over four 15-minute periods. In the area 10 to 20-miles from the NPP, background traffic continued to be loaded at a rate of one percent of the 10 to 20-mile total vehicles per 15-minute period for an additional 7 hours for a total of 8 hours. This rate was selected to provide an adequate amount of friction for the evacuating vehicles within the network. It was not intended to replicate any scenario beyond the general presence of ambient traffic throughout the entire region.

- Large population site model: Within the EPZ, background traffic was loaded at a rate of one percent of the total EPZ vehicles over each of two 15-minute seeding periods, prior to the siren. An additional 1 percent was loaded over the two 15-minute periods after the siren, prior to evacuees beginning to load the network. An additional 1 percent was loaded over the next 15-minute evacuation period coincident with evacuees beginning to enter the network. Thus, within the EPZ, background loading was implemented over five 15-minute periods. In the area 10 to 20-miles from the NPP, background traffic continued to be loaded at a rate of 1 percent of the 10 to 20-mile total vehicles per 15-minute period for an additional 6 hours and 45 minutes for a total of 8 hours.

3.3.3 Vehicle Volumes

NRC guidance provides that the populations for each demographic group be converted to vehicles for traffic simulation modeling. This is typically done by applying a person per vehicle ratio for each population group and is applicable to microscopic and macroscopic models. Because this study modeled a single population group combining populations of the general public, transients, schools, special facilities, and employees, an average vehicle loading was developed. Many current ETE studies were reviewed and data was gathered on the general public, transient, and employees, each of which are itemized in the ETE studies. The ratio for employees was typically 1.0 to 1.1 persons per vehicle. The ratio for general public typically ranged from 1.7 to 2.4. The ratio for transients was broader still, ranging from about 2 to over 4 persons per vehicle. Using the ratios and the contributions of each population group, an average persons per vehicle ratio of 2.0 was developed.

Vehicles were loaded into the model to represent the EPZ population, EPZ background, and EPZ pass-through traffic. Beyond the EPZ, the shadow population was loaded in the area from 10 to 15 miles from the plant, and background traffic was loaded onto the entire 10 to 20-mile area. Vehicle contributions for each model are identified in Table 3-3.

Table 3-3 Summary of Modeled Vehicle Contribution Inputs

Population Site Model	EPZ Population Vehicles	EPZ Background Vehicles	10-15 Mile Shadow Population Vehicles	Pass-through Traffic	10-20 Mile background Vehicles	Total Vehicles
Small	3,750	752	1,500	0[1]	6,350	12,352
Medium	100,000	4,000	15,000	5,000	48,220	172,220
Large	162,500	8,125	30,000	19,250	152,000	371,875

[1] Small population site model did not include pass-through traffic.

Vehicle loading was spatially distributed within 16 sectors (22.5-degree sectors) at one-mile distances, based on the assumed population density. In some instances, where large populations reside, multiple origin nodes were assigned to a single grid element. In other instances, where there was little or no population, no loading occurs within the sector. When multiple loading points were applied in a sector, the population was evenly divided among the number of loading points.

3.3.3.1 Vehicle Types

The models included two vehicles types, passenger cars and trucks (also referred to as heavy goods vehicles (HGVs)). The modeling of cars and trucks is applicable to microscopic and macroscopic models. The VISSIM model provides a variety of common types of cars and trucks from which to load the network and selects from a distribution of vehicle types to provide a broad vehicle mix for the scenario [21]. The performance characteristics of vehicles are specific to VISSIM; however, some characteristics—such as vehicle lengths—are applicable to microscopic and macroscopic models.

3.3.3.2 Percent Trucks

Current guidance does not address the percent of trucks in the vehicle fleet; however, it is well understood that the percent of trucks on the roadway impacts travel [21] [22] [37] [38]. Trucks, including all heavy vehicles with three or more axles, (e.g., buses, motor homes, and camper trailers) should be estimated for the evacuation scenario. The percent of trucks in a vehicle fleet is a contributing factor in developing ETEs for all types of models (e.g., microscopic and macroscopic). The parameter is important because trucks accelerate at a slower rate than passenger cars, and this slower acceleration can impact the throughput at intersections. Furthermore, speeds can decrease as grades increase. The number of trucks in the vehicle fleet also affects the sight distances in the microscopic model behavior parameters. The VISSIM User Manual illustrates (in Section 5.6.2.1 of the manual [21]) that an increase in percent of trucks produces a noticeable decrease in the saturation flow rate. A similar illustration of the impact of trucks is provided in the Oregon Protocol [24] showing that an increase of 5 percent of trucks reduces the saturation flow rate up to 5 percent.

Determining an appropriate percentage of trucks is a site-specific consideration for EPZs. Regional characteristics that include the extent of commercial activity within or near an EPZ could contribute to variations in truck percentage. The scenario being estimated (e.g., winter evening or summer daytime weekday) will also influence the percent of trucks to be modeled. Truck time-of-day patterns on urban and rural roads are consistent with other vehicular travel patterns, with truck traffic dropping substantially late at night [36]; thus, adjustments for evening scenarios may be appropriate.

Research has identified that heavy vehicle traffic has increased, and 8 to 10 percent of heavy trucks may be normal for urban roadways [36] [37] [38] [41]. A Baltimore Metropolitan Council study [41] identifies truck traffic as now accounting for over 10 percent of all traffic on major roadways. Additionally, because NPPs are typically located near major bodies of water, evacuees may be expected to own and evacuate with boats, trailers, and campers [39] [40]. From a modeling perspective, personal vehicles towing boats and trailers are modeled as heavy vehicles, which may suggest the use of a higher percent of heavy vehicles within the EPZ may be appropriate.

Urban roadways make up the prevalent transportation network within EPZs, with very few EPZs having significant freeway mileage within the area. Pass-through traffic, which would include all freeway heavy vehicles and some major arterial heavy vehicles, is expected to be controlled within 2 hours of the start of an evacuation [4]. As evacuees mobilize, they are largely in personal vehicles, and the percent of trucks becomes diluted. Assuming an initial 8 to 10 percent heavy vehicles within the EPZ, by the time EPZ residents are fully mobilized, the percent of trucks that potentially impact traffic conditions would likely be less. A range of 5 to 10 percent of trucks and heavy vehicles may be more appropriate for a typical day, with recognition that many sites are located around large bodies of water where there is typically a prevalence of recreational vehicles (RV), campers, and boats. However, given the large number of vehicles on the roadway during an evacuation, the total number of heavy vehicles would likely represent a small overall proportion of vehicles within the network. The base models used a value of 2 percent trucks.

3.4 Roadway Capacity

The capacity of a roadway is defined as the maximum rate at which vehicles can be expected to travel a section of roadway during a given period under specified roadway, traffic, and control conditions [22]. Microscopic and macroscopic simulation models calculate roadway capacity differently, with microscopic models estimating saturated flow and macroscopic models implementing the equations of the HCM. The HCM describes operating conditions as level of service (LOS) A through F, with LOS A as free-flow and LOS F as forced flow. Evacuation congestion can be significant, particularly with medium and large population sites, making capacity an important characteristic to measure accurately.

As roadways become congested (i.e., saturated), HCM methods are not adequate to represent aspects of traffic queue build-up and discharge and intersection turn lane spillback. Detailed analyses of these interactions can be performed using micro-level traffic simulation systems. These methods use numerical representations of individual driver behavior and project how these behaviors influence (and are themselves influenced by) vehicle-to-vehicle interactions considering traffic demand, roadway geometry, intersection control and other influences. Macroscopic models estimate roadway capacity for each segment based on a set of assumed or entered conditions. However, microscopic models use individual “microscopic” interactions to characterize maximum capacity through sections of roadway providing a more detailed analysis of the traffic phenomenon.

The concept of capacity, though quite specifically defined in the HCM, is an elusive number to quantify. Current research strongly suggests that capacity is a variable parameter, influenced by a number of constantly changing conditions [48] [49] [50] [51]. In a microscopic model, capacity, or the maximum rate of flow that can be achieved along a section of roadway, occurs when all vehicles are moving with minimum spacing (distance headway) and at maximum speed. The difficulty in using this definition in a microscopic model is that every leading-following vehicle pair is spaced with a different headway and traveling within a range of speeds. Because of this, traffic analysts characterize segment capacity with average headway and average speed even though in reality the maximum flow rate is likely to be constantly changing.

Tian and Urbanik, et al., compared VISSIM to CORSIM and Sim Traffic, which are all microscopic traffic simulation models [30]. The authors investigated the variations in the performance measures generated, focusing on capacity and delay estimates at a signalized intersection. The highest variation in each simulation model normally occurred when the traffic demand approached capacity. The study identified that many runs may be necessary to accurately estimate delay at, near, or over capacity. When the average values were considered from multiple runs, the throughput flow rates from all three models closely matched the input demand for under-capacity conditions. The three simulation models tested produced different results when the default traffic flow parameters from each simulation model were used. In general, VISSIM produced the highest capacity and lowest delay estimates, and SimTraffic produced the lowest capacity and highest delay estimates [30].

3.4.1 Roadway Types

An accurate depiction of the roadway network is needed to capture the roadway characteristics in traffic simulation modeling. This is required for the development of both microscopic and macroscopic simulation models. Representative roadway networks from actual EPZs were used in this analysis.

The types of roadways included in the networks are:

- Interstates and Freeways
- Interstate and Freeway Ramps
- Highways
- Major Arterials
- Minor Arterials
- Collectors

For small population EPZs, or for smaller study areas, it may be important to include residential streets in the analysis. But for the generic EPZs established for this project, the networks were well represented without the need for residential streets.

3.4.2 Roadway Geometry

Roadway geometry data was obtained by viewing aerial mapping of each network. The entire modeled network was reviewed using the aerial mapping to identify the following:

- Number of lanes in each direction
- Lengths of links/segments
- Right turn lane characteristics
- Left turn lane characteristics
- Types of signalized and non-signalized intersection control

Traffic simulation models (microscopic and macroscopic) define roadways via links and connectors (also called segments and nodes or other model specific terminology). Links are typically used to represent roadway segments that convey vehicles between geometric changes, such as intersections. Links typically proceed through a corridor with similar geometry. A connector is used to join links. Modeled roadway characteristics are presented in Table 3-4.

Table 3-4 General Roadway Characteristics

Characteristic	Value	Comment
Lane width	12 ft	Standard roadway width.
Desired Speed	25 to 70 mph	Estimated based on roadway classification (e.g., freeway, arterials).
Roadway grade	0%	All roadways were modeled as level terrain.

3.4.3 Roadway Grade

All roadways were modeled as level terrain for the base models. Guidance in NUREG/CR-7002 provides that grades greater than about 4 percent should be included in the analysis. Highway analysis studies have indicated that grades between negative 4 percent and positive 2 percent have a negligible impact on traffic performance. However, steep grades have the potential to significantly impact heavy vehicles [22]. When developing ETE studies, care should be taken

when modeling roads with a higher percentage of heavy vehicles if the NPP is in an area with grades steeper than 3 percent.

3.4.4 Intersections

Evacuation traffic can be significantly impacted by signalized intersections, particularly for evacuations in urban areas [31]. Capacity reduction and delay are both observed at sub-optimally performing intersections, which make up most intersections in the U.S. [48]. Oak Ridge National Laboratory (ORNL) studied capacity reduction and found that most capacity loss was due to less than optimal intersection performance on major arterials [48]. Although the authors were able to attribute the loss to intersections, they noted that most delay is unavoidable.

Microscopic and macroscopic models provide extensive capabilities in the modeling of signalized intersections. One of the major benefits of using microscopic simulation models is the ability to code signalized intersections with a high degree of representativeness to field conditions. Such detail can facilitate more accurate modeling of the traffic conditions, provided that enough data can be obtained on the intersection control (e.g., protected turn lanes) and cycle times. Several driver behavior parameters in VISSIM are related to signalized and non-signalized intersection throughput, including turning speeds, headway times, standstill distance, and the safety distance reduction factor. VISSIM can also model right and left turn lanes, either protected (left turn movement have the right-of-way) or unprotected (left-turn movements yield to oncoming through traffic or pedestrians). Given the importance of intersection control, current guidance provides that all signalized intersections within the evacuation network should be included in the traffic simulation modeling when developing an ETE study [4]. Guidance further identifies that it is not necessary to obtain actual traffic signalization timing for every intersection, because current signalization systems can change throughout the day, depending on traffic flow [4].

3.4.4.1 Signalized Intersection Coding

Typical types of traffic signals include actuated, fixed time, and combinations of these systems [42]. Actuated signals represent the state of practice for intersection control. These signals vary the allocation of green time in response to vehicle detectors, typically providing longer through times for the major streets [42]. For the base models, actuated intersection control was initially built into the medium and large population models with a high degree of detail. However, such specific representations for individual intersections in a large study area—as in the case of an NPP ETE study—is both labor intensive and impractical for such applications. Additionally, due to the large number of intersections, programming actuated signals within the model challenged the computational processing capability of the simulation software. The initial testing of actuated signals caused a fatal error in the program. It was determined that the most appropriate resolution was to implement fixed time signals. With fixed time signal control, the green, yellow, and red times were constant values that repeated. Because there was no detector looking to update the signal timing, this was a less computationally burdensome approach. Use of the fixed time signals also provided a benefit to this study in that it reduced variability in the system. Since the intent of this research is to assess the impact on evacuation times by varying select parameters of interest, reducing compounding effects, such as may be introduced with actuated signal controls, helped confine the change in evacuation time to the variable of interest.

Table 3-5 includes a summary description of the intersection signalization coded into the three base models. The table includes the approximate allocation of green time (i.e., phase splits) for

the major and minor approach directions. In general, the phase splits favored the major street approach at a ratio of two to one. The highest green time allocation to any direction was 280 seconds and the lowest was 5 seconds. These two allocations represent an intersection serving the maximum green time on the major approach and the minimum green time on the minor approach.

Table 3-5 Summary of Signalized Intersections

Population Site Model	Major Road Phase Time (seconds)	Minor Road Phase Time (seconds)	Major Road Protected Left-turn Phase Time (seconds)
Small	50	45	10
Medium	70	70	0
	220	90	0
	280	5	0
Large	50	33	0
	68	40	5
	68	65	10
	180	53	0

Once the decision was made to use fixed time control, all the intersections were then coded with permissive actions, which means that left turns and right turns were allowed after yielding to oncoming traffic. Conflict area functions were used to allow turning vehicles to stop in the intersection, wait for a gap in the oncoming traffic flow, and then proceed with the turn movement when the gap was acceptable. Upon completion of the fixed time intersection coding, interim test runs were conducted, and intersection performance was reviewed. When excessive congestion was observed at intersections, the intersection control was adjusted to support more efficient performance. This process is generally consistent with designing signalized intersection plans.

When significant control delay is observed (excessive congestion) an analysis of intersection level of service is conducted which can lead to the development of new signal timings, if justified [22]. The adjustments were generally focused on intersections that appeared to be operating inconsistent with the rest of the system, such as a congested intersection in-between two other intersections that were operating reasonably well. To improve the performance and reduce congestion, cycle times were adjusted or protected left turn control (exclusive left turn arrow) features were added. However, in some instances adjusting the green time allocation still did not allow for a reasonable approximation of traffic flow. The diminished intersection performance was because these intersections were very congested and required actuated control. Given the limitations discussed earlier, this was not practical. Therefore, to increase the efficiency of these intersections and compensate for not having actuation, the minor street signal head was removed in the model. Using the VISSIM conflict area function, the minor street was set to yield to the major street. When a gap was identified in the major street traffic, the minor street traffic was allowed to cross the major street. The signal on the major street stops traffic on this street at the specified red cycle time. The cycle length was set at 240 seconds. This approach to modeling these intersections reduced the queue length of the minor road while still permitting efficient traffic flow on the major road.

The difficulties associated with attempts to implement actuated signals on a large-scale in the microsimulation model, together with the assumptions required with respect to signal timing, suggest that care should be taken when developing the intersection control approach. Review of ETE studies conducted as part of this project found that modeling of actuated signals has not been identified as an issue with macroscopic models.

3.4.4.2 Non-signalized Intersection Coding

For intersections operating with a stop control, the stop sign was placed at the same location as the stop bar in the field. Conflict areas were used to assign the right-of-way. When an intersection consisted of yield entry, only conflict areas were utilized at the intersection.

3.4.4.3 Alternate Intersection Coding

In the large population site model, all un-signalized intersections were initially coded as stop control as determined through aerial mapping review of intersection characteristics. However, issues arose regarding system performance and excessive travel times. System errors were appearing in the output file identifying that some origin nodes were not loading all the vehicles onto the network during the model run.

To correct the system errors related to loading, alternative intersection control was employed at the origin nodes. All origin nodes, where vehicles were loaded onto the network, had been designed such that vehicles immediately entered a three-way stop-controlled intersection. The loaded vehicles were then forced to make a right-hand turn at the stop sign. These three-way intersections do not physically exist; however, it is common practice to build these into models specifically to load the network. The stop control at these loading intersections was causing delay in vehicles accessing evacuation routes. The delay was significant enough that the total vehicles assigned to the origin node were unable to enter the network during the time allocated for the simulation. The stop-controlled origin loading intersections were changed to a yield on the minor street and no control on the major street. These changes were implemented using the conflict area function in VISSIM. This allowed vehicles on the major street to pass through the intersections freely. Vehicles approaching from the yield side of the intersection proceed to turn right when sufficient gaps in traffic were available. In developing an actual ETE study, establishing additional loading origins, each with a smaller population, may be the more realistic approach to resolve such an issue. But for the test model, the simplified correction sufficed.

3.5 Vehicle Routing

Vehicle routing within traffic simulation models includes the process of directing vehicles to specific destinations. Vehicle routing is performed as part of the internal computational logic of many microscopic and macroscopic models. The VISSIM User Manual [21] explains that the static model assignment, implemented for the small population site, requires the analyst to specifically define the route vehicles will follow. Unless there is queuing and congestion, the inflow into any link in a static model is always assumed to be equal to the outflow. In the dynamic models, DTA tools address the needs of evacuation network performance under various scenarios using iterative algorithms to identify the best path [18] [46] [49]. Along with routing, the road network can have time-dependent characteristics (such as congestion that builds and discharges over time) that may be exacerbated during an evacuation, making dynamic assignment the most appropriate method. Dynamic network models are designed to represent the time-dependent characteristics (e.g., interaction of travel choices, traffic flows, and

time) [18]. DTA routing consists of providing an O-D for a vehicle, but the route used to achieve the O-D trip varies based on travel time, distance, or other factors.

These recognized benefits should not, however, suggest that DTA is without limitation, or that DTA is always the most appropriate method of routing for modeling all evacuation scenarios. In concept, DTA is founded on principles that are created to reflect routine normal daily traffic processes. As such, while many aspects of DTA are relevant to and appropriate for the modeling of evacuations, some are not. For example, DTA suggests that drivers are familiar with recurrent congestion patterns within the network and alternative routes to move around them. This results in an equilibrium assignment wherein traffic volume is relatively equally distributed among possible routes between origins and destinations in a network. An issue that can arise when applying these principles to an evacuation process is that, while they may appear logical, the driver population characteristics and network conditions that exist in such events may not be similar to a routine daily condition. However, given the comparatively small evacuation network for most NPP emergency scenarios and the assumption that a large majority of drivers would have an in-depth local knowledge of alternative routes, it was concluded that a DTA assignment process would be appropriate for the medium and large representative site models in this research.

It is well known that DTA algorithms have limitations in the logical routing of vehicles during an emergency. DTA seeks to assign vehicles to shortest time travel paths but this can result in illogical routing. A typical example was observed in this project where evacuees drove toward the hazard source, taking a circuitous route. In this research, measures were implemented in the control, connectivity and geometric features of the network to minimize such situations.

A static model was built for the small population site and dynamic models (with DTA) were used for the medium and large population sites. Static models were found to be inappropriate for the medium and large population sites due to the numerous potential routes available to evacuees and the difficulty of manual route assignment with a large number of evacuees. The Mississippi DOT has identified that analytic congestion functions used in static traffic assignment models are unable to realistically describe the propagation and dissipation of system congestion under time-varying traveler demand patterns [49]. Furthermore, as the size of a network increases, it becomes difficult to assign specific routes for vehicles and balancing traffic flow on the roadways involves judgment. A typical EPZ includes more than 300 square miles of roadway network with dispersed populations, plus the shadow evacuation area. Building a static model requires analysts to determine the specific routes evacuees would take. DTA provides a more reasonable representation of the routing evacuees would take to exit the EPZ.

During the seeding period for the static model, fixed turning movements of 20 percent left turns, and 30 percent right turns were assigned with the remaining 50 percent continuing straight through the intersection. This allowed the background vehicles to spread out and intermix randomly with the evacuee vehicles to ensure evacuees did not enter an empty road network. The fixed turning movements ceased within the EPZ after the two 15-minute seed periods at which time turning percentages were assigned individually at each intersection.

Evacuation routes were established for the static model evacuation portion of the analysis and turn percentages applied to all vehicles. Once the evacuation began, vehicles were generally routed radially away from the plant. This was done by establishing turning percentages of 100 percent through an intersection in the direction away from the plant. As roadways began to reach capacity, or when alternate routes were available that were also directionally away from the plant, turn percentages were in some cases allocated to these additional routes to help

balance the network. The vehicle loading was balanced through iterative runs, until the routing was determined to be reasonable.

A multi-destination assignment for the DTA in the medium and large population sites was implemented to ensure vehicles were routed away from the nuclear power plant to final destinations located in different sectors. It was observed in preliminary output that vehicles did not always follow a radial path and would return toward the NPP often following circuitous routes. This issue was identified in review of the longest vehicle travel path in test runs.

Figure 3-1 and Figure 3-2 identifies the destination locations used in the DTA for the medium and large population sites, respectively. In the medium population site, there were 13 unique destination zones (414 to 426) in different sectors as seen in Figure 3-1. The medium site had natural barriers that limited route choice (the large site did not). As such, the sectors with these natural barriers did not have destination zones assigned to them. Vehicles originating in the ENE and E sectors between the 5 and 10-mile rings were routed to destination zone 416 located in the NNW, NNE, E, and ESE sectors. In addition to the 13 main destination zones, two additional destination zones (427 and 428) were added in sectors with freeways (ESE and NNW). Origin parking lots within half a mile to the freeway were routed to either destination zones 427 (East quadrant) or 428 (North quadrant) depending on their proximity. These additional destination zones were added to the model after initial test runs showed vehicles originating near the freeways were oversaturating nearby frontage roads and not utilizing the freeways. Therefore, the additional destination zones allowed for routing vehicles more reasonably.

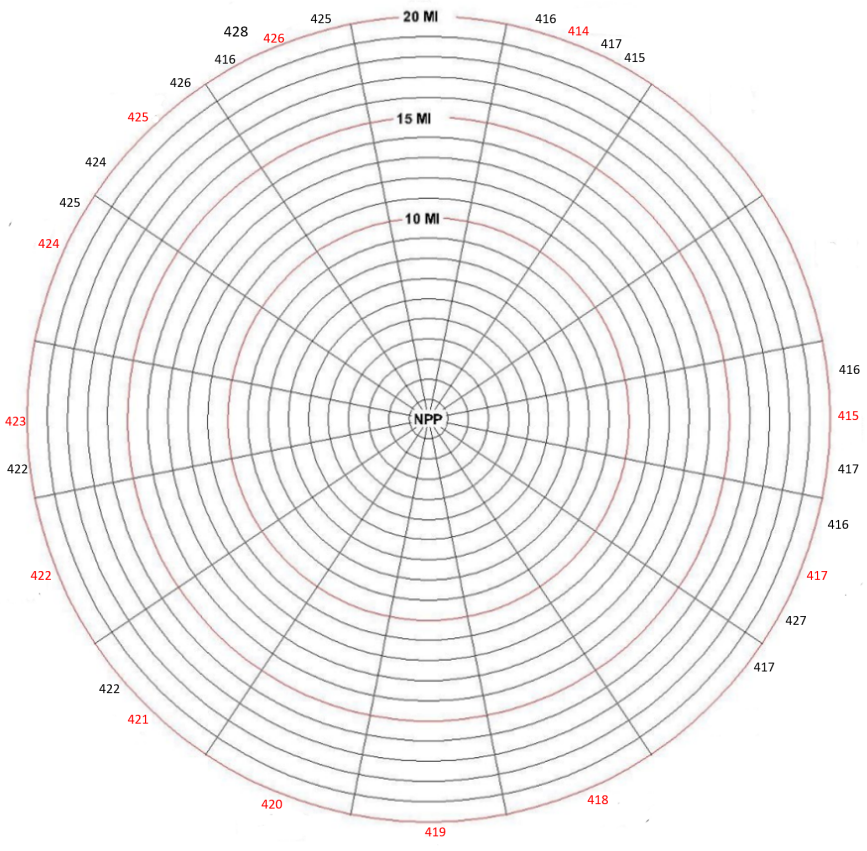

Figure 3-1 Destination Zones for the Medium Population Site Model

In the large population site illustrated in Figure 3-2, each sector was assigned one main destination zone (destinations zone numbers 458 to 473 colored in red) and two additional zones from adjacent sectors. Hence, three destination zones were available to each origin—the main destination zone on that same sector and that same destination zone located on two adjacent sectors. For example, Figure 3-3 shows that vehicles originating in the N sector would exit at destination zone number 458 located in either the NNW, N, or NNE sectors. In addition to the 16 main destination zone numbers in the large population site, two additional destination zones (474 and 475) were added in sectors with freeways (ESE, S, SSW, and WNW). These additional destination zones allowed for more reasonable routing of vehicles.

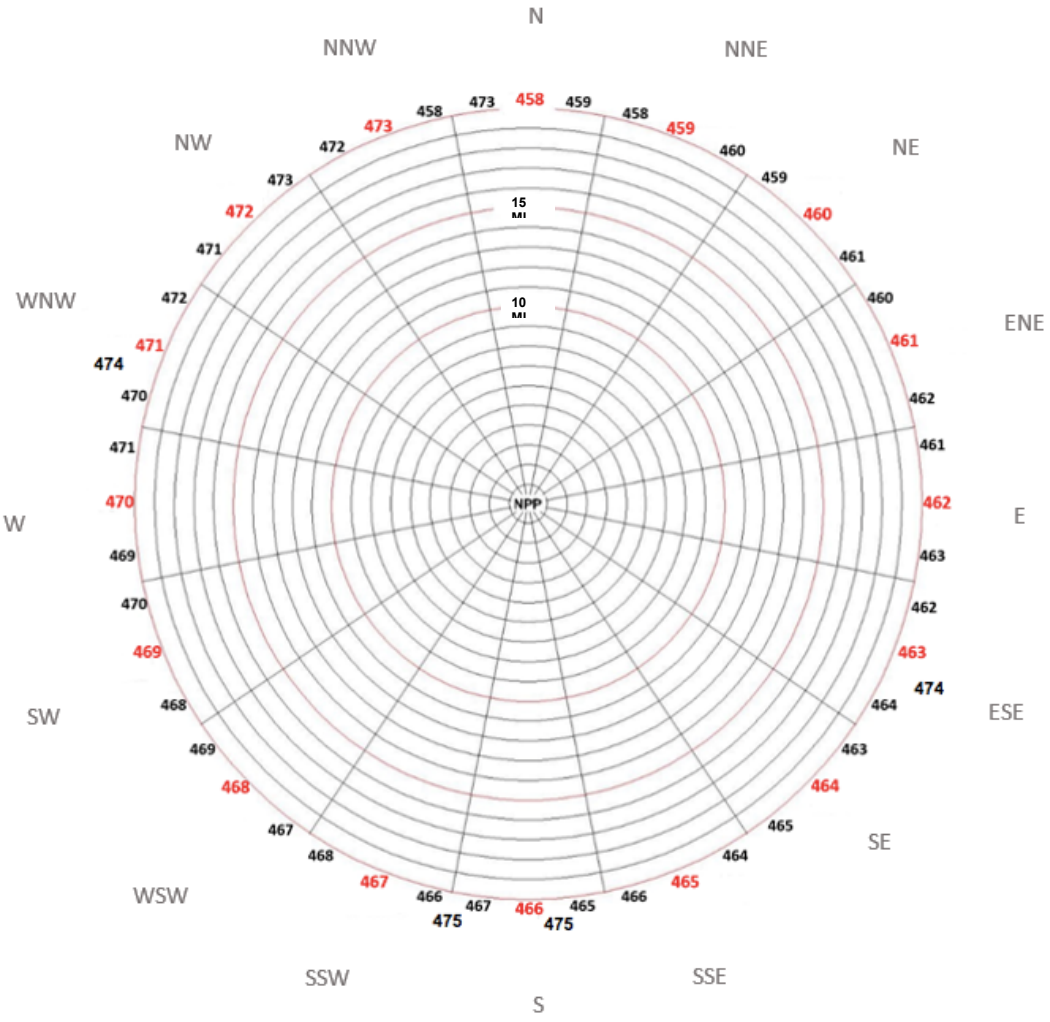

Figure 3-2 Destination Zones for the Large Population Site Model

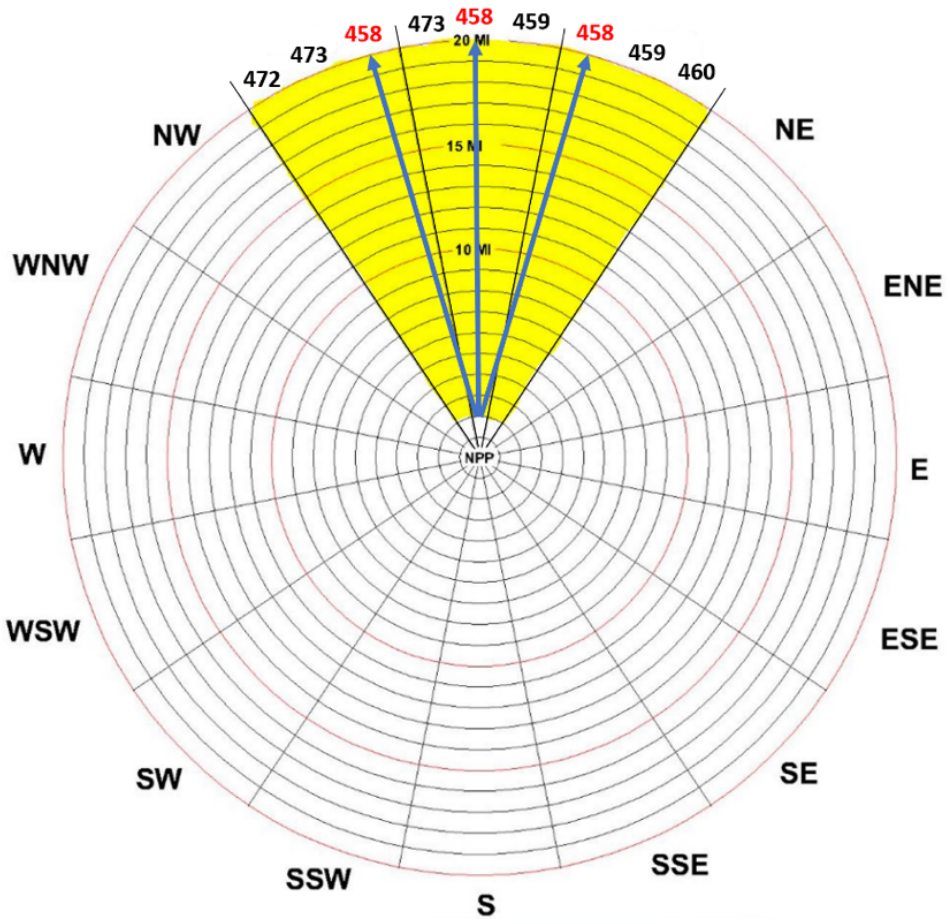

Figure 3-3 Illustration of Destination Assignments in the Large Population Site Model

The inset in Figure 3-4 illustrates the three-pronged outlet (e.g., destination zones 460, 461, and 462) that was used in the model to quickly dissipate vehicles at the exit points in the large population site model. This “pitch-fork” approach was also implemented in the medium site model because the ESE sector in the medium population site did not need to be restricted to an assumed radial evacuation. The vehicles generated inside the ESE sector were assigned to the SE, ESE, and E sectors as well as the NNE sector. This was done to take advantage of a north-bound high capacity road that was underutilized, exiting at the NNE sector.

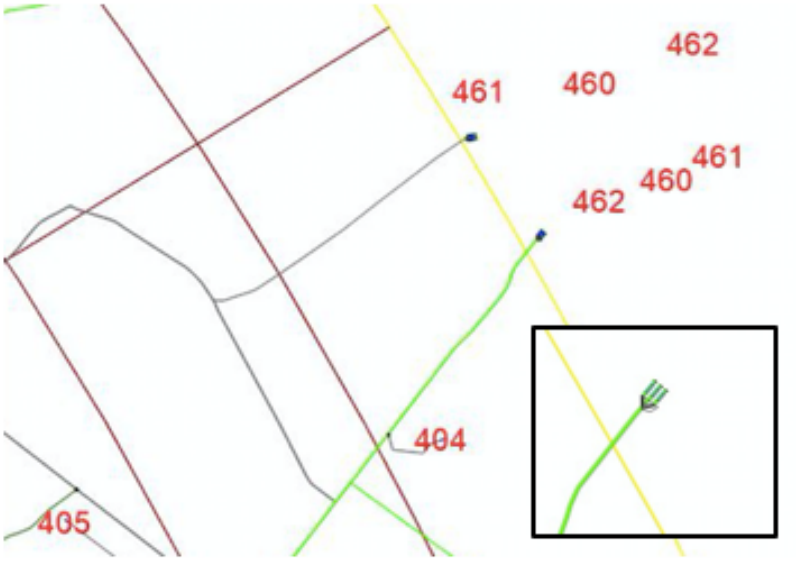

Figure 3-4 Illustration of Pitch-Fork Modeling Approach for Destination Zones

Realistic route choice was also achieved by assigning costs to routes. Travel time is a key component of the DTA computation process [21]. The common behavioral assumption of travelers is that they will choose a route that has the least cost (e.g., travel time) between their origin and destination and try to avoid routes that have the highest cost [21]. To set a hierarchy of road types, a cost per mile parameter was implemented in cost functions for the medium and large population site road networks as shown in Table 3-6. This function allowed for vehicles to distinguish between the classification of freeways, non-freeway evacuation routes, and local roads.

Table 3-6 Dynamic Traffic Assignment Cost Functions

Road Classification	Cost per Mile
Freeways	0
Non-freeway evacuation routes	1
Local roads	2

Additional controls, including closing in-bound lanes, were built into the model to prevent evacuee vehicles from returning into the EPZ. This directional approach constrains the evacuating vehicles to a narrower range of routes exiting the area and was specific to each of the base models.

3.6 Driver Behavior

The representation of driver behavior characteristics is a key component of microscopic models. Parameters that influence car following, lane changing, and gap acceptance behaviors govern traffic flow and effectively dictate factors such as capacity, throughput, queuing, congestion, and delay. These are not considered in macroscopic models, which employ computational processes similar to those of the HCM to determine capacities and delays.

VISSIM provides default values for the driving behavior model parameters to represent a generic, representative population. Although site-specific values of some these parameters are typically generated in traffic engineering projects through calibration and validation processes [45] [50], calibration was not undertaken in this study. This was acceptable due to the conceptual and non-site-specific nature of this project. The project used VISSIM default parameters which are representative of a typical driving population; however, some parameters were varied to reflect more realistic behavior as discussed in the following.

3.6.1 Car Following Models

The traffic flow model in VISSIM is a discrete stochastic model that contains a psycho-physical car following model for all interactions along the same lane [21]. VISSIM implements two car following models:

- Wiedemann 74 (W74): Model suitable for urban traffic and merging areas
- Wiedemann 99 (W99): Model for freeway traffic with no merging areas

The passenger car default values are provided in Table 3-7 and Table 3-8, respectively. A comprehensive list of the driver behavior parameters is provided in Appendix B. The default driver behavior values are identified in the VISSIM User Manual [21] and are provided as prepopulated values within the VISSIM model. VISSIM and by extension, the Wiedemann car-following models are widely used within the field of traffic simulation and found throughout the literature.

Table 3-7 Driver Behavior Parameters for Non-Freeways (Wiedemann 74)

Parameter	Description	Modeled Value	Default Value
Observed vehicles	The number of observed vehicles affects how well vehicles in the link can predict other vehicle movements and react accordingly.	4	4
Maximum look ahead distance	Maximum distance that a vehicle can see forwards in order to react to other vehicles either in front or to the side.	820.21 ft	820.21 ft
Maximum look back distance	Maximum distance that a vehicle can see backwards in order to react to other vehicles.	492.13 ft	492.13 ft

The W99 model uses ten Calibration Components (CC) listed in Table 3-8 as CC0 through CC9. The Wiedemann 99 parameters were only used on freeways, which require an on-ramp or off-ramp to enter or exit the roadway.

Table 3-8 Driver Behavior Parameters for Freeways (Wiedemann 99)

Parameter	Description	Modeled value	Default value
CC0 Standstill Distance	The average desired standstill distance between two stopped vehicles.	4.92 ft	4.92 ft
CC1 Headway Time	The distance in seconds which a driver wants to maintain while following another car.	0.9 s	0.9 s
CC2 Following Variation	How much more distance than the desired distance a driver allows before intentionally moving closer to the car in front (longitudinal oscillation).	13.12 ft	13.12 ft
CC3 Threshold for Entering Following	The number of seconds before reaching the safety distance. Controls the start of the deceleration process.	-8	-8
CC4 Negative Following Threshold	Defines negative speed difference during the following process. Low values result in more sensitive driver reaction to the acceleration or deceleration of the preceding vehicle.	-0.35	-0.35
CC5 Positive Following Threshold	Defines positive speed difference during the following process.	0.35	0.35
CC6 Speed Dependency of Oscillation	Influence of distance on speed oscillation while in the following process.	11.44	11.44
CC7 Oscillation Acceleration	Oscillation during acceleration.	0.82 ft/s^2	0.82 ft/s^2
CC8 Standstill Acceleration	Desired acceleration when starting from standstill.	11.48 ft/s^2	11.48 ft/s^2
CC9 Acceleration at 50 mph	Desired acceleration at 50 mph.	4.92 ft/s^2	4.92 ft/s^2
Maximum look ahead distance	Maximum distance that a vehicle can see forwards in order to react to other vehicles either in front or to the side.	820.21 ft	820.21 ft
Maximum look back distance	Maximum distance that a vehicle can see backwards in order to react to other vehicles.	492.13 ft	492.13 ft

3.6.2 Lane Change Parameters

The VISSIM lane change parameters used in all three models are identified in Table 3-9. A comprehensive list of lane changing parameters is provided in Appendix B. Default values were used, except for the *wait time before diffusion* value. This parameter required significant adjustment for the medium and large population models to perform under the saturated conditions of an evacuation. At the default value, vehicles became stuck in freeway congestion and were unable to exit at the designated point, as determined by the model. In such cases, VISSIM removes the vehicle from the system, causing a discrepancy between loaded vehicles and exiting vehicles. To eliminate the removal of vehicles, the wait time before diffusion was increased to 900 seconds. In the small population model, the value of 9,999 seconds was used.

Wait time before diffusion defines the maximum time vehicles wait on the freeway in a stopped position for a gap of sufficient distance to change lanes. A high value can result in excessive delay on the route, and a low value can result in vehicles being removed from the analysis. Both conditions may be unrealistic, and a balance is needed. In microscopic and mesoscopic traffic simulation models, the removal of a small number of vehicles is common and would be expected in any large scale ETE study. In general, it is common for this number to be in the range of two to three percent of the total number of vehicles modeled and would not impact the overall findings of an ETE study.

Table 3-9 VISSIM Lane Change Parameters

Parameter	Description	Modeled Value	Default Value
Maximum deceleration	Maximum deceleration technically possible.	-13.12 ft/s²	-13.12 ft/s²
Accepted deceleration	Upper bound of deceleration in prescribed cases.	-3.28 ft/s²	-3.28 ft/s²
Maximum deceleration of trailing vehicle	Maximum deceleration technically possible.	-9.84 ft/s²	-9.84 ft/s²
Accepted deceleration of trailing vehicle	Upper bound of deceleration in prescribed cases.	-3.28 ft/s²	-3.28 ft/s²
Wait time before diffusion	Maximum time vehicles wait on the freeway in a stopped position for a gap of sufficient distance to change lanes.	9999 s (small population site) 900 s (medium and large population site)	60 s
Minimum Headway front/rear	The minimum distance between two vehicles that must be available after a lane change, so that the change can take place.	1.64 ft	1.64 ft

3.6.3 Vehicle Speed

Speeds were implemented in the model using the VISSIM desired speed decision function. Desired speed, often referred to as free-flow speed, is defined in the VISSIM User Manual [21] as the speed at which a driver would travel, if not hindered by other vehicles or network objects. Such hindrances may include intersections, driveways, or other road interactions. Desired speed is typically higher than the posted speed value because it is a modeling feature and is not intended to be reflective of the posted speed. For posted speeds of 40 mph and lower, desired speeds were set with a range of 5 mph above and below the posted speed. For posted speeds of 45 mph and higher, desired speeds were set with a range of 10 mph above and below the posted speed. In all cases, the 85th percentile was set at the posted speed. The range of modeled speed values is provided in Table 3-10.

Table 3-10 Modeled Speed Values

Roadway type	Posted Speed (mph)	Lower Bound (mph)	Upper Bound (mph)
Residential or Collector	30	25	35
Residential or Collector	35	30	40
Minor Arterial	40	35	45
Minor Arterial/Major Arterial	45	40	50
Major Arterial	50	40	60
Major Arterial	55	45	65
Freeway/Rural Highway	60	50	70
Freeway	65	55	75
Freeway	70	60	80

When building the VISSIM model, the roadway speed is separate from the roadway type. At selected intersections, a speed decision point was established in each direction. When the modeled vehicle passed the decision point, a desired speed was assigned to the vehicle and the speed distribution profile was applied. In congested flow, the speed of the vehicle would be virtually the same as the vehicle in front. In uncongested flow, the speed profile may increase or decrease vehicle speed. The vehicle maintains the desired speed assignment until it crosses another speed decision point later in the network. For example, in the small population model, only one speed decision point was established in the 2-mile area and one in the 5-mile area. Further away from the plant, multiple speed decision points were assigned. In a site-specific ETE study, guidance would suggest that speeds be reflective of the roadway network, and additional speed decision points should be employed.

3.6.4 Base Model Loading

Loading a traffic simulation model network requires knowledge of the demographics, volume of vehicles evacuating, the rate at which vehicles enter the network, and the location at which the vehicles enter the network. In VISSIM, vehicles are input into the model at origin nodes, which are simply loading points for the model. The dispersion of origin nodes was generally based on the population density, such that higher density areas within the EPZ would have more origin nodes from which to load vehicles into the system. Vehicle loading rates were input at the grid element level using 16 sectors and one-mile rings to create the grid. For the medium and large

population models, loading was implemented via a short link built specifically to connect to a collector or arterial roadway. Typically, these connections were designed as yield entry points.

The trip generation time is the time elapsed for each population group from when the evacuation order was disseminated until the time when the evacuation trip begins [4]. It includes all activities necessary for evacuees to receive the notification and prepare to evacuate. The loading curves for the medium and large population sites were developed from an average of multiple ETEs from sites with similar populations. The loading curve used in the small population site was taken from a representative site. The loading curve data is provided in Figure 3-11.

Table 3-11 Traffic Simulation Loading Curves for Representative Models

Traffic simulation model time[1] (h:mm)	Evacuation interval number	Evacuation time (h:mm)	Evacuation period (minutes)	Small site EPZ loading	Medium site EPZ loading	Large site EPZ loading
Traffic simulation initialization period — 30 minutes[2]						
0:30	1	0:00	15	10%	0%	0%
0:45	2	0:15	15	25%	2%	0%
1:00	3	0:30	15	21%	6%	3%
1:15	4	0:45	15	16.5%	11%	10%
1:30	5	1:00	15	9.5%	15%	15%
1:45	6	1:15	15	8.5%	16%	15%
2:00	7	1:30	15	6.5%	13%	13%
2:15	8	1:45	15	2.5%	12%	12%
2:30	9	2:00	15	0.5%	8%	7%
2:45	10	2:15	15		6%	6%
3:00	11	2:30	15		4%	4%
3:15	12	2:45	15		2%	4%
3:30	13	3:00	15		2%	2%
3:45	14	3:15	15		1%	2%
4:00	15	3:30	15		1%	2%
4:15	16	3:45	15		1%	2%
4:30	17	4:00	15			1%
4:45	18	4:15	15			1%
5:00	19	4:30	15			1%
5:15	20	4:45	15			
5:30	21	5:00	15			
5:45	22	5:15	15			
6:00	23	5:30	15			
6:15	24	5:45	15			
6:30	25	6:00	15			
Total				100%	100%	100%

[1] Evacuation order is given at simulation clock time 0:30.

[2] A 30 minute initialization period is used to load background traffic onto the network prior to the evacuation.

Loading curves model the time of vehicle departures from their various points of origin. ETE studies typically gather loading curve information from telephone surveys and model resident's point of origin as their driveway. In this study, vehicles are loaded using connector links that do not capture residential streets or driveways. This modeling approach omits a portion of the time needed to drive from the driveway, but this is generally negligible. However, in some situations this modeling approach could have a larger impact and measures were taken within the base models to increase the efficiency of some stop-controlled intersections to compensate. The O-D approach provides a simplified and reasonable method for loading large numbers of vehicles at selected origin points and is consistent with the current state of practice in traffic simulation modeling. Following current guidance [4], the shadow evacuees were loaded consistent with the loading of the EPZ population.

3.7 Simulation Coding

3.7.1 Time Step

Time interval of processing is an input variable used in traffic simulation to control the rate of processing and response of vehicles to changes in traffic conditions. In the VISSIM microscopic simulation platform, the time interval of processing (referred as simulation resolution) influences the behavior of vehicles and their interactions [21]. The simulation resolution in VISSIM varies from 1 to 20 time steps per second. The simulation time step was set at 1 simulation per second for computational efficiency. This time step value is also consistent with the simulation resolution used for the signal control add-on analyses evaluated in Task 3 of the project.

3.7.2 Number of Runs

Microscopic model results are typically presented as an average of a set of runs where each run is performed with a random seed. VISSIM implements this approach because distributions are built into the code for some probabilistic parameters [21]. For each random seed, the model selects a value from the embedded distributions and executes the calculation. Different seed numbers produce different results, and results are presented as an average of the number of runs (with each run based on a different random seed).

A minimum of 10 runs is typically suggested to provide confidence in the averaged results [20] [24]; however, such recommendations do not consider the large size of the traffic networks modeled, the exact stochastic variation within the network, or project constraints such as time or computational resource limitations. The base models for each site were run 10 times and average results were presented. Using the 90 percent ETE as the most important metric, a statistical analysis was performed to determine the number of runs needed for each parametric analysis to achieve average results at the 95 percent confidence level.

$$n = \left(\frac{Z_{\propto/2} \cdot \sigma}{E}\right)^2 \quad 3.1$$

where,

- n is the required number of simulation runs
- $Z_{\propto/2}$ is the Z-score for a two-sided error of 2.5 percent (5 percent total) with $n-1$ degrees of freedom
- σ is the standard deviation from the initial sample of 10 runs from the base model

- E is the confidence interval of the true mean (acceptable error when estimating the mean)

The goal of this statistical analysis was to determine the number of runs required to sufficiently produce an average result that falls within the confidence interval of the unknown true mean. The analysis results were output in 5-minute increments. For the small population site, the 90 percent ETE from the 10 runs produced seven ETEs between 2:25 and 2:30 (h:mm), and three ETEs between 2:30 and 2:35. To determine the number of runs, it was assumed that the seven ETEs were 2:25 and the three higher value ETEs were 2:35, producing the largest possible standard deviation for the set. The number of vehicles exiting the network was collected over 5-minute intervals. Therefore, plus or minus five minutes represents the smallest measurable error for the ETE using the approach documented in this report. Based on an acceptable error of five minutes, the calculation results show that 4 runs are required to provide a 95 percent confidence interval. Subsequent analyses were performed for the medium and large population sites with an acceptable error of 10 minutes. The analyses suggested a total of 4 runs were required to produce average results suitable for the task analysis for both the medium and large population sites.

The approach to develop the number of runs required for the stochastic microscopic models requires judgment regarding the most important metric to be used in the equation. In the base models, the 90 percent ETE was used. ETE guidance [4] suggests that the 90 percent ETE be used to inform protective action recommendations, therefore, this was a reasonable metric on which to base the number of runs.

3.7.3 Validation and Model Adjustments

Murray-Tuite, et al., [31], emphasize the importance of validation stating, “Validation for evacuation models is a difficult but important task. With more complexity, the models will become more difficult to validate but this step cannot be ignored.” Model validation is a key aspect of simulation modeling. Because the base models do not represent an actual EPZ, no data or information would be available for the validation process. However, the base models for this study were developed to be representative, and VISSIM default parameters are calibrated and validated to represent a generic traffic scenario. Therefore, for the purpose of this research task, it was appropriate to use default parameter values instead of site-specific calibrated and validated ones.

Each model was loaded with a reasonable volume of background traffic distributed in a manner representing the population distribution. Speed and volume outputs were spot checked on key roadways during the background loading period (seeding period) similar to the method described in the Oregon Protocol [24]. This spot checking provided a verifiable method of quality assurance. Spot checking a set of roadways for vehicle volumes and speeds, prior to the start of evacuees entering the roadway network, provides an efficient means of verifying that important roadways in the network are performing as expected.

Review of interim model results was performed often throughout the model builds as a means to validate the reasonableness of the ETE. The evacuation time was the metric of interest for most of the internal reviews. When an ETE was determined to be excessive, the coding was reviewed to determine where issues may be occurring. Because controlled intersections usually present the initial point of congestion in a network, the review began with intersections. With the large number of intersections in the medium and large population models, an initial approach was to

look for intersections where congestion was occurring upstream or downstream of intersections that were performing well. Coding was reviewed for accuracy, and signal timing was reviewed for realism. As needed, cycle length or phase times were adjusted to allow the congested intersection to perform more efficiently. Intersections that could not be improved with signal timing were considered for traffic control points (TCP) in Task 3.

Testing and review of interim model results revealed sections of the roadway network that were substantially underutilized during the evacuation period. This was considered an unrealistic travel phenomenon for these roadway segments. Traffic simulation models attempt to replicate driver behavior and the model algorithms sometimes route vehicles along obscure paths that are not realistic. The VISSM cost function was adjusted to address this issue. “Cost,” with respect to traffic simulation modeling, applies a travel penalty to discourage use of one route and encourage use of another. Freeways are the more likely roadway of choice, so freeway costs were reduced. Arterial road costs were increased to make them a less desirable route choice. Additionally, for the large population site, two extra destination points were established to facilitate travel on the freeway over arterial roads. A reasonable final distribution of vehicles was established for these roadway segments after several iterations. The cost function is not applicable to the small population model because it was developed with static routes.

3.8 Base Model Data Collection and Analysis

The base models are relatively large and complex and VISSIM provides the capability to generate a significant amount of output data. A data collection and analysis methodology was developed to support the research objectives. Three measures of effectiveness (MOE) were selected preliminarily for comparison purposes:

- evacuation time estimate (ETE)
- average travel speed at selected locations
- hourly volume at selected locations

These measures are point location indicators and were collected at specific locations of interest within each model. In this report, the term “ETE” is applied primarily to the EPZ. The term “clearance time” is also used, but primarily to indicate the time needed to clear various sectors and distances outside of the EPZ.

3.8.1 Data Collector Locations

VISSIM requires data collection points to be established in the network prior to running the simulation. The initial set of collection points were established at EPZ outflow routes. Additional collection points were established at the 2, 5, 15 and 20-mile rings on various outflow routes to support study tasks. The small population site model had 109 collection points as shown in Figure 3-5. The medium model had 147 collection points and the large model had 308. These collection points are shown on maps in Appendix B.

3.8.2 Data Quantity and Data Representation

Clearance time, speeds and vehicle volumes—collected by vehicle designation (evacuee, background traffic, or shadow evacuee)—were collected in 5-minute intervals within each model. The number and frequency of data collection points created large amounts of data to be analyzed. To illustrate, the speed measure from one location in the large population site model for a scenario with a 10-hour clearance time created 120 data records for each vehicle

designation (10 hours × 12, 5-minute periods per hour). The large population model has 308 data collector locations so a single scenario run would yield 308 (data collection locations) × 120 (data records), or 36,960 data records for each vehicle designation. Since there are three primary MOEs (volume, speed, and ETE/clearance time) of interest, one run resulted in 36,960 (records) × 3 (MOEs), for a total 110,880 MOE data records.

Carrying this forward to the task analyses, testing individual parameters may require two to six scenarios to model the possible parameter variation. Assuming an average number four scenarios, data collection in the large population site would produce 4 scenarios × 110,880 data records per scenario, or 443,520 data records per parameter of interest. Assuming that the medium and small population site yield data records within the same order of magnitude, combined, one run of all three models to study one parameter of interest would yield about one million data records. The large data set challenged the project staff to condense and summarize data to discern meaningful results.

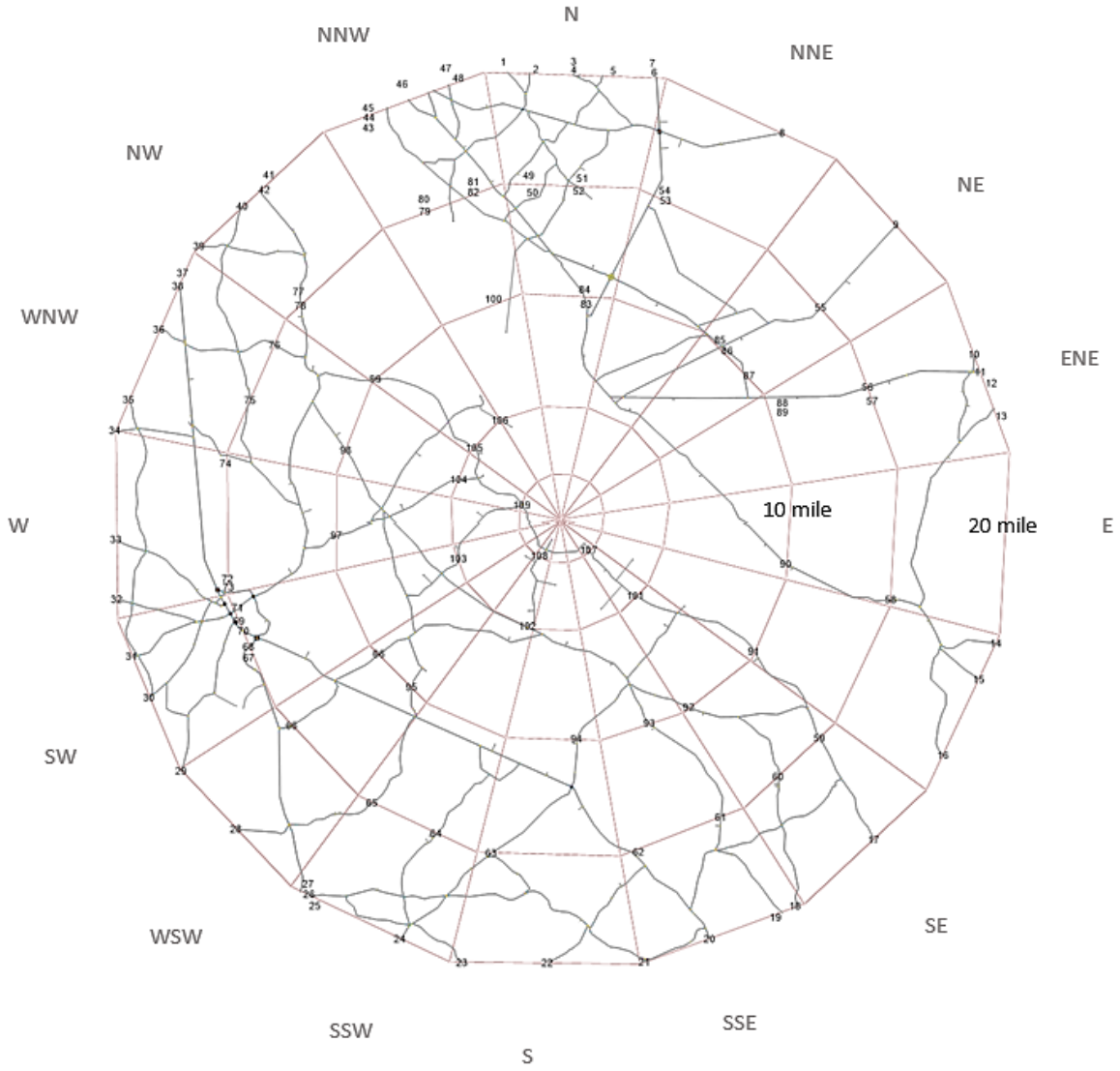

Figure 3-5 Data Collector Points for the Small Population Site Model

3.8.3 Other Performance Indicators

The medium and large population site models showed extensive vehicle queuing at intersections along evacuation routes throughout all periods of the evacuation. Queue formation began early and extended over entire roadway corridors. The queue growth on some routes became indistinguishable from congestion resulting from high traffic volume. Early in the model development process, observations of system performance suggested that useful information could be obtained by collecting some additional performance indicators.

Additional performance data were collected during the simulation that was stratified by vehicle type (background vehicles and pass through vehicles, EPZ evacuee vehicles, and shadow evacuee vehicles). Data collected included: average vehicle delay; number of stops; total delay; average speed; vehicle hours traveled; vehicle miles traveled; number of vehicles arriving at destination and number of vehicles still active when the simulation completed. These additional MOEs were used to provide a quality assurance check on the model during development stages and for the task analyses. It should be noted that VISSIM performs vehicle averages over the entire model area and simulation time and does not evaluate average parameters in subregions. For example, it was not possible to evaluate vehicle miles traveled within the EPZ and outside the EPZ, nor was it possible to segregate out the statistics collected after the seeding period.

3.8.4 Base Model MOE Results

Base model results were the average of 10 runs (10 different random seeds) for each site model. The primary MOE was EPZ ETEs. However, speed, volume and clearance times at distances beyond the EPZ were also collected to provide insight into the dynamics of the evacuation process. Additional MOES were collected as discussed in Section 3.8.3.

3.8.4.1 Base Model Evacuation and Clearance Times

The 90 and 100 percent ETEs were tabulated at the 2, 5, and 10-mile rings of the EPZ for each population model. As an additional level of analysis, clearance times were also recorded along the 15 and 20-mile rings. ETEs and clearance times for the base models at 90 and 100 percent evacuation are shown in Table 3-12.

Table 3-12 Base Model Average ETEs and Clearance Times

Population Site Model	2-Mile ETE (h:mm)		5-Mile ETE (h:mm)		10-Mile ETE (h:mm)		15-Mile Clearance Time (h:mm)		20-Mile Clearance Time (h:mm)	
	90%	100%	90%	100%	90%	100%	90%	100%	90%	100%
Small	1:35	2:18	1:35	2:21	1:44	2:31	1:55	2:41	2:00	2:45
Medium	2:41	4:03	2:51	5:18	4:59	7:22	5:41	8:04	5:58	8:23
Large	3:39	5:06	4:02	7:16	4:40	9:02	5:14	9:41	5:43	10:07

Table 3-12 shows that the 100 percent ETE for the small population site was 2:31 and the 90 percent ETE was 1:44. This difference of 37 minutes suggests that the last 10 percent of evacuees increased the evacuation time by about 35 percent. This finding was consistent with prior observations that the evacuation tail significantly increases evacuation time [16]. The small population site ETEs reflect the assumed loading times (Table 3-11). This phenomenon is expected in evacuations where road network capacity is sufficient to keep traffic flowing at or

near free-flow speeds and minimizing delay. Because of this, loading time tends to be the dominant contributor to the ETE for small population sites. Figure 3-6 illustrates the ETE profile for the small population site.

The ETE times at various ring distances provide insights into traffic flow conditions throughout the small population site model. As expected, the clearance times increased at further distances, however, the relatively small incremental time increases reflect high vehicular travel speeds. The ETE data shows consistency between the 90 and 100 percent evacuations in that the time required to evacuate the last 10 percent at the 2, 5, 10, 15, and 20-mile rings took about the same time, approximately 40 minutes.

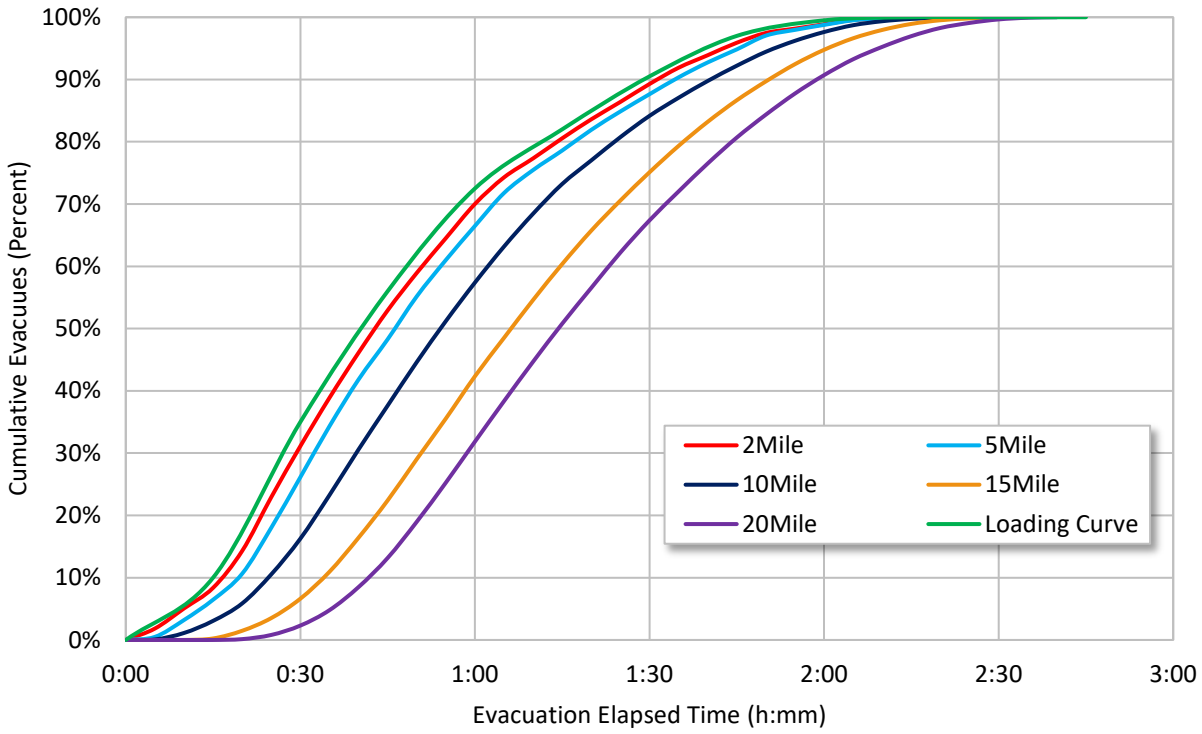

Figure 3-6 ETE Curves for the Small Population Site Base Model

The 100 percent average ETE for the medium population site was 7:22, approximately 2 hours and 23 minutes longer than the 90 percent ETE time (4:59) and 3 hours and 22 minutes longer than the loading time of 4:00. The last 10 percent of evacuees increase the ETE by nearly 48 percent. The time elapsed between the loading curve and the 100 percent ETE suggest congestion caused approximately 3 hours of delay as demand exceeded the available capacity.

The loading curve, ETEs, and clearance times for the medium population site can be seen in Figure 3-7. The ETEs for the 2 and 5-mile rings mirror the loading curve. This is expected since the areas nearest the NPP have low population density and free-flow would result. Beyond the 5-mile ring, the population density increases resulting in a divergence between the loading curve and the 10-mile ETE. This trend continues as population density increases further from the NPP. As the evacuation progresses, the network traffic begins to clear, and after congestion has abated travel times would be expected to reflect free-flow conditions.

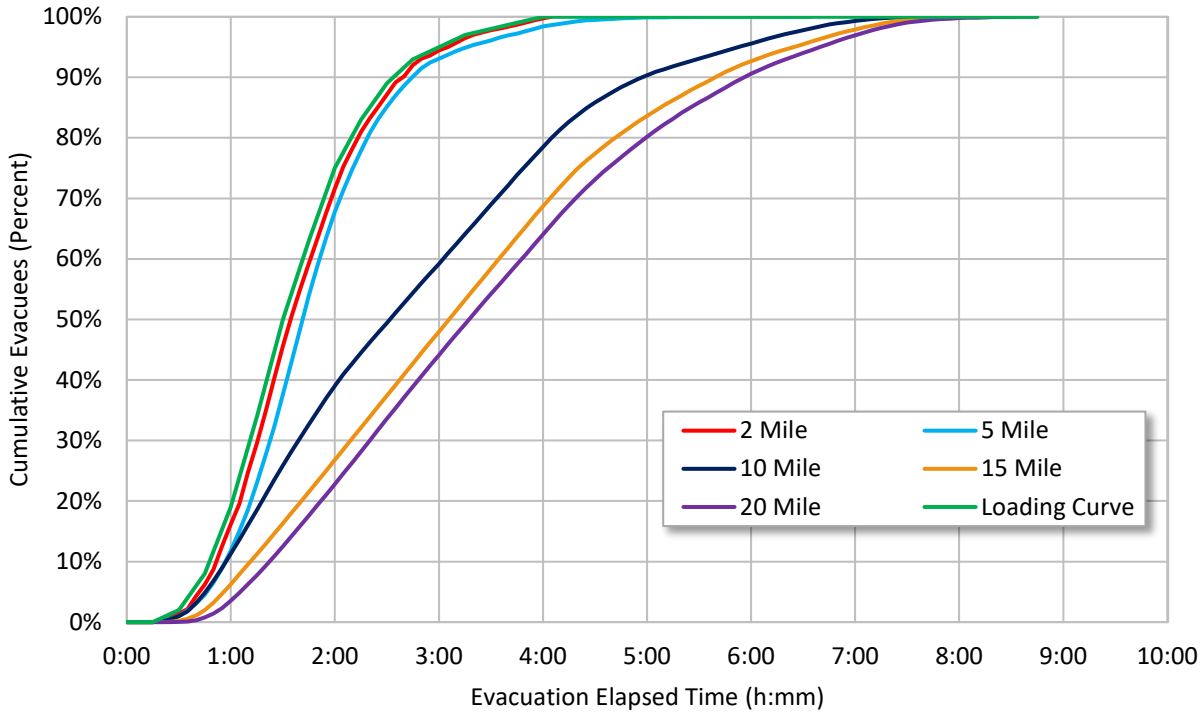

Figure 3-7 ETE Curves for the Medium Population Site Base Model

The 100 percent ETE for the large population site was 9:02. This was 4 hours 22 minutes longer than the 90 percent ETE and 4 hours and 47 minutes longer than the loading curve. The spatial and temporal distribution of demand, generated by the loading of evacuees, generated as much as 5 hours of added travel time during portions of the evacuation. This was the result of severe congestion, as demand exceeded the available capacity. This relationship can also be seen in Figure 3-8 for the large population site model.

Figure 3-8 illustrates the traffic conditions within the large population site model. There is considerably more congestion throughout the EPZ due to the large population loading on the network. Beyond the 10-mile EPZ boundary, although congestion remains, it takes 39 minutes to clear the 15 mile-ring and only 26 minutes after that to clear the 20-mile ring (for the 100 percent evacuation). This reflects the increasing robustness of the network with additional routes and capacity available to traffic as it moves into more distant and more populated areas of the region.

Table 3-13 identifies the 100 percent ETE and clearance times for the specified distances of the four 90-degree quadrants of each site. This information was useful in understanding the variation of clearance times by quadrant and comparing the values to the population distributions. These numbers report the clearance times of that quadrant at the mileage ring only. Multiple collectors are typically located on each ring, but some quadrants had no collector points at a given ring. The maximum value for the quadrant is presented in the table. The other collectors within each quadrant had values equal to or less than those in the table. It should be noted that these values do not necessarily compare to the ETE times. As discussed below, due to the stochastic nature of VISSIM and simulation modeling in general, the maximum time to clear all vehicles from a network may not always be a realistic representation of the ETE.

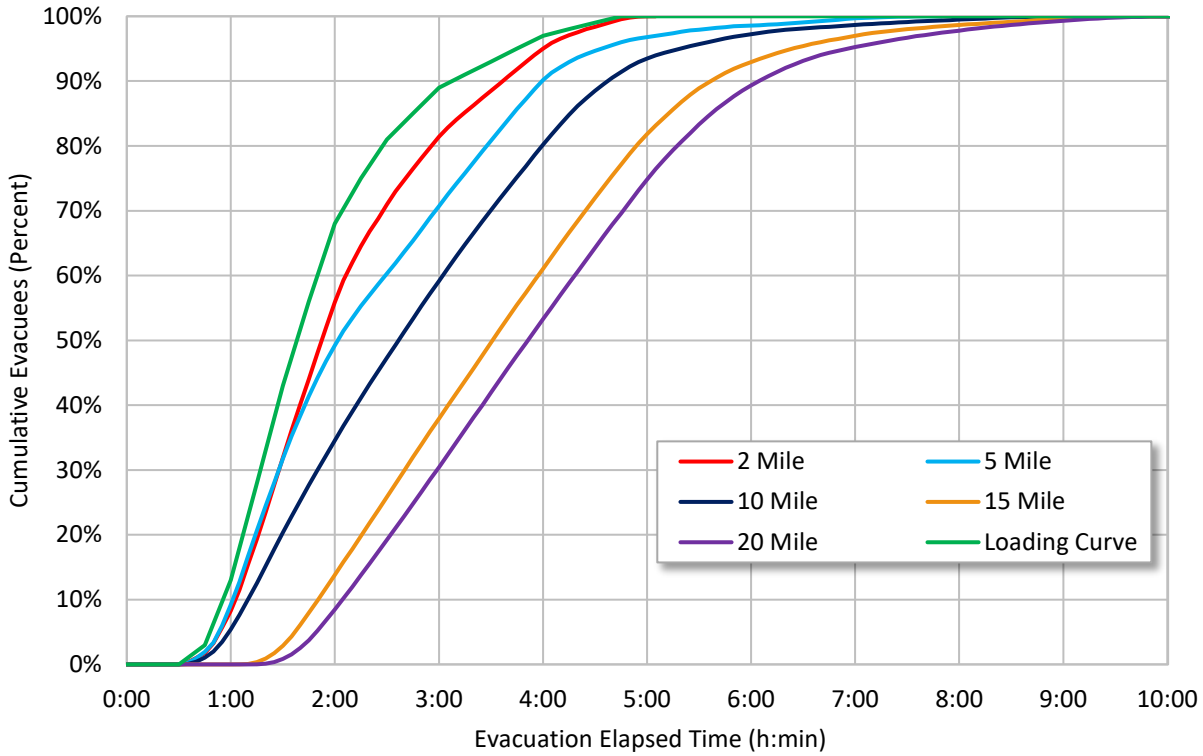

Figure 3-8 ETE Curves for the Large Population Site Base Model

Table 3-13 ETEs and Clearance Times by Quadrant

Site Quadrant	2-Mile 100% ETE (h:mm)	5-Mile 100% ETE (h:mm)	10-Mile 100% ETE (h:mm)	15-Mile 100% Clearance Time (h:mm)	20-Mile 100% Clearance Time (h:mm)
Small N	NC[1]	NC	2:15	2:35	2:45
Small E	NC	NC	2:10	2:20	2:25
Small W	2:20	2:20	2:35	2:45	3:05
Small S	2:20	2:25	2:35	2:40	2:50
Medium N	NC	6:35	7:40	8:30	8:45
Medium E	NC	NC	6:15	7:25	7:35
Medium S	4:03	4:20	4:30	4:40	5:25
Medium W	NC	4:05	7:30	7:00	8:45
Large N	5:05	6:30	9:05	10:50	9:35
Large E	5:00	6:25	9:10	9:20	9:45
Large S	5:00	6:35	6:45	7:10	7:25
Large W	5:10	7:50	7:35	10:40	11:20

[1] NC indicates no collector was located in the quadrant.

Clearance time calculations for areas beyond the EPZ consider the full population evacuating to the 20-mile ring. NUREG-0654/FEMA-REP-1, Revision 1 [5], recommends that relocation centers be located at least five miles and preferably 10 miles beyond the EPZ. Results of a national telephone survey of EPZ residents found that 34 percent of respondents were likely to go to reception centers [8]. The base models do not consider that portions of the population may

cease their travel at some point within the 10 to 20-mile region. Table 3-14 provides the high, low, and mean clearance time results for the 10 and 15-mile rings for the three population site models.

Table 3-14 Low, Mean, and High ETE and Clearance Time Results

Population Site Model	10 Mile ETEs (h:mm)			15 Mile Clearance Times (h:mm)		
	Low	Mean	High	Low	Mean	High
Small	2:30	2:31	2:35	2:40	2:41	2:45
Medium	7:05	7:22	7:40	7:45	8:04	8:30
Large	8:55	9:02	9:10	9:10	9:41	10:50

As shown in Table 3-14, the stochastic nature of VISSIM creates variation in the ETEs among the ten individual runs. This variation is intended to reflect the normal variation in traffic conditions and driver behavior from day-to-day and even minute-to-minute. The variation among the ten runs for each of the sites was relatively low for the 10-mile EPZ. It was about 5 minutes (3 percent of the mean) for the small population site, 35 minutes (8 percent of the mean) for the medium site, and about 15 minutes (3 percent of the mean) for the large population site model. The medium population site likely experienced the most variation within the EPZ because it showed the highest levels of congestion among the models and because the base population was set intentionally high. Variation was more pronounced for the clearance of the 15-mile area surrounding the large population site NPP. These runs showed a 100 minute difference between the low value and high value or about 17 percent of the mean value. These results suggest that it is important to use the mean value for a set of runs that establishes a level of variation.

These results also emphasize an important aspect of microsimulation that should be taken into account when computing ETEs. Because no simulation is a perfect representation of reality, certain situations arise where vehicles may become stuck in the system or take arbitrarily long routes to exit. In these cases, a few final vehicles in the evacuation tail could take a disproportionately long time to exit the network. Waiting on one or two vehicles to exit the network could add a significant amount of time to the ETE or clearance time beyond the EPZ. As such, a volume cutoff was applied in some cases so that clearance times were not artificially distorted. Typically, the “last vehicle” 100 percent clearance time would be declared once 10 or fewer evacuation vehicles remained in the network at a particular radial distance. For the medium and large population site models, this represents less than 0.01 percent of evacuation vehicles.

3.8.4.2 Base Model Travel Speeds

Average travel speeds observed at collector points were used to assess travel conditions. Speeds were recorded for individual vehicles then grouped into averages in 5-minute increments. To accomplish this, detector locations were grouped into 16, 22.5-degree, compass sectors (N, NNE, NE, ENE, E, etc.). Within these sectors, speeds were averaged and grouped by time period and summarized within each of the concentric compass rings. In this way, variations in speed could be displayed over time and in various exit directions away from the NPP. Figure 3-9, 3-10, and 3-11 display the progression of travel speeds at the exit of the EPZ for the small, medium, and large population sites, respectively.

The speed data showed results consistent with the ETE for the small population site. In general, operating speeds tended to be high throughout the small population model. In many cases, speeds averaged above posted speeds in the network. This was consistent with observations made during peak hour traffic where volumes are below capacity. Traffic speeds tend to be higher than posted speed as drivers travel at their desired speed. VISSIM allows for this by modeling individual vehicles and their desired speed as opposed to setting the maximum speed of a link, as is common with macroscopic models.

Figure 3-9 illustrates several key features of the early periods of the small population site evacuation at the 20 percent base case shadow participation level. The most obvious of these is the consistency of speeds during the early portion of the evacuation. The three curves align almost exactly. This suggests that there was not much speed change over the first hour and a half of the evacuation. It further suggests that there was little-to-no build up and discharge of congestion and delay during this time period. The figure also shows zero speeds in the NNE, SSW, and WSW sectors of the figure. These do not mean that vehicles were not moving, rather they reflect that that no traffic moved out of the EPZ on routes within these sectors. Conversely, the high speeds in the southeasterly and northwesterly quadrants of the figure suggest that there was little-to-no congestion, and traffic was effectively moving at free-flow speeds through these regions of the EPZ.

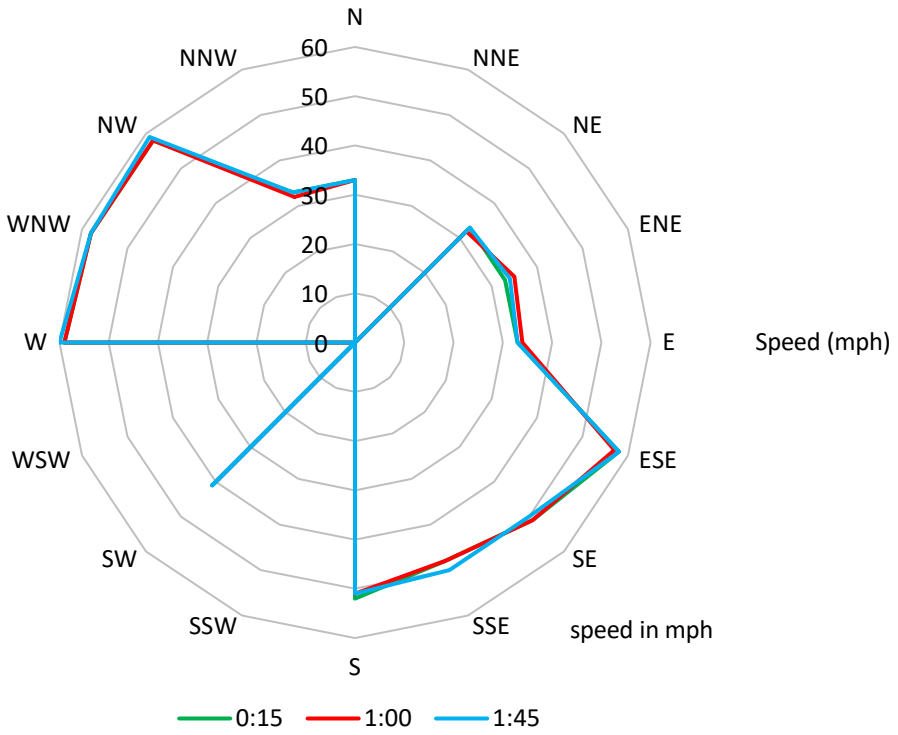

Figure 3-9 EPZ Average Exit Speeds (mph) for the Small Population Site Base Model at Various Times in the Evacuation

Figure 3-10 shows much greater speed variation during the evacuation for the medium population site. The curves of this figure illustrate decreases in speed within several of the sectors. However, not every sector saw a decrease in speed and some sectors experienced a decrease in speed early in the evacuation but then recovered. This suggests the population density within the medium population site was not uniformly distributed, as is the case. The

speed data also suggest that some sectors, predominately those exiting further downstream to the south and southeast, were impacted greatly by the evacuation. This was expected because these sectors have the highest population density. Sectors in the north and northwest have about half the population density as in the southeast. The decrease in travel speeds and eventual recovery in the north-northwest and east sectors suggests the formation of congestion in those areas during the middle periods of the evacuation and then a gradual recovery to free-flow speeds in the later stages of the clearance process. These data suggest the network was able to eventually recover, and as expected, conditions would converge to free-flow toward the end of the evacuation.

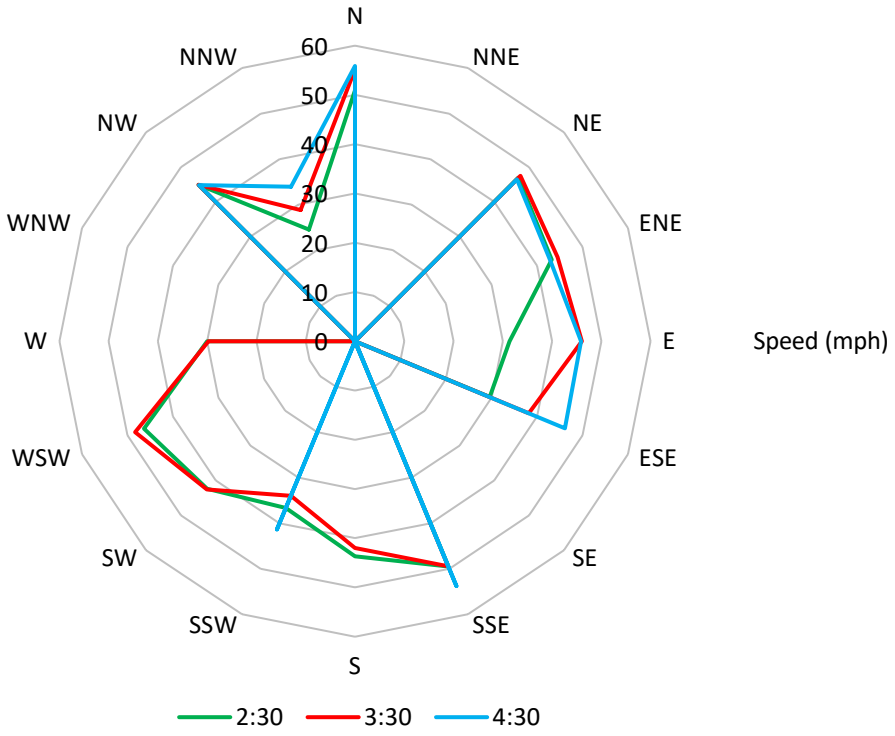

Figure 3-10 EPZ Average Exit Speeds (mph) for the Medium Population Site Base Model at Various Times in the Evacuation

Figure 3-11 shows the EPZ average exit speed data for the large population site. Similar to the medium population site, this figure shows a diversity of travel speeds at various times during the evacuation. However, speed decreases in this model were not as severe as they were in the medium population model and speeds were typically able to recover by the end of the simulation. This suggests that the large population site was better able to cope with evacuation traffic when compared to the medium population site. This was likely because the large population site had a higher concentration of roads to accommodate the evacuating vehicles. The road network in the large population site was not restricted with as many bodies of water and had more available exit routes to accommodate traffic. While the large population did cause significant congestion, the abundance of exit routes made this site more resilient and better able to cope with the added stress of the evacuating vehicles.

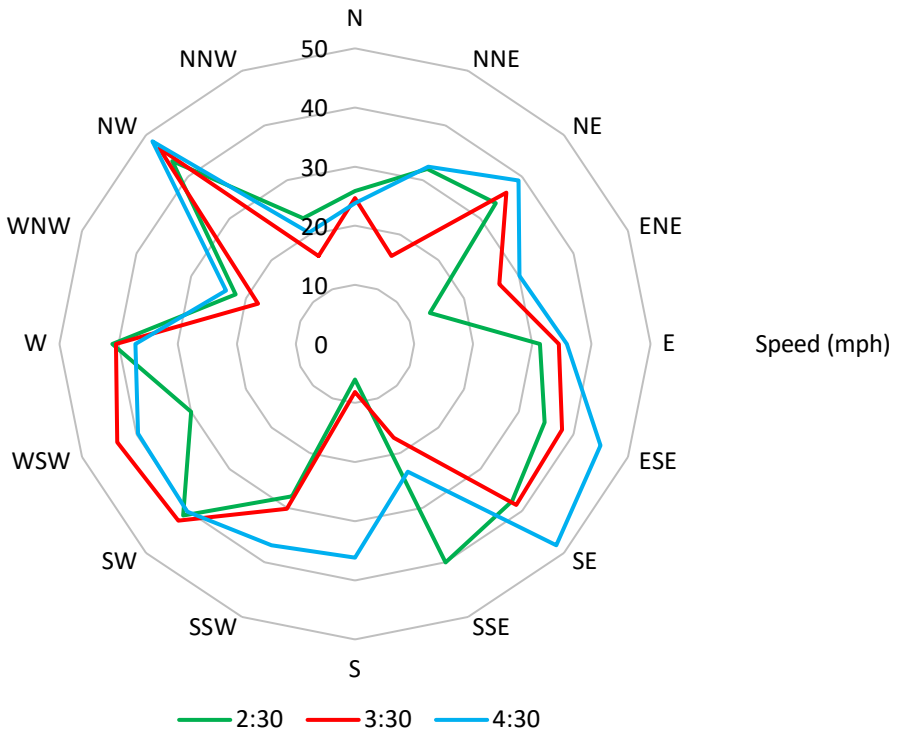

Figure 3-11 EPZ Average Exit Speeds (mph) for the Large Population Site Base Model at Various Times in the Evacuation

3.8.4.2.1 High Travel Speed Issue

Although the speeds at some locations in the models appear to be high, such conditions are not unreasonable within traffic simulations. These higher speeds are likely the result of certain coding decisions made in the models that were necessary tradeoffs between model detail and effort. Although traffic simulation models are designed to produce realistic results, there are many simplifications that are introduced during the model development process that require adjustments to maintain reasonable representations of physical systems and driver behaviors. Following a practical and commonly utilized approach, the simulation models developed as part of this project were constructed using the concept of desired speed and a simplification of lengthy segments of roadway link by nodes connecting to successive links at intersections.

3.8.4.2.2 Effect of Desired Speed Settings

Because of the rural nature of the small population site model, most desired speeds on routes within the EPZ were coded between 55 and 60 mph. In traffic simulation models, desired speeds are often set at 5 mph to 10 mph above posted speeds using rule of thumb estimates [43]. However, as explained previously in Section 3.6.3, to reflect recognized real-world driver behavior, desired speeds were set with a range of 10 mph above and below the posted speed on routes with posted speeds of 45 mph and higher.

The distribution of speeds above posted speed limits is thought to be likely in rural, small population sites. The effect of the high speeds on the ETE is that evacuees travel faster as they evacuate. This results in ETE and clearance times that are shorter than they would be if speeds were constrained to lower values; however, this difference is on the order of a few minutes or

less in the small population site. For the medium and large population site models, and in general, intersection performance is the primary contributor to longer travel times in traffic networks. It is expected that using higher desired speeds minimally changes the travel times.

3.8.4.2.3 Effect of Simplified Link Representation

The occurrence of higher than expected speeds could be related to certain roadway representations within the models. One of these conditions was loading large vehicle volumes at single points of origin. With respect to speeds in the small population site, rural roadways within the representative network were reviewed using various online data sources and it was found that driveways, curves, and minor street crossings were frequently present on evacuation routes throughout the analysis area. To maintain a practical coding effort, however, not all these detailed features were coded into the model. Rather, the model was limited to arterial roadways and significant geometric features. It is recognized that this decision limited the model to higher speed roadways and tended to eliminate segments of reduced speed limits. It also largely eliminated the influence of vehicles entering routes in the network from driveways, access points, and obstructions as would slow the movement of evacuating vehicles in the network in real life. An unintended effect was the creation of more segments with unobstructed traffic flow than would exist if the minor streets were included. This issue is common, and Volume II of the FHWA toolbox [19] describes this specific issue as a model limitation, explaining that models cannot address the impact of numerous minor driveways along a link. The issue was exacerbated in the small site model due to the infrequent number of loading origins.

The insight from this analysis is that roadway characteristics and evacuation characteristics are a key consideration in establishing the speed ranges for evacuation traffic models [40] [43]. Each of the hundreds (sometimes thousands) of vehicles that were loaded into the models developed for this research did so at a single origin point. In a real system, it would be expected that they would enter the network via residential driveways eventually connected to rural highways, likely impeding flow on connecting roads along the way. However, it is impractical to represent every driveway and other obstruction in models of significant size. To compensate, it is important that origin nodes be sized and spaced appropriately.

3.8.4.2.4 Effect of Dynamic Traffic Assignment

Another potential contributor to elevated speeds was the use of DTA. Since DTA facilitates the distribution of vehicles on the most beneficial routes to the destination points, major roadways within the EPZs were used as evacuation routes. Current ETE guidance provides that the average speed for each major evacuation route be included in the ETE study. Other methods of displaying outputs, such as graphics that illustrate LOS or speed at selected times within the evacuation, were identified in the associated review of ETE studies. These methods were found to achieve the same objective of providing an understanding of evacuation route performance.

3.8.4.3 Base Model Vehicle Volumes

Vehicles were generated using three different sets of vehicle classifications including:

- evacuee vehicles
- background vehicles (including pass-through traffic in medium and large population model)
- shadow evacuee vehicles

A fourth category, total vehicles, was generated using the summation of all vehicles in the network. In addition to determining the clearance time based on the "last vehicle" exiting the EPZ, the volumes were captured from vehicles passing over the data collectors. This allowed tracking of model input volumes and output volumes and provided a basis for assessing the dispersion and destination of vehicles within the analysis areas.

Table 3-15 summarizes the number of vehicles generated within and exiting the EPZ, and the shadow vehicles generated and moving through the shadow evacuation areas. The values in the table represent averaged values from the ten runs conducted for each site.

Table 3-15 Summary of EPZ and Shadow Evacuation Vehicle Inputs and Exits

Model	EPZ Evacuee Vehicles Input / Exit	Shadow Evacuee Vehicles[1] Input / Exit
Small	3,750 / 3,747	1,500 / 1450
Medium	100,000 / 98,894	15,000 / 14,955
Large	162,500 / 160,836	30,000 / 29,866

[1] Shadow output is measured at the 20 mile data collectors.

The table shows that a few vehicles that were generated failed to exit the EPZ. These vehicles were "lost" in the analysis. This is a feature of many micro scale models and can occur for reasons ranging from vehicles unable to move for an extended amount of time to unrealistic routing. In VISSIM, the system allows vehicles to disappear or be removed from the analysis when certain conditions occur that prevent a vehicle from executing a desired function. Because this was generally a small number of vehicles within the overall traffic process, there was no effort to identify the cause of the lost vehicles. During model development, the number of lost vehicles was used to help calibrate the DTA and to check performance of the model geometry. Within the base models for this research the percentage of "lost" vehicles was maintained under four percent.

3.8.4.4 Base Model Additional Metrics

Table 3-16 provides a summary of other selected metrics for the three sites. These metrics are commonly used in traffic engineering analyses to assess various performance aspects of traffic processes and road facilities. In this research these metrics were collected for a more detailed understanding of the performance of the small, medium, and large population site networks and to aid in the debugging through identification of non-standard performance. The numbers in the table below represent averages within the entire 20-mile study area.

Table 3-16 Model Output Summary Metrics

Metrics	All Vehicles	Background Traffic Vehicles	EPZ Evacuee Vehicles	Shadow Vehicles
Small Population Site 20-Mile Metrics				
Average delay (minutes)	2	1	6	2
Total delay (hours)	507	116	348	44
Average number of stops	25	4	68	20
Average speed (mph)	44	47	43	44
Vehicle hours traveled (VHT)	3860	1410	1989	461
Vehicle miles traveled (VMT)	171,510	66,357	84,880	20,273
Active vehicles	3	0	3	0
Medium Population Site 20-Mile Metrics				
Average delay (minutes)	46	13	70	21
Total delay (hours)	131,723	12,444	114,146	5,133
Average number of stops	86	27	129	37
Average speed (mph)	16	29	13	22
Vehicle hours traveled (VHT)	194,639	94,314	89,720	64,944
Vehicle miles traveled (VMT)	3,069,490	915,733	1,932,023	221,734
Active vehicles	0	0	0	0
Large Population Site 20-Mile Metrics				
Average delay (minutes)	32	8	62	13
Total delay (hours)	198,111	24,865	166,685	6,561
Average number of stops	285	68	561	95
Average speed (mph)	19	31	15	27
Vehicle hours traveled (VHT)	339,597	77,979	245,445	16,173
Vehicle miles traveled (VMT)	6,418,796	2,406,175	3,576,547	436,075
Active vehicles	694	5	689	0

Travel distance was investigated to gain an understanding of the vehicle routing out of the EPZ. The average distance evacuees travelled to exit the 20-mile collector for the small, medium, and large population site models was 22.6 miles, 19.9 miles, and 22.7 miles, respectively. These average distances are reasonable because evacuation routes would rarely be direct. Most evacuees would need to make multiple turns and follow routes that are not oriented directly away from the NPP.

During the model development and testing, excessive travel distances were observed for many vehicles. Investigation revealed that some vehicles were circulating within the EPZ. This issue could have been caused in many ways. The most likely was the routing calculated by the DTA algorithm, which does not always behave as an evacuating driver with knowledge of the roadway network. To limit circuitous routing, a “three destination path” approach was implemented.

The vehicle type for background traffic was used for background vehicles generated within the EPZ, background vehicles generated outside the EPZ, and pass through traffic. Because background vehicles generated outside the EPZ are more numerous and travel routes typically shorter, the average travel distance for background traffic was lower compared to EPZ evacuees. Furthermore, because the small population site model does not incorporate pass-through traffic, which typically traverse some portion of the diameter of the model, travel distances for background traffic in the small population site were the shortest.

The travel time for background traffic in the small population site was also considerably less than the other vehicle groups due to the shorter distances traveled on average. Results from the large population site also showed shorter travel times for background traffic than for evacuee traffic, but slightly longer than the shadow population. Given that a significant percentage of the background traffic was generated within the EPZ, this was consistent with expectations since travel time for the shadow would be expected to be less than that of the background traffic.

4 TASK 1 SHADOW EVACUATION ANALYSIS

The goal of this task was to enhance understanding of the effect shadow evacuation traffic has on NPP ETEs. This work is of interest because shadow evacuations have the potential to create congestion that may extend into the EPZ and increase the ETE for evacuees exiting the EPZ.

NRC regulatory guidance recognizes this potential impact and requires ETE studies to include a shadow evacuation of 20 percent of the population out to 15 miles from the NPP. The 20 percent participation rate is based, in part, upon a telephone survey of EPZ populations [8] that indicated about 20 percent of the population might evacuate if others are under an evacuation order even if they are not. Fifteen miles was selected as a reasonable analysis distance. Additionally, NRC/FEMA guidance [54] provides information for use by government agencies to effectively communicate protective action direction in order to reduce shadow evacuation.

While a 20 percent shadow evacuation is a useful assumption for planning purposes, it is not possible to know the exact size of a shadow evacuation for any given event. The NRC staff saw benefit in an analytical study of shadow evacuation size and impact on ETEs to inform regulatory guidance. The focus of this task will be to examine the congestive conditions of incrementally increasing rates of shadow participation and their potential, if any, to increase evacuation time.

To quantify potential impacts of shadow evacuation on the evacuation of NPP EPZs, Task 1 sought to address the following:

- Determining the sensitivity of ETEs to shadow evacuation participation rate.
- Determining site characteristics that exacerbate the effect of shadow evacuation.
- Comparing the current 20 percent shadow evacuation guidance in NUREG/CR-7002 to study results.

The objectives of this task included determining the size of the shadow that would be necessary to increase evacuation times significantly. For the purpose of this study this is defined as an ETE increase of 30 minutes.

4.1 Background

A shadow evacuation occurs when residents evacuate from areas beyond the officially designated evacuation area [4] [6] [11]. Shadow evacuees tend to mobilize and evacuate after they monitor the progression of the emergency and when they observe evacuees traveling through the area. There are no sirens within the shadow area outside the EPZ, thus awareness propagates by way of news broadcasts, social interaction, and social media. Based on the perceived threat, residents make individual decisions of whether to evacuate. Typically, when residents decide to evacuate, they need to have received and understood the warning before they act [31] [52].

Zeigler et al., originally defined the shadow evacuation in 1981 as the tendency of an official evacuation advisory to cause departure from a much larger area than intended [11]. The authors observed this phenomenon in response to the accident at Three Mile Island (TMI). Shadow evacuations have since been observed in many large-scale evacuations but have generally not affected the efficiency of these evacuations [6]. However, under certain conditions, such as a large number of shadow evacuees in areas with limited roadway capacity, the

shadow has the potential to impact evacuees from a declared evacuation area. Limited roadway capacity does not necessarily suggest fewer streets. It could be caused by EPZ evacuee vehicles traveling through the area using the available capacity. Such an impact could result in longer travel times for evacuees.

At the time of the TMI accident, minimal emergency planning existed around NPPs and coordination among OROs and decision makers was not well defined. Since TMI, the NRC and FEMA have developed detailed and extensive emergency planning regulations and guidelines which have now been in place and implemented for more than 35 years [5]. The regulations and guidance have resulted in robust emergency planning and infrastructure for NPPs. The emergency preparedness regimen includes detailed onsite and offsite communication protocols, siren systems with secondary and backup alert systems, prepared EAS messages, and many more response elements regulated by the NRC. Guidance on implementation of these regulations is provided in NUREG-0654/FEMA-REP-1, Rev. 1 [5], the FEMA Program Manual for Radiological Emergency Preparedness [53], and other documents. The NPP offsite emergency response plans are demonstrated biennially in full-scale exercises that are documented in FEMA After Action Reports.

Federal regulation requires that provisions exist for prompt communications to emergency personnel and the public. Supplement 3 to NUREG-0654/FEMA-REP-1, Rev. 1 identifies that an informed population contributes to reducing evacuation times by potentially reducing the size of the shadow evacuation [54]. Hurricane research identified that a low percentage of shadow evacuees in response to Hurricane Ike was attributed to effective evacuation warnings from authorities [44]. Additionally, NRC has conducted research regarding the understanding and response expectations of the general public residing within the EPZ and found that the public largely understands what to do in an NPP emergency [8]. Through this research and the study of evacuations [6] [7], a shadow evacuation estimate of 20 percent of residents in the 5-mile area beyond the EPZ was identified for use in the ETE analysis [4]. The guidance in NUREG/CR-7002 identifies that people within the shadow region, but closer to the hazard area are more likely to shadow evacuate than people farther from the hazard area [4]. In March 2013, the Government Accountability Office (GAO) recommended the NRC improve their understanding of the effect of shadow evacuation [55].

Research has found that shadow evacuations typically do not impact the efficiency of the evacuation from the hazard area [6]. Furthermore, if a shadow evacuation occurs and the original evacuation area ultimately needs to be expanded, a percentage of people from the expanded area will have already left as shadow evacuees. During emergency response planning, the potential impact to evacuees from the declared evacuation area can be estimated by including the shadow evacuation contribution in the ETE analysis. The parametric analysis conducted herein provides observations and insights on potential impacts on the ETE for the small, medium, and large population EPZs.

4.1.1 Shadow Evacuation Literature Review

The over response to evacuation orders for Hurricane Rita in 2005 has often been described as a large shadow evacuation that caused so much congestion that many residents returned home rather than continue their evacuation. Many studies have described the over response as a shadow evacuation, causing undue concern with regard to the effects of a shadow evacuation. However, the evacuation orders for the hurricane were actually thought to be the cause, combined with the recent devastation from Hurricane Katrina just weeks prior. This was not an issue of people evacuating because they were near a hazard and believed they were at risk,

these residents evacuated because they believed they were within the hazard area, as described by the OROs [60]. Hurricane Ike was the next major hurricane following Rita, and the improved offsite response messaging was attributed to decreasing the shadow evacuation [44].

In discussions with emergency response personnel during research on evacuations, they often explain that shadow evacuations are observed, but attempts are not made to quantify the shadow because the focus is on the residents in the declared evacuation zone. Researchers have attempted to quantify the shadow, but the results are difficult to interpret because published reports do not always adhere to the specific criteria of the shadow definition [15] [56] [57]. In other instances, research was found to cite the Zeigler definition precisely or otherwise define the shadow appropriately [6] [7] [31] [59] [61]. Although the shadow evacuation was defined quite explicitly from the very beginning [11], even Zeigler and Johnson [58] interchanged spontaneous evacuation and shadow evacuation terms, and this may have contributed to the misuse of the term.

Shadow evacuations are somewhat spontaneous because residents leave without having been ordered to do so, but the definition of spontaneous evacuation is more appropriately applied to residents who leave before the official evacuation advisory or order is issued, such as those who observe or receive direct information on the hazard and respond prior to any issuance of a protective action order. Thus, it has a temporal component that the generally accepted definition of shadow evacuation does not. In post-evacuation research of the 2005 Graniteville train accident, which had a declared evacuation area of a one-mile radius, Mitchell, et al., [56] determined that 59 percent of the residents from one to two miles had evacuated as a shadow. However, the study also noted that more than half of these residents were specifically instructed to evacuate, mostly from Reverse 911 or fire/police officials knocking on their door. Anyone that was directed to evacuate should not have been included in the shadow contribution because this was not due to the tendency of the advisory to cause evacuation, it was a direct order from OROs.

Weinisch and Bruekner [62] reviewed 48 ETE studies to determine impacts from shadow evacuations. Each of the ETE studies reviewed included a sensitivity analysis that increased the size of the shadow from 20 percent to 60 percent of the public residing in the 5-mile area beyond the EPZ. Of the 48 ETEs reviewed, only 7 showed an increase of 30 minutes or more for the 100th percentile ETE, and more than 70 percent of the sites showed little to no change in the ETE [62]. Based on their study, a shadow evacuation that begins coincident with the EPZ evacuation has little impact on the ETE [62]. A more detailed literature review of evacuations, ETEs, and shadow evacuations are provided in Appendix A.

4.1.2 Shadow Evacuation Assumptions

As described in Section 3.1 of this report, many assumptions were made in the development of the three base models for this research. Several additional assumptions related to this task were also made:

- Consistent with current guidance [4], a 20 percent shadow contribution was used for the base models.
- The shadow contribution was assumed to be a fixed rate throughout the 5-mile area beyond the EPZ, also consistent with current guidance [4].
- The start of the shadow evacuation is coincident with the EPZ evacuation, consistent with current guidance [4].

- A maximum shadow contribution of 40 percent of the public within the shadow region is available to evacuate as a shadow for the medium and large population sites.

4.1.3 Shadow Evacuation Contribution

The shadow evacuation is defined as "the tendency of an official evacuation advisory to cause departure from a much larger area than intended," [11]. As simple as this may sound, there is an implied detail in the definition. First, the shadow occurs from areas beyond the declared evacuation area. This implies that there must be an officially declared evacuation area. Secondly, an advisory[2] must have been issued to define the officially declared area.

Given the difficulties in accurately quantifying the shadow [15] [56] [57], bounding the shadow provides a means of estimating potential impacts. The assumption for many NRC consequence analyses is a winter, weekday, and daytime evacuation [34]. On a typical winter weekday, in the shadow evacuation area, people are working, children are at school, and government, commercial, and retail establishments are open for business. Most residents engaged in these activities would not be available to participate as a shadow. Schools and government facilities would not evacuate, unless they were ordered to do so; thus, they cannot, be a contributor to the shadow evacuation. A small percent of parents may choose to leave work and remove their children from school, but this would be done at the individual decision level, not as an organized response. These population groups may be quantified using the U.S. Census Bureau data on schoolchildren, preschool through college, which shows that nationally, 25.6 percent of the U.S. population attends school.

A national GALLUP poll found that 17 percent of residents say they work for the local, state, or federal government [63]. Residents who need assistance to evacuate would also not be included in a shadow. Organizing wheelchair vans, ambulances, and other specialized equipment to evacuate these residents would only occur when an evacuation order has been declared for an area. In a national survey of residents of EPZs [8], 8 percent of respondents identified as not being able to evacuate without help from outside the home. A range of 6 to 10 percent of residents, who would require assistance, has also been identified in hurricane related research [31]. The total of just these categories represents 51 percent of the public, using the 8 percent transit-dependent value. In addition, residents of nursing homes, hospitals, and prisons would only be evacuated when ordered to do so in a declared and organized manner.

Furthermore, throughout an NPP emergency, state and local officials would continuously update the public. Supplement 3 to NUREG-0654 provides guidance that OROs inform areas beyond the EPZ that they are not under official orders to evacuate [54] in part, to reduce the potential shadow evacuation. Although it is possible that some small businesses may choose to close and allow employees to leave, large businesses are not expected to close in areas where no evacuation order has been declared. To the contrary, commercial and service industries outside of designated evacuation areas are often observed to stay open and provide for the needs of the evacuating public.

Based on all of these studies and statistics, it was regarded as reasonable to assume that at least 60 percent of the public is not readily able to participate in a shadow evacuation for any defined scenario. A review of prior ETE studies also shows this percentage is a valid assumption. Through site-specific survey results it was found that, on average, 18 percent of the

[2] The initial evacuation advisory, also called the evacuation order, is typically the EAS message that informs residents of specific protective actions. This would be broadcast after sirens are sounded within an EPZ.

non-evacuating population may decide to evacuate if advised to take shelter at home. The majority (80 percent) of survey responses were less than 20 percent. Only 2 survey results were higher than 30 percent, with the maximum being 40 percent. Thus, based on practical considerations and survey data, a maximum contribution of 40 percent of the shadow evacuation area population was established for use in this project for the medium and large sites.

The timing of the response of the shadow evacuation is another consideration. As the number of vehicles on the roadway increase, the capacity may be exceeded, causing congestion. Because the shadow receives information on the emergency indirectly (e.g., EAS messages are not directed to this population group), they would generally be expected to mobilize after EPZ evacuees. This would put shadow evacuees on the roadways at the same time as the EPZ evacuees are passing through the shadow area.

4.1.4 Analysis of Shadow Participation

Following the guidance in NUREG/CR-7002 [4] the base model was set up with an assumed shadow contribution of 20 percent of the public in the area from 10 to 15 miles from the NPP. This was in addition to the background traffic in this region. The base model response curves are described in Section 3 and were established with the shadow evacuee response consistent with the general public response from the EPZ [4]. The shadow evacuation populations implemented in the base models included:

- Small population site: 3,000 shadow evacuees; 1,500 vehicles
- Medium population site: 30,000 shadow evacuees; 15,000 vehicles
- Large population site: 60,000 shadow evacuees; 30,000 vehicles

The criteria in Appendix E to 10 CFR Part 50 and NUREG/CR-7002, which identify a 25 percent increase in the ETE or 30 minutes, were used to determine whether the ETE was impacted significantly. To determine the size of the evacuation that would be necessary to increase ETEs significantly, comparisons were made to the base values for the 10-mile ETEs. All parameters and input values to the base models were held constant and only the shadow population was adjusted. The 90 and 100 percent ETEs were tabulated for each quadrant of the small, medium, and large population sites. The largest ETE value was selected from each quadrant for comparison to the ETE from the same collector point in the base model results. Shadow analysis data was collected at 2, 5, and 10-mile radial distances from the NPP site.

4.2 Shadow Participation Rate Analysis

The guiding principle of this task, and all the tasks in this research, was to inform NRC understanding of evacuation processes. This task sought to determine if a 20 percent shadow evacuation participation rate is a reasonable assumption for ETEs and more broadly the effect shadow evacuations have on ETEs.

4.2.1 Analysis Scenarios

The shadow participation rate was varied at increments of 0 percent, 20 percent, 30 percent and 40 percent. The small population model used a 100 percent participation rate rather than 30 and 40 percent simulation runs because the shadow is likely to have minimal effect on the ETE. A 100 percent participation rate is included for research purposes only. A 20 percent participation

rate is included in the base case simulation runs for each model as described in Section 3. These simulations resulted in a total of 11 data sets which are summarized in Table 4-1.

Table 4-1 Scenarios for Shadow Analysis

Population Site Model	Shadow Participation Rate
Small	0
	20[1]
	100
Medium	0
	20
	30
	40
Large	0
	20
	30
	40

[1] 20 percent shadow participation scenario is recommended in NRC guidance and served as the base case.

4.2.2 Data Collection and Measures of Effectiveness

Task 1 analyses included four simulation runs for the large and medium population sites and 10 for the small population site and the average value of these runs was taken as the performance metric. These average values account for VISSIM model stochastic variations. They also help to lessen the likelihood of data interpretation being made on a single run that could have potentially produced an "outlier" result.

The MOEs that served as the bases of comparison for Task 1 were the 90 and 100 percent evacuation time, average travel speed, and outflow volume on all links exiting the EPZ. All data were collected in increments of 5 minutes at the 2, 5, 10, 15, and 20-mile rings. Evacuation time and average travel speed results were also assessed by compass sector quadrant (i.e., North, East, South, and West). Quadrant analysis was thought to reveal site characteristics that exacerbate shadow evacuation effects. A presentation of the quantitative results and an associated discussion of notable aspects of these results for the three models are included in the sections that follow.

4.2.3 Shadow Participation Rate Results

This section discusses results of varying shadow population participation rates on evacuation time. The ETE for each model (small, medium, and large) was calculated for the 2, 5, 10-miles rings. Additionally, the sector evacuation time (North, South, East, West) was also calculated for the varying shadow participation.

4.2.3.1 Small Population Site Model Evacuation Time Results

Shadow evacuation had minimal effect on ETE for the small population site. Previous ETE studies performed sensitivity analyses of shadow evacuation at small population sites and also did not identify significant impact. As discussed earlier, a reasonable maximum contribution for

the shadow evacuation is 40 percent of the residents in the shadow area. However, analysis of 100 percent participation rate demonstrated that there was no impact on the ETE.

Table 4-2 Average ETEs, Small Population Site Shadow Analysis

Shadow Participation Rates	2-Mile		5-Mile		10-Mile	
	90% ETE	100% ETE	90% ETE	100% ETE	90% ETE	100% ETE
0%	1:35	2:18	1:35	2:21	1:44	2:31
20%	1:35	2:18	1:35	2:21	1:44	2:31
100%	1:35	2:18	1:35	2:21	1:44	2:31

Figure 4-1 shows the cumulative percent evacuated for the small population site at the 10-mile EPZ boundary. This figure is a visual representation of the evacuation process that led to the 90 percent and 100 percent ETE times shown in Table 4-2. The figure also displays the evacuee loading curve for reference. In the figure, the 10-mile ETEs for 0 percent, 20 percent, and 100 percent shadow population particpation rate are indistinguishable, demonstrating the particpation rate of the shadow evacuation had minimal effect on ETE.

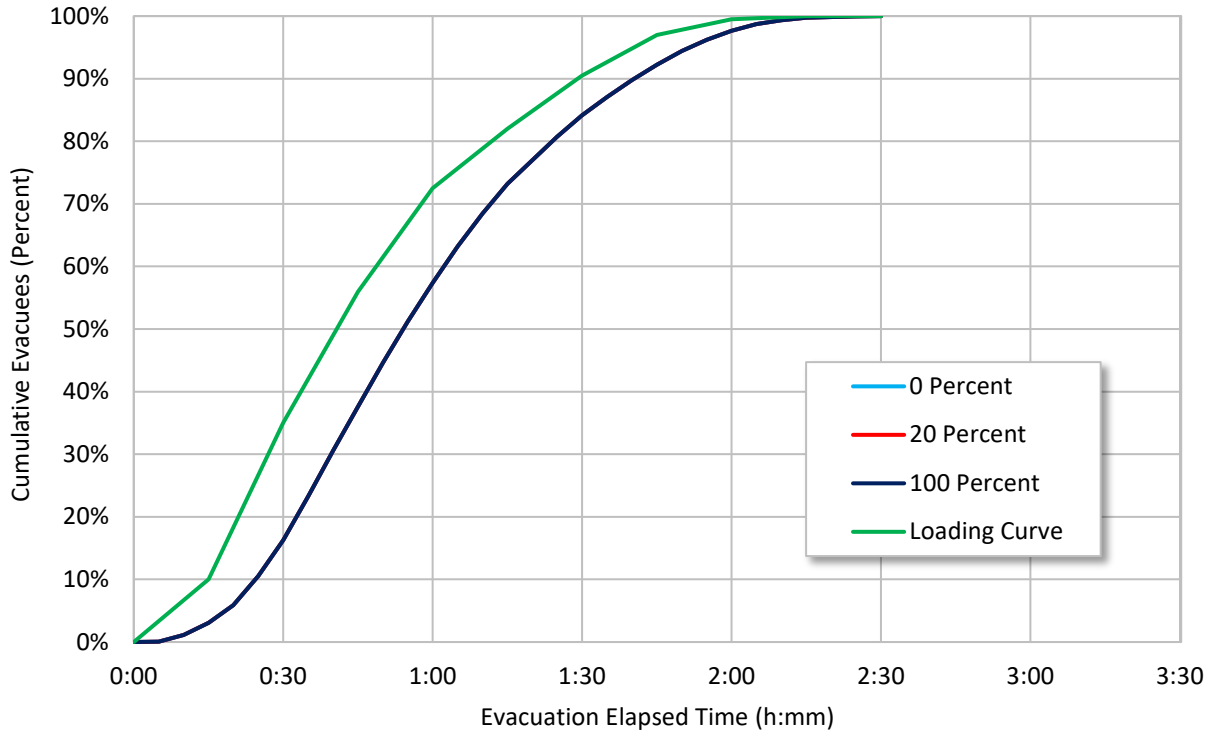

Figure 4-1 Ten Mile ETE Curves, Small Population Site Shadow Analysis

Table 4-3 identifies the evacuation times by quadrant for the small population site EPZ and increasing shadow participation rate. No discernable difference in ETEs is seen. This finding suggests that shadow evacuation analyses for small population sites do not provide important information for protective action strategy development or evacuation planning.

Table 4-3 Ten Mile ETEs by Quadrant, Small Population Site Shadow Analysis

Quadrant	0% Shadow Participation		20% Shadow Participation		100% Shadow Participation ETE	
	90% ETE	100% ETE	90% ETE	100% ETE	90% ETE	100% ETE
North	1:39	2:09	1:39	2:09	1:39	2:09
East	1:43	2:21	1:43	2:21	1:43	2:21
South	1:44	2:30	1:44	2:30	1:44	2:30
West	1:44	2:29	1:44	2:29	1:44	2:29

4.2.3.2 Medium Population Site Model Evacuation and Clearance Time Results

Due to the high demand and low availability of roads, the medium population site might be expected to show a significant impact from an increased shadow evacuation participation rate. However, with the exception of one sector, this was generally not the case. Table 4-4 shows the 90 percent and 100 percent ETEs for the 2, 5, and 10-mile rings and Table 4-5 shows the results by quadrant. It was expected that the 0 percent shadow participation rate would consistently result in the lowest ETEs, followed by 20 percent, 30 percent and 40 percent runs. Table 4-4 shows slight variations in ETE times that contradict this notion. This suggests that the variability in the simulation model runs, compounded by the high level of congestion and competing effects of the DTA, likely impacted the VISSIM calculations. For example, the 0 percent shadow participation rate, 5-mile 100 percent ETE was 24 minutes longer than the ETE corresponding to 40 percent shadow participation. This was likely caused by the stochastic nature of VISSIM, particularly the variability in route choice by the DTA and the variability in clearing the last few vehicles that determine the 100 percent ETE.

When comparing the 90 percent ETEs, the results are more consistent and within a 5-minute margin of error. This same phenomenon was also seen in the large population site. Table 4-4 shows results that consistently suggest the 10-mile 90 percent and 100 percent ETE were similar regardless of the shadow participation rate. The ETE resulting from 0 percent shadow participation and 40 percent participation rates differed by 22 minutes. Thus, while there is some impact by the shadow evacuation, it is not significant. The 20 percent participation resulted in a 100 percent ETE that was only 4 minutes higher than the 100 percent ETE for the 40 percent shadow participation scenario and is likely due to a combination of VISSIM stochasticity and DTA. This result shows that shadow evacuation participation rate is not a dominant factor in determining evacuation times even for capacity constrained sites.

Table 4-4 Average ETEs, Medium Population Site Shadow Analysis

Shadow Participation Rates	2-Mile		5-Mile		10-Mile	
	90% ETE	100% ETE	90% ETE	100% ETE	90% ETE	100% ETE
0%	2:40	4:03	2:48	5:26	4:56	7:10
20%	2:40	4:03	2:47	5:17	5:00	7:36
30%	2:40	4:03	2:43	5:10	5:11	7:21
40%	2:40	4:03	2:43	5:02	5:13	7:32

Figure 4-2 displays the cumulative percent evacuated from the medium population site at the 10-mile EPZ boundary. The figure illustrates the clustered nature of the ETEs that resulted from varying shadow participation rates. In a non-congested network, as seen in the small population site (Figure 4-1), the shape of the cumulative percent evacuated curve closely matches the shape of the loading curve. Without congestion, these two curves are only separated by the free-flow travel time between the origins and destinations. When congestion is present, the shape of the cumulative percent evacuated curve tends toward linear, as vehicles queue near the EPZ exit and leave the network at a uniform rate. The cumulative percent evacuated curve for the medium population site clearly shows the impact of congestion at all levels of shadow evacuee participation, including a zero percent participation rate.

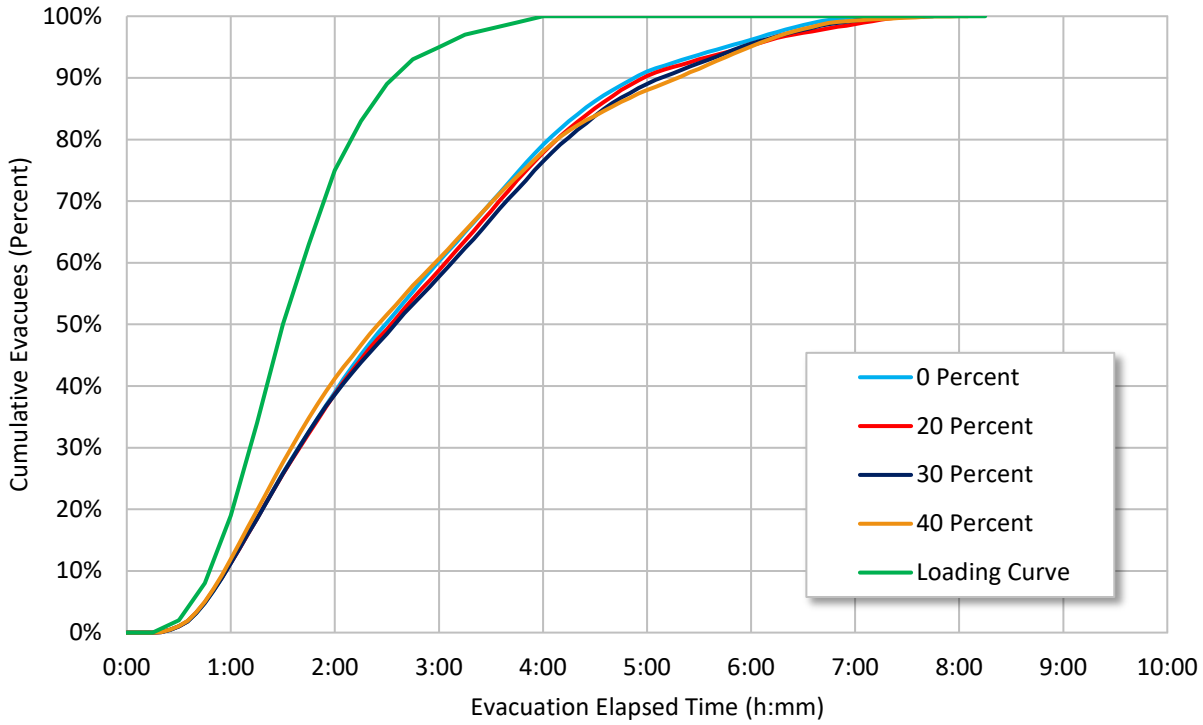

Figure 4-2 Ten Mile ETE Curves, Medium Population Site Analysis

Table 4-5 shows evacuation time estimates by quadrant for the medium population site. The South quadrant was the least congested and resembles free-flow conditions. In the medium population site model, evacuees primarily exit the 20-mile ring along routes in the North-Northwest and South-Southeast sectors. The impact of the shadow population along these routes is reflected in the population density and network capacity in these sectors. The shadow population in the Northwest is diffusely distributed. Thus, while a 20 percent shadow has a significant impact on the 100 percent ETE in the North quadrant due to the added volume of vehicles, further increases in the participation rate do not exacerbate the effect of the already congested network. In the South-Southeast sector, evacuation routes pass through a more densely populated shadow region. Because the network capacity is greater in this sector (reflective of the population density) a significant impact of the shadow is not observed in the East quadrant until the shadow participation rate reaches 40 percent. In fact, the network was able to adjust to the 20 percent shadow participation with no noticeable impact on the ETE (compared to 0 percent shadow). The largest difference between the 20 percent and 40 percent participation rate evacuation times was 43 minutes and occurred in the East quadrant. This suggests that population density along evacuation routes in the shadow region can exacerbate

the impact of the shadow evacuation. However, it should be noted that the overall evacuation time in the East quadrant was significantly less than the time to evacuate along the North quadrant. This again demonstrates that while the shadow evacuation may have an impact, it is not the dominant factor controlling the ETE.

Table 4-5 Ten Mile ETEs by Quadrant, Medium Population Site Analysis

Quadrant	0% Shadow Participation		20% Shadow Participation		30% Shadow Participation		40% Shadow Participation	
	90% ETE	100% ETE	90% ETE	100% ETE	90% ETE	100% ETE	90% ETE	100% ETE
North	5:37	7:06	6:02	7:36	5:50	7:21	5:40	7:32
East	4:02	5:31	4:03	5:20	4:21	5:53	4:46	6:03
South	2:46	4:22	2:46	4:22	2:46	4:22	2:46	4:22
West	5:48	6:41	5:40	6:26	5:55	6:50	5:51	6:41

4.2.3.3 Large Population Site Model Evacuation and Clearance Time Results

Table 4-6 shows the large population site 90 percent and 100 percent ETEs for 0, 20, 30, and 40 percent shadow participation rates. The 100 percent 10-mile ETE varied by less than 30 minutes between the 0 and 40 percent participation rate. The 100 percent ETE was relatively insensitive to the shadow participation rate. This is likely because congestion in the network begins to clear during the start of the evacuation tail. However, the 90 percent ETE shows more sensitivity to the shadow evacuation. Comparing the 20 percent and 40 percent participation rates, the 90 percent ETE varied by 41 minutes, nearly a 15 percent increase in ETE. This may appear to be significant, but the incremental change of 90 percent ETEs between shadow participation rates was not significant. This suggests that an assumed participation rate anywhere within the range of 0 to just above 30 percent would likely not impact the ETEs. When the shadow participation rate increases beyond 30 percent, evacuees may begin to see longer delays. However, an ETE corresponding to 40 percent shadow participation may disproportionately impact the analysis. Additionally, the difference in 100 percent ETEs is compounded by the stochasticity of VISSIM and should not necessarily be attributed to the impact of a shadow evacuation.

Table 4-6 Average ETEs, Large Population Site Shadow Analysis

Shadow Participation Rates	2-Mile		5-Mile		10-Mile	
	90% ETE	100% ETE	90% ETE	100% ETE	90% ETE	100% ETE
0%	3:40	5:05	3:58	6:52	4:32	9:02
20%	3:38	5:05	4:01	7:07	4:40	9:00
30%	3:41	5:05	4:08	6:55	4:56	9:05
40%	3:42	5:18	4:12	6:58	5:21	9:28

Figure 4-3 shows the cumulative percent evacuated at the 10-mile ring for the large population site. A comparison with the loading curve suggests the evacuees experienced moderate to severe congestion. The figure also illustrates the 100 percent ETEs tended to converge in the tail of the evacuation. While little impact was ultimately made by the shadow participation rate on the 10-mile 100 percent ETE, this figure illustrates the impact of the shadow on the 90

percent ETE. A key insight in this analysis is that 50 and perhaps up to 60 percent of the evacuees were able to exit the EPZ before an impact of the shadow participation was seen inside the EPZ. The figure suggests the impact of the shadow evacuation at the EPZ boundary was felt by the remaining 40 percent of evacuees only for a few hours toward the latter end of the evacuation.

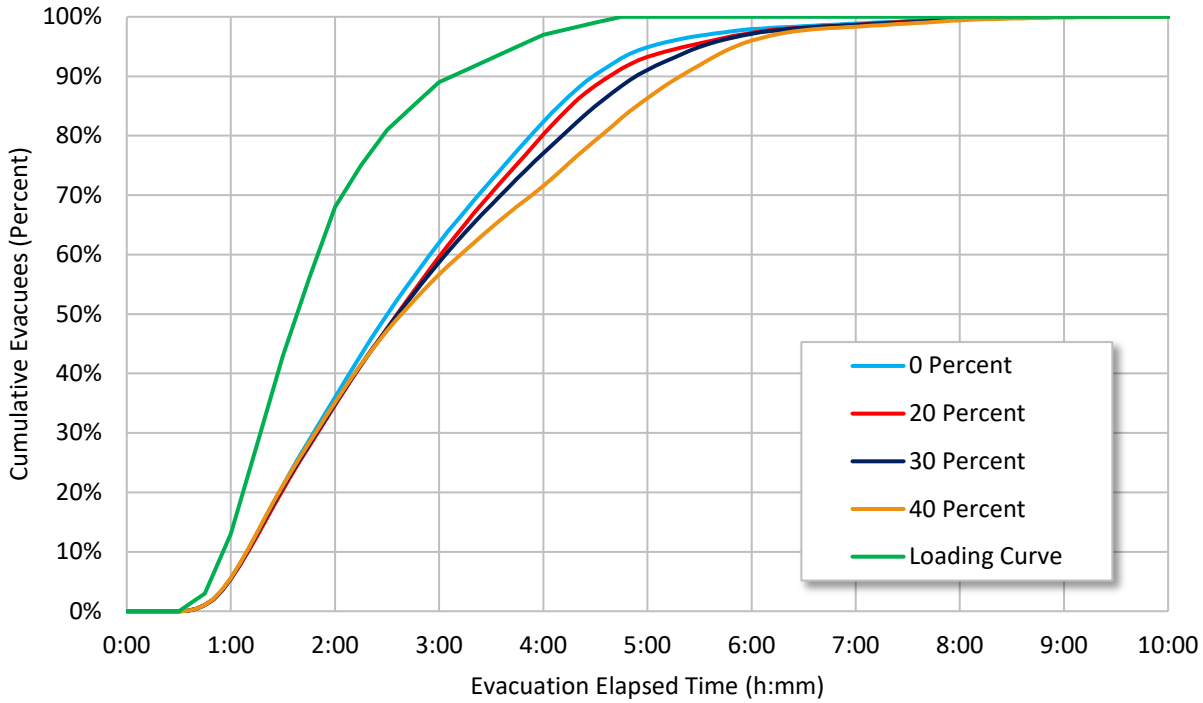

Figure 4-3 Ten Mile ETE Curves, Large Population Site Shadow Analysis

Table 4-7 shows the impact of shadow participation on clearance time by quadrant. The table shows that the 100 percent ETE was not significantly impacted by shadow evacuation participation rate. The table also shows that 90 percent ETEs for the East and South quadrants experienced significant delays caused by increasing the shadow participation. The shadow region within the South and East quadrant had the highest population density within the large population site. Similar to the results of the medium population site model, this result suggests that high population densities within the shadow region can exacerbate the impact that shadow evacuation has on ETE times.

Table 4-7 Ten Mile ETEs by Quadrant, Large Population Site Shadow Analysis

Quadrant	0% Shadow Participation		20% Shadow Participation		30% Shadow Participation		40% Shadow Participation	
	90% ETE	100% ETE	90% ETE	100% ETE	90% ETE	100% ETE	90% ETE	100% ETE
North	4:51	8:12	5:01	8:27	5:05	8:16	5:22	8:22
East	4:35	9:02	4:36	9:00	4:52	9:05	5:31	9:28
South	4:12	5:56	4:17	6:13	4:50	6:08	4:58	6:12
West	4:23	6:17	4:53	6:51	4:52	6:26	5:08	6:40

Another key finding in these analyses is the observation that the 2-mile and 5-mile ETEs were not affected by the shadow participation rate. This was demonstrated in each of the representative site models. Thus, the population residing closest to the site of a potential release of radioactive material would be unimpeded in their evacuation by a large shadow evacuation. This is a significant finding since most of the risk of early health effects from a serious NPP accident would occur close to the plant.

4.2.4 Average Travel Speed Results

Travel speeds at detector locations were grouped in 16 compass sectors (N, NNE, NE, ENE, E, etc.) and speeds were averaged for various time periods at each of the concentric compass rings. In this way, speed increases and decreases could be displayed over various time spans in the various exit directions away from the NPP. This method of displaying speed data provided a reasonable means of comparing speeds between different models over the same time period.

4.2.4.1 Small Population Site Model Average Travel Speed Results

Figure 4-4 and Figure 4-5 show the average travel speed in the small population site EPZ boundary at 0:15 and 1:45 into the evacuation for the 0, 20, and 100 percent shadow participation rates, respectively. The average speeds at 0:15 are indicative of free-flow conditions and exemplify the “best case” scenario within each sector. No impact of shadow participation is seen in Figure 4-4 because the data captured a time when evacuees are just beginning to enter the EPZ and shadow region. Figure 5 was taken at 1:45 into the simulation when most evacuees were loaded onto the road network. This figure shows the average travel speeds for the various shadow participation rates overlapped in the figure. This suggested that the shadow population participation rate had little to no impact on average travel speed in the small population site. Furthermore, by comparing Figures 4-4 and 4-5, it can be concluded that evacuees are able to travel at or near free-flow speed throughout the evacuation. This indicates that the model was uncongested even at 100 percent particaption of the shadow population.

4.2.4.2 Medium Population Site Model Average Travel Speed Results

Figure 4-6, Figure 4-7, and Figure 4-8 show the average travel speed in the medium population site EPZ boundary at 2:30, 3:30, and 4:30 into the evacuation for the 0, 20, 30, and 40 percent shadow participation rates, respectively. At 2:30 minutes into the evacuation, Figure 4-6 shows the onset of congestion in the North-Northwest sector and travel speeds are beginning to be impacted by the shadow participation rate. One hour later, the impact of congestion still dominates the North-Northwest sector; however, speeds have begun to recover even for the largest shadow participation rates. In the East-Southeast sector, only the 40 percent shadow participation rate creates a significant reduction in speed. The other quadrants of the model appear to be less affected by the shadow region. By 4:30, congestion in the Northwest quadrant is still noticeable, but speeds continue to increase. At this point, the shadow evacuation region has little impact. And by this time, the South and West quadrants have mostly completed their evacuations. Taken as a whole, these three figures show that shadow participation did impact travel speeds at the EPZ boundary, but not enough to increase the ETE 30 minutes or 25 percent overall.

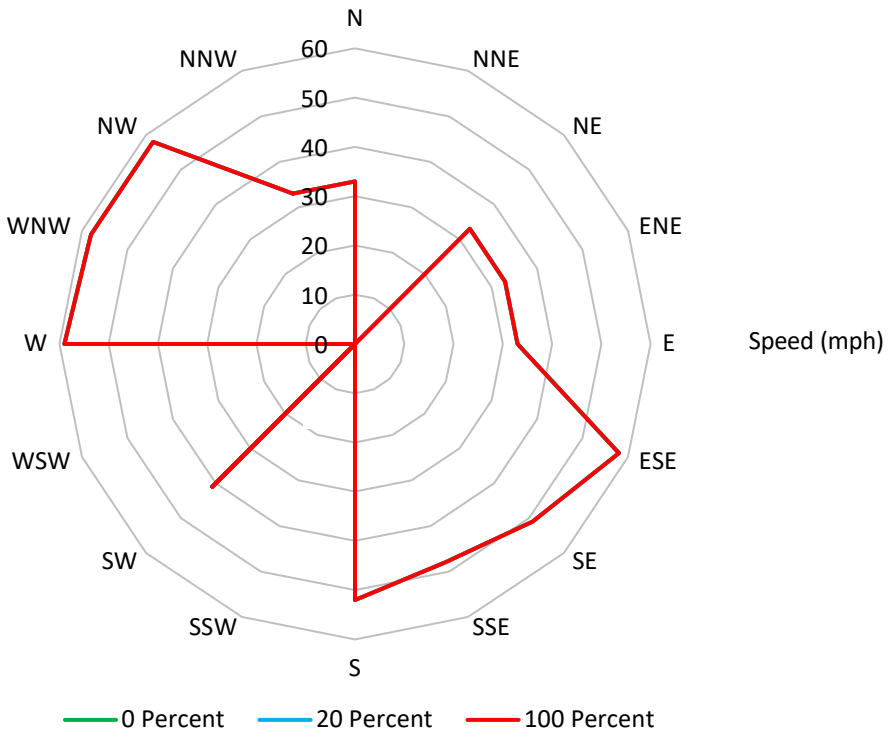

Figure 4-4 Average Exit Speeds at 0:15, Small Population Site Shadow Analysis

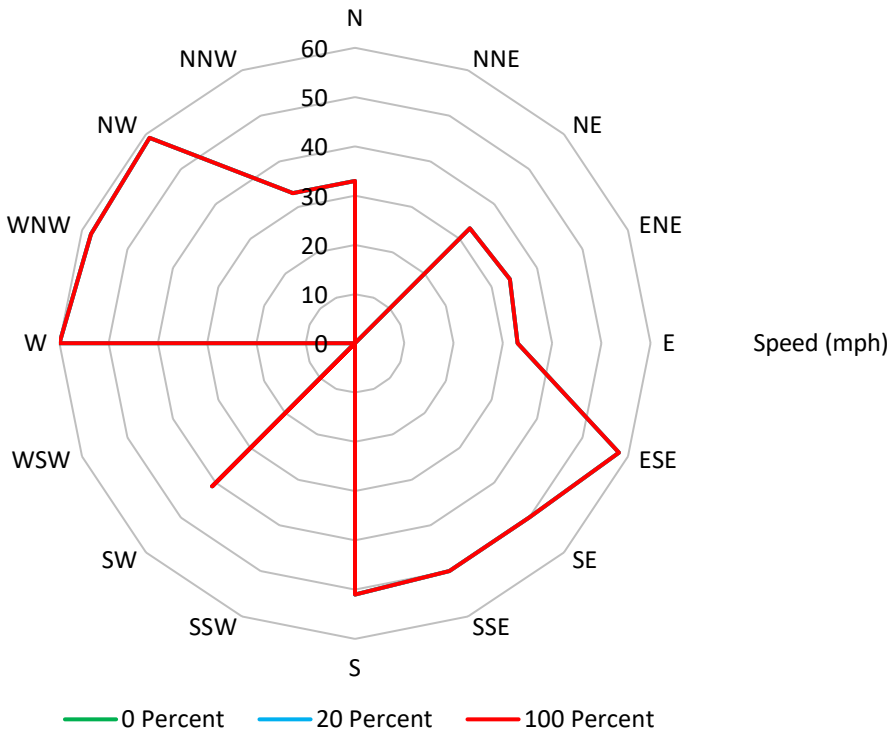

Figure 4-5 Average Exit Speeds at 1:45, Small Population Site Shadow Analysis

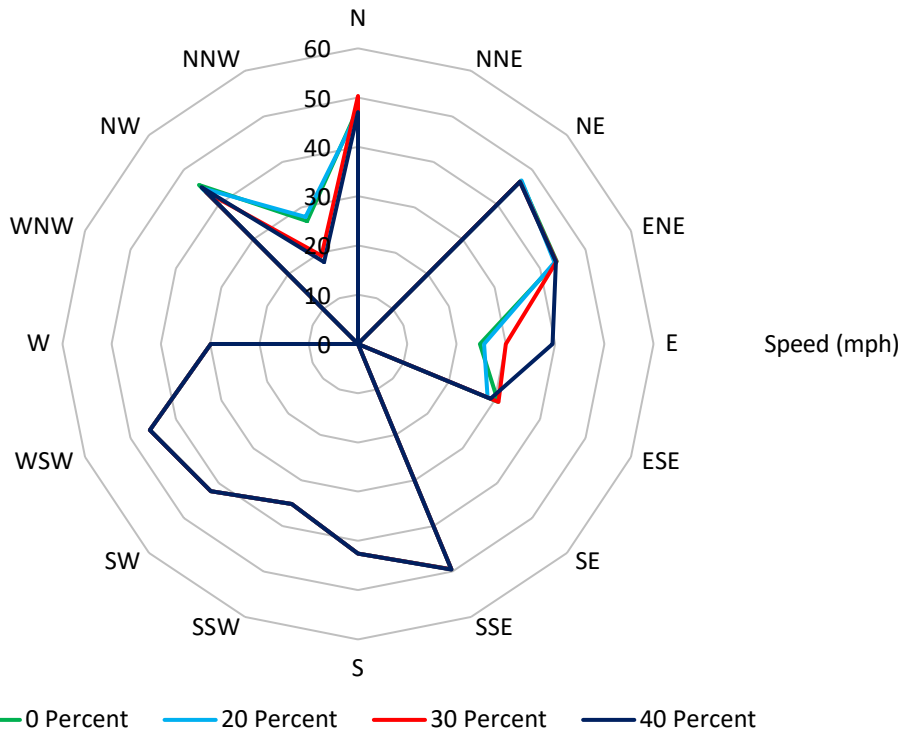

Figure 4-6 Average Exit Speeds at 2:30, Medium Population Site Shadow Analysis

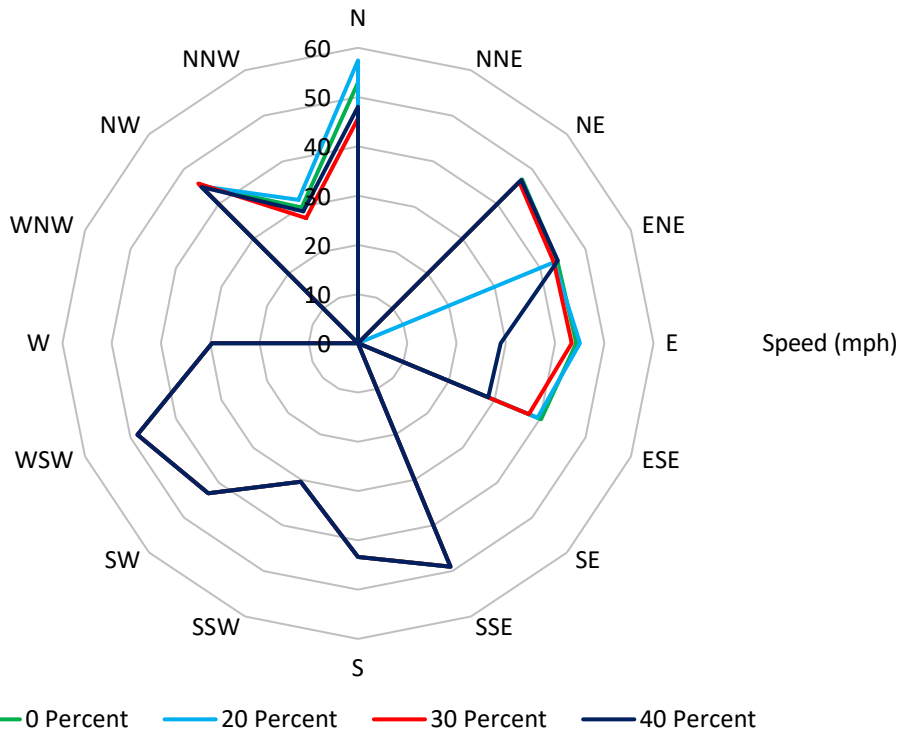

Figure 4-7 Average Exit Speeds at 3:30, Medium Population Site Shadow Analysis

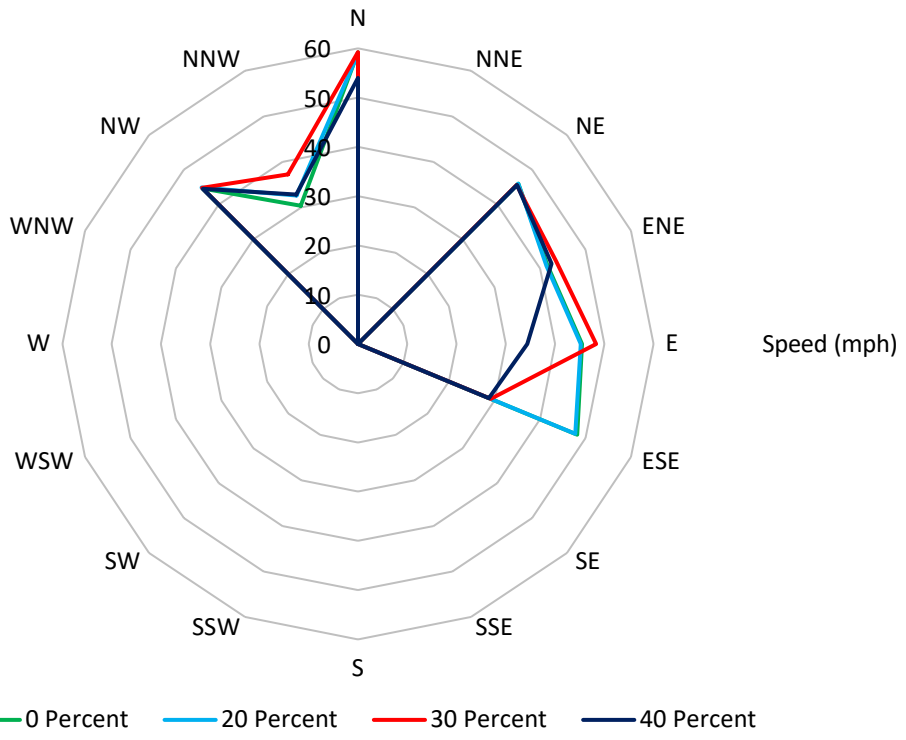

Figure 4-8 Average Exit Speeds at 4:30, Medium Population Site Shadow Analysis

4.2.4.3 Large Population Site Model Average Travel Speed Results

Figure 4-9, Figure 4-10, and Figure 4-11 show the progression of average travel speed in the large population site EPZ boundary at all shadow participation levels during evacuation times of 2:30, 3:30, and 4:30, respectively. The average travel speeds shown in Figure 4-9 at 2:30 into the evacuation show the most diversity of speeds between the various shadow participation levels compared to the zero participation rate. This figure shows unique speed profiles when there is a shadow participation (20, 30, 40 percent) early in the evacuation. This finding may indicate the shadow population could have impacted the level of congestion early on in the simulation and route choice by the DTA. However, as shown in Figure 4-10, by 3:30 into the evacuation the speed profiles for the various participation rates have converged and differences are noticeable at the same exit points for the various shadow participation rates. Figure 4-11 shows a similar consistency of average speed for the various shadow particpation rates but with larger variations in speed for the South and East quadrants. These findings support the hypothesis that large population densities within the shadow region may exacerbate the impact of the shadow evacaution. The speed analysis also suggests that when sigificant congestion builds in an area, average speed tends to converge, regardless of the shadow participation rate. The shadow particpation rate may have played a role in when the speed drop occurred but, ultimately, with congestion building inside the EPZ, an overall drop in average speed was likely unavoidable.

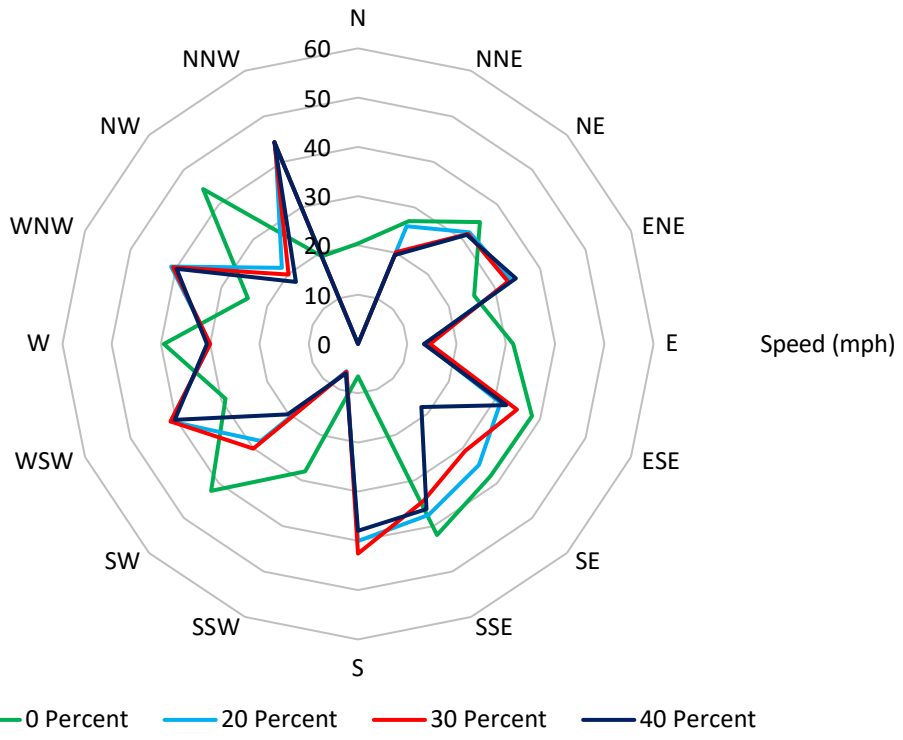

Figure 4-9 Average Exit Speeds at 2:30, Large Population Site Shadow Analysis

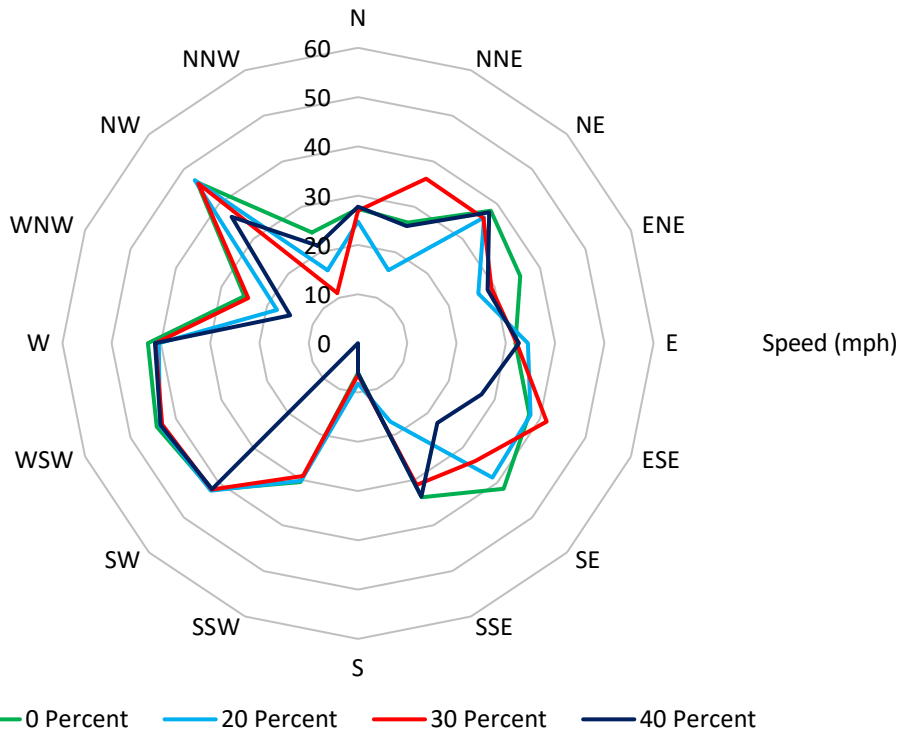

Figure 4-10 Average Exit Speeds at 3:30, Large Population Site Shadow Analysis

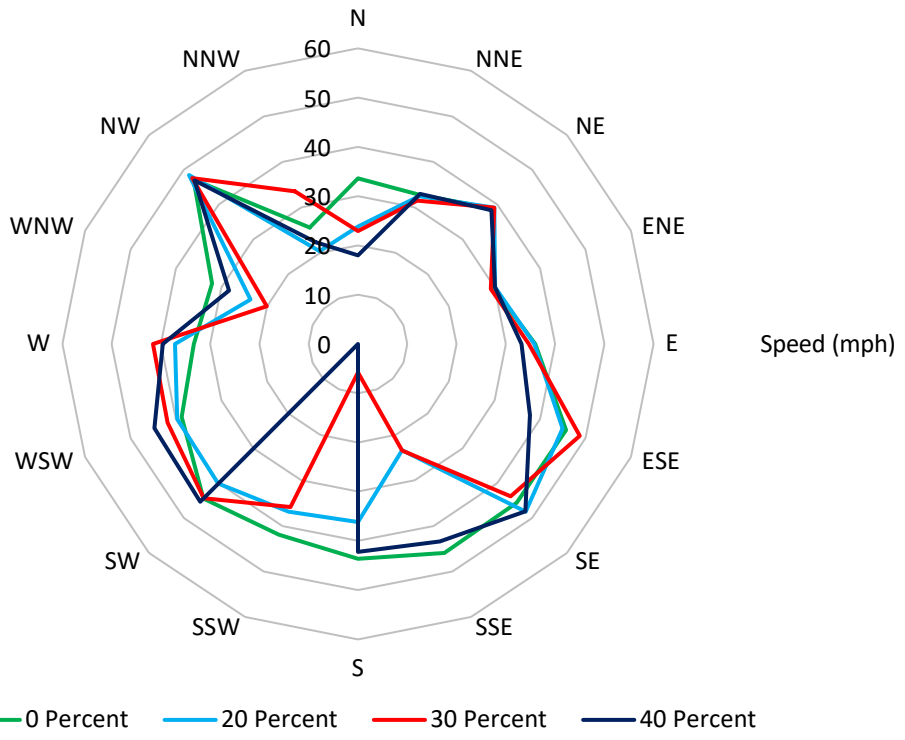

Figure 4-11 Average Exit Speeds at 4:30, Large Population Site Shadow Analysis

4.2.5 EPZ Exit Volume Results

The EPZ exit flow rate is the number of vehicles that exit the 10-mile ring during each 5-minute data collection interval. This flow rate is converted into vehicles per hour as is the standard practice in traffic engineering. The exit flow rate measures diffusion of evacuation vehicles out of the EPZ and into the shadow evacuation region. It was expected that a high shadow participation might impact the rate at which vehicles were able to exit the EPZ in the medium and large population site models.

4.2.5.1 Small Population Site Model EPZ Exit Flow Rate Results

Figure 4-12 shows the small population site EPZ exit volumes for 0, 20, and 100 percent shadow participation rates. The figure shows that the small population site 10-mile ring exit volumes were not sensitive to the shadow participation rate. This reflects the fact that the shadow area did not experience congestion during the 100 percent participation rate scenario and EPZ evacuees were not slowed by shadow evacuee traffic.

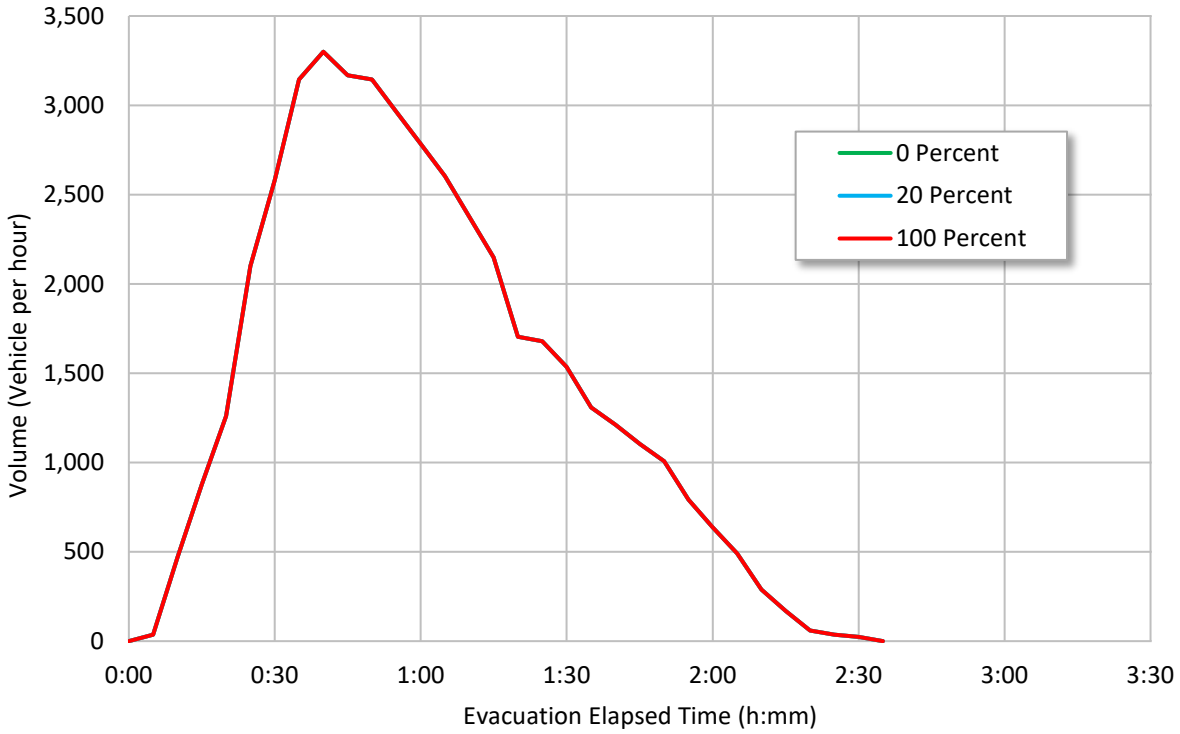

Figure 4-12 EPZ Exit Volumes, Small Population Site Shadow Analysis

4.2.5.2 Medium Population Site Model EPZ Exit Flow Rate Results

Figure 4-13 shows the medium population site EPZ exit volumes for 0, 20, 30, and 40 percent shadow participation rates. The figure suggests the shadow participation rate did not significantly impact the exit volume of the EPZ at rates less than 40 percent. However, as previously discussed, the 40 percent participation rate does appear to affect the exit flow rates beginning at approximately 3:00 and continuing for 2 hours and 30 minutes. This is mostly due to the impact in the Southeast sector. However, after this the exit flow rate increases beyond that of the base model and the traffic network was able to effectively dissipate the additional traffic queue, resulting in a 100 percent ETE similar to the base model. This shows that while the 40 percent shadow participation rate did impact the EPZ exit volumes, it was not enough to increase the overall ETE significantly (i.e., 30 minutes or 25 percent).

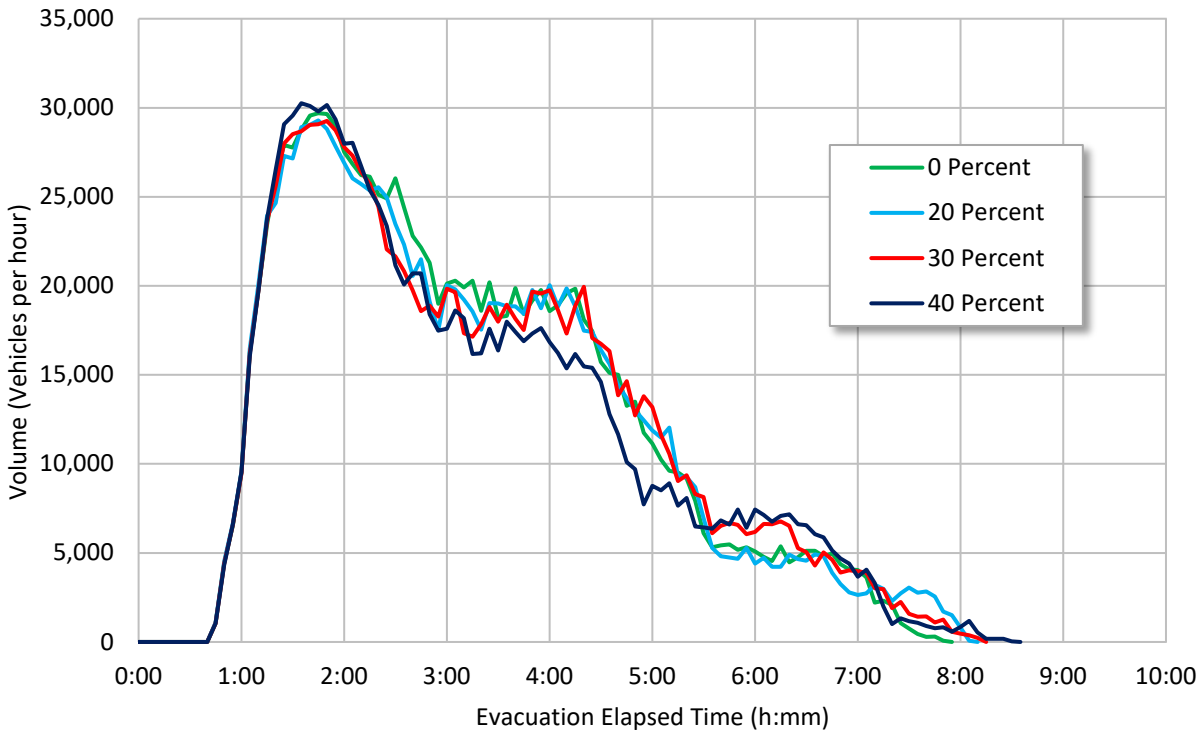

Figure 4-13 EPZ Exit Volumes, Medium Population Site Shadow Analysis

4.2.5.3 Large Population Site Model EPZ Exit Flow Rate Results

Figure 4-14 shows the large population site EPZ exit volumes for 0, 20, 30, and 40 percent shadow evacuation participation rates. The figure shows that exit volumes increase steadily, for all participation rates, until the exit links reach capacity at approximately 50,000 vehicles per hour. This was consistent with results seen in the small population site and indicates that ETEs are not sensitive to shadow participation rates while the network is uncongested. Once the model reached its exit capacity, the exit volumes diverged. The figure shows the extent to which each participation rate affects exit volume. The figure shows that the exit volumes for the various participation rates stabilized from around 3:00 to 4:20 as the evacuees cleared the EPZ. The 40 percent shadow participation rate had a significant impact on the exit volume indicative of downstream congestion in the shadow region. As congestion abated the flow rates recovered, increasing the 100 percent ETE minimally. This finding may explain why he 90 percent ETE was significantly impacted by shadow participation and the 100 percent was not. The analysis of exit flows suggests that the evacuation tail extends the evacuation time and allows the evacuees delayed by congestion in the shadow area to “catch up” and exit the EPZ at about the same time. However, the 90 percent ETE is more sensitive to the impact of delayed vehicles.

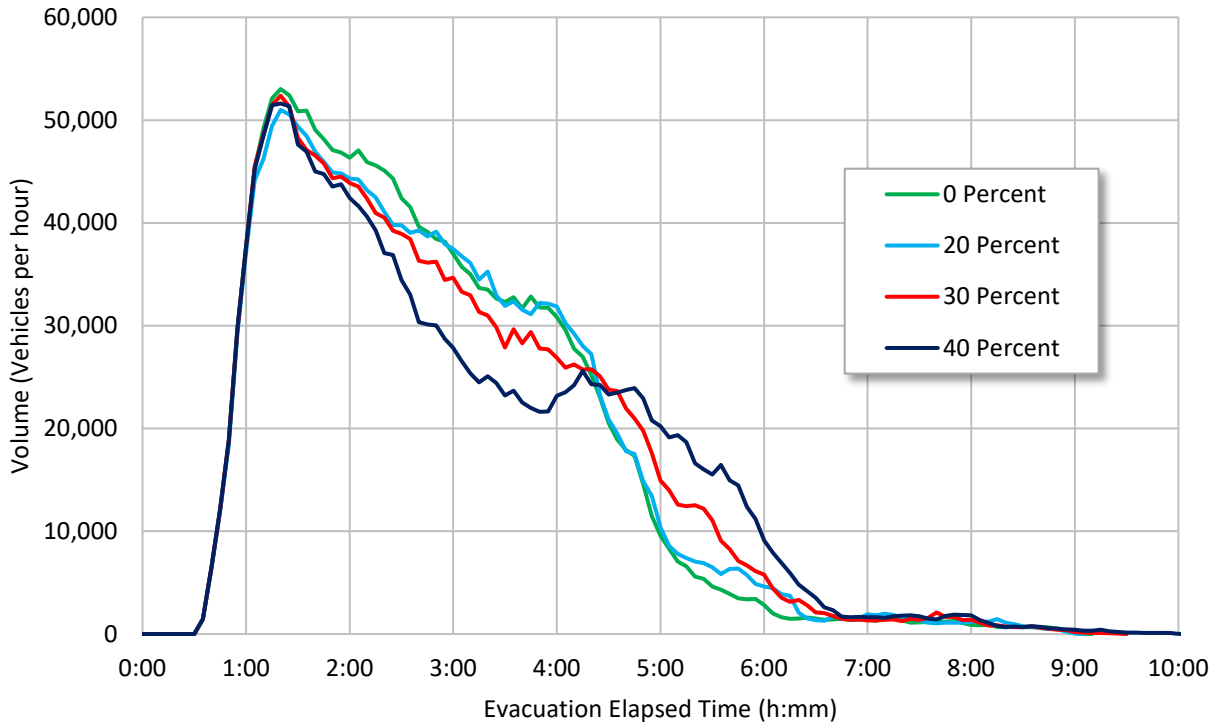

Figure 4-14 EPZ Exit Volumes, Large Population Site Shadow Analysis

4.3 Site Characteristics that Exacerbate the Impact of a Shadow Evacuation

As described in Section 3, at the most fundamental level evacuation processes can be described in terms of supply and demand relationships. Of significance in this study, is the occurrence of a shadow evacuation and the potential to impact the ETE by impacting supply and demand of the network, and in particular under what conditions this impact be would be exacerbated. In terms of site-specific characteristics, these conditions can be narrowed down. Based on this research, influential conditions have been identified.

4.3.1 Demand-Related Site Characteristics

The analysis of the three representative sites used relatively similar spatial and temporal processes for the generation of demand. Most notably, the evacuee behavioral response assumptions used to load shadow evacuees into the network was the same as those assumed for the EPZ population. As such, there was not a time lag between the two sub-areas of the evacuation analysis region. In an actual NPP emergency, these could differ between sites, especially in large population sites with denser populations where the visible departure of people by potential shadow evacuees could encourage like-minded behavior. The impact on the ETE, however, would depend on the time lag. If shadow evacuees left significantly before or after EPZ evacuees the impact is likely to be much less than if a simultaneous evacuation is assumed, as performed in this study.

As evidenced in the medium and large site models, the population density of the shadow population can impact the ETE within localized regions. However, there are many other factors that contribute to this effect, including the local network capacity and the extent to which this

capacity is modeled, particularly in the design of the links used to load the shadow evacuees into the network.

Two other demand-related factors that could exacerbate the impact of the shadow evacuation on the clearance of the EPZ are the amount of pass-through and background traffic. Once again, based on the assumption that higher population sites would tend to have higher levels and pass-through and background traffic, it would logically follow that these higher levels of traffic could impact the rapid clearance of the EPZ. These assumptions were borne out by the simulation model runs, although not as obvious as might be expected. The influence of background traffic is explored separately in Task 4.

4.3.2 Supply-Related Site Characteristics

Traffic engineering fundamentals would suggest that any characteristic that reduces roadway capacity including intersection control, number of lanes, speed limits, geometric roadway characteristics (e.g., grade, lane width, etc.) and driver behavior (for microsimulation) would likely result in increased clearance times. However, no modifications were made within the models to test these ideas explicitly. The research associated with the additional tasks of this study will be able to demonstrate broad effects on a model-wide level. As such, the results and findings of these tasks would be applicable to the shadow region.

4.4 Review of Current Shadow Evacuation Guidance

If the EPZ permanent resident population increases such that the longest ETE increases by 30 minutes or by 25 percent, the ETE must be updated [1]. The 30 minute period was developed, in part, from discussions with OROs, that indicated they would likely not make protective action decisions (PAD) to any higher degree of fidelity than 30 minutes. This was not to suggest that a PAD would change if an ETE changed by 30 minutes, but rather that 30 minutes was a minimum time to consider whether alternate PADs might be appropriate.

The results of increasing the shadow contribution were compared against the 30 minute or 25 percent increase criteria and generally showed no significant impact on the ETE from a base assumption of 20 percent shadow participation. Although significant increases in the ETEs were observed in the medium and large population site models, these increases were only observed for the highest shadow participation rate and were limited to specific quadrants of the EPZs where high population densities exist within the shadow region. Furthermore, the maximum increase was 41 minutes. This impact is within the variation of the clearance times typically observed at large population sites when performing ETEs using the various scenarios of NUREG/CR-7002 [4]. Such variation in ETE is accounted for in site-specific protective action strategies. Another interesting finding was that in even in congested conditions, approximately 50 percent of the evacuees exited the EPZ before any influence of the shadow region could be seen within the EPZ and nearly 70 percent exited before the impact could be classified as significant. Thus, a shadow evacuation can only impact a small portion of the evacuating population, even at the highest participation rates. Additionally, when compared to the results of Tasks 2, 3, and 4 of this study, the impact of the shadow evacuation appears not to be a dominant component of the ETE.

Based on the analyses conducted with the three base models for the generic EPZs, it is apparent that assuming a shadow participation rate between 20 percent and 30 percent is reasonable to capture effects of evacuees from areas beyond the EPZ. Therefore, this task analysis leads to the conclusion that the current 20 percent shadow guidance is appropriate.

However, any value greater than 0 percent and equal to or less than 30 percent could be justifiable and would likely lead to similar results. Furthermore, for small population sites, consideration of a shadow region may not be warranted given the consistent finding of no impact in this report and other previously conducted ETE studies. However, this also depends on the supply and demand characteristics of a particular site. It is possible that circumstances could arise in a small population site to cause a larger increase in ETE times, but as shown herein, the increase would need to be substantial to have a meaningful impact.

5 TASK 2 DISTANCE OF EVACUATION TRAVEL

A critical component in the development of ETEs is the establishment of an appropriately sized model and adequate boundary conditions. At the point where vehicles exit the model, they no longer create traffic queues or influence the upstream traffic in any way. If vehicles were to exit the simulation at the EPZ boundary, the lack of traffic congestion may detract from the veracity of the simulation.

ETEs provide information to offsite response organizations that can lead to changes in protective action strategies, identification of congestion areas, and changes in traffic control plans. The assessment of clearance times for EPZ regions generally does not require detailed aspects of most traffic processes. However, there are times when transportation facility-specific conditions, like an intersection, merge area, or even a driveway entrance can significantly influence operations along an entire travel route. In such instances, the approach and departure of vehicles at intersections, passing and turning movements along roadway segments, and the loading and unloading of vehicles into an evacuation road network can be of interest and importance because they can impact key performance indicators of the evacuation system, like congestion, delay, travel time, and—most importantly for ETE studies—EPZ clearance time.

This task examines the effects of downstream conditions in the road network beyond the shadow region of an ETE study to determine the factors that can impact EPZ clearance time. A valuable performance indicator observable in micro- and macro-level models is the build-up and discharge of vehicle queues. Queuing characteristics yield insight into roadway capacity and can identify bottlenecks by their effect on constraining movements within the network. For example, a queue resulting from a lane drop or a major shopping center that exists just beyond the boundary of a study network may create congestive effects that back-propagate into a study area. This task investigated incremental increases of network modeling size for the purpose of informing ETE development. This task also explored evacuee travel times beyond the EPZ.

5.1 Background

Current NRC guidance for ETEs recommends accounting for the impact of traffic congestion beyond the 10-mile EPZ. The guidance recommends modeling the road network to 15 miles from the NPP. Modelling the evacuation network beyond the EPZ can include the effect of nearby more heavily populated areas. Areas with more traffic may create congestion extending upstream into the EPZ and increase the ETE. For this reason, analysts often examine the road networks, population distributions, and traffic generators and attractors beyond the 15-mile study boundaries to assess the potential to create downstream queuing and congestion that could impact an ETE.

The need to model areas beyond the shadow region depends on the potential to impact the ETE and the additional coding effort that would be required. For example, inclusion of the road network and population conditions in a five-mile ring between 15 and 20 miles from the NPP would encompass an area 175 percent larger than the entire EPZ, 140 percent larger than the 10 to 15-mile ring, and nearly 80 percent as large as both together. The additional modeling is a significant task that should only be necessary if it provides information important to public health and safety.

5.1.1 Queue Spillbacks

Traffic flow is influenced by vehicle demand, traffic composition, traffic control, network topology, driver behavior, and the geometrics of the road [22]. Traffic conditions on surrounding roads and other parts of the transportation network also have influence as a road merges or diverges onto others in a series of interconnected links that make up the transportation network [74]. When demand exceeds the available capacity queues start to form, and the tail of the queue could propagate to upstream segments. This is a traffic phenomenon referred to as queue spillover or queue spillback [75]. Even in cases where the upstream link has sufficient capacity to serve the demand, a queue regulates the outflow capacity of the upstream link [76]. Queues could also partially or fully block intersections, oversaturate them, and potentially create gridlock in the network.

Modeling queue spillbacks in traffic simulations is important to obtain representative results. The study of Knoop et al., assessed the effect of evacuation processes with and without queue spillback modeling using macroscopic simulation [78]. The study suggested that the overall output flow is affected by the queue spillbacks. An impact of less than eight minutes was seen on the 90 percent ETE when queue spillback was not modeled in different driver routing scenarios. However, the 90 percent ETE increased by as much as 83 minutes when spillbacks were built into the model [78]. This suggested that the modeling of queue spillbacks captures the impact of congestion.

5.1.2 Spatial Boundary Limits for Traffic Simulation Studies

The state of the practice for traffic modelers is to investigate the area outside the study boundaries to identify traffic conditions that could affect traffic operations within a study area. Transportation authorities in some states have developed guidelines to assess the boundary conditions for traffic simulation studies and for extending the study boundaries when appropriate. Florida, Oregon, and Washington State DOTs have available handbooks and guidelines that address this issue. The Oregon and Washington State DOT guidelines are specific to the VISSIM software [24] [25].

In general, the selection of the spatial boundary limits depends on the transportation network topology and roadway functional classification (e.g., freeways and arterial roads), and the traffic control and operational characteristics of the road network. Typically, the model network extends for two miles outside a study area to capture conditions in what is referred to as the ‘zone of influence’, which affects the study area. Analysis of freeways in urban areas may require to be extended at least two interchanges or two miles [24] [25]. The zone of influence for arterial roadways depends upon the road network configuration, frequency of traffic signals, and the level of congestion within the project area [77]. However, these recommendations were developed for application in traffic/roadway engineering as opposed to evacuation modeling where traffic is predominately directed outbound [24] [25] [77].

Typically, the selection of the spatial boundary limits could be based on the presence of one of the following:

- Downstream bottlenecks that affect traffic flow out of the zone of influence with queue spillback into the study area.
- Queues that extend beyond the study area.
- Interchanges that affect lane-changing behavior (merge/diverge or weaving operations, toll plazas, ramp meters).

- Adjacent intersections that affect the formation of vehicle platoons; for example, a signal coordination.

Identification of the zone of influence in selection of study boundaries can focus analysis efforts.

5.1.3 Spatial Boundary Limits for Hurricane Evacuation Studies

The issue of model extent is not unique to NPP ETE analyses—it is critical in all applications of traffic modeling and simulation. A model that does not adequately capture key congestion creating or relieving features of a road network would not accurately determine its performance. Such a condition is important in an evacuation simulation because congestion and queuing can impact the clearance time of the area under threat and increase travel time.

Hurricane evacuations are particularly good illustrations of the need to include zone of influence considerations in traffic simulation models. Hurricanes create large evacuations that can involve the movement of many thousands of vehicles over long distances. Evacuation traffic will inevitably pass through downstream populated areas that intersect with other routes. These conditions can result in traffic congestion and travel delay that can propagate widely, quickly, and significantly throughout entire regions.

Three examples of hurricane evacuations where such traffic conditions occurred include the evacuation of Galveston Island, Texas; New Orleans, Louisiana; and The Florida Keys. These case studies illustrate situations in which remote downstream network characteristics impacted the evacuation process and how simulation modeling beyond the evacuation zone was applied to mitigate problems. Each of them is briefly described below.

5.1.3.1 Houston-Galveston

Coming only two weeks after Hurricane Katrina, Hurricane Rita threatened to devastate the southwest Texas region in 2005. Among the most critically threatened areas of this region were the coastal communities on Galveston. Galveston is effectively an island some 30 miles south of Houston. With a population of thousands of people only a few feet above sea level, a complete mandatory evacuation of the island was deemed necessary. To reach areas of safety, most islanders needed to drive through Houston. Unfortunately, this occurred at a time when a substantial portion of the Houston metropolitan region of more than six million people was also evacuating. The recognition of this condition made it necessary to create a staged evacuation plan for the region in which the most vulnerable and critically threatened areas of the region (like Galveston Island) would be ordered to evacuate first, then move to and through the Houston metropolitan area before the onset of traffic congestion from the evacuation of greater Houston. As such, it was necessary to model the entire Houston region to determine a clearance time for Galveston Island.

5.1.3.2 New Orleans

The evacuation plan for New Orleans illustrates an even more extreme case of the effect of downstream congestion and the need for network modeling outside of the immediate road network. Traffic count observations collected from several evacuations of the southeast region of Louisiana showed that major evacuations of New Orleans and its surrounding region brought significant traffic flows into and beyond Baton Rouge as evacuees sheltered in the city and points beyond. Although it was about 80 miles away, Baton Rouge was critical in the development of the New Orleans evacuation plan in two respects. First, like Houston, there was

a concern that routine traffic in Baton Rouge would interfere with pass-through evacuation traffic creating the potential to queue all the way upstream into New Orleans. The second was the fact that all westbound traffic moving through this region could only do so by crossing over one of two bridges spanning the Mississippi River. These two bridge crossings were critical from the standpoints of both evacuation traffic movement and simulation modeling.

The bridge crossings in Baton Rouge effectively dictated the capacity of all westbound traffic moving beyond Baton Rouge. This point could also be argued for all westbound traffic evacuating from New Orleans and traveling toward Baton Rouge, Houston, and any destination before, after, or in between. Effectively, the bridges over the Mississippi River in Baton Rouge created a capacitated network within which evacuation traffic flow was limited to the maximum flow that is attainable to the capacity of the bridges. During a regional evacuation when demand is great, the maximum flow prior to Baton Rouge (and potentially all the way back to New Orleans) would also be dictated by the bridge capacity. This could occur due to the build-up and back propagation of queues from these bridges.

From a modeling perspective, the Baton Rouge issue presented a number of challenges. At a conceptual level, some simple calculations were used to estimate the queue formation and discharge characteristics within this corridor. Additionally, some high-level macroscopic simulation of this segment was performed. However, neither of these were able to assess specific conditions associated with local traffic volume that was added from the Baton Rouge area or the influence of confluence congestion created by the merging of two major interstate freeways into a single route. Given the limits of the technology of the day, two separate micro-level simulation models were used to first determine the flow out of the New Orleans region, then—assuming that the volumes stayed relatively uniform during the 80 mile journey between the two cities—to use that outflow volume as the inflow volume (and added local volume) into the Baton Rouge model [79].

The separate, though coupled, micro-simulation modeling approach to evacuation modeling in this area was critical to understanding the expected conditions associated with an evacuation of New Orleans in Baton Rouge and to plan for them. In fact, the model was pivotal in creating a regional phased plan in which major public sector employers in Baton Rouge (including state government offices and Louisiana State University) may be called to close during an evacuation of New Orleans to keep local traffic to a lower level. None of these conditions would have been recognized without extending the modeling area 80 miles beyond the areas ordered to evacuate.

5.1.3.3 Florida Keys

A final example illustrating the critical nature of model extent was seen in the planning for hurricane evacuations in the Florida Keys. The Florida Keys are unique from several perspectives. From a geographical standpoint, the area is unlike most other threatened areas because there is only a single route of egress and the travel distance to the first available shelter locations is in excess of 100 miles for most of the evacuees. From environmental and socio-demographic perspectives there is a great emphasis on preserving the natural beauty and character of the islands. Various citizen constituencies have vocal opposition to adding roads within the island chain. As a result, evacuations were facilitated by adding outbound capacity with added contraflow lanes and using shoulders. Even so, it was evident that the potential controlling factor of the Keys evacuation was the capacity of downstream segments well beyond the boundary of the Keys.

To address this concern, studies were conducted of two critical locations on the Florida mainland south of Miami. The first study was an improved operational plan for the signalized intersection near Florida City in which geometric and control improvements would permit unimpeded outbound flow through the area leading up to the southern entry point of the Florida Turnpike [80]. The second study—which is still being debated because of its complexity and manpower requirements—was the Florida Turnpike's "One-Way Evacuation Plan" [81] [82], which would permit a one-way northbound evacuation traffic operation on the Florida Turnpike between Florida City and Orlando.

Each of these real-world examples illustrates the need for modeling beyond the assumed boundary of an ordered evacuation zone and, in some cases, well beyond. Research by Dixit and Wolshon, suggested the application of a "Maximum Evacuation Flow Rate" and a "Maximum Sustainable Evacuation Flow Rate" [40]. The maximum evacuation flow rates can be thought of as the effective capacity of the roadway during emergency evacuation conditions that is attributable to a downstream bottleneck(s). The maximum sustainable evacuation flow rates are the flow rates that can be sustained after a peak in the evacuation flow rate. This research encourages modelers to use the maximum evacuation flow rate as capacity values in dynamic macroscopic and dynamic mesoscopic simulation models, or for validating microscopic simulation models. The maximum sustained evacuation flow rates can also be used to conduct sketch planning analysis or input-output based analysis to determine delays, queue length, and evacuation time estimates.

Clearly, there are trade-offs between the additional required time, effort, data, and cost that must be expended to build and evaluate larger modeled areas. Even a relatively small additional area beyond an EPZ has the potential to significantly increase the modeling effort. This would be particularly true for NPP sites that border on or are within the relative vicinity of highly populated areas with considerably denser road networks. Another key point of model extent determination is to locate downstream capacity constraint points with the potential to impact the evacuation process within the EPZ and model them as appropriate. This is often done by extending the model in one area to include the constraint point. One potentially more practical and streamlined approach might be to create models that use outflow volume from an upstream representation area to feed inflow volume into a downstream model. However, the use of wholly separate models to represent a single area can miss some of the complexities of travel into, out of, and across boundaries due to the way traffic is generated in most traffic simulation systems.

5.2 Task 2 Analysis

This task was developed to quantify the impact of travel distance on ETEs. Task 2 included two subtasks: 1) a sensitivity analysis of the effect of more or less distance traveled in order to determine the impact that model extent has on the ETE, and 2) an analysis of the travel times beyond the EPZ boundary to determine the value of such analyses. The modeled distance, more specifically, the inclusion or exclusion of bottlenecks (capacity reductions) and population centers (demand generators) could potentially impact congestion and vehicle routing by the DTA algorithm, thereby impacting the simulation within the EPZ. Current NRC guidance requires model development out to 15 miles for the inclusion of a five-mile shadow region. Therefore, the shortest evacuee travel distance outside of the EPZ is 5 miles. The base models for this research model representative transportation networks out to a distance of 20 miles. For this task, the base models were systematically truncated at one-mile increments from 20 miles to 15 miles. Each increment was compared to the base model to quantify the impact of travel distance on ETEs.

5.2.1 Model Truncation

Model truncation is the separation of the influence of traffic from one area to another. Model truncation is accomplished by deleting the model beyond a certain point. For the small population site, where static traffic assignment was used, the model was truncated by deleting all links beyond a given truncation radius. This approach was acceptable for the small population site model because there was no impact of model extent on route choice with the static route assignment. However, the use of DTA in the medium and large population site did not permit the altering or changing of the network geometry as was done in the small population site. Therefore, truncating the medium and large population site required a separate methodology.

The small population site was truncated at five radii: 19 miles, 18 miles, 17 miles, 16 miles, and 15 miles, in three primary steps. Step one was to bisect the roadway links within VISSIM immediately downstream of the truncation line. The second step was to delete all the links and connectors beyond (radially away from the NPP) the bisected link, and the final step was to add data collection points at the line of truncation to collect measures of effectiveness (MOEs) to compare with the base model.

The DTA algorithm used in the medium and large population sites generates a pool of potential paths for each origin-destination pair. When a vehicle is generated, the DTA algorithm evaluates the generalized cost of each potential path within this pool and assigns the vehicle to the path with the lowest cost. The generalized cost is a function of the travel time and also the travel distance and delay. When selecting a route, travel time typically governs. However, other factors may impact a driver's route selection such as the number of signalized intersections, the use of limited access freeways, the travel distance, etc.

When evaluating the impact of model extent, it was important not only to capture the impact of queue propagation, but also to consider the impact of the added network on the equilibrium of the DTA algorithm. For example, a model that is inclusive of a major bottleneck will tend to distribute traffic away from the bottleneck. However, if this model is truncated and the bottleneck section removed, the DTA is likely to add vehicles to this path, altering the vehicle assignment from the base model. The same would be seen with the inclusion or exclusion of a major population center. It should be emphasized that the DTA is attempting to optimize route choice for the entire model extent, not just within the EPZ. As the model extent is increased, the DTA algorithm will be more influenced by factors outside of the EPZ. This is acceptable for purposes of this task, and no attempt was made to optimize evacuation routes from the EPZ within each truncated model.

In order to keep the pool of paths consistent while truncating the model an approach was developed that left the network geometry unchanged from the base model. Any change applied to the network geometry would render the base model pool of paths unusable in the task analysis. Therefore, the base model for the medium and large sites were truncated by diverting vehicles to newly added destinations just past the radial line of truncation. A vehicle would leave its origin destined for the same parking lot it was assigned in the base model but would then be diverted to a new parking lot at the truncation line. The radial lines of truncation used for the medium and large population site were the same as the small population site (19 miles, 18 miles, 17 miles, 16 miles, and 15 miles).

The model truncation for the medium and large population sites was accomplished in three primary steps. The first step was adding destination parking lots downstream of the various lines

of truncation. The second step was programming a route detour which directed vehicles to these parking lots instead of the base model destinations. The third step was to place data collection points upstream of the line of truncation to collect MOEs for comparison with the base model

5.2.2 Analysis Results

The results presented in this section represent the average of several simulation runs, each with varying random seed values. As was done with the Task 1 results, the small population site results represent an average of ten simulation runs, whereas the medium and large site results represent an average of four runs. The MOEs used to evaluate Task 2 were evacuation and clearance time, average travel speeds, and vehicular volumes exiting the EPZ. Travel time collectors were also placed on key evacuation routes in the models to collect travel time beyond the EPZ to the various lines of truncation. The data was collected and analyzed over 5-minute increments and segregated to display results for 90 percent of the evacuating EPZ vehicles and 100 percent, where applicable. The results of the Task 2 analysis are presented for each model in the following sections.

5.2.2.1 Evacuation Time Results

This section discusses the results of varying the extent of each model, thereby varying evacuee travel distance and clearance time. Evacuation times were calculated at the 2, 5, and 10-mile rings. Additionally, the evacuation times by sector are shown graphically for the medium and large population sites for the 90 and 100 percent ETEs. Model truncation caused variation in clearance times by altering the equilibrium paths selected within the DTA, and in some cases, by the inclusion of bottlenecks that could propagate congestion back into the EPZ. Backpropagation is likely only to impact the 10-mile ETE, whereas changes to the DTA path selections could impact the clearance times at the 2 and 5-mile rings as well.

5.2.2.1.1 Small Population Site Model ETE Results

The small population site used a static route choice model. Changing the model size should not impact the 2 and 5-mile ETEs unless severe congestion propagated back from beyond the 15-mile ring deep into the EPZ. For small population areas, varying the size of the model beyond the 15-mile shadow region was not expected to impact the 2, 5, or even 10-mile ETE. In order to influence traffic significantly, a bottleneck beyond the EPZ would have to cause a queue length of at least five miles, and with such low population densities within the small population site, this was unlikely. Table 5-1 shows the ETE for each truncation iteration. It can be seen that model extent beyond the shadow region did not impact the ETE for the small population site. This suggests that either no significant bottlenecks exist beyond the shadow region capable of causing significant queues or that the traffic volume on bottleneck links was not high enough to propagate back into the EPZ.

Table 5-1 Small Population Site Average ETEs for Models of Varying Distance

Model Extent (miles)	2-Mile		5-Mile		10-Mile	
	90% ETE	100% ETE	90% ETE	100% ETE	90% ETE	100% ETE
15	1:35	2:18	1:35	2:21	1:44	2:31
16	1:35	2:18	1:35	2:21	1:44	2:31
17	1:35	2:18	1:35	2:21	1:44	2:31
18	1:35	2:18	1:35	2:21	1:44	2:31
19	1:35	2:18	1:35	2:21	1:44	2:31
20	1:35	2:18	1:35	2:21	1:44	2:31

Figure 5-1 shows the small population site resident populations, road network, and truncation distances beyond the 15-mile shadow region. Figure 5-2 shows the cumulative percent evacuated for the small population site at the 10-mile ring. This figure is a visual representation of the ETE process that led to the 90 percent and 100 percent ETE times shown in Table 5-1. The figure also displays the evacuee loading curve for reference. From Figure 5-2, the 10-mile ETE for the truncated models were identical to the base model curve. This indicates the reduction of the modeled network size from the base (20 miles) to 15 miles had no impact on the small population site ETE.

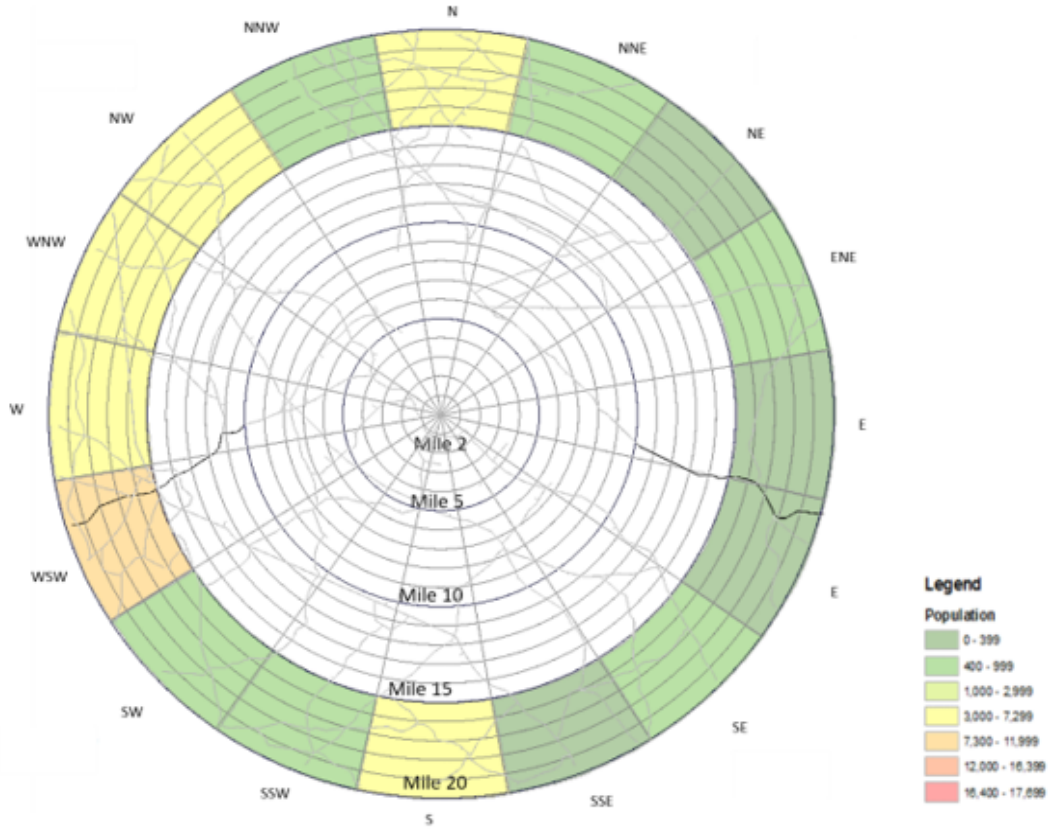

Figure 5-1 Small Population Site Model Population Beyond the Shadow Region

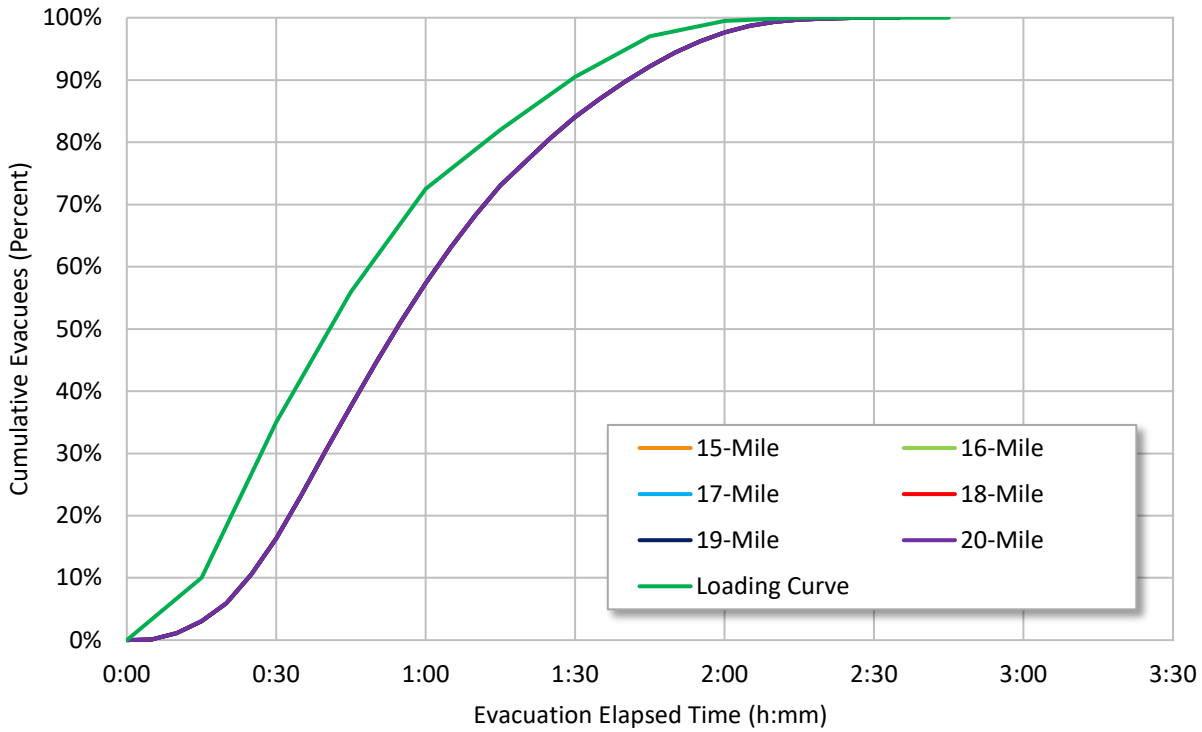

Figure 5-2 Ten Mile ETE Curves, Small Population Site Travel Distance Analysis

5.2.2.1.2 Medium Population Site Model ETE Results

The medium population site 90 percent and 100 percent ETEs times are provided in Table 5-2 for each ring within the EPZ and by sector in Figure 5-3 and Figure 5-4. It was expected that changes to the model extent would impact the DTA route choice and had the potential to impact the 2, 5, and 10-mile ETEs. Table 5-2 shows that ETEs were approximately the same once the model extended beyond 18 miles (model sizes 18, 19, and 20). This suggests that the path selection did not change significantly between these three models. Models truncated at the 15, 16, and 17-mile ring affected the DTA path selection and significantly impacted ETEs. This was likely the result of a combination of factors encountered as the model was extended including: 1) the increase in background traffic in the eastern quadrant, 2) the decreasing roadway network in the eastern quadrant as the model extended outward, and 3) the increase in population in the northern quadrant.

Table 5-2 Medium Population Site Average ETEs for Models of Varying Distance

Model Extent (miles)	2-Mile		5-Mile		10-Mile	
	90% ETE	100% ETE	90% ETE	100% ETE	90% ETE	100% ETE
15	2:40	4:03	3:13	5:48	5:28	8:08
16	2:40	4:03	5:51	7:00	6:17	9:06
17	2:40	4:03	4:38	5:57	5:43	7:46
18	2:40	4:03	2:55	5:05	5:07	7:45
19	2:40	4:03	2:46	4:46	5:02	7:45
20	2:40	4:03	2:47	5:05	5:03	7:41

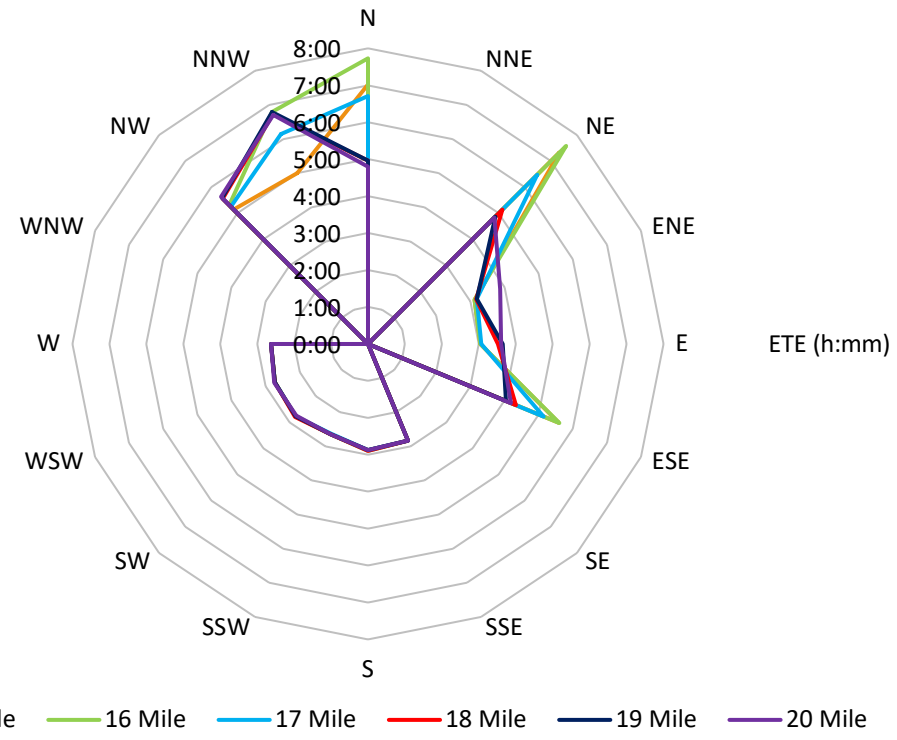

Figure 5-3 Ten Mile 90 Percent ETE by Sector, Medium Population Site Travel Distance Analysis

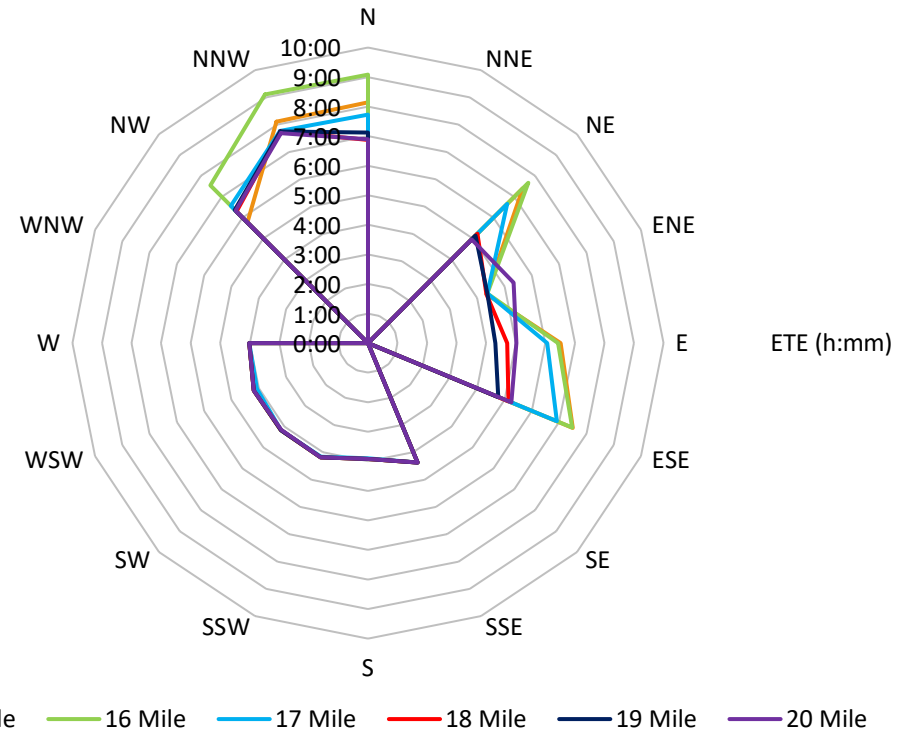

Figure 5-4 Ten Mile 100 Percent ETE by Sector, Medium Population Site Travel Distance Analysis

Figure 5-5 shows the medium population site resident populations, road network, and truncation distances beyond the 15-mile shadow region. As the model extends outward in the eastern direction, higher populations within this area will increase the amount of background traffic making eastern paths less desirable. The eastern quadrant also approaches a major body of water (not shown). As the network expands toward that body of water the road network in this region becomes less dense, resulting in more congestion and less desirable routes. As the model extends outward in the northern quadrant, the population density also increases, adding background vehicles and congestion. The model truncation removed various portions of the network and thus various locations of congestion. In general, this played a significant role in route selection and resulted in different route utilization by the DTA algorithm with each new truncation.

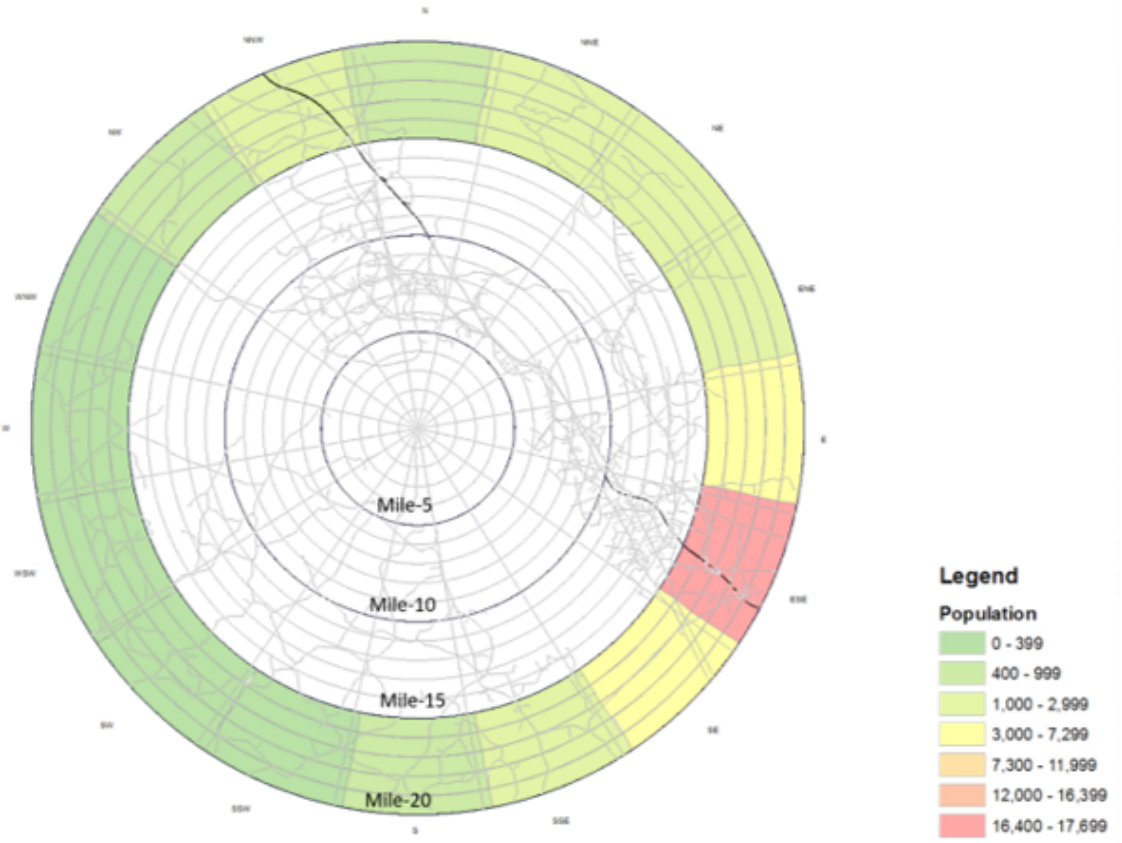

Figure 5-5 Medium Population Site Model Population Beyond the Shadow Region

When the model was built out to 18 miles or more, the DTA algorithm was “aware” of the restrictions and path selection did not significantly deviate from the base model paths. The ETE times from the 18-mile network were similar to the 19 and 20-mile networks because the model extent included enough of the 20-mile network to produce a similar DTA result within the EPZ. However, when the model truncation excluded some or all of these factors, the equilibrium paths within the EPZ were impacted. This resulted in the DTA algorithm assigning evacuees to paths, which may not have been representative of actual route choice behavior given the knowledge of the downstream network characteristics. This finding suggests that major population generators and changes in the roadway network characteristics need to be modeled to ensure the DTA algorithm can assign vehicles based on information that would be known to

the local population. For example, an evacuee may select (or not select) a path because it passes through a populated/congested area or if a path is known to have stretches of severe congestion (bottlenecks). Simulation models need to have these factors built in to them to inform the DTA and to allocate traffic in an appropriate and realistic manner.

Figures 5-6, 5-7, 5-8 show the medium population site cumulative percent evacuated at the 2-mile, 5-mile, and 10-mile rings, respectively. These figures are visual representations of the ETE process that led to the 90 percent and 100 percent ETE times in Table 5-2. Figure 5-6 shows no variation in the cumulative percent evacuated at the two-mile ring, regardless of the model extent. This was an expected finding because the DTA had only a limited number of vehicles and available paths leading out of this area and therefore the paths remain consistent with the base model. Figure 5-7 and Figure 5-8 show that models inclusive of the 18, 19, and 20-mile ring, have ETEs that are similar, whereas the models truncated at 15, 16, and 17 miles show more variation in the ETE, particularly for the 5-mile ring. This suggests that the paths selected for these models was different than those selected for the 18, 19, and 20-mile model truncations. These longer ETE times were not unexpected. The base model DTA paths were calibrated for the 20-mile model. If different paths are used, these vehicles could be routed improperly resulting in vehicles looping in the network or getting stuck or trapped. Calibrating the DTA paths used in the 15, 16, and 17-mile truncated network would have prevented these erroneous paths, but was not necessary for the Task 2 analysis. Showing that model extent has a significant impact on path selection was enough to achieve the goals of this task.

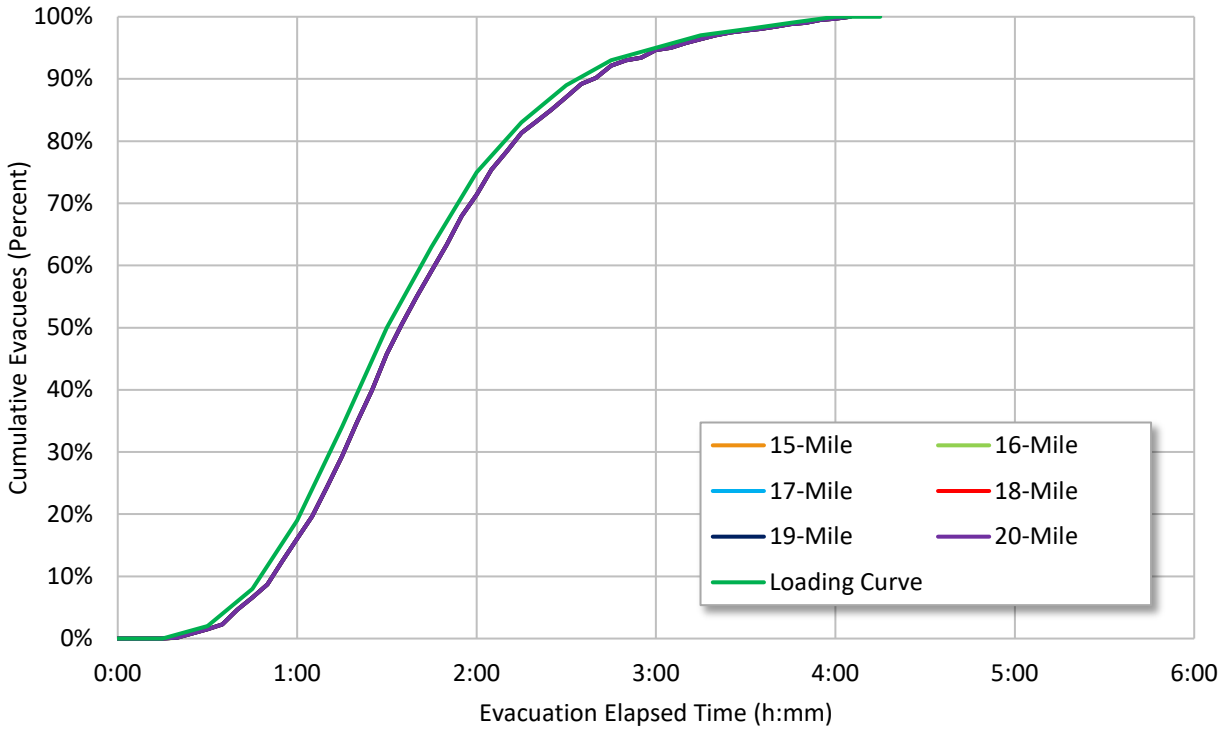

Figure 5-6 Two Mile ETE Curves, Medium Population Site Travel Distance Analysis

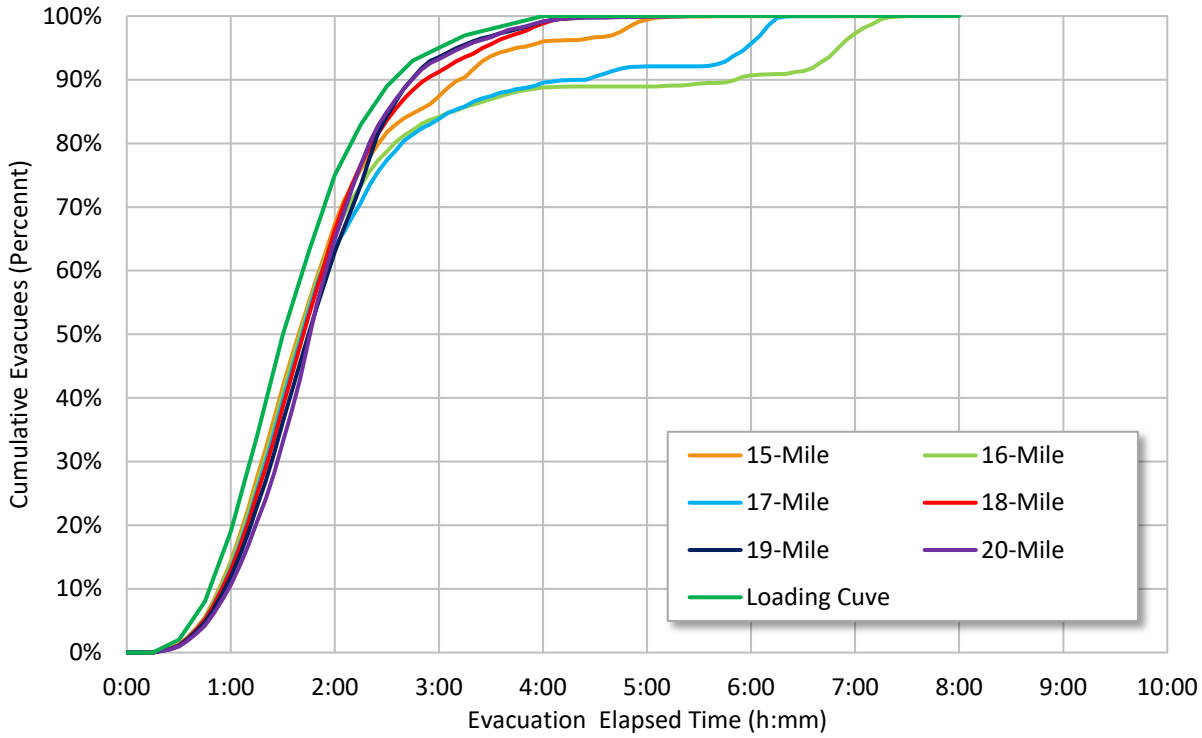

Figure 5-7 Five Mile ETE Curves, Medium Population Site Travel Distance Analysis

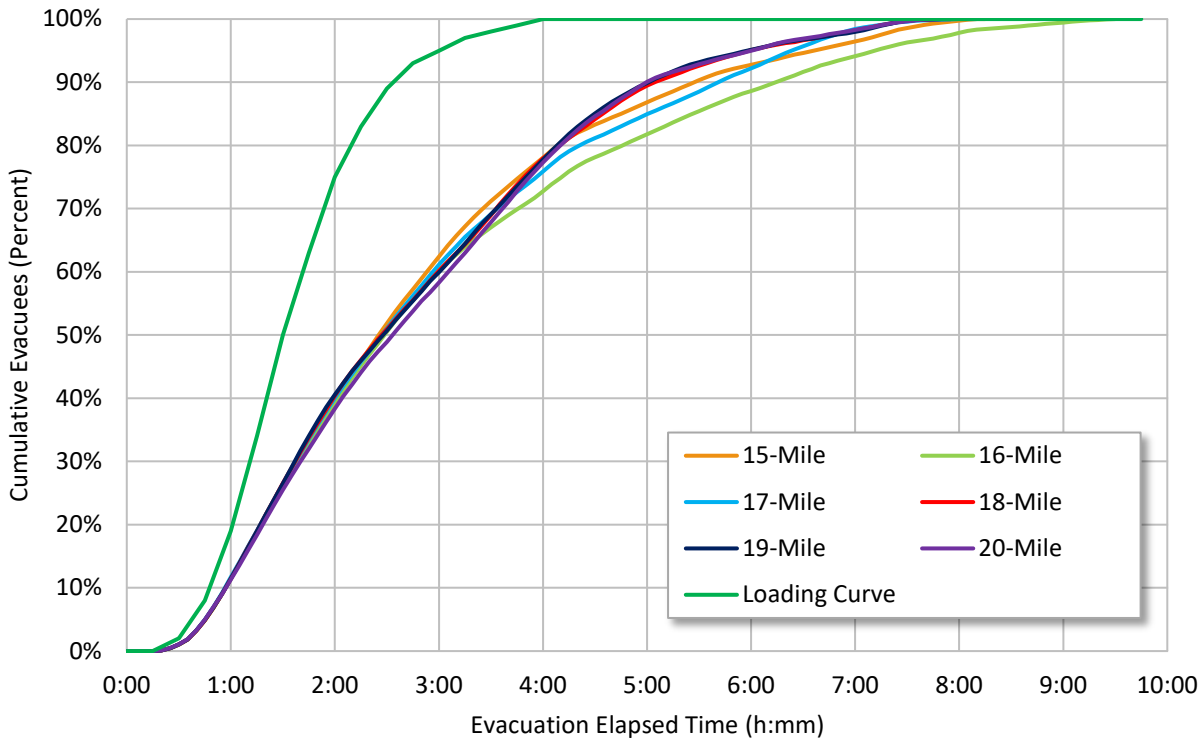

Figure 5-8 Ten Mile ETE Curves, Medium Population Site Travel Distance Analysis

5.2.2.1.3 Large Population Site Model ETE Results

The large population site average ETEs for the 2, 5, and 10-mile rings are shown in Table 5-3. The table shows that ETEs remained consistent between model sizes. This suggests the vehicle paths selected by the DTA algorithm within the EPZ did not vary significantly between model sizes. Table 5-3 also shows that the 5-mile 90 percent ETE was higher than the 10-mile 90 percent ETE. This was possible because the population density between the 5-mile and 10-mile ring is substantially higher than the population density within the 5-mile ring. Therefore, within the 5-mile ring, the number of vehicles that make up the ten percent tail of the evacuation is less than the 90 percent of the larger 10-mile ring population. This makes it possible to evacuate 90 percent of the population from the 10-mile ring while the 5-mile ring has not yet reached the same level percentage-wise.

Figure 5-9 and Figure 5-10 show the clearance time by sector and are consistent with the findings in Table 5-3. Figure 5-11 shows the large population site resident population, road network, and truncation distances beyond the 15-mile shadow region. High population areas in the east, east-southeast, and southeast sectors were anticipated to influence the route selection within the EPZ. However, consistent ETEs and clearances time values suggest that route selection within the EPZ was sufficiently similar to the base model to generate comparable ETEs. Given the extensive road network that exists beyond the EPZ boundary in the east, east-southeast, and southeast sector, it is likely that after exiting the network vehicles were routed away from high-density areas. Because of the diversity of path options that exist beyond the EPZ boundary in these sectors, evacuees were able to select the fastest route out of the EPZ and still avoid major population generators. Without such diversity of road network, this would not have been possible, as is demonstrated in the medium population site results.

Table 5-3 Large Population Site Average ETEs for Models of Varying Distance

Model Extent (miles)	2-Mile		5-Mile		10-Mile	
	90% ETE	100% ETE	90% ETE	100% ETE	90% ETE	100% ETE
15	4:20	8:42	6:31	9:17	6:17	10:10
16	4:20	8:10	6:37	9:35	6:25	10:16
17	4:58	8:47	6:28	9:37	6:20	10:20
18	3:57	8:27	6:12	9:36	6:16	9:56
19	4:03	8:20	5:23	10:06	5:53	10:28
20	4:11	8:26	6:10	9:35	6:15	10:13

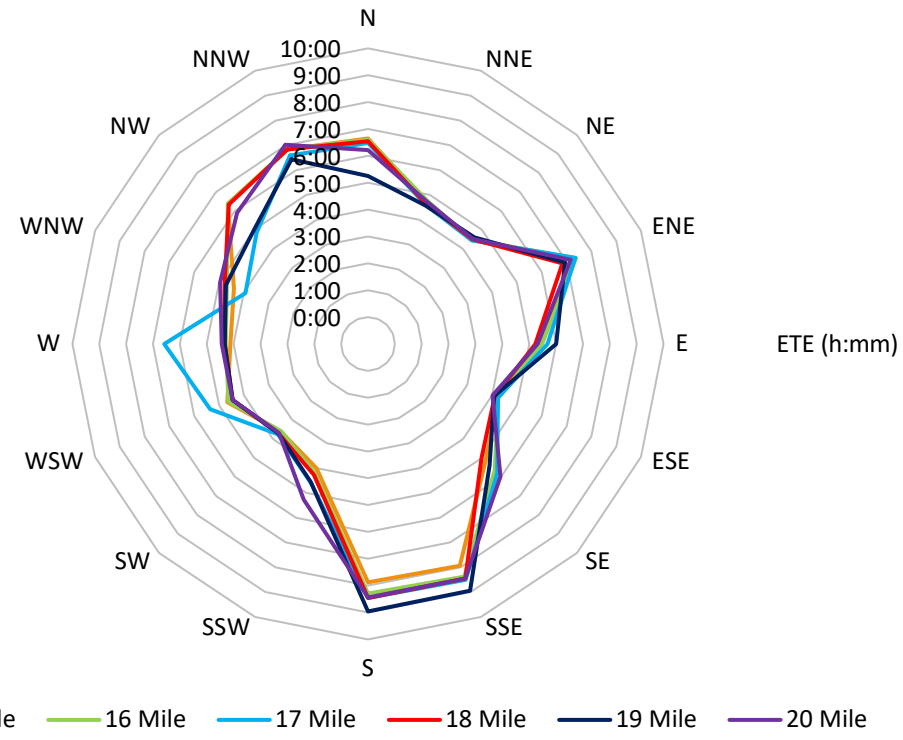

Figure 5-9 Ten Mile 90 Percent ETE by Sector, Large Population Site Travel Distance Analysis

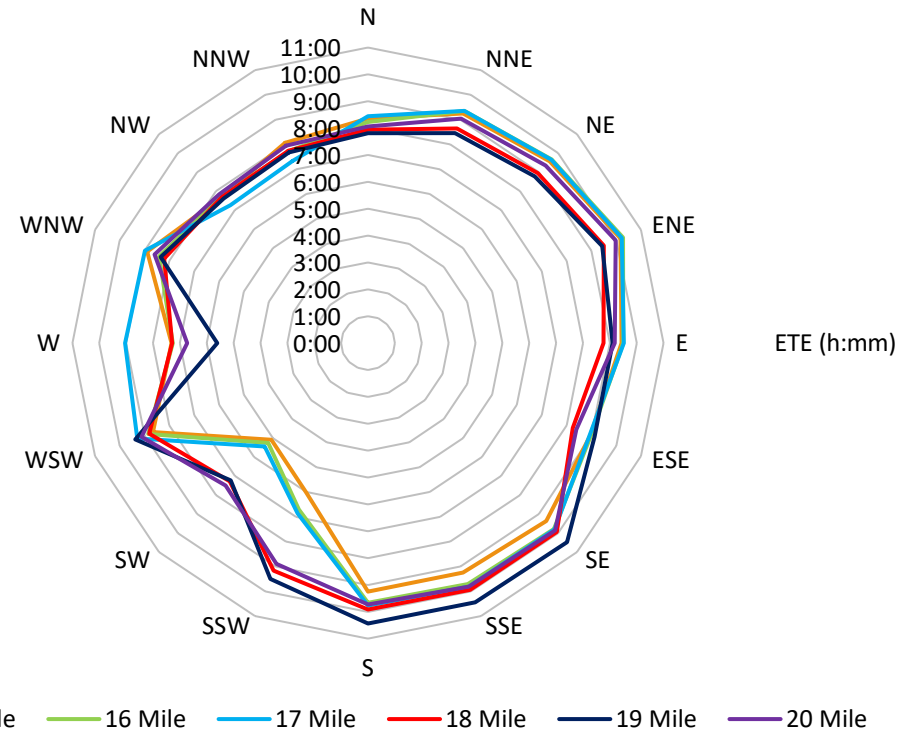

Figure 5-10 Ten Mile 100 Percent ETE by Sector, Large Population Site Travel Distance Analysis

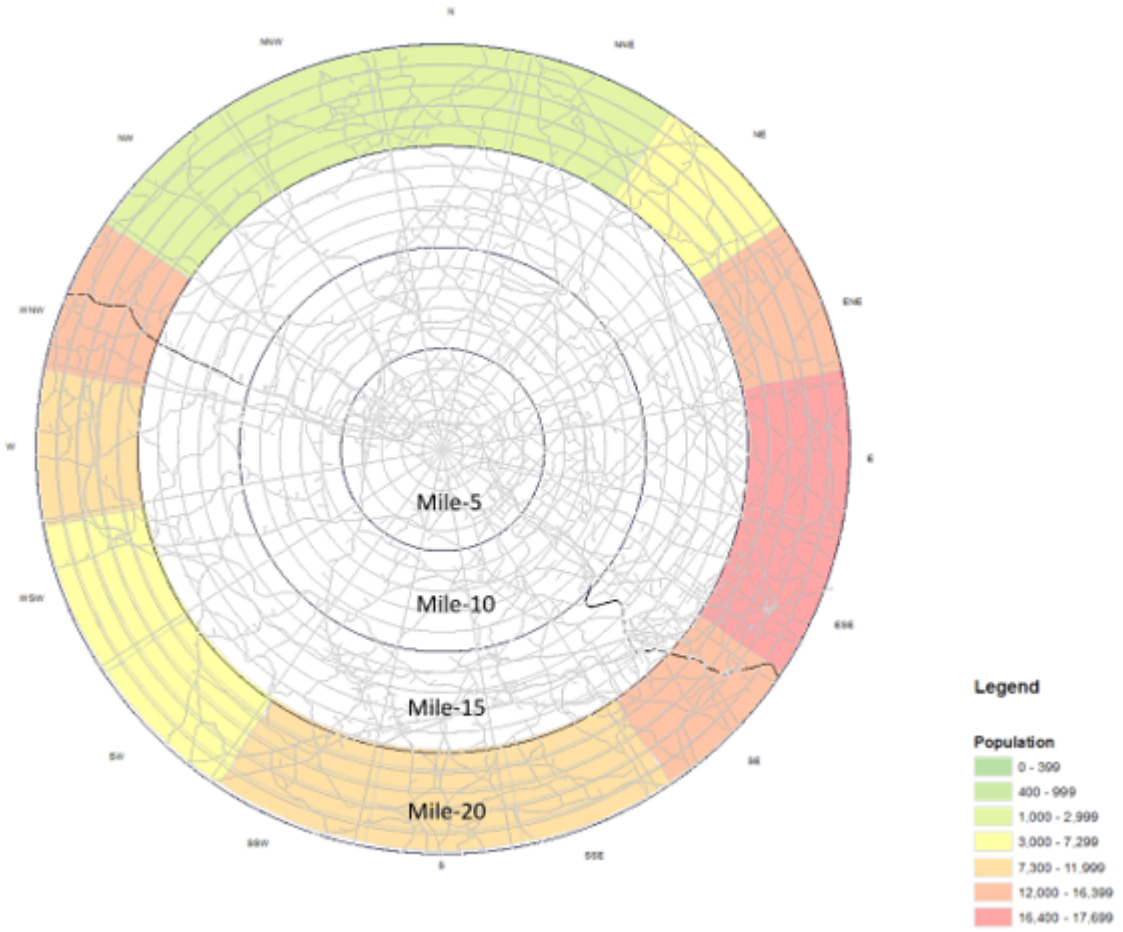

Figure 5-11 Large Population Site Model Population Beyond the Shadow Region

Figure 5-12, Figure 5-13, and Figure 5-14 show the cumulative percentage evacuated at the 2, 5 and 10-mile rings, respectively, for the large population site. These figures suggest that not only are the 90 percent and 100 percent ETEs consistent between models, but the entire evacuation process was generally consistent with similar percentages of the population exiting the EPZ at approximately the same time. This could only occur if the paths used to exit the EPZ were similar in each model. Some significant variation can be seen in the 2-mile ring when the model was truncated at 17-miles, however this is not reflected in the 5 and 10-mile rings for that model. Such variations could indicate fluctuations in the level of congestion and route selection, or may be the result of the randomness of the simulation software. In either event, these fluctuations were not significant to the evacuation process within in the EPZ overall. Additionally, as seen in the results of the shadow evacuation analysis, in general the impact from model extent is observed mostly during a narrow window of the evacuation time, between 60 to 90 percent cumulative evacuation.

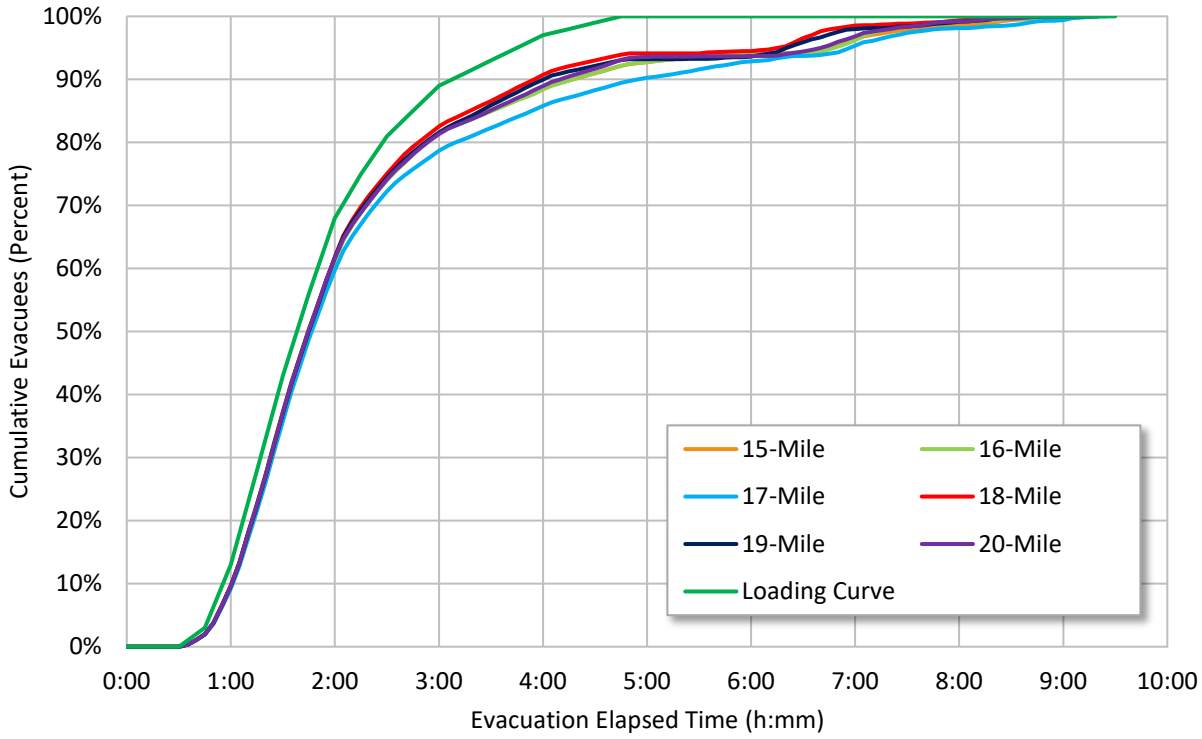

Figure 5-12 Two Mile ETE Curves, Large Population Site Travel Distance Analysis

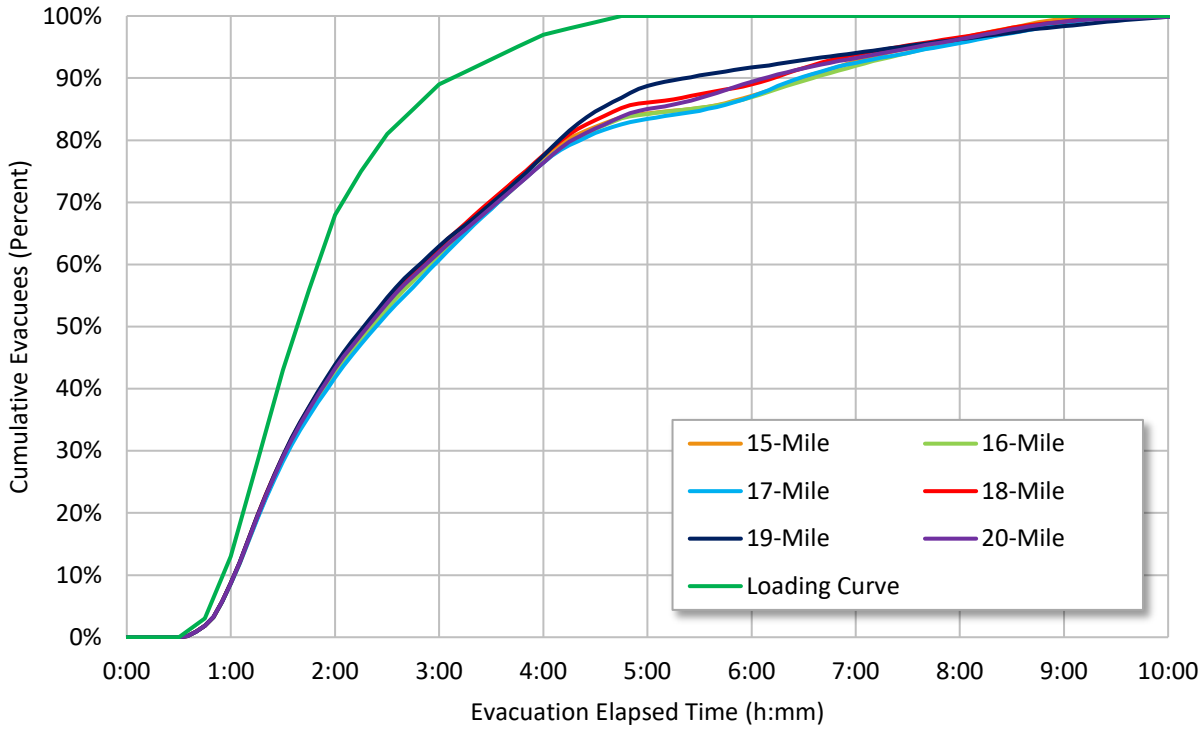

Figure 5-13 Five Mile ETE Curves, Large Population Site Travel Distance Analysis

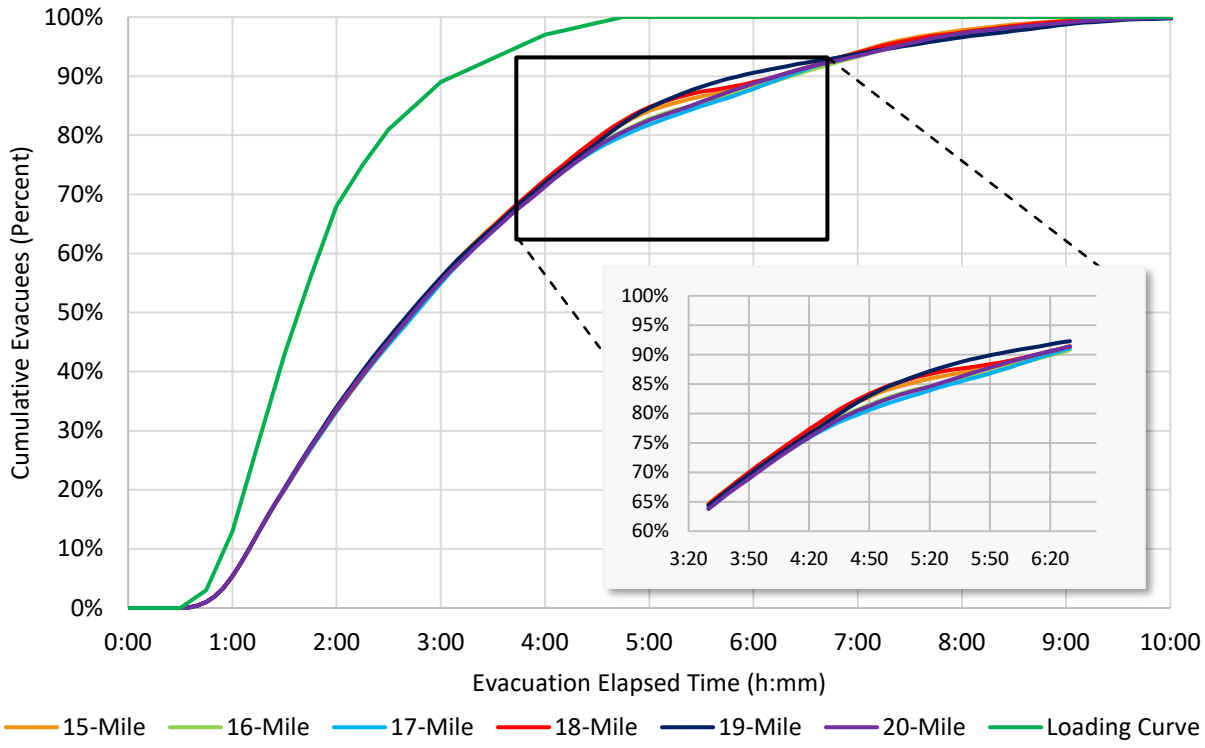

Figure 5-14 Ten Mile ETE Curves, Large Population Site Travel Distance Analysis

5.2.2.2 Average Travel Speed Results

The average travel speed of vehicles exiting the EPZ at the 10-mile ring was grouped into 16 compass sectors (N, NNE, NE, ENE, E, etc.). These average speeds are shown at various time periods into the simulation to illustrate the progression of the evacuation event. Speed decreases signify congestion at the interface of the EPZ and shadow region. This analysis may indicate whether bottlenecks beyond the shadow region were influencing traffic behavior within the EPZ. In such a case, models that incorporate this bottleneck would have a distinct speed drop whereas models that excluded the bottleneck would not. The average speed analysis may also indicate when the DTA was changing the route selection between the truncated models. If the DTA was shifting vehicles within the EPZ due to traffic patterns outside the EPZ, then routes that received higher volumes of vehicles would show lower speeds and vice versa. This would result in a diverse range of speeds between the truncated models as opposed to a single distinct drop as would be the case in the event of a bottleneck.

5.2.2.2.1 Small Population Site Model Average Travel Speed Results

Figure 5-15 and Figure 5-16 show the average travel speed in the small population site at 0:15 and 1:45 into the evacuation, respectively, for 15, 16, 17, 18, 19, and 20-mile ring truncations. The average speeds at 0:15 are indicative of free-flow conditions and exemplify the “best case” scenario within each sector. Varying model size should not have an impact on the free-flow speed. The results shown in Figure 5-15 confirm this. Figure 5-16 was taken at 1:45 into the evacuation when most of the evacuees were loaded onto the road network.

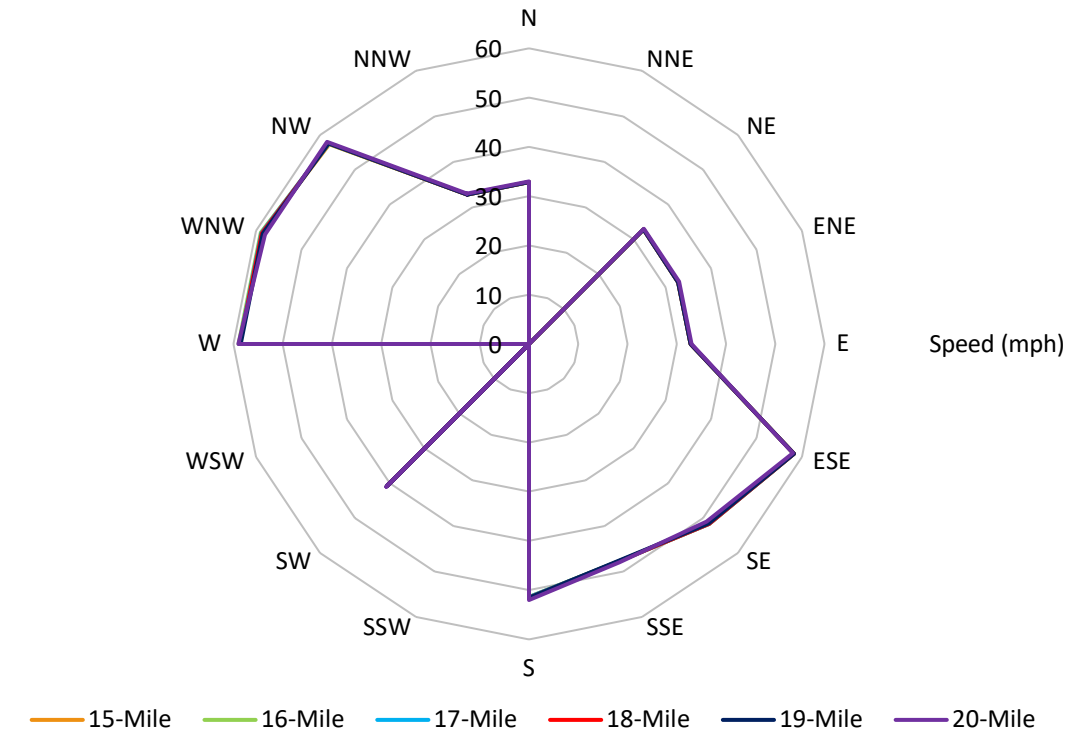

Figure 5-15 Average Speeds at 0:15, Small Population Site Travel Distance Analysis

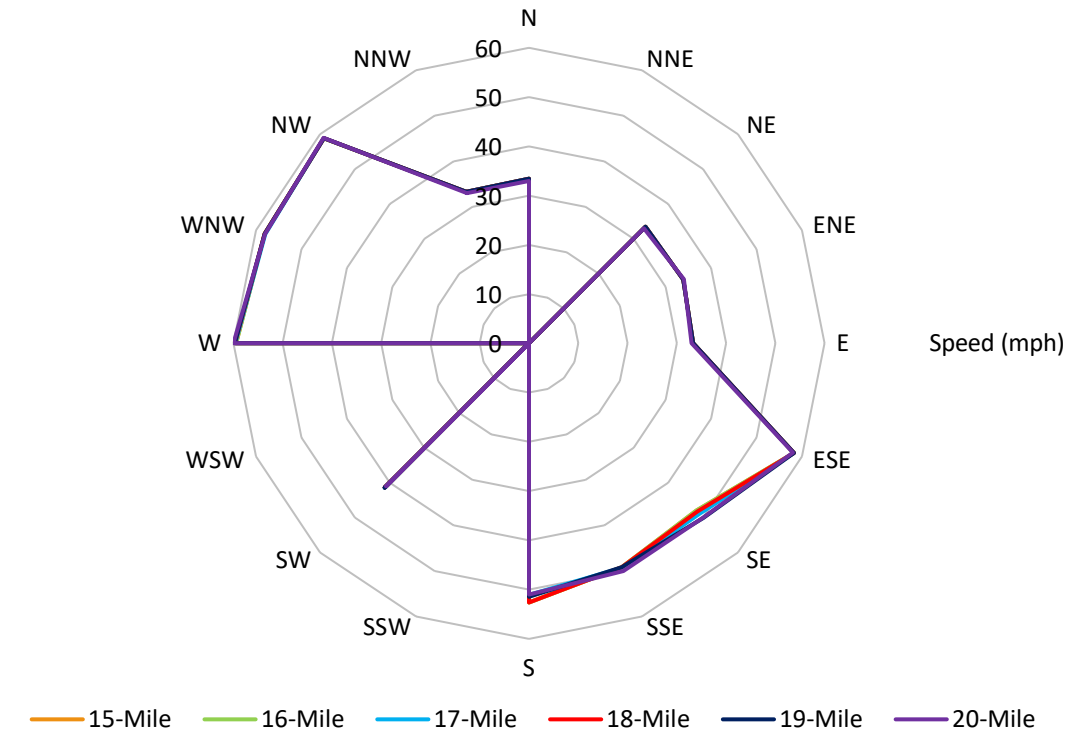

Figure 5-16 Average Speeds at 1:45, Small Population Site Travel Distance Analysis

In general, the model truncation produced average speed lines that overlap with the base model, indicating no impact. A slight speed discrepancy was seen in the southeast and south sectors. However, this speed difference was less than a few miles per hour and likely resulted from the stochastic nature of the model.

5.2.2.2.2 Medium Population Site Model Average Travel Speed Results

Figure 5-17, Figure 5-18, and Figure 5-19 show the average travel speed in the medium site model at 2:30, 3:30, and 4:30 into the evacuation, respectively, for 15, 16, 17, 18, 19 and 20-mile ring truncations. These times correspond to when most of the evacuees were loaded onto the road network. The figures show a wide diversity of average speeds exiting the EPZ when the model was truncated at various lengths. As the model extends outward, there is an increase in background traffic, which could be slowing down evacuees leaving the EPZ. Also, the DTA may be allocating vehicles to different exits of the EPZ in an attempt to avoid congestion that exists outside the EPZ. This was important because it suggests the model extent plays a significant role in DTA path selection within the EPZ. It should be re-emphasized that the DTA is attempting to optimize route choice for the entire model extent, not just within the EPZ.

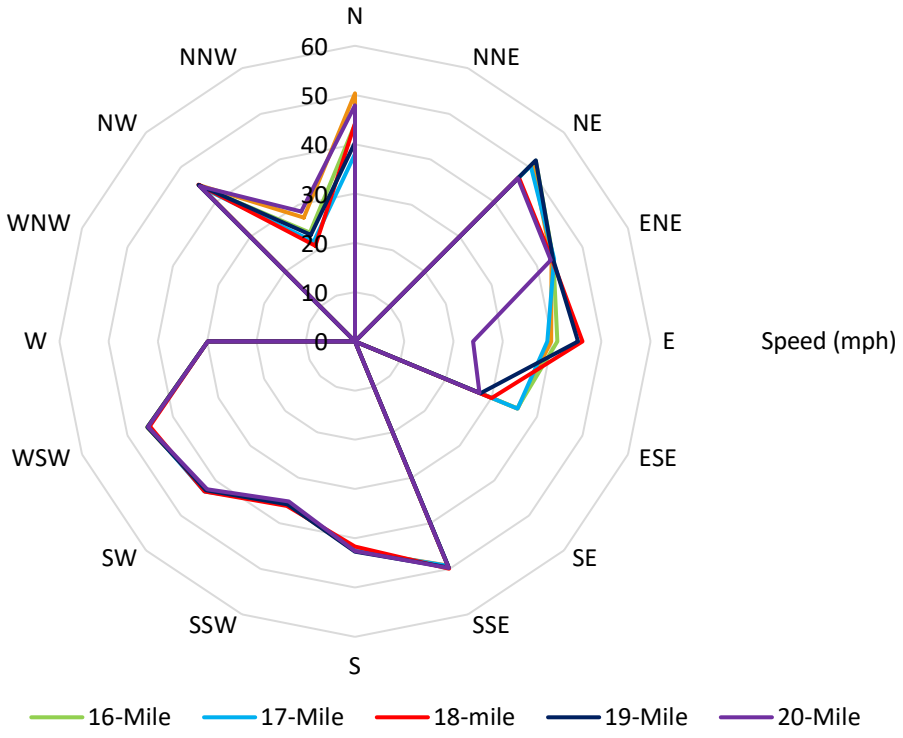

Figure 5-17 Average Speeds at 2:30, Medium Population Site Travel Distance Analysis

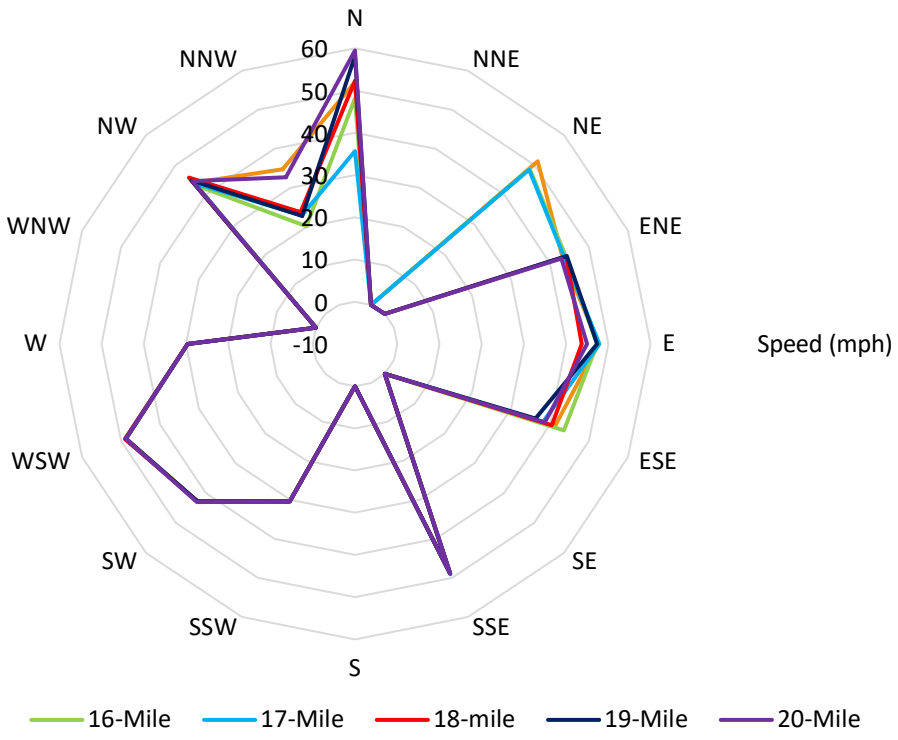

Figure 5-18 Average Speeds at 3:30, Medium Population Site Travel Distance Analysis

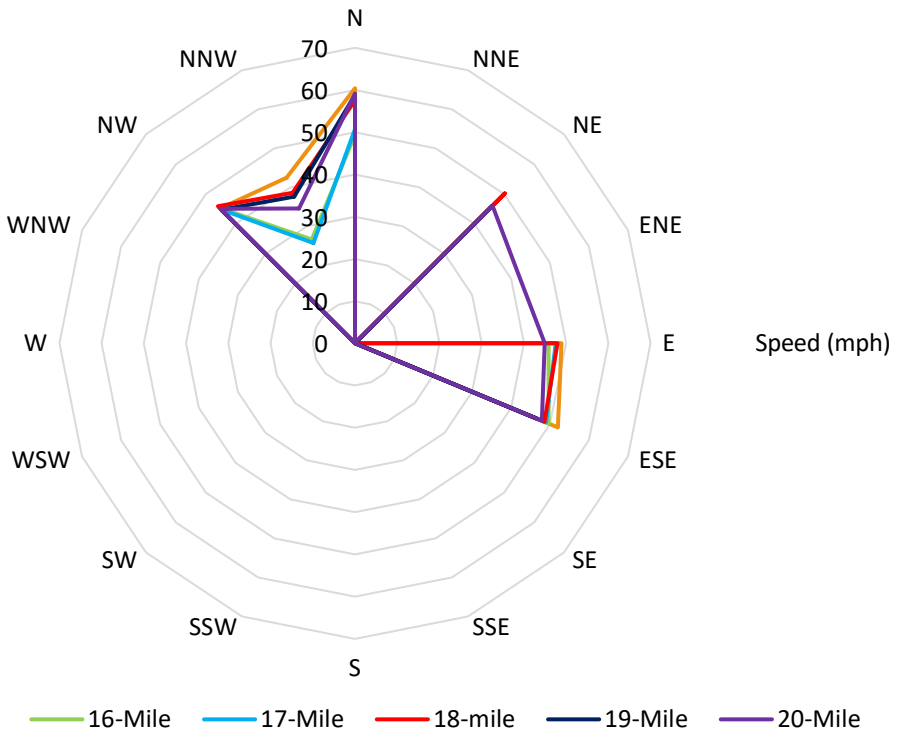

Figure 5-19 Average Speeds at 4:30, Medium Population Site Travel Distance Analysis

5.2.2.2.3 Large Population Site Model Average Travel Speed Results

Figure 5-20, Figure 5-21, and Figure 5-22 show the average travel speed in the large site model at 2:30, 3:30, and 4:30 into the evacuation, respectively, for 15, 16, 17, 18, 19 and 20-mile ring truncations. These times correspond to when most of the evacuees were loaded onto the road network. In general, the figures show consistent average speeds exiting the EPZ. This may suggest that vehicle paths within the EPZ were not significantly impacted by the model size and that congestion patterns were fairly consistent. Some variations were seen in the south and west-northwest sectors but were not evident until the model extent approached 19 miles. As the model extends outward, the decrease in speeds in the south and west quadrants shown in Figure 5-22 is likely due to a combination of factors including additional background vehicles, and additional intersections and traffic controls at intersections. The persistence of congestion at 4:30 into the evacuation can be seen in the speeds of the extended models as compared to the results of the 15-mile truncated model that shows an increase in speeds to the south, indicating an earlier ease in congestion.

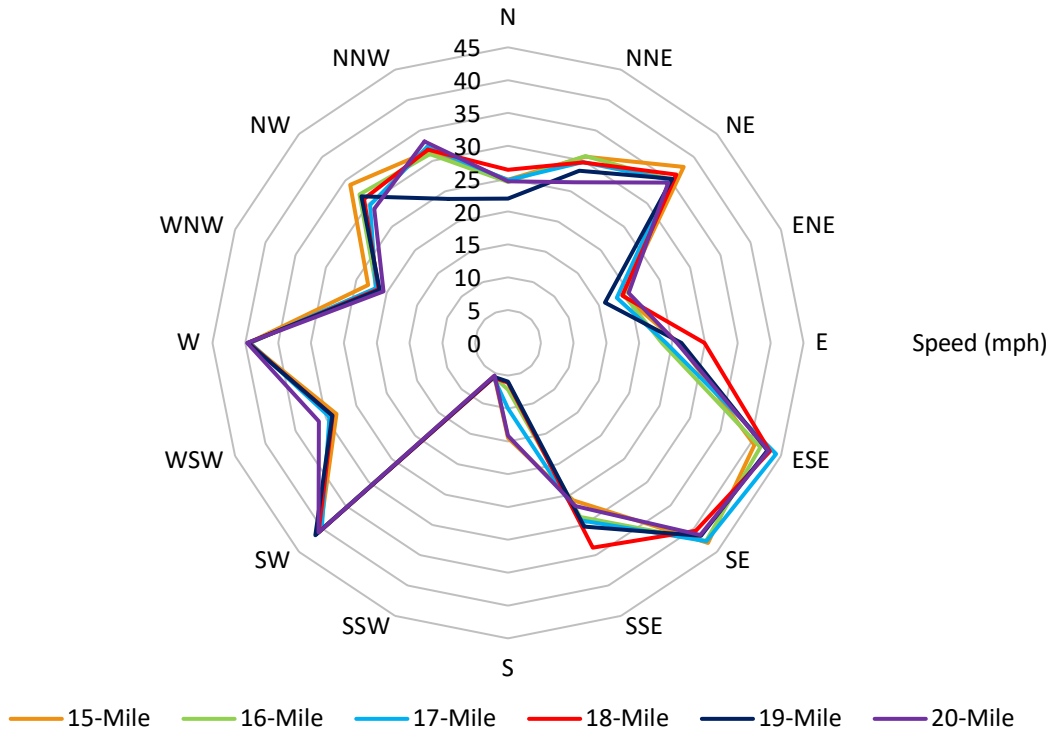

Figure 5-20 Average Speeds at 2:30, Large Population Site Travel Distance Analysis

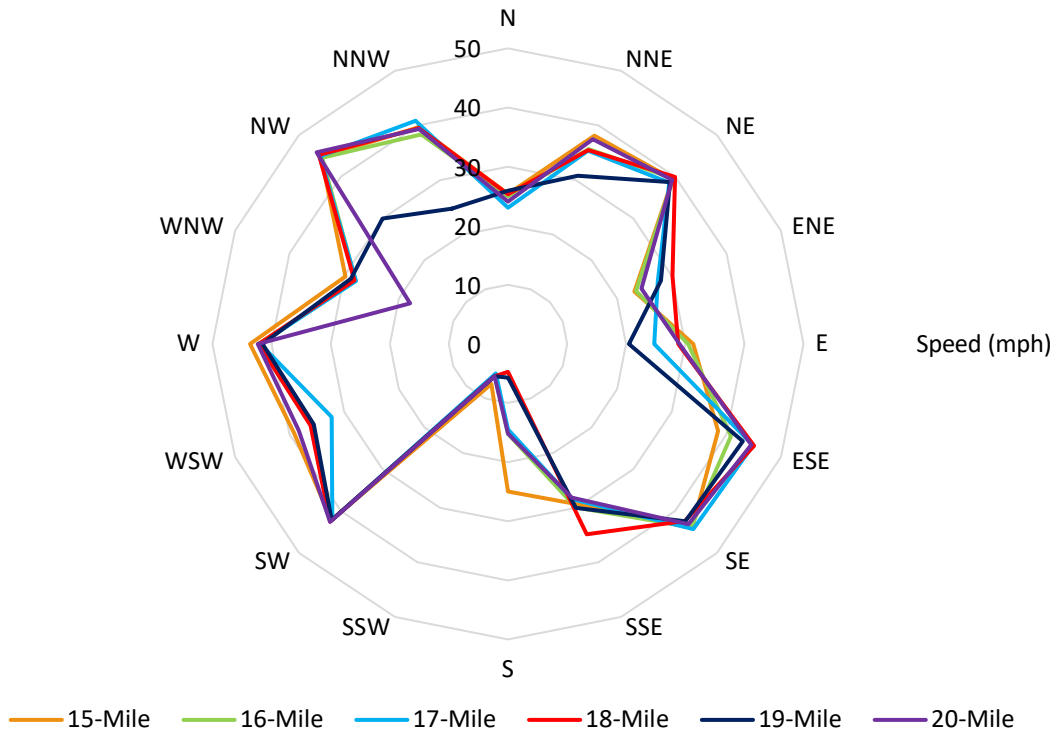

Figure 5-21 Average Speeds at 3:30, Large Population Site Travel Distance Analysis

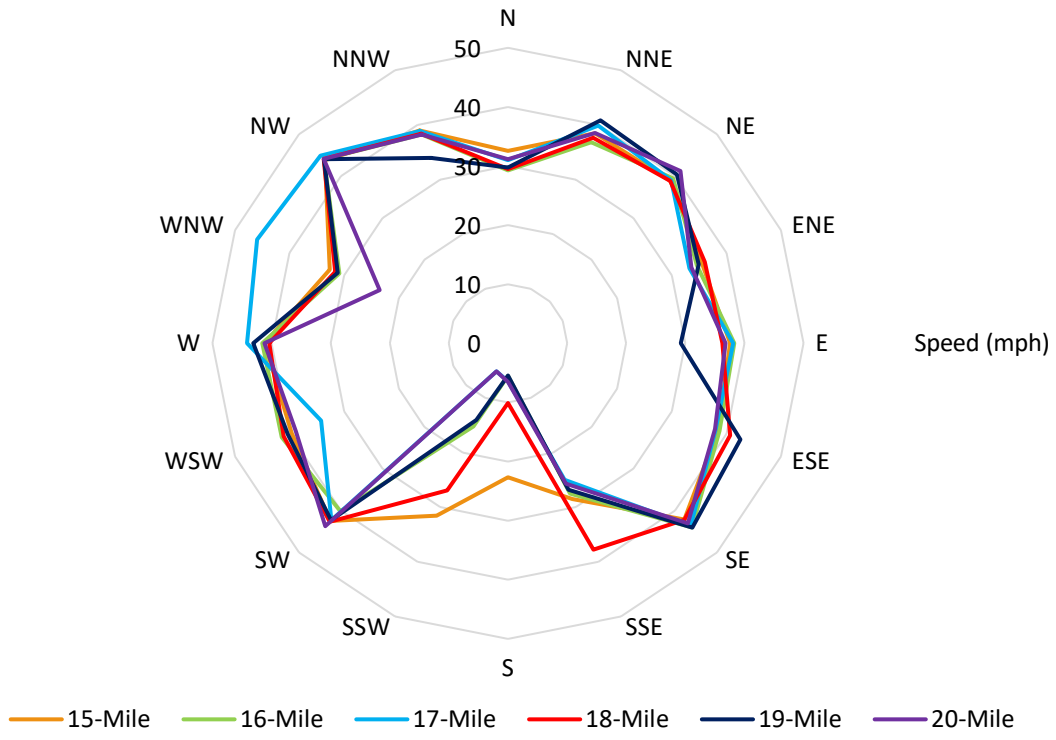

Figure 5-22 Average Speeds at 4:30, Large Population Site Travel Distance Analysis

5.2.2.3 EPZ Exit Flow Rate Results

The EPZ exit flow rate is the number of vehicles that exited the 10-mile EPZ over each 5-minute data collection interval. This flow rate was converted into vehicles per hour to be consistent with the standard practices of traffic engineering. Fundamentally, the 10-mile EPZ exit flow rate measured the diffusion of evacuation vehicles out of the EPZ and into the shadow evacuation region. It was expected that if the size of the model impacted the ability of evacuees to exit the EPZ, then discrepancies in the exit flow rate could be identified using this analysis.

5.2.2.3.1 Small Population Site Model EPZ Exit Flow Rate Results

Figure 5-23 shows the small population site exit volumes at the 10-mile ring resulting from truncations at 15, 16, 17, 18, 19-miles and the base model (20-mile) flow rates. The figure shows significant overlap between the models. Variations in exit flow rates are not systematically impacted by the model extent and likely resulted from the stochasticity of the simulation software.

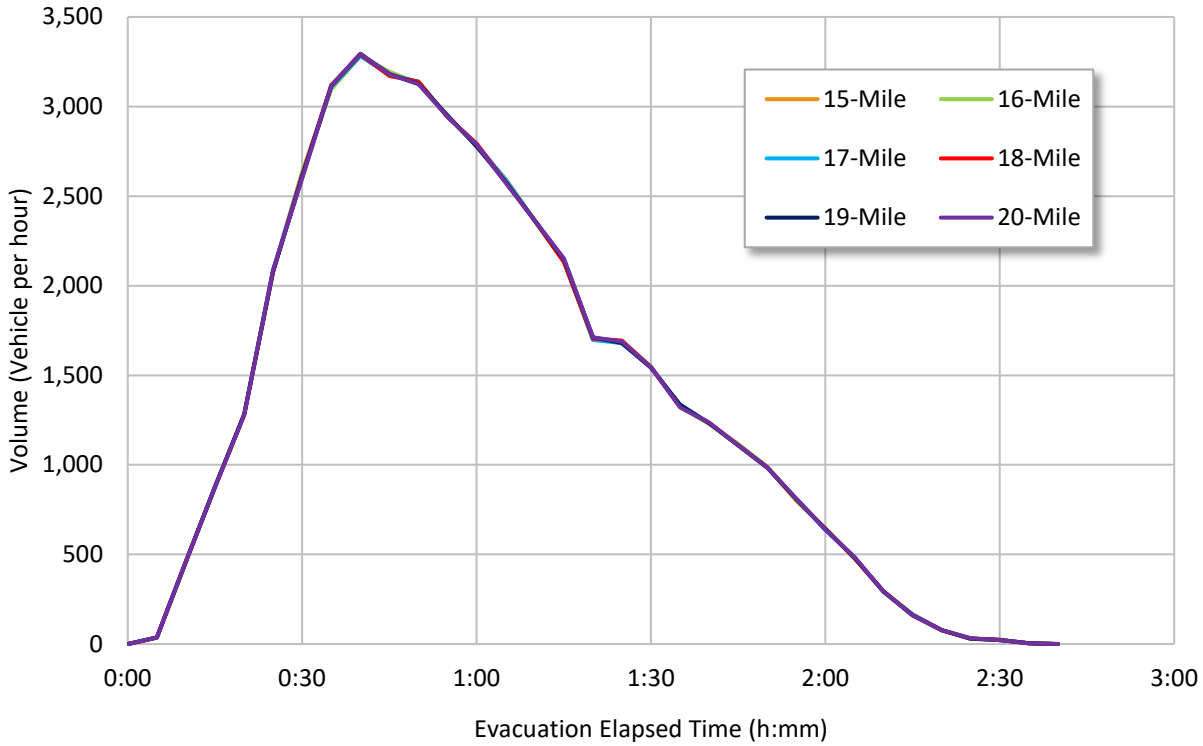

Figure 5-23 EPZ Exit Volumes, Small Population Site Travel Distance Analysis

5.2.2.3.2 Medium Population Site Model EPZ Exit Flow Rate Results

Figure 5-24 shows the medium population site exit volumes at the 10-mile ring resulting from truncations at 15, 16, 17, 18, 19-miles and the base model (20-mile) flow rates. The figure shows a diverse range of exit rates between models of different sizes. This was likely the result of the DTA shifting routes between models in response to added demand and is consistent with the clearance time and average speed results.

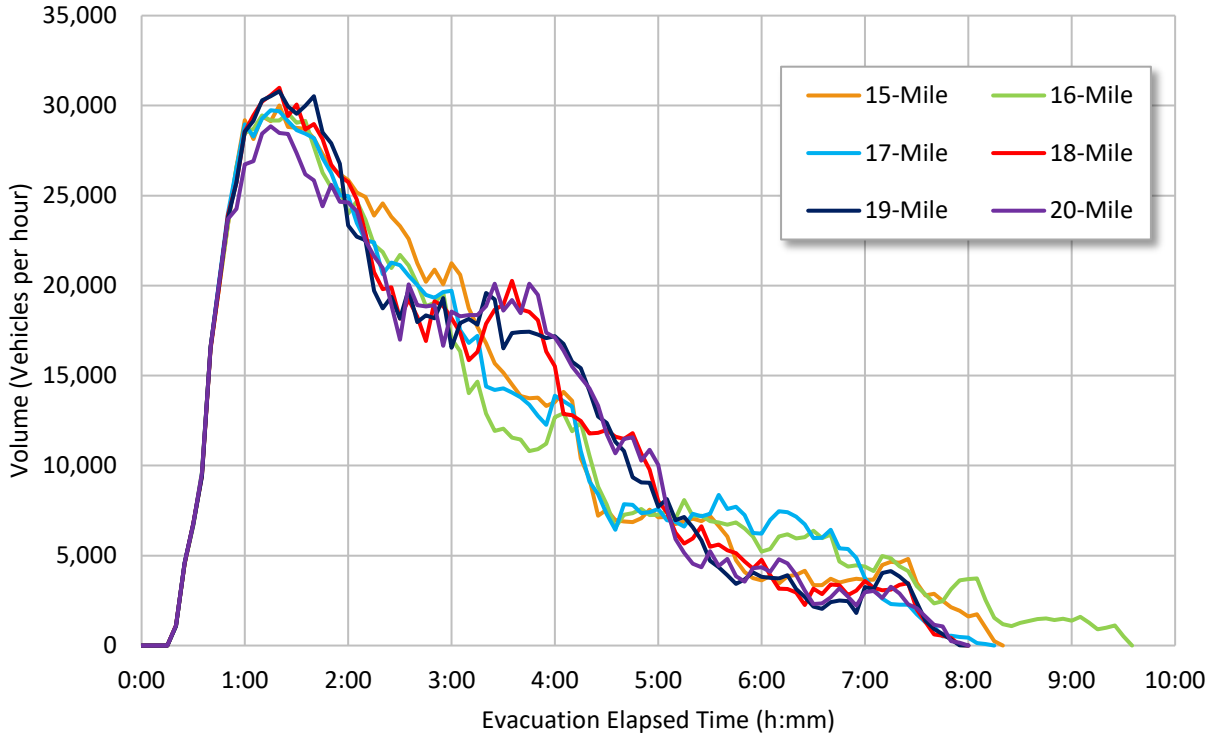

Figure 5-24 EPZ Exit Volumes, Medium Population Site Travel Distance Analysis

5.2.2.3.3 Large Population Site EPZ Exit Flow Rate Results

Figure 5-25 shows the large population site exit volumes at the 10-mile ring resulting from truncations at 15, 16, 17, 18, and 19-miles and the base model (20-mile) flow rates. The figure shows significant overlap between the models. This further supports the finding that paths within the EPZ of the large population site were not significantly impacted by the model truncations.

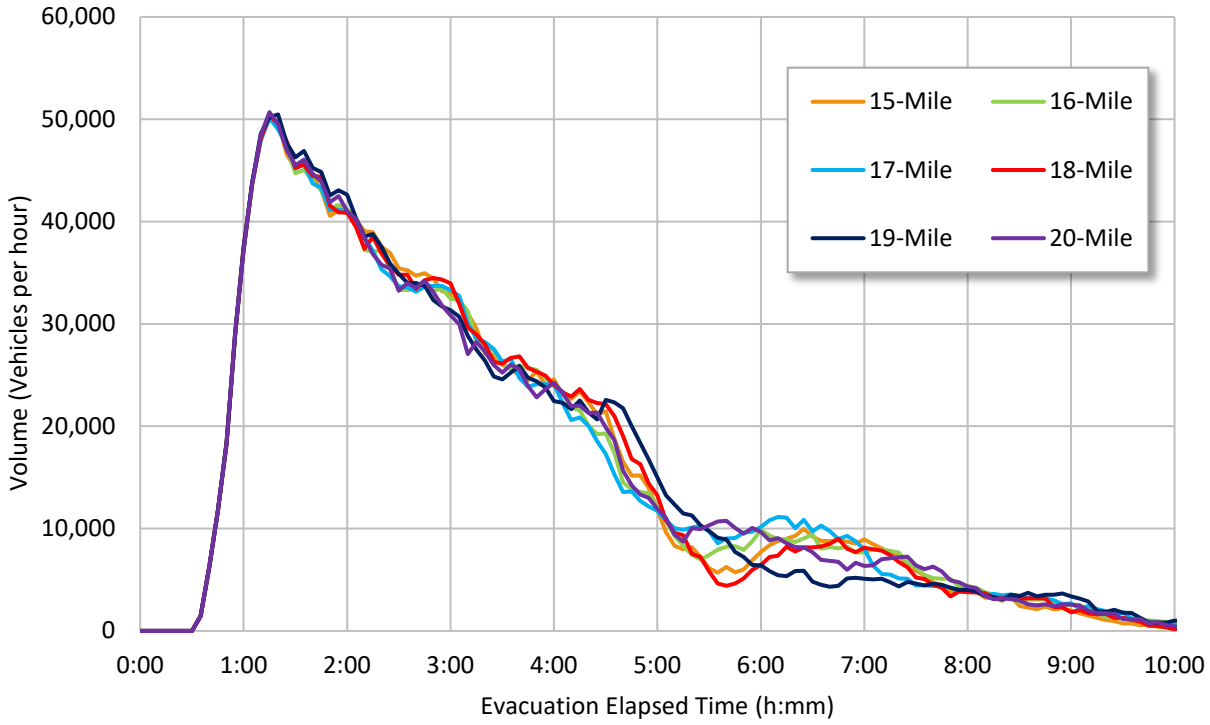

Figure 5-25 EPZ Exit Volumes, Large Population Site Travel Distance Analysis

5.2.2.4 Travel Time Results

Travel time can be used to estimate the generalized cost of a link or path as seen by the DTA algorithm. Travel times beyond the EPZ were collected and analyzed to determine the value of such information for inclusion in ETE reports. Travel time collectors were placed on major evacuation routes departing the EPZ in each model. Travel times were collected between the 10-mile ring and the 15, 16, 17, 18, 19, and 20-mile rings for each truncated model. It was expected that as the model size increased, the average travel time would also increase representing a longer distance traveled. In an uncongested model, this travel time increase would be linear (constant rate of change) and representative of free-flow conditions. If significant congestion was present on a route, the travel time would likely increase with model size, but in a non-linear fashion. Travel time decreases could occur and would indicate a change in the DTA path selection between model truncations. This is because the only way to increase the length of a road while at the same time decrease the travel time is to allocate fewer vehicles to it and thus reduce the congestion.

5.2.2.4.1 Small Population Site Model Travel Time Results

Travel time collectors were placed on major routes in the west and east regions of the small population model. These routes were selected because they were predominately used by evacuees and span the network between the 10 and 20-mile rings. Table 5-4 and Table 5-5 show the results for the west and east routes, respectively. Each row represents the travel time in seconds beginning at the 10-mile ring and ending at another ring within the model. Each column represents the travel time value taken from each of the truncated models. It was not possible to collect travel times in the truncated portion of the network and therefore these values are blank within the table.

The travel times presented in Table 5-4 and Table 5-5 show steadily increasing travel time as the small population site model size increased. The small population site utilized static route choice and was predominately uncongested. As would be expected, the travels times shown were representative of a model with minimum congestion and no deviation in route choice. Any bottlenecks that may have been considered in the model, as the model increased in size, did not have a significant impact on route travel time.

Table 5-4 Small Population Site Travel Times, Major Route in West-Southwest Sector

Segment	Travel Time (seconds)					
	20-Mile (Base)	19-Mile Truncation	18-Mile Truncation	17-Mile Truncation	16-Mile Truncation	15-Mile Truncation
10 to 20	898					
10 to 19	824	823				
10 to 18	755	755	754			
10 to 17	695	695	692	687		
10 to 16	587	586	585	582	584	
10 to 15	460	458	457	458	458	458

Table 5-5 Small Population Site Travel Times, Major Route in East-Southeast Sector

Segment	Travel Time (seconds)					
	20-Mile (Base)	19-Mile Truncation	18-Mile Truncation	17-Mile Truncation	16-Mile Truncation	15-Mile Truncation
10 to 20	683					
10 to 19	626	624				
10 to 18	549	548	549			
10 to 17	470	470	470	470		
10 to 16	391	391	391	391	391	
10 to 15	329	329	329	329	329	329

5.2.2.4.2 Medium Population Site Model Travel Time Results

Travel time collectors were placed on major routes leading out of the medium population model EPZ in the east-southeast and west-northwest directions. These routes are bolded in Figure 5-5 and show the assumed resident population and road network that was modeled beyond the EPZ. The paths selected for the travel time analysis were chosen because they were major routes out of the EPZ, carried predominately evacuee traffic, and led in the direction of major population generators.

Table 5-6 shows the travel time on the east-southeast route leading away from the NPP. The travel time between the 10-mile ring and 15-mile ring tripled from 316 seconds to 1067 seconds when the model was extended from 15 miles to 20 miles in radius. This suggests significantly higher levels of congestion, as the model grew in size. This was likely the result of increased background traffic and more vehicles being routed to this link because of the limited number of available alternative routes. This has the potential to significantly change the path selections within the EPZ and impact ETE times.

Table 5-6 Medium Population Site Travel Times, Major Route in East-Southeast Sector

Segment	Travel Time (seconds)					
	20-Mile (Base)	19-Mile Truncation	18-Mile Truncation	17-Mile Truncation	16-Mile Truncation	15-Mile Truncation
10 to 20	1,690					
10 to 19	1,627	1,333				
10 to 18	1,544	1,263	960			
10 to 17	1,489	1,204	899	445		
10 to 16	1,325	1,070	803	389	374	
10 to 15	1,067	915	700	331	316	316

Table 5-7 Medium Population Site Travel Times, Major Route in North-Northwest Sector

Segment	Travel Time (seconds)					
	20-Mile (Base)	19-Mile Truncation	18-Mile Truncation	17-Mile Truncation	16-Mile Truncation	15-Mile Truncation
10 to 20	938					
10 to 19	876	866				
10 to 18	787	777	797			
10 to 17	711	707	726	735		
10 to 16	643	643	665	667	438	
10 to 15	567	561	580	590	387	392

Table 5-7 shows the travel time on a major route in the north-northwest portion of the medium population site. The population in this area increased as evacuees leave the EPZ. The travel times corresponding to the 15 and 16-mile network show minimal congestion. However, models built out to 17 miles or more experience moderate congestions levels. This likely played a role in the path selection within the EPZ and could account, in part, for the differences seen in the ETEs.

5.2.2.4.3 Large Population Site Model Travel Time Results

Travel time collectors were placed on major routes exiting the large population EPZ toward the southeast and west-northwest directions. These routes are bolded in Figure 5-11 and show the assumed resident population and road network that was modeled beyond the EPZ. These paths were selected because they were major routes out of the EPZ, carried predominately evacuee traffic, and led in the direction of major population generators. Furthermore, the west-northwest path experiences a major bottleneck at approximately 18 miles from the NPP, generating significant congestion at this location. This bottleneck is primarily the result of a series of traffic lights along the route.

Table 5-8 shows the travel times on the southeast route to various distances within each of the truncated models. The travels times were indicative of moderate congestion and in general, were increasing. However, when the model was extended to the 20-mile ring, the travel times decreased. This suggests that as the model extended into the more populated southern region, the DTA selected paths that would alleviate some of this congestion by spreading the traffic demand to other routes. Because the majority of this route appears to be operating efficiently, it

was likely the alternative routes selected did not vary drastically from those of the preceding models until it reached the 18 or 19-mile rings.

Table 5-8 Large Population Site Travel Times, Major Route in South-East Sector

Segment	Travel Time (seconds)					
	20-Mile (Base)	19-Mile Truncation	18-Mile Truncation	17-Mile Truncation	16-Mile Truncation	15-Mile Truncation
10 to 20	912					
10 to 19	836	841				
10 to 18	743	747	752			
10 to 17	662	670	674	654		
10 to 16	595	606	609	590	584	
10 to 15	526	532	535	516	511	515

Table 5-9 Large Population Site Travel Times, Major Route in West-Northwest Sector

Segment	Travel Time (seconds)					
	20-Mile (Base)	19-Mile Truncation	18-Mile Truncation	17-Mile Truncation	16-Mile Truncation	15-Mile Truncation
10 to 20	4,915					
10 to 19	4,321	4,500				
10 to 18	4,137	4,239	1,718			
10 to 17	3,406	3,608	804	810		
10 to 16	2,094	2,083	707	728	675	
10 to 15	1,237	862	589	599	575	570

Table 5-9 shows the travel times on the west-northwest route to various distances within each of the truncated models. In general, the travel times corresponding to a model extending out 18 miles or less showed only moderate congestion. However, when the model was built out beyond 18 miles, severe congestion resulted in excessively long travel times. This was caused, in part, by a bottleneck, which persisted beyond the 18-mile ring due to a series of traffic lights. The inclusion of this bottleneck likely contributed to the drastic rise in travel time on this route. It was expected that such a rise in travel time would prompt the DTA to select alternative paths. However, this route is a high capacity route, and unlike the east, east-southeast, and southeast sectors, it did not have many alternatives likely making the congestion unavoidable.

As the modeled distance was increased, the DTA algorithm attempted to balance the proportion of vehicles allocated to this route. Approximately 19,500 vehicles traveled along the main route, but when the model was built to 17 miles, prior to crossing the 15-mile boundary, the DTA routed approximately 4000 more vehicles to the adjoining west-southwest. However, this only eased congestion along the west-northwest route temporarily, because as the model was extended further, the traffic routed to the west-southwest could take northerly routes and ultimately rejoin the west-northwest traffic. As such, the DTA again adjusted travel volumes keeping most of the exiting vehicles on the main west-northwest route.

When the model was built out to 19 miles, travel times increase non-linearly. This increase in travel time was due to a number of factors including an increased numbers of traffic lights,

circuitous routes for some evacuee vehicles, as well as increasing numbers of background vehicles from densely populated surrounding areas. However, because of the bottleneck location, seven to eight miles past the 10-mile ring, the congestion did not impact the ETE, travel speeds, or exit flow rate.

5.2.3 Analysis Findings

This section highlights the results found in the Task 2 analysis and presents it within the broader context of the research goals.

5.2.3.1 Small Population Site Model

The small population site utilized static route choice that allowed quantification of model extent without any influence from the DTA algorithm. Therefore, any influence of traffic patterns within the EPZ would have to originate beyond the shadow region and propagate backward a distance greater than five miles. While this level of queue propagation is often seen in hurricane evacuations which generate hundreds of thousands of evacuees, an NPP emergency evacuation is unlikely to generate demand necessary to propagate several miles back upstream into an EPZ. The number of evacuating vehicles from even the largest of NPP sites is much smaller in comparison to the evacuation that can be generated from a hurricane.

For the small population site, the 100 percent ETE resulting from the traffic model built out to 20 miles was 2:31, matching that of the 15-mile model. Furthermore, an analysis of average speed and flow rate of vehicles leaving the EPZ showed no significant change in performance, regardless of model size. From this analysis, there would appear to be no significant benefit captured by modeling a small population site out to 20 miles when compared to a model completed to 15 miles. These results suggest two primary conclusions: 1) the road network geometry of the area beyond the small population site shadow region did not have significant capacity reduction locations or 2) the traffic volume on routes with significant bottlenecks was never high enough to create a queue which could propagate back into the EPZ. Given the low traffic volumes typical of rural, low population sites, the findings suggest that it is unlikely that a significant reduction in capacity, such as a lane drop on a major evacuation route would significantly impact the traffic pattern within the EPZ.

5.2.3.2 Medium Population Site Model

The medium population site provided an opportunity to examine the impact of model extent in combination with the DTA path selection and assignment process of the simulation system. The medium population site is assumed to be located in the vicinity of a large body of water to the East. As the model extends toward this body of water, the population density increases and the road network becomes limited. From the perspective of the DTA, this is a “one-two punch” which causes both the congestion and path cost to increase significantly. As the model extends into this region, what was once considered a viable, low cost path changes drastically. This can be seen in Table 5-6 where the travel time (a proxy variable for path cost) more than tripled from 316 seconds to 1,067 seconds. As a result, the DTA worked to change paths to keep the network travel time at a minimum. The key finding here is that modifying the equilibrium paths causes significant changes to the travel patterns within the EPZ. These changes account for the variable average speeds, EPZ exit flow rates and ultimately for an 85 minute difference in ETEs seen in Table 5-2. However, this difference is likely exaggerated because the truncated model paths were not calibrated, as was done in the base model. From the analysis of the medium population site it was apparent that in congested regions with limited route options, simulation

models may need to consider major bottlenecks and population generators beyond the 15-mile shadow region to ensure DTA paths accurately represent evacuee decision-making.

5.2.3.3 Large Population Site Model

The large population site case analyzed the role that model extent had on the DTA path selections within the EPZ. However, unlike the medium population site that had increasing demand with a shrinking supply of roads, the large population site had a denser roadway network. Table 5-3 shows that ETE times were largely unaffected by the change of model extent. The data summarized in Figure 5-14 shows that evacuation clearance times between truncation distances were similar. This result suggests that the DTA route paths within the EPZ remained unchanged between model sizes. These findings were supported by the average travel speed and EPZ exit flow rate results.

Travel times from the southeast portion of the model, shown in Table 5-8 were consistent across cases even though EPZ evacuation traffic encountered a significant increase in background traffic from a larger population generator. This suggests that the dense roadway network in the region allowed DTA to minimize travel time by diverting traffic. It appears that DTA was able to maintain the same or similar paths within the EPZ. This finding is significant because it suggests that a dense road network allows the DTA to compensate for population fluctuations in areas beyond the EPZ without impacting traffic or the paths within the EPZ.

Table 5-9 shows the travel times collected in the west-northwest portion of the large population site. This table shows increasing travel times as model extent increases, which is assumed to result primarily from a large bottleneck located between the 18 and 19-mile ring. The increase in travel time suggests the DTA was unable to use rerouting strategies to alleviate the congestion. Under most conditions, it would be expected that the DTA would route vehicles away from this region, potentially impacting route selection within the EPZ. However, the characteristics of the bottleneck and the surrounding road network made it difficult to find suitable routes with adequate capacity to reassign traffic or avoid this congestion. Since the DTA had no choice but to allocate vehicles to this route, regardless of the extremely long travel times, the combined effect of these phenomena resulted in the EPZ having similar path selections regardless of model extent, and therefore, similar evacuation behavior within the EPZ.

5.3 Conclusion

A key factor in using traffic simulation is maintaining confidence in the validity of the computational processes that govern the representation of traffic movements in the model. The simulation needs to be reasonably similar to the traffic patterns that can or will occur in an actual situation. The two research objectives of interest in this task were associated with the extent of a simulation model. More specifically, the research sought to determine if the ETE would be impacted by conditions well beyond the EPZ boundary and to quantify travel times beyond the EPZ.

The findings from this task reveal a few important considerations related to traffic modeling. This task analyzed the impact extent of travel can have on EPZ ETEs. The study showed that in certain cases there may be an impact but that DTA algorithms can impact ETEs as much as physical characteristics of the network. The processes observed and the results obtained followed well established theories of traffic flow—the most fundamental of these is the basic relationship between network capacity and travel demand. From an understanding of the basic relationships of traffic capacity and demand volume, the results of the research show that a

change in outflow capacity (the “supply” component of the network) or in traffic volume (the “demand” component of the network) had an impact on travel within the test networks. If such effects occurred beyond the limits of a model, then their direct local effect and their impact in the EPZ clearance time was not recognized. However, when captured, the level of the impact and the movement of congestive effects over time and through the networks were influenced by network topology, routing alternatives, and the demand in the network modeling beyond the typical 15-mile boundary.

From a computational perspective, the research results showed that the size of the simulation network can influence the travel behavior under the influence of DTA. Fundamentally, the DTA algorithm seeks to minimize the overall travel cost or travel time, from evacuee origin to destination. Because the DTA is focused on minimizing the overall travel cost and not necessarily the travel cost within the EPZ, an optimal route selected by DTA that is influenced more by the downstream conditions, could result in higher travel times within the EPZ. However, effects are likely exaggerated because the DTA paths used in the truncated networks were never calibrated, as was done for the base model and would be done in an actual ETE study. While the impact of the DTA should have been similar to simulations of routine traffic conditions, consistent with the principles of DTA, the overall level of influence and impact within the context of an evacuation was new knowledge gained from this research. As such, a key issue to developers of ETE studies should be to ensure that the competing effects of site physical characteristics and simulation system DTA are properly modeled in the ETE.

DTA is predicated on commuter-oriented driving assumptions in which drivers are able demonstrate high levels of knowledge to select routes that minimize travel time, based on their history and understanding of traffic conditions that permit them to make judgments between alternatives built up over repeated driving experiences. While it is debatable whether such an assumption would hold under the fluid and variable conditions of an emergency evacuation, many experienced professionals believe this to be so. Emerging technologies such as mobile phone based real-time route guidance systems will also support and strengthen these opinions into the future. Regardless, this research demonstrated the potential impact of DTA on an evacuation traffic simulation.

This task only evaluated the DTA algorithm within the VISSIM simulation system. It may be beneficial to validate the findings in this report against the adequacy of other systems with respect to their DTA algorithms. This research also demonstrates the potential influence of a modeler. The professional judgment of a modeler who must make decisions on which route to include and how to code them into a simulation can have a large effect, especially when it is recognized that the availability, arrangement, and connectivity of available routes will significantly impact the DTA process and vice versa.

In reality, there is no single answer of what an ETE will be, but rather, what would likely come from a distribution of potential times. When examining ETE reports, issues of delays and congestion, or a lack thereof, should be assessed from the perspective of their source. Specifically, consideration should be given to what extent conditions result from the physical characteristics of the system (including the capacity, control, and volume, etc.) and to what extent they are reflective of, or heavily influenced by, the dynamic traffic assignment process (assigned route choice). This task to study the impact of model extent clearly illustrated the influence of modeling assumptions about both the system characteristics and the DTA computational processes.

6 TASK 3 MANUAL TRAFFIC CONTROL STUDY

Manual traffic control (MTC) is a common intersection control strategy in which trained personnel, typically police law enforcement officers, allocate intersection right-of-way to approaching vehicles. The assumed benefit from this form of control comes from the belief that traffic enforcement officers, with their ability to directly observe and react to changing traffic conditions and periodic surges in volume, can directly allocate right-of-way at intersections in response to changing demand [83]. This is thought by many to yield an advantage over pre-timed traffic signals that operate on pre-set timings and phase patterns which repeat regardless of the traffic conditions. Manual signal control is also thought to provide significant benefits over actuated signalization—even though both are responsive to changing traffic conditions—because police-conducted MTC has the added benefit of "boots-on-the-ground" authority to observe conditions, respond to problems, and project the presence of a command and control during times of crisis [84].

The use of manual control is most frequently associated with abnormally high, unbalanced, or widely varying directional and intersecting traffic demand. While such conditions can occur at any time, they are particularly common before and after special events and for emergencies such as power outages and evacuations. MTC has generally been used to minimize congestion, expedite emergency traffic, exclude unauthorized vehicle entries, and protect the public. As such, MTC is of interest as a method to expedite traffic flow in an evacuation.

In practice, manual traffic control is typically implemented using one of two methods. The first is the traditional "officer-in-the-intersection" approach. The other is the more modern "clicker" method. The officer-in-the-intersection involves the placement of uniformed personnel near the center of the intersection to direct vehicles and pedestrians using hand gestures and whistle commands. The advantages of this method are that it is quick and easy to deploy, can be used at any intersection with little-to-no preparation, and can be stopped rapidly. It can also be used at both signalized and unsignalized intersections and even ramp junctions. The major disadvantage of the officer-in-the-intersection control is that it can be unsafe for the officer and is prone to inefficiencies that result from vehicles slowing down through the intersection and, oftentimes, completely stopping to ask the officer questions on a variety of subjects [122] [83].

The "clicker" method, in contrast, permits a police officer to allocate right-of-way using an existing traffic signal by changing the phase lengths that serve conflicting streams of traffic approaching the intersection. Operators can change which approach directions and movements will receive a green indication from the controller with the "click" of a button (colloquially referred to as a "pickle" because of its shape and size). Button controllers are typically wired directly into the installed controller hardware and are accessible through a small door in a signal controller cabinet that can be unlocked by the police. This configuration permits officers to control the signal timing while sitting inside a patrol vehicle parked next to the controller cabinet (or stand near it, instead of standing in the intersection. The advantages of this method are two-fold: 1) it improves safety for officers because they do not have to stand in traffic, and 2) it eliminates many of the inefficiencies in traffic flow that result from drivers who slow down because of the officer standing in the intersection. In fact, because the timing is relayed to, and displayed by, the existing signal faces, most drivers do not even realize the signal is under manual control.

Evolving practices in emergency management have resulted in changes to the roles and responsibilities of transportation and law enforcement officials. In addition to their enforcement responsibilities, police personnel have expanded the many important roles they play before,

during, and after emergencies. These include maintaining law and order, providing security in impacted areas, serving as first responders, and conducting rescue operations [86]. Despite its perceived advantages during emergencies, manual traffic control exposes officers to increased safety risks, requires significant manpower, and may be a poor utilization of limited police resources during emergencies [87]. For these reasons it is suggested that conventional signal control can provide a safer, more efficient, and more effective option for moving traffic [122] [115] [116] [119]. Because of these conflicting views, a disagreement exists among those who believe manual traffic control is an essential element of special event and emergency traffic management and those who believe traffic would flow more efficiently using conventional signal control. A review of the current state-of-the-practice has shown that the administration, implementation and execution of manual traffic control is based on expert judgment, local knowledge, past experience, and, in some cases, public perception.

There is no single, universally recognized authoritative source or set of guidelines that govern manual traffic control, in both practice and its representation for analysis in tools like traffic simulation models. Interestingly, the virtual absence of information on how an officer directs traffic and allocates right-of-way has also rendered the topic a virtually un-researched field within the transportation community. For example, no studies have been conducted to understand the stimulus-response relationship between operational traffic stream characteristics and officer decision-making while directing traffic. Without an understanding of the fundamental processes of how and why police allocate green time, it is not possible to assess how, or even if, the performance of manual traffic control differs from or is better than fixed pre-timed or actuated traffic signal control from a systematic engineering point-of-view.

This study has applied state-of-the-art research and methods on the quantification and representation of police manual traffic control into simulation models to represent its effect on an evacuation. More specifically, this task sought to examine how the implementation of manual traffic control at key locations within the region of a nuclear power plant EPZ could impact the traffic flow and clearance time conditions during an emergency evacuation. Included in this research were quantitative comparisons of manual traffic control to other control strategies under emergency conditions, including automatic actuated control. The expectation is that the results of this research can be used to inform the allocation of right-of-way at oversaturated intersections during an emergency evacuation; the stimulus-response relationship between the traffic stream and officer decisions while directing traffic; the traffic stream variables with strong and weak correlation to observed officer actions; and the benefit-detriment (in terms of clearance time) relationship between MTC and automatic traffic control.

6.1 Background

It is well recognized that traffic simulation is a valuable tool to plan, design, and operate transportation systems. Its many applications include support of the design and evaluation of traffic management plans for special events (festivals, parades, and sporting events) and emergencies (evacuations, traffic accidents, and road closures). Through simulation, engineers evaluate the effect of congestion mitigation alternatives and strategies. The current state-of-the-practice in evaluating traffic operations and control employs traffic simulation modeling. However, due to the previously un-quantified nature of manual traffic control, it has not been possible to accurately represent or calibrate simulation models to fit empirical observations. As a result, current special event and emergency evacuation simulations have been unable to realistically model the essence of neither manual traffic control nor the results that are produced by it. Without this ability, the traffic management plans developed for these situations cannot be tested in advance via traffic simulation.

Many event traffic management plans and emergency traffic management plans call for the use of manual traffic control in response to oversaturated traffic conditions. Expediting traffic flow is a particularly high priority during emergencies when the effective movement of traffic may be a matter of public health and safety. However, during emergencies, police personnel are also in great demand for other non-traffic related duties. During non-emergency events, police presence can have a high economic cost because it often requires overtime or extra duty pay. It is therefore essential to identify the benefits and costs, as well as the trade-offs, advantages, and disadvantages associated with manual intersection traffic control. There is also a need to quantify the operational effects of manual traffic control on intersection performance for comparison to signalized intersection control. This will enable the travel-time savings (if any) from manual traffic control to be weighed against the cost of deploying the police officer at the intersection. Without such comparisons, there can be no quantitative metric to evaluate manual traffic control.

Under manual traffic control, police officers must make decisions of phase length and phase sequence while directing traffic. By definition, these decisions have an impact on traffic operations of the intersection. The actions taken by the officer may have significant consequences (positive or negative) for potentially hundreds of people approaching the intersection. It has been observed that the likelihood of inadequate green time allocation is greater if the officer is inexperienced or has not been properly trained [122]. If an officer provides inadequate green time to one phase of an intersection, the resulting queue can propagate upstream interfering with the operations of adjoining intersections. Traffic simulation is a relatively inexpensive tool used to evaluate proposed traffic management strategies for effectiveness and efficiency. However, no simulation software can simulate the effect that a police officer directing traffic has on roadway operations. A model capable of effectively representing manual traffic control would be useful for the purpose of evaluating traffic flow in traffic simulations. Such a model would help identify where, how, and when manual traffic control should be implemented to better utilize officer resources and intersection right-of-way.

The guidance in NUREG/CR-7002, “Criteria for the Development of Evacuation Time Estimate Studies,” states that traffic simulation modeling should consider manned traffic control as a possible intersection control strategy and states “in general, it may be assumed that staffed traffic controlled intersections operate most efficiently” compared with unsignalized, fixed-time signals and actuated signals [4]. NUREG/CR-7002 supports the use of traffic simulation in the development of evacuation time estimates and recommends that if MTC is proposed as part of a traffic management plan, then the ETE study should simulate the implementation of MTC. The document proposes modeling MTC as an actuated signal with a signal-timing plan that reflects more efficient operations. However, without full knowledge of MTC operations, simulating MTC as an actuated signal may not be realistic. Furthermore, no guidance was given on how to make the simulated actuated signal more efficient or how to simulate the actuated signal to produce results similar to those of MTC.

A review of current ETEs provided to the NRC identified several key assumptions, functions, and considerations for MTC used to develop traffic management plans in response to NPP emergencies. In general, ETEs assume personnel with the appropriate knowledge and training are available to conduct MTC along with any necessary equipment (cones, flares, reflective vest, etc.). It is also generally assumed that personnel conducting MTC have knowledge of the traffic management plans which identify preferred evacuation directions and any road closures at each traffic control point (TCP) location. It is typically further assumed that Access Control Points (ACP) are stationed within 2 hours of the advisory to evacuate and that TCPs are

stationed over time beginning with the advisory to evacuate. ETEs have further identified several functions for personnel directing traffic. These are to:

- Facilitate the movement of vehicles through the intersection
- Discourage movements toward the NPP
- Provided guidance and information to unsure travelers
- Observe and report the progress of the evacuation to the emergency operations center

Furthermore, ETEs have based the development of their traffic management plans on:

- The existing TCPs and ACPs identified by offsite agencies
- An analysis of traffic simulations of the evacuation event
- Field observations and site visits
- Consultation with emergency managers and law enforcement agencies
- Prioritization of potential TCP and ACP points

6.2 Research Task

The goal of Task 3 was to determine the value of manual traffic control at intersections toward enhancing traffic flow during NPP evacuations and to improve assumptions used to develop ETEs. Specific objectives were:

Objective 1: To identify and review existing documentation of manual traffic control practices and training for police officers during emergency and major events and to develop an understanding of the expected resources and timing required to implement.

Objective 2: To identify and review available video observations of MTC and use it to quantify the allocation of right-of-way by police officers at oversaturated intersections during major events. This was to include the determination of cycle length and vehicle volume to assess the rate at which vehicles flow through an intersection.

Objective 3: To conduct a quantitative analysis on the stimulus-response relationship between the traffic stream and officer decisions while directing traffic and to determine traffic stream variables with strong and weak correlations to observed officers' actions.

Objective 4: To benchmark the development of a MTC model for simulated test intersections and conduct comparisons of performances between simulated MTC and video observations; between simulated MTC to observed traffic control within an alternative study area for cross-validation; and simulated MTC and actuated traffic control.

Objective 5: To determine the benefit-detriment relations between MTC and automatic traffic control in terms of ETE within three representative sites.

Objective 6: To determine the ETE sensitivity to the number of MTC intersections.

The following sections document the accomplishment of each of the six research objectives. The next section provides a literature review, followed by the data collection and processing of video footage of police officers directing traffic. This will be followed by a quantitative analysis of the stimulus-response relationship between the traffic stream and officer decision making, followed by the development of the MTC model for application within traffic simulation software and the comparisons of performance. Next, the impact of manual traffic control, as compared to automated control will be evaluated on three representative NPP sites. Finally, the results of an ETE sensitivity analysis conducted on the number of MTC intersections will be presented.

6.3 Literature Review

The design, implementation, and maintenance of traffic control devices in the United States has been an evolutionary process. Police officers were the first true traffic control devices. Over time, however, police officers were replaced by simple traffic signals, which were later improved by introducing advanced traffic control systems. For the development of this research, a literature review was conducted in several topical areas including: the manual of uniform traffic control devices, police traffic control training, manuals and handbooks, special event and emergency planning, and empirical studies on manual traffic control.

6.3.1 Manual of Uniform Traffic Control Devices (MUTCD)

The Manual of Uniform Traffic Control Devices (MUTCD) is the document that sets the national standards for all traffic control devices governing streets, highways, bikeways and roadways otherwise open to public travel in the United States. The MUTCD designates a traffic control device as any signs, signal, markings or any other devise used to regulate, warn or guide motor vehicles, bicyclist or pedestrians (MUTCD, 2009). Prior to the publication of the first MUTCD in 1935, two previous manuals governed traffic control devices in the U.S. [88]. The first published in 1927 then revised in 1929 was the Manual and Specifications for the Manufacture, Display and Erection of U.S. Standard Road Markers and Signs. The American Association of State Highway Officials (AASHO) in conjunction with the National Conference on Street and Highways Safety (NCSHS) sponsored this document. AASHO is now known as the American Association of State Highway Transportation Officials (AASHTO). This manual provided standards for rural roads and did not include standards for traffic signals; manual, automatic or otherwise [89]. The other predecessor to the MUTCD was the Manual on Street Traffic Signs, Signal and Markings, also sponsored by the National Conference on Street and Highway Safety (NCSHS). This manual, in contrast to the Manual and Specifications for the Manufacture, Display and Erection of U.S. Standard Road Markers and Signs, was designed to accommodate urban traffic signs, markings and was the first national standard for traffic signal regulation in the U.S. However, having two set of national regulations governing roadway sign, signals and markings was undesirable. Therefore, the MUTCD was created to bring uniformity and establish a single source for regulating the design of road sign, signals and markings (MUTCD, 2009).

The National Conference on Street and Highway Safety was responsible for the Manual on Street Traffic Signs, Signal and Markings. This document makes no mention of manual traffic control but does note “Traffic officers stationed in roadways shall be illuminated at night, by flood lights if necessary, in the interest of safety” [90]. However, the NCSHS, in an attempt to bring uniformity to city traffic laws published a model set of municipal traffic ordinances in 1930 [91]. In this document, the authors recognized the role of police and the need for their authority in directing traffic:

It shall be the duty of the Police Department of this city to enforce the provisions of this ordinance. Officers of the Police Department are hereby authorized to direct all traffic either in person or by means of visible or audible signal in conformance with the provisions of this Ordinance, provided that in the event of a fire or other emergency or to expedite traffic or safeguard pedestrians, officers of the Police or Fire Department may direct traffic, as conditions may require, notwithstanding the provision of this Ordinance [91].

The most recent MUTCD published in 2009 makes little mention of manual traffic control of intersections. The document discusses traffic incidents and states, “if manual traffic control is needed it should be provided by qualified flaggers or uniformed law enforcement” (MUTCD,

2009). The manual does, however, specify that officers directing traffic are subject to the same high-visibility safety apparel as flagmen when operating near the roadway. Furthermore, the MUTCD developed a Traffic Control Point Sign (EM-3) to be used at locations where manual traffic control is used on a regular basis (MUTCD, 2009). Other than these three instances, the 862 page document publishing the national standards for all traffic control makes no mention of manual traffic control despite its frequent use during planned special events and emergencies.

6.3.2 Police Training For Traffic Control

The effectiveness of a police officer at directing traffic is a function of training and experience. Prior to formal regulations, officer training was conducted entirely within each department. Specialized training for law enforcement officers first emerged in 1935 with the founding of the FBI National Academy [92]. Between the years of 1935 and 1944 the FBI National Academy sent instructors to 1,513 local, county and state police agencies. In 1946 alone the academy instructed 1,785 schools attended by almost 90,000 law enforcement officials. Due to the size and scope of the traffic problem the FBI national Academy included traffic training from its founding in 1935 [93]. As director of the Federal Bureau of Investigations (FBI), J. Edgar Hoover institutionalized uniform training programs and training templates for police traffic control. Hoover believed that “the development of police executives and instructors cannot be accomplished without adequate training in traffic law enforcement” [93]. The FBI made police traffic control training available to local law enforcement in urban and rural areas. In 1949 over 150 police training schools were held specializing in traffic control. Small stations, which did not have an adequate number of officers to justify holding an entire course at their department, could go to “Zone Schools” which allowed officers from many neighboring communities to attend [92] [93].

6.3.2.1 Northwestern University Traffic Institute

Private traffic control training for law enforcement officers began in 1936 with the founding of the Traffic Safety Institute at Northwestern University [94]. The Traffic Safety Institute, later known as the Traffic Institute, trained officers in crash prevention, traffic supervision and police management. Traffic supervision had three direct functions, accident investigation, traffic law enforcement and traffic direction [95]. Since the founding of the Traffic Institute it has published several documents on manual traffic control.

Police traffic direction is defined by the Northwestern University Traffic Institute (NUTI) as “telling drivers and pedestrians how and where they may or may not move or stand at a particular place, especially during periods of congestion or in emergencies” [95]. Published in 1952 the article Directing Traffic, what it is and what it does, was the first of its kind in providing a cross-jurisdictional standard for manual traffic control. While manual control had become more-or-less standardized in practice, this article was the first to publish and disseminate the procedure. The article states that officers while directing traffic must answer inquiries, tell drivers and pedestrians what to do and what not to do and in the cases of emergency traffic control, make rules for the flow of traffic when usual rules are inadequate. The article tells officers to act as a traffic light operating in coordination with neighboring signals, never allowing more vehicles through the intersection which the downstream intersection cannot handle [95]. However, the article does not provide guidance on how to effectively and efficiently direct traffic in practice.

In 1960, the NUTI put out the first edition of Signals and Gestures for Directing Traffic. This publication was revised five times; the most recent version was released in 1986. The article explained, through illustration, how a police officer should communicate with vehicles and

pedestrians while directing traffic. First, it explained different postures and then went on to illustrate how each hand gesture corresponded to a vehicle movement or action. The article then moved on to controlling traffic using the “clicker” method, however, the article implied that the “officer in the intersection” approach was more effective at directing traffic. Finally, the article concluded by explaining the role of the baton and whistle, and how to cope with directing traffic at night [96]. The article may be a good instructional guide for communications while directing traffic but does not lend any insight on how to effectively or efficiently direct traffic.

The follow-up publication of NUTI to Signals and Gestures for Directing Traffic was Directing Vehicle Movements, published in 1961. This article was unique in that it employed traffic engineering concepts to assist in the effectiveness of manual traffic control. The guide stated that manual control is only necessary when an intersection is oversaturated for its current control technique (e.g., signal control, stop controlled, priority controlled), citing that motorists will exercise undue caution when entering an intersection governed by a police officer in the same fashion that drivers will hesitate to overtake a police patrol vehicle while driving on the highway. The presence of an officer inevitably led to a loss of efficiency and, thus, an officer should only direct traffic in situations where manual traffic control will offset the initial loss in efficiency. Therefore, an officer was only able to direct traffic when needed in oversaturated conditions.

The article instructed officers to equitably distribute delay time between movements based on volume. Delaying one car for 30-seconds is equivalent to delaying 30 cars for one second, as such low volume movements should be delayed for longer periods. To maximize saturation flow rate, officers were instructed to hold a movement’s initial arrival until a group of vehicles formed, and then switch to that direction and keep them there so long as vehicles depart one right after the next. It stated officers should not keep vehicles waiting for longer than a minute in the hope of collecting a group and officers should not prolong green time for a single vehicle. The article stresses the importance of preventing queues from propagating into neighboring intersections. It instructed officers to force vehicles to detour if the queue is threating the upstream intersection.

At an intersection where cross-street traffic and main-street traffic were equal, the officers were told to increase cycle length to reduce start-up lost-time and increase effective green time. Also, it stated officers should never waste green time; if an exit lane was blocked, officers were told to immediately switch to a free-flowing movement until adequate room would allow the previously-blocked movement to continue. When switching between movements, officers were informed to wait until a natural gap in the traffic stream appeared. If no gap existed, officers were instructed to stop the flow of vehicles after a heavy truck. By letting the heavy truck pass the intersection, the start-up lost-time of having to halt and restart the large vehicle was reduced. In addition to informing officers on how to increase efficiency, officers were instructed on how to improve safety. Officers are told where to stand in the intersection, how to cope with wet and icy environments, and how to remain safe in intersections with irregular geometries [97]. The article assumed that the “officer in the intersection” approach was more efficient than the “clicker” method, which may not be true today given the advancements in traffic signal controllers.

6.3.2.2 Modern Police Training for Traffic Control

In 1973 the International Association of Chiefs of Police (IACP) collaborated with the National Highway Traffic Safety Administration (NHTSA) to develop a comprehensive collection of police traffic service polices for best practice. This partnership developed the Police Traffic Service Basic Training Program [98]. The goal of this program was to improve the effectiveness of the National Highway Safety Program by establishing national standards on jurisdictional law

enforcement training to provide police officers with basic, uniform training in police traffic services. This national training program was targeted at six major areas; 1) policy and traffic service, 2) traffic law, 3) traffic direction and control, 4) traffic law enforcement, 5) traffic management, and 6) traffic court. The traffic direction and control section of the training program stated that an officer had three goals when directing traffic: safe movement of vehicles and pedestrians, the mitigation of traffic congestion, and ensuring drivers comply with traffic laws. The training program also discussed instances where police traffic control should be used, areas of periodic congestion (e.g., rush hour choke points), special events, and around hazardous scenes. However, the training program did not include guidance in determining when it may be more beneficial to use police in lieu of signalized control, when it should be used, where it can best be implemented, or how to evaluate its effect on the overall movement of traffic during emergencies, events, or routine traffic conditions.

By 1977, the IACP and NHTSA partnership had developed a system for evaluating police traffic services for the nation. This guide was intended to assist police agencies in determining the quantity and quality of services provided by their traffic control division. The manual was designed to evaluate an individual police officer's performance. It was possible to measure and evaluate the performance of traffic control for a department if aggregated for the entire police force. The manual evaluated an officer based on several factors related to traffic control. An officer's performance while directing traffic was based on the traffic flow through the intersection and eyewitness reports of the officer's actions (NHTSA, 1977).

In 1986, the IACP and NHTSA published the Manual of Model Police Traffic Services Policies and Procedures. This document consolidated, revised, and updated the work done in the previous decade. This effort was motivated by the need for police officials to remain compliant with traffic-related standards set by the Commission on Accreditation for Law Enforcement Agencies. The document detailed traffic control functions, such as staff and administrative service, traffic law enforcement, accident management, traffic direction and control, traffic engineering and ancillary motorist services. Under traffic direction and control, the document provided guidance on general policy and procedure, including identifying locations for traffic control, implementing temporary traffic control devices and traffic direction for special events, fire scenes, and adverse road conditions [99]. An important note here was that only the policy differs with regard to directing traffic for regular operations, special events, and fire scene—not the procedure. The procedure for directing traffic remained the same regardless of the application.

Over the years, numerous other manuals were developed to describe the proper functioning of police traffic control [100] [83]. However, these documents focus primarily on the role of police in accident reduction, selective traffic law enforcement, and the development of a traffic-orientated police force. They also provided guidelines for officer safety by identifying where and how to move within a congested intersection. The book by Weston (1996) provided a comprehensive reference for ensuring safety while directing traffic, but it did not specify when it may be more beneficial to use police in lieu of signalized control, when it should be used, where it can best be implemented, or how to evaluate its effect on the overall movement of traffic during emergencies, events, or routine traffic conditions [83].

6.3.2.3 Technical Manuals, Handbooks and Published Guidelines

An extensive amount of unpublished or otherwise not widely disseminated practitioner training references exist for manual traffic control. In general, they are designed to be a quick reference for an individual new to manual traffic control. These documents were usually developed by

individual police departments and used as a jurisdictional guideline for new police officers. Most of these documents were for “in-house” use, authored by senior officers on the force with years of manual traffic control experience.

Despite being developed to meet local traffic control needs, these manuals showed consistency in several key points. All of the reviewed documents shared the following:

- The use of reflective vest at all times
- The use of lighting for directing traffic in adverse weather
- The need for additional lighting at night from the police vehicle or additional flood lights
- Where to stand within the intersection
- How the officer should position his/her body to command vehicles Uniform hand signals to start and stop the flow of traffic Safety when directing conflicting turn movements
- The use of traffic control tools such as flashlights, whistle, illuminated batons and flares

While consistent, these documents have been inadequate in providing guidance on how to effectively distribute intersection right-of-way. These documents provided a “how to” for directing traffic; after reading one of these manuals an officer would know “how to” start and stop the flow of vehicles but would not know when or why. Without a basic understanding of traffic engineering concepts behind intersection control, which police officers developed with experience, new officers would likely perform poorly [101-111].

A review of the technical manuals, handbooks and published guidelines finds a varied and brief discussion on the resources needed to conduct MTC. In general, if an officer is directing traffic from the controller box (the “clicker” method) then only one officer is typically required. The same is true for intersections with small geometric footprints. These are typically stop or yield control intersections. If it is desired to block or limit access to one or more approaches, additional officers may be needed. Larger intersections with more diverse movements would also require additional personnel to direct traffic effectively. Beyond personnel, MTC requires safety equipment such as vest and lighting as well as transportation cones, barricades, flares, and patrol vehicles are also required, especially when restricting movements. Communication, in the form of walkie-talkies or radios is also necessary.

It is generally accepted that an average police response time to a life and death 911 call is approximately 10 minutes. However, the time required to dispatch police to intersections during an NPP emergency is wholly unstudied. In many cases, police departments will have to call in off-duty police officers, who may be in the process of evacuating themselves, to report to TCPs to direct traffic. Depending on the number of TCPs within a police jurisdiction and the number of police officers available at the time of notification, the time required could be as little as 10 minutes and as long as several hours for police to report to the police department and be dispatched to TCPs.

6.3.3 Special Event and Emergency Planning

Nearly all major planned special events have had a traffic management plan. And most municipalities have an emergency operations or emergency evacuation plan on some level (Region, State, County, City, etc.). Traffic management plans for special events and emergencies are often developed based on a set of common guidelines. For an emergency evacuation plan, the guidelines may include government regulations that require planning action. For planned special events, the guidelines are more of a collection of best practices

aimed at assisting municipalities in event planning and management. This section looks at the guidelines used by authorities for developing these plans.

6.3.3.1 Special Event Planning

The National Cooperative Highway Research Program (NCHRP) has a mission to collect, evaluate and disseminate information on common highway problems faced by highway administrators, engineers and researchers. The NCHRP synthesis series present the state-of-the-practice in how these everyday problems were solved around the nation. One such problem, transportation planning and management for special events is addressed by NCHRP Synthesis 309. This document is a compendium of the best knowledge available on the practice of special event traffic management planning. NCHRP Synthesis 309 makes frequent reference to the use of police officers for manned traffic control points. “The advantage of using staffed traffic posts over signalized control is the presence of authority and the ability to make dynamic changes to the traffic flow”. Based on the survey conducted in NCHRP 309, manual traffic control of intersections for special events was a common traffic management technique used around the country. Therefore, any agency looking to develop a special event traffic management plan was encouraged to use manual traffic control. Furthermore, these agencies were encouraged to use traffic simulation in the development of management plans. However, any event utilizing manual traffic control currently would have no reliable way of simulating the process for a comparative analysis.

6.3.3.2 Emergency Planning and the National Response Framework

The National Response Framework (NRF) was designed to assist governmental, commercial, and non-governmental organization officials in the response and recovery needed from a major disaster. The NRF includes various guidance documents to assist State and local governments in creating emergency traffic management plans for an all-hazards emergency (FEMA, 2009). The Emergency Support Function #13, Public Safety and Security Annex provides federal assistance to local and state governments in order to maintain safety and security. Within this annex, the federal government may provide assistance to local agencies for traffic control operations, namely traffic direction and control for vehicles and large crowds (ESF#13, 2009). The Mass Evacuation Incident Annex provides the criteria needed for federal support to assist in a mass evacuation. This annex states that local police should be used to control the flow of vehicles on federal and state routes. This document references ESF #13 for the administration of traffic direction and control.

ETEs are primarily used for protective action decision-making. However, ETEs are also used in the development of traffic management plans to support an evacuation. The NRC guidance for ETEs (NUREG/CR-7002) highlights manual traffic control stating, “In general, it may be assumed that manned traffic-controlled intersections operate most efficiently” when compared to un-signalized, fixed-time signals and actuated signals. This document also supports the use of traffic simulation in the development of ETEs. It recommends that if manual traffic control is proposed as a part of a traffic management plan, then the simulation model should simulate the effects of manual traffic control. The document proposes modeling manual traffic control as an actuated signal with a signal timing plan that reflects more efficient operations [4]. However, no guidance was given on how to make the simulated actuated signal more efficient or how to simulate the actuated signal to produce results similar to that of manual traffic control.

6.3.4 Manual Traffic Control and Empirical Studies

Since the first studies to evaluate the effectiveness of manual traffic control in the 1920's relatively little work has been conducted on this form of control. Since the 1920's, manual traffic control under routine conditions in urban intersections was no longer commonplace [113]. After this time, manual traffic control has been primarily used for special events and emergency situations. However, in rare situations, manual traffic control is still used to supplement automated traffic controllers during peak hour periods in urban and rural areas. This was the case in Fort Belvoir, Virginia in 1953. At that time, a traffic study of ten intersections with narrow-width approaches (total width of two-way streets is less than thirty feet) was conducted to determine if the approach widths needed to be expanded [114]. Of the ten intersections studied, six were manually controlled by police officers (some using the "stand in the intersection" method and others using the "clicker" method), two were controlled under fixed time settings, one was an actuated controller, and the final one was all-way stop controlled. The highest capacities were observed using manual traffic control strategies. Officers extending the green time to the priority approach at the cost of the cross-street traffic accomplished this. The report stated that during the 15 minute peak period, 31 approaches where found to be overloaded, however only two were recommended for widening. The study suggested that this was due to the added capacity of manual traffic control at the intersection and thus widening of the approach lanes was not necessary. Unfortunately, the study did not discriminate between manual traffic control conducted by the "officer in the intersection" approach or the "clicker" approach. This would have allowed more insight into the operational advantages of manual traffic control.

A study conducted in Brisbane, Australia evaluated manual traffic control at an un-signalized priority-controlled intersection during peak periods. From the rooftop of a nearby building, researchers used stopwatches to observe and time an officer directing traffic. The researchers recorded parameters such as phase length, number of vehicles and type, maximum queue length, and the time to clear each queue. These values were then used to compare the officer's performance to a hypothetical pre-timed and actuated traffic controller. The study found that saturation flow rate was not affected by manual control, but average approach delay was slightly lower than expected when compared to a pre-timed isolated intersection. The paper concluded that it was unable to prove that an officer was superior to a traffic signal [115]. However, this conclusion is not generalizable based on the evidence that the study only considered one intersection under police control and observed this intersection for only one hour. Furthermore, the article states that the intersection was under-saturated. One of the primary applications for manual traffic control is for special events and emergency traffic, almost certainly operating in oversaturated conditions.

In some developing countries with high levels of congestion, manual traffic control during peak periods remains common for critical intersections. May and Montgomery (1988) evaluated pre-timed signal control settings as an alternative to manual traffic control for isolated and linked intersections in Bangkok, Thailand [116]. An isolated intersection was studied for six days during evening peak periods. On days one, three, and five of the study pre-timed signalized control was used at the intersection. On days two, four, and six manual "clicker" control was used. Over the course of the experiment, the pre-timed signal control cycle and phase length settings were adjusted to increase their effectiveness. The results showed that at isolated intersections with over-saturated conditions, police out-performed pre-timed signal control based on delay, queue length, and total throughput. The authors noted that saturation flow rate decreased over time, which represented inefficiencies in manual control as a result of long phase lengths.

May and Montgomery (1988) also applied their methodology to evaluate the performance of pre-timed signal control at four linked intersections as a replacement to manual control [116]. The study evaluated the four pre-timed signal settings over five consecutive days and compared the results of manual control to the following four days (excluding Saturday and Sunday). The results showed that a 21 percent decrease in travel time and a 29 percent increase in travel speed were possible using pre-timed coordinated signals as opposed to manual traffic control. However, it was necessary to have manual intervention when the corridor capacity was affected by major traffic incidents. The conclusions of this research were also backed by a quantitative analysis but, based on the high variation of the traffic demand between observation days, the small sample size was not sufficient to draw a statistically confident conclusion.

Another comparison of manual traffic control and automated control was conducted in Israel [117]. This research compared manual traffic control of two isolated intersections to control by an actuated signal in oversaturated conditions. The first intersection was observed for two days under actuated signal control and four days under manual control. The second intersection was observed for one day of each. It was found that in over-saturated conditions, the actuated control performed similar to a pre-timed setting due to the recall of the maximum green. The research used total throughput and degree of saturation as measures of effectiveness. The study results showed that manual control was correlated to a decrease in lost-time by as much as 60 percent and an effective green time increase of 15%. This reduction in lost-time was attributed to the use of the longer cycles associated with manual control, resulting in fewer cycles per hour.

Confirming the findings of May and Montgomery (1988) [116], the Israeli research study also identified a decrease in saturation flow rate as phase length increased, despite the persistence of long queues. The authors quantified this phenomenon showing that 55 seconds into the phase, saturation flow rate decreased rapidly. This observation suggested that a trade-off exists between long phase length (increases in effective green time) and efficient use of green time (decreasing saturation flow rate). Further analyses of intersection throughput found that manual traffic control increased intersection capacity by as much as 9 percent, confirming the result found by Sutermeister (1956) [114]. A comparison of the degree of saturation suggested that manual control could increase capacity to such an extent that it could surpass demand. This conclusion is based on a comparison assuming constant cycle length and green splits for manual control. Research conducted by Marsh (1927) found that officers directing traffic do not operate in this manner [122]. Furthermore, many of the advantages of manual traffic control can be hindered by such assumptions. Therefore, the conclusion suggested by Mahalel, Gur and Shiftan, (1991) is confirmed by previous research; but due to the stated assumptions the magnitude of the capacity increase caused by manual traffic control may be larger [117]. With a simulation tool for manual control these assumptions would not have been necessary.

During peak hours, roundabout intersections may also be supplemented with police control if demand warrants. A comparison of a police-controlled roundabout to a traditional four-leg intersection was undertaken by Al-Madani (2002) [118]. Selecting two intersections (one roundabout and one traditional signalized four-leg) with similar traffic and geometric characteristics, video detection was used to produce vehicle trajectories. From these trajectories, vehicle delay was plotted against queue length for both intersections. The results showed that at distances less than 262ft (80m), the police-controlled roundabout significantly out preformed the four-leg signalized intersection. However, when queue length surpassed this threshold, the four-leg signalized intersection reduced delay considerably when compared to the police-controlled roundabout. It is uncertain whether the cause of this phenomenon could be attributed to the police control or the effect of an over-congested roundabout. Given the small

sample size, the conclusions of this paper may not be widely generalizable to other locations and sets of conditions.

Manual traffic control has also been used frequently at all-way-stop controlled intersections before and after special events. Traffic volume at these intersections typically does not justify installing a traffic signal but during these instances of high, non-recurring congestion, manual traffic control is used to assist intersection operations. Using traffic simulation modeling, a comparison of manual traffic control and pre-timed signal control of an all-way-stop controlled intersection during a special event was undertaken by Ye, Veneziano and Lassacher (2008) [119]. This research determined the saturation flow rate from a 1 hour and 30 minute video recording of manual control operations. The saturation flow rate at this location was estimated to be 1,300 vehicles per hour. This is considerably less than the results of an earlier study by Pretty (1974) where the saturation flow rate was found to be nearly 1,700 vehicles per hour per lane [115].

During the observation period Ye, Veneziano and Lassacher observed the saturation flow rate decrease overtime; confirming the findings of Mahalel, Gur and Shiftan (1991) [117] and May and Montgomery (1988) [116] though not to the same extent. The manually controlled intersection was simulated as a pre-timed signal control using average cycle and phase lengths observed during the peak period of the special event traffic. These results were then compared to an optimized pre-timed signal plan within a traffic simulation environment. The results of the simulation showed that the optimized signal plan reduced vehicle delay by over half when compared to manual control. However, to simulate manual traffic control, this research assumed constant cycle lengths and phase splits in the same fashion as Mahalel, Gur and Shiftan, (1991) [117] and contradicting Marsh (1927) [122].

6.3.5 Summary of Literature Review Findings

Previous research has shown that in oversaturated conditions, manual traffic control can outperform automated control at isolated intersections [114] [116] [117]. However, in the case of under-saturated intersections, automated control prevails [115] [119]. Research conducted before the 1930s found that automated signal control outperformed manual control for coordinated systems [122] [85]. Similar results were shown using a quantitative approach in more recent research [116]. These studies also showed that under manual control, saturation flow rate decreases over time as phase lengths increase [116] [117] [119]. However, research on manual traffic control has been generally based on small sample sizes leading to questionable conclusions based on implied statistical significance. Furthermore, the previous research has only investigated the officer's effect on the traffic stream and not what events in the traffic stream affect the officer's decision making. Studies attempting to simulate manual traffic control have done so by assuming officers act like traffic lights, with constant cycle lengths and phase splits [115] [117] [119]. However, empirical observations show this is not the case. Furthermore, Marsh (1927) suggested that many of the advantages of manual traffic control come from not having constant cycle length and phase splits [122]. The advantages of manual traffic control are in an officer's ability to extend green time when needed, cut phases short, and accommodate unbalanced and uneven traffic volumes [122] [120] [121]. Simplifying manual traffic control in simulation models by assuming constant cycle length and phase splits could lead to an unfair comparison between manual traffic control and automated control.

A review of the resources and timing required to conduct MTC found that often, more than one officer is needed per TCP; intersections with large geometric footprints and ones that require roadblocks typically need additional personnel. Officers also need reflective vest, lights, cones,

flares, barricades, communications, and transportation. No research has been conducted on the time required to deploy officers to TCPs during NPP emergencies. The time needed would likely vary depending of the number of TCP within a jurisdiction and officers available when the evacuation order is given.

A review of past research studies and other documents showed that there is a gap in the knowledge base. No studies have been conducted using a statistically significant sample size to evaluate MTC for planned special event and emergencies. Additionally, no research has been conducted on the stimulus-response relationship between the traffic stream and officer decision making while directing traffic. As such, no research to date has ever programmed the traffic light to act as an officer, having phase length dictated by stimuli in the traffic stream. The research proposed in this report seeks to fill the gaps in knowledge by developing a discrete choice model able to replicate the actions taken by a police officer while directing traffic. The discrete choice model will then be programed into a traffic simulation model. By incorporating the discrete choice model into the simulation model, the oversimplification and broad assumptions made by Pretty (1974), Mahalel, Gur and Shiftan (1991) and Ye, Venexiano and Lassacher (2008) are not required, allowing for a more equitable comparison of manual traffic control and automated control [115] [117] [119].

6.4 Video Data Collection and Processing

The data requirements needed to quantify the stimulus-response relations between traffic stream variables and officer right-of-way allocation decisions were extensive. Data was collected from four intersections after five college and professional football games in Baton Rouge, LA and Miami Gardens, FL. In both study areas, intersections were chosen because of their proximity to the football stadiums and their location on heavily used routes. In total, video data from more than 320 hours of special event traffic was collected, viewed, and cataloged. From the video footage, a total of 26 hours and 27 minutes (less than 10 percent of the total footage collected) were of police officers actively directing traffic.

In Baton Rouge, three intersections were selected for data collection during four Louisiana State University football games. These intersections were Stanford and Perkins, Nicholson and Roosevelt, and Nicholson and Lee. In Miami Gardens, cameras were placed at the intersection of Southwest 183rd Street and Southwest 27th Avenue near Hard Rock Stadium for one football game. In all observations, traffic conditions were generally oversaturated and officers in these jurisdictions directed traffic from the controller box using the “clicker” method.

Through a data reduction process, the video footage was systematically categorized into numeric observations. The product of data reduction was a timeline capturing the events (phase changes, phase length, lane groups, vehicle departures, etc.) that took place in the intersection. This process was completed in two steps. The first step required manually recording lane groups, phase length, and phase sequence for the periods immediately before, during, and immediately after the officer was directing traffic. During this time, observations of red light running, emergency vehicle movements, and other abnormal road user behavior were also noted.

The next step was to time-stamp individual vehicle departures, platoon gaps, and intersection blockages. Vehicle departures were time-stamped manually. Temporary gaps in the traffic platoon, which typically occur when vehicle platoons break up because of poor coordination, lack of demand, or travel conditions between intersections, were also cataloged. In addition, durations in which vehicles were stopped or prevented from proceeding through the intersection

because of downstream congestion were noted. With the use of the coded data, a second-by-second timeline was created to incorporate departures for all intersection movements, lane groups, phase length and phase sequence, and intersection blockages and gaps.

Table 6-1 shows the observed traffic signal timing under MTC. The Average Time column and Standard Deviation column show the average phase length and standard deviation of phase lengths observed in the field, respectively. The average cycle length and standard deviation are also provided. The individual phases were labeled using the standard convention. For example, the northbound left and southbound left lane group was labeled as NBL & SBL and eastbound and westbound through movements were labeled EBT & WBT the table shows that cycle length typically ranged between 200 and 400 seconds and had standard deviations as high as 80 seconds. For reference, a typical actuated controller will have phase length of 60 to 120 seconds and standard deviations less than 5 seconds.

Table 6-1 Observed MTC Signal Timing

Phase	Average Time (seconds)	Standard Deviation (seconds)
Intersection: Nicholson & Roosevelt		
NBL & SBL	8.33	1.11
NBT & SBT	158.81	45.16
WBT & EBT	46.2	20.43
Cycle length	216.67	56.88
Intersection: Nicholson & Lee		
NBT & SBT	210.13	77.03
NBL & SBL	20.94	4.23
WBT & EBT	76.6	56.11
Cycle length	302.07	75.78
Intersection: Stanford & Perkins		
EBL & WBL	53.69	24.31
EBT & WBT	80.08	33.89
NBL & SBL	36.92	8.41
NBT & SBT	211.62	81.19
Cycle length	398.92	102.4
Intersection: NW 183 Street & NW 27 Avenue		
EBL & WBL	20.43	15.07
EBT & WBT	27.59	11.94
NBL & SBL	34.7	19.68
NBT & SBT	111.35	32.64
Cycle length	194.08	50.38

6.4.1 General Observations

This section describes the general video observations from a qualitative perspective. These observations provided an idea of the concepts and principles that may (or may not) contribute to the way in which officers direct traffic. These observations, along with the literature review, informed all subsequent analysis.

While viewing the video it was not clear what prompted the police officer to start directing traffic. Some officers started immediately while others did not. In general, it may have been a relationship with phase failure (the inability of a phase to discharge its queue). Likewise, the criterion for ending manual traffic control was unclear. In general, the officers stopped when traffic was light or when the required cycle length needed to service all approach queues was low. Furthermore, the police officers tended to have a build-up effect, where cycle length increased to a peak and then tapered off. This was likely due to the peaking nature of traffic arrivals, but it was not present at every observed intersection. There were a number of instances where the phase length between cycles jumped drastically, but in general, phase length was increased and decreased incrementally over the period of a few cycles. It was also observed that emergency vehicles (police cars, ambulances, and fire trucks) did have an impact on the officer. Some instances resulted in a green-extension or red truncation in response to the emergency vehicle. Interestingly, many times after an emergency vehicle would leave the intersection, the officer would immediately change phases, irrespective of what phase or how long it had been green.

Watching the video, it became obvious that the police officers do not like to waste any green time. Gaps in the traffic stream, generally from the breaking up of vehicle platoons, promptly resulted in a phase change. Also, the officers had inherent priorities for certain directions. For some directions the officer was willing to tolerate more frequent and longer gaps when compared to other directions. At every oversaturated intersection, the downstream queue would inevitably propagate and block the study intersection. Each officer addressed this in different ways and there was not a consistent approach to remedy this situation. Also, it did not appear that pedestrians had any effect on the officer. Furthermore, red light running occurred at all study intersections but seemed more prevalent in Baton Rouge as compared to Miami Gardens (this effect could be due to the number of observations in the sample).

6.5 Variables Influencing MTC

At signalized intersections, police officers direct traffic from the controller box. Using a push-button device within the controller cabinet, an officer can switch between signal phases. Fundamentally, an officer directing traffic with this method is faced with a binary discrete choice process: to change the signal during a time interval or let the current phase remain green. Phase sequence, the order in which one phase leads to the next, was not decided by the police officer. Once the officer pushes the button, the signal changes to the next default option. This action is a function of the controller and its programing and not the officer. The controllers in Baton Rouge and Miami Gardens functioned in this manner under MTC. To model the choice by the officer to push the button, binary logit modeling was used. Other discrete choice models were applicable for this purpose, but since the simulation model must ultimately calculate the choice probabilities every time step, it was assumed that a more complex choice model would increase the computation time during the simulation process.

The logit model choice probability that an officer (*n*) would change phases (choose alternative *i* over alternative *j)* was a function of the utility of changing phases (U_{in}). This relationship is shown in Equation 6.1:

$$P_n(i) = \frac{e^{U_{in}}}{e^{U_{in}} + e^{U_{ij}}} \quad 6.1$$

The utility of changing phases in any time interval was dependent on a vector of independent variables (X_{in}) observed in the traffic stream and the degree to which these variables influenced this decision (vector β_k). For example, if x_1 was a variable determined to affect the officer's decision making, then x_1 contributed to the utility of changing phases by a factor of β_1, as observed in Equation 6.2. The parameter coefficient vector β_k was econometrically inferred from a sample of *N* observations with the maximum likelihood estimation procedure.

$$U_{in} = \beta_o + \beta_1 X_{in1} + \beta_2 X_{in2} + \cdots + \beta_k X_{ink} + \varepsilon_{in} \quad 6.2$$

6.5.1 Variable Selection

The data collection and reduction process resulted in a second-by-second timeline of events that took place in the traffic stream. This timeline was then used to develop the dependent and independent variables for the logit model analysis. The time interval used in this research was one second. As a result, the discrete choice represented by the logit model was between an officer changing phases during a one second interval (dependent variable $y = 1$) and the officer not changing phases during this second ($y = 0$). Before the generation of the independent variables, the intersection clearance time (the yellow and all-red times, which transition between signal phases) was removed from the timeline to avoid biasing the model toward selecting the intervals.

There were three independent variables used in this research: time, gap, and phase. The time variable was the phase length duration, or how long a phase has received a green indication. The gap variable accounted for periods of time in which no vehicles entered an intersection despite having a green indication (time headways greater than four seconds). These gaps were generally the result of the breaking down of vehicle platoons. The gap variable took a value of one if one of the intersection approaches had a gap, two if two of the approaches had a gap during the same time interval, and zero if no gap was present. The phase variable was a set of four binary variables that indicated which phase was receiving the green indication. Each of these four variables represented a phase (northbound–southbound through, northbound–southbound left, etc.). The four phase variables were labeled according to the priority they received from the police officers. They are primary, secondary, tertiary, and quaternary.

The primary variable represented the phase that received the largest proportion of the green time allocated by the officer. For example, if the northbound–southbound through phase received more green time than any other phase, this phase would be labeled the primary phase. This was done to compare primary phases between intersections regardless of the intersections' geometric characteristics. As such, secondary, tertiary, and quaternary represented the phases' green time proportions. It was also hypothesized that the effect on the officer's decision making of time and the presence of gaps varied for each direction. These variables were tested for their interaction and included in the study. The variable representing the interaction of the priority phase and time was labeled *P-Time*. As such, the interaction between the gap variable and the priority phase was labeled *P-Gap*. The same labeling system was used for the interaction between secondary, tertiary, and quaternary phases for time and gap (*S-Time*, *S-Gap*, *T-Time*, *T-Gap*, *Q-Time*, *Q-Gap*). Results indicated that interaction did occur and the contribution to the decision-making process made by the time and gap varied depending on which phase was green.

6.5.2 Logit Model Coefficients

A total of nine logit models were estimated for this research, one from each observation event, not including the pilot study data. These events are referenced in the tables by their intersection initials followed by the data collection date. For example, the model estimated for the intersection of Nicholson and Roosevelt in Baton Rouge, collected on 10/13/12 is labeled as "N & R 10/13".

The logit model results are divided into five tables, one for each of the four phase priority variables (Primary, Secondary, Tertiary, and Quaternary) and one for the constant variable. This allowed for a comparison of the coefficient values by showing the results based on their perceived importance by the officer instead of their geometric layout (northbound, southbound, eastbound, and westbound). Each of the five tables shows a *Coefficient (Coef.)*, *Standard Deviation (STD), P*>|*z*|, and *Observations* column. The *Coef* column represents the variable coefficient value estimated for the utility function in Equation 6.2 and the *STD* value is the standard deviation of the coefficient value. The *P*>|*z*| column displays the p-value result of a single sample t-test comparing the coefficient value to zero. P-values less than 0.05 indicated that the coefficient value was not equal to zero at a 95 percent confidence interval and therefore had a significant impact on the dependent variable. P>|z| values less than 0.001 are rounded to 0.00 within the table. The *Obs*. column is the number of observations from which these parameters were estimated. Each table is followed by a statistical analysis of coefficient values, testing if these values were consistent between the models estimated.

The coefficient values are then compared between observation events. This was done to determine if the coefficient values estimated by the logit models from different locations and days were statistically equivalent. If so, this may suggest that police officers were directing traffic in a similar fashion between observations.

6.5.2.1 The Constant Variable

Table 6-2 shows the constant variable for each of the logit models estimated. This coefficient value represents the cumulative effect of all error within the model. The negative coefficient values indicate the officer prefers not to change phases, i.e., all things being equal the officer would not change phases. The p-value suggests that the cumulative error had a significant impact on the decision-making process (all p-values are less than or equal to 0.05).

Table 6-2 Constant Variable for MTC Logit Model

Intersections	Coefficient	Standard Deviation	P>|z|	Observations
N & R 10/13	-3.79	65.3	0.00	7534
N & R 11/03	-5.61	163.4	0.01	6385
N & R 11/10	-3.75	65	0.00	3141
N & R 11/17	-3.86	64.8	0.00	3134
N & L 11/03	-4.76	41.2	0.00	6898
N & L 11/10	-7.31	95.7	0.00	4581
S & P 11/10	-3.39	35.6	0.00	3486
S & P 11/17	-7.56	104.4	0.00	3987
183 & 27 01/07	-3.29	22	0.00	6541

These values of the constant variable were compared using a two-tailed, two sample student t-test or a one-way ANOVA test, where applicable. The constant variable estimated from data collected at the intersection of Nicholson and Roosevelt (models *N & R 10/13*, *N & R 11/03*, *N & R 11/10* and *N & R 11/17*) are compared in Table 6-3 and labeled *N & R*. Likewise, a t-test was conducted on the observations collected from Nicholson and Lee and Stanford and Perkins, these are labeled *N & L* and *S & P*, respectively. Additionally, an evaluation was conducted on all three-phase intersections (intersection which had a three phase sequence) and four phase intersections, these are labeled *Three Phase* and *Four Phase*, respectively. The three phase intersections in the study were Nicholson and Roosevelt and Nicholson and Lee. The four phase intersections were Stanford and Perkins and NW 183 St. and NW 27 Ave. Finally, an ANOVA test was completed which included all of the constant variables estimated from the logit models. This comparison is labeled *All* in Table 6-3.

Table 6-3 Statistical Testing for the MTC Constant Variable

Comparison	Test	Statistics	P>|z|
N & R	ANOVA	0.658	0.58
N & L	T-TEST	1.962	0.05
S & P	T-TEST	2.246	0.02
Three phase	ANOVA	1.049	0.39
Four phase	ANOVA	7.016	0.00
All	ANOVA	1.173	0.31

The statistical analysis was unable to reject the null hypothesis that the constant variable terms generated from the different intersection were statistically different. This indicates that the value estimated for the constant variable could be equal across all intersections in the study. In other words, the constant term estimated from one intersection was not statistically different (within the statistical boundary) when compared to most other intersections. This suggest that the models were capturing (or not capturing) the same decision-making characteristics at all study intersections.

6.5.2.2 Primary Variable

The coefficients of the *Primary* variable and the interactions between the primary variable and *Time* and *Gap* variables are discussed in this section. Table 6-4 shows the coefficient values, standard deviation and statistical significance for each to these variables estimated by the nine logit models developed for each data collection event. In this table, as in all remaining tables in this chapter, p-values less than 0.001 are rounded to 0.00 for ease of display. Looking at the table horizontally shows the result of the single model estimate on the given day. Looking vertically, the table shows how the coefficient values varied for data collection events. From the p-values it is apparent that all three variables are statistically significant in explaining the phase change decision. The negative coefficient of the *Primary* variable suggests that when the primary direction was green, the officer preferred not to change phases, as compared to other directions. This was to be expected for all phase variables that receive some degree of priority (all phase variables except *Tertiary* for three phase intersections and *Quaternary* for four phase intersections, as these receive no preferential treatment from the police officer). The positive coefficients observed for *P-Time* and *P-Gap* suggest that when these two values increased, so too, did the likelihood the office would change phases. This was expected; as phase length increases and the traffic stream thins, the officer was more likely to change phases.

Table 6-4 Primary Direction Variables

Intersections	Primary			P-Time			P-Gap			Obs.
	Coef.	STD	P>|z|	Coef.	STD	P>|z|	Coef.	STD	P>|z|	
N & R 10/13	-5.34	83.7	0.00	0.01	0.115	0.00	2.81	44.9	0.00	5712
N & R 11/03	-2.23	152.6	0.30	0.01	0.153	0.00	1.03	31.5	0.02	5004
N & R 11/10	-7.56	79.7	0.00	0.02	0.239	0.00	3.28	28.6	0.00	2389
N & R 11/17	-4.35	90.6	0.02	0.02	0.205	0.00	1.05	60.9	0.39	2461
N & L 11/03	-2.45	45.1	0.00	0.02	0.194	0.00	0.47	21.3	0.16	4162
N & L 11/10	0.34	93.5	0.83	0.01	0.174	0.00	-0.18	23.8	0.67	3326
S & P 11/10	-8.06	90.9	0.00	0.01	0.200	0.00	2.66	41.1	0.00	2319
S & P 11/17	-3.91	111.7	0.10	0.02	0.269	0.00	2.04	30.6	0.00	2249
183 & 27 01/07	-5.56	50.7	0.00	0.03	0.291	0.00	1.48	20.2	0.00	3975

The variables were compared in Table 6-5 using a two-tailed, two sample student's t-test or a one-way ANOVA test. The table indicates that coefficient values collected from Nicholson and Roosevelt are statistically indistinguishable in providing priority to the *Primary* phase but handle time and gaps for this phase differently. The intersection for Nicholson and Lee and Stanford and Perkins, showed that the model coefficient values remained consistent across data collection days. In other words, the officers directing traffic at these intersections treated the primary phase similarly for every event. The Four Phase evaluation found that data collected from the intersection of Stanford and Perkins in Baton Rouge and data collected from the intersection of NW 183 St. and NW 27 Ave. in Miami Gardens were not statistically different; the officers directing traffic were likely treating the priority direction similarly in both cities.

Table 6-5 Statistical Testing of the Primary Direction Variables

Comparison	Test	Primary		P-Time		P-Gap	
		Statistics	P>|z|	Statistics	P>|z|	Statistics	P>|z|
N & R	ANOVA	1.414	0.24	7.006	0.00	2.761	0.041
N & L	T-TEST	1.696	0.09	1.766	0.08	1.233	0.218
S & P	T-TEST	1.378	0.17	1.058	0.29	0.576	0.564
Three phase	ANOVA	2.453	0.03	5.42	0.00	4.817	0.000
Four phase	ANOVA	1.492	0.23	2.097	0.12	1.168	0.311
All	ANOVA	2.434	0.01	4.552	0.00	3.697	0.000

6.5.2.3 Secondary Variable

This section provides a similar discussion for the Secondary direction and the coefficients are provided in Table 6-6. The Secondary direction was the direction which received the second largest proportion of green time allocated by the police officer. The negative coefficient signs for the *Secondary* variables indicate again that the officer preferred not to change phases when the secondary direction was green. The table also shows that in general officers put less emphasis on time and more emphasis on the presence of gaps. This makes sense because the *Secondary* phase was shorter in duration than the *Primary*, suggesting less of a reliance on time.

Table 6-6 Secondary Direction Variables

Intersections	Secondary			S-Time			S-Gap			Obs.
	Coef.	STD	P>|z|	Coef.	STD	P>|z|	Coef.	STD	P>|z|	
N & R 10/13	-2.01	36.7	0.02	0.02	0.261	0.01	1.23	13.5	0.00	5712
N & R 11/03	0.41	71.6	0.84	0.00	0.196	0.68	2.12	13.0	0.00	5004
N & R 11/10	-2.42	37.4	0.09	0.04	0.429	0.03	1.61	18.4	0.02	2389
N & R 11/17	-1.32	32.4	0.31	0.03	0.300	0.03	1.41	10.0	0.00	2461
N & L 11/03	-0.42	29.3	0.51	0.01	0.210	0.00	0.31	18.7	0.44	4162
N & L 11/10	2.82	47.9	0.06	0.01	0.205	0.20	-0.24	11.8	0.51	3326
S & P 11/10	-3.10	28.8	0.01	0.03	0.311	0.04	1.51	10.8	0.00	2319
S & P 11/17	1.08	58.4	0.59	-0.01	0.427	0.39	3.25	19.2	0.00	2249
183 & 27 01/07	-2.44	20.8	0.00	-0.02	0.398	0.21	2.21	11.1	0.00	3975

A statistical analysis was conducted to test if the officers were directing traffic in a similar fashion across the data collection events. The results are provided in Table 6-7. The statistical analysis of the officers directing traffic at the intersection of Nicholson and Roosevelt was unable to reject the null hypothesis that these officers were providing the same consideration toward the secondary direction with respect to time and the presence of gaps. This suggests that the values estimated by the logit models from the various data collection days are statistically similar. This was also true for the intersection of Stanford and Perkins. Furthermore, the statistical analysis conducted on all three phase intersections was unable to distinguish between data collection days or location. This suggested that police officers treated the secondary direction statistically similar across time and space. This was also shown to be true for four phase intersections. However, the statistical analysis comparing the officers directing traffic at three phase intersections and four phase intersections rejected the null hypothesis that these values were similar. This suggested that police officers treated the secondary direction differently for three phase and four phase intersections and implies that an officer's approach to directing traffic at a four phase intersection was not a "three phase plus one" approach but an entire reallocation of priority.

Table 6-7 Statistical Testing of the Secondary Direction Variables

Comparison	Test	Secondary		S-Time		S-Gap	
		Statistics	P>|z|	Statistics	P>|z|	Statistics	P>|z|
N & R	ANOVA	0.725	0.54	2.180	0.09	0.968	0.41
N & L	T-TEST	2.365	0.02	0.623	0.53	0.868	0.39
S & P	T-TEST	1.555	0.12	1.871	0.06	1.925	0.05
Three phase	ANOVA	2.023	0.07	1.869	0.10	3.931	0.00
Four phase	ANOVA	2.514	0.08	2.369	0.09	2.586	0.08
All	ANOVA	1.965	0.05	2.905	0.00	5.293	0.00

6.5.2.4 Tertiary Variable

The tertiary direction received the third largest proportion of the green time allocation. For three phase intersections this was the lowest possible priority, i.e., no priority. Because of this the value of the *Tertiary* variable for three phase intersections must be equal to zero. In Table 6-8, the *Tertiary* variable for S & P 11/17 was estimated to be -30.99 and the *T-Gap* variable was

estimated at 17.46, two relatively extreme values. This occurred because every observation of a phase change occurred when *T-Gap* was equal to two, that is, the phase changed only when gaps on both approaches of the phase were present. Furthermore, the coefficient and p-values indicate a heavier reliance on *Time* and *Gap* variables when compared to other directions.

Table 6-8 Tertiary Direction Variables

Intersections	Tertiary			T-Time			T-Gap			Obs.
	Coef.	STD	P>|z|	Coef.	STD	P>|z|	Coef.	STD	P>|z|	
N & R 10/13	0.00	0.0	1.00	0.07	0.565	0.17	2.02	4.7	0.00	5,712
N & R 11/03	0.00	0.0	1.00	-0.04	0.227	0.01	0.20	15.4	0.04	5,004
N & R 11/10	0.00	0.0	1.00	0.49	1.680	0.03	1.05	4.7	0.09	2,389
N & R 11/17	0.00	0.0	1.00	1.19	3.272	0.02	0.01	4.4	0.98	2,461
N & L 11/03	0.00	0.0	1.00	0.04	0.392	0.03	1.32	7.0	0.00	4,162
N & L 11/10	0.00	0.0	1.00	0.28	1.194	0.00	1.35	5.6	0.00	3,326
S & P 11/10	-1.61	18.7	0.11	-0.03	0.481	0.30	2.40	18.7	0.02	2,319
S & P 11/17	-30.99	0.0	0.00	0.03	0.394	0.07	17.46	11.3	0.00	2,249
183 & 27 01/07	-1.52	16.4	0.01	-0.02	0.582	0.29	1.70	10.1	0.00	3,975

The statistical testing results of the *Tertiary* direction are presented in Table 6-9. The p-values indicate that the *Tertiary* direction was relatively unique to the data collection day when compared to the other directions; only *T-Time* for the four phase analysis and the *T-Gap* for the three phase analysis were consistent between observations. This may indicate that the officers did not allocate much attention to these directions given the lower demand that led to lower priority. This may also reflect a desire by the officer to move past this phase quickly to service the demand on the competing approaches. Also, for three phase signals, the *Tertiary* direction represented the smallest number of observations when compared to the *Primary* and *Secondary* directions.

Table 6-9 Statistical Testing of the Tertiary Direction Variables

Comparison	Test	Tertiary		T-Time		T-Gap	
		Statistics	P>|z|	Statistics	P>|z|	Statistics	P>|z|
N & R	ANOVA	0.000	1.00	14.143	0.00	0.592	0.62
N & L	T-TEST	0.000	1.00	4.299	0.00	0.050	0.96
S & P	T-TEST	37.343	0.00	1.940	0.05	15.164	0.00
Three phase	ANOVA	0.000	1.00	17.271	0.00	0.751	0.59
Four phase	ANOVA	833.541	0.00	2.045	0.13	291.661	0.00
All	ANOVA	439.358	0.00	22.244	0.00	113.892	0.00

6.5.2.5 Quaternary Variable

The *Quaternary* direction was only present for four phase intersections. Therefore, the three phase intersections have been excluded from this analysis. The *Quaternary* direction had the lowest priority for the four phase intersections and as such the coefficient for the *Quaternary* variable must be equal to zero as seen in Table 6-10. The p-value for the *Q-Time* variable was not statistically different for any of the four phase intersections. This indicated a stronger reliance on the presences of gaps in the decision making process for the police officers.

Table 6-10 Quaternary Direction Variables

Intersections	Quaternary			Q-Time			Q-Gap			Obs.
	Coef.	STD	P>|z|	Coef.	STD	P>|z|	Coef.	STD	P>|z|	
S & P 11/10	0.00	0.0	1.00	0.11	1.158	0.13	0.95	12.7	0.25	2,319
S & P 11/17	0.00	0.0	1.00	0.06	1.035	0.26	1.93	15.5	0.02	2,249
183 & 27 01/07	0.00	0.0	1.00	-0.05	0.610	0.07	1.90	7.7	0.00	3,975

The statistical results from the Quaternary direction analysis are provided in Table 6-11. The officers directing traffic at the intersection of Stanford and Perkins treated the quaternary direction statistically indistinguishable at a 95 percent confidence interval. When compared with the intersection of NW 183 St. and NW 27 Ave., the officers treated the gaps for this phase similarly but not the phase time.

Table 6-11 Statistical Testing of the Quaternary Direction Variables

Comparison	Test	Q-Time		Q-Gap	
		Statistics	P>|z|	Statistics	P>|z|
S & P	T-TEST	0.566	0.57	0.805	0.42
Four phase	ANOVA	3.168	0.04	0.615	0.54

Generally, it was observed that direction coefficients were negative in value and the coefficients for time and the presence of gaps were positive. This suggests that officers show priority to certain directions as compared to others and as phase length grows or if gaps were present, the officer was more likely to change phase. These observations were made in almost all instances and show that the models were intuitively correct in predicting phase changes. The models developed from multiple observation days at the same intersection generally produced coefficient values that were statistically indistinguishable. However, logit models generated from the three phase intersection and four phase intersection did not produce statistically similar values. This suggests that an officer's approach to directing traffic at a four phase intersection was not a "three phase plus one" approach but an entire reallocation of priority. The only exception to this was seen with the constant variable, which was statistically indistinguishable for all intersections within a 95 percent confidence interval. This suggests that the cumulative effect of the error was consistent between all models and was an indication the models were capturing (or not capturing) the same decision making characteristics.

The most significant finding was the statistical similarities between intersections despite being collected at separate intersections in different cities. The statistical analysis was unable to determine that the officers directing traffic in Baton Rouge, LA were doing anything different than the officers in Miami Gardens, FL. This may suggest that police directing traffic in Baton Rouge and Miami Gardens use a similar approach.

6.5.3 Goodness-Of-Fit

Goodness-of-fit for logit models is a measure of how well the predicted choice outcomes match the observed data. Goodness-of-fit for this research was quantified using three metrics: the pseudo R-squared (ρ^2) value, the Hosmer-Lemeshow chi-squared statistic (χ^2) and the area under the receiver operator curve (ROC). These measures of goodness-of-fit are provided in Table 6-12. Also shown in this table are the p-values corresponding to the chi-squared statistic

with eight degrees of freedom for the Hosmer-Lemeshow Test. In general, the model fit was in the "good" to "outstanding" range. However, the models estimated at the intersection of Nicholson and Lee did drop into the "acceptable" range [123]. The p-value indicated the estimated probabilities made by the logit model were statistically similar to those observed in the data within a 95 percent confidence interval.

Table 6-12 Logit Model Goodness-of-Fit

Intersections	ρ^2	χ^2	P>|z|	ROC
N & R 10/13	0.277	7.47	0.49	0.864
N & R 11/03	0.223	4.53	0.81	0.855
N & R 11/10	0.338	4.81	0.45	0.935
N & R 11/17	0.287	7.59	0.47	0.886
N & L 11/03	0.145	13.13	0.11	0.828
N & L 11/10	0.190	10.46	0.23	0.817
S & P 11/10	0.224	5.71	0.68	0.891
S & P 11/17	0.366	1.92	0.98	0.958
183 & 27 01/07	0.221	5.05	0.75	0.874

6.5.4 Model Transfer and Validation

The goal of the model validation was to show that the parameters estimated by the models (the officer's decision making) were temporally and spatially consistent. This was done by using *model transfer*. For each intersection, the coefficient values from one or more data collection days were projected onto the data collected from a different day. The pseudo R-squared *(ρ^2)* value was then used as a measure of model validation. If the officer's decision making was consistent between observation days, then the pseudo R-squared value estimated from the validation data should fall into the acceptable range (greater than 0.1). For the purposes of validation, the intersections were broken up into two datasets: calibration and validation. The calibration dataset represents the models that were transferred. The validation dataset represents the data on which the calibration parameters were being transferred to. This is shown in Table 6-13.

Table 6-13 MTC Calibration and Validation Datasets

Intersections	10/13/12	11/03/12	11/10/12	11/17/12	01/07/13
Stanford & Perkins	N/A	N/A	C	V	N/A
Nicholson & Roosevelt	C	C	C	V	N/A
Nicholson & Lee	N/A	C	V	N/A	N/A
NW 183 & NW 27	N/A	N/A	N/A	N/A	C

C = Calibration dataset; V = Validation dataset

The intersection of Nicholson and Lee was validated by transferring the coefficients estimated on 11/03/12 to the data collected on 11/10/12. Likewise, the validation of Stanford and Perkins was conducted by transferring coefficients estimated by the model for 11/10/12 onto the data collected on 11/17/12. Since only one data collection day was available for the intersection of NW 183 St. and NW 27 Ave. this intersection was validated using the model estimated for Stanford and Perkins on 11/10/12. The only intersection that required having more than one

intersection data collection day combined into one model was Nicholson and Roosevelt. This was because Nicholson and Roosevelt was the only intersection with more than two observation events.

The other intersections only required one set of coefficients to be used to estimate pseudo R-squared *(ρ^2)* on the validation dataset. The combined Nicholson and Roosevelt model was estimated by combining the data collected from three of the data collection days (10/13/12, 11/013/12 and 11/10/12) into a single dataset and estimating a new logit model. These coefficients were then used to estimate a pseudo R-squared value for the fourth data collection day (11/17/12). The Bayesian Updating approach to model transfer was considered, but because the original dataset was available from the estimated models, Bayesian Updating was not needed and would likely lead to less accurate results [124].

Table 6-14 shows the model coefficients estimated by the combined Nicholson and Roosevelt dataset. The number of observations used to estimate the model was 17,060 and the pseudo R-squared *(ρ^2)* was 0.235, suggesting good model fit. The p-value indicated that all model variables were statistically significant at a 95 percent confidence interval. The sign value for each of the variables appeared to be intuitively correct with the exception of *T-Time*. This may have resulted from the relatively small number of observations when the *Tertiary* direction was green. To validate the Nicholson and Roosevelt model, these values were used on data collected on 11/17/12 to estimate the pseudo R-squared.

Table 6-14 Nicholson and Roosevelt Combined Logit Model Parameters

Variable	Coefficient	STD	P>|z|
Primary	-5.423	83.33	0.00
Secondary	-2.429	67.08	0.00
P-Time	0.007	0.13	0.00
S-Time	0.009	0.51	0.02
T-Time	-0.052	1.78	0.00
P-Gap	2.143	46.53	0.00
S-Gap	1.567	28.98	0.00
T-Gap	1.199	32.00	0.00
Constant	-2.977	56.05	0.00

6.5.4.1 Validation Results

Table 6-15 shows the logit model validation results. The *Model* column indicates which log-likelihood value is being compared. *$L^*(0)$* refers to the log-likelihood when only the constant term was estimated. This value was used as the basis of comparing the pseudo R-squared value for the validation process. The *$L^*(\theta_0)$* refers to the model estimate using the data from which it was collected. This is the goodness-of-fit measure provided in Table 6-12. The values in Table 6-12 are the upper bound for the validation goodness-of-fit (no model would fit better on the validation dataset than calibration data). The *$L^*(\theta)$* represents the log-likelihood value estimated by completely transferring the calibration model onto the validation dataset and the *$L^*(\theta')$* was the result of updating the transferred model's constant term. This resulted in the *$L^*(\theta')$* model always producing better results than the *$L^*(\theta)$.* The *LL* column is the log-likelihood value estimated and the *C* value is the constant term used for each calculation.

The ρ^2 value for model validation was estimated according to Equation 6.3 [124]:

$$\rho^2 = 1 - \frac{L^*(n)}{L^*(0)} \quad 6.3$$

where,

- *L*(0)* is the log-likelihood corresponding to market shares
- *L*(n)* is the log-likelihood of the validation statistics (*L*(θ_o), L*(θ), or L*(θ')*)

Table 6-15 Logit Mode Validation Results

Model	N & R			N & L			S & P			183 & 27		
	LL	ρ^2	C	LL	ρ^2	C	LL	ρ^2	C	LL	ρ^2	C
L(0)*	-235		-4.2	-248		-4.6	-223			-725		-3.7
L(θ_0)*	-168	0.287	-3.8	-201	0.190	-7.3	-141	0.366	-7.5	-565	0.221	-3.2
L(θ)*	-185	0.212	-2.9	-375	-0.514	-4.8	-182	0.185	-3.6	-647	0.108	-3.3
L(θ')*	-178	0.242	-2.3	-255	-0.028	-6.6	-169	0.241	-4.3	-646	0.109	-3.5

From Table 6-15 it was observed that in general the model transfer results were in the "acceptable" to "good" range, except for Nicholson and Lee [123]. Nicholson and Roosevelt showed the most successful model transfer. This was likely due to the larger dataset which was used to estimate the transfer model. The intersection of Stanford and Perkins also showed good transferability. This too was not surprising given that the original model had the highest goodness-of-fit measure. The intersection of NW 183 St. and NW 27 Ave. showed results that were on the lower end of the "acceptable" range. This was to be expected given that this was the only model transferred to a different location from which it was estimated. Nicholson and Lee started with the lowest ρ^2 value, and therefore, was not expected to transfer well [124].

6.5.5 Summary of Logit Model Findings

The logit models estimated from the signal operation data were able to reasonably capture the choice behavior of the police officers directing traffic. This was evident in the goodness-of-fit statistics provided in Table 6-12. In general, the variables which were determined to effect when the officer changed direction (*Priority*, *Time*, and *Gap*) were both intuitive and statistically significant. Generally, logit models produced statistically similar coefficient values, indicating that officers placed in similar situations will likely direct traffic in a similar fashion. This was consistent both spatially and temporally. However, stronger correlations were observed for officers directing traffic at the same intersection but on different days as compared to officers directing traffic at different intersections. The statistical analysis also indicated that officers directing traffic at a three phase intersection allocate green time differently than those at a four phase intersection. It was also apparent that officers directing traffic in Baton Rouge, LA and Miami Gardens, FL did so in a similar fashion. These results were verified by validating the logit models through model transfer. This showed that choice behavior estimated from one observation (in the case of Nicholson and Roosevelt, three) were statistically similar when evaluated on data from another observation, provided they had the same number of phases (three phases or four phases).

6.6 MTC Model Development and Comparisons of Performance

The predictive logit models quantify the police officers' phase change decisions observed in the field. These models were integrated into a microscopic simulation software, VISSIM 5.3, for the purpose of simulating the officer's decision making. The traffic simulation was conducted in three steps. The first step was to program the geometric design and special event traffic demand for each observation into the simulation software. The second step was to program the logit models developed in the previous section into VISSIM to act as the signal controller. The final step was to conduct a comparison of performance between the simulated MTC and video observations; simulated MTC to observed traffic control within an alternative study area; and simulated MTC and an actuated signal. This was done for the purposes of benchmarking, calibrating, validating, and evaluating the proposed MTC model. Because simulating MTC using the logit models requires the tracking of individual vehicles, the models might not be readily implemented in macroscopic or mesoscopic traffic simulation platforms.

6.6.1 Geometric Design and Demand Modeling

The coding of the simulation model required the geometric design of the intersections and the vehicle demand as model inputs. The geometric design of the four study intersections was programmed into VISSIM 5.3 with the use of open-source high-resolution satellite images provided through an online search. The accuracy of the measurements taken from the images was verified during site visits. With the traffic count and turning movement information from the intersection event timelines, the intersection discharge flow rate observed in the videos was aggregated into 15-min flow rates and programmed into the simulation.

6.6.2 Logit Model Programing

The integration of the logit models into VISSIM was accomplished with the Vehicle Actuated Program (VAP) interface. VAP allowed for a real-time exchange of information between the simulation software and a VAP program file, which contained the logit models. The VAP received the intersection detector information to create the independent variables used in the logit model. From these variables and the logit model parameters, it was possible to estimate the probability of a phase change.

Through the VAP interface, the phase change probability was calculated every simulation time step (one second). These probabilities were then compared with a threshold value. If the probability of changing phases was higher than or equal to the threshold value, the VAP notified the signal controller inside the VISSIM model to change phases and proceed to the next time step. If the threshold value was not reached, the VAP allowed VISSIM to proceed with the next time step without a phase change.

The threshold value was assumed to be a random variable from a uniform distribution. By randomly changing the threshold value, phase to phase, it was possible to more accurately represent the variability of MTC, which was observed in the field. At the end of each phase, the threshold value for the next phase was calculated by use of Equation 6.4. The threshold value (K_p) of phase p was computed by adding and subtracting a pseudo-random number to a static threshold value (S_p) as follows:

$$K_p = S_p \pm \alpha_p \left[\frac{(aX_n+c) \bmod m}{m}\right] \quad 6.4$$

where,

- K_p = threshold value of phase *p*
- S_p = static cut-point value
- α_p = calibration parameter
- X_n = random number generated in previous or initial time step
- *a* = 1,597
- *c* = 51,749
- *m* = 244,944

The value of the static cut-point value was empirically derived from the data collection video. For example, if 30 phase changes were observed in the video, the static cut-point (S_p) was set to the value of the 31st highest choice probability estimated by the logit model. This approach ensured that, on average, 30 phase changes would likely occur during the same time period, permitting the simulation and observed intersections to have approximately the same number of phase changes.

The upper and lower bounds of the random number were confined by the calibration variable α_p, and allowed the degree to which the threshold value varied to be calibrated to match the observations in the field. This step was done by adjusting this variable up or down until the standard deviation for the simulated phase lengths was equal to the standard deviation observed in the videos. The calibration variable α_p was multiplied by a pseudo-random number between zero and one. This value was calculated with a linear congruential random number generator [124]. The generation of the pseudo-random number also required a seed value to calculate the initial random variable. The value of the seed number varied for each simulation.

6.6.3 Comparisons of Performance

Three comparisons of performance were conducted to verify and evaluate the performance of the developed MTC model within the simulation platform. The first comparison of performance evaluated if the simulation model produced similar signal timings and intersection throughput as those observed in the video observations. The second comparison of performance evaluated how well the MTC model functioned when applied to an alternative study area. This comparison evaluated how well the MTC simulation tool would transfer to other locations and if this model could be used to signify a “representative” police officer directing traffic. The third comparison of performance was used to evaluate how the MTC model performed in contrast to an actuated signal controller.

6.6.3.1 MTC Model Calibration

Before performance comparisons could be conducted, the MTC model needed calibration. The goal of the calibration process was to have the simulation output match the field measurements with statistical certitude. The calibration process was important because not all model parameters could be directly observed in the video footage. There were three parameters that needed to be estimated through the calibration process that were unique to each simulated intersection: the logit model coefficients (β_k), the variance of the cut-point (α_p), and the approach demand.

The calibration of these three parameters was conducted in parallel because each of these parameters was interdependent. For example, by adjusting the logit model coefficients, the signal timing would change, altering the intersection throughput. An added complexity was the stochastic nature of the simulation runs. As a result, multiple simulation runs were required to estimate if the changes observed in the simulation model were a result of calibrating the relevant parameters or of the stochastic nature of the simulation model.

Once the calibration was done, an analysis was conducted to determine the number of simulation runs required to estimate reliable results. This analysis used the average cycle length to estimate the number of simulation runs required. It was determined that anywhere between three to nine simulation runs were required for each model to ensure that the average cycle length was consistent between runs. Therefore, to ensure consistent results, each event was simulated 10 times and the results were averaged.

The estimated logit model coefficients provided a range of values within the 95 percent confidence interval. The values of the coefficients that result in the correct green time allocation can fall anywhere within this range. Therefore, the coefficient values for each variable used in the logit model was calibrated within the range of the 95 percent confidence interval until the average simulated phase length matched the field observations. Adjusting these values affected the mean value of the simulated signal. To adjust the variance of this mean, the calibration variable (α_p) had to be estimated through an iterative process until the standard deviation of each phase length approximately matched the observed standard deviation.

6.6.3.2 Simulated MTC to Observed MTC

The comparison of performance made between the simulated MTC and Observed MTC investigated two key elements: 15-minute vehicle counts and signal timing. It was believed that if the 15-minute vehicle counts and the average phase and cycle lengths were statistically similar, this would show strong evidence the MTC model was producing similar signal timing and having a similar impact on intersection performance.

6.6.3.2.1 15-Minute Vehicle Count Comparison

The simulated 15-minute vehicle counts were compared to the observed 15-minute vehicle counts using a chi-squared test and a regression analysis. The chi-squared test compared the average 15-minute counts of the simulated runs to the expected count frequencies in the video footage. The results of this test are presented as the p-value shown in Table 6-16 under the *P*>|*z*| column. P-values greater than 0.05 indicated that the simulated counts are statistically similar to the observed traffic counts at a 95 percent confidence interval. The regression analysis plotted the average simulated vehicle counts and the observed counts for every 15-minute observation pair. The R^2 column of Table 6-16 shows the resulting Pearson Correlation Coefficient that provides an indication of the proportion of the variance between observed and simulated vehicle counts. The results show, for the most part, the simulated throughput matches that of the throughput collected from the video data in the field. When viewed in context of the signal timing, presented in the next section, it can be inferred that the simulated intersection approach demand was similar to that observed during the data collection periods.

Table 6-16 Simulated MTC Vehicle Counts vs. Observed and Statistical Evaluation

Intersections	P>|z|	R^2
N & R 10/13	0.08	0.984
N & R 11/03	0.42	0.992
N & R 11/10	0.29	0.996
N & R 11/17	0.83	0.997
N & L 11/03	0.22	0.983
N & L 11/10	0.00	0.930
S & P 11/10	0.00	0.986
S & P 11/17	0.00	0.930
183 & 27 01/07	0.00	0.986

6.6.3.2.2 Signal Timing Comparisons

With the beta coefficients (β_k) and cut-point variable (α_p) calibrated, the signal timing results for each observation were compared to those obtained in the simulation model. These results are provided in Table 6-17. This table displays the observed average phase length, the simulated average phase length and their respective standard deviations. To compare the observed phase length and standard deviation from the video footage to the simulation model, a two-sample student t-test and f-test were conducted; p-values for these tests are provided in the table. P-values larger than 0.05 indicated that the observed phase length and the simulated phase length were statistically similar at a 95 percent confidence interval.

Table 6-17 Simulated MTC Signal Timing vs. Observed MTC and Statistical Evaluation

Phase	Observed		Simulated		P>|z|	
	Avg Time (s)	STD (s)	Avg Time (s)	STD (s)	T-Test	F-Test
Intersection: Nicholson & Roosevelt 10/13/12						
NBL & SBL	10.11	6.42	10.45	2.68	0.87	0.09
NBT & SBT	224.69	110.02	218.37	81.89	0.86	0.32
EBT & WBT	69.77	33.4	70.14	19.11	0.97	0.2
Cycle length	304.65	107.43	299.13	85.62	0.87	0.36
Intersection: Nicholson & Roosevelt 11/03/12						
NBL & SBL	16.18	22.34	17.75	13.03	0.84	0.2
NBT & SBT	232.45	91.38	237.24	55.03	0.88	0.22
EBT & WBT	56.82	32.9	59.18	37.49	0.86	0.58
Cycle length	305.45	104.7	314.46	69.87	0.81	0.27
Intersection: Nicholson & Roosevelt 11/10/12						
NBL & SBL	9.07	1.67	9.05	0.72	0.98	0.1
NBT & SBT	164.27	31.16	161.36	35.69	0.83	0.58
EBT & WBT	51.27	17.4	54.53	16.62	0.64	0.47
Cycle length	224.6	34.03	225.53	39.56	0.95	0.59
Intersection: Nicholson & Roosevelt 11/17/12						
NBL & SBL	8.33	1.11	9.51	0.53	0	0.13
NBT & SBT	158.81	45.16	167.81	46.03	0.63	0.51

EBT & WBT	46.2	20.43	40.55	19.74	0.49	0.48
Cycle length	216.67	56.88	217.62	49.61	0.97	0.42
Intersection: Nicholson & Lee 11/03/12						
NBT & SBT	139.26	35.41	128.33	25.2	0.37	0.3
NBL & SBL	22.6	10.7	23.91	10.76	0.74	0.5
EBT & WBT	75.16	41.1	80.81	47.2	0.72	0.58
Cycle length	235.74	69.4	232.77	55.58	0.9	0.37
Intersection: Nicholson & Lee 11/10/12						
NBT & SBT	210.13	77.03	230.91	74.77	0.51	0.48
NBL & SBL	20.94	4.23	20.64	2.43	0.84	0.2
EBT & WBT	76.6	56.11	73.53	47.24	0.89	0.4
Cycle length	302.07	75.78	327.01	91.08	0.46	0.61
Intersection: Nicholson & Lee 11/10/12						
EBL WBL	44.44	27.36	31.06	28.56	0.31	0.53
EBT & WBT	68.56	30.24	67.4	29.4	0.93	0.48
NBL & SBL	34.5	6.16	32.62	9	0.62	0.72
NBT & SBT	294.88	103.78	287.2	79.73	0.86	0.34
Cycle length	455	106.24	416.76	83.63	0.4	0.36
Intersection: Nicholson & Lee 11/17/12						
EBL & WBL	53.69	24.31	58.69	17.16	0.59	0.3
EBT & WBT	80.08	33.89	64.34	27.98	0.25	0.38
NBL & SBL	36.92	8.41	38.96	9.74	0.6	0.59
NBT & SBT	211.62	81.19	203.23	67.2	0.8	0.39
Cycle length	398.92	102.42	366.08	85.07	0.43	0.39
Intersection: NW 183 Street & NW 27 Avenue 01/07/13						
EBL WBL	20.43	15.07	22.98	12	0.63	0.36
EBT & WBT	27.59	11.94	32.43	10.98	0.26	0.45
NBL & SBL	34.7	19.68	36.66	22.2	0.79	0.57
NBT & SBT	111.35	32.64	112.57	25.75	0.91	0.36
Cycle length	194.08	50.38	204.64	37.64	0.55	0.33

The results showed that in all but one instance, the analysis must accept the null hypothesis that the simulated phase lengths were statistically similar to the observed. The exception to this was observed in Table 6-17 for the intersection of Nicholson and Roosevelt collected on 11/17/12. In this table, the northbound left, southbound left phase did not statistically match the simulated phase length. The average value was approximately 8.33 seconds with a standard deviation of 1.11 while the simulated intersection had a phase length of 9.51 seconds with a standard deviation of 0.53. Due to the short duration and relatively small standard deviation observed in the field, the simulation model had difficultly matching this phase. Despite this single t-test failure, the results of the comparison suggest that the simulated models statistically replicated the observed phase length and standard deviation of this length, within a 95 percent confidence interval. The results showed, with statistical certitude, that the simulation matched the observed video data with respect to 15-minute approach counts, signal phase length and standard deviation of this length.

6.6.3.3 Simulated MTC to Observed Traffic Control

This comparison of performance evaluates how well the MTC model, developed from one study area transfers spatially and temporally. In effect, this process would be like moving an officer directing traffic at one intersection to a different time or location. The comparison of MTC to observed performance was accomplished using model transfer by transferring the calibrated VAP files from one intersection to another. For purposes of this research, a successful transfer was considered achieved when the transferred model produced statistically similar results, temporally and spatially, with the observations made in the field. To achieve this, the intersections were split into two data sets: calibration and validation. The calibration dataset represents the models that were transferred. The validation data set represents the data to which the calibration parameters were being transferred. The intersection of Nicholson and Lee was validated by transferring the model estimated on November 3, 2012, to the data collected on November 10, 2012. Likewise, the validation of Stanford and Perkins was conducted by transferring the model estimated on November 10, 2012, onto the data collected on November 17, 2012. Because only one data collection day was available for the intersection of NW 183rd Street and NW 27th Avenue, this intersection was validated with the model for Stanford and Perkins on November 10, 2012. The intersection of Nicholson and Roosevelt was validated by combining the data collected on October 13, 2012, November 3, 2012, and November 10, 2012, and testing this combined model on data collected on November 17, 2012. Table 6-18 displays the traffic signal timing results for the validation dataset. Present in the tables are the average time (phase length), the standard deviation of this phase length, the two sample, two-tailed t-test results comparing the mean values and a two sample, f-test comparing the standard deviations. P-values larger than 0.05 suggest that the signal timings were statistically similar at a 95 percent confidence interval.

The analysis from a two-sample, two-tailed student t-test failed to reject the null hypotheses for all but one observation, suggesting that the transferred models performed in a similar fashion when compared with the observed officers directing traffic in the alternative study area. The single exception was seen for the tertiary direction at the intersection of Nicholson and Roosevelt and was likely the result of an extraordinarily small standard deviation observed during the validation data set. *F*-testing conducted on the variance of these values also showed them to be statistically similar (failure to reject the null hypothesis that these values are equal) for every observation with the exception noted previously. Therefore, in general, the transferred models were able to approximate the signal timing reasonably well. This suggests the principles used to direct traffic were sufficiently similar such that representative officers would likely make similar right-of-way allocations as those predicted by the MTC model. While some instances failed the statistical test conducted, overall the models were consistent.

6.6.3.4 Simulated MTC to Actuated Control

The third comparison of performance was to evaluate the simulated MTC model against an actuated signal controller. For this analysis, an actuated controller was programed into the simulation model for all nine study areas. The total throughput, signal timing, and network performance were then used to compare and evaluate the two control types. The signal controller data for the intersections located in Baton Rouge, LA was obtained from the Baton Rouge Department of Public Works. The signal timing information was not available for the intersection of NW 183 St and NW 27 Ave in Miami Gardens, FL. The signal timing for this intersection was estimated from the video footage collected prior to the arrival of the police officer. The actuated controllers were simulated 10 times and their results averaged as was done in the MTC simulations.

Table 6-18 Simulated MTC Signal Timing vs. Observed Within Alternative Study Area

Phase	Observed		Simulated		P>|z|	
	Avg Time (s)	STD (s)	Avg Time (s)	STD (s)	T-Test	F-Test
Intersection: Nicholson & Roosevelt						
NBL & SBL	8.33	1.11	10.57	1.95	0	0.81
NBT & SBT	158.81	45.16	200.27	56.97	0.05	0.64
WBT & EBT	46.2	20.43	67.42	22.13	0.02	0.55
Cycle length	216.67	56.88	277.68	65.31	0.02	0.58
Intersection: Nicholson & Lee						
NBT & SBT	210.13	77.03	235.59	71.02	0.41	0.45
NBL & SBL	20.94	4.23	21.02	2.32	0.96	0.18
WBT & EBT	76.6	56.11	83.57	49.88	0.75	0.43
Cycle length	302.07	75.78	340.4	87.2	0.26	0.59
Intersection: Stanford & Perkins						
EBL & WBL	53.69	24.31	37.33	24.2	0.12	0.50
WBT & EBT	80.08	33.89	79.9	23.22	0.98	0.28
NBL & SBL	36.92	8.41	34.26	8.27	0.47	0.49
NBT & SBT	211.62	81.19	303.52	77.91	0.01	0.47
Cycle length	398.92	102.4	456.62	81.94	0.17	0.37
Intersection: NW 183 Street & NW 27 Avenue						
EBL & WBL	20.43	15.07	20.85	21.09	0.95	0.70
WBT & EBT	27.59	11.94	61.4	27.09	0	0.89
NBL & SBL	34.7	19.68	32.16	12.66	0.7	0.25
NBT & SBT	111.35	32.64	323.24	86.01	0	0.93
Cycle length	194.08	50.38	438.25	88.43	0	0.81

6.6.3.4.1 Total Throughput

The total throughput was collected from the intersections and converted into volumes (veh/hr). The results are presented in Table 6-19. The *ATC* column displays the average throughput volume of the intersection under fully actuated signal control. The *Observed* column shows the total throughput volume observed in the field under manual traffic control. The *MTC* column shows the total throughput volume of the simulated manual traffic control model. The table indicated that the actuated controller, the observed and the manual traffic control model produced approximately the same amount of throughput. This was to be expected since the simulation model was calibrated based on 15-minute count data. This indicated that the actuated controller was performing at least as well as the manual traffic control model, in terms of intersection throughput. Had the actuated controller not performed as well this would likely have caused a reduction in throughput.

Table 6-19 Intersection Throughput: Observed, Actuated Control, and Simulated MTC

Intersections	Observed (vehicles/hr)	ATC (vehicles/hr)	MTC (vehicles/hr)
N & R 10/13	1092	1092	1090
N & R 11/03	1033	1019	1015
N & R 11/10	1692	1640	1645
N & R 11/17	1983	1982	1973
N & L 11/03	1546	1540	1535
N & L 11/10	1544	1567	1381
S & P 11/10	2622	2516	2613
S & P 11/17	3197	3393	3157
183 & 27 01/07	3460	3390	3640

6.6.3.4.2 Signal Timing

The average signal timing for the actuated controllers and the manual traffic control model is presented in Table 6-20. The *Avg Time* column displays the average phase length, the *STD* column shows the standard deviation of this time and the *Obs.* column shows the number of times this phase was observed during the simulation. The actuated controller displayed lower cycle length and standard deviation when compared to the MTC model. Furthermore, the number of observations suggested that the actuated controller was able to skip over phases, resulting in a lower number of observations for phases with low demand. This was not present in the manual traffic control model, as officers directing traffic using the “clicker” method do not have the ability to skip over phases. Therefore, the number of observations for the MTC model is approximately the same for each phase.

6.6.3.4.3 Network Performance

The actuated controller was evaluated for overall network performance and compared to the MTC model. The network evaluation metrics used were average delay, average number of stops, average speed, average stop delay, total delay, total number of stops, total stop delay and total travel time. The parameter values corresponding to manual control are compared to actuated signal control for each intersection in Table 6-21. These tables show the average parameter value for each of the 10 simulation runs under the column headers *MTC* and *ATC*, respectively. Also shown is the percent difference between the control types for each metric and the p-value of a two-sample, two-tailed student t-test. P-value less than 0.05 suggest the difference between the traffic control types was statistically significant.

The results showed that the actuated controller outperformed the police officer in nearly every metric. The exception to this was seen in the average number of stops and total number of stops at the intersection of Stanford and Perkins on 11/17/12 and NW 183 St. and NW 27 Ave. on 01/07/13. Other than two instances, every metric indicated that the actuated controller would have performed better than the officer directing traffic. The t-test results showed, for the most part that these findings were statistically significant at a 95 percent confidence interval. There are two likely causes for the poor performance of manual traffic control when compared to the actuated controller. The first of which was a substantial decrease in saturation flow rate as phase length progressed. This finding was consistent with the previous literature on manual traffic control [116]. The other likely cause was the ability of the actuated controller to skip phases when demand was not present.

Table 6-20 Simulated MTC Signal Timing vs. Simulated Actuated Control

Phase	Simulated Actuated Control			Simulated MTC		
	Avg Time (s)	STD (s)	Obs.	Avg Time (s)	STD (s)	Obs.
Intersection: Nicholson & Roosevelt 10/13/12						
NBL & SBL	16.75	1.10	15	10.45	2.68	27
NBT & SBT	44.14	0.05	92	218.37	81.89	26
EBT & WBT	15.83	0.29	92	70.14	19.11	26
Intersection: Nicholson & Roosevelt 11/03/12						
NBL & SBL	13.97	0.76	7.3	17.75	13.03	19
NBT & SBT	44.20	0.09	74.2	237.24	55.03	19
EBT & WBT	13.96	0.37	75.3	59.18	37.49	19
Intersection: Nicholson & Roosevelt 11/10/12						
NBL & SBL	14.83	0.94	6	9.05	0.72	15
NBT & SBT	44.04	0.08	44	161.36	35.69	15
EBT & WBT	14.76	0.27	45	54.53	16.62	14
Intersection: Nicholson & Roosevelt 11/17/12						
NBL & SBL	17.14	0.83	16	9.51	0.53	18
NBT & SBT	43.98	0.00	49	167.81	46.03	17
EBT & WBT	14.71	0.78	50	40.55	19.74	17
Intersection: Nicholson & Lee 11/03/12						
NBT & SBT	63.58	0.54	73	128.33	25.2	29
NBL & SBL	11.68	0.16	66	23.91	10.76	29
EBT & WBT	25.09	0.42	72	80.81	47.2	28
Intersection: Nicholson & Lee 11/10/12						
NBT & SBT	65.34	1.05	46	230.91	74.77	12
NBL & SBL	11.70	0.39	40	20.64	2.43	12
EBT & WBT	22.94	1.02	45	73.53	47.24	11
Intersection: Stanford & Perkins 11/10/12						
NBT & SBT	103.87	27.16	21	287.2	79.73	8
NBL & SBL	16.71	3.58	21	32.62	9.00	9
EBT & WBT	31.54	11.81	21	67.40	29.40	9
NBL & SBL	19.33	3.83	21	31.06	28.56	9
Intersection: Stanford & Perkins 11/17/12						
NBT & SBT	82.74	23.39	28	203.23	67.20	13
NBL & SBL	25.49	8.31	28	38.96	9.74	13
EBT & WBT	44.89	11.03	27	64.34	27.98	13
NBL & SBL	21.19	4.88	27	58.69	17.16	13
Intersection: NW 183 Street & NW 27 Avenue 01/07/13						
NBT & SBT	65.39	11.77	56	112.57	25.75	35
NBL & SBL	24.03	10.30	55	36.66	22.20	35
EBT & WBT	20.40	4.54	55	32.43	10.98	36
NBL & SBL	19.86	0.68	55	22.98	12.00	36

Table 6-21 Simulated MTC Network Performance vs. Simulated Actuated Control

Parameter	MTC	ATC	Percent Difference	P>|z|
Intersection: Nicholson & Roosevelt 10/13/12				
Average Delay (s)	42.1	11.7	72.15%	0.00
Average Number of stops	0.4	0.4	14.98%	0.00
Average Speed (mph)	12.3	22.4	-81.69%	0.00
Average Stop delay (hr)	37.9	8.0	78.90%	0.00
Total delay (hr)	30.3	8.4	72.12%	0.00
Total number of stops	1112	946	14.89%	0.00
Total stop delay (hr)	27.2	5.8	78.88%	0.00
Total travel time (hr)	48.5	26.7	44.98%	0.00
Intersection: Nicholson & Roosevelt 11/03/12				
Average Delay (s)	33.7	7.7	77.12%	0.00
Average Number of stops	0.4	0.3	27.99%	0.00
Average Speed (mph)	13.7	24.9	-81.23%	0.00
Average Stop delay (hr)	30.3	5.0	83.40%	0.00
Total delay (hr)	17.2	3.9	77.12%	0.00
Total number of stops	670	482	28.05%	0.00
Total stop delay (hr)	15.4	2.6	83.40%	0.00
Total travel time (hr)	29.5	16.3	44.82%	0.00
Intersection: Nicholson & Roosevelt 11/10/12				
Average Delay (s)	27.7	12.5	54.70%	0.00
Average Number of stops	0.4	0.4	2.29%	0.35
Average Speed (mph)	15.2	21.6	-41.82%	0.00
Avg. Stop delay (hr)	23.0	7.5	67.33%	0.00
Total delay (hr)	16.9	7.7	54.58%	0.00
Total number of stops	875.4	857.6	2.03%	0.45
Total stop delay (hr)	14.1	4.6	67.25%	0.00
Total travel time (hr)	31.7	22.7	28.27%	0.00
Intersection: Nicholson & Roosevelt 11/17/12				
Average Delay (s)	44.7	19.4	56.67%	0.00
Average Number of stops	0.7	0.6	12.32%	0.00
Average Speed (mph)	13.6	20.4	-49.44%	0.00
Avg. Stop delay (hr)	39.4	14.5	63.08%	0.00
Total delay (hr)	36.6	15.9	56.68%	0.00
Total number of stops	1927	1690	12.28%	0.00
Total stop delay (hr)	32.3	11.9	63.09%	0.00
Total travel time (hr)	62.8	42.1	32.96%	0.00
Intersection: Nicholson & Lee 11/03/12				
Average Delay (s)	61.2	18.2	70.23%	0.00
Average Number of stops	0.7	0.6	17.51%	0.00
Average Speed (mph)	11.1	20.7	-86.40%	0.00
Average Stop delay (hr)	56.0	13.4	76.02%	0.00
Total delay (hr)	32.3	9.6	70.25%	0.00

Total number of stops	1277	1052	17.59%	0.01
Total stop delay (hr)	29.5	7.1	76.04%	0.00
Total travel time (hr)	48.7	26.1	46.34%	0.00
Intersection: Nicholson & Lee 11/10/12				
Average Delay (s)	24.0	8.3	65.51%	0.00
Average Number of stops	0.4	0.3	28.03%	0.00
Average Speed (mph)	16.3	24.3	-48.87%	0.00
Average Stop delay (hr)	19.8	4.9	75.32%	0.00
Total delay (hr)	11.2	3.9	65.52%	0.00
Total number of stops	668.7	481.1	28.05%	0.00
Total stop delay (hr)	9.2	2.3	75.34%	0.00
Total travel time (hr)	22.4	15.1	32.72%	0.00
Intersection: Stanford & Perkins 11/10/12				
Average Delay (s)	97.6	72.3	25.91%	0.00
Average Number of stops	1.0	1.5	-49.55%	0.00
Average Speed (mph)	9.1	11.4	-25.87%	0.00
Average Stop delay (hr)	89.7	60.8	32.13%	0.00
Total delay (hr)	75.0	51.5	31.43%	0.00
Total number of stops	2757	3814	-38.36%	0.00
Total stop delay (hr)	68.9	43.3	37.18%	0.00
Total travel time (hr)	103.8	79.1	23.79%	0.00
Intersection: Stanford & Perkins 11/17/12				
Average Delay (s)	122.6	80.9	34.02%	0.00
Average Number of stops	2.6	2.2	16.27%	0.00
Average Speed (mph)	7.9	10.8	-36.34%	0.00
Average Stop delay (hr)	107.6	65.3	39.30%	0.00
Total delay (hr)	143.9	94.6	34.30%	0.00
Total number of stops	11075	92230	16.66%	0.00
Total stop delay (hr)	126.4	75.4	39.55%	0.00
Total travel time (hr)	190.0	141.3	25.64%	0.00
Intersection: NW 183 Street & NW 27 Avenue 01/07/13				
Average Delay (s)	58.0	56.9	1.93%	0.13
Average Number of stops	1.5	2.2	-42.59%	0.00
Average Speed (mph)	13.2	13.4	-1.31%	0.08
Average Stop delay (hr)	46.4	42.0	9.42%	0.00
Total delay (hr)	132.9	127.2	4.27%	0.00
Total number of stops	12649	17607	-39.20%	0.00
Total stop delay (hr)	106.4	94.0	11.58%	0.00
Total travel time (hr)	223.6	215.8	3.47%	0.00

Historically, police officers have been able to decrease lost time by extending phase length, resulting in fewer phases per cycle per hour and thus less lost time overall. However, when using the “clicker” method the officer did not have the ability to skip phases and therefore had to service the minimum green time for phases even when demand was not present. Continually serving phases without demand negates any benefit the officer has in decreasing lost time. The inability of the officer to skip phases resulted in an overall increase of lost time despite having fewer cycles per hour. An example of this is presented in Figure 6-1.

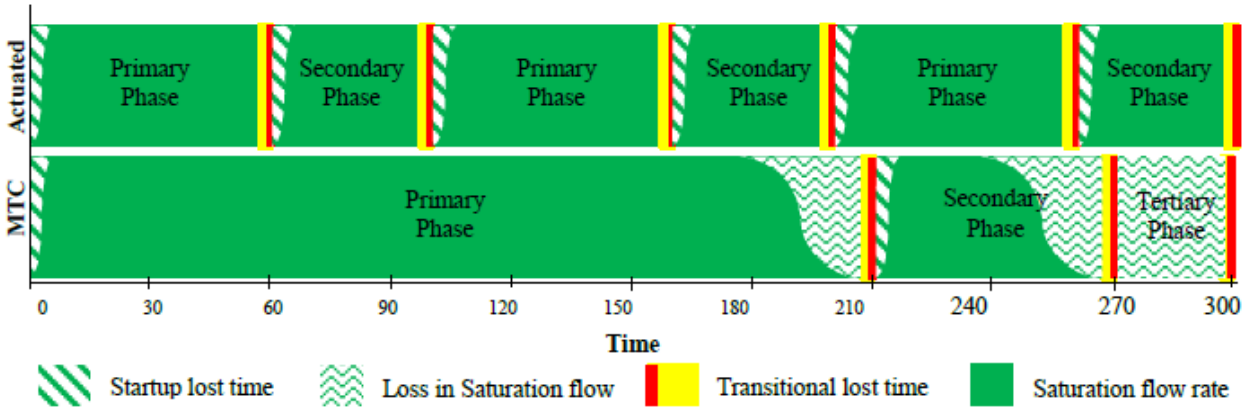

Figure 6-1 Saturation Flow Rate and Lost Time Diagram

Figure 6-1 shows a 5-minute (300 second) phase diagram illustration of a hypothetical example of what was likely occurring during the simulation. Two controller strategies for the same intersection are shown for actuated and MTC. Both controllers were three phase but the actuated controller could skip phases if demand was not present. The actuated controller had a 100 second cycle length and the manual traffic control shown here had a 300 second cycle length. The time when the intersection was operating at saturation flow is shown in green. Lost time and loss in saturation flow are also presented in the diagram. For this example, demand was not present for the *Tertiary* phase. This illustration shows how the decrease in saturation flow rate and the inability to skip phases has a drastic impact on the total lost time of the intersection when compared to actuated signal control. The officer directing traffic has the ability to minimize the saturation loss but cannot eliminate the lost time seen in the *Tertiary* phase.

6.6.4 Summary of Findings

The MTC model was shown to be statistically similar to the observed police controlled intersections in respect to phase length, standard deviation of phase length and intersection throughput. The model was validated on a separate dataset, which yielded consistent results. This suggests that the MTC model described herein could potentially serve as generalized model of a representative officer directing traffic. After the MTC model was calibrated and validated in the simulation, it was used to compare manual traffic control to an actuated controller. The results of the simulation showed that actuated control outperformed police control in nearly every metric. This performance was likely the result of the actuated controller’s ability to skip phases when demand was not present. A police officer directing traffic using the “clicker” method does not have a similar capability. As a result, any lost time saved by the officer was negated.

6.7 NPP Representative Site Analysis

Current NRC guidance suggests that MTC is a more efficient means of controlling an intersection compared to other traditional methods. NUREG/CR-7002 proposes modeling MTC as actuated signals and adjusting the signal timing to reflect more efficient operations. However, without full knowledge of MTC operations, simulating MTC as an actuated signal may not be realistic. This task seeks to quantify the impact of MTC by evaluating ETEs with and without the use of MTC at key intersections throughout the study areas. Because the base simulation models used in this study have pre-timed signal settings, the deployment of actuated traffic control was also evaluated as a comparison scenario for select intersections. Insights gained from this analysis can be used to evaluate current assumptions regarding MTC used by evacuation planners and Offsite Response Organizations (ORO).

6.7.1 Modeling MTC for the ETE Study

This research task was carried out in five primary steps. The first step was to review prior ETE studies and identify a typical number of TCPs that would be representative of a small, medium, and large population sites. The second step was to determine which intersections within the base models would receive MTC. The third step was to develop the first evaluation scenario and program the MTC model at TCPs intersections. The fourth step was to program the second evaluation scenario and replace the MTC model with an actuated controller at signalized TCPs. The final step was to evaluate the MTC model, actuated traffic control (ATC), and base model using the performance measures of clearance time, average travel speed, and EPZ exit flow rates.

6.7.1.1 Intersection Selection

A review of prior ETE studies found that most ETE plans rely on OROs to identify many, if not most of the TCPs and ACPs within the study region. Most ETEs use simulation results to identify critical intersections that experience pronounced congestion. This information is augmented by field surveys and by interviewing local officials. Because the base models developed in this research are for representative sites, it was not possible to consult with local officials to identify the number and location of TCPs. Therefore, the number of TCPs to be modeled with MTC was selected based on an analysis of current ETEs. Table 6-22 shows the basic statistics on the number of TCPs used at small, medium, and large population sites. The number and location of these TCPs and ACPs served as a starting point for selecting intersections to be modeled with MTC in the base models. Based on these statistics, it was determined that a representative number of TCPs for a representative small, medium, and large population site would be 25, 50, and 100 respectively.

Table 6-22 Traffic Control Point Statistics and Number Modeled in Representative Sites

Statistics	Small Population Sites	Medium Population Sites	Large Population Sites
Mean number of TCP	27	65	127
Median number of TCP	24	52	102
Minimum number of TCP	0	6	6
Maximum number of TCP	68	176	306
Modeled number of TCP	25	50	100

The base model results were reviewed to determine optimal intersections to model as TCPs. For the medium and large population site models, average intersection-node delays were calculated to identify potential locations for TCPs. The 50 intersection-nodes with the highest average delay within the medium population site EPZ and the 100 highest delay intersection-nodes within the large population site EPZ were selected as the initial pool of potential TCP locations. The final selection of TCPs was made based on an iterative process and visual inspection to minimize intersection congestion. The TCPs within the small population site were selected by visual inspection of the base model simulation. Signalized intersections and intersections which experienced long queues were identified for MTC. Figures 6-2, 6-3, and 6-4 show the locations of the intersections modeled with MTC within the small, medium, and large population sites, respectively.

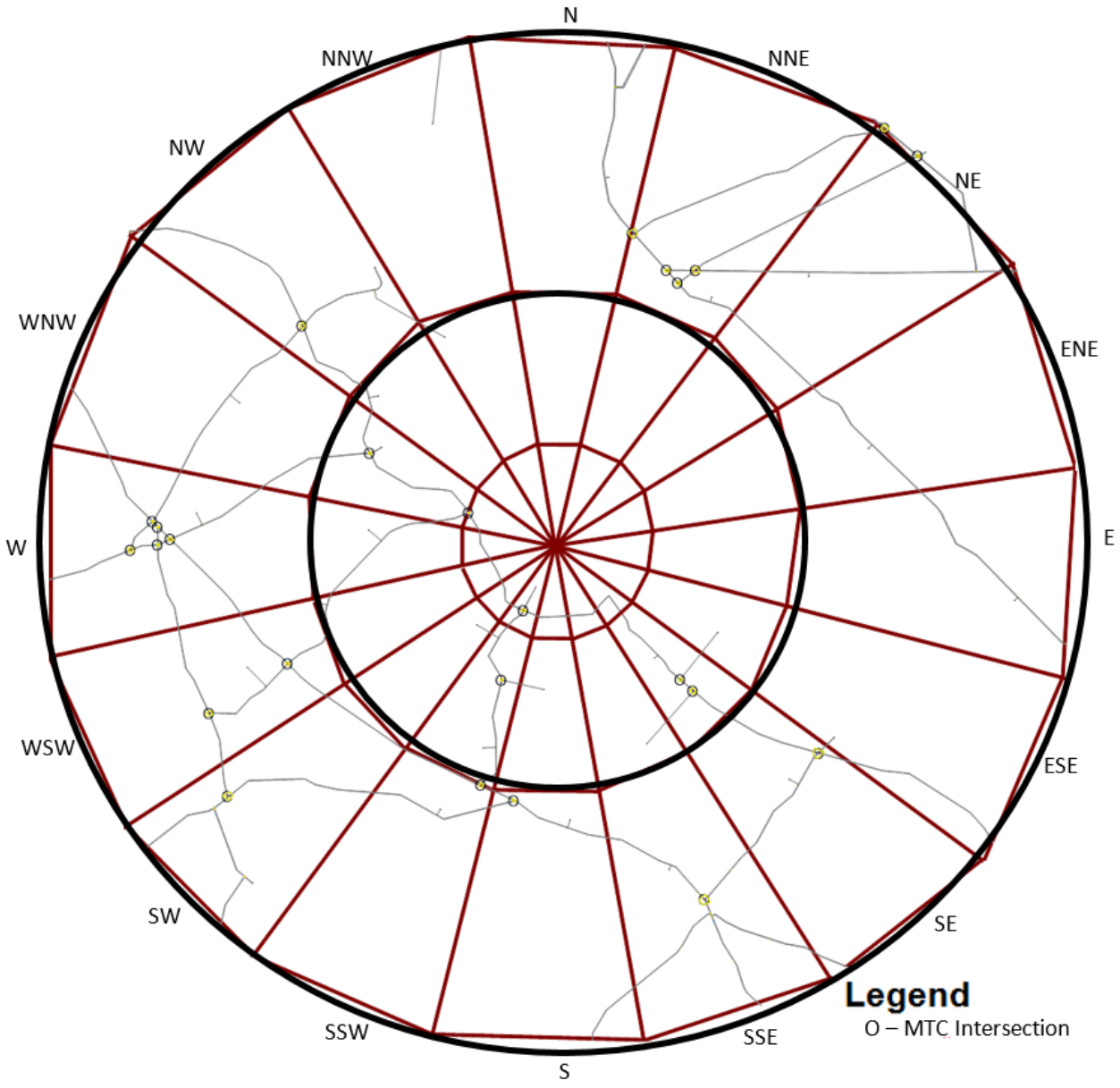

Figure 6-2 Small Population Site Model MTC Intersections in the 10-Mile EPZ

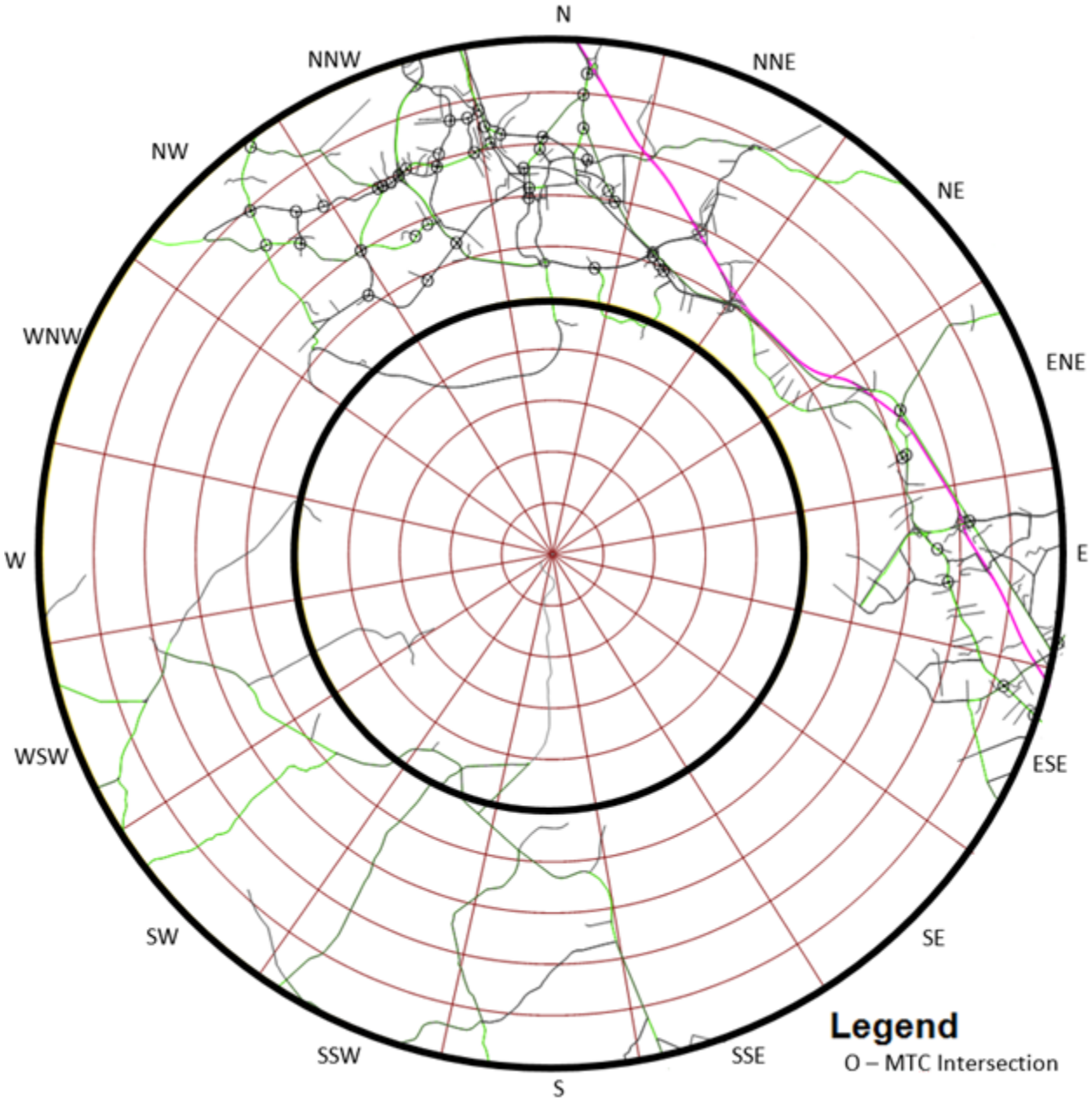

Figure 6-3 Medium Population Site Model MTC Intersections in the 10-Mile EPZ

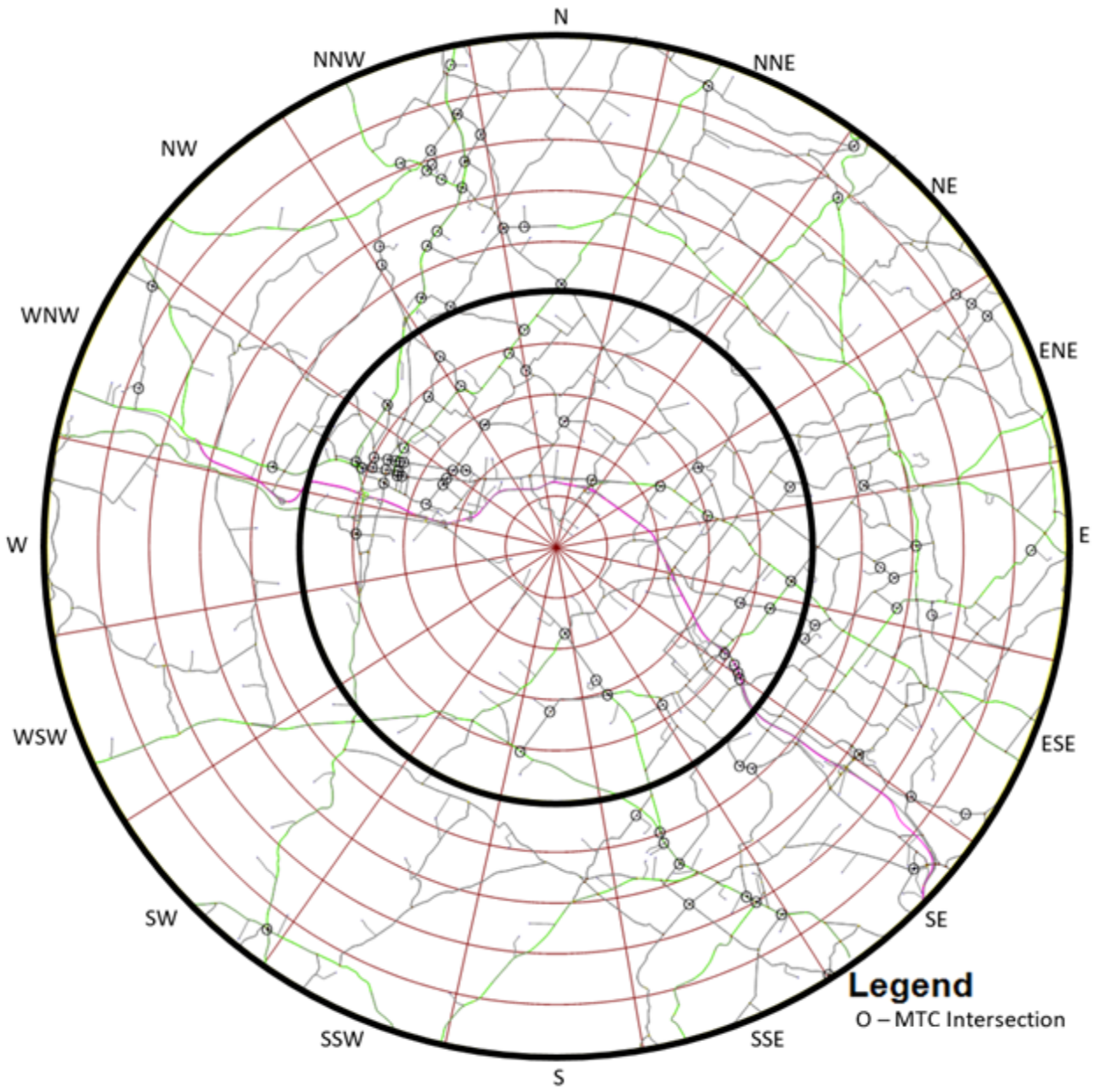

Figure 6-4 Large Population Site Model MTC Intersections in the 10-Mile EPZ

6.7.1.2 Intersection Modeling

Initially, all the identified TCPs were modeled as MTC. The MTC model described in this report was slightly modified to allow for permissive left turn movements, in effect allowing the MTC model to skip phases. This capability was added because the observed intersection from which the MTC model was developed did not allow permissive left turns when conducting MTC from the signal controller box. This does not represent all traffic controllers and could bias the results of this study if not accounted for. By allowing permissive left turns, the MTC model would have the ability to skip low priority phases and provide a better basis of comparison with ATC, which already has this ability. The MTC model was programed into VISSIM using the Vehicle Actuated Program (VAP) interface and utilized 300 ft stop-bar detectors to represent an officer's ability to look upstream. The MTC model was programed with two variations, northbound-southbound

dominant and eastbound-westbound dominant. Each TCP was evaluated to determine which variant of the MTC was best suited on a case-by-case basis. The MTC model remained active throughout the simulation run. While this may not represent a typical deployment of TCPs during an evacuation— as MTC would normally require time for an officer to arrive at the intersection and prepare—it is a useful implementation for this study in order to quantify the impact of MTC at various stages of the evacuation process and to provide comparison to actuated signal control.

After data collection for the MTC model was complete, the TCPs were programmed with actuated signal control. The signal timing used for the actuated controller in this study was selected be to representative of a typical controller and not optimized or tailored for any individual intersection. Two variations of the same basic signal timing plan were utilized for the analysis. The actuated controllers used a two-phase signal, with an eastbound-westbound dominant and northbound-southbound dominant variation. The basic signal timing plan, featuring a two-phase signal with eastbound-westbound preference, is provided in Table 6-23. The actuated controller used 50 ft stop-bar detectors and was allowed to have variable cycle length. This is referred to as ATC within the results section.

Table 6-23 Representative Actuated Signal Control Timing Four-Phase EB-WB Dominate

Signal timing (seconds)	Phase 2	Phase 4	Phase 6	Phase 8
Minimum green	7	15	7	15
Vehicle extension	2	5	2	5
Maximum 1	15	30	15	30
Yellow	4	4.5	4	4.5
Red clearance	1	1	1	1
Walk	8	8	8	8
Red clear	12	12	12	12
Maximum 2	30	99	30	99
Added initial	0	3.5	0	3.5
Minimum gap	0	3.5	0	3.5
Reduce after	0	20	0	20
Time to reduce	0	20	0	20
Splits	20	74	15	74
Transition maximum	24	88	24	88

6.7.2 Impact of MTC

The results presented in this section represent the average of several simulation runs, each with different random seed values. As was done in the previous task analyses, the small population site results represent an average of ten simulation runs, whereas the medium and large site results represent an average of four runs. The measures of effectiveness used to evaluate the impact of MTC were evacuation and clearance times, average travel speeds, and vehicular volumes exiting the EPZ. The data was collected and analyzed over five minute increments and segregated to display results for 90 percent of the evacuating EPZ vehicles and 100 percent, where applicable. The results of this analysis are presented for each model in the following sections.

6.7.2.1 Evacuation and Clearance Time Results

This section discusses the results of modeling TCPs with MTC by replacing the base model traffic control technique with the MTC model developed in Section 6.6. The results for Actuated Traffic Control (ATC) are also presented. Evacuation clearance times were calculated at the 2, 5, and 10-mile rings. Additionally, the quadrant clearance times (North, South, East, and West) were calculated. It was anticipated that the various traffic control strategies could impact evacuation and clearance times by altering the flow of traffic throughout the network, by changing the loading pattern of vehicles onto the network, or by decreasing congestion near the EPZ boundary.

6.7.2.1.1 Small Population Site Model Evacuation and Clearance Time Results

The small population site is predominately rural and was modeled with 25 TCPs. The small population site analysis allowed for an investigation of MTC when the network was under-saturated and with limited use of signalized intersections. It was anticipated that by replacing stop and yield control intersections with MTC, the network would be better able to facilitate the movement of traffic and ultimately decrease the clearance time. Table 6-24 and Table 6-25 show the ETE and clearance time by quadrant (respectively) for the base model, MTC and ATC scenarios. The results suggest no impact resulted from changing the traffic control scenario at the 25 TCPs selected within the small population site. MTC and ATC may have increased the carrying capacity for intersections that were previously signalized or pre-timed; however, within the uncongested model this made little impact on the overall ETE and clearance times. This was likely because the added capacity was not needed at these intersections and ultimately not realized, or any increase in the performance gained at one intersection was lost when these vehicles joined in with the rest of traffic at downstream intersections and bottlenecks, or a combination of both effects.

Table 6-24 Small Population Site Average ETEs for Varying Traffic Control

Traffic Control	2-Mile Ring		5-Mile Ring		10-Mile Ring	
	90% ETE	100% ETE	90% ETE	100% ETE	90% ETE	100% ETE
ATC	1:35	2:18	1:35	2:21	1:44	2:32
MTC	1:35	2:18	1:36	2:22	1:45	2:33
Base (Fixed timing)	1:35	2:18	1:35	2:21	1:44	2:31

Table 6-25 Small Population Site Average ETEs by Quadrant for Varying Traffic Control

Quadrant	ATC		MTC		Base	
	90% ETE	100% ETE	90% ETE	100% ETE	90% ETE	100% ETE
North	1:39	2:09	1:39	2:10	1:39	2:09
East	1:43	2:22	1:44	2:22	1:43	2:21
South	1:43	2:29	1:45	2:31	1:44	2:30
West	1:44	2:30	1:45	2:31	1:44	2:29

Figure 6-5, Figure 6-6, and Figure 6-7 show the cumulative percent evacuated for the small population site at the 2, 5, and 10-mile rings, respectively. The figures show no significant impact of varying the traffic control strategy at the 25 TCPs.

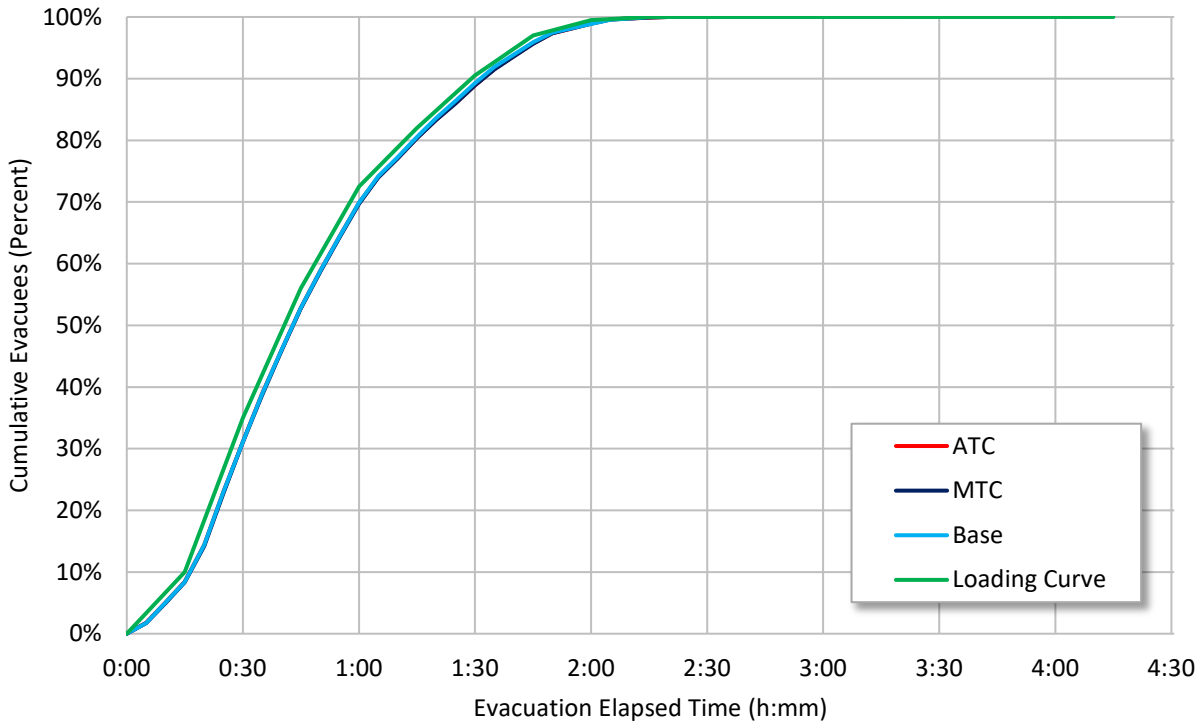

Figure 6-5 Two Mile ETE Curves, Small Population Site Manual Traffic Control Analysis

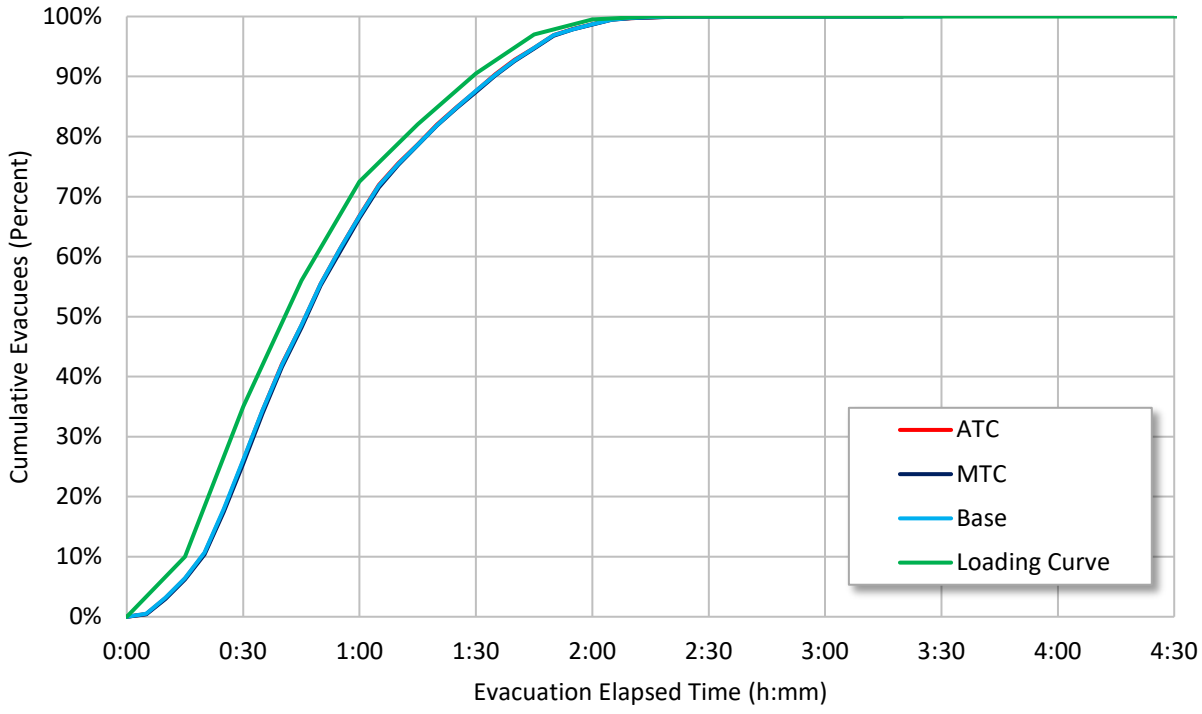

Figure 6-6 Five Mile ETE Curves, Small Population Site Manual Traffic Control Analysis

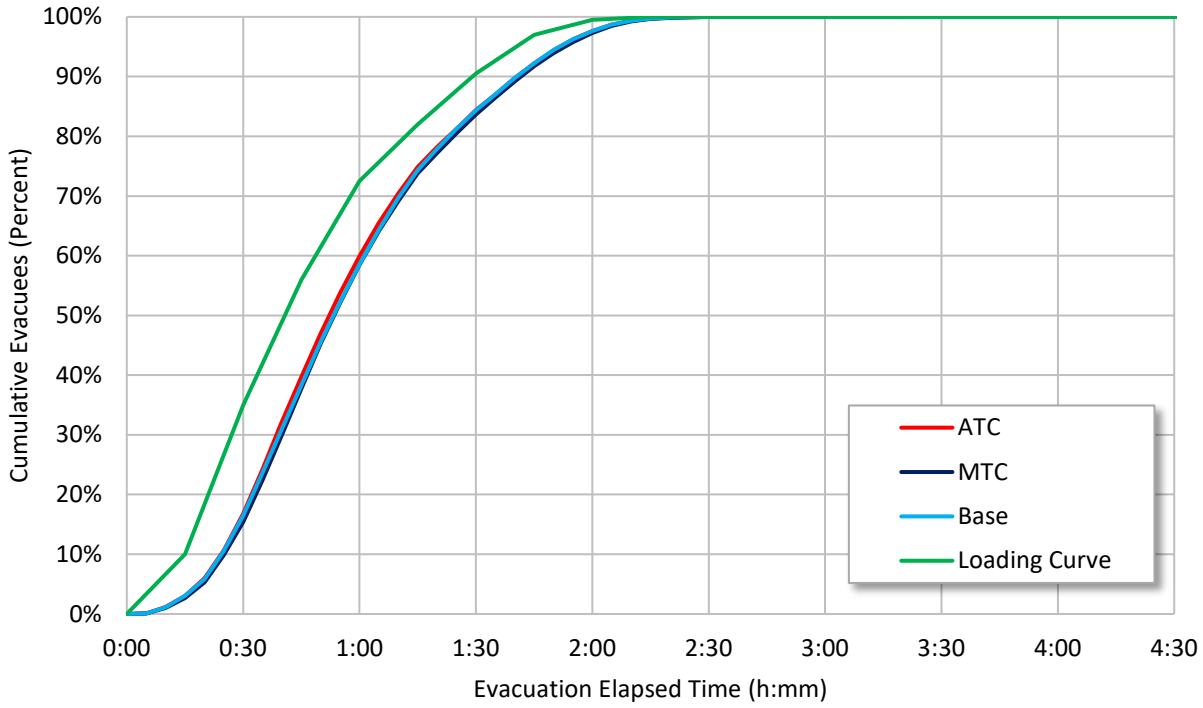

Figure 6-7 Ten Mile ETE Curves, Small Population Site Manual Traffic Control Analysis

6.7.2.1.2 Medium Population Site Model Evacuation and Clearance Time Results

The evacuation and clearance time results for the medium population site are provided by ring in Table 6-26 and by quadrant in Table 6-27. As shown in these tables, the 2-mile ring and the South quadrant were insensitive to the traffic control strategy deployed at the 50 TCPs within the medium population site. This was likely because, similar to the small population site, these areas are predominately rural with smaller populations, and with fewer TCPs. However, significant differences were seen in the 5-mile and 10-mile rings and in the North, West, and East quadrants. The differences seen between the MTC and the base model were likely caused by two factors: 1) interruption of the pretimed cycle phase length and 2) long cycle lengths typically used during MTC.

The pretimed signals used in the base model all had the same cycle length and operated in coordination with each other. The pretimed signals did not utilize signal offsets, the process by which green time at one intersection is timed to match the neighboring intersection according to the travel time between them. However, the pretimed signals all turned green at the same time, allowing some vehicles to pass several closely spaced intersections during a single green phase. The introduction of a MTC or ATC signal interfered with this process and resulted in longer queue lengths and lower overall corridor capacity.

Also impacting the performance of the network during MTC was the longer cycle lengths. During the simulated evacuation, the longer cycle lengths used in MTC caused long queues at these intersections. Because demand at these intersections was very high, these queues extended upstream and blocked nearby intersections and network loading links. As these queues extended, they mixed with other long queues from neighboring intersections (some of which were also controlled by MTC). This intermingling of intersection queues caused localized

gridlock within the model. The long queue lengths, combined with areas of gridlock, prevented vehicles from accessing the network. Once the gridlock cleared, the blocked vehicles were able to exit the model, but only after significant delay.

Table 6-26 Medium Population Site Average ETEs for Varying Traffic Control

Traffic Control	2-Mile Ring		5-Mile Ring		10-Mile Ring	
	90% ETE	100% ETE	90% ETE	100% ETE	90% ETE	100% ETE
ATC	2:40	4:03	4:46	7:52	7:16	10:03
MTC	2:40	4:03	5:03	8:11	7:36	10:05
Base (Fixed timing)	2:40	4:03	2:47	5:05	5:03	7:41

Table 6-27 Medium Population Site Average ETEs by Quadrant for Varying Traffic Control

Quadrant	ATC		MTC		Base	
	90% ETE	100% ETE	90% ETE	100% ETE	90% ETE	100% ETE
North	8:10	9:50	8:08	9:50	6:12	7:41
East	4:08	7:56	4:15	8:11	4:05	5:22
South	2:47	4:22	2:47	4:22	2:47	4:22
West	8:47	10:03	8:37	10:05	5:32	6:20

Figure 6-8, Figure 6-9, and Figure 6-10 show the cumulative percent evacuated for the medium population site at the 2, 5, and 10-mile rings, respectively. These figures are a visual representation of the evacuation process that led to the 90 percent and 100 percent ETE times shown in Table 6-26. The figures also display the evacuee loading curve for reference. Figure 6-8 shows no significant impact of MTC or ATC on the 2-mile ETE curve. Again, this was likely because of the low population and sparse roadway network in this region of the model. Figure 6-9 shows that ATC and MTC performed similar to the base model for the first 60-65 percent of the evacuation. However, after that point, long queues, caused by interrupting the pretimed coordination, and long cycle lengths resulted in gridlock which prevented vehicles from exiting the network. In this figure it can be seen that after approximately 65 percent of the evacuees have exited the model, the ETE curves for the MTC and ATC model become approximately linear. This suggests vehicles were queuing in the model, unable to exit and is consistent with the existence of gridlock. Figure 6-10 for the 10-mile ring shows similar results. However, the ATC and MTC models diverge from the base model after only 20 percent of the evacuation.

It is important to note that the gridlock that developed under MTC and ATC was also observed during development of the base models using the fixed signal timing. This was eliminated in the base model through model calibration and is not unexpected in the MTC and ATC results, since the model was not calibrated specifically for these scenarios. It is likely that a model calibrated with MTC or ATC in place would not result in such extensive gridlock. However, these results still provide a useful comparison between MTC and ATC operating under similar conditions.

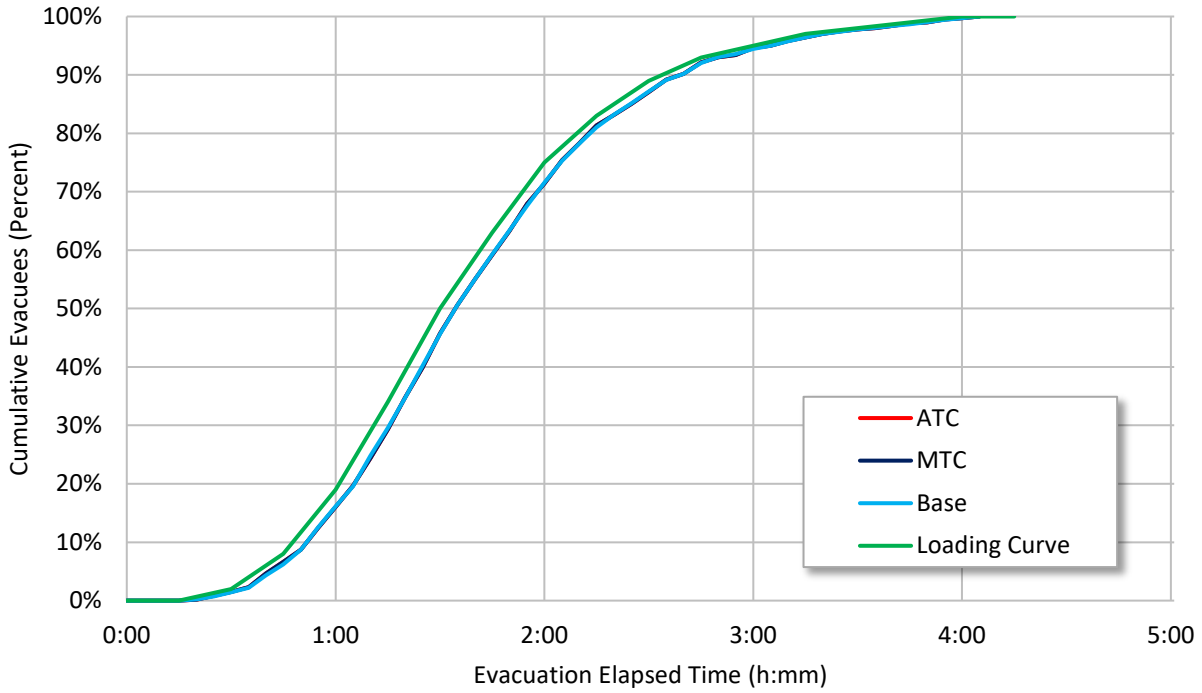

Figure 6-8 Two Mile ETE Curves, Medium Population Site Manual Traffic Control Analysis

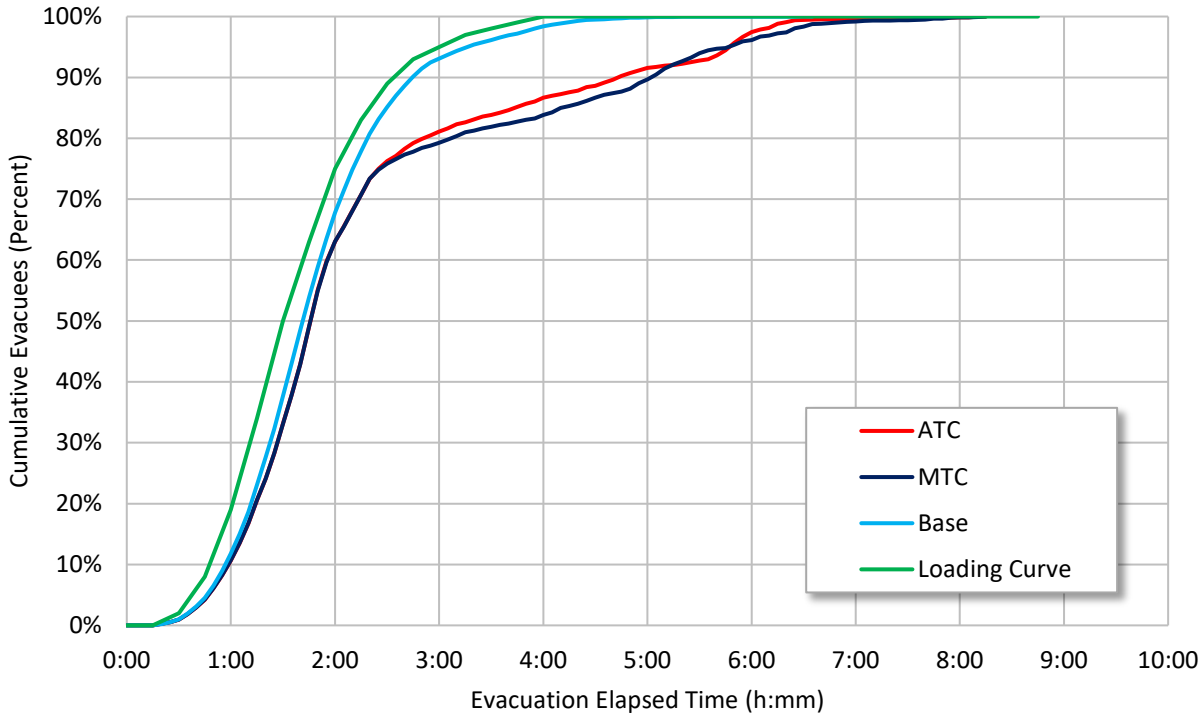

Figure 6-9 Five Mile ETE Curves, Medium Population Site Manual Traffic Control Analysis

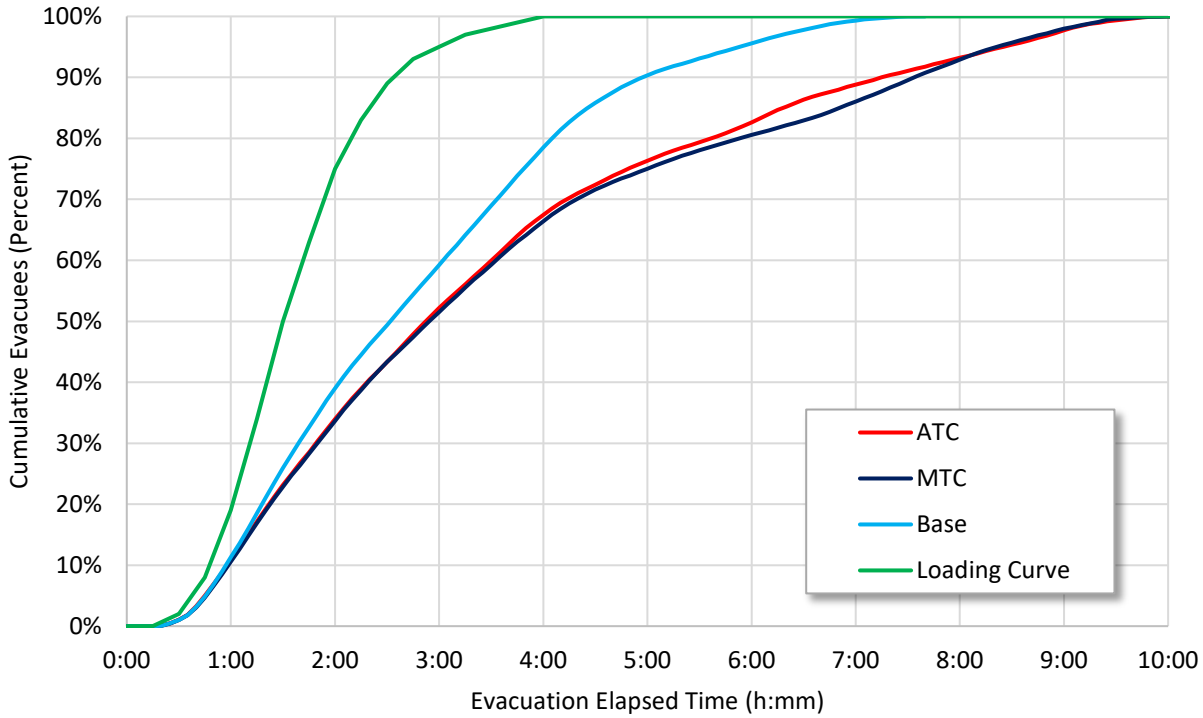

Figure 6-10 Ten Mile ETE Curves, Medium Population Site Manual Traffic Control Analysis

6.7.2.1.3 Large Population Site Model Evacuation and Clearance Time Results

The evacuation and clearance time results for the large population site are provided by ring in Table 6-28 and by quadrant in Table 6-29. Significant differences in the 100 percent ETE were seen at the 2, 5, and 10-mile rings and in nearly every quadrant. The 90 percent ETEs were more consistent with the base models. However, significant differences persisted for the 90 percent ETE at the 5-mile ring, 10-mile ring, and in the North and East quadrants. This suggests the traffic control type impacted the evacuation tail more significantly than for the majority of evacuees. For the MTC intersections this is likely because the large population site utilized 100 TCPs throughout the network. To illustrate, if an evacuee traveled along a major arterial, passing ten intersections using MTC with an average cycle length of 5 minutes, then this vehicle could experience up to 50 minutes of stop delay, even in an uncongested network. Conversely, for ATC this same vehicle could see significantly less stop delay because of the actuated controller. In the absence of congestion, prior research studies show the actuated controller should outperform MTC [115] [119]. At the 10-mile ring, the ATC scenario decreased the ETE significantly by over an hour despite having a 90 percent ETE that was significantly longer than the base model. This is because the actuated controller was better able to accommodate the lower volumes seen during the tail end of the evacuation. The MTC model was not able to accomplish this and resulted in an extended tail, significantly increasing the 100 percent ETE. However, because MTC would likely only be used during the most heavily congested period of the evacuation, it is unlikely that officers would continue to direct traffic during the uncongested evacuation tail, as was programmed here. Therefore, it is more likely that the evacuation tail for the MTC scenario would be truncated during an actual evacuation.

Table 6-28 Large Population Site Average ETEs for Varying Traffic Control

Traffic Control	2-Mile Ring		5-Mile Ring		10-Mile Ring	
	90% ETE	100% ETE	90% ETE	100% ETE	90% ETE	100% ETE
ATC	3:41	6:21	4:15	7:18	5:28	7:47
MTC	4:08	8:43	4:40	9:23	5:55	10:15
Base (Fixed timing)	3:40	5:05	3:57	6:35	4:43	9:01

Table 6-29 Large Population Site Average ETEs by Quadrant for Varying Traffic Control

Quadrant	ATC		MTC		Base	
	90% ETE	100% ETE	90% ETE	100% ETE	90% ETE	100% ETE
North	6:20	7:45	6:41	9:33	4:55	8:00
East	5:27	7:01	6:16	10:15	4:42	9:01
South	4:40	6:35	4:36	7:53	4:40	5:50
West	4:42	7:30	4:41	8:58	4:37	6:07

Figure 6-11, Figure 6-12, and Figure 6-13 show the cumulative percent evacuated for the large population site at the 2, 5, and 10-mile rings, respectively. These figures are a visual representation of the ETE process that led to the 90 percent and 100 percent ETE times shown in Table 6-28. The figures also display the evacuee loading curve for reference. Figure 6-11Figure 6-11 for the 2-mile ring, shows similarity among the control strategies, with the exception of the evacuation tail. The 5-mile ETE curve, shown in Figure 6-12, displays some of the characteristics of queueing seen in the medium population site, which may indicate some gridlocking occurred within the 5-mile ring when MTC was used. However, some benefits of control can be seen during the early stages of the evacuation. This was likely the result of replacing stop controlled intersections with actuated control, resulting in more efficient loading of the network.

Figure 6-13 shows the 10-mile ETE curves and a divergence of the ATC scenario from the MTC and base models. This figure suggests that during times of high congestion, after approximately 60 percent of the evacuees were loaded into the network, the coordination effect of the pretimed signals outperformed the actuated controllers. However, because the actuated controllers were better able to accommodate the tail of the evacuation, this strategy was able to outperform the 100 percent ETE despite having a significantly longer 90 percent ETE. This figure also suggests the gridlock seen in the medium population site was not as pronounced within the large population site or occurred only on a limited scale. This indicates that either the traffic demand or the intersection spacing did not trigger the propagation and intermingling of intersection queues on the same level as the medium population site. Also seen at the 10-mile ring was a slight benefit from ATC early on in the evacuation. Again, this suggests the ATC strategy may have assisted in loading the network at access links.

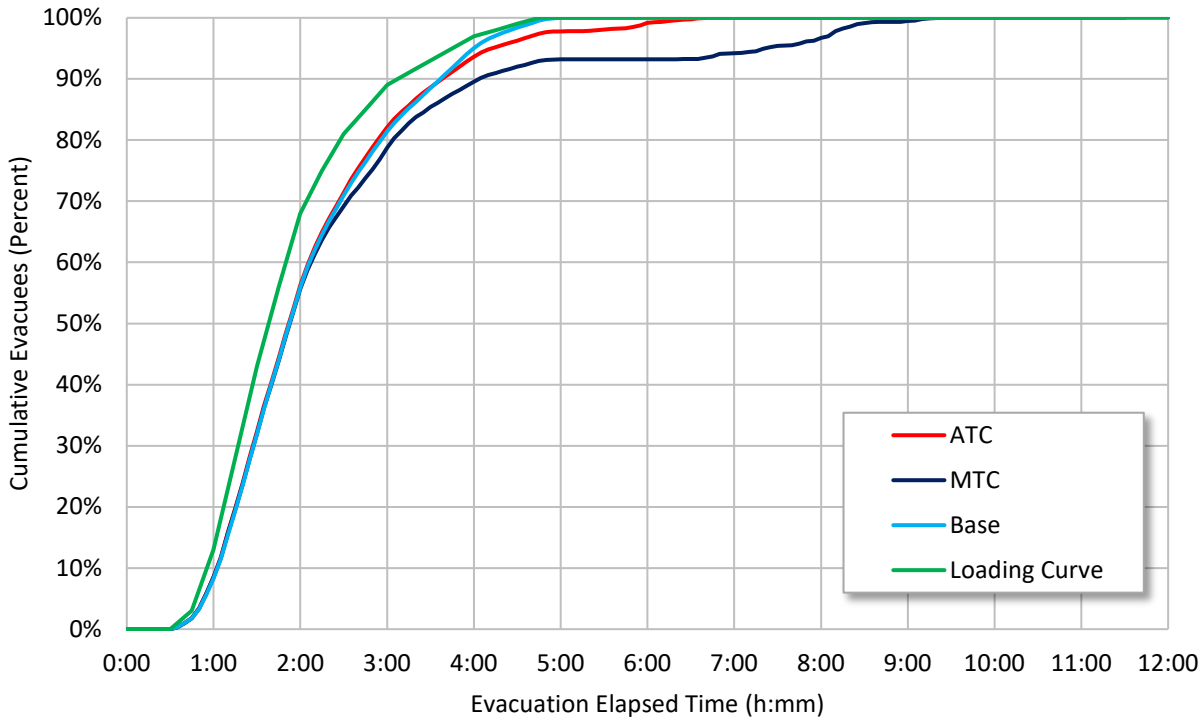

Figure 6-11 Two Mile ETE Curves, Large Population Site Manual Traffic Control Analysis

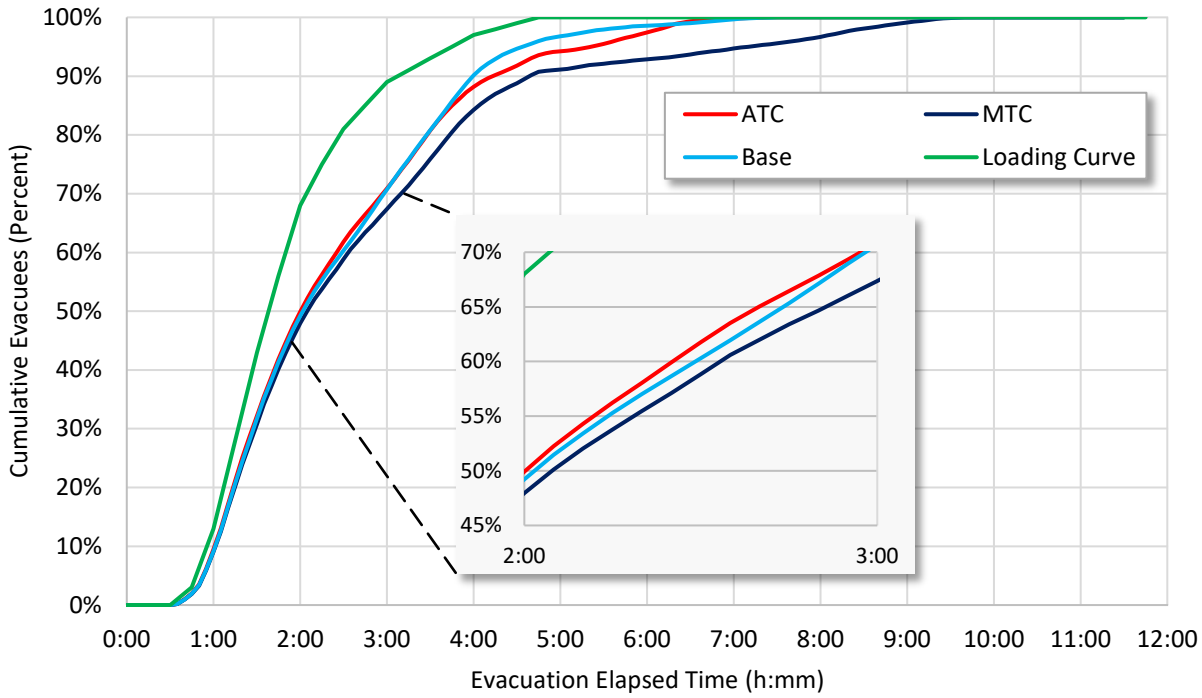

Figure 6-12 Five Mile ETE Curves, Large Population Site Manual Traffic Control Analysis

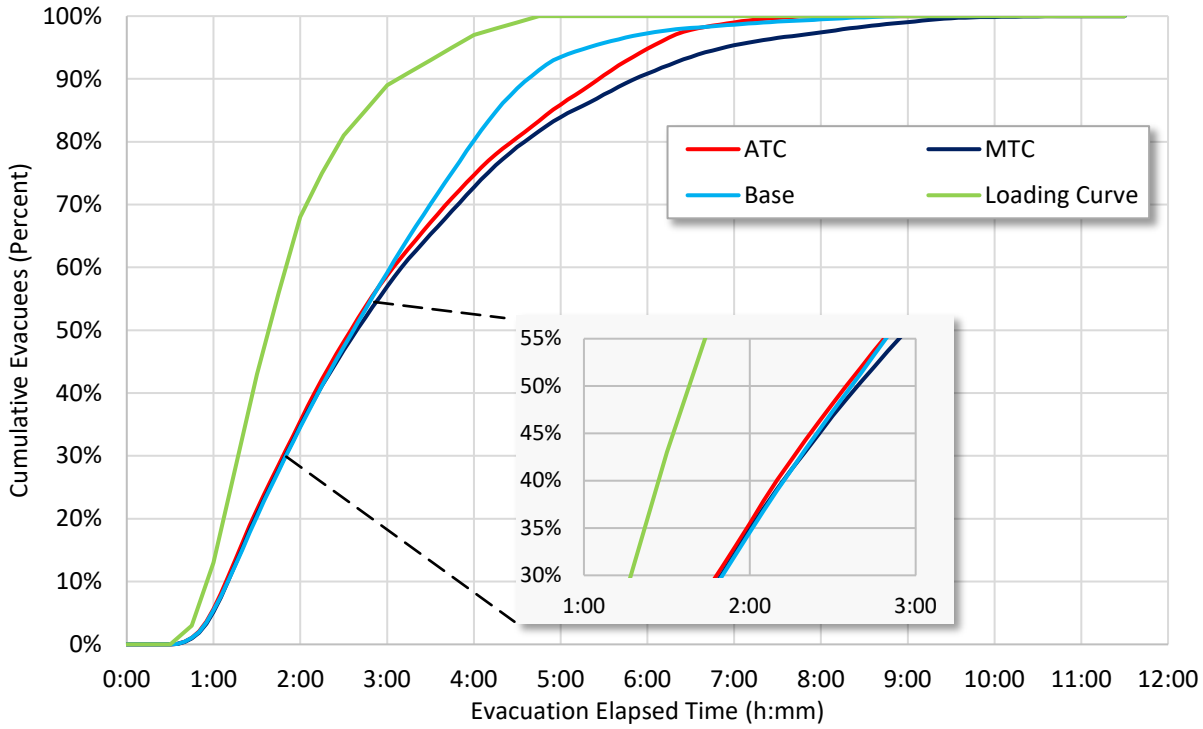

Figure 6-13 Ten Mile ETE Curves, Large Population Site Manual Traffic Control Analysis

6.7.2.2 Average Travel Speed Results

The average travel speed of vehicles exiting the EPZ (10-mile ring) was grouped into 16 compass sectors (N, NNE, NE, ENE, E, etc.). These average speeds are compared at various time periods into the simulation to illustrate the progression of the evacuation event. Speed increases and decreases signify congestion at the interface of the EPZ and shadow region. It is not anticipated that the traffic control strategy will have a meaningful impact on the travel speed exiting the EPZ. For signal control strategies to significantly impact travel speed, signal coordination—the programmed offset between signalized intersections which provides a progression of green lights to drivers traveling down the street—would be needed. Prior research has shown that police officers directing traffic typically do not coordinate, and signal coordination was not studied as part of this research task. However, variation in average travel time could occur depending on the volume of vehicles exiting the 10-mile EPZ within each 5-minute time bin. This would alter the weighted average of travel speeds.

6.7.2.2.1 Small Population Site Model Average Speed Results

Figure 6-14 shows the average travel speed in the small population site at 1:45 into the evacuation. No significant impact can be seen in the small population site average speed at this time. This finding was consistent throughout the evacuation. This was likely because the traffic control strategy does not significantly impact the travel speed and the exit of vehicles from the 10-mile EPZ.

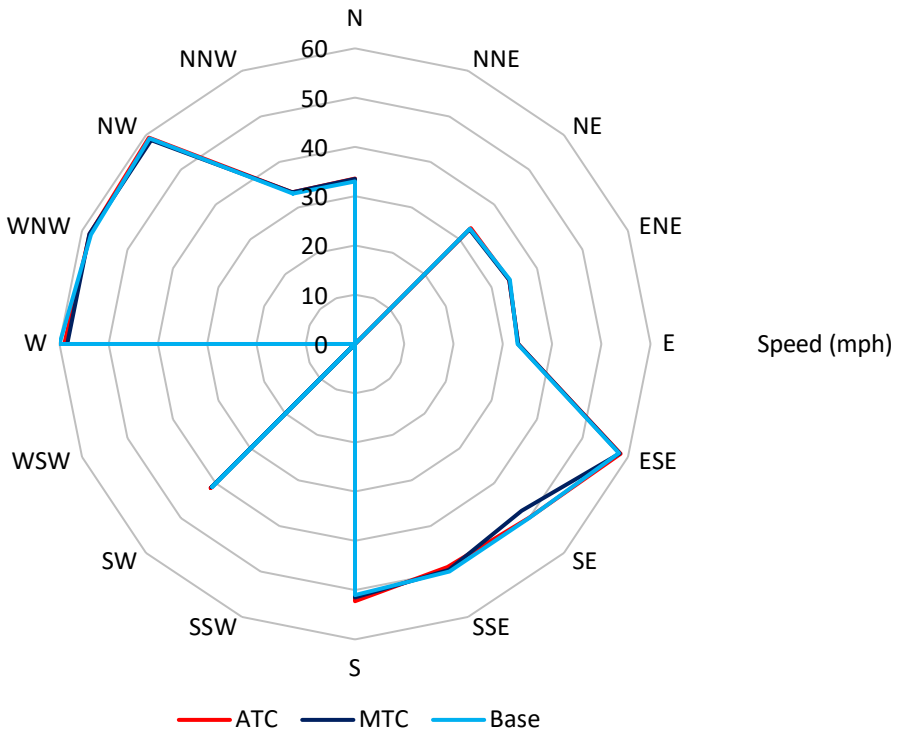

Figure 6-14 Average Speeds at 1:45, Small Population Site Manual Traffic Control Analysis

6.7.2.2.2 Medium Population Site Model Average Speed Results

Figure 6-15, Figure 6-16, and Figure 6-17 show the average travel speed in the medium site model at 2:30, 3:30, and 4:30 into the evacuation, respectively. These values show more variation when compared to the small population site model, with higher speeds seen in the north-northwest sector. With longer green times at intersections near the 10-mile EPZ exit, it was possible for vehicles to exit the network at higher speeds when compared to the base model. Also, the actuated controller allows for green times to be extended if a vehicle is approaching the intersection. This likely allowed for vehicles to pass through intersections near the EPZ at higher speeds. It is also likely that gridlock, caused by longer queue inside the EPZ, restricted the flow of vehicles, causing fewer vehicles to exit the model at the same time. This resulted in less congestion and higher speeds near the EPZ boundary.

6.7.2.2.3 Large Population Site Model Average Speed Results

Figure 6-18, Figure 6-19, and Figure 6-20 show the average travel speed in the large site model at 2:30, 3:30, and 4:30 into the evacuation, respectively. In general, the MTC and ATC scenarios resulted in the higher average speeds when compared to the base model. This was likely because of the longer green time afforded the MTC and ATC. With pretimed signals periodically changing phase regardless of demand, lower average spot speeds would be expected.

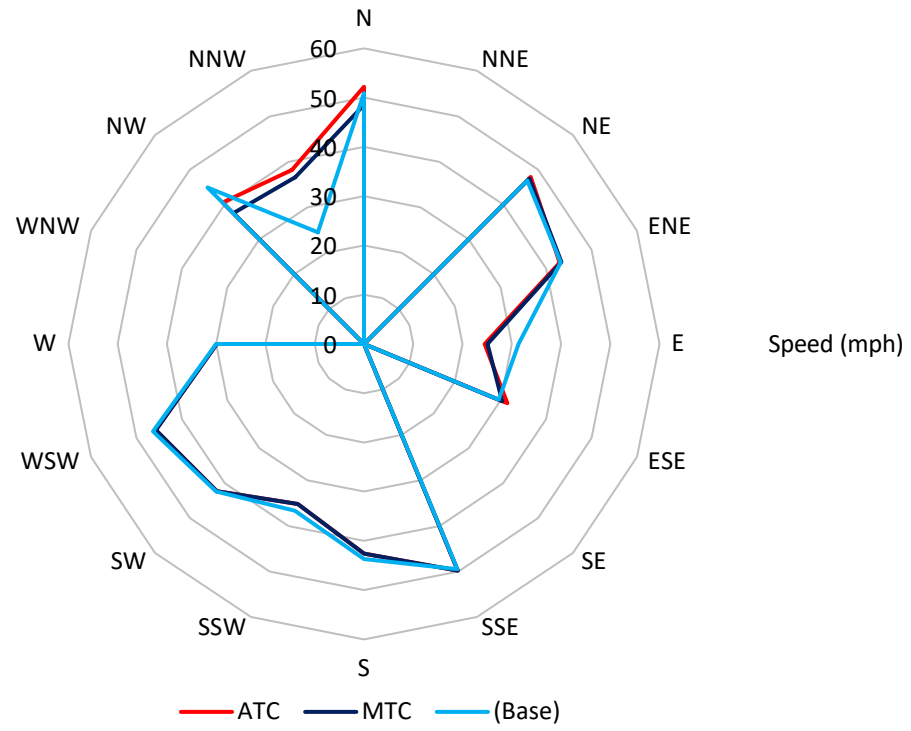

Figure 6-15 Average Speeds at 2:30, Medium Population Site Manual Traffic Control Analysis

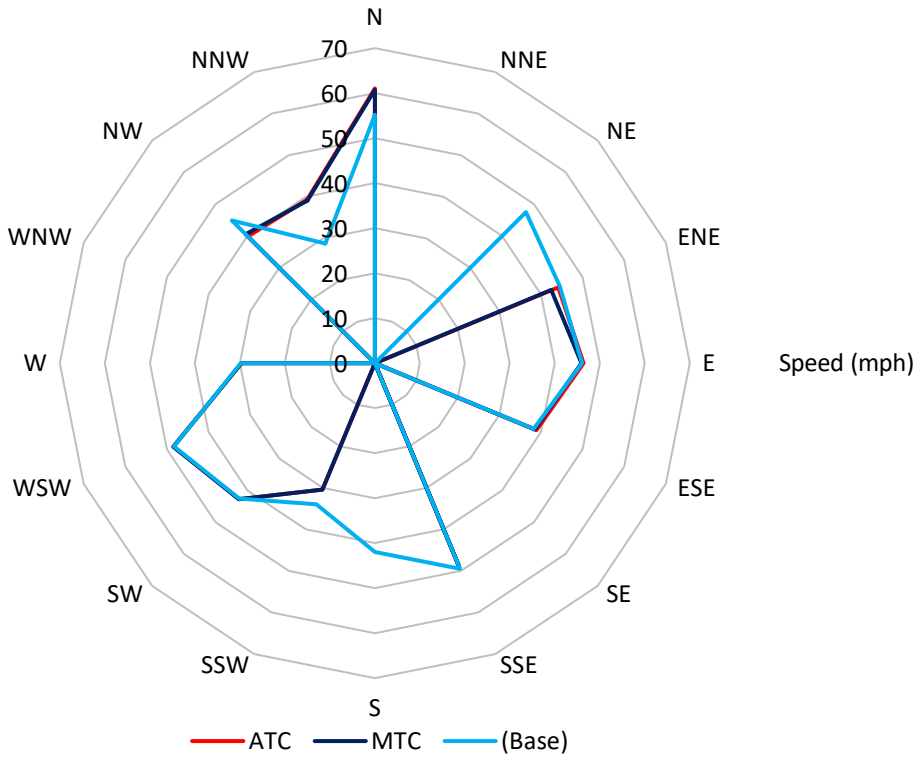

Figure 6-16 Average Speeds at 3:30, Medium Population Site Manual Traffic Control Analysis

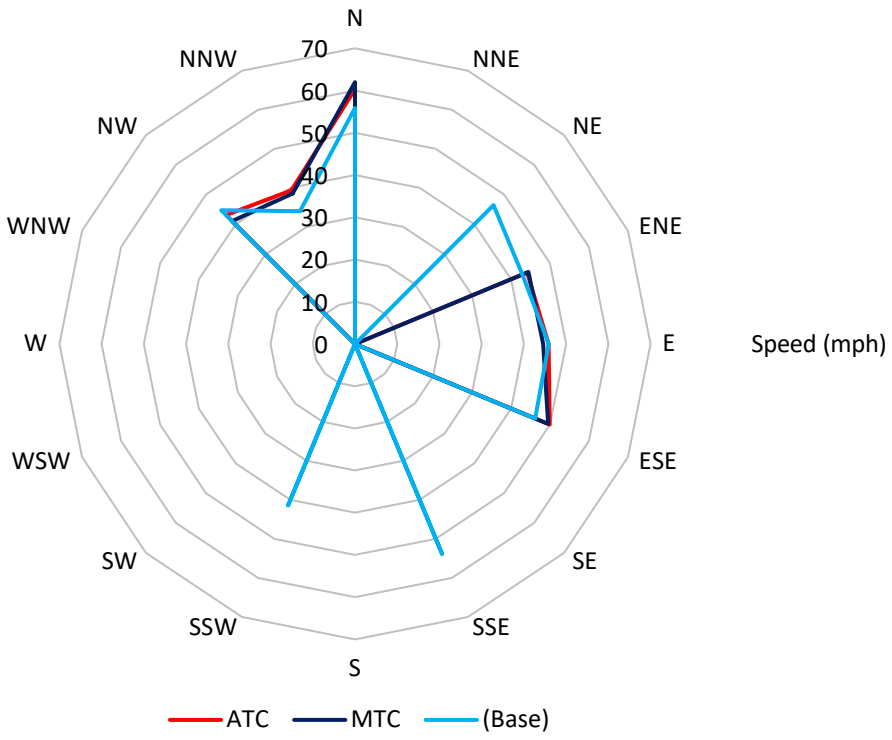

Figure 6-17 Average Speeds at 4:30, Medium Population Site Manual Traffic Control Analysis

Figure 6-18 Average Speeds at 2:30, Large Population Site Manual Traffic Control Analysis

Figure 6-19 Average Speeds at 3:30, Large Population Site Manual Traffic Control Analysis

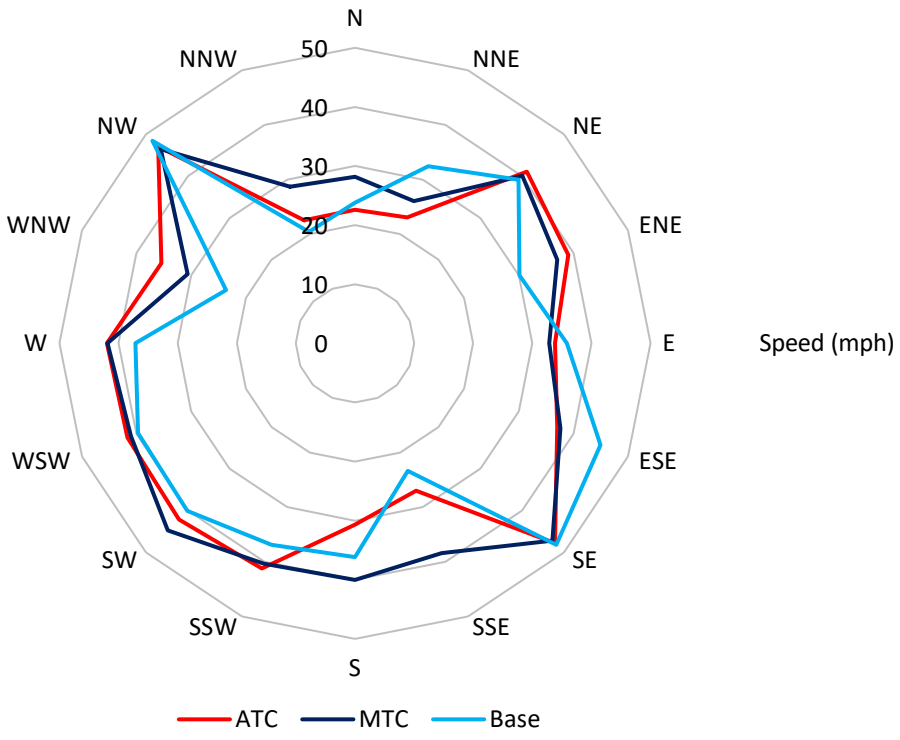

Figure 6-20 Average Speeds at 4:30, Large Population Site Manual Traffic Control Analysis

6.7.2.3 EPZ Exit Flow Rate Results

The EPZ exit flow rate is the number of vehicles that exit the 10-mile EPZ over each 5-minute data collection interval. This flow rate was converted into vehicles per hour, consistent with the standard practices of traffic engineering. Fundamentally, the 10-mile EPZ exit flow rate measures the diffusion of evacuation vehicles out of the EPZ. It was expected that if one of the traffic control scenarios were able to increase the exit flow rate over the base model, this might suggest that congestion within the model was adversely impacting the exit routes. By easing this congestion, the model could more efficiently load traffic onto exit routes, increasing the exit flow rate. A competing hypothesis would be that if the traffic control strategies loaded the network access links onto collector/distributor roads more efficiently, then the network could ultimately discharge vehicles more quickly, increasing the exit flow rate.

6.7.2.3.1 Small Population Site Model EPZ Exit Flow Rate Results

Figure 6-21 shows the small population site exit volumes at the 10-mile ring. The 2 and 5-mile ring exit flow rates were not impacted by the traffic control types. However, the 10-mile ring shows a distinctive increase in the exit flow rates when MTC was deployed. This was likely because many of the intersections within the small population site were unsignalized before the introduction of MTC. This may also suggest that MTC was able to load vehicles from connector links onto arterial roads more efficiently or that MTC intersections were able to marginally increase intersection performance during the early stages of the evacuation. The flow rates for MTC and ATC were similar suggesting the traffic control types may have a similar impact on traffic. This may also suggest that these control types were better able to load evacuees from network access links onto the collector/distributor roads. The more efficient loading of vehicles from low capacity side streets on to larger arterials is consistent with the common application of MTC used for routine traffic. For example, police officers are often deployed to facilitate church traffic. During the week, these facilities do not generate enough traffic demand to warrant signalization. However, following Sunday services, police officers are used to help facilitate the egress of church-goers from side streets to the main arterial. The more efficient loading would be indicative of a higher exit flow rate earlier in the evacuation, when the road network is less congested. It would be expected that this benefit would not be sustained as roadways approach capacity.

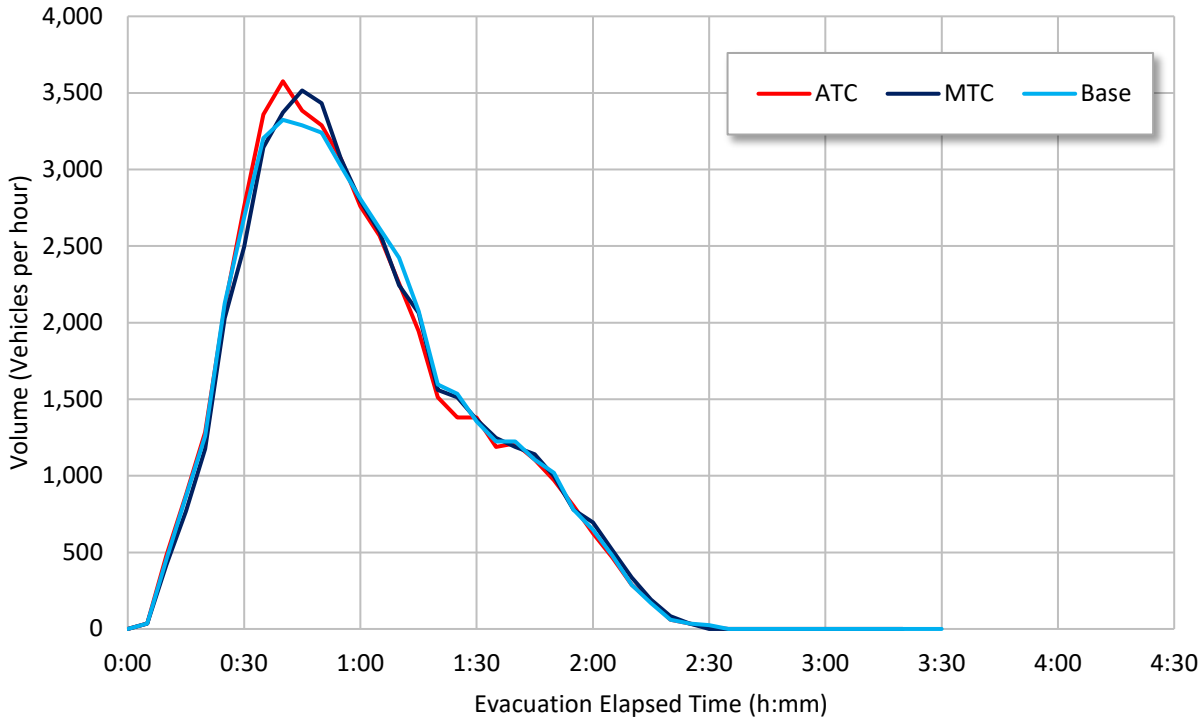

Figure 6-21 EPZ Exit Volumes, Small Population Site Manual Traffic Control Analysis

6.7.2.3.2 Medium Population Site Model EPZ Exit Flow Rate Results

Figure 6-22, Figure 6-23, and Figure 6-24 show the medium population site exit volume at the 2, 5, and 10-mile rings, respectively. The 2-mile ring shows no significant impact from the traffic control strategies. This was likely because of the low population and limited road network of this region within the model. Figure 6-23 for the 5-mile ring shows a delay in the peak exit volume and overall fewer exiting vehicles within the first four hours of the evacuation when MTC and ATC were deployed, as noted by the area under these curves. This suggests the loading of vehicles on the network was inhibited, significantly by the control strategies. This supports the finding that the alternative control strategies interrupted the coordination of the pretimed signals and introduced long queues which blocked links from loading vehicles into the network. This is in contrast to the small population site, where MTC and ATC may have assisted in the loading of the network. Because the small population site had fewer vehicles and intersections spaced at greater distances, it was less likely that downstream congestion, caused by long queues at MTC intersections would inhibit side street access. However, in the highly congested medium population site, long queues caused by the long cycle lengths used by MTC prevented vehicles from accessing the arterial roads. Figure 6-24 of the 10-mile ring captures this phenomenon well because it clearly shows the base model's pretimed signals loading the newtork more efficiently than the alternative control strategies. Ultimately, lower exit flow rates ealier in the evaucation resulted in longer ETE times because the delayed vehicles eventually had to be loaded after the gridlock was cleared. This resulted in higher exit flow rates at the tail of the evacuation for MTC and ATC.

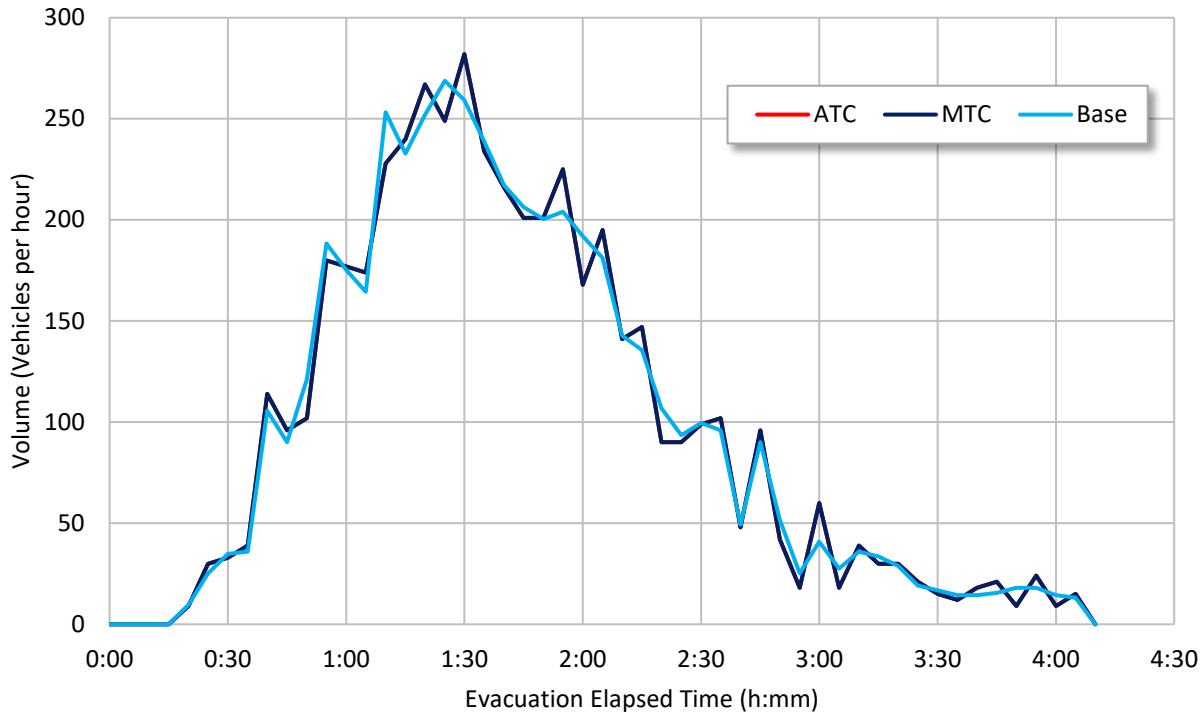

Figure 6-22 Two Mile Exit Volumes, Medium Population Site Manual Traffic Control Analysis

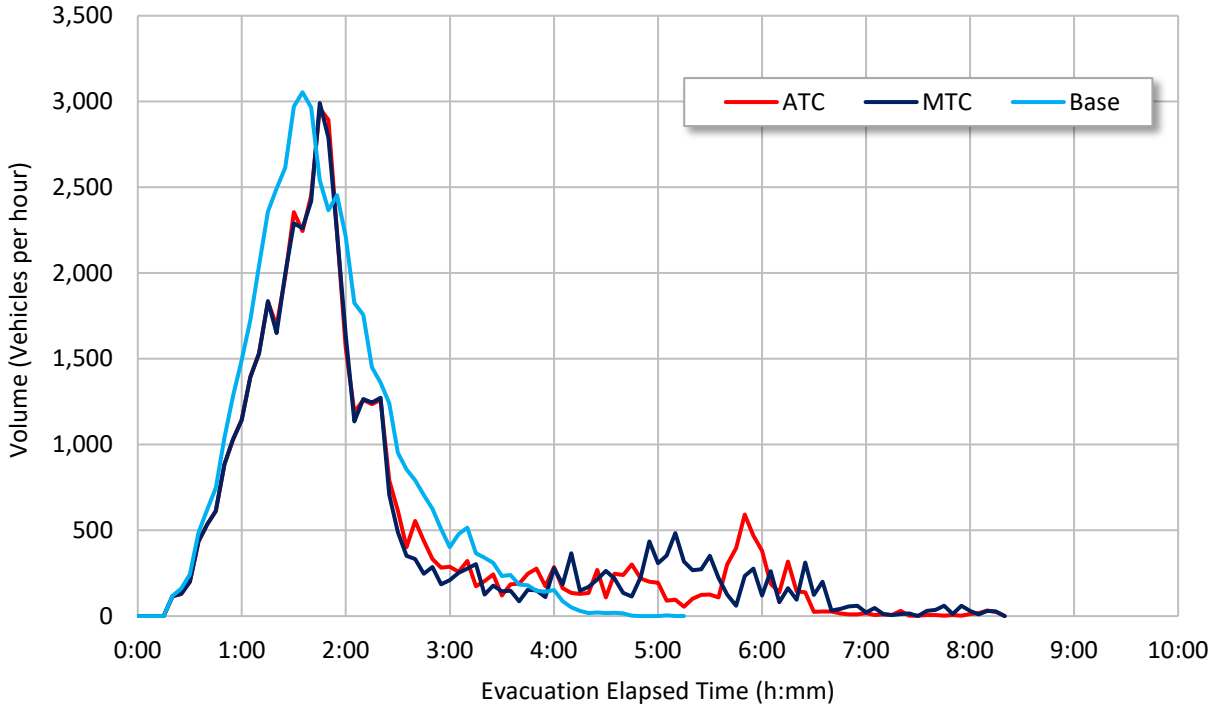

Figure 6-23 Five Mile Exit Volumes, Medium Population Site Manual Traffic Control Analysis

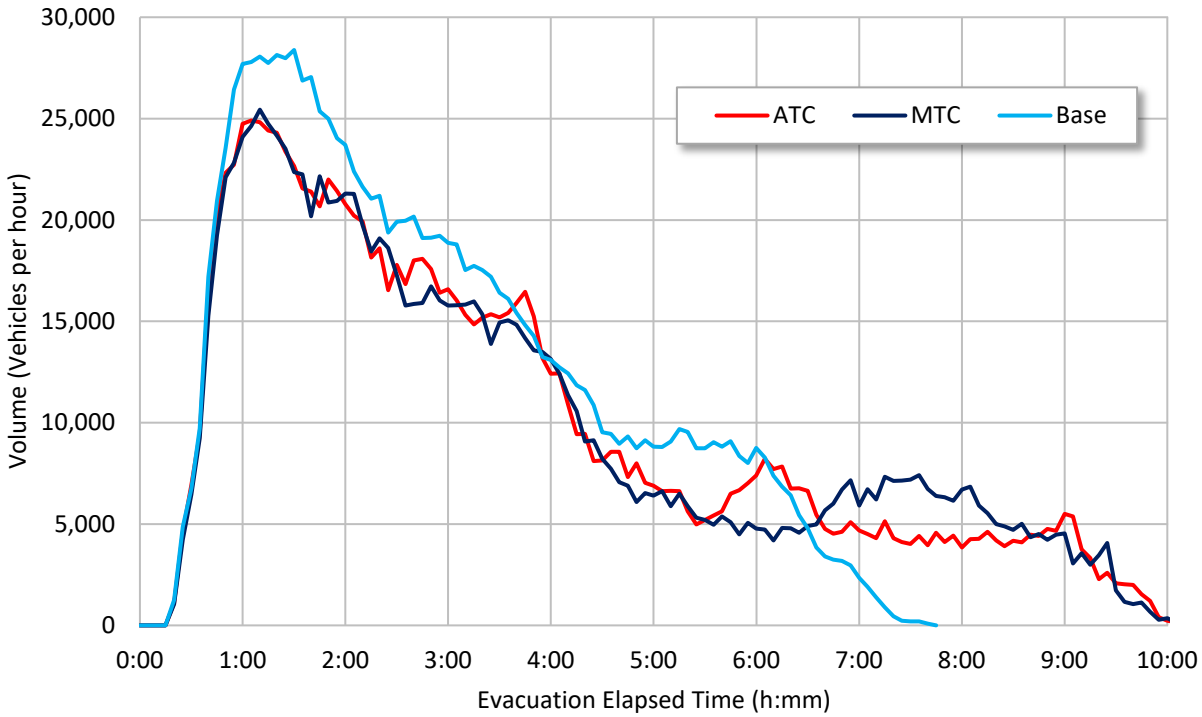

Figure 6-24 Ten Mile Exit Volumes, Medium Population Site Manual Traffic Control Analysis

6.7.2.3.3 Large Population Site Model EPZ Exit Flow Rate Results

Figure 6-25, Figure 6-26, and Figure 6-27 show the large population site exit flow rates at 2, 5, and 10-mile rings, respectively. The 2-mile ring shows consistent exit flow rates with the exception of an extended tail. The 5-mile ring shows no significant distinction between the traffic control strategies. The 10-mile exit flow rates show a marginal increase in the EPZ exit flow rates when MTC and ATC was utilized, similar to the results seen at the 10-mile ring in the small population site. Again, this may have been caused by increasing the loading rate of vehicles onto collector/distributor roads or better performance of the MTC and ATC traffic control during the early stages of the evacuation.

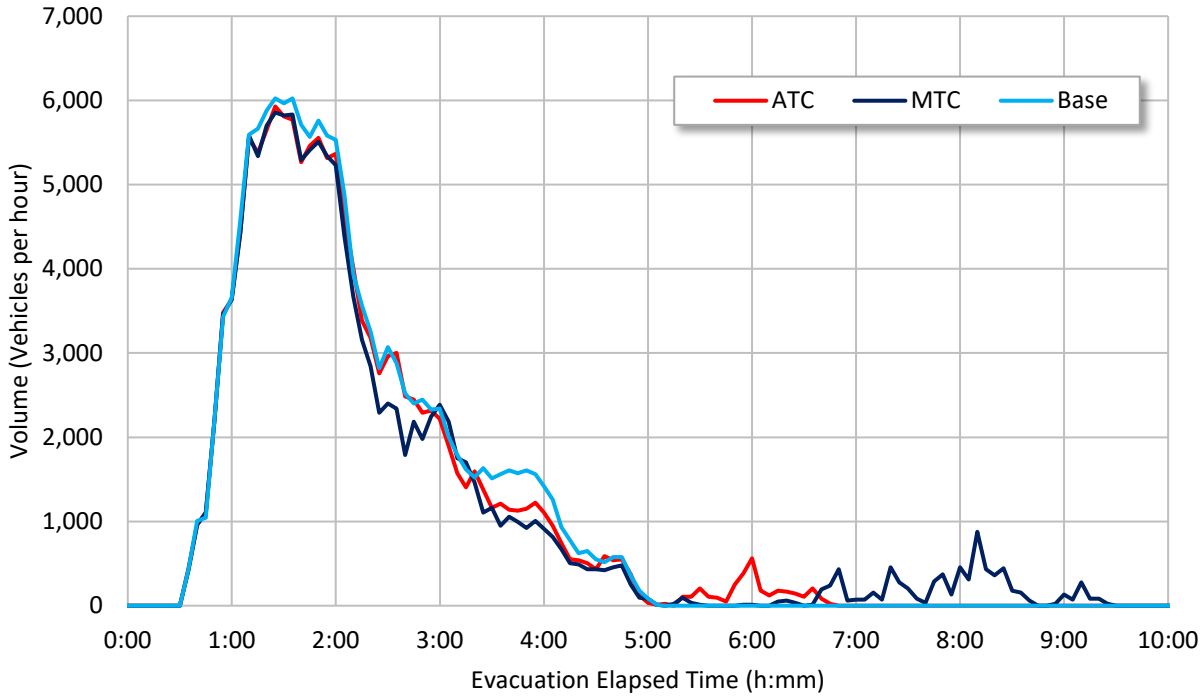

Figure 6-25 Two Mile Exit Volumes, Large Population Site Manual Traffic Control Analysis

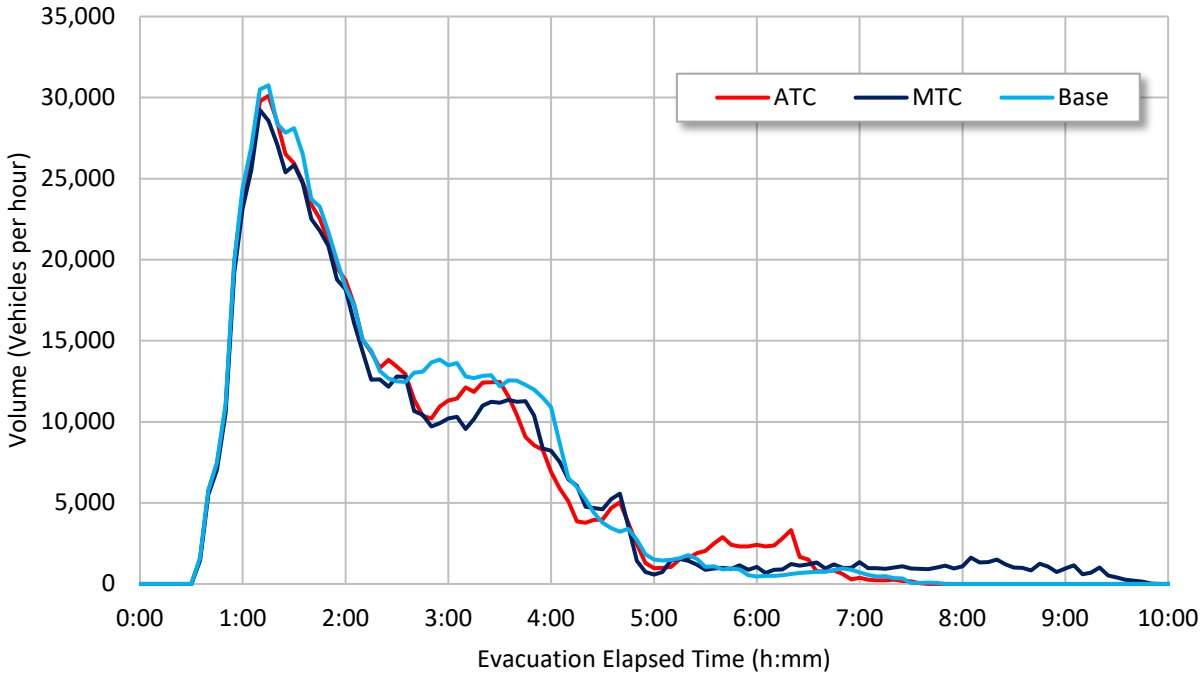

Figure 6-26 Five Mile Exit Volumes, Large Population Site Manual Traffic Control Analysis

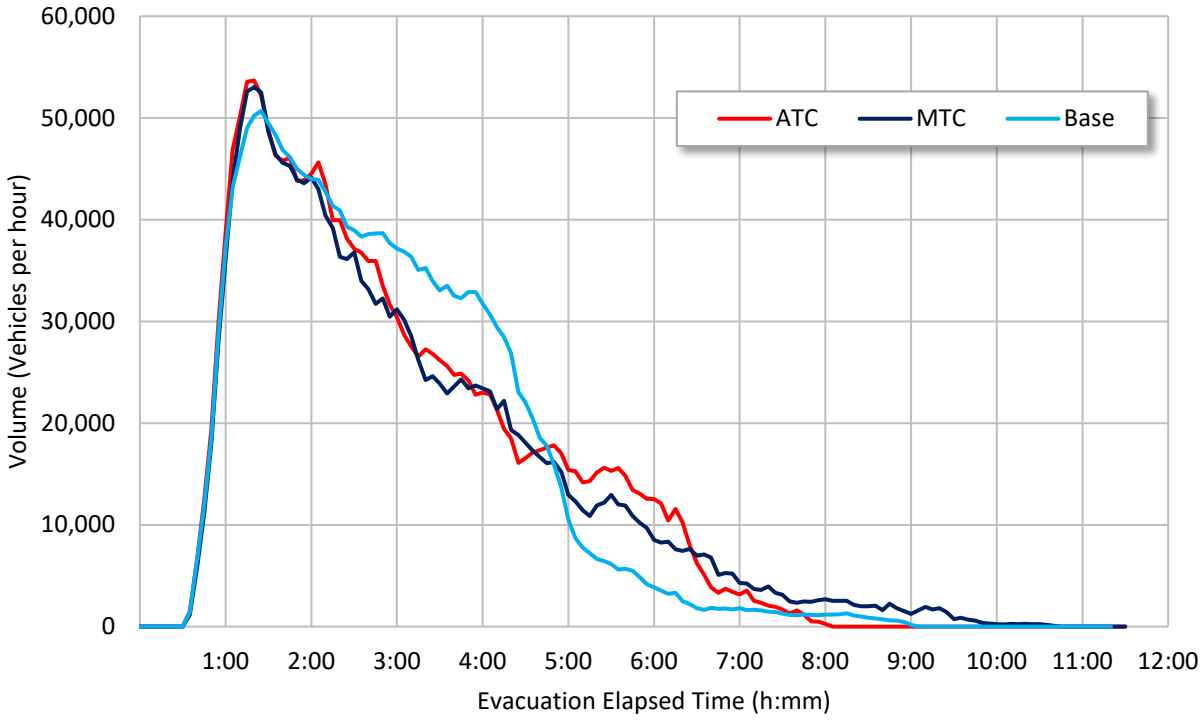

Figure 6-27 Ten Mile Exit Volumes, Large Population Site Manual Traffic Control Analysis

6.7.2.4 Significant Findings

The analysis of the 90 percent and 100 percent ETE saw no significant gains from the application of MTC. Conversely, instances were observed where the 90 percent and 100 percent ETE increased when MTC was deployed. The analysis suggested that for highly congested urban areas, with closely spaced intersections, the long cycle length associated with MTC resulted in significant queues and subsequent gridlock. This effectively paralyzed regions of the model, preventing vehicles from passing through these areas or loading onto the network. In rural or less congested urban areas, the findings suggested that MTC may not significantly impact the 90 percent ETE and may benefit intersection performance and the loading of vehicles from oversaturated local roads on to arterial streets. This is similar to the manner in which police officers load vehicles out of congested parking lots following special events or church services. However, these efficiencies in network performance and loading did not constitute a significant gain over the base model. Based on these findings and the simulation modeling methodology used in the analysis, it does not appear that MTC conducted on a limited but, representative number of TCPs can significantly decrease the 90 percent or 100 percent ETE and in some cases may increase these values.

The application of MTC on select TCPs was likely able to increase the capacity of these individual intersections. However, a vehicle that receives a 5, 10, or even 20 percent decrease in delay at one intersection does not signify a network-wide benefit nor would it be expected to decrease the ETE. While MTC may increase the performance of a single intersection, it interferes with signal coordination which is likely to result in reduced overall performance of the evacuation corridor. Based on the analysis conducted here, to achieve a meaningful decrease in clearance times, MTC would have to be applied on a scale and coordination that is impractical given the range of TCPs proposed in recent ETE studies. This research also found

that actuated controllers operate in a similar fashion to MTC, by identifying tradeoffs in phase length and saturation flow rate (time and gaps). The ATC strategy applied produced results similar to the more advanced MTC model developed as part of this research. This suggest that modeling MTC intersections with a modified actuated controller is an appropriate modeling simplification for ETE studies. The cycle length should be in the range of 200-400 seconds and randomized to capture the variability seen in MTC.

6.7.3 Sensitivity to the Number of MTC Intersections

This research objective explores the impact that the number of TCPs selected for MTC has on the 2, 5, and 10-mile ETEs for the representative small, medium, and large population sites. This was accomplished by replacing select pretimed traffic controllers within the base model with the MTC model developed in Section 6.6. Various increments of selected intersections were investigated from each of the representative models. These increment are provided in Table 6-30. Beginning with the base model, MTC was programed into the larger, higher volume intersections until the first test increment was reached. The model was run and the results evaluated for this task. Then more intersections were added, again beginning with intersections that carried higher volumes of vehicles, until the next interval was reached. The process continued for each model until the final increment was achieved. The small population site model representing 25 MTC intersections, the medium population model representing 50 MTC intersections, and the large population site model with 100 MTC intersection were used for the MTC scenarios seen in Section 6.7.2.

Table 6-30 Increments of MTC Intersection Scenarios

Population Site Model	Number of MTC Intersections
Small	0[1]
	5
	10
	25
Medium	0[1]
	10
	25
	50
Large	0[1]
	10
	25
	50
	100

[1] Base model scenario.

6.7.3.1 Sensitivity to Number of MTC Intersection Results

This section discusses the results of varying the number of TCPs modeled with MTC within the representative models. Evacuation clearance times were calculated at the 2, 5, and 10-mile rings. Additionally, the quadrant clearance times (North, South, East, and West) were calculated. It was anticipated that varying the number of intersection modeled with MTC could identify an optimum number of TCPs or provide additional insight into the utility of MTC.

The results presented in this section represent the average of several simulation runs, each with different random seed values. As was done in the previous task analyses, the small population site results represent an average of ten simulation runs, whereas the medium and large site results represent an average of four runs. The measure of effectiveness used to evaluate the ETE sensitivity to the number of MTC points was the evacuation and clearance times and EPZ exit flow rates. The data was collected and analyzed over five minute increments and segregated to display results for 90 percent of the evacuating EPZ vehicles and 100 percent, where applicable. The results of this analysis are presented for each model in the following sections.

6.7.3.1.1 Small Population Site Model Evacuation Time Results

Within the small population site, the number of TCPs selected for MTC varied between 5, 10, and 25 intersections. Table 6-31 shows the 90 percent 100 percent ETEs resulting from each of these increments, and the base model results which did not include MTC intersections. Table 6-2 shows this same information, by quadrant. From these tables, only slight differences in ETE times can be seen between the increments and none of these resulted in a significant impact on the ETE. This was likely because of the uncongested driving environment in the small population site.

Table 6-31 Small Population Site ETEs for Varying MTC Intersections

Traffic control	2-Mile Ring		5-Mile Ring		10-Mile Ring	
	90% ETE	100% ETE	90% ETE	100% ETE	90% ETE	100% ETE
5 MTC	1:35	2:18	1:35	2:21	1:44	2:31
10 MTC	1:35	2:18	1:35	2:21	1:45	2:33
25 MTC	1:35	2:18	1:36	2:22	1:45	2:33
Base (0 MTC)	1:35	2:18	1:35	2:21	1:44	2:31

Table 6-32 Small Population Site ETEs by Quadrant for Varying MTC Intersections

Quadrant	5 MTC		10 MTC		25 MTC		Base (0 MTC)	
	90% ETE	100% ETE	90% ETE	100% ETE	90% ETE	100% ETE	90% ETE	100% ETE
North	1:39	2:10	1:39	2:10	1:39	2:10	1:39	2:09
East	1:42	2:23	1:42	2:23	1:44	2:22	1:43	2:21
South	1:44	2:28	1:44	2:30	1:45	2:31	1:44	2:30
West	1:44	2:29	1:45	2:31	1:45	2:31	1:44	2:29

Figure 6-28 shows the 10-mile EPZ ETE curve for the small population site that resulted from varying the number of TCPs modeled with MTC. The figure suggests there was no significant impact from increasing the number of MTC intersections from zero in the base model, to 5, 10, or even 25 intersections. Again, this was likely because the area was not congested and therefore, little was gained or lost as the result of intersection delay.

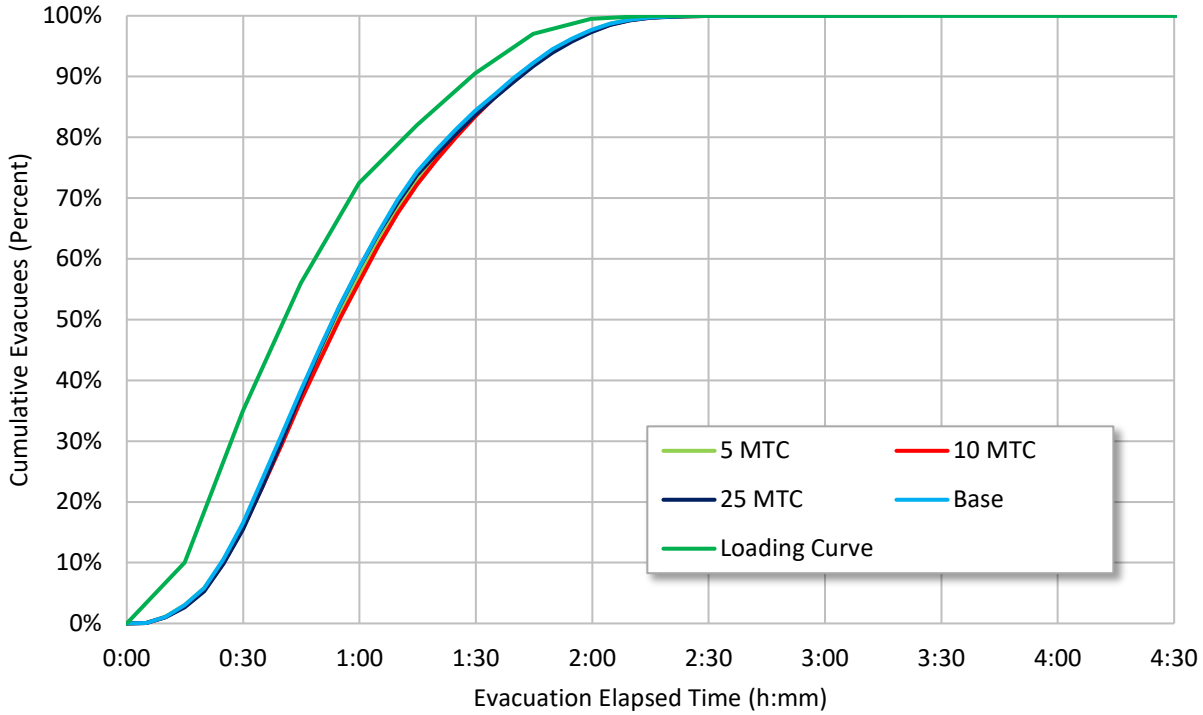

Figure 6-28 Ten Mile ETE Curves, Small Population Site Varying MTC Intersections

6.7.3.1.2 Medium Population Site Model Evacuation Time Results

The medium population site varied the number of TCP selected for MTC from 10 intersections, to 25 and then 50. Table 6-33 shows the ETEs resulting from these increments and the base model results at the 2, 5, and 10-mile rings. Table 6-34 shows these results by quadrant. The results show the 2-mile ring and the South quadrant were insensitive to the number of MTC intersections. Based on the findings in the small population site, this was expected because these regions of the medium population site were predominately rural with low congestion. In general, the ETEs increased with higher numbers of MTC intersections. This supports the previous finding that MTC with long cycle lengths can lead to significantly long queues forming at intersections. These queues propagate upstream, spanning several intersections, and can influence the queues from other intersections or bottlenecks. This interaction between queues causes conditions which can lead to localized gridlock. Because the first increment of ten intersections selected for MTC were the largest and most highly traversed in the network, even this low number of intersections utilizing MTC led to significant delays.

Table 6-33 Medium Population Site ETEs for Varying MTC Intersections

Traffic control	2-Mile Ring		5-Mile Ring		10-Mile Ring	
	90% ETE	100% ETE	90% ETE	100% ETE	90% ETE	100% ETE
10 MTC	2:40	4:03	4:32	7:23	7:07	10:37
25 MTC	2:40	4:03	4:46	7:47	7:10	10:52
50 MTC	2:40	4:03	5:03	8:11	7:36	10:05
Base (0 MTC)	2:40	4:03	2:47	5:05	5:03	7:41

Table 6-34 Medium Population Site ETEs by Quadrant for Varying MTC Intersections

Quadrant	10 MTC		25 MTC		50 MTC		Base (0 MTC)	
	90% ETE	100% ETE	90% ETE	100% ETE	90% ETE	100% ETE	90% ETE	100% ETE
North	7:45	10:07	7:53	10:52	8:08	9:50	6:12	7:41
East	4:16	9:05	4:13	8:25	4:15	8:11	4:05	5:22
South	2:47	4:22	2:47	4:22	2:47	4:22	2:47	4:22
West	8:48	10:37	8:47	10:01	8:37	10:05	5:32	6:20

Figure 6-29, Figure 6-30, and Figure 6-31 show the 2, 5, and 10-mile ring ETE curves for the varying increments of MTC intersections used within the medium population site, respectively. Figure 6-29 shows no impact from the use of MTC within the 2-mile ring. Figure 6-30 shows significant deviation from the base model beginning after approximately 60-65 percent of the evacuees have been loaded into the network. This corresponds to the results seen in the previous section and indicated MTC used at ten of the highest volume intersections had approximately the same impact on the ETE curve as when 50 of the highest volume intersections were selected. This may suggest that MTC is not ideally suited for larger, higher volume intersections located in congested urban corridors. Figure 6-31 for the 10-mile EPZ show results similar to the 5-mile ring.

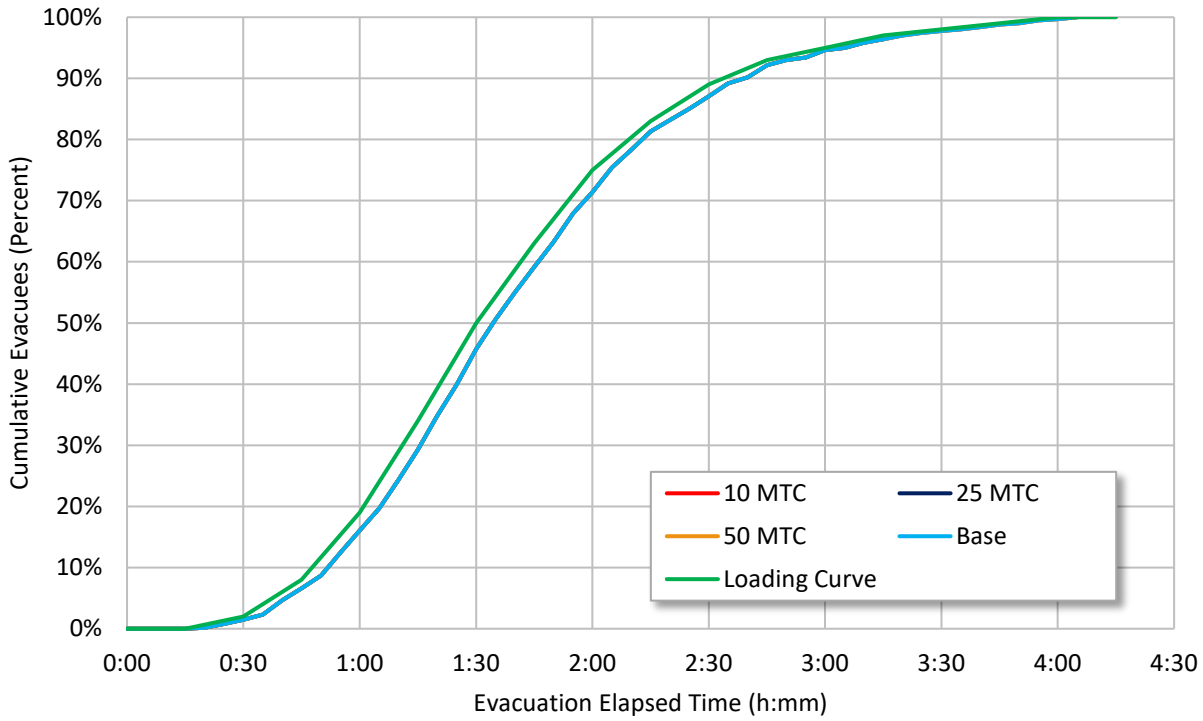

Figure 6-29 Two Mile ETE Curves, Medium Population Site Varying MTC Intersections

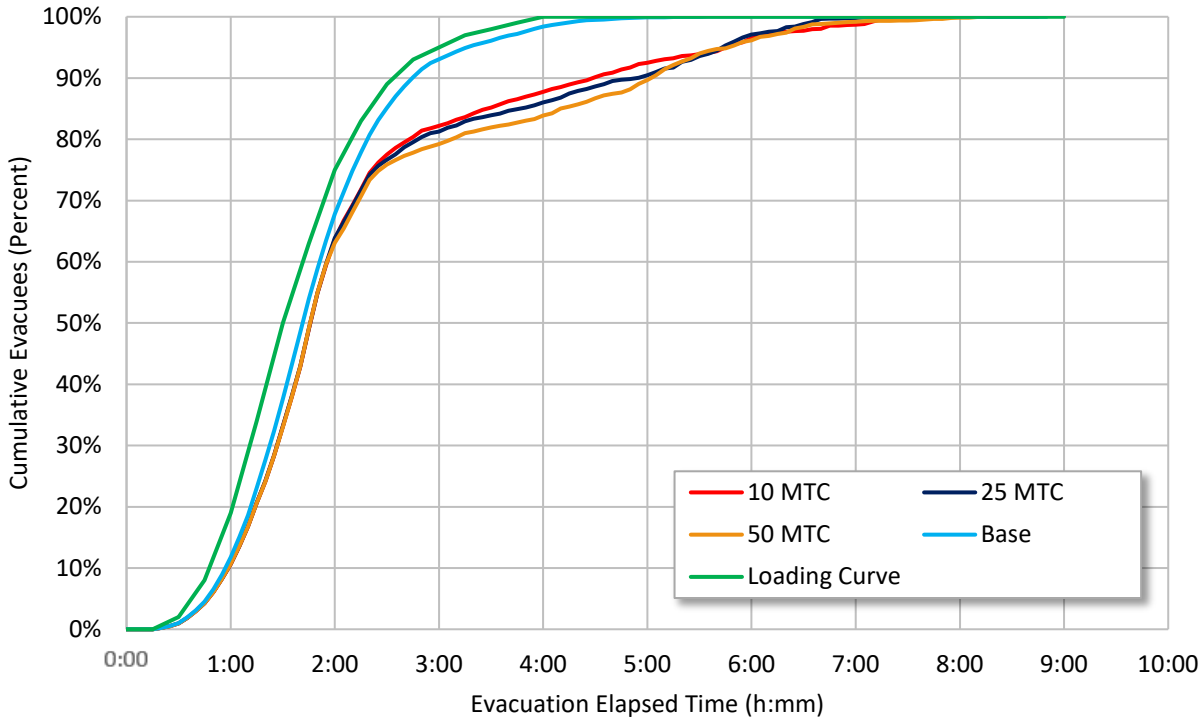

Figure 6-30 Five Mile ETE Curves, Medium Population Site Varying MTC Intersections

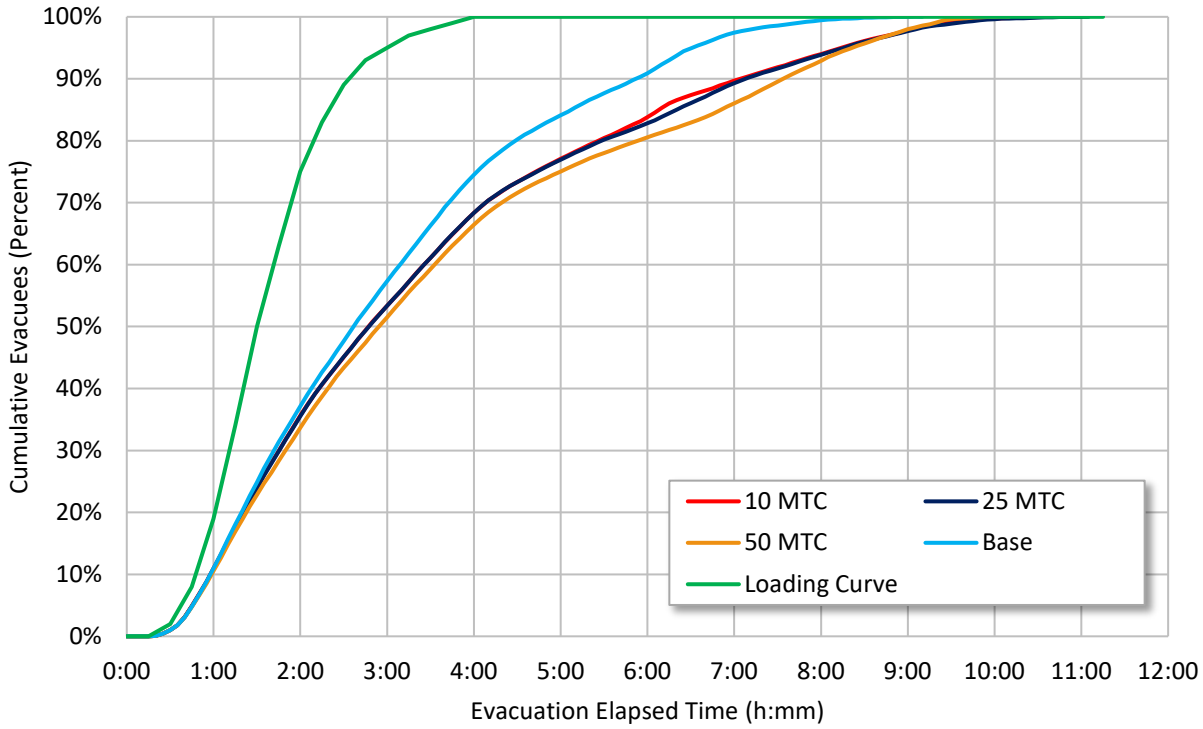

Figure 6-31 Ten Mile ETE Curves, Medium Population Site Varying MTC Intersections

6.7.3.1.3 Large Population Site Model Evacuation Time Results

Table 6-35 shows the ETEs for the large population site by ring, corresponding to the varying number of MTC intersections. These results are displayed by quadrant in Table 6-36. In general, the 90 percent ETE was insensitive to the number of MTC intersections within the 2 and 5-mile rings. However, the 100 percent ETE at the 2, 5,and 10-mile rings and the 90 percent ETE at the 10-mile ring all significantly increased compared to the base model. This suggests the evacuation tail may have been disproportionately impacted by the application of MTC. This is consistent with findings of the previous section. In general, the ETEs increased with the number of MTC used. However, this was not always the case, as the scenario utilizing 50 MTC marginally outperformed the 25 MTC scenario, in some cases.

Table 6-35 Large Population Site ETEs for Varying MTC Intersections

Traffic control	2-Mile Ring		5-Mile Ring		10-Mile Ring	
	90% ETE	100% ETE	90% ETE	100% ETE	90% ETE	100% ETE
10 MTC	3:37	6:21	4:28	7:07	5:41	10:07
25 MTC	3:40	6:32	4:42	7:18	5:46	10:03
50 MTC	3:36	6:20	4:22	7:05	5:41	10:13
100 MTC	4:08	8:43	4:40	9:23	5:55	10:15
Base (0 MTC)	3:40	5:05	3:57	6:35	4:43	9:01

Table 6-36 Large Population Site ETEs by Quadrant for Varying MTC Intersections

Quadrant	10 MTC		25 MTC		50 MTC		100 MTC		Base (0 MTC)	
	90% ETE	100% ETE	90% ETE	100% ETE	90% ETE	100% ETE	90% ETE	100% ETE	90% ETE	100% ETE
North	6:25	7:50	6:31	7:51	6:27	7:45	6:41	9:33	4:55	8:00
East	5:36	10:07	5:41	10:03	5:40	10:13	6:16	10:15	4:42	9:01
South	4:45	8:37	4:48	8:41	4:51	8:46	4:36	7:53	4:40	5:50
West	4:53	7:16	5:06	7:28	4:42	7:23	4:41	8:58	4:37	6:07

Figure 6-32, Figure 6-33, and Figure 6-34 show the ETE curves at the 2, 5, and 10-mile rings, respectively, corresponding to the number of intersections programed for MTC. At the 2-mile ring, there was no significant deviation from the base model ETE curves until after 90 percent of the evacuees were loaded into the network. The 5-mile ring does not show significant distinction from the base model until nearly 85 percent of the vehicles have been loaded. However, at the 10-mile EPZ, this distinction begins when approximately 60 percent of the vehicles were loaded. In general, the ETE curves suggest the scenarios utilizing 10, 25, and 50 MTC intersections performed similar to each other whereas the 100 MTC scenario under preformed, specifically at the 2 and 5-mile ring.

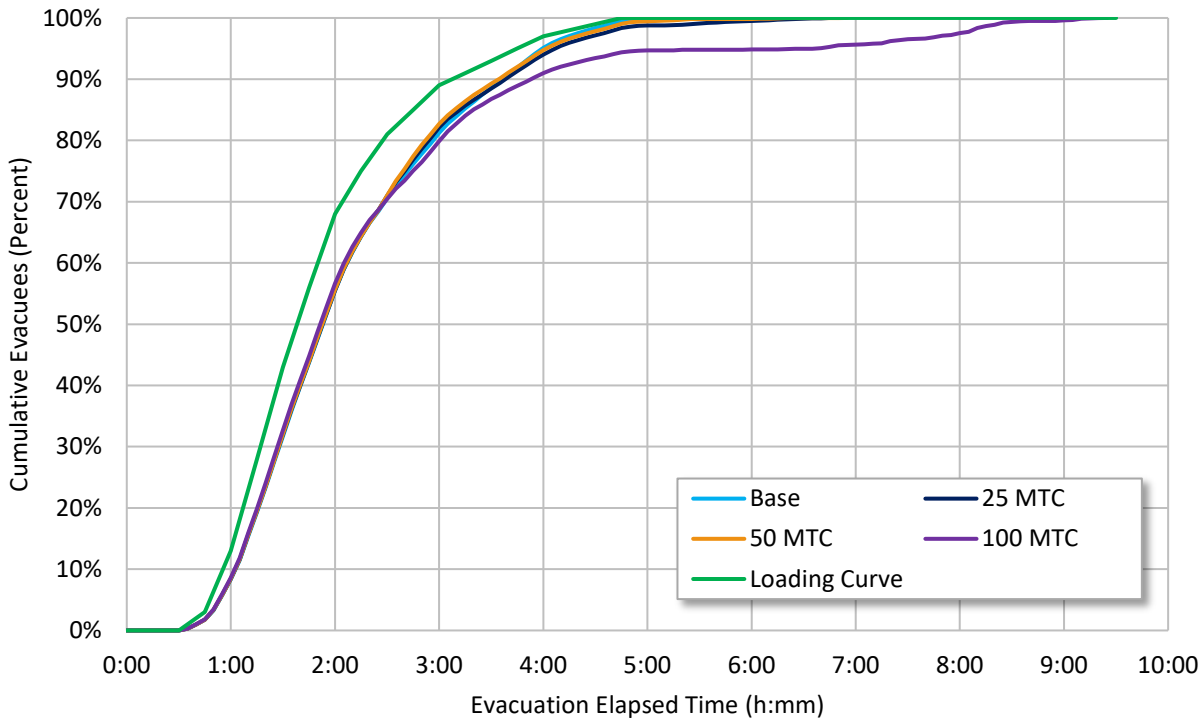

Figure 6-32 Two Mile ETE Curves, Large Population Site Varying MTC Intersections

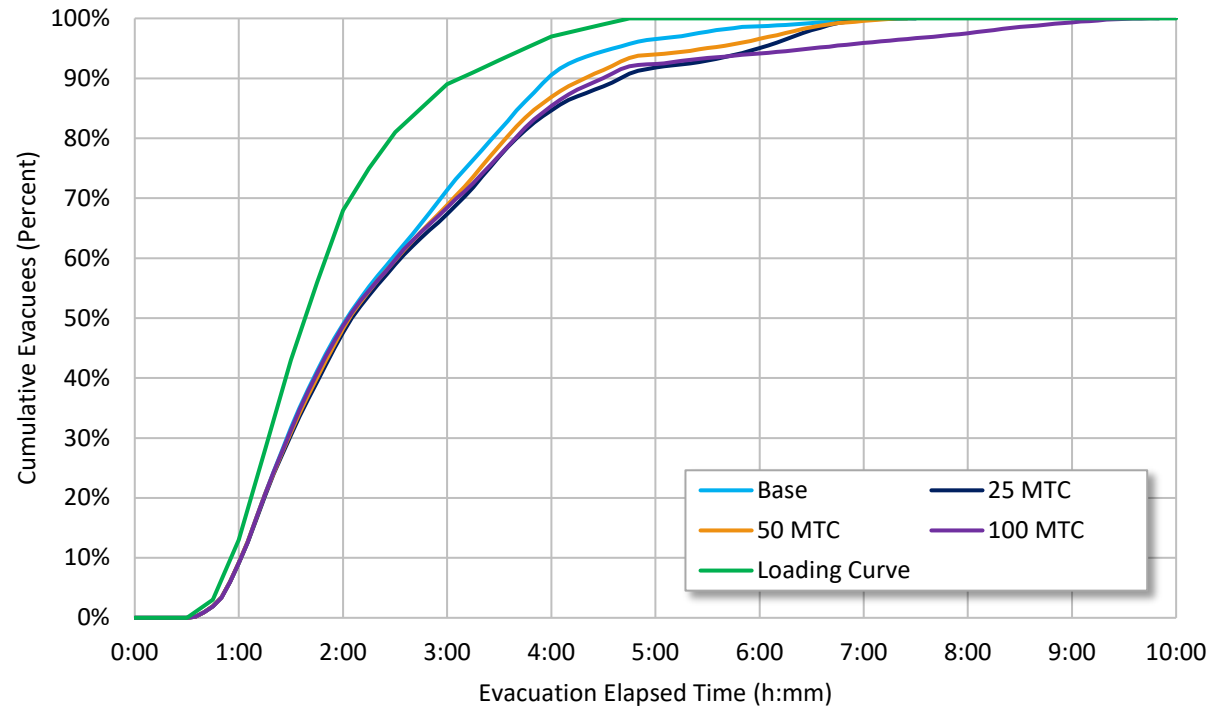

Figure 6-33 Five Mile ETE Curves, Large Population Site Varying MTC Intersections

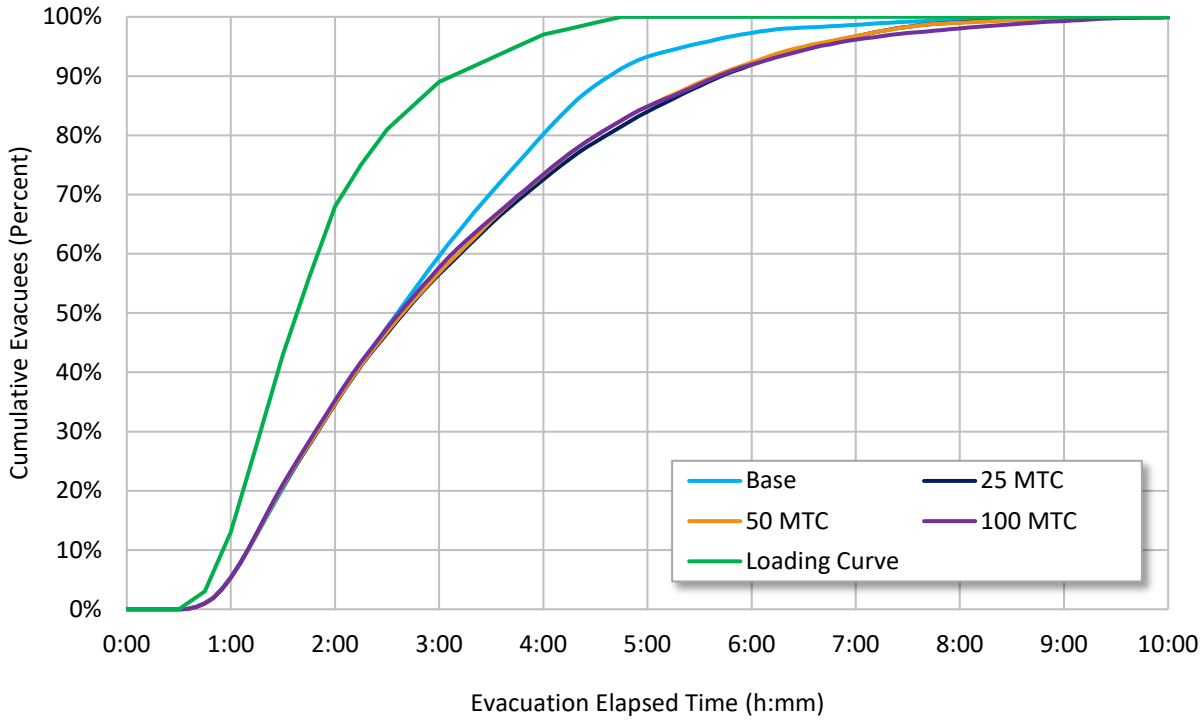

Figure 6-34 Ten Mile ETE Curves, Large Population Site Varying MTC Intersections

6.7.3.2 EPZ Exit Flow Rates Results

The EPZ exit flow rate is the number of vehicles that exit the 10-mile EPZ over each 5-minute data collection interval. This flow rate was converted into vehicles per hour, consistent with the standard practices of traffic engineering. Fundamentally, the 10-mile EPZ exit flow rate measures the diffusion of evacuation vehicles out of the EPZ. In the prior section, MTC and ATC strategies were able to marginally increase the exit flow rates in the small and large population sites. The increase could have been caused by more efficient loading of vehicles onto the network or from a slight increase in performance of MTC and ATC earlier in the evacuation. The investigation conducted here aimed at determining which of these two factors contributed to the bump in exit flow rates seen in the prior section. If MTC resulted in better loading of vehicles from side streets on to arterials, than it would be expected the increase in exit flow rate would only be present when larger numbers of intersections used MTC. This is because scenarios with fewer MTC intersections utilized intersections that were predominately large, with high volumes and not network loading links, whereas scenarios with more intersections selected for MTC were more likely to include network loading links. If the gain in exit flow rate was accomplished through loading the network at these locations, then the increase in exit flow rates should only be present in the scenarios with more MTC intersections and not present in scenarios with fewer. However, if the exit flow rates increased as a result of better intersection performance earlier in the simulation, then it would be expected that these gains would be visible when fewer, more heavily traversed intersections were modeled with MTC.

6.7.3.2.1 Small Population Site Model EPZ Exit Flow Rate Results

Figure 6-35 shows the small population site exit flow rates corresponding to changing the number of intersections programed as MTC. The figure shows a small increase in EPZ exit flow rates when 25 intersections were selected for MTC. This increase was not present when the number of MTC intersections was reduced to five or ten. This finding suggest the modest gains seen were likely caused by increased efficiency in loading the network and not necessarily from an increase in individual intersection performance manifest on a network wide level.

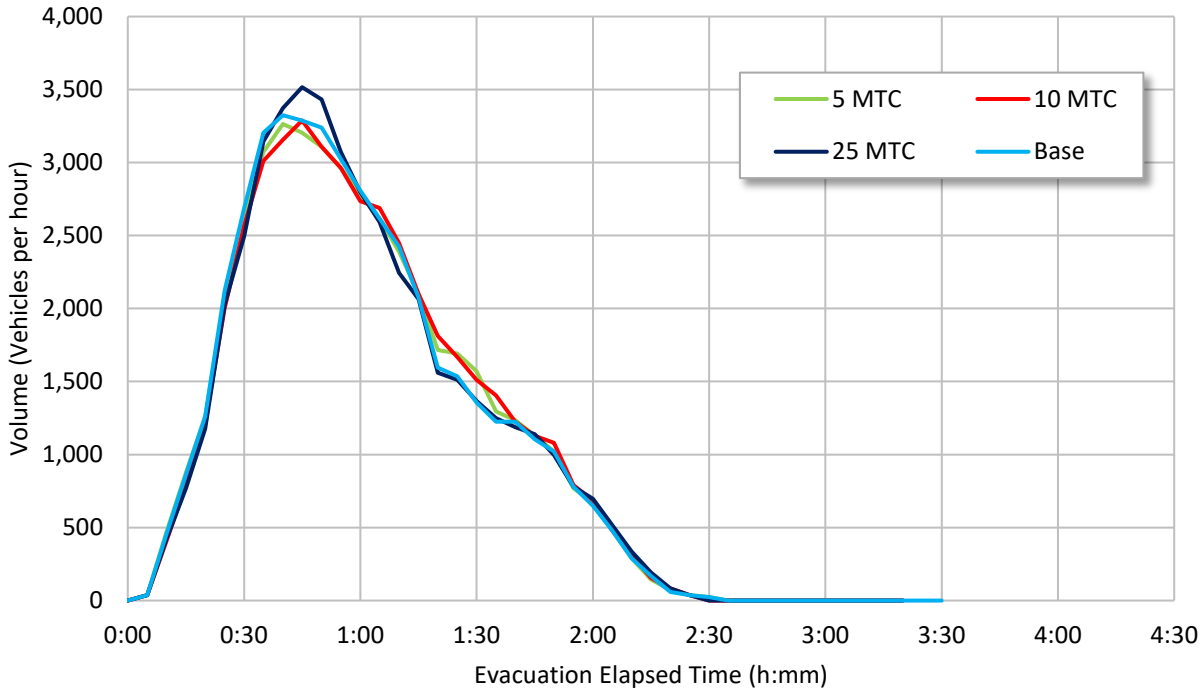

Figure 6-35 EPZ Exit Volumes, Small Population Site Varying MTC Intersections

6.7.3.2.2 Medium Population Site Model EPZ Exit Flow Rate Results

Figure 6-36 shows the EPZ exit flow rate for the medium population site corresponding to the number of intersections selected for MTC. The figure suggests that the exit flow rate was adversely impacted by the implementation of MTC. This decrease in performance became more prevalent as the number of MTC intersections increased. This supports the finding that MTC likely led to localized gridlock within the congested network, resulting in fewer vehicles accessing and moving through the EPZ.

6.7.3.2.3 Large Population Site Model EPZ Exit Flow Rate Results

Figure 6-37 shows the large population site 10-mile EPZ exit flow rates corresponding to the various numbers of MTC intersections. A small increase in exit flow rates can be seen when 10 of the highest volume intersections were modeled as MTC. This could have resulted in a larger number of vehicles passing through the network during the initial stages of the evacuation. Ultimately, these gains were marginal and lasted only briefly because of the long queues which resulted from the longer cycle length.

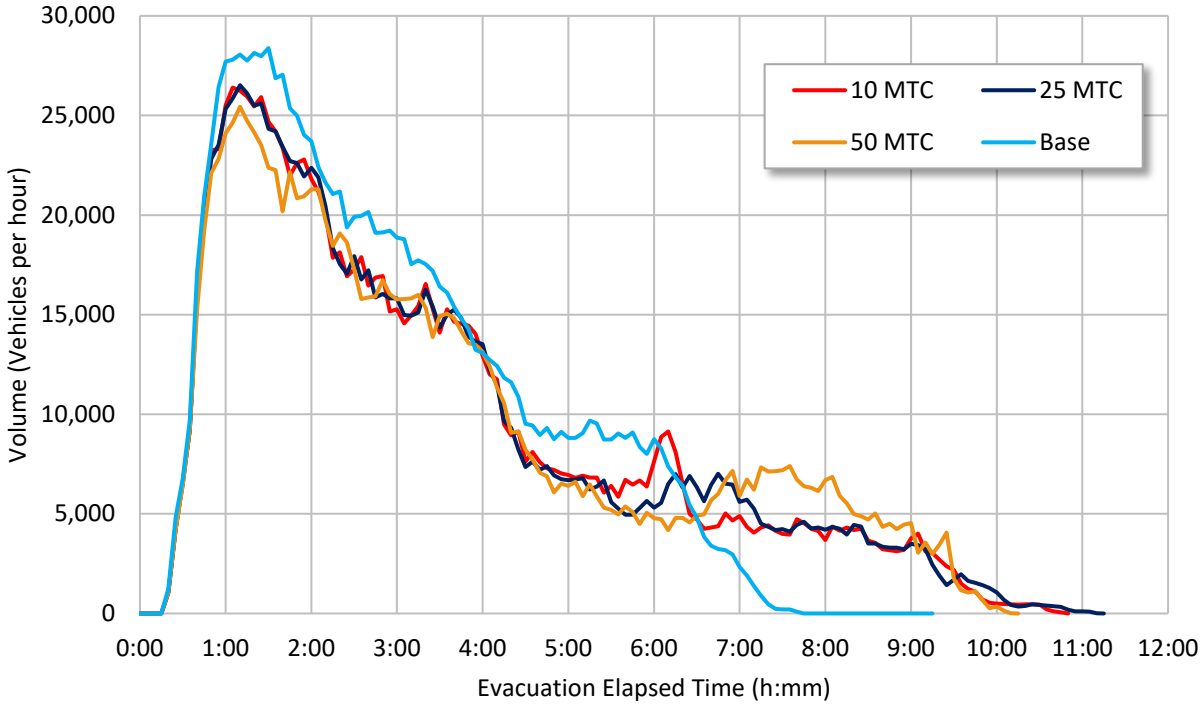

Figure 6-36 EPZ Exit Volumes, Medium Population Site Varying MTC Intersections

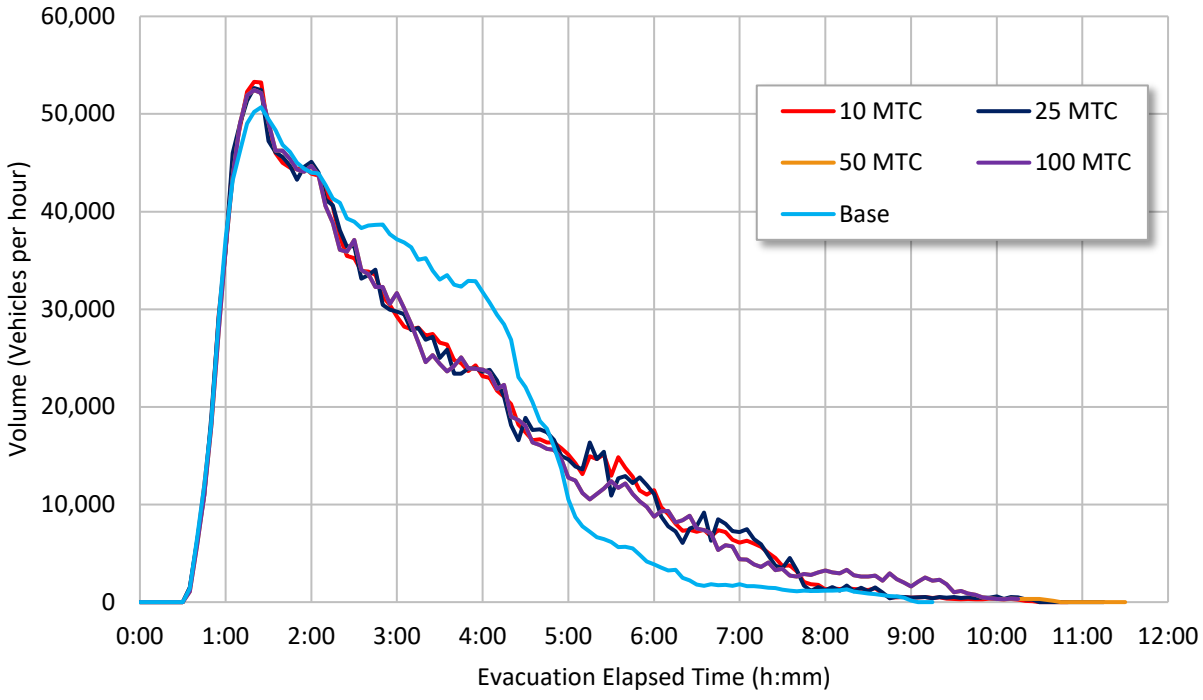

Figure 6-37 EPZ Exit Volumes, Large Population Site Varying MTC Intersections

6.7.3.3 Significant Findings

In general, the analysis found that the representative sites were insensitive to the number of intersections selected for MTC. This finding was likely because the lowest increment of TCPs tended to include intersections with the highest volumes of vehicles. Because these intersections served a larger proportion of vehicles, any significant changes to these intersections would likely impact the ETE. The exit flow rate resulting from the small population site suggested that MTC likely increased the efficiency of the modeled intersections. This was because many of the intersections in the small population site were unsignalized. Replacing an unsignalized intersection with MTC most certainly increased the intersection capacity. This assisted in the loading of vehicles into and through the road network. However, because the small population site was uncongested, these gains did not significantly impact the ETE. The large population site also saw a brief period of marginally higher exit flow rates at the 10-mile EPZ. This increase may have resulted from better performance at the MTC intersections during the earlier stages of the evacuation. However, these increases could not be maintained and ultimately, the 90 percent and 100 percent ETE were adversely impacted by MTC.

6.8 Conclusion

Manual intersection control is a valuable and effective tool to manage traffic during emergencies and planned special events. The reasonable assumption is that a human being—with the ability to directly observe and respond to prevailing traffic conditions—would provide a significant advantage in the movement of traffic over and above what could be achieved by a fixed-time or traffic actuated signal. From the standpoint of a nuclear power plant evacuation, this could mean decreased travel times, less extensive queuing, and increased operating speeds which, in turn, would yield lower evacuation times. The purpose of this task was to investigate these ideas and assumptions about MTC through the use of state-of-the-art models and simulation tools. It is worth noting that, despite the long history of manual traffic control use throughout the world and its assumed effectiveness, there have been no quantitative, systematic studies of when, where, and how MTC should be used or how it performs compared to automated signals. A recent review of MTC practices and training [126] identified standardized methods for communicating with drivers, where and how to position police and vehicles to direct traffic, and resource needs. Additionally, documents detailing the practice and training of officers on MTC typically do not provide guidance on how to effectively distribute intersection right-of-way. In addition to the personnel requirements, which are extensive, officers are also likely to require reflective vests, lights, cones, flares, barricades, communications, and transportation. Furthermore, no research to date has been conducted on the time needed to deploy officers to TCPs during NPP emergencies. It stands to reason the time required varies depending on the number of TCPs and available officers. Prior ETE studies suggest this could take as few as 10 minutes and as long as 2 hours.

Building from a practical understanding of MTC and a limited amount of existing research, the goal of this task was to determine the value of manual intersection traffic control toward enhancing traffic flow during NPP evacuations. This was accomplished in a series of steps that was based on the application of a recently developed technique that quantified the effect of MTC on intersection operations by reviewing video of police officers directing traffic and benchmarking the development of a discrete choice model (logit model) to represent their actions. The outcome of the logit models was the computation of the green time extension (or truncation) for high demand directions based on an attempt by the officers to avoid long gaps or waste in the traffic stream. As was noted in the original research, the logit model processes were very consistent with the general concept of a traffic signal, wherein right of way is allocated

to serve the needs of competing and conflicting traffic movements, but also limited by the requirement to minimize the average approach delay incurred by drivers on these same approaches.

These logit models demonstrated a strong correlation between directional priority, time, and gap variables within the traffic stream and an officer's decision to allocate right-of-way. The practical effects of the resulting logit model were tested by programming its logic into a microscopic traffic simulation software to serve as the signal controller and act as a representative police officer directing traffic. The comparison of performance between MTC and actuated signal control showed that MTC replicated the observed traffic stream data within acceptable statistical tolerances and was generally transferable to alternative study areas. The comparison of performance between the different forms of control also showed the limitations of some traffic controllers that would diminish an officer's ability to conduct MTC effectively and that MTC could possibly increase intersection performance without this limitation.

6.8.1 Summary of Results

The results of the analysis of MTC through use of an algorithm to represent police manual intersection control within the three representatives NPP site traffic simulations suggest that MTC tended to increase the 90 percent or 100 percent ETEs. Although some benefits, in terms of increased flow rates, were observed at TCPs, these gains were ultimately lost when vehicles rejoined queues downstream of MTC intersections where traffic was slowed and stopped because of a downstream flow restriction. These restrictions included both signalized and unsignalized intersections, lane reductions, and volume increases that resulted from the introduction of demand from downstream generators. The findings also suggest that on congested urban corridors, with closely spaced intersections, the long cycle lengths of MTC led to long queues of vehicles. These queues propagated upstream and blocked neighboring intersections causing subsequent queues and gridlock. Therefore, it may not be advisable to use any intersection control timing plan with excessive cycle lengths when intersections are closely-spaced and congestion is high.

The model results suggest that when MTC was used to provide better access to collector/distributor roads from network loading links, system wide performance increased, resulting in higher EPZ exit rates. This was an expected finding because officers are typically used during special events to load collector roads from adjoining parking lots. Once the parking lot has emptied, these vehicles can access the greater road network. The same phenomenon also commonly occurs at church parking lots, where officers are routinely deployed to provide access to collector roads after worship services are complete. These benefits were manifest in improved ETE curves (albeit not significant at the 90 percent or 100 percent level) and slightly increased EPZ exit capacity. The research also found that while MTC may increase the performance of a single intersection, it interferes with signal coordination which is likely to result in reduced overall performance of the evacuation corridor. It was also found that the representative models were, in general, insensitive to the number of MTC intersections. A comparison against ATC also showed no noticeable benefit of one control strategy over the other. Looking at the research in its totality, it could be generalized that an actuated controller with longer and variable cycle length could generally influence traffic in a sufficiently similar manner as a police officer directing traffic.

Within the context of ETE analyses, existing methods of representing MTC using actuated signal control appear to be equivalent to more detailed and sophisticated logit models that have been developed through research and observation of actual traffic enforcement police actions in

the field. This is a positive development because it obviates the need to include sophisticated algorithms and site-specific calibration data. However, the ability of an officer to influence traffic is limited to his or her immediate surroundings, and global impact is difficult to achieve by deploying MTC to a limited number of intersections.

7 TASK 4 PARAMETERS OF IMPORTANCE

Traffic simulation models require many assumptions be made to represent traffic movement within a roadway network. These assumptions dictate parameter values used in the traffic simulation. Developing a basis for assumptions requires a substantial effort. ETE developers conduct telephone surveys and roadway inspections and review traffic management plans and state/county roadway related documents. If the most important assumptions/parameters were known, ETE developers and reviewers could prioritize the effort and focus attention on the most important aspects of simulation development and analysis. The focus of Task 4 was identifying the most important assumptions and parameters used in ETE studies.

Three main objectives in this study are:

- Identify parameters that are most likely to significantly influence calculation of ETEs.
- Conduct systematic sensitivity analyses to assess the influence of each parameter.
- Compare the resultant MOEs to base model results to determine the effect of varying each parameter.

In the sections that follow, the parameters of interest, the bases for selecting baseline values and the ranges for testing, and the results of the sensitivity analysis are described. Combined with the insights from the previous tasks, the outcomes of this task revealed a number of key insights into the competing factors of traffic supply and demand which provide a better understanding of the impact of certain parameters on the simulation of evacuations and enhance the overall efficacy of ETE studies.

7.1 Background

Evacuation traffic simulations are influenced by the transportation related aspects of traffic supply and demand and by the representation of physical processes in the modeling. In simulation modeling, traffic demand parameters include variables that describe the temporal and spatial generation, movement, and characteristics of traffic during an evacuation. Traffic supply parameters are those that are used to influence the overall capacity that exists within a system. Simulation parameters are not as directly related to the representation of the physical conditions of a system, but govern the computational routines of simulation models; these parameters include the duration of system state updating (commonly known as “processing time step” or “simulation resolution”) and random seeds for stochastic models. All simulation parameters can be generally categorized as relating to traffic demand, traffic supply, or simulation process.

7.1.1 Parameters of Importance

A total of nine input parameters were selected for study. The identification and selection of these parameters were based on a number of sources including a review of relevant literature, guidance documents, prior ETE studies, and the use of expert judgement. Selected parameters for study are:

- Traffic Demand: population, mobilization time, background traffic, and heavy vehicles
- Network Supply: free-flow speed, adverse weather, and roadway impact
- Simulation Process: computation processing time step and random seed uncertainty

Each of these parameters were studied in the three representative population site models. The sensitivity analysis consisted of uniformly varying each parameter within a range of values while keeping everything else constant. A brief description of these parameters and the range of values studied in the representative population site models is summarized in Table 7-1, Table 7-2, and Table 7-3. The selection of specific values was influenced by several considerations such as: characteristics of each representative site model; recommendations in NUREG/CR-7002; findings from relevant research; preliminary tests performed in this study; broad application to all types of traffic simulation and avoidance of parameters unique to VISSIM. In the sections that follow, the parameters of interest, and the bases for selecting the baseline values and the ranges for testing are described in detail.

Table 7-1 Traffic Demand Parameters Description and Range

Input parameter	Description	Population Site Model	Minimum	Base	Maximum	Number of Scenarios
Population (evacuees)	Range of EPZ evacuation population leading to vehicle demand.	Small	7,500	7,500	27,375	9
		Medium - North	71,500	192,000	240,000	10
		Medium - South	7,990	8,000	55,000	5
		Large	130,000	325,000	390,000	10
Mobilization time (h:mm)	Loading curves that capture slower and faster mobilization of evacuees.	Small	2:15	2:15	6:30	9
		Medium	2:30	4:00	10:00	11
		Large	2:30	4:45	10:00	11
Background traffic (vehicles)	Number of background vehicles (demand shown is outside the EPZ).	Small	3,175	6,350	9,525	4
		Medium	24,110	48,220	96,440	4
		Large	76,000	152,000	304,000	4
Heavy vehicles (percent)	Percentage of trucks and RVs (recreational vehicles).	Small	0	2	20	4
		Medium	0	2	20	4
		Large	0	2	20	4
Total number of scenarios						**89**

Table 7-2 Network Supply Parameters Description and Range

Input parameter	Description	Population Site Model	Minimum	Base	Maximum	Number of Scenarios
Free-Flow speed decrease (percent)	Uniform percent decrease in free-flow speed on all roads.	Small	10	0	35	6
		Medium	10	0	35	6
		Large	10	0	35	6
Adverse weather (rain & snow)	Uniform percent decrease in free-flow speed (FFS) and uniform increase in headways based on W74 parameters: Bx_{add} and Bx_{mult}, and W99 CC1 parameter.	Small	0% FFS Bx_{add}=2 Bx_{mult}=3	0% FFS Bx_{add}=2 Bx_{mult}=3	35% FFS Bx_{add}=3 Bx_{mult}=4	5
		Medium	0% FFS Bx_{add}=2 Bx_{mult}=3	0% FFS Bx_{add}=2 Bx_{mult}=3	35% FFS Bx_{add}=3 Bx_{mult}=4	5
		Large	0% FFS Bx_{add}=2 Bx_{mult}=3 CC1=0.9	0% FFS Bx_{add}=2 Bx_{mult}=3 CC1=0.9	10% FFS Bx_{add}=2.6 Bx_{mult}=3.6 CC1=1.3	5
Roadway impact (links closed)	Temporary loss of capacity from localized roadway disruptions using lane closures.	Small	N/A	0	1	1
		Medium	N/A	0	2	2
		Large	N/A	0	2	2
					Total number of scenarios	38

Table 7-3 Simulation Process Parameters Description and Range

Input parameter	Description	Population Site Model	Minimum	Base	Maximum	Number of Scenarios
Processing Time Step (time steps/second)	Number of time steps per simulation second.	Small	1	1	10	3
		Medium	1	1	10	3
		Large	1	1	10	3
Random Seed Uncertainty Analysis (number of seeds)	Number of random seed runs for data averaging.	Small	10	10	50	2
		Medium	4	10	50	2
		Large	4	10	37	2
					Total number of scenarios	15

7.1.1.1 Population

The population of a region is a key variable in transportation simulation because it dictates the vehicle demand from points of origin in a roadway network. Evacuee demand depends on vehicle occupancy, number of vehicles and drivers in households, and participation rates. Population is important because vehicle demand can significantly influence the formation and release of congestion. Population is converted into vehicles based on participation rates (for ETEs this is modelled as 100 percent participation) and based on vehicle occupancy rates for the various population groups involved in the evacuation process (residents, transients, etc.). Household characteristics such as vehicle ownership, number of persons in the household, and the decision to evacuate together or bring as many vehicles as possible would vary the occupancy rate during an evacuation.

7.1.1.1.1 Literature Review

NUREG/CR-7002 provides general ranges of vehicle occupancies for different population groups. For example, residents are likely to evacuate with average vehicle occupancy rates of 1 to 2 persons per vehicle [4]. ETE studies also typically estimate average vehicle occupancy rates for transients in recreational areas and transient employees. In most ETE studies occupancy rates for the EPZ resident population are based on telephone surveys that provide household characteristics such as vehicle ownership, number of persons in the household, and whether they would evacuate together or bring as many vehicles as possible. Vehicle occupancy rates for employees and transients are typically obtained from surveys of major employers and facilities that attract transients (e.g., universities, campgrounds, golf courses, expo centers, etc.).

A review of vehicle occupancy rates documented in prior ETE studies showed occupancy rates for residents between a minimum of 1.55 and a maximum of 2.37 persons per vehicle across small, medium and large population sites. The average vehicle occupancy rate reported for large population sites was the highest (2 persons per vehicle with a standard deviation of 0.20 persons per vehicle) followed by medium population sites (average occupancy of 1.88 persons per vehicle). Small population sites had the lowest average occupancy rates (1.81 persons per vehicle). For the employee population group (i.e., people who work in the EPZ but reside outside the EPZ), average vehicle occupancy rates varied between a minimum of 1 and a maximum of 1.25 persons per vehicle across small, medium and large population sites. The maximum occupancy rate was observed in small population sites. The estimate of vehicle occupancy rates is important as it dictates the number of vehicles loaded in a traffic simulation model. For example, 100,000 people with an average vehicle occupancy rate of 1.6 results in 62,500 evacuating vehicles, but an average vehicle occupancy rate of 1.8 results in 55,600 evacuating vehicles. The difference in number of vehicles can impact the ETE.

The sensitivity of ETEs to population has been previously investigated. Pel et al., (2010) assessed the sensitivity of roadway network performance (capacity) during a flood evacuation in a metropolitan area using EVAQ, a macroscopic traffic simulation tool. The authors of the study found that demand and capacity had a quasilinear impact on network conditions (e.g., congestion) and evacuation timing [141].

The NRC sponsored a sensitivity study documented in NUREG/CR-4874, “The Sensitivity of Evacuation Time Estimates to Changes in Input Parameters for the I-DYNEV Computer Code,” [13]. The study suggested that ETEs remain unchanged when the EPZ population is varied below a certain threshold value defined as “Point A” in Figure 7-1. This was because capacity

was adequate at demand (evacuating population) below that threshold. As such, there was enough capacity to serve the demand and no significant delay other than that produced by vehicle interactions occurred. After the threshold value, however, the networks become capacity constrained and ETEs increased linearly at a rate dependent on the relationship between demand and capacity.

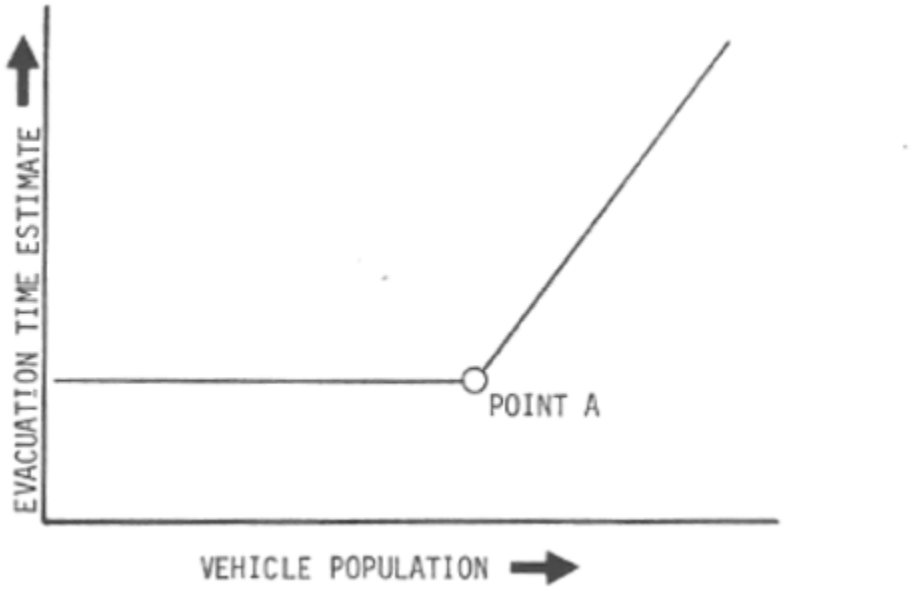

Figure 7-1 Theoretical Relationship Between Population and ETEs

The study of population in this research is expected to deepen the understanding of the effect of population variability and its relationship to emergency evacuations. In addition, this research is expected to illustrate the role that network topology plays, which might influence population distributions and the number of available routes in such areas (e.g., topological features such as geographic constraints, rivers, bays, and other bodies of water, etc.). Ultimately all of these factors come together to affect an evacuation clearance process.

7.1.1.2 Mobilization Time

Mobilization time is an important variable that accounts for the timing of travel departures of people and vehicles from their points of origin. Mobilization time is defined as the period from the time an evacuation order is received to the time vehicles depart from their origins. An individual's mobilization time may be influenced by several factors including securing of properties, caring for pets, gathering family members, or shutting down business operations. Mobilization time can also vary based on factors related to population group characteristics, season of the year, and time of day. As such, mobilization times can vary widely.

Mobilization times are often estimated from telephone surveys that collect information related to evacuee departure behaviors (e.g., time to leave work, time to pack, snow removal, etc.). This information is used to develop loading curves that reflect the rate at which vehicles would be loaded onto the transportation network. Mobilization time is important because the loading curve can greatly affect the location and level of congestion in a roadway network. For example, if 10,000 trips are expected on a section of road, the capacity needed to carry the traffic would be completely different if these vehicles were expected over a 2-hour period rather than a 10-hour period. A secondary issue is the formation of and recovery from traffic queuing, because it can

be a slow process to recover from congestion once it has begun. This element of the task assessed the effect of mobilization time variability on the ETE.

7.1.1.2.1 Literature Review

Prior research has investigated the sensitivity of ETEs to mobilization time. Ozbay et al., (2006) conducted a sensitivity analysis to evaluate the effect that changes in the loading curves would have on the clearance process of Cape May, New Jersey, based on a multiple origin and single destination network [142]. The study suggested that slow, medium, and fast loading rates had a nonlinear effect on network performance and that the characteristics of this effect were mainly influenced by network capacity. In addition, it was observed that clearance times were directly affected by the loading rate of 50 percent of the population. Similar observations were made in NUREG/CR-4874 [13].

A later study conducted by Pel et al., (2010) used the macroscopic traffic simulation model EVAQ to assess the sensitivity of network performance to changes in demand and capacity in the evacuation of Rotterdam in the Netherlands [141]. Their research also found that loading rates had a nonlinear impact on clearance times, particularly when the total demand was high. Tamminga et al., (2011) conducted a sensitivity analysis to investigate the influence of mobilization times on network performance during an evacuation [135]. The study used the microscopic simulation software S-Paramics to model evacuation departure times spanning from 7 hours to 16 hours. The results of the study showed that clearance times for 85 percent of the population were observed to increase with longer total departure times. However, ETEs for 90 percent of the population were observed to decrease slightly and then increase. Short mobilization times were observed to influence the network performance significantly as the simulation period ended before all the vehicles exited the area under evacuation. In general, it was concluded from that study that outflow from an evacuation is a function of network capacity and that loading vehicles faster deteriorates performance.

NUREG/CR-4874 showed that for low population density sites, the 100 percent ETE approached the total mobilization time [13]. As such, it was suggested that sites with small populations clear faster with shorter mobilization times. This is because demand does not exceed network capacity regardless of the loading rate.

The studies reviewed identified important aspects of an evacuation process that affect the overall clearance process. In particular, mobilization times were found to be an important variable. However, most studies did not consider scenarios with lower demand or variations in network topology, both of which were noted in those studies as important factors that could influence the evacuation performance. Although, there is no clear measure that captures the relationship between mobilization time and network topology, nor a range of mobilization times where an ETE may be most sensitive, it is expected that some difference would be observed in regions with different network and demand characteristics.

7.1.1.3 Background Traffic

Vehicular traffic in both real roadway networks and simulation models, come from several sources. The focus of modeling is typically on the traffic generated by or attracted into a network under study. The representation of traffic in a realistic way must include all traffic that might exist within a network, including background traffic.

Background traffic can be thought of as any traffic that would have been present in a network whether or not any new generator, attracter, or activity existed. For the purposes of this study

background traffic refers to vehicles in the network that are not part of the initial active evacuation [31]. Background traffic includes residents and transients assumed to be travelling within the EPZ conducting general activities when the initial evacuation notification occurs. Background traffic also includes traffic outside the EPZ that is not part of the evacuation but is thought to affect the movement of evacuees traveling between their origins and destinations.

Background traffic is important because the additional vehicles occupy physical space (i.e., available capacity) on the roadway that could otherwise be used by evacuating vehicles. Including background traffic creates more realistic conditions in the computation of ETEs, but relatively little information is available about the amount of background traffic that would be present during an evacuation [143]. This element of the task assessed the effect of various levels of background traffic on ETEs across the three representative site models.

7.1.1.3.1 Literature Review

Background traffic varies throughout the day and nighttime, and dawn scenarios have a lower volume than daytime. The general approach to modeling background traffic is to use available traffic data for the study area under non-emergency conditions [137] [138] [139] [140]. For example, the study conducted by Zheng et al., (2010) used O-D tables provided by planning agencies or derived from static data. Their study also considered the routing of background traffic by considering whether the origin and destination was inside or outside the hazard area [140].

Traffic management plans call for background traffic mitigation by closing facilities such as schools and government offices in anticipation of evacuation. As an example, in Baton Rouge, there exists a regional phased plan in which major public sector employers, state government offices, and Louisiana State University, may be called to close during an evacuation of New Orleans to keep local traffic to a lower level. These conditions were recognized by modeling background traffic in the area 80 miles beyond the areas under mandatory evacuation [79]. This study showed that expected demand from background traffic can be as important as the roadway infrastructure and traffic control. The importance of background traffic in ETE studies may provide insight to governmental agencies in developing traffic management plans.

7.1.1.4 Heavy Vehicles

Vehicles like trucks, busses, and recreational vehicles (i.e., heavy vehicles) with their large size, sweeping turning radii, lowered acceleration and deceleration characteristics, and reduced ability to climb steep grades, tend to slow traffic streams and take up space on roadways. These conditions are known to be even more pronounced in hilly and mountainous terrain where climbing over long uphill grades is necessary, and in urbanized areas where stop-and-go movements are more prevalent and frequent turning and lane changing is necessary. There is little research or observation of the effects of such heavy vehicles during evacuations. Although seemingly minor, some evacuees are known to load up trucks and trailers, trailer boats, or drive recreational vehicles (RVs) when fleeing threats like hurricanes and floods. The element of the task will assess the impact of various levels of heavy vehicle traffic on ETEs.

7.1.1.4.1 Literature Review

The Highway Capacity Manual (HCM) defines a heavy vehicle as “any vehicle having more than four wheels on the ground during normal operation” [22]. Heavy vehicles can be categorized as trucks, buses, or recreational vehicles (RVs). Per HCM specifications, trucks include single-unit

trucks with double rear tires (pickup trucks with only four wheels on the ground are considered passenger cars), and triple-unit tractor-trailer combinations. RVs include self-contained motor homes, cars or small trucks with trailers, or other conveyances [22].

A literature review indicates that 8 to 10 percent heavy trucks may be normal for urban roadways [36] [37] [38] [41]. A Baltimore Metropolitan Council study [41], identified truck traffic as now accounting for over 10 percent of all traffic on major roadways. These percentages can be even higher on interstates. However, urban roadways make up the prevalent transportation network in EPZs, and there are very few EPZs with significant interstate mileage within the area.

Heavy vehicles impact network capacity because of their operational characteristics. At signalized intersections, trucks reduce traffic passing through the intersection due to their size and slow acceleration. In freeways, multilane highways and two-lane highways, heavy vehicles have been found to affect average headways [144].

A study by Krammes et al., (1986) looked at empirical data from freeways under different traffic conditions and heavy vehicle compositions. Their study found headways varied by traffic conditions and vehicle type. For example, passenger car headways were slightly larger when following a heavy vehicle than when following a passenger car [145]. In addition, headways were observed to decrease as congestion increased. More recently, Ahmed et al., (2013) assessed the impact of heavy vehicles during congested conditions using empirical data from a freeway corridor [146]. The study found that passenger cars maintained significantly longer headways when following heavy vehicles. In addition, passenger car headways, when following a heavy vehicle, decreased as speed increased from 10 to 50 mph. The largest headways were observed when travel speeds were less than 10 mph. It was suggested that this was because drivers of passenger cars experience sight limitations while following heavy vehicles. In particular, longer headways allow for sufficiently large stopping distances in case of sudden stops [146].

Heavy vehicles are modeled as equivalent number of passenger cars using a conversion factor referred to as Passenger Car Equivalent (PCE) [22]. PCEs provide the equivalent number of passenger cars that will result in the same operational conditions as a single type of heavy vehicle. PCEs are tabulated in the HCM for freeways, multilane highways and two-lane highways and for different types of trucks, buses, and RVs. The HCM provides PCEs for heavy vehicle percentages between 2 and 25 on segments with upgrades and between 5 and 20 percent in segments with downgrades.

PCEs also account for acceleration and deceleration limitations of trucks in different grades. For example, the tabulated PCEs for upgrades lower than 2 percent (flat terrain), are the same for trucks percentages between 2 and 25 [22]. However, for upgrades of 2 percent or more and downgrades larger than 4 percent, the impact of trucks on freeways and multilane highways has been observed to decrease as the percent of trucks increase for the same grade. This is due to the tendency of heavy vehicles to group as their proportion increases on steep grades, decreasing adverse impact [130]. This is also the case for RVs. It is important to note that PCE factors in the HCM were derived from a limited field database and calibrated for steady flow (uncongested) conditions. Therefore, the impact of trucks in congestion conditions may not be well captured with the HCM method. For example, the study conducted by Ahmed et al., (2013) found a PCE of 1.76 in level terrain during congested conditions when the proportion of heavy vehicles was 9 percent. This PCE value is higher than the HCM 2010 recommended value of 1.5 under steady-flow conditions for a similar grade and heavy vehicle composition [146].

7.1.1.5 Free-Flow Speed

Free-flow speed (FFS) is a term used in traffic engineering to define the maximum possible speed that a driver chooses when it is not impeded by other vehicles on the road. It represents the speed a driver wants to travel, not necessarily the speed a driver is able to travel. Free-flow speed is influenced by conditions such as roadway geometry, posted speed limits, complexity of the driving environment, and weather conditions [22]. In traffic engineering practice, free-flow speeds could be used to estimate road capacity based on the HCM method.

Variation in free-flow speeds can influence travel times, particularly in very low traffic conditions where vehicles are traveling in freely-flowing conditions. Effectively, travel times can increase as free-flow speeds decrease. It has also been suspected that the impact of free-flow speed reductions can have varying significance depending on the road types. For example, compared to freeways, the opportunity to travel at free-flow speed on interrupted flow facilities like arterial freeways is limited by the presence of intersections. As such, vehicles must frequently slow or stop based on right-of-way. Thus, the impact on ETEs also depends on the relative number of intersections and opportunities to travel at the desired speed. In congested conditions vehicle movements are often governed by the discharged rate of traffic queues. As such, changes in free-flow speed may not impact the ETEs significantly. However, at the network-wide level, reduced free-flow speeds could slow down vehicle platoons (where the first vehicle is traveling at free-flow speeds) which may create some impact.

Given the extent of the average travel distance within the EPZ, the percent change in free-flow speed will likely translate into very small changes in travel time in roads that have low speed limits. As such, ETEs will likely not be significantly impacted by changes in free-flow speed.

This element of the task will assess the impact of variation in FFS on ETEs. Because driving in adverse weather conditions is known to impact free-flow speed, this parameter was considered separately in this task, prior to the study of adverse weather in order to separate the impacts of free-flow speed from other weather-related driving behaviors.

7.1.1.5.1 Literature Review

The sensitivity study in NUREG/CR-4874 found that variations in free-flow speed had a minimal effect on ETE [13]. Varying the free-flow speed plus or minus 5 mph from the base speed on individual links had no impact in most cases. At constant free-flow speeds of 30 mph and 60 mph throughout the network, there was an observed increase in the ETE by up to 30 minutes. But this was believed to be the result of other factors including the time interval of processing, capacity reduction factors, and a function that limited the rate of change of vehicle travel time on a segment.

The study by Pel et al., (2010) found network outflow rates and network accumulation to be insensitive to changes in free-flow speeds [141]. The study also observed that decreases in free-flow speeds caused evacuees to select longer routes with faster free-flow speeds. However, ETEs remained unaffected by this variation.

7.1.1.6 Adverse Weather

The history of highway travel in adverse weather has demonstrated inherent safety risks and negative impacts to the flow of traffic. Over 1.5 million crashes each year and 500 million hours of delay are associated with adverse weather in the U.S. [151]. This is related to the adverse

weather impacts on road, driver, and vehicle performance which limits the ability to effectively accelerate, brake, and steer [134]. As such, these conditions tend to reduce driver speeds and road capacities which can lead to significant vehicle delays. The magnitude of these impacts, however, depend on the type and intensity of the weather event. This element of the task will assess the impact of varying adverse weather parameters on ETEs.

7.1.1.6.1 Literature Review

The effects of rain and snow have been widely investigated in the literature. Research has found more pronounced impacts on traffic flow during snow than in rain [152] [128]. A FHWA study "Empirical Studies on Traffic Flow in Inclement Weather," used data collected from Saint Paul and Minneapolis to assess the effects of inclement weather on traffic stream parameters: roadway capacity (q_c), free-flow speed (u_f), speed-at-capacity (u_c), and jam density (k_j) [128]. These traffic stream parameters were observed to decrease more pronouncedly during snow than rain except for jam density which remained the same.

Precipitation intensity has also been found to influence the magnitude of the effects on traffic flow. In rainy conditions, the research conducted by Lamm et al., (1990) suggested that heavy rain impacted travel speeds more than in light rain because of poor visibility in heavy rain [153]. Similarly, Liang et al., 1998 found that reduced visibility and winds were the primary factors affecting travel speeds. In snowy conditions, speeds have also been observed to decrease more based on precipitation intensity [128]. Although research suggested travel speeds vary based on rain and precipitation intensities, roadway capacity was found to be insensitive. Regional differences and driver familiarity with rainy and snowy conditions also have been suggested to influence the impact of adverse weather on traffic flow [152] [128]. For example, more significant reductions in speeds under snowy conditions were observed in areas that experience higher snowfall because drivers are more aware of potential dangers [128].

7.1.1.6.2 Modeling and Simulation of Adverse Weather

Research has focused on finding methods to model the effect of adverse weather on driving. To model traffic flow under adverse weather conditions, adjustment factors can be used to modify either the roadway capacity (macroscopic models) or driver behavior (microscopic models). One example of this can be found in Exhibit 10-15 of the HCM, which includes freeway capacity adjustment factors for different weather conditions including different intensities of rain, snow, wind, temperature, and visibility. The recommended range of capacity reduction varies from 1 to 18 percent in rain and from 3 to 28 percent in snow [22]. The impact of adverse weather on capacity is shown in Figure 7-2.

Although the HCM procedures are widely used for transportation applications in the U.S., these procedures are generally limited to the analysis of a single roadway segment. This is not ideal for traffic modeling because the performance of an isolated intersection or road segment can be affected by conditions system wide, most notably, conditions on adjacent roadways [18]. In addition, the HCM procedures are not as effective in analyzing traffic performance beyond moderate congestion [18]. Traffic simulation, however, can account for congested states and network conditions beyond those possible with the HCM method [155].

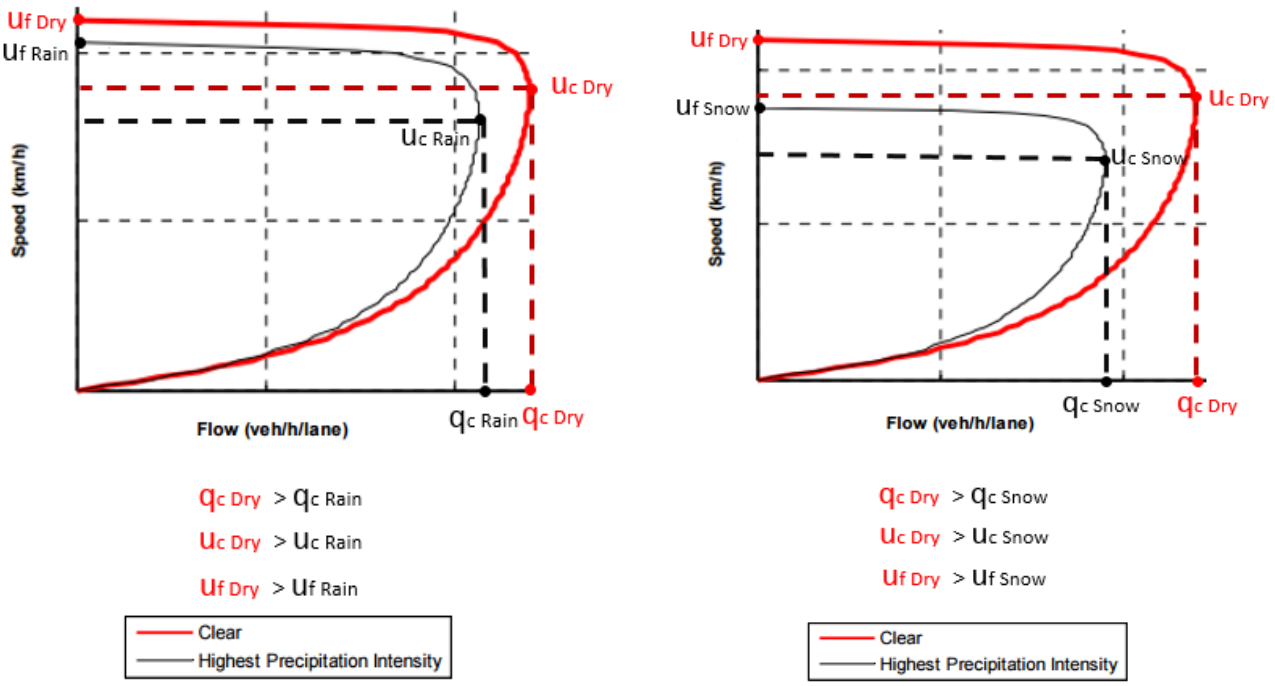

Figure 7-2 Adverse Weather Impact on Macroscopic Traffic Flow

7.1.1.6.3 Micro-level Traffic Simulation of Adverse Weather

The FHWA Traffic Analysis Tools (TAT) program developed a module titled, "Traffic Analysis Toolbox Volume XI: Weather and Traffic Analysis, Modeling and Simulation," to guide traffic engineers and transportation operations managers in analyzing and modeling weather impacts on highway traffic movement [127]. Included in the module are a summary of the effects of adverse weather that have been observed on traffic stream parameters (e.g., roadway capacity, volume, free-flow speed, and speed at capacity). Free-flow speed reductions between 2 to 9 percent for rain and 2 to 36 percent for snow have been observed. Similarly, reductions in roadway capacity of approximately 4 to 30 percent and 3 to 27 percent have been observed in rain and snow, respectively. In addition, effects at the intersection level were quantified as impacts to saturation flow, saturation headway, and lost startup time (i.e., time taken by the first few vehicles to react to the start of a green phase and to accelerate from a stopped position) as shown in Table 7-4 [127].

Table 7-4 Inclement Weather Impacts on Traffic Flow

Typical Impacts	Weather Event	
	Rain	Snow
Capacity	-4 ~ -30%	-3 ~ -27%
Volume	-20%	-6 ~ -26%
Speed at Capacity	-8 ~ -14%	-5 ~ -19%
Saturation Flow	-2 ~ -6%	-4 ~ -21%
Lost Startup Time	+7.6 ~ 31.5%	+18.5 ~ 65.2%
Saturation Headway	+2.5 ~ 13.2%	+4.4 ~ 30.9%
Free-Flow Speed	-2 ~ -9%	-3 ~ 36%

Over the last decade, the modeling of adverse weather using key input parameters of microscopic traffic simulation has been investigated. The FHWA study, “Identifying and Assessing Key Weather-Related Parameters and Their Impacts on Traffic Operations Using Simulation,” reports the findings of a sensitivity analysis conducted using CORSIM, a microscopic traffic simulation tool [155]. The relative sensitivity of traffic volumes, average speed, average density, and average delay to a wide variety of simulation input parameters was investigated considering different congestion levels in freeways, arterial roads and intersections. In freeways, four different congestion levels were investigated: *low* (v/c ratio of 0.42), *medium* (v/c ratio of 0.63), *high* (v/c ratio of 0.83), and *very high* (v/c ratio of 1.0). The analysis was conducted separately on freeway segments and freeway elements (merge, weave and diverge areas). Free-flow speed was considered in the sensitivity analysis along with parameters from the freeway car following and lane changing models in CORSIM. Car following parameters investigated included: 1) *car following sensitivity factor* which is used in the calculation of the desired time headway, 2) *car following sensitivity multiplier* which is a link-specific multiplier of the car-following sensitivity factor; 3) *Pitt car following constant* which is the minimum distance between the rear of the lead vehicle and front of the following vehicle, regardless of vehicle speeds; 4) *lag acceleration/deceleration time* which is the time delay for motorist starting to accelerate or decelerate; 5) *maximum non-emergency deceleration* which is the maximum deceleration on level grade and dry pavement in non-emergency conditions related to driving habit (not vehicle capability); and 6) *jerk value* which is the maximum change in acceleration between consecutive intervals [155].

Arterial segments and intersections were also considered in the sensitivity analysis at various congestion levels: *low* (v/c ratio of 0.4), *medium* (v/c ratio of 0.6), *high* (v/c ratio of 0.8), and *very high* (v/c ratio of 1.0). Free-flow speed and parameters from CORSIM’s car following and lane changing models were considered in the sensitivity analysis. The car following parameter considered in the sensitivity study only included the *Time to react to sudden deceleration of lead vehicle* which is the amount of time needed for a driver to begin decelerating after the leader begins a sudden deceleration due to perception/reaction time [155]. Several lane changing parameters were considered including *minimum deceleration for a lane change* and *time to react to sudden deceleration of the lead vehicle* [155].

The results of the freeway sensitivity analysis suggested that most of the parameters investigated in the study were insensitive at lower congestion levels and most sensitive in *high* congestion [155]. At *very high* congestion (at-capacity), the sensitivity was not as much compared to *high* congestion (just below capacity). This was likely because at *very high* congestion levels, there were closer spaced vehicles with less maneuverability and therefore less variability [155]. It was also found that average delay was the most sensitive MOE while volume and vehicle miles traveled (VMT) were the least sensitive. Average speed and average density were equally sensitive. In addition, it was observed that by increasing the road segment complexity (e.g., one lane vs. three lanes, etc.), the sensitivity increased. However, the study was based on a segment-level analysis and did not consider a network wide analysis which could influence the sensitivity of the MOEs. The FWHA study also suggested that free-flow speed is an important parameter when modeling adverse weather on freeways [155]. In particular, the mean free-flow speed had the highest sensitivity of all parameters studied. The car following parameter found to be most sensitive was the *car following sensitivity multiplier* which is a link-specific multiplier of the car-following sensitivity factor used in the calculation of the desired time headway. The *lag acceleration/deceleration time* had a medium sensitivity effect on the MOEs. The MOEs worsen as its value increased. Regarding the sensitivity of the lane changing parameters investigated, the sensitivities were generally not as stable as the car following parameters. This was because many of these lane changing parameters produced no

clear trends in the MOEs [155]. As such, the understanding of key weather-sensitive lane changing parameters in freeways was limited.

For the arterial sensitivity results it was found that the parameters were slightly more sensitive at the just-below capacity (v/c ratio around 0.83) than the at-capacity conditions [155]. However, the car following parameter studied, t*ime to react to sudden deceleration of lead vehicle,* was found to degrade the MOEs significantly under all congestion levels. In the case of the lane changing parameters, the *time to react to sudden deceleration of the lead vehicle* was also found to degrade the MOEs under all congestion levels. Similar to what was observed in the freeways, the MOEs were the most sensitive to changes in the mean free-flow speed parameter. From the intersection analysis, it was found that the MOEs degraded when the v/c ratio approached 1.0 and the *time to react to sudden deceleration of lead vehicle* showed slightly less sensitivity in the intersection analysis than in the arterial analysis [155].

Continuing the efforts to model adverse weather using microscopic traffic simulation, the FHWA study, "Microscopic Analysis of Traffic Flow in Inclement Weather – Part 2," illustrated a step-by-step application to model adverse weather conditions at a signalized intersection using VISSIM [156]. In this study, the following simulation input parameters were adjusted: 1) desired speeds (i.e., free-flow speed), 2) driving behavior parameters in the Wiedemann 74 car following model, and 3) gap acceptance at intersections. The Wiedemann 74 car following model in VISSIM is used to model driving behavior in urban traffic and merging areas and it has several associated parameters (see Appendix B, Table B-1). The FHWA study modeled adverse weather at an intersection by adjusting *average standstill distance* (*ax*), the *additive part of safety distance* (BX_{add}), and the *multiplicative part of safety distance* (BX_{mult}) [156]. The *average standstill distance* (*ax*) is the spacing from the front bumper to the rear bumper of the vehicle ahead when they are both in a stopped position [156]. BX_{add} is used to adjust the time requirement values for the computation of the desired safety distance in the Wiedemann 74 car following model [21]. BX_{mult} is also used in the computation of the safety distance to modify its distribution [21]. BX_{mult} is related to BX_{add} based on Equation 7.1.

$$BX_{mult} = BX_{add} + 1 \quad (7.1)$$

The desired safety distance has a direct relationship to saturation flow rate. Increasing BX_{mult} increases the desired safety distance and decreases the saturation flow rate as shown in Figure 7-3 [21]. In the FHWA study, the value of the Wiedemann 74 car following model parameters were adjusted based on the relationship between the desired safety distance and the estimated values of the traffic stream parameters capacity (q_c), free-flow speed (u_f), and jam density (k_j) during adverse weather conditions as described in Equation 7.2. In this equation, α is the ratio of the maximum following distance to the minimum following distance, which ranges from 1.5 to 2.5.

$$E(BX) = 1000\sqrt{3.6}\sqrt{uf}\left(\frac{1}{\alpha q_c} - \frac{1}{k_j u_f}\right) \quad (7.2)$$

BX is related to BX_{add} and BX_{mult} based on Equation 7.3. In this equation, *RND* is a normally distributed random variable with a default mean value of 0.5 and a standard deviation of 0.15 [156]. BX_{mult} can be found from Equation 7.3 based on the known relationship between BX_{add} and BX_{mult} given in Equation 7.1.

$$BX = BX_{add} + BX_{mult} * RND \quad (7.3)$$

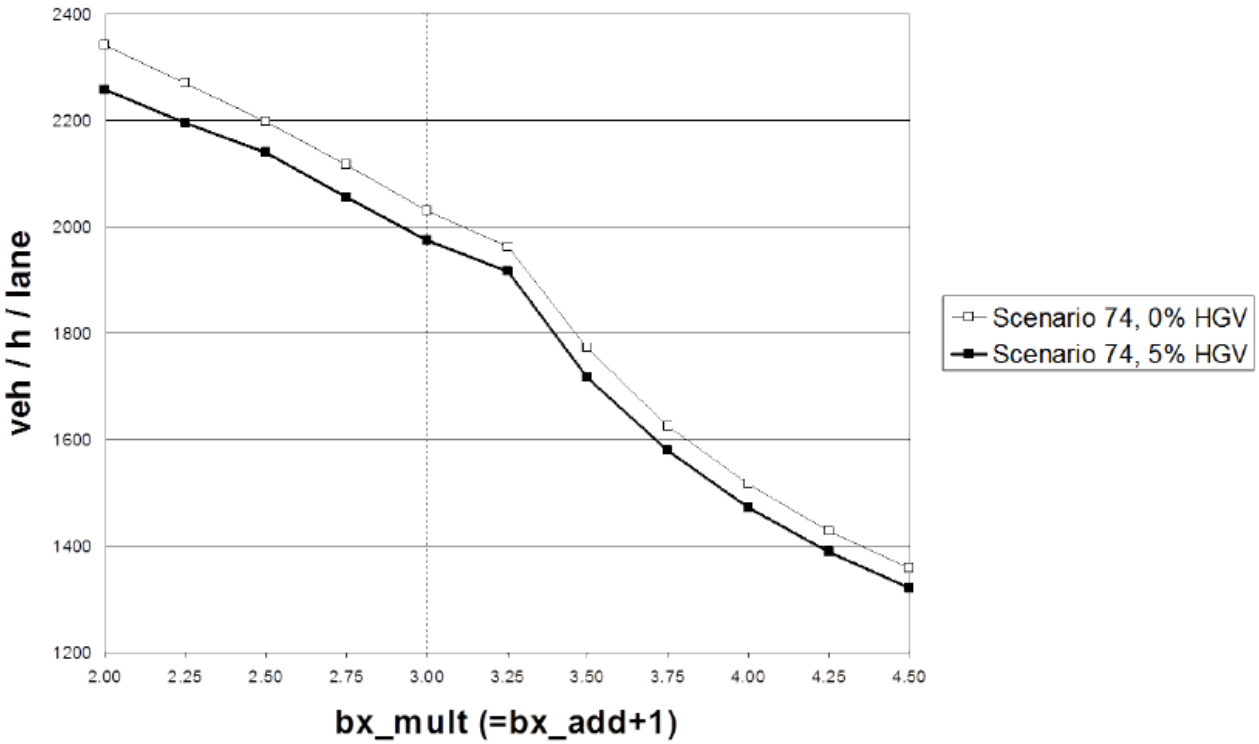

Figure 7-3 Relationship Between Saturation Flow Rate and the Multiplicative Part of the Safety Distance (BX_{mult}) in the Wiedemann 74 Car Following Model

Wiedemann 99 is another car following model used to model driving behavior in freeways with no merging areas [21]. VISSIM has several input parameters associated with Wiedemann 99 (see Appendix B, Table B-2). The FHWA study, "Microscopic Analysis of Traffic Flow in Inclement Weather – Part 2," also suggested to adjust CC1 and CC0 in the Wiedemann 99 model when modeling adverse weather using VISSIM. CC0 is the average desired standstill distance between two vehicles [21]. It is the difference in the standstill spacing between two vehicles, which is the distance from front bumper to front bumper and the average vehicle length (L_{avg}). The standstill spacing is the inverse of jam density (k_j). Therefore, CC0 can be found using Equation 7.4.

$$CC0 = \frac{1000}{k_j} - L_{avg} \quad 7.4$$

The distance CC1 is the headway time which is defined as the distance in seconds that a driver wants to maintain while following another car at a certain speed. CC1 is used to compute the average safety distance (dx_{safe}). The safety distance is defined as the minimum distance a driver will maintain while following another vehicle. It is the sum of CC0 and CC1 multiplied by speed (v) as shown in Figure 7-4 and Equation 7.5. The higher the value of CC1, the more cautious the driver. In the case of high volumes, this distance has a determining influence on capacity [21].

$$dx_{safe} = CC0 + CC1 * v \quad 7.5$$

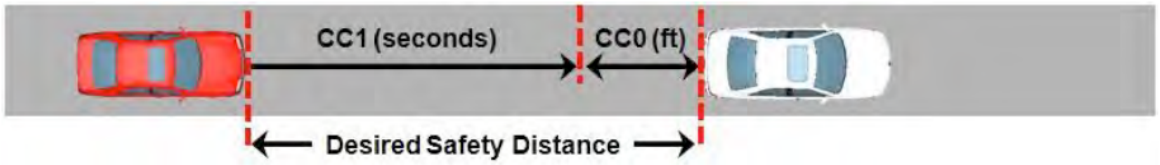

Figure 7-4 Relationship Between Desired Average Safety Distance and Wiedemann 99 Car Following Parameters Headway Time (CC1) and Standstill Distance (CC0)

CC1 can be found based on the relationship between the desired safety distance and the estimated values of the traffic stream parameters capacity (q_c), free-flow speed (u_f), and jam density (k_j) using Equation 7.6

$$CC1 = 3600\left(\frac{1}{q_c} - \frac{1}{k_j u_f}\right) \quad 7.6$$

As mentioned earlier, the desired safety distance has a direct relationship to saturation flow rate. Increasing CC1 from its default value of 0.9 seconds increases the desired safety distance and decreases the saturation flow rate as shown in Figure 7-5. Scenario 99-2 in the figure refers to driving conditions on American freeways with 15 percent heavy vehicles. The remaining scenarios shown in the figure are relevant to driving behavior in German freeways.

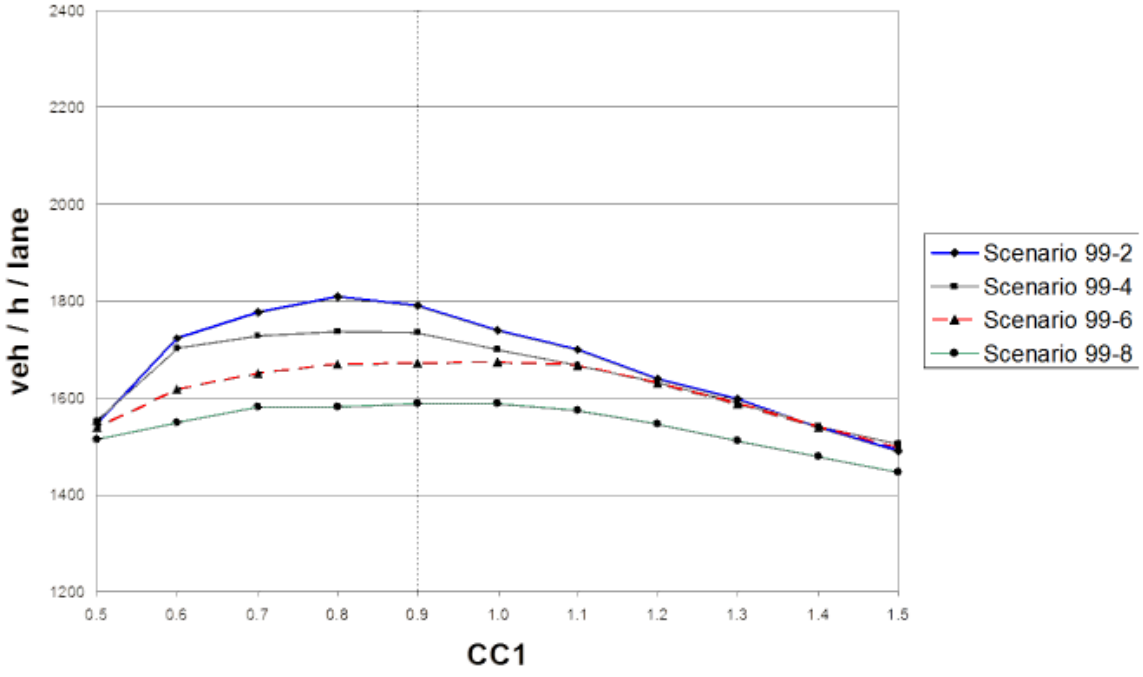

Figure 7-5 Relationship Between Saturation Flow Rate in veh/h/lane and Wiedemann 99 CC1 Car Following Parameter (Headway Time)

The study conducted by Jung et al., (2011) modeled adverse weather conditions using VSSIM microscopic traffic simulation to assess the effect on traffic safety and operations on a freeway [157]. Adverse weather was modeled by adjusting the desired speed distribution, desired deceleration rate function, and headway time (a value of 1.1 seconds was used). The adjustment of the parameters was done through a comparison of the simulation results and

empirical data (model calibration). Desired speed distribution and acceleration rate function were found to be key weather-related sensitive parameters [157].

Asamer et al., (2012) investigated the sensitivity of saturation flow rate and start-up delay to desired speed, desired acceleration, desired deceleration, and Wiedemann 74 parameters BX_{add}, and BX_{mult} [158]. The sensitivity analysis suggested that all the parameters except the desired deceleration had a large effect on saturation flow and start-up delay as shown in Figure 7-6 [158]. The figure shows that the saturation flow rate increased with increasing values of BX_{add}, and BX_{mult}. Similarly, average start up delay decreased as the values of BX_{add}, and BX_{mult} increased from the VISSIM default values of 3 and 2, respectively.

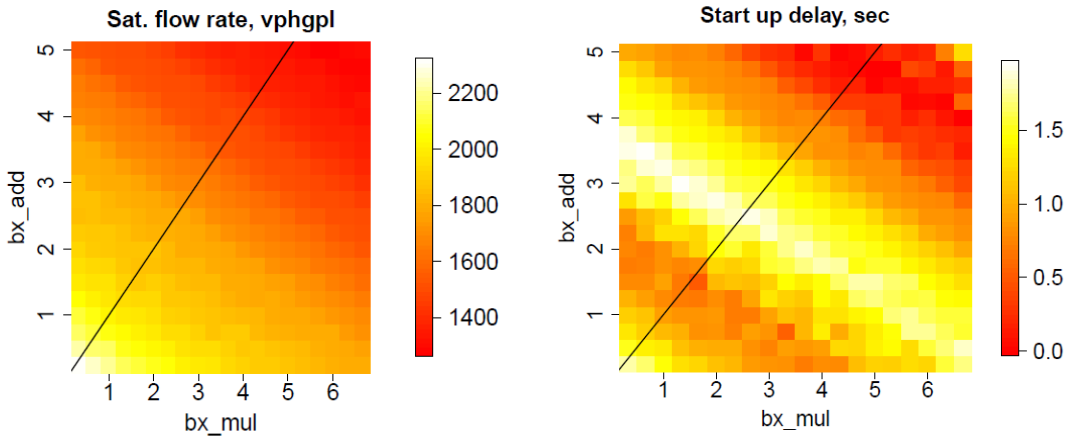

Figure 7-6 Relationship Between (a) Saturation Flow Rate and (b) Start-up Delay to the Multiplicative Part (BX_{mult}) and Additive Part (BX_{add}) of the Safety Distance in the Wiedemann 74 Car Following Model. Black Line Indicates Combined Parameters (BX_{mult} and BX_{add})

Prior ETE studies have widely use simulation at the macroscopic level and have used capacity and free-flow speed reduction factors to model adverse weather conditions. The models and simulation systems used in this research, however, provided a unique opportunity to assess the impacts of adverse weather through the influence on driver behavior. The methods used in this research made it possible for comparing microscale simulation results to those from macroscale simulation at the network level.

7.1.1.7 Roadway Impact/Disruptions

The capacity of a network depends on the capacity of individual roadway links. Roadway capacity is defined as the maximum traffic flow rate in a unit of time under prevailing conditions [22]. Congestion reduces capacity and is accounted for in traffic simulation models. However, unexpected or transitory events such as vehicular accidents, broken down vehicles, lane closures, work zones and debris also reduce roadway link capacity. When a network has a particularly high volume of traffic, even localized events can have effects that propagate rapidly and widely throughout the road network.

The modeling of roadway capacity in traffic simulation tools varies by level of abstraction. Macroscopic traffic simulation tools require an estimated value of the base capacity associated with each roadway segment. This base capacity can be modified using a “capacity reduction factor” to account for congested conditions or adverse weather. The HCM provides capacity reduction factors for various road types. However, for microscopic simulation tools, capacity is the result of the interaction among vehicles, characteristics of the roadway, and driving behavior. This element of the task assesses the effect of capacity reducing road closures on ETEs.

7.1.1.7.1 Literature Review

Capacity losses may be detrimental to the operational performance of roads or transportation systems as a whole. Consequently, drivers may experience delay, rerouting, limited accessibility, or a combination of these. The overall magnitude of the effect is dependent on the relationship between capacity and traffic demand. For example, a lane closure resulting from a traffic incident reduces the capacity of that road temporarily; this disruption may cause excessive delay when the traffic volumes are high (e.g., during peak-hour periods). However, the same incident may cause little or no delay when the traffic volumes are low [22]. A road is capable of fully servicing demand when the ratio of volume to capacity (v/c) is less than or equal to 1. As demand approaches capacity, the performance of the system begins to decrease, congestion develops, and the rate of vehicles that can be serviced decreases.

Losses in roadway capacity depend on the characteristics of the disruption (e.g., complete or partial lane closure, duration, extent, etc.). The impact of temporary capacity losses varies by the characteristics of the disruption, the measure of how critical that roadway is to the overall highway system, and the number of alternate routes (network redundancy) available for vehicles to take [133]. High volume roads with a limited number of alternative routes are most likely critical roadway segments that may significantly affect traffic performance when a disruption occurs on that road. This suggests that critical road segments are not necessarily those that are located on the highest traffic volume routes since the availability of alternate routes is also a key factor.

Dotson and Jones (2005) reviewed 50 previous evacuation cases and found only four traffic incidents that occurred in these events [147]. Of those four incidents, three of them were caused by vehicles running out of gas and the fourth was caused by heavy fire smoke, downed power lines and abandoned vehicles. Although the sample of traffic incidents during evacuations is small each of them caused the degradation of capacity. More specifically, chi-squared testing showed that traffic incidents had a strong relation to evacuation efficiency. The final ranking of issues that affected evacuations showed that traffic incidents were third most important after information dissemination and roadway availability.

The effect of capacity disruptions also depends on the characteristics upstream and downstream of the disruption. For example, the study of Bahaaldin et al., (2016) examined the effect of traffic incidents during a no-notice emergency evacuation in the Eastern St. Louis Metropolitan area using VISSIM [148]. The analysis conducted in that study utilized incident locations based on historical data. Average delay was used as a measure of effectiveness. Three main traffic incident locations were used to compare the results to the “no-incident” base scenario. In the first two scenarios, a traffic incident occurred on a bridge and on a section of an interstate. The results showed that delay only changed slightly compared to the base scenario. It was noted in the study that these two locations were both upstream of bottleneck locations. The third scenario investigated in the study was a traffic incident at a section of an interstate.

The results showed a significant effect on delay. This location was located just over one mile downstream of a bottleneck. Overall, this study found that incident locations upstream of key bottlenecks do not significantly change traffic delay during a no-notice evacuation. However, incidents downstream of bottlenecks can significantly increase the evacuation clearance time [148].

Fonseca et al., (2013) assessed the impact of traffic incidents on the overall evacuation travel time in two different evacuation scenarios. In the first scenario, a low evacuation demand was assumed and in the second scenario a high flux of departing traffic was used. Their study suggested that incidents are more of a safety concern rather than flow-disturbing events [149]. The study showed that total travel time increased by only 0.13 percent for low demand and 0.09 percent for high demand situations compared to a no-incident scenario. Other studies have found that traffic incidents were predicted to increase evacuation duration by up to 8 percent [139]. Robinson et al., (2009) studied the impact of traffic incidents in Hampton Roads during hurricane evacuations. The research involved simulation of evacuation traffic over a 70-hour period and averaged almost 200 vehicular accidents and 1,400 incidents. The simulated scenarios were extracted from traffic databases and the incident locations, severities and durations were randomly selected from available historic traffic data. The authors found that if catastrophic events occur which completely close the main interstate exit in Hampton Roads, the evacuation clearance time would increase by approximately 10 percent [150].

NUREG/CR-7002 recommends ETE studies consider a roadway impact scenario to represent a variety of conditions that may impact a roadway segment such as construction, flooding, vehicle accidents, etc. The guidance recommends studying the following cases:

- Case 1: Road closure of one segment in one of the top five highest volume roadways
- Case 2: Lane closure of single outbound lane on an interstate highway

A review of ETE studies showed that the roadway impact scenarios typically included a single lane closure on an interstate. In a few instances, bridges were closed to traffic. This is reasonable as bridges often provide an important egress route. Additionally, a few ETEs used scenarios with multiple roadway closures, such as might occur due to flooded roads due to heavy rain. It was found that disruptions occurring on one roadway may shift demand to an alternate route that was not considered critical until the disruption. Roadway impacts were modeled both inside and outside the EPZ, as appropriate to the site.

The result of roadway impact scenarios with single lane closures showed that the 90 percent ETEs can increase by over 90 minutes in medium population sites. In large population sites, the maximum increase was much less, about 35 minutes. Small population sites showed little impact from roadway impact scenarios, although one site was impacted almost 2 hours. The median values for the impact to the 90 percent ETEs observed in the review of prior ETE studies was 10, 15, and 20 minutes in small, medium and large population sites, respectively.

7.1.1.8 Processing Time Step

In addition to the assumptions and models used to represent physical characteristics and processes of traffic flow through road networks, there are a number parameters that simulation systems use to control the computational processing of the simulation code. These computational control parameters are generally used by all simulation systems. An important parameter is the one that governs the system state updates within the model.

The system state describes the current status of all entities within the model at a moment in time. In traffic simulation this can include location, speed and acceleration of each vehicle in the network and the traffic signal indications visible to vehicles. As the simulation progresses, the state of each of these parameters for every element in the system is updated. The time interval between system states is known as the processing time step. The duration of this time step determines how often event updating occurs. For example, the position of a vehicle traveling at 60 miles per hour within a single-second processing step “moves” about 90 feet during each step. However, if the time step is ten seconds the vehicle will move 900 feet.

Traffic simulation is made up of a string of these small incremental changes. An hour-long simulation with one-second state updating is actually an accumulation of 3,600 state changes. The complexity of state updating in systems like VISSIM is considerable because state changes in one variable can influence changes in many others. For example, within a queue of vehicles approaching a changing traffic light, this results in changes in the relative vehicle spacing, speed, acceleration, or lane changing maneuvers as governed by the models. Because of the computational processing speed of modern computers, these minute updates are nearly transparent and appear to occur continuously in real-time. However, in reality, the quantitative results and visualizations occur as a series of small discrete steps, advancing from one time step period to the next. The time step in VISSIM can be an integer from 1 to 20 time steps per second. Selection of the time step requires a tradeoff between model fidelity and computational processing time. The default value setting within VISSIM is 10 time steps per second, however, the developers state that using a processing time between 5 and 10 time steps per second will produce accurate results [21]. When modeling systems as complex as those in this research, such processing rates can add significant computational run time. In some cases, a single scenario would require several hours to run. As a result, a processing time step of 1 step per second was selected in this research.

At this processing rate small state changes can be “lost” in the simulation. Driver reaction times can take place in half-a-second real time and a 1-second processing time step can introduce artificial time delays. The quantitative impact of varying the time step parameter in microscopic simulation codes is not well known. NUREG/CR-4874 assessed the sensitivity of ETEs to different processing times using the macroscopic tool I-DYNEV. The results showed that in some instances larger processing time steps decreased ETEs by 15 minutes but in other instances no effect was observed. It is desirable to have an understanding of the tradeoff between processing capability and VISSIM platform performance against the desired fidelity and accuracy of the simulation results. This element of the task will assess the impact of varying the time step parameter.

7.1.1.9 Random Seed Uncertainty Analysis

Most microscopic traffic simulation systems incorporate routines that reflect the stochastic variation inherent in traffic flow processes. This random variability reflects operating conditions that might exist as traffic and drivers vary from day-to-day and even moment-to-moment. Computationally, this is accomplished by performing multiple runs for a single set of model conditions using different random seeds to produce different stochastic variations. Typically, it is recommended to average the results from at least 10 random seeds [20] [24] or at least five seeds in congested corridors [129]. However, the number of runs needed can depend on a number of factors including the complexity of the model, the acceptable error, and the objectives and constraints of the research. This element of the task will assess the impact of varying the random seed and validate the prior assumption that using four random seeds was adequate (see Section 3.7.2).

7.2 Description of Scenarios

This section describes the approach to simulating the parameters of this task within VISSIM, and the range of values that were simulated. Parameter values for the minimum, maximum, and increment quantities were established from a review of prior ETE studies, relevant literature related to each variable, and expert judgment. The ranges were also influenced by the characteristics of the site models; the capabilities of the simulation tool used in this research; and results obtained from preliminary tests performed in support of this task.

7.2.1 Population

The base population for each model was uniformly varied with all other parameters held constant. As in the base model, the population was converted to number of vehicles assuming two passengers per vehicle. For research purposes, population was increased or decreased beyond reasonably expected population growth. A review of decennial census data for the year 2000 and the year 2010 showed an average population growth in the U.S. of 10 percent. The maximum population growth observed by state was 35 percent (state of Nevada). While local population growths can exceed these values, in general, very large percent population changes are not often observed, particularly in regions that are already heavily populated. Additionally, the study in NUREG/CR-4874 found ETEs to be sensitive to population above a certain threshold value. As such, this study of population included increases and decreases in population beyond what would be considered realistic short-term population changes. This was done to assess overall trends in the sensitivity analysis.

The study of population also considered significantly larger population growths without considering the likely improvements in the infrastructure to accommodate the increase in demand. In reality, roadway networks are expected to adapt over time to serve routine demand based on population. Changes in available roadway infrastructure to adapt to changes in demand was not considered in this study because the interest was to capture the effect of population alone. Table 7-5 shows the range of the population parameter studied for the small population site. The EPZ population was uniformly increased from 7500 people (base value) to 27,375 evacuees (approximately 265 percent increase). This maximum was selected based on preliminary tests and a review of prior ETE studies which suggested that a large population increase would be required to observe a significant change in ETE.

Table 7-5 Small Population Site Model Population Parameters

Scenario Number	Total EPZ Population	Total EPZ Vehicles	Population Change (%)
1 (Base model)	7,500	3,750	0
2	10,125	5,063	35
3	11,625	5,813	55
4	14,250	7,125	90
5	16,875	8,438	125
6	19,500	9,750	160
7	22,125	11,063	195
8	24,750	12,375	230
9	27,375	13,688	265

The study of population in the medium population site model followed a different approach to account for the non-homogeneous spatial distribution of the population on each side of a body of water running through the WNW and SE sectors. The EPZ region was divided into two distinct parts: a “medium-north” portion with a large population (96 percent of the overall population) and a “medium-south” portion with a low population (4 percent of the overall population) as shown in Figure 7-7. This spatial breakdown was done to isolate the effect of population in the north and south portions. Without this spatial breakdown, a uniform variation in the overall EPZ population would have caused the population in the northern region to overwhelm any data from the southern region. As a result, ETEs would have been dominated by the traffic conditions in the northern region. The medium population site model was designed not to have infrastructure connecting the north and the south portions in order to facilitate the task analyses.

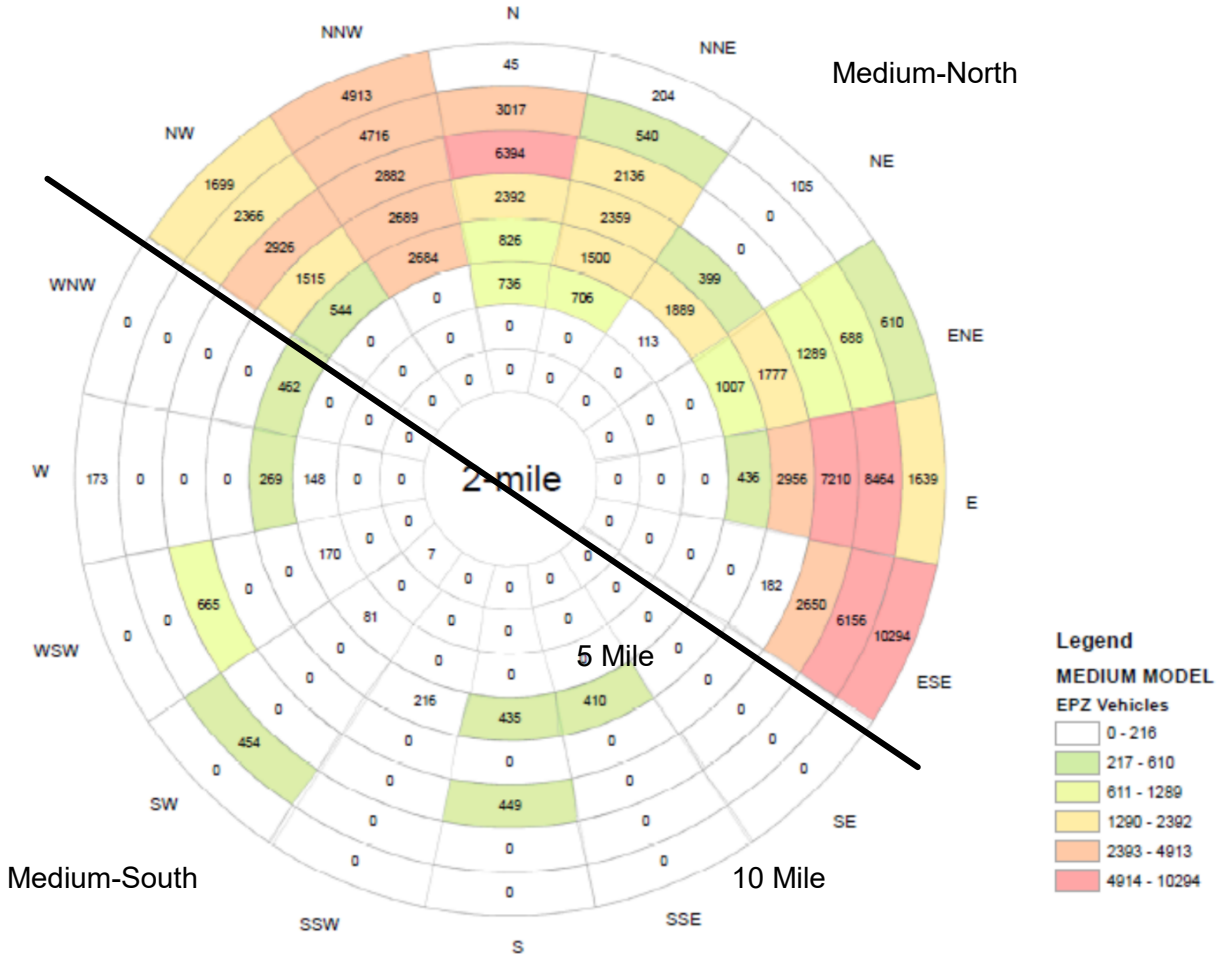

Figure 7-7 Spatial Population Breakdown in the Medium Population Site Model

The EPZ population was uniformly increased and decreased by specific percentages in the north and south portions for each scenario. As shown in Table 7-6, the EPZ population in the north was decreased to a minimum of 71,500 evacuees (63 percent decrease) and incrementally increased to a maximum of 240,000 evacuees (25 percent increase).

Table 7-6 Medium-North Population Site Model Population Parameters

Scenario Number	EPZ Population	EPZ Vehicles	Population Change (%)
1	71,500	35,750	-63
2	110,000	55,000	-43
3	130,000	65,000	-32
4	150,000	75,000	-22
5	170,000	85,000	-11
6 (Base model)	192,000	96,000	0
7	210,000	105,000	9
8	220,000	110,000	15
9	230,000	115,000	20
10	240,000	120,000	25

The EPZ population in the southern region was increased from a minimum of 7,990 (base value) to a maximum of 55,000 evacuees (588 percent increase) as shown in Table 7-7.

Table 7-7 Medium-South Population Site Model Population Parameters

Scenario Number	EPZ Population	EPZ Vehicles	Population Change (%)
1 (Base model)	7,990	3,995	0
2	17,500	8,750	119
3	27,500	13,750	244
4	37,500	18,750	369
5	55,000	27,500	588

The population for the large population site model was varied from 130,000 (a 60 percent decrease) to 390,000 evacuees (a 20 percent increase) as shown in Table 7-8. These values were selected based on a review of previous ETE studies and preliminary analyses.

Table 7-8 Large Population Site Model Population Parameters

Scenario Number	Total EPZ Population	Total EPZ Vehicles	Population Change (%)
1	130,000	65,000	-60
2	162,500	81,250	-50
3	227,500	113,750	-30
4	282,750	141,375	-13
5	308,750	154,375	-5
6 (Base model)	325,000	162,500	0
7	341,250	170,625	5
8	357,500	178,750	10
9	373,750	186,875	15
10	390,000	195,000	20

7.2.2 Mobilization Time

Loading curves derived from prior ETE studies and from the literature were used to assess the sensitivity of ETEs to mobilization times. Loading curves were selected to capture differences in both the loading rate and the total loading time.

Table 7-9 summarizes the selected mobilization time ranges and scenarios studied in each model. In the small population site model, the base mobilization time was 2:15. Therefore, it was desired to test slower loading conditions and longer mobilization times. A total of 11 different mobilization times were tested in the sensitivity analysis in the small model site spanning from 2:15 (base model) to 6:30. In the medium and large population site models, the base mobilization times were 4:00 and 4:45, respectively. Therefore, it was desired to test both faster loading conditions with shorter mobilization times and slower loading conditions with longer times. A total of nine mobilization times spanning from 2:30 to 10:00 were included in the sensitivity analysis for these sites.

Table 7-9 Mobilization Time Scenarios

Population Site Model	Range of Mobilization Times (h:mm)	Mobilization Time Scenarios (h:mm)
Small	2:15 to 6:00	2:15 (Base Model), 2:30, 2:45, 3:00, 4:00, 4:30 5:00, 6:00, 6:30
Medium	2:30 to 10:00	2:30, 2:45, 3:00, 4:00 (Base Model), 4:00, 4:30, 5:00, 6:00, 6:30, 8:00, 10:00
Large	2:30 to 10:00	2:30, 2:45, 3:00, 4:00, 4:45 (Base Model), 4:30, 5:00, 6:00, 6:30, 8:00, 10:00

As described earlier, loading curves model the rate at which evacuees begin to evacuate during a certain time interval. The loading rates used for each scenario in the small, medium, and large population site models are summarized in Table 7-10, Table 7-11, and Table 7-12, respectively.

An important aspect of loading curves is that loading rates can vary widely for the same mobilization time. The medium population site model includes two 4:00 mobilization times. As shown in Table 7-10 the difference in these loading curves is in the rate of loading, with the base model having a slower initial loading rate. For example, in the base model, about 80 percent of the evacuees are loaded into the network within 2 hours and 15 minutes, while in the second 4:00 mobilization time scenario about 80 percent of the evacuees are loaded into the network within 1 hour and 30 minutes. Network conditions could vary widely for those scenarios even though the overall mobilization times are the same. This study will assess the sensitivity of ETEs to both the loading rate and the overall mobilization time.

Table 7-10 Traffic Simulation Loading Curves for Small Population Site Model

Loading Start Time (h:mm)	Loading End Time (h:mm)	Mobilization Time Scenarios								
		2:15 (Base)	2:30	2:45	3:00	4:00	4:30	5:00	6:00	6:30
Loading starts after 30 minutes of simulation time to populate the network										
0:00	0:15	10%	1%	1%	2%	1%	2%	1%	0%	1%
0:15	0:30	25%	10%	8%	13%	9%	20.5%	5%	5%	10%
0:30	0:45	21%	23%	20%	26%	23%	20.5%	16%	15%	20%
0:45	1:00	16.5%	27%	25%	24%	11.5%	15.5%	19%	17%	17%
1:00	1:15	9.5%	19%	20%	14%	11.5%	15.5%	15%	12%	10%
1:15	1:30	8.5%	9%	11%	11%	26%	10%	13%	13%	10%
1:30	1:45	6.5%	5%	6%	5%	5%	7%	5%	5%	4%
1:45	2:00	2.5%	3%	5%	1%	1%	2%	2%	5%	4%
2:00	2:15	0.5%	2%	3%	2%	3%	1.5%	6%	6%	4%
2:15	2:30		1%	0.5%	1%	4%	1.5%	6%	6%	4%
1:00	2:45			0.5%	0.5%	2%	1%	3%	2.5%	1.75%
2:45	3:00				0.5%	1%	1%	1%	2.5%	1.75%
3:00	3:15				2%	0.5%	0%	1.25%	1.5%	1.75%
3:15	3:30					0.5%	1%	1.25%	1.5%	1.75%
3:30	3:45					0.5%	0.25%	1.25%	2%	0.5%
3:45	4:00					0.5%	0.25%	1.25%	2%	0.5%
4:00	4:15						0.25%	0.75%	0.5%	0.5%
4:15	4:30						0.25%	0.75%	0.5%	0.5%
4:30	4:45							0.75%	0.5%	0.25%
4:45	5:00							0.75%	0.5%	0.25%
2:00	5:15								0.5%	0.25%
5:15	5:30								0.5%	0.25%
5:30	5:45								0.5%	1.5%
5:45	6:00								0.5%	1.5%
6:00	6:15									1.5%
6:15	6:30									1.5%
Total		100%	100%	100%	100%	100%	100%	100%	100%	100%

Table 7-11 Traffic Simulation Loading Curves for Medium Population Site Model

Loading Start Time (h:mm)	Mobilization Time Scenarios										
	2:30	2:45	3:00	4:00 (Base)	4:00	4:30	5:00	6:00	6:30	8:00	10:00
Loading starts after 30 minutes of simulation time to populate the network											
0:00	1%	1%	2%	0%	1%	2%	1%	0%	1%	0%	0%
0:15	10%	8%	13%	2%	9%	20.5	5%	5%	10%	1%	1%
0:30	23%	20%	26%	6%	23%	20.5	16%	15%	20%	2%	1%
0:45	27%	25%	24%	11%	11.5	15.5	19%	17%	17%	4%	1%
1:00	19%	20%	14%	15%	11.5	15.5	15%	12%	10%	6%	1%
1:15	9%	11%	11%	16%	26%	10%	13%	13%	10%	7%	2%
1:30	5%	6%	5%	13%	5%	7%	5%	5%	4%	8%	3%
1:45	3%	5%	1%	12%	1%	2%	2%	5%	4%	8%	3%
2:00	2%	3%	2%	8%	3%	1.5%	6%	6%	4%	7%	3%
2:15	1%	0.5%	1%	6%	4%	1.5%	6%	6%	4%	7%	4%
2:30		0.5%	0.5%	4%	2%	1%	3%	2.5%	1.75	6%	4%
2:45			0.5%	2%	1%	1%	1%	2.5%	1.75	6%	5%
3:00				2%	0.5%	0%	1.25	1.5%	1.75	6%	6%
3:15				1%	0.5%	1%	1.25	1.5%	1.75	4%	7%
3:30				1%	0.5%	0.25	1.25	2%	0.5%	3%	6%
3:45				1%	0.5%	0.25	1.25	2%	0.5%	3%	5%
4:00						0.25	0.75	0.5%	0.5%	3%	4%
4:15						0.25	0.75	0.5%	0.5%	2%	4%
4:30							0.75	0.5%	0.25	2%	4%
4:45							0.75	0.5%	0.25	2%	3%
2:00								0.5%	0.25	2%	3%
5:15								0.5%	0.25	1%	3%
5:30								0.5%	1.5%	1%	3%
5:45								0.5%	1.5%	1%	3%
6:00									1.5%	1%	2%
6:15									1.5%	1%	2%
6:30										1%	2%
6:45										1%	2%
7:00										1%	2%
7:15										1%	2%
7:30										1%	2%
7:45										1%	1%
8:00											1%
8:15											1%
8:30											1%
8:45											1%
9:00											0.5%
9:15											0.5%
9:30											0.5%
9:45											0.5%
Total	100%	100%	100%	100%	100%	100%	100%	100%	100%	100%	100%

Table 7-12 Traffic Simulation Loading Curves for Large Population Site Model

Loading Start Time (h:mm)	Mobilization Time Scenarios										
	2:30	2:45	3:00	4:00	4:30	4:45 (Base)	5:00	6:00	6:30	8:00	10:00
Loading starts after 30 minutes of simulation time to populate the network											
0:00	1%	1%	2%	1%	2%	0%	1%	0%	1%	0%	0%
0:15	10%	8%	13%	9%	20.5	0%	5%	5%	10%	1%	1%
0:30	23%	20%	26%	23%	20.5	3%	16%	15%	20%	2%	1%
0:45	27%	25%	24%	11.5	15.5	10%	19%	17%	17%	4%	1%
1:00	19%	20%	14%	11.5	15.5	15%	15%	12%	10%	6%	1%
1:15	9%	11%	11%	26%	10%	15%	13%	13%	10%	7%	2%
1:30	5%	6%	5%	5%	7%	13%	5%	5%	4%	8%	3%
1:45	3%	5%	1%	1%	2%	12%	2%	5%	4%	8%	3%
2:00	2%	3%	2%	3%	1.5%	7%	6%	6%	4%	7%	3%
2:15	1%	0.5%	1%	4%	1.5%	6%	6%	6%	4%	7%	4%
2:30		0.5%	0.5%	2%	1%	4%	3%	2.5%	1.75	6%	4%
2:45			0.5%	1%	1%	4%	1%	2.5%	1.75	6%	5%
3:00				0.5%	0%	2%	1.25	1.5%	1.75	6%	6%
3:15				0.5%	1%	2%	1.25	1.5%	1.75	4%	7%
3:30				0.5%	0.25	2%	1.25	2%	0.5%	3%	6%
3:45				0.5%	0.25	2%	1.25	2%	0.5%	3%	5%
4:00					0.25	1%	0.75	0.5%	0.5%	3%	4%
4:15					0.25	1%	0.75	0.5%	0.5%	2%	4%
4:30						1%	0.75	0.5%	0.25	2%	4%
4:45							0.75	0.5%	0.25	2%	3%
2:00								0.5%	0.25	2%	3%
5:15								0.5%	0.25	1%	3%
5:30								0.5%	1.5%	1%	3%
5:45								0.5%	1.5%	1%	3%
6:00									1.5%	1%	2%
6:15									1.5%	1%	2%
6:30										1%	2%
6:45										1%	2%
7:00										1%	2%
7:15										1%	2%
7:30										1%	2%
7:45										1%	1%
8:00											1%
8:15											1%
8:30											1%
8:45											1%
9:00											0.5%
9:15											0.5%
9:30											0.5%
9:45											0.5%
Total	100%	100%	100%	100%	100%	100%	100%	100%	100%	100%	100%

ETE Loading curves are typically determined through telephone survey of the EPZ population. Respondents are asked how they would prepare to evacuate, and the information is used to generate an estimated network loading curve. The ETE is sensitive to the shape of the loading curves in addition to the duration. Rapid loading early in the evacuation can overload the network and cause long duration congestion. Alternately, more gradual loading reduces instantaneous network demand and stress on the network. The loading curves used in this assessment are shown in Figures 7-8 and 7-9 illustrating faster and slower mobilization times, respectively. A variety of loading rates and durations were used in the analyses. For example, in Figure 7-8, the loading curves for 2:30 and 3:00 mobilization time scenarios load 90 percent of the vehicles within the first 1 hour and 30 minutes and are likely to produce similar 90 percent ETEs. In Figure 7-9 the loading curve for the 4:30 mobilization time scenario shows that approximately 95 percent of the vehicles are loaded more rapidly than the 4:00 mobilization time scenario. This may have an impact on the development of congestion in the network.

The loading rates start to flatten out after 90 percent of the vehicles begin their evacuation trip. Therefore, the tail of the evacuation (remaining 10 percent of evacuees) take significantly longer to begin their evacuation trip. The loading curve for the 10:00 mobilization time scenario loads vehicles the most gradually and slowly among all scenarios.

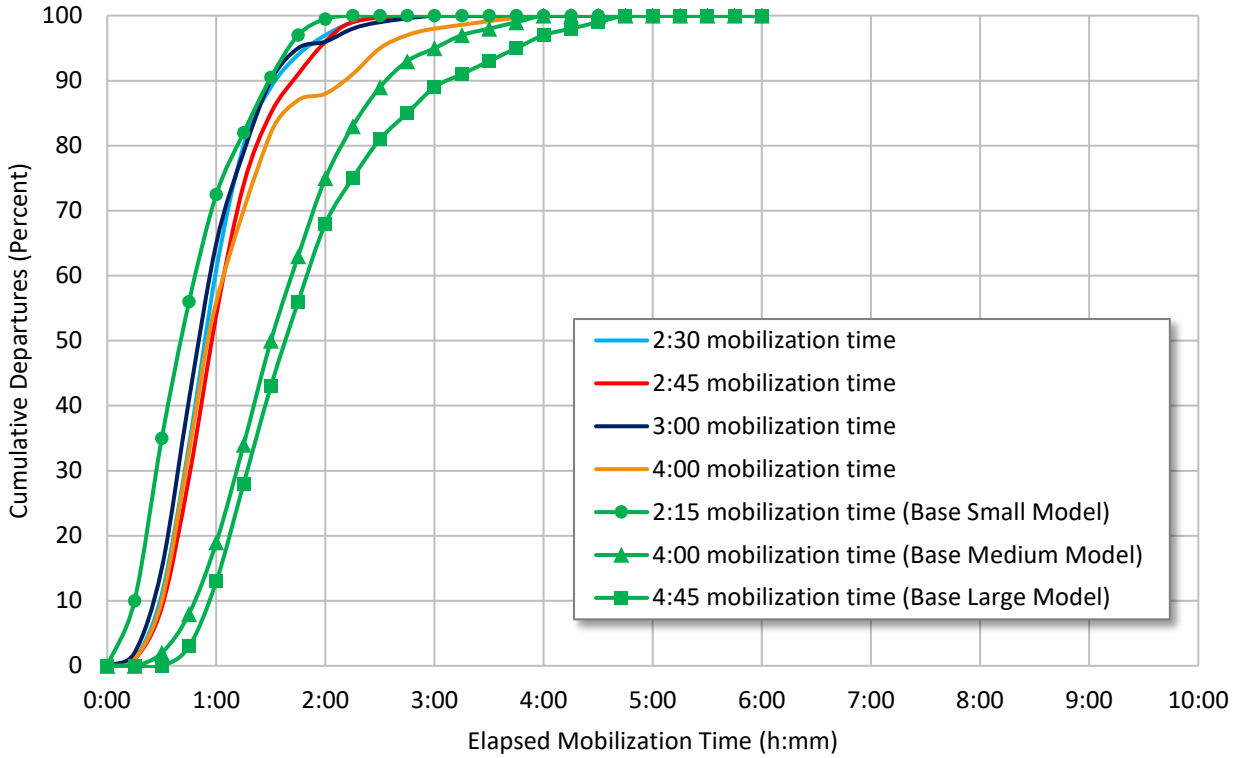

Figure 7-8 Faster Mobilization Time Curves and Base Scenario Loading Curves

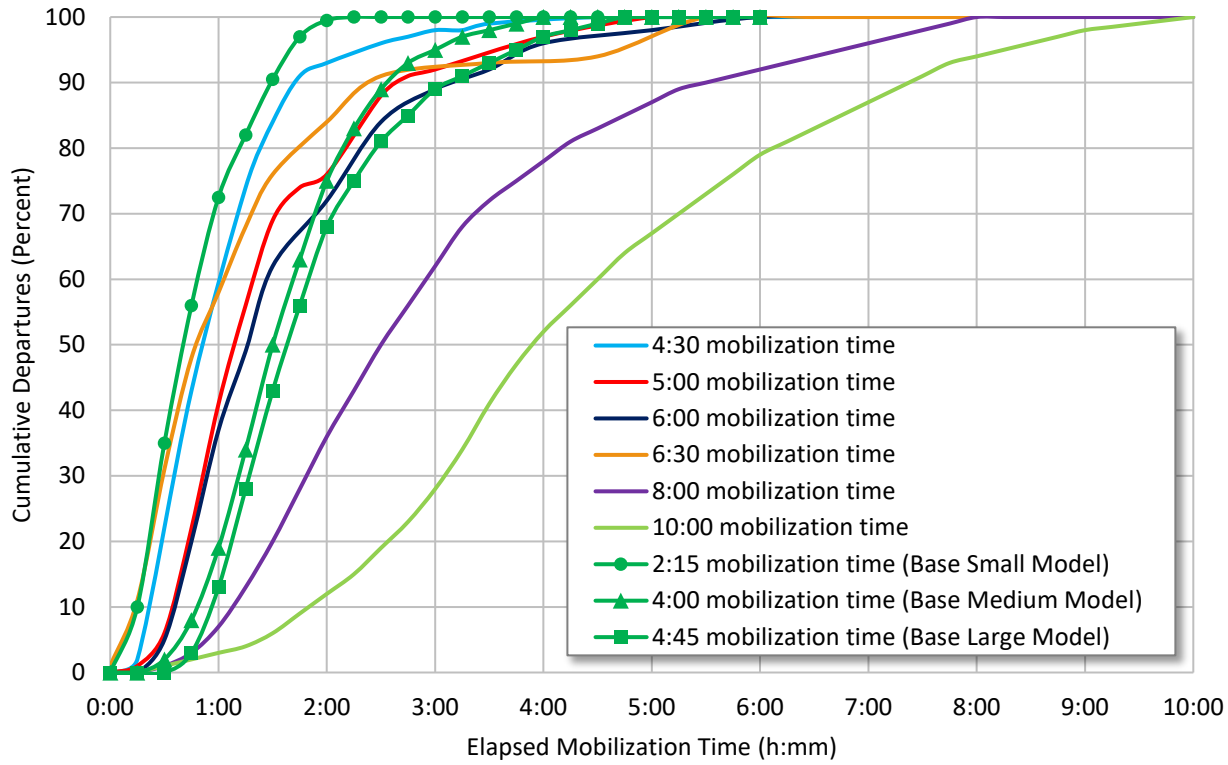

Figure 7-9 Slower Mobilization Time Curves and Base Scenario Loading Curves

7.2.3 Background Traffic

The sensitivity of ETEs to background traffic was assessed by decreasing and increasing the number of background vehicles loaded onto the network inside and outside the 10-mile EPZ. The loading rate, vehicle composition, routing characteristics and origination points of background traffic was kept the same as in the base models. Pass-through traffic was not varied as it was assigned to specific routes in the medium and large population models. Background traffic would join those routes in normal course and increase demand.

Background traffic loading rates were the same as in the base models. As described in the model development, background traffic inside the EPZ was loaded during a 30-minute seeding period prior to the evacuation notification and continued for a period of time into the evacuation. This was done to reflect background traffic existing within the EPZ at the start of the evacuation and being routed away as these vehicles become part of the active evacuation. Extending the loading time of background traffic ensured that the friction created by these vehicles was present as evacuees entered the network. The background traffic outside the EPZ was similarly seeded, but continued throughout the duration of the analysis to represent trips that are not part of the evacuation but could affect the movement of evacuees as they travel to their destinations. Since no actual traffic existed for the hypothetical NPPs modeled in this study, background traffic was estimated as a percent of the EPZ vehicles in each of the representative population site models.

Table 7-13 contains the scenarios for background vehicles. Each model was tested with a background traffic percentage lower than the base model to determine the effect of less traffic on ETE. The background traffic was increased incrementally to determine when a significant change in ETE occurred. Maximum background percentages were selected to exceed what

would normally be expected. The background traffic volumes were adjusted separately inside and outside of the EPZ because background traffic inside the EPZ is assumed to eventually become part of the evacuation.

Table 7-13 Background Traffic Scenarios

Population Site Model	Scenario Number	EPZ Background Traffic Vehicles	10-20 Mile Background Traffic Vehicles	EPZ Background Traffic (%)	10-20 Mile Background Traffic (%)
Small	1	375	3,175	10	14
	2 (Base model)	752	6,350	20	27
	3	900	7,620	24	34
	4	1,125	9,525	30	42
Medium	1	2,000	24,110	2	16
	2 (Base model)	4,000	48,220	4	32
	3	4,800	57,860	5	38
	4	6,000	72,330	6	48
	5	8,000	96,440	8	64
Large	1	4,060	76,000	2.5	16
	2 (Base model)	8,125	152,000	5	32
	3	9,750	182,400	6	38
	4	12,185	228,000	7.5	48
	5	16,250	304,000	10	64

7.2.4 Heavy Vehicles

The sensitivity of ETEs to heavy vehicles was assessed by varying the composition of passenger vehicles and heavy vehicles generated in each of the representative site models; the adjustment of vehicle composition was applied for all vehicle types (evacuees, background, and shadow population). The scenarios for the three representative site models are given in Table 7-14.

Four different scenarios were implemented in the three representative site models. In the first scenario, no heavy vehicles were modeled, and only cars were loaded onto the network. This minimum was selected to assess the effect the absence of heavy vehicles would have on an ETE and to better assess the impact of increasing this parameter. The second scenario modeled 10 percent of the vehicles loaded as heavy vehicles and 90 percent of passenger cars and SUVs to make up for the 100 percent. The last scenario modeled 20 percent heavy vehicles and 80 percent of cars.

Table 7-14 Heavy Vehicle Scenarios

Population Site Model	Scenario Number	Percent Heavy Vehicles	Heavy Vehicles	Passenger Vehicles	Total EPZ Vehicles
Small	1	0%	0	3,750	3,750
	2 (Base model)	2%	75	3,675	3,750
	3	10%	375	3.375	3,750
	4	20%	750	3,000	3,750
Medium	1	0%	0	100,000	100,000
	2 (Base model)	2%	2,000	98,000	100,000
	3	10%	10,000	90,000	100,000
	4	20%	20,000	80,000	100,000
Large	1	0%	0	162,500	162,500
	2 (Base model)	2%	3250	159,250	162,500
	3	10%	16,250	146,250	162,500
	4	20%	32,500	130,000	162,500

Vehicle dynamics in VISSIM vary by vehicle type. Heavy vehicles (e.g., trucks and RVs) can be modeled using the "HGV" vehicle type in VISSIM. In addition, the power-to-weight ratio or specific truck power can be adjusted accordingly. The lower limit of the power-to-weight ratio can vary from 1 to 10 kW/t and the upper limit from 11 to 1000 kW/t. The default range of power-to-weight ratio is 7.00 kW/t to 30.00 kW/t which represents a range of weight-to-power ratios varying from 45 lb/hp to 192 lb/hp. Since many NPPs are located around large bodies of water and the prevalence of motor homes, campers, and boats could be large, the study of heavy vehicles in Task 4 varied the compositions of both trucks and RVs. The proposed ranges were selected to capture the impact of trucks and RVs on level terrain (grades less than two percent) since the roads in the base models were flat and variations in grades were not considered.

7.2.5 Free-Flow Speed

Free-flow speeds were implemented in the base models using VISSIM's desired speed decision function. This function assigns a speed distribution profile for freely-flowing vehicles. The speed distribution is bounded below and above by a fixed speed. In the base model, speed decision points were added in each direction at selected intersections and road segments. When vehicles drove over a decision point, a desired speed was assigned to the vehicle based on the assigned speed distribution profiles. In free-flowing conditions, vehicles would maintain the desired speed assignment until driving over another speed decision point later in the network. The sensitivity of ETEs to free-flow speed was assessed by varying the desired speeds for individual links in VISSIM. The scenarios tested included a range of values that captured speed reductions identified for rainy and snowy conditions. This was done to assess the effect of free-flow speed alone prior to assessing the combined effect of adverse weather. The free-flow speed distributions were varied as shown in Figure 7-10. The screen capture on the left of this figure shows an example of a desired speed distribution in the base model with a lower bound of 45 mph and upper bound of 65 mph and an 85th percentile at 60 mph. The screen capture on the right shows the lower and upper bounds when a 25 percent decrease is implemented for this desired speed decision. This procedure was followed to vary all the desired speed distributions in the network.

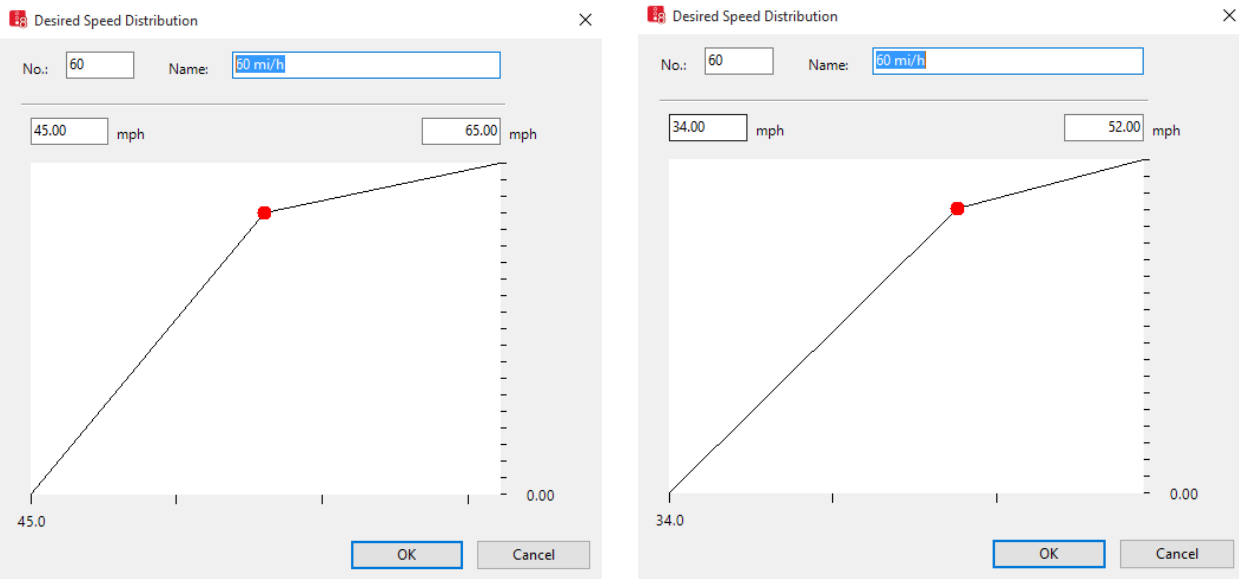

Figure 7-10 Desired Speed Distribution in VISSIM

In this study, the desired speed distributions from the base scenario were decreased by 10, 20, 25, 30, and 35 percent as shown in Table 7-15. A zero percent change in free-flow speed indicates base model free-flow speeds.

Table 7-15 Free-flow Speed Scenarios

Population Site Model	Scenario Number	Free-flow Speed Decrease (%)
Small	1 (Base model)	0
	2	10
	3	20
	4	25
	5	30
	6	35
Medium	1 (Base model)	0
	2	10
	3	20
	4	25
	5	30
	6	35
Large	1 (Base model)	0
	2	10
	3	20
	4	25
	5	30
	6	35

7.2.6 Adverse Weather

Adverse weather impact can be modeled by reducing free-flow speed and roadway capacity for varying degrees of rain and snow conditions. Free-flow speed was varied in the same fashion as was done for the independent analysis of this parameter. Roadway capacity was varied by modifying car following parameters as described in the Federal Highway Administration guidance [156]. VISSIM has two car-following models, Wiedemann 74 (W74) which is used to model urban traffic and freeway merging areas, and Wiedemann 99 (W99) which is used to model freeway traffic excluding merging areas. The safety distance parameter of the W74 car following model was adjusted to represent a reduction in roadway capacity. Using Equation 7.3 the value of *BX* was estimated. The values for BX_{add} and BX_{mult} from the base model (default value of $BX_{add} = 2$ and $BX_{mult} = 3$) were used. Link capacity (q_c) was estimated in the base model using Equation 7.2 and using known free-flow speeds (u_f) and jam density (k_j). To model rain and snow, different values of BX_{add} and BX_{mult} were first assumed for different free-flow speed reductions. Link capacity (q_c) was then estimated for each combination of BX_{add} and BX_{mult} using Equation 7.1 and Equation 7.2. The resulting capacity obtained from this step was then compared to the estimated capacity in the base model scenario to compute the reduction in capacity. Values of BX_{add} and BX_{mult} were selected for each combination of capacity and free-flow speed reductions in rain and snow that fell within the range provided in Federal Highway Administration guidance [127].

The W99 car following parameter CC1 (headway time) was modified to represent capacity reduction on freeways. To find the range of values of CC1 to be used in the analysis, link capacity (q_c) was estimated in the base model using Equation 7.6 and the known value of CC1 (default of 0.9 seconds) and known free-flow speeds for individual links. Then, different values of CC1 were assumed for free-flow speed reductions of 10 and 35 percent and capacity (q_c) was estimated for each combination using Equation 7.6. The estimated capacity from this step was compared to the estimated capacity in the base model scenario to calculate the reduction in capacity. Values of CC1 were selected for each combination of capacity and free-flow speed reductions in rain and snow that fell within the range provided in FHA guidance [127].

Table 7-16 summarizes the rain and snow scenarios for the small, medium, and large population site models. Two rain and snow scenarios were run in the small and medium population site models to assess the sensitivity of ETEs to various degrees of rainy and snowy conditions. These scenarios included a 10 and 35 percent decrease in free-flow speed with variations in BX_{add} and BX_{mult} parameters in the Wiedemann 74 car following model that gave an approximate capacity reduction between 9 and 20 percent in rainy conditions and between 28 and 30 percent in snow as estimated using Equation 7.2.

Rainy and snowy conditions were modeled in the large population site model by varying the BX_{add} and BX_{mult} parameters in the Wiedemann 74 car following model and also by varying the CC1 parameter in the Wiedemann 99 car following model since there were more lane-miles of freeway inside the EPZ in the large population site model. CC1 varied between 0.9 seconds (default value) and 1.3 seconds. The scenarios included a 10 and 35 percent reduction in free-flow speed.

Table 7-16 Adverse Weather Scenarios

Population Site Model	Scenario Number	Weather Condition	Estimated Capacity Reduction (%)	Free-flow Speed Decrease (%)	Driver Behavior Parameters
Small	1 (Base)	Fair[1]	-	0	Bx_{add}=2.0; Bx_{mult}=3.0
	2	Rain	9	10	Bx_{add}=2.1; Bx_{mult}=3.1
	3	Rain	19-20	10	Bx_{add}=2.5; Bx_{mult}=3.5
	4	Snow	28-30	10	Bx_{add}=3.0; Bx_{mult}=4.0
	5	Snow	27-28	35	Bx_{add}=2.9; Bx_{mult}=3.9
Medium	1 (Base)	Fair	-	0	Bx_{add}=2.0; Bx_{mult}=3.0
	2	Rain	9	10	Bx_{add}=2.1; Bx_{mult}=3.1
	3	Rain	19-20	10	Bx_{add}=2.5; Bx_{mult}=3.5
	4	Snow	28-30	10	Bx_{add}=3.0; Bx_{mult}=4.0
	5	Snow	26-28	35	Bx_{add}=2.9; Bx_{mult}=3.9
Large	1 (Base)	Fair	-	0	CC1=0.9; Bx_{add}=2.0; Bx_{mult}=3.0
	2	Rain	9-16	10	CC1=0.95; Bx_{add}=2.05; Bx_{mult}=3.05
	3	Rain	16-22	10	CC1=1.1; Bx_{add}=2.2; Bx_{mult}=3.2
	4	Snow	26-29	10	CC1=1.3; Bx_{add}=2.6; Bx_{mult}=3.6
	5	Snow	24-31	35	CC1=1.1; Bx_{add}=2.05; Bx_{mult}=3.05

[1] Fair weather refers to conditions where roadways are clear and dry, and visibility is not impaired.

7.2.7 Roadway Impact

The roadway impact scenario assessed the sensitivity of ETEs to disruptions on the transportation network. Each scenario tested here consisted of a lane closure that remained active for the duration of the simulation to represent a work-zone due to major construction (e.g., roadway widening). The lane closures were of varying length and were implemented on segments of freeways and arterial roads carrying the highest volumes.

Although NUREG/CR-7002 indicates that a road closure or a lane closure could be used in the roadway impact analysis, this study only considered lane closures. This was selected because disruptions on routes without alternative paths have been, in general, identified as having a larger impact since vehicles are forced to stay on that road if their destinations do not change. The locations where the lane closures were implemented in this study, had alternative paths; however, vehicle re-routing was not allowed. It is likely that actual drivers would route around the congestion, but eliminating that behavior allows the impact of roadway disruptions to be quantified.

Table 7-17 summarizes the scenarios studied for the roadway impact in the small, medium, and large population site models. The roadway disruption in the small population site model consisted of a lane closure on Link 647 located inside the EPZ and close to the 10-mile EPZ boundary as shown in Figure 7-11. Two lane closures at different road segments were implemented in the medium and large population site models as shown in Figure 7-12 and Figure 7-13. Lane closures did not extend through intersections and did not involve lanes with on-ramps or off-ramps so that vehicles remained on their respective paths. Vehicles whose original path included the lane closure, remained on that road.

Table 7-17 Roadway Impact Scenarios

Population Site Model	Scenario Number	Link # Closed	Roadway Classification	Number of Lanes	Length of Closure (miles)
Small	1 (Base model)	-	-	-	-
	2	647	Arterial	2	0.66
Medium	1 (Base model)	-	-	-	-
	2	133	Freeway	3	0.18
	3	222	Freeway	2	1.82
Large	1 (Base model)	-	-	-	-
	2	150	Freeway	2	0.63
	3	32909	Arterial	3	0.16

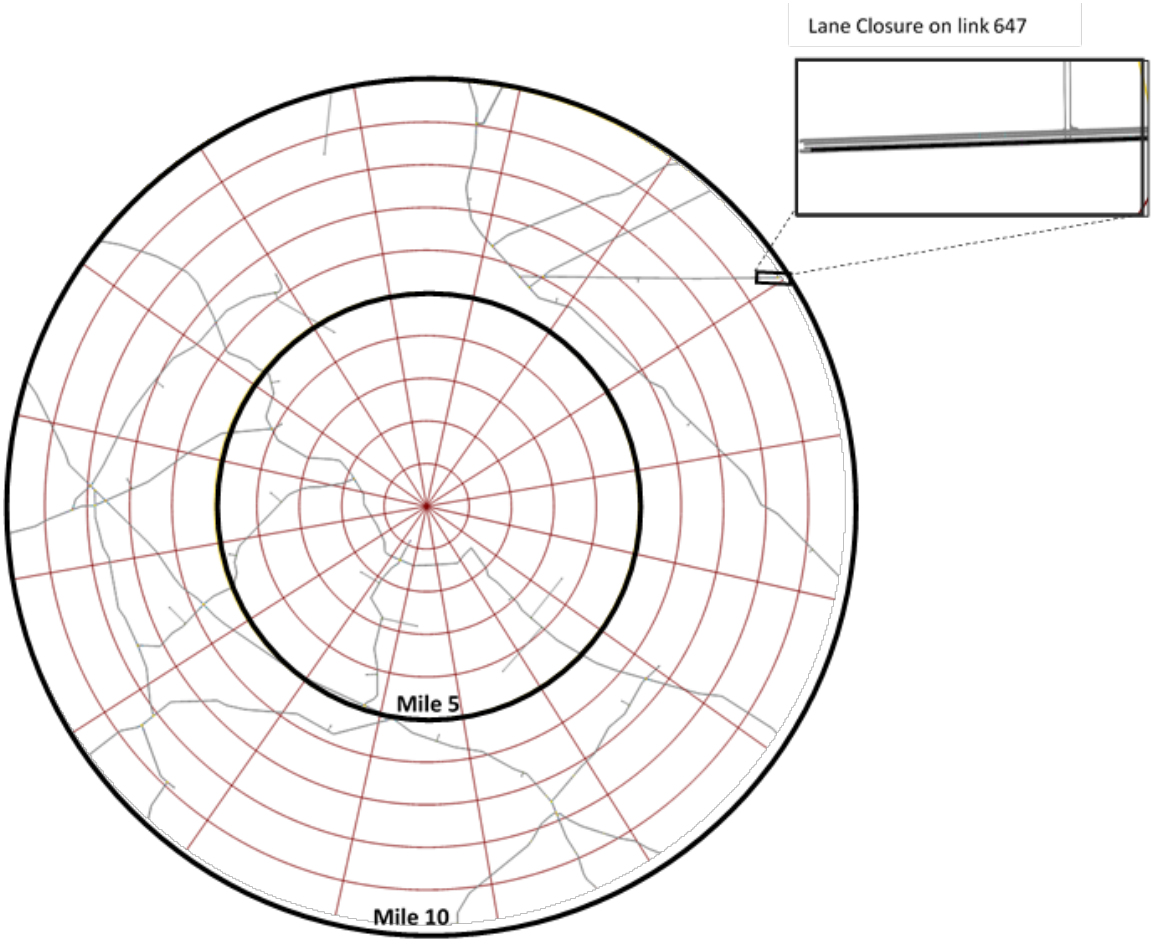

Figure 7-11 Small Population Site Model Roadway Impact Location

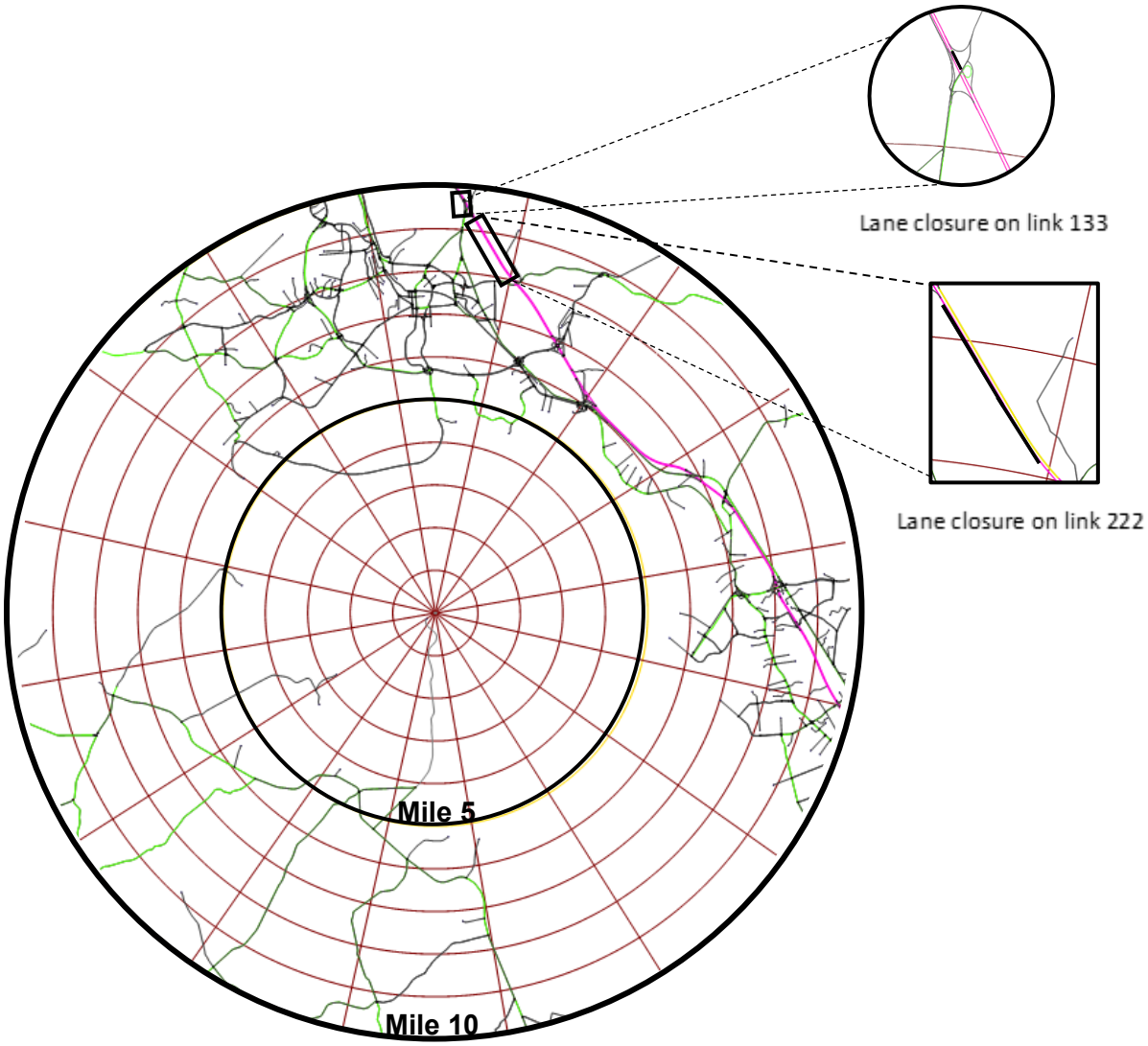

Figure 7-12 Medium Population Site Model Roadway Impact Locations

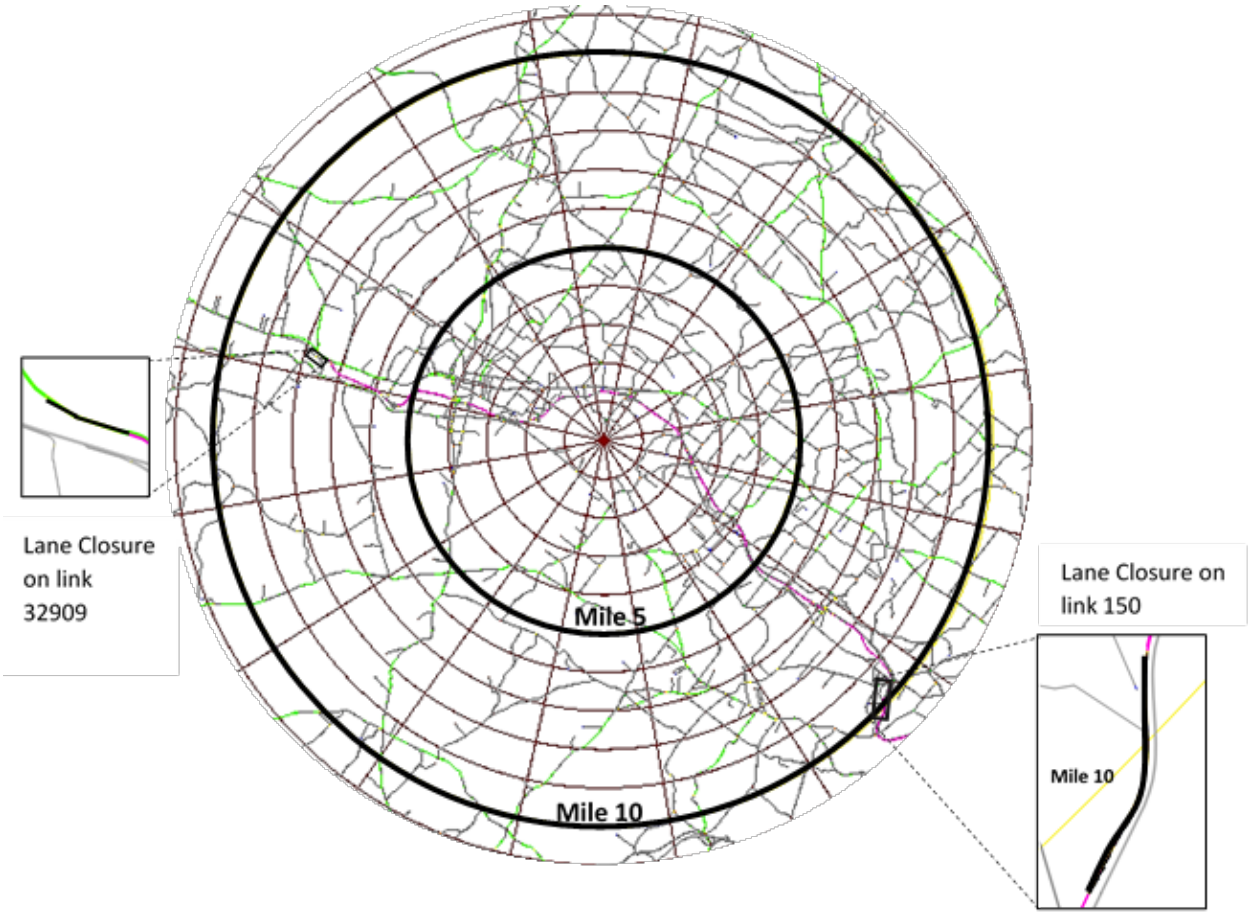

Figure 7-13 Large Population Site Model Roadway Impact Locations

7.2.8 Processing Time Step

The processing time step (simulation resolution) in VISSIM can range from 1 to 20 time steps per second. The selection requires a trade-off between model fidelity and computational processing time. The default value setting within VISSIM is 10 time steps per second, and the developers recommend using a processing time between 5 and 10 time steps per second to produce more accurate results [21]. However, when modeling systems as large and complex as those in this research, such processing rates can add enormous amounts of time to individual model runs—in some cases requiring more than 24 hours for a single model scenario.

Three scenarios were tested using the base models to assess the impact of time step selection as shown in Table 7-18. The first scenario was the base model with 1 time step per second to allow for faster runs. The simulation resolution was then increased to 5 and 10 time steps per second to test the minimum and maximum values recommended in the VISSIM manual.

Table 7-18 Processing Time Step Scenarios

Population Site Model	Scenario Number	Processing Time Step (time steps/second)
Small	1 (Base model)	1
	2	5
	3	10
Medium	1 (Base model)	1
	2	5
	3	10
Large	1 (Base model)	1
	2	5
	3	10

7.2.9 Uncertainty Analysis

This analysis assessed the degree to which stochastic effects introduced by various random seeds impacted model performance. In the small and medium sites, a total of 50 random seeds were run for the uncertainty analysis. These included the 10 seeds used in the base models. In the large site, 37 seeds were run. These also included the 10 seeds used in the base model. The uncertainty analysis is expected to provide an understanding of how the stochastic nature of the simulation affected the model results and its relationship to ETE.

7.3 Task 4 Results

This section discusses the results for the average of several simulation runs, each with varying random seed values. Similar to Task 1, 2, and 3, the small population site model results represent an average of ten simulation runs and the medium and large population site model results represent an average of four runs. The measures of effectiveness used to evaluate Task 4 outputs were primarily evacuation time, average travel speeds, and vehicular volumes exiting the EPZ. Network wide average vehicle delays were also analyzed to obtain additional information about the dynamics of the evacuation process. Depending on the parameter that was investigated, other MOEs (e.g., average queue length) were used to supplement and support the interpretation of the ETE and the evacuation process.

The parameters followed a one-at-a-time sensitivity analysis approach by isolating a parameter and adjusting its value while keeping all other parameters constant. This analysis provided an opportunity to analyze elements of traffic flow theory in an evacuation context under a range of different operational characteristics. Output data was collected and analyzed over 5-minute increments and segregated to display results for the 90 and 100 percent ETE at the 2, 5, and 10-mile rings. The analyses are a comparison of the base case output to the results of the various parameter tests. Significant differences to the base model results were identified as increases or decreases in ETEs of 30 minutes or more. The results are presented for each of the 9 parameters studied through 245 scenario runs.

7.3.1 Population Parameter Results

Variations in the population represent changes in demand and the number of vehicles loaded into a network. Three distinct network traffic states were observed in the assessment of changes in population: a non-congested state, a transition state, and a congested state. The physical and operational elements of the network including network topology and connectivity, number of lane-miles, traffic control, traffic composition, and vehicle dynamics, primarily governed the travel times and travel speeds in the non-congested state independent of demand. In non-congested networks, ETEs are relatively insensitive to population and roughly equate to the mobilization time plus some travel time. As demand increases, the interaction among vehicles and the infrastructure begins to influence the network performance and ETEs slightly increase. In this transition state, network performance deteriorates gradually as demand approaches some threshold value related to the network's service ability. In the congested state, ETEs increase approximately linearly with population increase as there is more demand than can be serviced. This is due to a combination of effects including: activating existing bottlenecks sooner; creating bottlenecks at the boundary of or within the EPZ; or extending queues at existing bottlenecks that can limit demand that can be served. It is important to note that the level of congestion is not uniform within the network. However, congestion is captured in the network-wide performance which drops significantly as the network becomes increasingly congested.

The results showed that the population threshold values for the 90 percent ETEs were less discernable than those for 100 percent ETEs in the three representative site models. This is because 90 percent ETEs are typically more sensitive to traffic conditions while 100 percent ETEs are most likely to be influenced by the tail of the evacuation independent of the traffic conditions.

Although not specifically analyzed, longer mobilization times with more gradual loading rates would be expected to have larger population thresholds in the same site because higher populations would be needed to increase the flow rate into the network. Similarly, the network characteristics and the spatial distribution of the population will influence network performance through local rates of vehicle loading. Even for similar populations and mobilization times, if the spatial distribution of demand is different, local arrival rates are expected to vary. As such, local bottlenecks are more likely to occur in higher population density locations because higher demands are achieved with relatively small increases in population.

7.3.1.1 Small Population Site Model Population Parameter Results

The 90 and 100 percent ETEs for the small population site model at the 2, 5, and 10-mile rings are provided in Table 7-19. The base EPZ population for the small population site was 7,500 evacuees. The base model was assumed to initially be in the non-congested region. As such decreasing the base population was not a consideration in this study.

A transition state can be observed once the number of evacuees exceeds 150 percent of the base population (11,625 evacuees). A threshold is observed starting at populations of 16,875 evacuees or more and the 100 percent ETE increased significantly (by 30 minutes or more) at the 5 and 10-mile rings. These results are evidence that the ETE increased slightly up to a threshold, and then scaled more rapidly after the threshold due to increasing congestion with increasing demand. The ETE at the 2 mile ring increased significantly only for EPZ populations at the extreme end of the range where population was increased by over 250 percent.

Average evacuee delay is shown in Table 7-19. In the non-congested state average evacuee delay was fairly constant. As the threshold value is approached, delay increases, and continues to increase with further increases in the population demand.

Table 7-19 Small Population Site Population Analysis

Scenario Number	Total EPZ Population	Average Evacuee Delay (minutes)	2-Mile		5-Mile		10-Mile	
			90% ETE	100% ETE	90% ETE	100% ETE	90% ETE	100% ETE
1[1]	7,500	14	1:35	2:18	1:35	2:21	1:44	2:31
2	10,125	11	1:35	2:19	1:40	2:22	1:49	2:31
3	11,625	15	1:35	2:19	1:48	2:23	1:55	2:35
4	14,250	22	1:35	2:20	2:02	2:36	2:06	2:57
5	16,875	28	1:36	2:20	2:19	3:03	2:21	3:25
6	19,500	34	1:54	2:22	2:40	3:31	2:38	3:51
7	22,125	37	2:19	2:47	2:59	3:57	2:56	4:19
8	24,750	38	2:45	3:15	3:21	4:25	3:15	4:47
9	27,375	46	3:09	3:43	3:41	4:53	3:36	5:14

[1] Base model.

Figure 7-14 and Figure 7-15 show the cumulative percent evacuated for the small population site model at the 2 and 10-mile rings, respectively. These figures are a visual representation of the overall evacuation process. The loading curve is also provided to illustrate the transition point where demand begins to exceed capacity. The 2-mile ETE for populations of 16,875 evacuees or less were very similar to the base model which indicates that the rate of egress out of the 2-mile region was controlled by the loading curve and suggesting conditions of minimal congestion. However, the egress rate decreases after about 45 minutes to an hour into the evacuation with higher EPZ populations which may suggest queues propagating back into the 2-mile area. The separation among the ETE curves becomes larger for populations higher than 16,875 evacuees, reflected in increased delays.

A threshold in the population is evident in the data. As shown in Figure 7-22, after a threshold point of 11,625 evacuees, the 100 percent ETE increased approximately linearly with population, as expected. Figure 7-23 suggests that a population threshold value may not be observable in the 90 percent ETE. Figure 7-15 illustrates the growing congestion and the departure from the loading curve as the population increases past the transition point population.

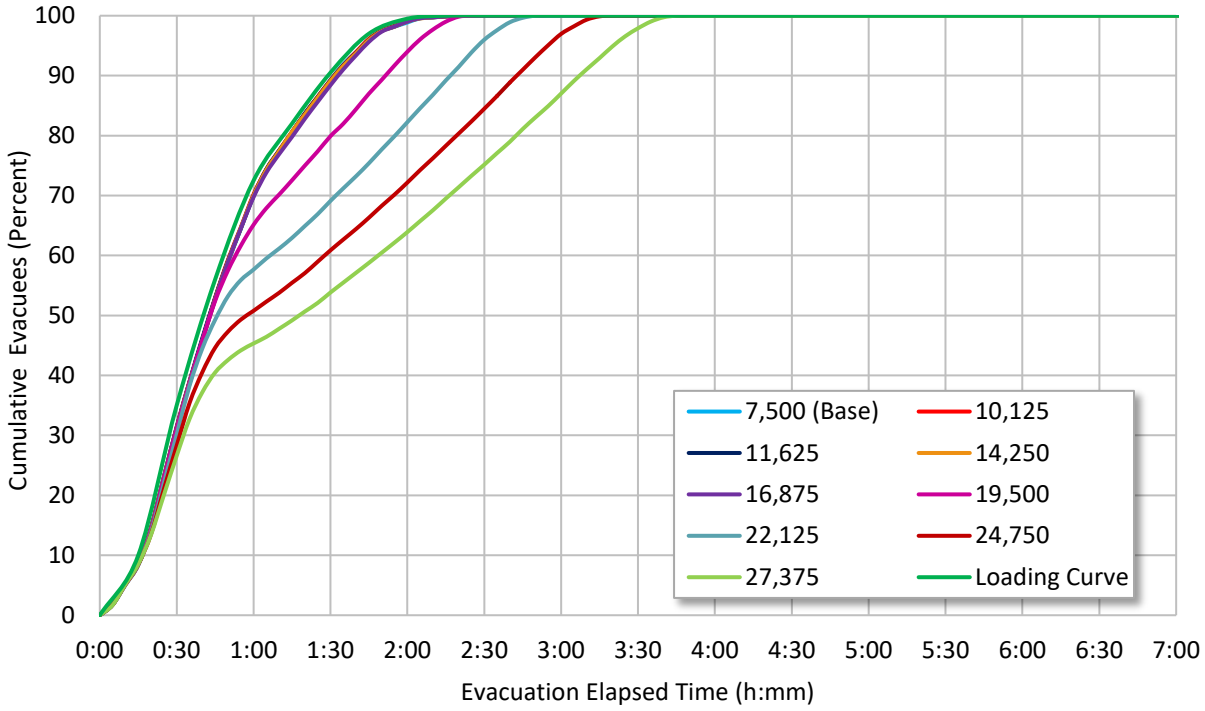

Figure 7-14 Two Mile ETE Curves, Small Population Site Population Analysis

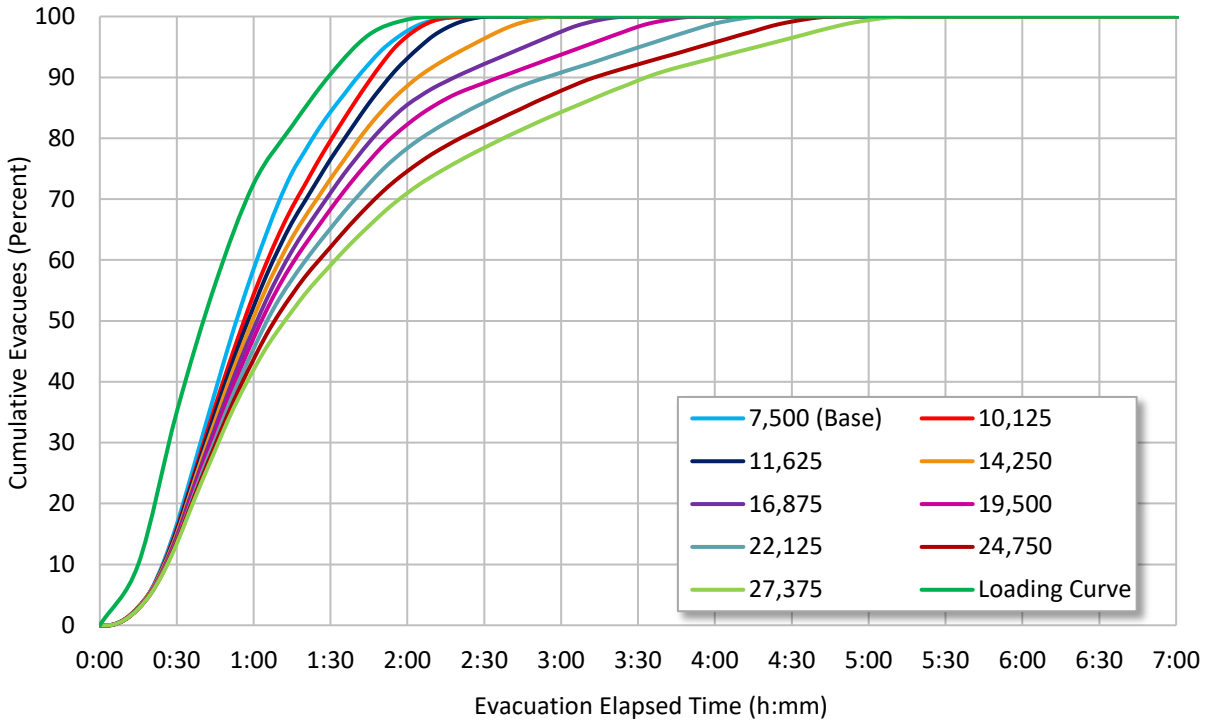

Figure 7-15 Ten Mile ETE Curves, Small Population Site Population Analysis

7.3.1.2 Medium-South Population Site Model Population Parameter Results

In the medium population site model, the ETEs were estimated and provided separately for the north and south sides according to the geographic break-down described in Section 7.2.1 and illustrated in Figure 7-7. The base EPZ population for the southern portion of the medium model was approximately 7,990 evacuees and was increased at exceedingly high rates compared to the small population site to minimize the number of scenarios. This level of population increase is not expected to actually occur, but was performed to test the response to higher population densities in a rural network. Decreasing the base population was not necessary since the medium south population site model was in the non-congested state in the base condition.

The 90 and 100 percent ETEs for each population scenario are shown in Table 7-20. Figures 7-16 through 7-17 show the evacuation clearance curves for the medium-south population site model at the 2 and 10-mile rings. This region is similar to the small population site and increasing population does not significantly affect the ETEs until a very high population is modeled. The curves in Figure 7-16 for the 2-mile EPZ show little impact on ETE until the population reaches 55,000 evacuees and then congestion spills back into the zone. The curves in Figure 7-17 for the 10-mile EPZ show a significant effect on ETE at a population of 27,000. Again, growth in population of that magnitude (more than 300 percent) within the time period between decennial censuses is highly unlikely. The increase in average evacuee delay for the medium-south side population site model was not generally discernible. This is because the average evacuee delay is the average for the entire network which is dominated by conditions in the north. Not until population is excessively high in the southern region does it begin to impact the average delay (increases by 3 minutes). In all scenarios, the number of vehicles not exiting the EPZ remained less than 1.5 percent.

Table 7-20 Medium-South Population Site Population Analysis

Scenario Number	South EPZ Population	Average Evacuee Delay[2] (minutes)	2-Mile		5-Mile		10-Mile	
			90% ETE	100% ETE	90% ETE	100% ETE	90% ETE	100% ETE
1[1]	7,990	70	2:40	4:05	2:42	4:11	3:30	4:22
2	17,500	68	2:40	4:05	2:45	4:10	3:30	4:25
3	27,500	68	2:40	4:05	3:02	4:10	4:51	5:55
4	37,500	70	2:40	4:05	4:07	5:35	6:16	7:40
5	55,000	73	4:46	5:42	6:42	7:40	8:46	11:25

[1] Base model.

[2] Evacuee delay is based on network average.

Figures 7-22 and 7-23 compare ETEs between the small site and medium-south models. The difference in ETEs is driven primarily by mobilization time, with the medium model having a base loading time of 4:00 and the small model 2:15. However, once the threshold value is reached, the linear rates of change in ETE with population are approximately the same. Again, a clear threshold for the 90 percent ETE is not observed.

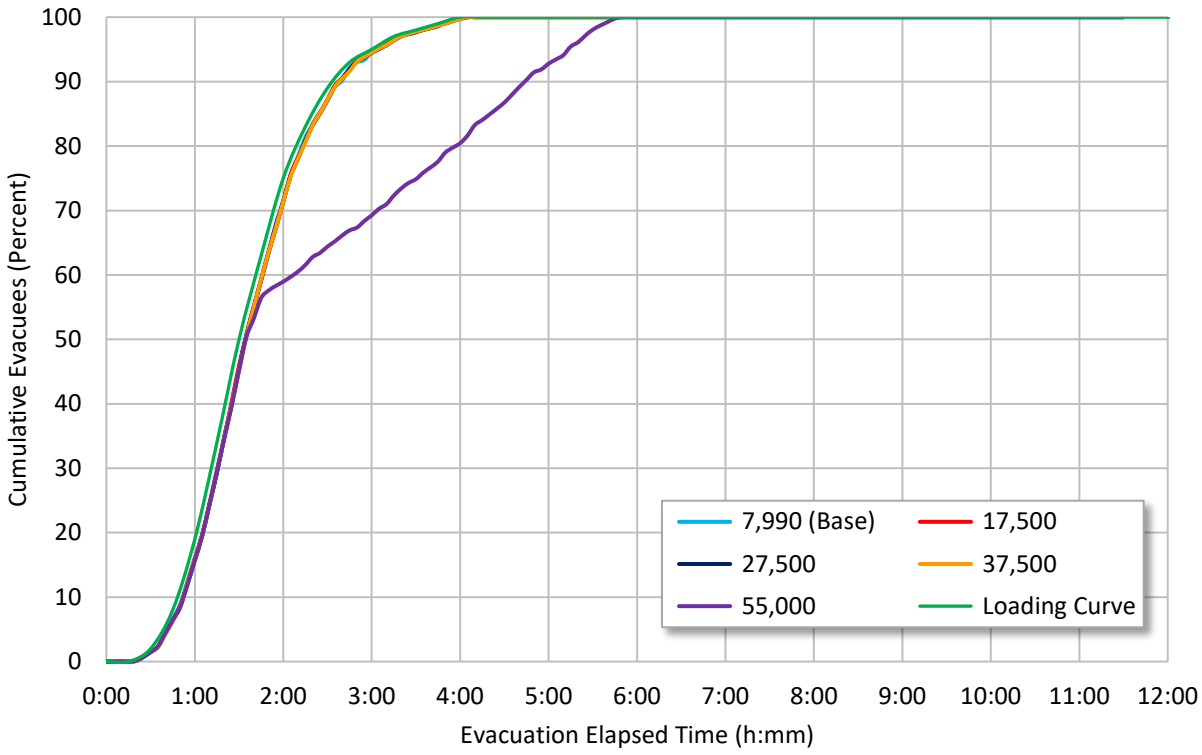

Figure 7-16 Two Mile ETE Curves, Medium–South Population Site Population Analysis

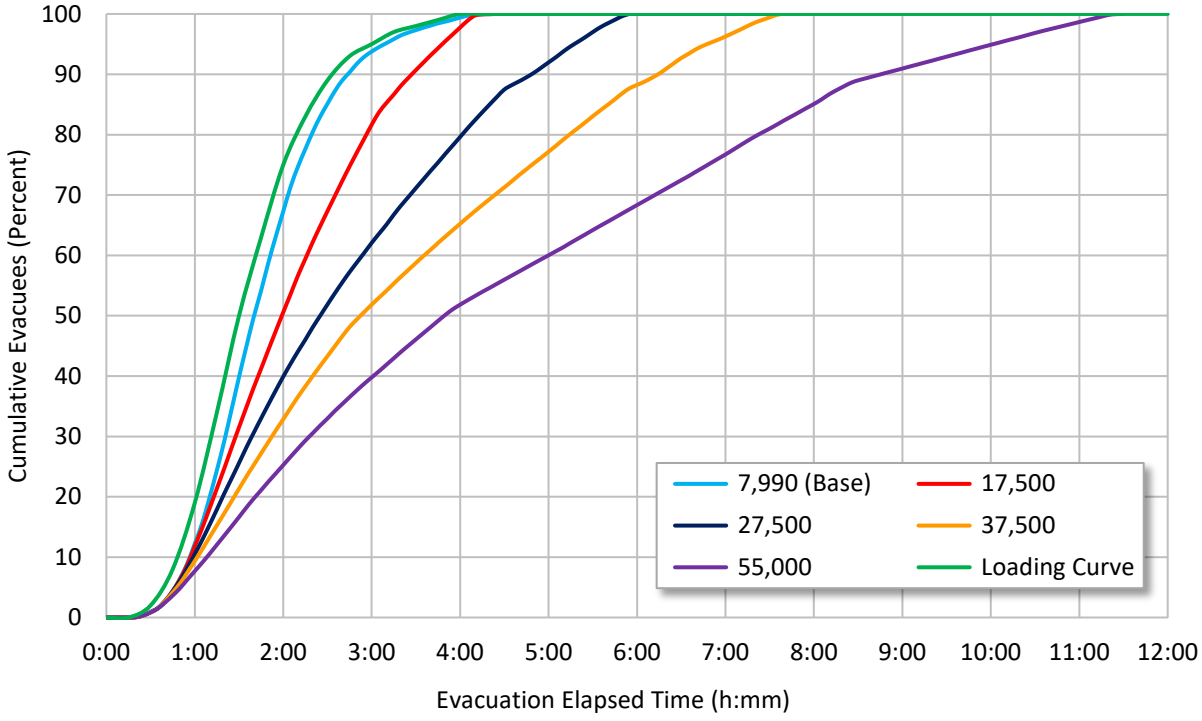

Figure 7-17 Ten Mile ETE Curves, Medium–South Population Site Population Analysis

7.3.1.3 Medium-North Population Site Model Population Parameter Results

The base EPZ population for the medium-north population site was approximately 192,000 evacuees. In the base conditions, the EPZ was in the congested state. Therefore, the base population was increased and decreased at different rates to minimize the number of scenarios while capturing the sensitivity of ETEs and the population threshold. The 90 and 100 percent ETEs were available only for the 5 and 10-mile rings in the north side since there were no vehicle generators inside the 2-mile area.

The 90 and 100 percent ETEs for the north side are shown in Table 7-21. The population threshold for the 10-mile 100 percent ETE in the north side was estimated to be around 110,000 evacuees with a mobilization time of 4:00 and loading rates specified by the base loading curve for this site. This is shown in Figure 7-25. Similar to the small population site model, a population threshold for the 90 percent ETE is not observable, as evidenced in Figure 7-25. In all scenarios, the number of vehicles not exiting the EPZ remained less than 1.5 percent.

Table 7-21 Medium-North Population Site Population Analysis

Scenario Number	North EPZ Population	Average Evacuee Delay (minutes)	2-Mile		5-Mile		10-Mile	
			90% ETE	100% ETE	90% ETE	100% ETE	90% ETE	100% ETE
1	71,500	11	-	-	2:40	4:12	2:48	4:27
2	110,000	30	-	-	2:38	4:12	3:20	4:35
3	130,000	43	-	-	2:40	4:11	3:40	5:22
4	150,000	50	-	-	2:40	4:18	4:02	6:01
5	170,000	60	-	-	2:41	4:45	4:32	6:46
6[1]	192,000	70	-	-	2:50	5:05	5:03	7:41
7	210,000	78	-	-	4:21	6:32	5:33	8:17
8	220,000	81	-	-	4:32	6:38	5:45	8:28
9	230,000	85	-	-	5:20	7:50	5:56	8:56
10	240,000	90	-	-	6:37	8:05	6:22	9:15

[1] Base model.

Figure 7-18 shows the 5-mile ETE curve for the EPZ population scenarios on the north side of the medium site model. From this figure, it can be observed that the rate of egress out of the 5-mile area for EPZ populations of 210,000 evacuees and higher decreased significantly during the period from 2:30 to 5:00 into the evacuation compared to lower population scenarios (including the base model). This suggests there is significant congestion during this time period. However, this was an expected response based on preliminary results from the model development stage because the base model population was intentionally set high to stress the network. The flattening of the ETE curve when EPZ population reaches 240,000 evacuees is indicative of gridlock conditions. Visual inspection of the simulation showed major congestion in the 5 to 10-mile area, causing queue spillbacks inside the 5-mile area in the north sector. The 10-mile ETE curve in Figure 7-19 does not have as much separation between curves or flat areas as observed in the 5-mile area, suggesting that the congestion did not result in gridlock conditions at the EPZ boundary.

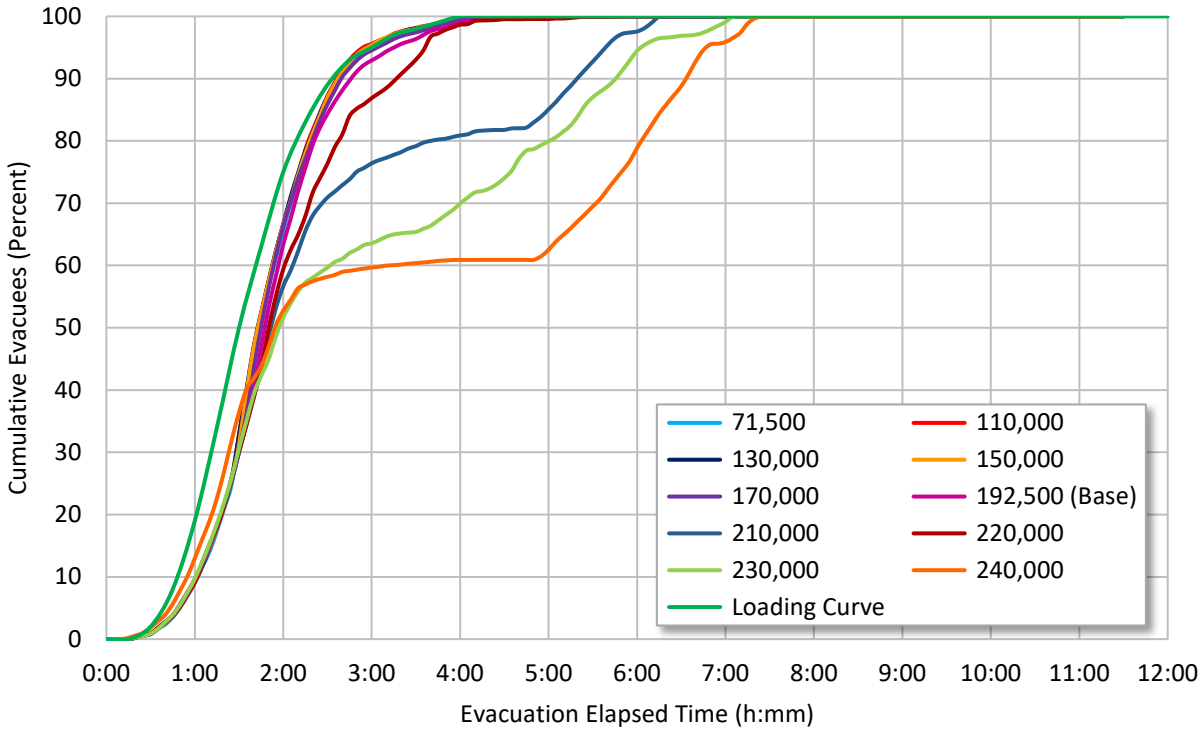

Figure 7-18 Five Mile ETE Curves, Medium–North Population Site Population Analysis

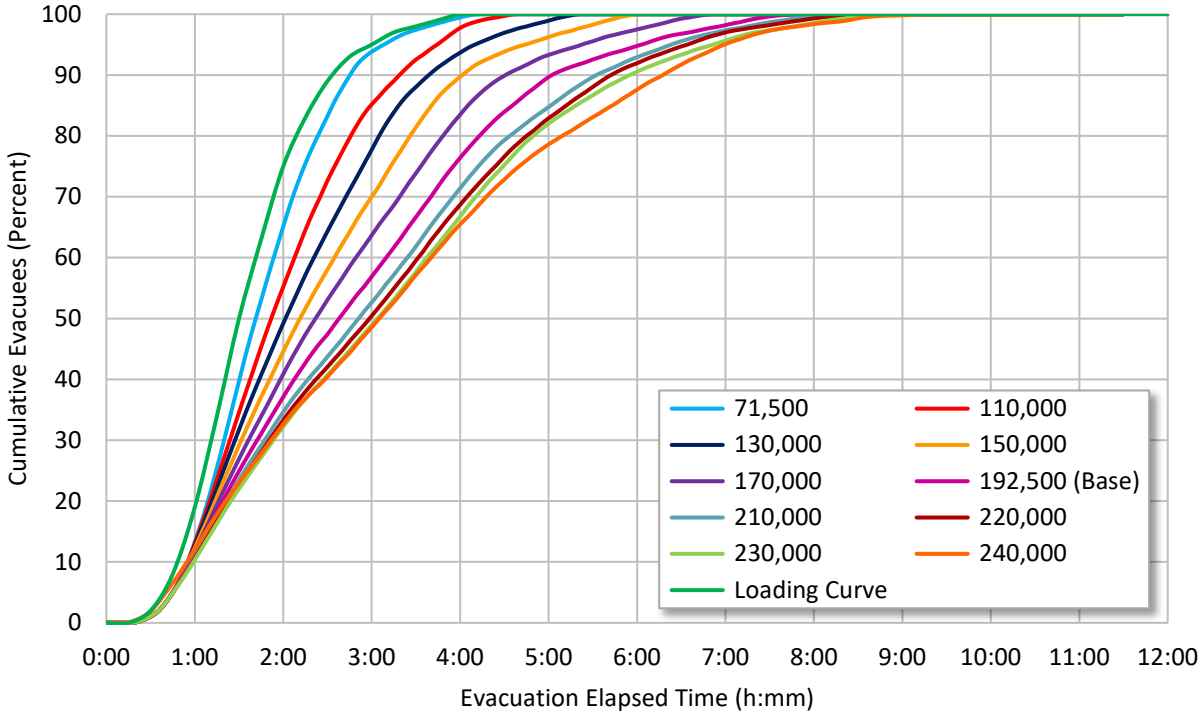

Figure 7-19 Ten Mile ETE Curves, Medium–North Population Site Population Analysis

7.3.1.4 Large Population Site Model Population Parameter Results

The large site model had a base population of 325,000 and was in a congested state; therefore, the EPZ population was increased and decreased to capture the population threshold. Table 7-22 shows the 90 and 100 percent ETEs at the 2, 5, and 10-mile rings for the large population site model. In all scenarios, the number of vehicles not exiting the EPZ remained less than 0.6 percent.

The threshold for the large site was estimated to be somewhere around 227,500 evacuees. This is close to the 200,000 EPZ population range for large sites as defined in this research and is significantly below the base model population. It would suggest that in ETE studies of large population sites, any change in vehicle population would result in proportional changes to the ETE.

Table 7-22 Large Population Site Population Analysis

Scenario Number	Total EPZ Population	Average Evacuee Delay (minutes)	2-Mile		5-Mile		10-Mile	
			90% ETE	100% ETE	90% ETE	100% ETE	90% ETE	100% ETE
1	130,000	13	3:33	4:58	3:20	5:10	3:25	6:10
2	162,500	20	3:35	5:06	3:20	5:10	3:30	6:15
3	227,500	36	3:35	5:01	3:20	5:12	3:48	6:33
4	282,750	51	3:33	5:05	3:30	5:28	4:20	7:56
5	308,750	56	3:40	5:03	3:45	6:11	4:31	8:33
6[1]	325,000	62	3:40	5:05	3:57	6:35	4:43	9:01
7	341,250	64	3:43	5:02	4:12	7:13	4:53	9:30
8	357,500	70	3:50	5:16	4:23	7:36	5:03	10:00
9	373,750	71	4:02	5:42	4:42	8:22	5:22	10:20
10	390,000	73	4:05	6:08	5:16	8:55	5:41	10:58

[1] Base model.

Figure 7-20 and Figure 7-21 show the cumulative percent evacuated for the large population site at the 2 and 10-mile rings, respectively. From the figures it can be observed that the rate of egress out of the 2-mile area for 90 percent of the population was not significantly affected by the population changes. Gradual variations of ETE with population were observed in the ETE curves at the 5-mile (not shown) and 10-mile rings (Figure 7-21).

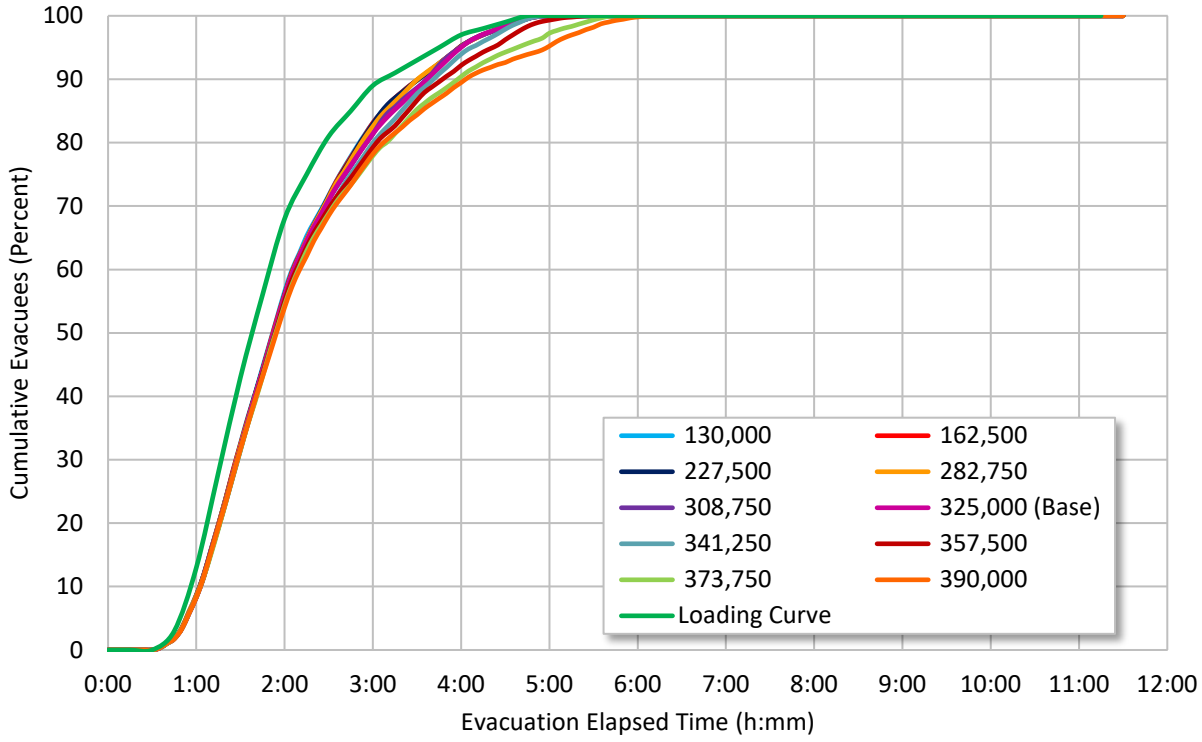

Figure 7-20 Two Mile ETE Curves, Large Population Site Model, Population Analysis

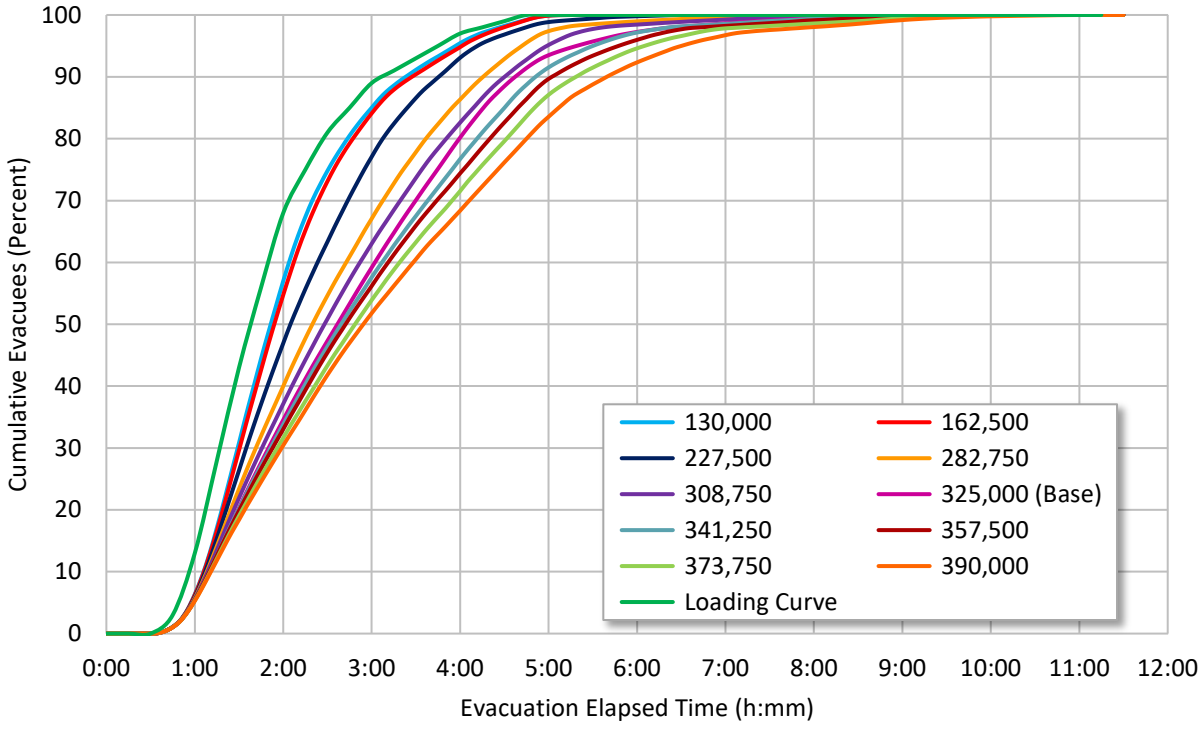

Figure 7-21 Ten Mile ETE Curves, Large Population Site Model, Population Analysis

7.3.1.5 Sensitivity of Population Parameter

Figure 7-22 illustrates the 10-mile 100 percent ETE for the small and medium-south population sites for the demand scenarios investigated. Figure 7-23 shows the 10-mile 90 percent ETE for the same scenarios. Similar data for the medium-north and large population site models are provided in Figure 7-24 and Figure 7-25. The point where the curves deflect is the approximate transition to congested conditions. Beyond the threshold point, the 100 percent ETEs increase linearly with population increase. It may be noted that the 90 percent ETE curve does not show a distinct threshold but continues increasing monotonically in all cases.

Comparing graphs, it can be seen that the 90 percent ETE is less sensitive to changes in population than the 100 percent ETE. This is likely due to the impact of congestion and long queues influencing the evacuation tail. This is an important insight with regard to protective action recommendations that make use of the 90 percent ETE. In particular, the results from the medium and large population site models show that it takes population increases of around 10 percent to significantly impact the 90 percent ETE. This finding suggests that the 90 percent ETE is unlikely to change significantly due to population alone during the 10-year period between decennial censuses.

Figures 7-24 and 7-25 illustrate a geographic element that occurs at coastal (and other) NPP sites which explains why the medium-north ETE is higher than the large population site ETE. The northern region of the medium population model has a large population in about half the size of a full EPZ. Additionally, there are fewer evacuation route alternatives, with traffic predominately following the main routes to the NW and SE. While the overall population of this EPZ ranks as medium, the population density in the northern region is as high as a large population site. In Figure 7-24, for an 8-hour 100 percent ETE, the large site evacuates about 100,000 people more than the medium site. A similar comparison can be made with the 90 percent ETE data. This illustrates the important interplay between capacity and demand as it relates to evacuation efficiency.

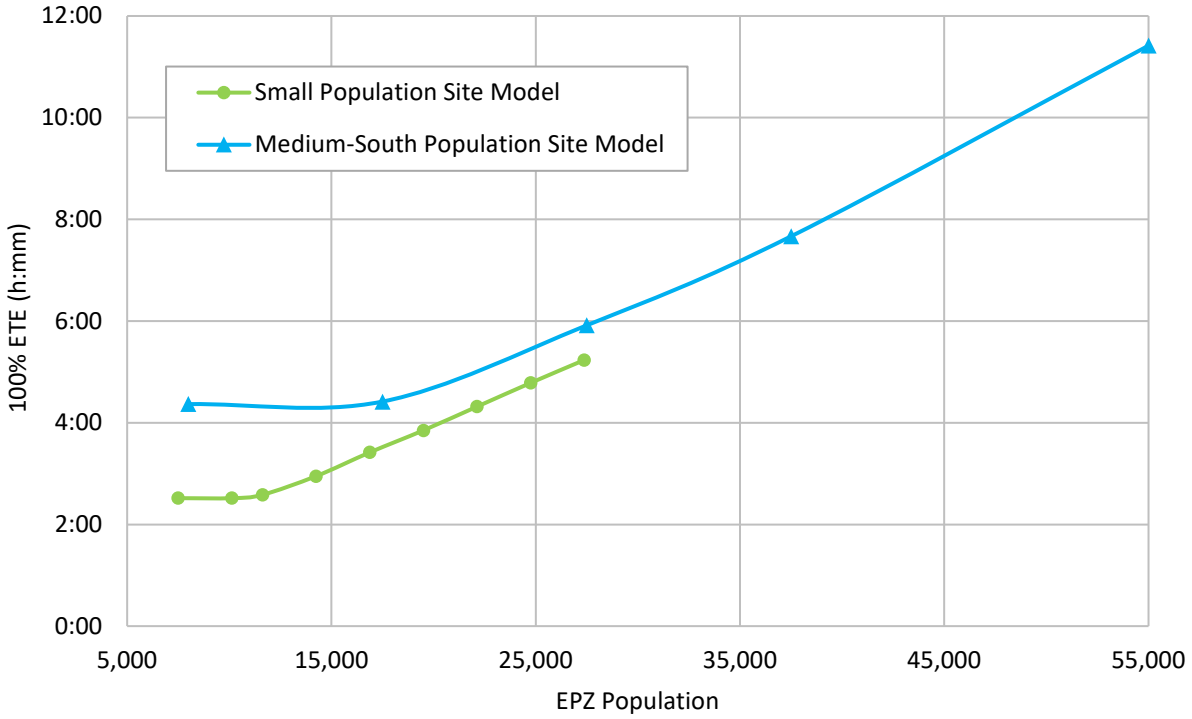

Figure 7-22 Ten Mile 100 percent ETEs, Small and Medium-South Site Population Analyses

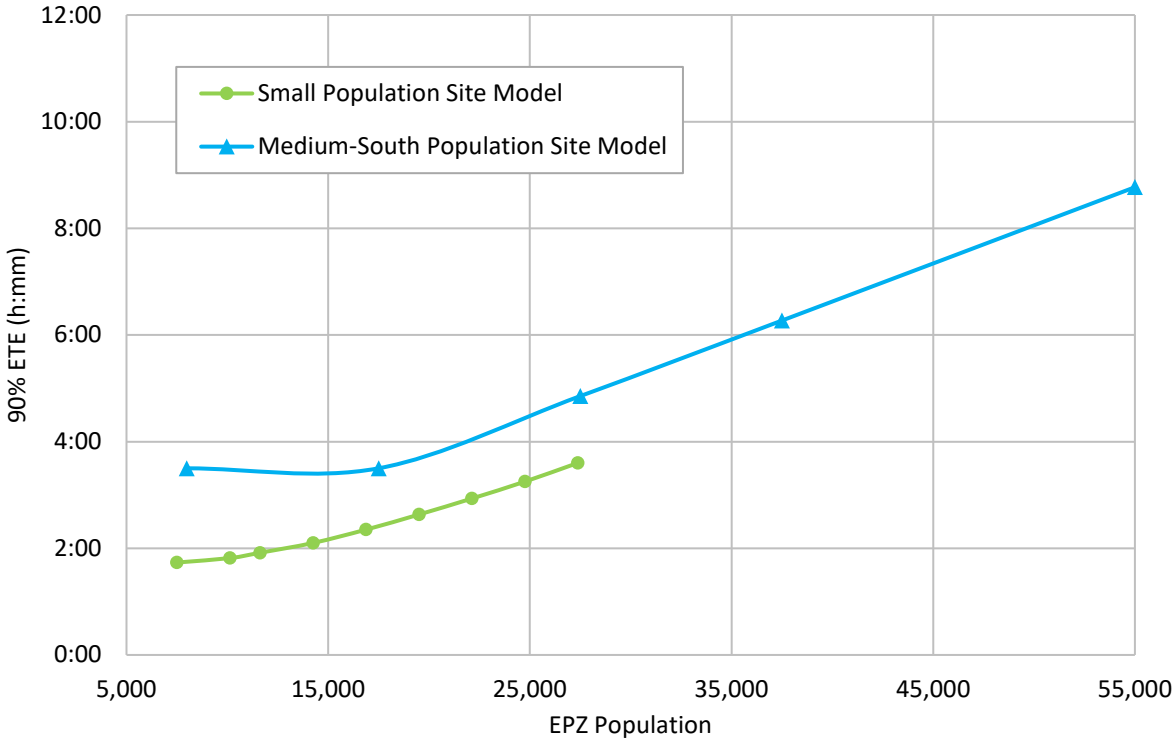

Figure 7-23 Ten Mile 90 percent ETEs, Small and Medium-South Site Population Analyses

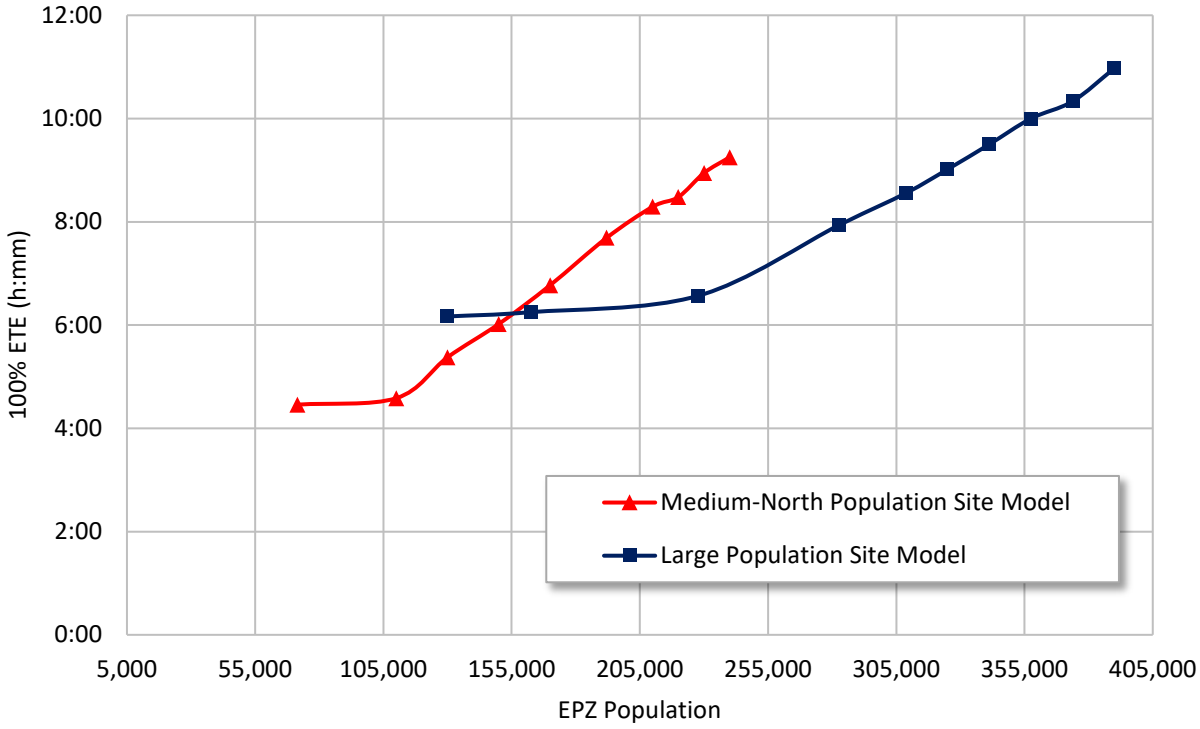

Figure 7-24 Ten Mile 100 percent ETEs, Medium-North and Large Site Population Analysis

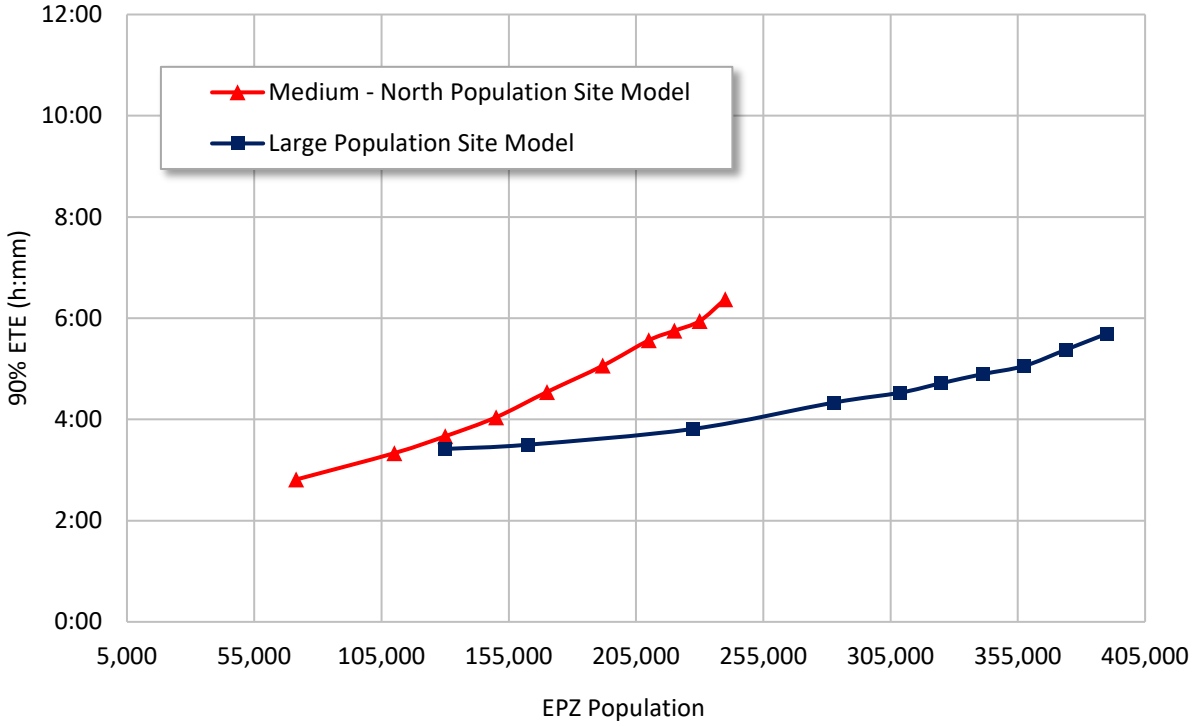

Figure 7-25 Ten Mile 90 Percent ETEs, Medium-North and Large Site Population Analysis

7.3.1.6 Exit Volume Results for Population Parameter

The EPZ exit flow rate is the number of vehicles that exit the 10-mile EPZ per hour. Vehicle counts were collected at the EPZ boundary in 5-minute intervals and converted into vehicles per hour consistent with the standard practices of traffic engineering.

Figure 7-26 shows the rate of vehicles leaving the 10-mile EPZ in the small population site. It can be seen that the rate of egress increases as the population increases with a peak at approximately 8,500 vehicles per hour. Each scenario consistently reached a peak exit rate approximately 45 minutes into the evacuation. Additionally, each scenario reached a higher exit volume indicating capacity continued to serve increased demand. For the largest population scenarios, the graph flattens for a period of time before the evacuation is finished, suggesting a constant rate of outflow and queue dissipation along select routes.

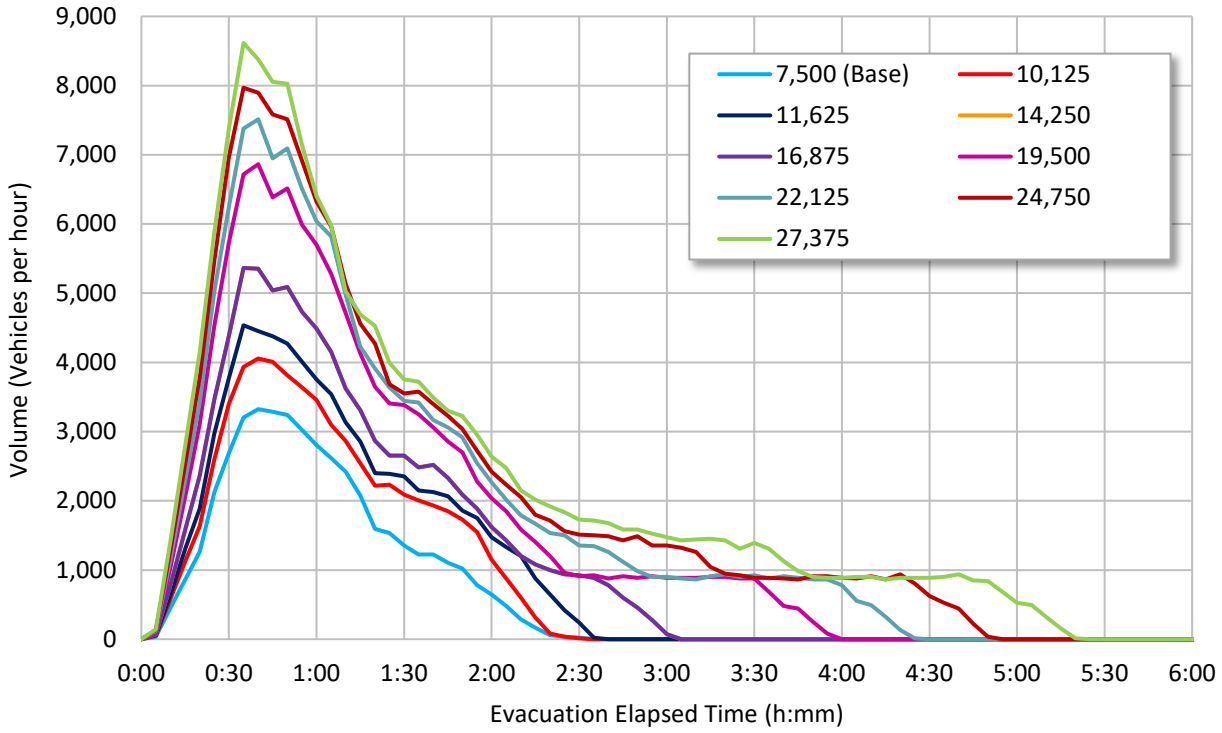

Figure 7-26 EPZ Exit Volumes, Small Population Site Population Analysis

Figure 7-27 shows the rate of vehicles leaving the 10-mile EPZ in the medium population site, southern region. It illustrates that the peak exit rate increased with each scenario. This indicates that roadway capacity was accommodating demand, even with congestion. This is another indication of the robustness of roadway capacity in low population areas. Each scenario consistently reached a peak at approximately 1:30 into the evacuation. Compared to the peak in the small population site model, this indicates that the peak outflow is also related to mobilization time. Again, the graphs were observed to flatten for a period of time before the evacuation finished only for the scenario with an EPZ population of 55,000 people. This suggests a constant rate of outflow and queue dissipation.

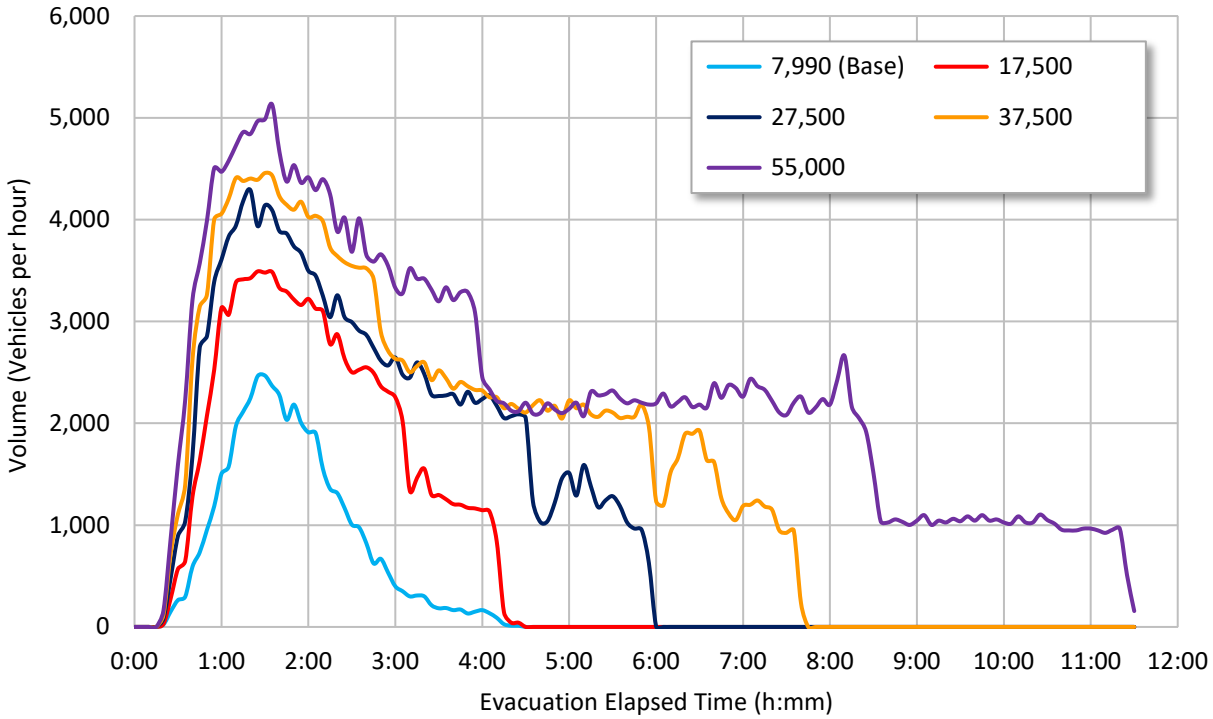

Figure 7-27 EPZ Exit Volumes, Medium-South Population Site Population Analysis

Figure 7-28 shows the rate of vehicles leaving the 10-mile EPZ in the medium-north side. The graph shows that several of the scenarios, including the base, peaked at about 27,000 vehicles per hour. That indicates the maximum rate the roadway capacity can handle. Each scenario reached a peak consistently at approximately 1:15 into the evacuation. The graphs were not observed to flatten for a period of time before the evacuation finished like in the small and medium-south population site models. This would suggest that there were queues dissipating at the 10-mile boundary that formed somewhere inside the EPZ.

Figure 7-29 shows the exit rate from the 5-mile ring for the medium population site, northern region. The graph illustrates that the base case of 192,000 people achieves the maximum exit rate indicating the roadway capacity limit within the 5-mile ring. The peak exit flow rates follow the same pattern as traffic at the 10-mile boundary in that as population increases, the peak times come slightly earlier. It can also be observed that peak exit flow rates drop about 500 vehicles per hour as population increases. This is likely due to congestion in the 5-10 mile region limiting the outflow. It can be seen that for larger EPZ populations the exit volume decreases significantly reaching approximately 0 vehicles per hour (gridlock conditions) at one point. The standstill traffic at the 5-mile boundary is consistent with the observations made during visual inspection of the simulation. There are only four egress points within the 5-mile region which limits the routes out of the area.

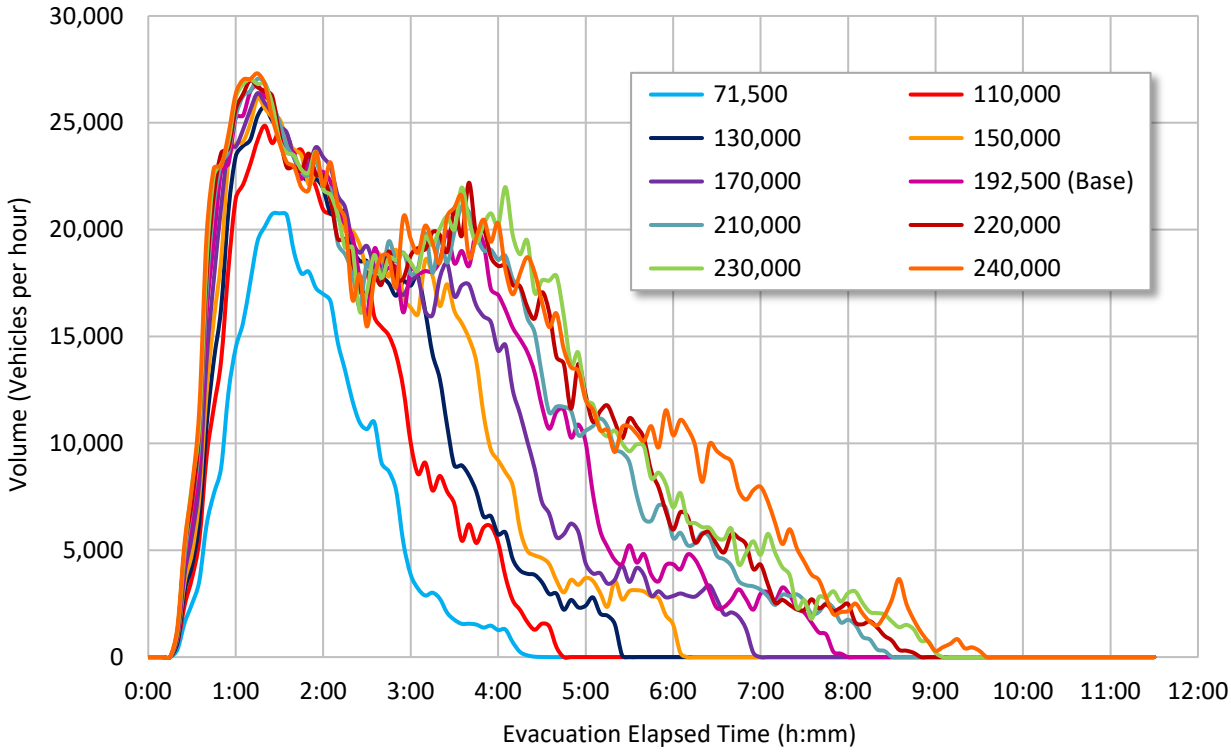

Figure 7-28 EPZ Exit Volumes, Medium-North Population Site Population Analysis

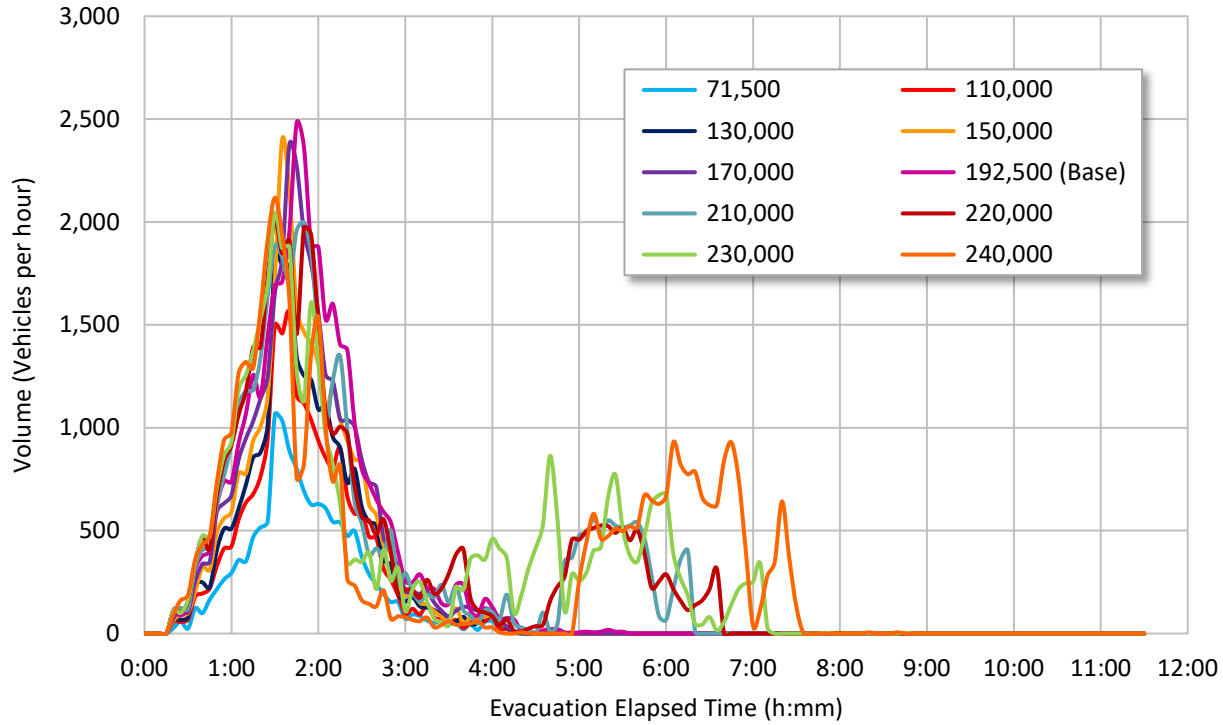

Figure 7-29 Five Mile Exit Volumes, Medium-North Population Site Population Analysis

Figure 7-30 shows the rate of vehicles leaving the 10-mile EPZ in the large site. The figure shows that the rate of egress increases as the population increases with the highest peak at approximately 55,000 vehicles per hour. Each scenario consistently reached a peak at approximately 1:15 minutes into the evacuation. The graphs were observed to flatten for a period of time before the evacuation finished which was the result of a few vehicles arriving at the EPZ boundary after they were discharged out of queue somewhere inside the EPZ and not at a queue at the EPZ boundary. Visual inspection of the simulation showed that there was a local bottleneck between the 6 and 7-mile rings. This internal bottleneck extended the 100 percent ETE although congestion everywhere else inside 10-mile EPZ had already been cleared.

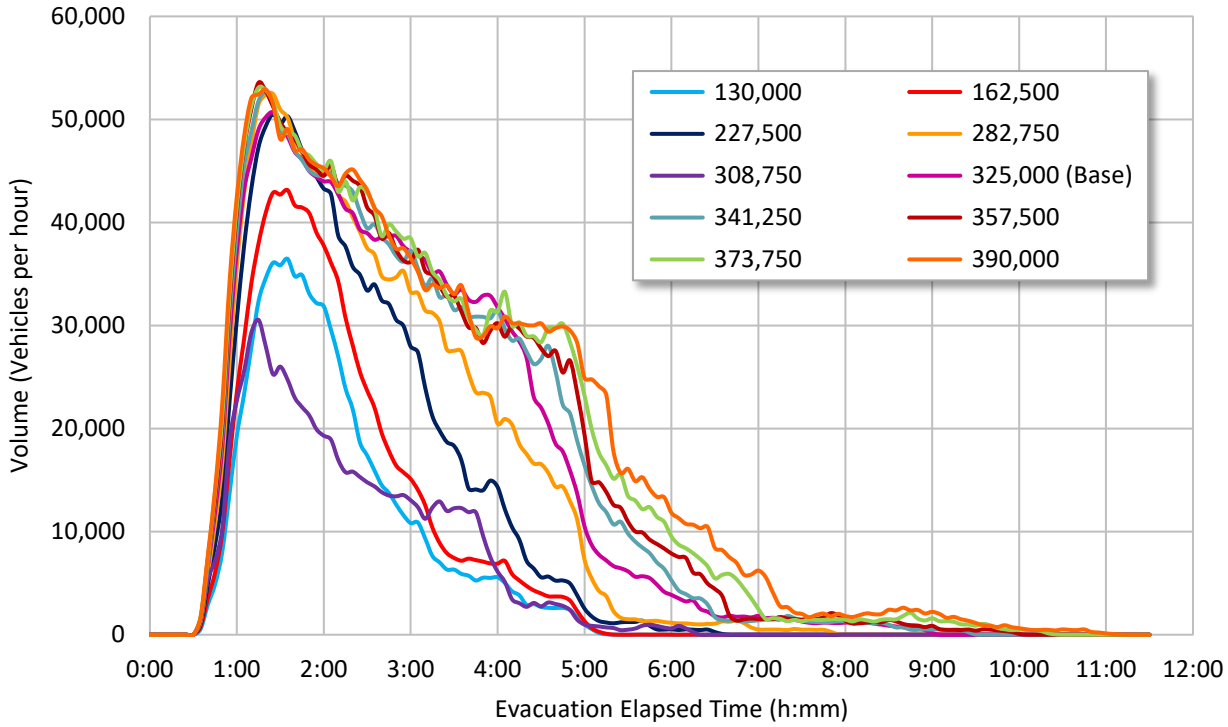

Figure 7-30 EPZ Exit Volumes, Large Population Site Population Analysis

7.3.1.7 Broader Findings, Population Parameter Results

This element of Task 4 sought to determine the importance of population in the development of ETEs. Intuitively, population would be a key parameter as it determines demand on the roadway network. These results illustrate well-recognized fundamental relationships in traffic engineering that relate travel demand and road capacity. The findings from the three models showed that as the population increased above a certain threshold, the impact on ETEs was more pronounced.

In particular these results illustrate how demand and capacity interact to influence the formation of congestion. This was shown to occur in all three sites whenever travel demand approached the capacity of the road network. However, the assessment showed that ETEs at low population sites are not sensitive to realistic population growth. The scenarios used for the assessment increased population without improving the roadway network. This is not a reflection of reality where roadway infrastructure would expand with growing population, at least to some extent. The assessment also determined that ETEs at high population sites and capacity constrained

areas such as the medium population site northern region are sensitive to modest increases in population.

In relation to the evacuation of NPP EPZs in particular, a key consideration would be the specifics of how and when travel in networks is influenced by localized conditions. The results from the medium site show that ETEs can vary significantly due to population distribution and network characteristics. In locations where localized capacity restrictions or population density distributions have the potential to result in significant congestion and delay (e.g., coastal locations), demand that approaches network capacity has the potential to significantly impact ETEs. This would suggest that performing a separate analysis by sectors with heterogeneous characteristics could provide a better understanding of the evacuation process and enhance protective action strategies. This would be especially important when considering staged evacuations and may provide useful insight for the development of protective action strategies. In practice, ETE studies provide these type of sector analyses which take into account wind direction and ERPA designations for the study of keyhole and staged evacuations [4]. Although this may be of benefit to medium-to-large population sites, the effort to produce these separate analyses may not be warranted for small population sites because lower populations are more likely to have relatively small differences by sector.

The percentage of vehicles removed from the simulation was small for these analyses. If the percentages were not small, it could have artificially lowered the ETE. For NPPs, an artificially lower ETE could potentially affect the protective action strategy. The percentage of vehicles removed from the simulation due to code algorithms could be important information for ETE studies.

Taken together, these insights suggest that periodic population assessments between decennial censuses provide useful information for large population sites or area with capacity constraints, but less so for low population sites unless population is known to be significantly increasing.

7.3.2 Mobilization Time Results

Developers of ETE studies must obtain information from EPZ residents regarding how quickly they would or could mobilize for evacuation. The information is gathered by telephone survey and various loading curves are developed from this data. The loading curve is accepted as a reasonable estimate of public behavior. This element of Task 4 seeks to determine the importance of this parameter.

This study considered the overall mobilization time and also the rate at which vehicles are loaded on to the network. Faster loading rates were expected to stress the network resulting in early activation of bottlenecks or extension of queues at existing bottlenecks which, in some cases could spillback to upstream locations. The queue spillback to these locations could deactivate some bottlenecks, however, the network would remain severely congested. The findings demonstrate that in some cases there is a tradeoff between mobilization time and evacuation efficiency and that faster mobilization times can lead to increased evacuee delay even while reducing the overall evacuation time.

7.3.2.1 Small Population Site Mobilization Time Parameter Results

The 10-mile 100 percent ETE in the small population site was observed to increase with increasing mobilization times as shown in Table 7-23. The 2, 5, and 10-mile 100 percent ETEs increased by 30 minutes or more with mobilization times of 3 hours or longer. The 90 percent ETE was less sensitive to the extended mobilization times. This is because the 100 percent ETE is governed by the tail of the evacuation and is more impacted as the total mobilization time extends. Significant increases in ETE was driven by the longer mobilization times and not by congestion. This is demonstrated by a consistent 14 to 17 minute difference between the 100 percent ETE and the corresponding mobilization time in all scenarios. The results suggest that there was little to no congestion in the network and the 15 minute difference is the approximate average network travel time to the EPZ boundary after approximately 100 percent of the vehicles had been loaded into the network. Average evacuee delay was also observed to decrease slightly with longer mobilization time durations.

Figure 7-31 shows the loading curves for the faster mobilization time scenarios (dashed lines) and cumulative percent evacuees (solid lines) for the small population site model at the 10-mile ring. Figure 7-32 shows the corresponding data for slower loading rates. The ETE curve is very close to the loading curve due to the lack of congestion in all mobilization time scenarios.

Table 7-23 Small Population Site Mobilization Time Analysis

Scenario Number	Mobilization Time (h:mm)	Average Evacuee Delay (minutes)	2-Mile		5-Mile		10-Mile	
			90% ETE	100% ETE	90% ETE	100% ETE	90% ETE	100% ETE
1[1]	2:15	14	1:35	2:18	1:35	2:21	1:44	2:31
2	2:30	14	1:38	2:34	1:39	2:38	1:46	2:47
3	2:45	13	1:46	2:48	1:48	2:50	1:55	2:59
4	3:00	14	1:35	3:03	1:35	3:06	1:44	3:15
5	4:00	12	2:15	4:02	2:12	4:05	2:15	4:15
6	4:30	12	1:49	4:30	1:46	4:34	1:50	4:44
7	5:00	9	2:45	5:03	2:35	5:07	2:45	5:17
8	6:00	8	3:11	6:03	3:00	6:07	3:04	6:17
9	6:30	9	3:25	6:35	3:10	6:38	3:10	6:47

[1] Base model.

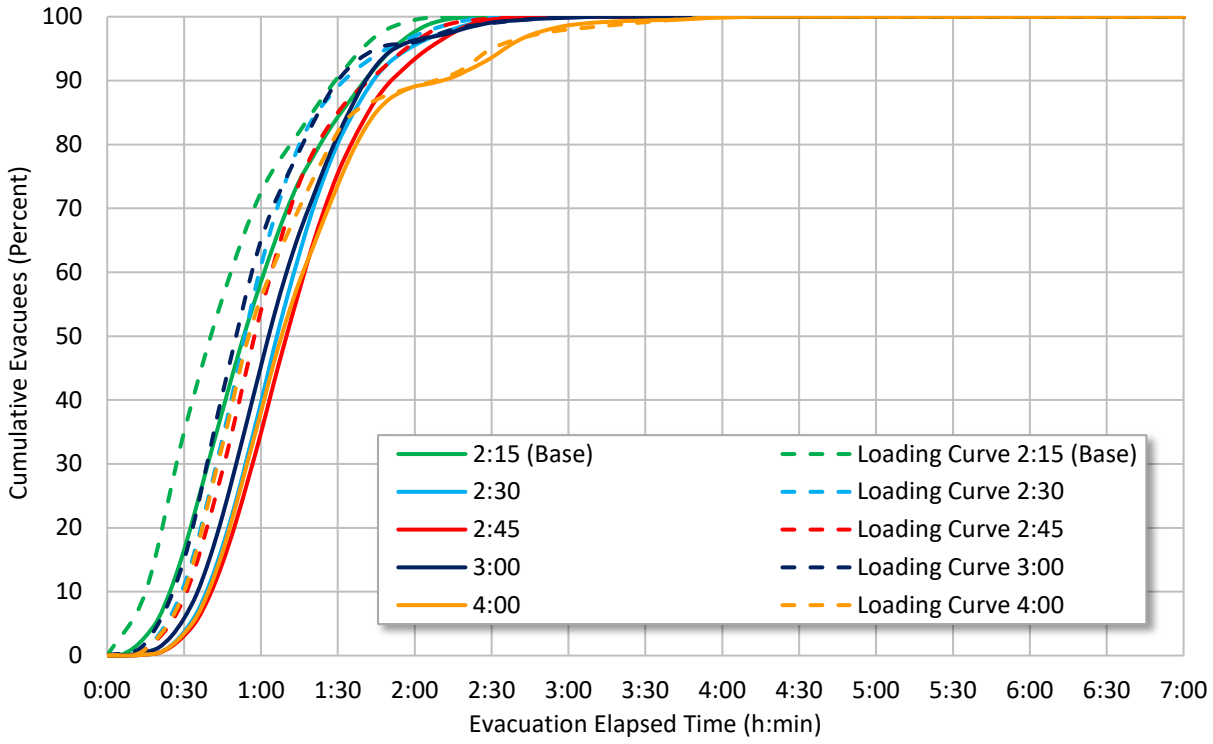

Figure 7-31 Ten Mile ETE Curves, Small Population Site Faster Mobilization Times

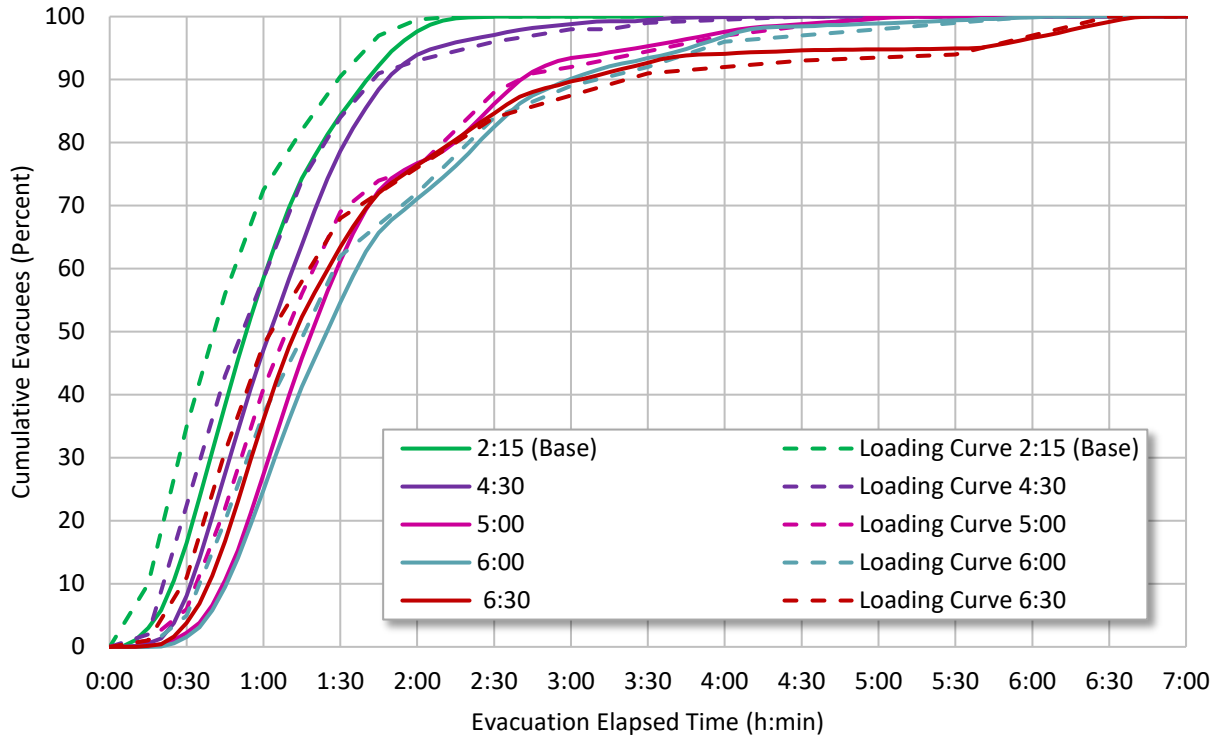

Figure 7-32 Ten Mile ETE Curves, Small Population Site Slower Mobilization Times

7.3.2.2 Medium Population Site Mobilization Time Parameter Results

Table 7-24 shows the ETE at the 2, 5, and 10-mile rings in the medium population site model. This site has a geography that is reflected in the results. The 2-mile ETE only involves the rural southern region and is largely free of congestion regardless of loading curve. The simulation reported that approximately 10,000 vehicles did not exit the 10-mile EPZ for scenarios 1, 2, 3, 5, and 6. Visual inspection of the simulation showed complete gridlock in a few areas. This suggests the medium population site model was very sensitivity to short mobilization times and the simulation could not handle the faster rate of vehicles loaded into the network.

As expected, the 10-mile 100 and 90 percent ETEs were observed to increase significantly with mobilization times of 8:00 and 10:00 in the medium population site model. However, the more gradual loading of the demand improved travel conditions and may have removed some bottlenecks in the network. This was evidenced by the significant reduction in average evacuee delay as shown in Table 7-24.

Figure 7-33 and Figure 7-34 show the loading curves for each scenario (dashed lines) and cumulative percent evacuees (solid lines) for the medium population site at the 10-mile ring. In general, it can be seen that the separation between the loading curve and the ETE curve is wider for faster mobilization times, indicating congested conditions. The separation narrows for the 8:00 and 10:00 mobilization time scenarios suggesting improvements in traffic conditions.

Table 7-24 Medium Population Site Mobilization Time Analysis

Scenario Number	Mobilization Time (h:mm)	Average Evacuee Delay (minutes)	2-Mile		5-Mile		10-Mile	
			90% ETE	100% ETE	90% ETE	100% ETE	90% ETE	100% ETE
1	2:30	106	1:55	2:48	2:42	4:30	4:33	6:15
2	2:45	100	2:05	3:02	2:26	4:38	4:33	6:21
3	3:00	108	1:50	3:12	2:41	4:23	4:30	6:18
4[1]	4:00	70	2:40	4:03	2:47	5:05	5:03	7:41
5	4:00	97	2:22	3:17	3:17	4:32	4:32	6:13
6	4:30	112	2:03	4:40	2:45	5:02	4:32	6:26
7	5:00	65	3:02	5:17	4:22	6:15	5:02	7:07
8	6:00	63	3:30	6:13	4:46	6:33	5:13	7:18
9	6:30	64	3:41	6:50	4:46	6:56	5:25	7:18
10	8:00	36	5:37	8:03	5:30	8:10	6:30	8:35
11	10:00	16	7:20	10:00	7:26	10:08	7:25	10:30

[1] Base model.

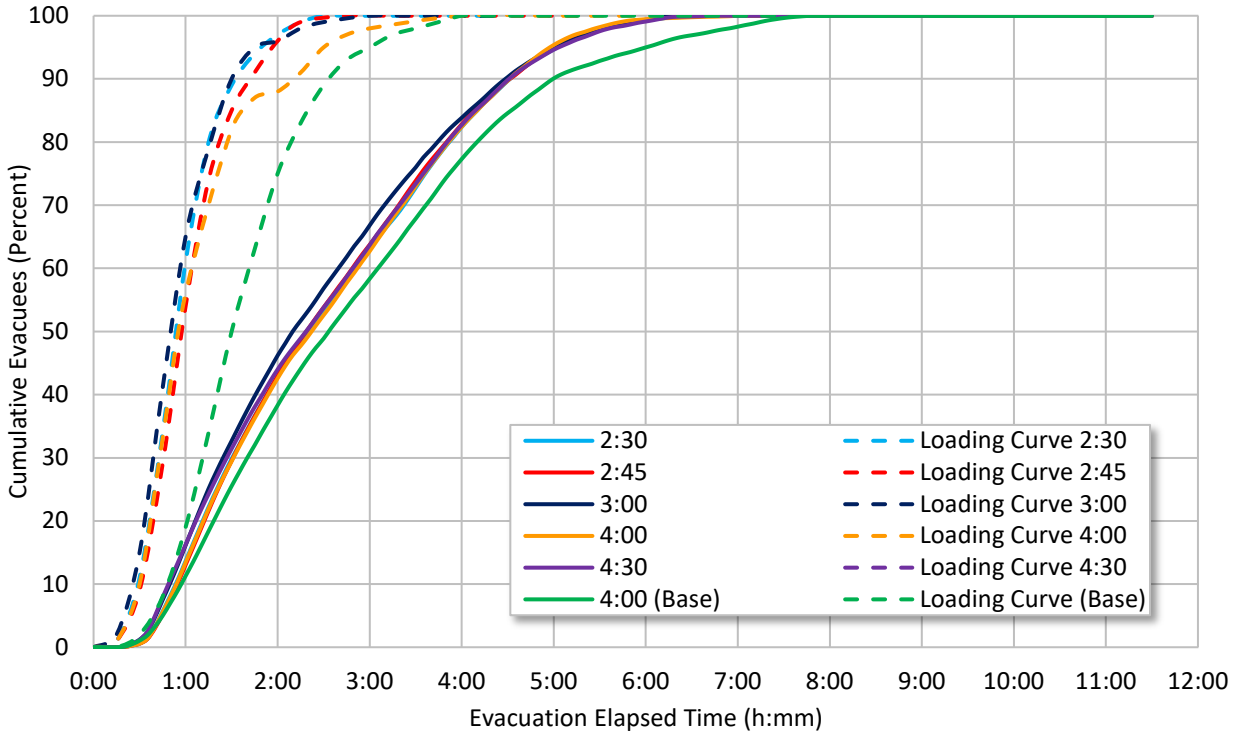

Figure 7-33 Ten Mile ETE Curves, Medium Population Site Faster Mobilization Times

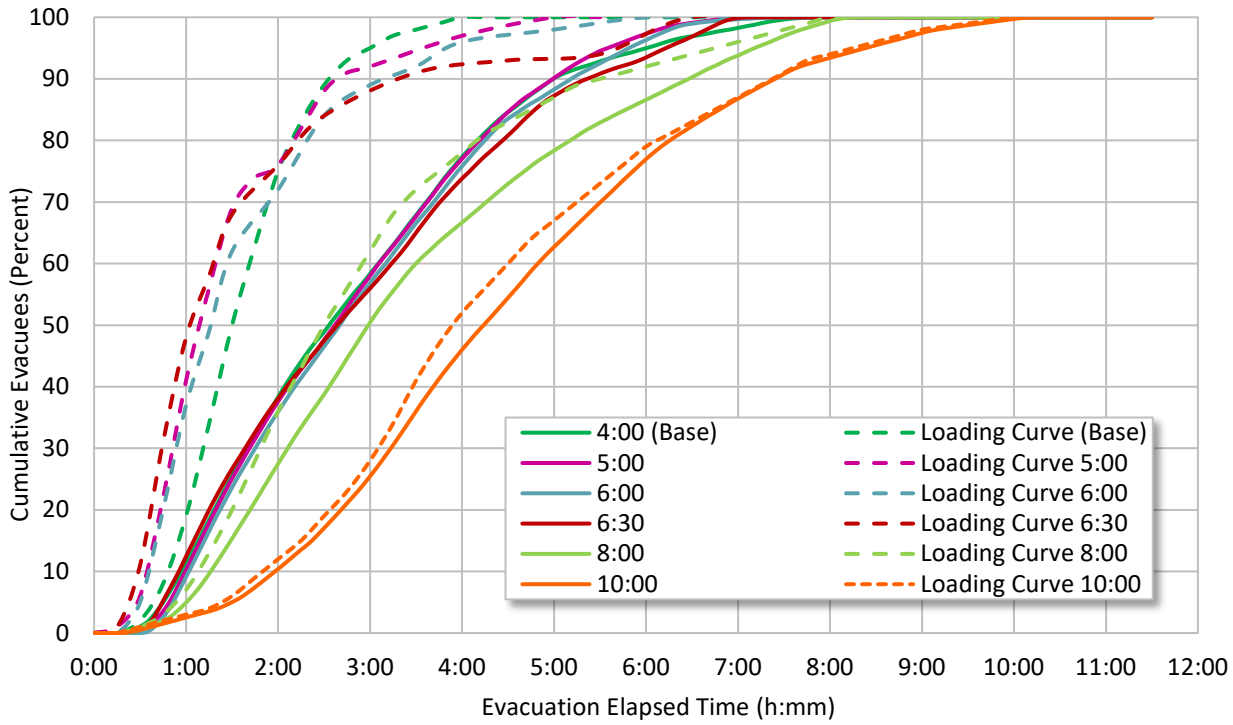

Figure 7-34 Ten Mile ETE Curves, Medium Population Site Slower Mobilization Times

7.3.2.3 Large Population Site Mobilization Time Parameter Results

Table 7-25 shows the 90 and 100 percent ETEs for the 2, 5, and 10-mile rings for the large population site model. Figures 7-35 and 7-36 show the loading curves and ETE curves for the site. The curves were split among the figures for ease of viewing. The figures show that the roadway network capacity meets demand at most of the mobilization times tested. Evacuation curves group at about the same congestion level as the base case and do not exceed the significance level of a 30 minute increase or decrease. The 2, 5, and 10-mile ETEs are not significantly affected by mobilization time until scenarios 10 and 11 where the ETEs follow the mobilization times. In scenarios 10 and 11, congestion decreases as shown by the evacuation curves following the loading curves more closely than the base case and by the decrease in average evacuee delay as shown in Table 7-25. After a certain threshold is reached, ETE times increase linearly with the increased mobilization times as in the small and medium population site models. In all scenarios, the number of vehicles not exiting the EPZ remained less than 1.2 percent.

Table 7-25 Large Population Site Mobilization Time Analysis

Scenario Number	Mobilization Time (h:mm)	Average Evacuee Delay (minutes)	2-Mile		5-Mile		10-Mile	
			90% ETE	100% ETE	90% ETE	100% ETE	90% ETE	100% ETE
1	2:30	73	2:45	4:45	4:15	6:47	4:50	9:21
2	2:45	72	2:45	4:53	4:13	7:03	4:53	9:18
3	3:00	73	2:58	5:02	4:11	6:26	4:51	9:15
4	4:00	69	3:13	4:47	4:12	7:16	4:48	9:13
5	4:30	69	3:17	5:17	4:07	7:17	4:52	9:02
6[1]	4:45	62	3:40	5:05	3:57	6:35	4:43	9:01
7	5:00	60	3:50	5:45	4:17	7:30	4:57	9:07
8	6:00	61	4:01	6:42	4:21	7:16	5:01	9:12
9	6:30	55	3:58	6:50	4:11	7:05	5:06	9:40
10	8:00	31	5:11	8:20	6:26	8:33	6:26	9:28
11	10:00	21	7:17	10:15	8:18	11:30	8:08	11:30

[1] Base model.

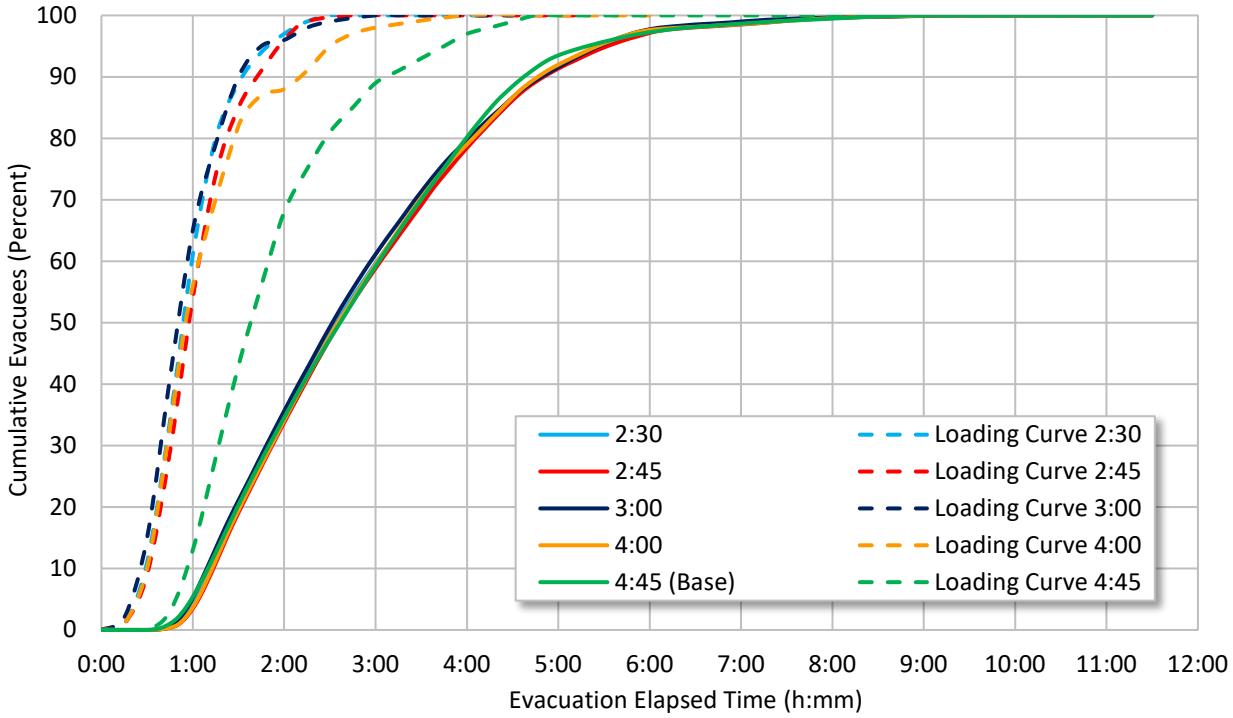

Figure 7-35 Ten Mile ETE Curves, Large Population Site Faster Mobilization Times

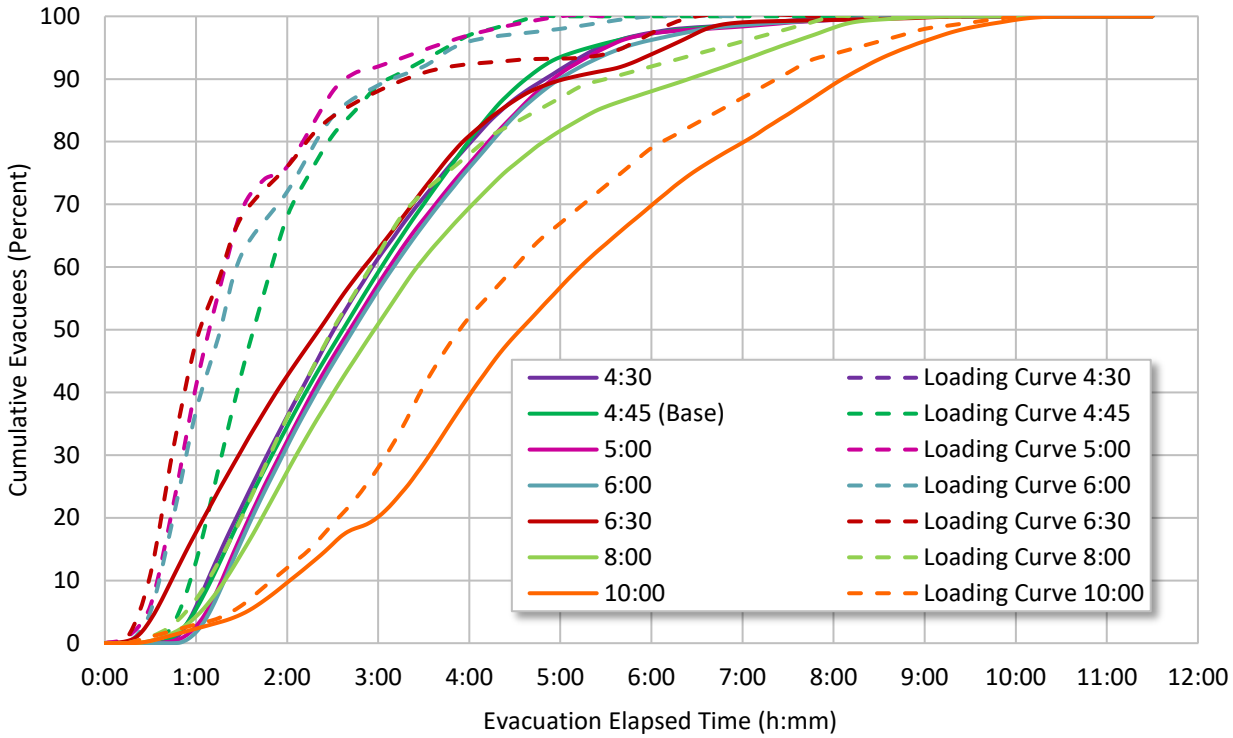

Figure 7-36 Ten Mile ETE Curves, Large Population Site Slower Mobilization Times

7.3.2.4 Comparison of Mobilization Time Parameter Results

Figure 7-37 illustrates the sensitivity of the 10-mile 100 percent ETEs to mobilization time for each representative site. The results reveal the impact of mobilization time within congested and uncongested states. In the congested state, ETEs are governed by the relationship between demand and capacity. For sites in the uncongested traffic state, which are typically observed in areas with small populations, mobilization time governs the ETEs [13] [31]. Under such assumptions, uncongested sites can clear faster with shorter mobilization times. This is clearly illustrated in the results for the small population site model where the 100 percent ETEs increased linearly as mobilization time increased. Based on this relationship, ETEs can be approximated by the mobilization time plus a constant equal to the average network travel time after 100 percent of the vehicles have been loaded onto the network. For the small population site, the approximate value of this travel time varied from 14 to 17 minutes in the mobilization time scenarios tested.

For the medium and large population site models, the relationship is more complex. In many cases, the medium and large population site model ETEs appeared to be insensitive to mobilization times. Further investigation of the large population site model revealed that the reason for this was related to the loading of vehicles onto the network. More specifically, the "actual" loading of 100 percent of the evacuees in the large population site model was consistently observed to be between 8:30 and 9:00 across all the mobilization time scenarios (except for the 10:00 mobilization time scenario) because congestion limited the rate at which vehicles could physically access the network. Even though vehicles were mobilized (generated in the network) at different times, congestion prevented quick access the network evacuation routes. Furthermore, it was found that such loading was related to local traffic conditions limiting the entrance of evacuees from origin nodes located between the 6 and 7-mile rings. This network constraint caused vehicles to continue to enter the network even after the rest of the network was empty. Therefore, the ETE remained about the same for many of the scenarios. However, eventually a threshold point is reached, beyond which the ETE increases linearly with mobilization time.

The results for the medium population site model revealed that the network struggled to handle faster loading rates. An increase in average evacuee delay of up to 50 minutes (compared to the base model) was observed for this site. In addition, there were signs of severe congestion and gridlock in scenarios with faster mobilization times and some vehicles did not exit the simulation. This observation was consistent for all the random seeds used to test each scenario. From the perspective of NPP evacuations, average evacuee delay can be important from a protective action strategy standpoint. A longer delay time would result in a higher potential of exposure to the plume. As a result, there may be no advantage in attempting to get everyone mobilized quickly, because it may actually increase the risk of exposure as evacuees drive to their destinations. Previous research in evacuation modeling has suggested that MOEs other than ETEs could be used to account for traffic conditions and exposure to hazards over time and space [28]. Evacuee delay time appears to be an important MOE for characterizing the evacuation process. Overall, it was seen that faster mobilization times reduced ETEs, but increased delay. This was clearly observed in the two scenarios having equal mobilization time spans of 4:00 for the medium population site model. The loading curve for one scenario loaded about 82 percent of the evacuees onto the network within 1:30 while the other scenario loaded about 83 percent of the evacuees loaded onto the network within 2:15. The ETEs are significantly different from each other; more notably, the average evacuee delay was 37 percent higher for the faster 4:00 mobilization time scenario as compared to the base model 4:00 scenario, even though the ETE was shorter.

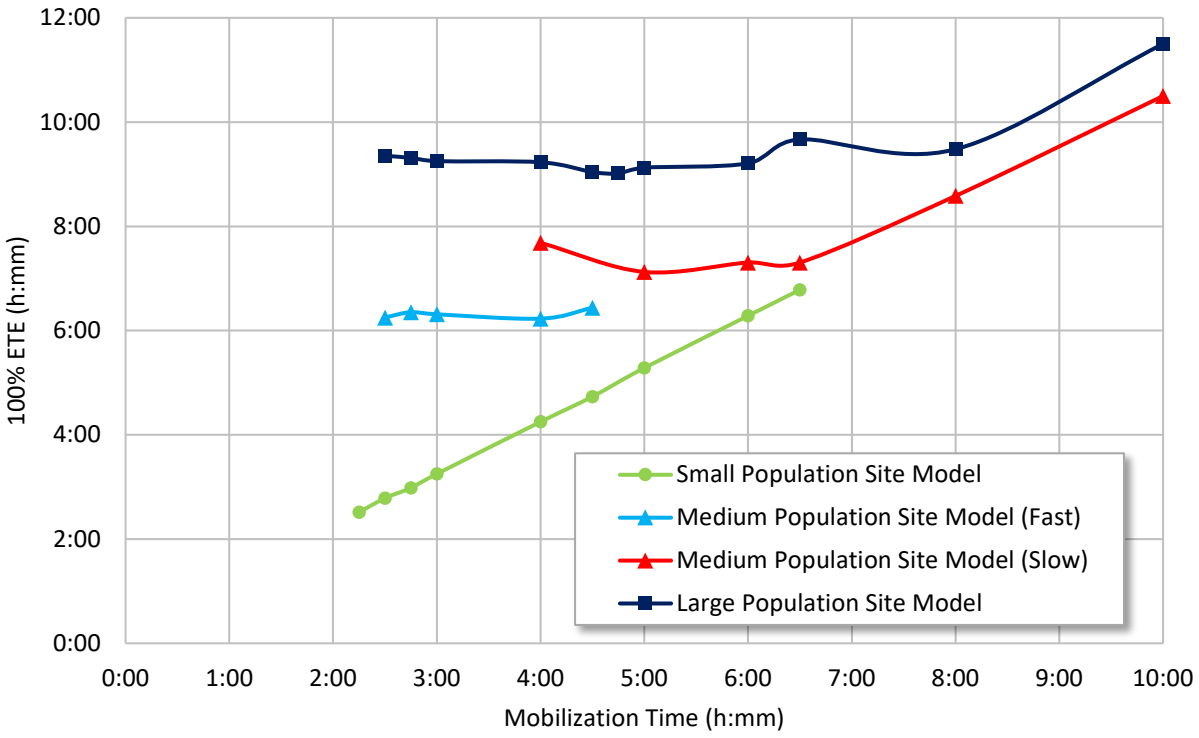

Figure 7-37 Ten Mile 100 Percent ETEs, Small, Medium, and Large Population Site Mobilization Time Analysis

7.3.2.5 Exit Volume Results for Mobilization Time Parameter

Flow rate was measured as the number of vehicles that exited the 10-mile EPZ over 5 minute data collection intervals. Flow rate was then converted into vehicles per hour.

Figure 7-38 shows the exit volumes out of the 10-mile EPZ for the small population site model. In general, the maximum volume of vehicles leaving the EPZ decreased with longer mobilization times. This is because the rate of loading of vehicles was generally decreased. The exit volume for the 6:30 scenario was observed to decrease to approximately 0 vehicles per hour for about 2 hours and then pick up again. However, this was not due to traffic conditions inside the EPZ. The volume exiting the EPZ was extended because of the loading rate characteristics of this scenario which loaded vehicles very rapidly at the beginning and then slowly for the rest of the duration (refer to the loading curve).

Figure 7-39 shows the exit volumes out of the 10-mile EPZ for the medium population site model. In general, the maximum volume of vehicles leaving the EPZ decreased with longer mobilization times. This is because the rate of loading of vehicles was decreased and was not due to worsening traffic conditions inside the EPZ. This is evidenced, in particular, for the 8:00 and 10:00 mobilization time scenarios. The 10-hour mobilization scenario shows periods of static exit flows interspersed in the time to reach the peak exit flow rate. This again is related to the slow loading of vehicles into the network.

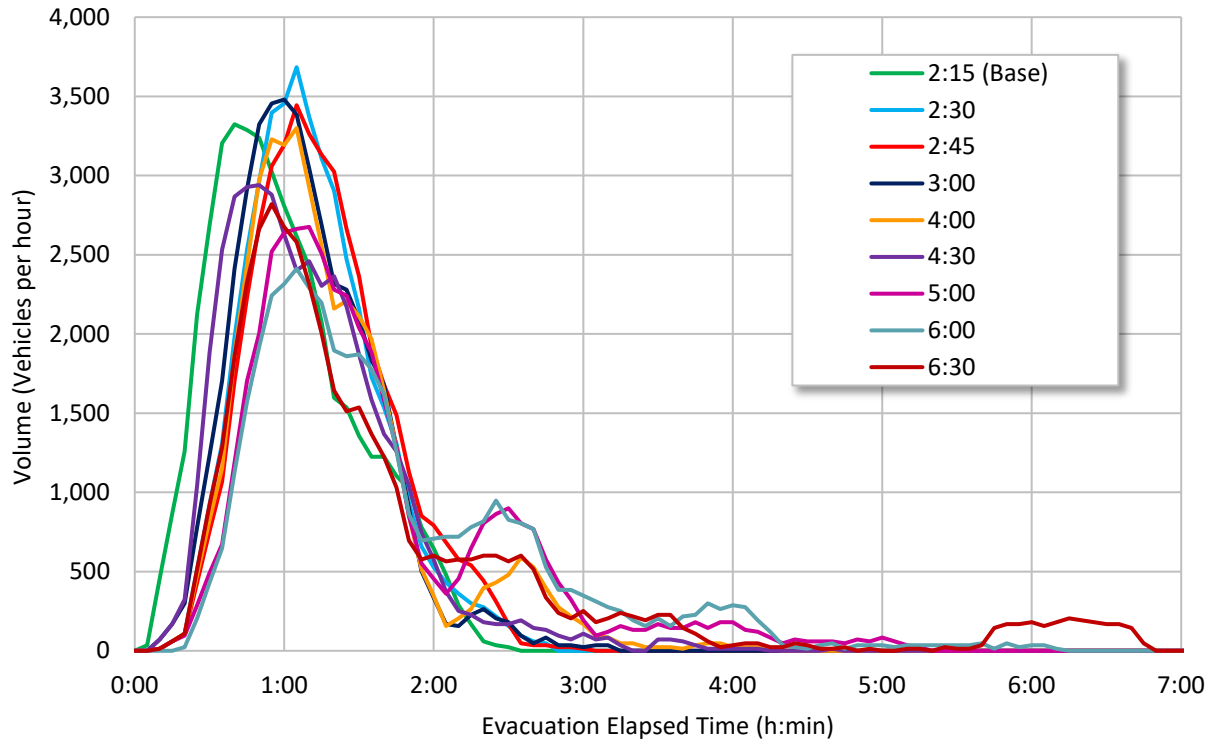

Figure 7-38 EPZ Exit Volumes, Small Population Site Mobilization Time Analysis

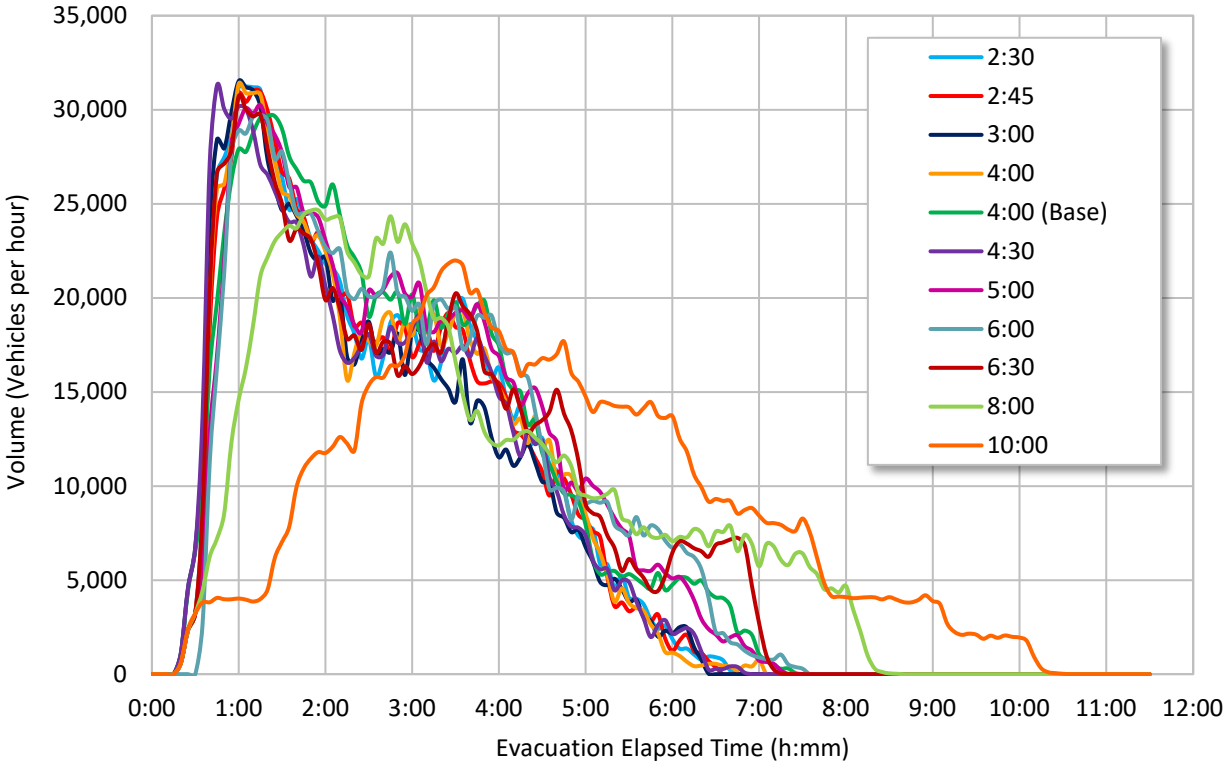

Figure 7-39 EPZ Exit Volumes, Medium Population Site Mobilization Time Analysis

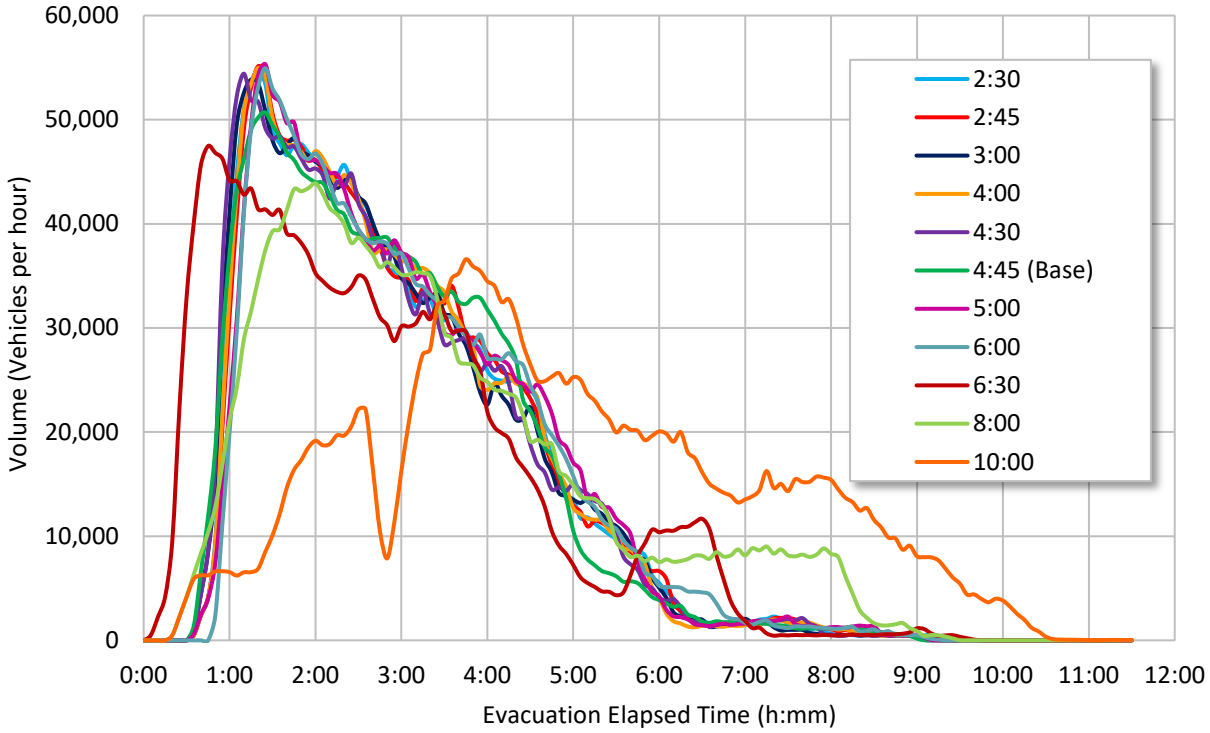

Figure 7-40 EPZ Exit Volumes, Large Population Site Mobilization Time Analysis

Figure 7-40 shows the exit volumes out of the 10-mile EPZ for the medium population site model. As in the other models, the maximum volume of vehicles leaving the EPZ decreased with longer mobilization times. The exit volumes for the 10-hour mobilization time scenario drop significantly at around 2 hours and 45 minutes into the evacuation compared to the other scenarios and then increased again. This significant drop in the volume is related to the mobilization time. Since the vehicles are loaded very slowly into the network at different geographic locations, vehicles may still be traveling towards the EPZ around that time.

7.3.2.6 Broader Findings, Mobilization Time Parameter Results

The mobilization time analysis results were consistent with previous demand loading and egress scenarios observed during evacuations for other hazards (like hurricanes) and reported in related research. Mobilization time has a direct relationship with ETE for areas with minimal congestion during evacuation and short travel times. Unlike the population parameter, this sensitivity to the mobilization time was most evident at the 2-mile ring in all three of the representative site models.

Congested site ETEs for the 10-mile EPZ are less affected within a range of mobilization times. More in depth reviews of the traffic process within these models suggested that the effects associated with longer and slower loading times were from the “metering effect” that existed for departures within the network. This gradual release into the system limited the formation of congestion despite the creation of the same large demand. However, even though ETEs appeared to be relatively insensitive for a range of mobilization times, faster mobilization times result in significant increases in the average evacuee delay time and decreased system performance. As mobilization times increased, eventually a threshold was met beyond which ETEs followed mobilization time in a linear fashion as in the non-congested small population site

model. The results also indicate there may be an optimal loading rate: one that balances the demand, leaving some excess capacity, while minimizing both ETE and delay time. However, such a consideration is only of academic interest, since it would be impractical to try and control mobilization time to a fine degree in an evacuation.

Another important consideration is that high delays due to congestion may also cause vehicle breakdowns, crashes, and vehicle abandonment due to running out of gas. These situations have been commonly observed in large-scale evacuations, for example, the evacuation of Houston during Hurricane Rita in 2005. Unfortunately, these specific issues are not always immediately accounted for in traffic simulation tools. This is because these tools do not model factors such as the amount of fuel remaining in evacuating vehicles, their accessibility to gas stations, or probability of vehicle mechanical failures (e.g., engine overheating). Some of these conditions could be coded “manually” so that they are represented in a simulation. However, this would require a mathematical model to estimate the amount and location where these would occur.

Mobilization time is an important parameter as the 90 percent ETE—utilized in formulating protective action strategies—can increase with mobilization time almost directly. The assessment showed that the loading curve can affect the ETE through both duration and rate of loading. As such, the methods used to determine mobilization times and develop the loading curve should be better understood. While congested site loading curves may not affect ETEs as directly as free-flowing sites, the shape of the loading curve can significantly affect evacuation dynamics.

7.3.3 Background Traffic Parameter Results

Fundamentally, background traffic represents vehicles on the roadway that physically take up available capacity that evacuating vehicles could otherwise utilize. In this sense, background traffic acts like a friction factor impeding the movement of evacuees. Ingress into the EPZ is controlled by local authorities at some point after the emergency is declared. However, background vehicles continue to enter the region outside the EPZ and use the same roads that evacuees travel. This element of Task 4 assessed the impact to the ETE from background traffic inside and outside the EPZ.

The amount of background traffic was not significant enough to alter the travel dynamics in the models. While additional congestion and delay were present, it did not cause major congestion to the extent that the evacuating vehicles were significantly impacted from exiting the EPZ. A significant sensitivity to background traffic could only be observed at the highest levels of assumed activity of background vehicles for the medium and large population site models. The results presented below involved increases and decreases in background traffic both inside and outside the EPZ. For the medium and large population site models, the background traffic was predominately increased outside of the EPZ. Table 7-13 contains the number of background traffic vehicles modeled inside the EPZ for each scenario.

7.3.3.1 Small Population Site Model Background Traffic Parameter Results

The 90 and 100 percent ETE at the 2, 5, and 10-mile rings are summarized for the small population site model in Table 7-26. The results showed no significant impact on the 90 or 100 percent ETEs. This predominately rural area did not have any major congestion. Therefore, the road network capacity was able to accommodate the demand created by a higher volume of background vehicles without significantly impeding the evacuating traffic.

Figure 7-41 shows the cumulative percent evacuated for the small population site model at the 10-mile ring. The ETE curves for each scenario overlap indicating the evacuation process is not being impacted by background traffic. Higher demands would be needed to affect the evacuation process as was evidenced in the study of EPZ population.

Table 7-26 Small Population Site Background Traffic Analysis

Scenario Number	10-20 Mile Background Traffic Vehicles	Average Evacuee Delay (minutes)	2-Mile		5-Mile		10-Mile	
			90% ETE	100% ETE	90% ETE	100% ETE	90% ETE	100% ETE
1	3,175	12	1:35	2:19	1:35	2:21	1:45	2:31
2[1]	6,350	14	1:35	2:18	1:35	2:21	1:44	2:31
3	7,620	16	1:35	2:19	1:35	2:21	1:44	2:31
4	9,525	17	1:35	2:19	1:35	2:22	1:44	2:31

[1] Base model.

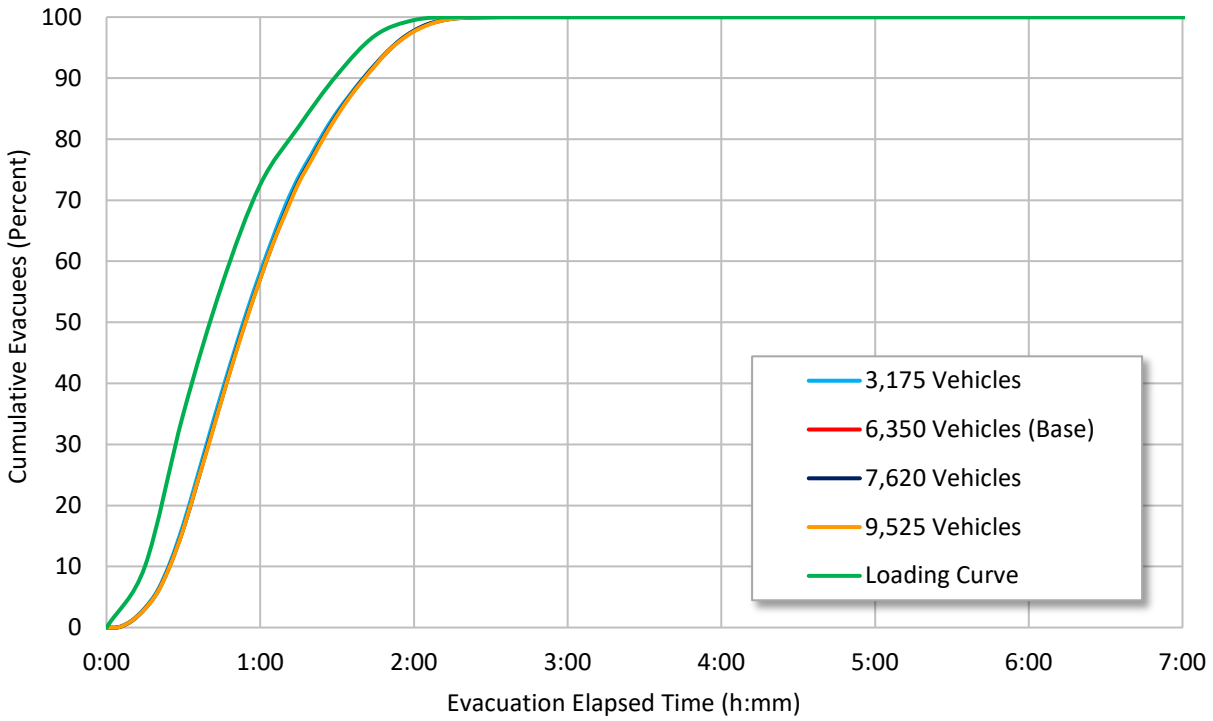

Figure 7-41 Ten Mile ETE Curves, Small Population Site Background Traffic Analysis

7.3.3.2 Medium Population Site Model Background Traffic Parameter Results

The 90 and 100 percent ETE at the 2, 5 and 10-mile rings are summarized for the medium population site model in Table 7-37. Background traffic did not significantly affect the ETEs until it was doubled from the base model value. Overall, the average evacuee delay was observed to increase with increased background traffic which is indicative of degradation of the network-wide travel conditions. In all scenarios, the number of vehicles not exiting the EPZ remained less than 2 percent.

Table 7-27 Medium Population Site Background Traffic Analysis

Scenario Number	10-20 Mile Background Traffic Vehicles	Average Evacuee Delay (minutes)	2-Mile		5-Mile		10-Mile	
			90% ETE	100% ETE	90% ETE	100% ETE	90% ETE	100% ETE
1	24,110	63	2:40	4:03	2:47	5:00	5:00	7:43
2[1]	48,220	70	2:40	4:03	2:47	5:05	5:03	7:41
3	57,860	75	2:40	4:03	2:48	5:18	5:00	7:43
4	72,330	83	2:40	4:05	2:46	5:18	5:03	7:55
5	96,440	95	2:40	4:03	2:50	5:35	5:51	7:55

[1] Base model.

Figure 7-42 shows the cumulative percent evacuated for the medium population site model at the 10-mile ring. The figure illustrates that most of the ETE curves overlap showing about the same congestion and ETE. A doubling of the background traffic did show an effect, but only for a limited duration and conditions improved towards the end of the evacuation. This impact is likely to have been caused by the increased background traffic outside the EPZ as the conditions worsen almost mid-evacuation, which is after background traffic inside the EPZ was loaded into the network.

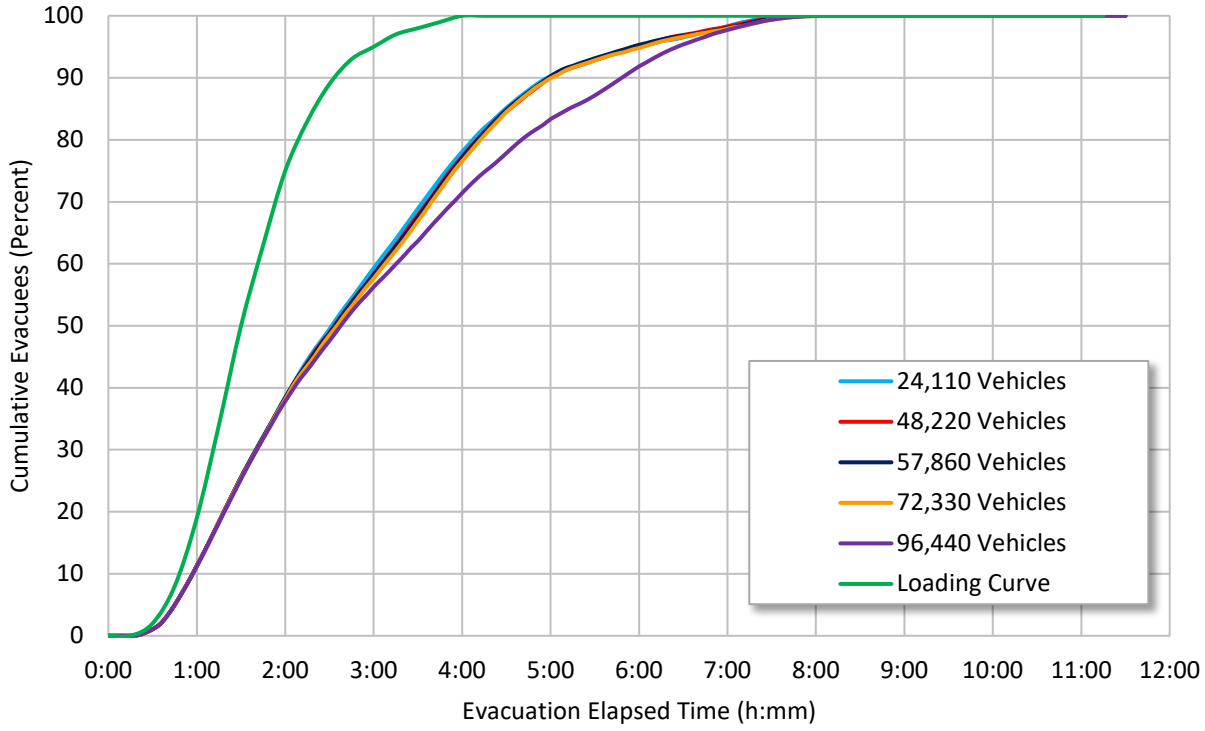

Figure 7-42 Ten Mile ETE Curves, Medium Population Site Background Traffic Analysis

7.3.3.3 Large Population Site Model Background Traffic Parameter Results

Table 7-28 shows the ETEs for the 2, 5 and 10-mile ETE for the large population site model. The 90 percent ETEs were not significantly impacted by the background traffic in most scenarios tested. At the highest amount of background, the ETE was observed to drop and the average evacuee delay in the network increased to more than 2 hours. This suggests travel conditions outside the EPZ caused major gridlock that prevented about 18 percent of the EPZ vehicles (evacuation tail) to exit before the simulation ended. The remaining vehicles would be expected to extend the 10-mile 100 percent ETE for that scenario beyond the reported 8:22. This scenario, however, represents a significant demand on the system with more than 500,000 vehicles simulated. Such a high demand would be unlikely in an evacuation event surrounding an NPP. In all other scenarios, the number of vehicles not exiting the EPZ remained less than 1.5 percent.

Table 7-28 Large Population Site Background Traffic Analysis

Scenario Number	10-20 Mile Background Traffic Vehicles	Average Evacuee Delay (minutes)	2-Mile		5-Mile		10-Mile	
			90% ETE	100% ETE	90% ETE	100% ETE	90% ETE	100% ETE
1	76,000	51	3:41	5:05	3:56	6:38	4:35	8:53
2[1]	152,000	62	3:40	5:05	3:57	6:35	4:43	9:01
3	182,400	65	3:40	5:03	4:01	6:48	4:51	9:01
4	228,000	77	3:41	5:01	4:08	6:41	5:05	9:03
5	304,000	160	3:38	5:06	4:22	7:06	4:53[2]	8:22[2]

[1] Base model.

[2] Approximately 18 percent of vehicles did not exit the EPZ during simulation.

Figure 7-43 shows the cumulative percent evacuated for the large population site model. The ETE curves are very close to each other indicating a minimal impact within the EPZ from increasing background traffic. The evacuation curve for the highest background rate is closer to the loading curve than some other scenarios. This is because about 18 percent of the vehicles did not exit the 10-mile EPZ. The code removes vehicles when severe congestion develops, and this appears to have improved exit flow for a time in this scenario. The other scenarios had less than 1.5 percent vehicles not exiting the EPZ. This result emphasizes the value of using multiple MOEs, such as the number of evacuating vehicles, to assess the quality of the ETE data.

7.3.3.4 Exit Volume Results for Background Traffic Parameter

The EPZ exit flow rate was measured as the number of vehicles that exited the 10-mile EPZ over each 5-minute data collection interval. This flow rate was converted into vehicles per hour and the results are presented in Figures 7-44, 7-45, and 7-46 for the small, medium, and large population sites, respectively. In general, background traffic has a relatively minor impact on the evacuation out of the EPZ as compared to the population and mobilization time parameters. At higher rates of background traffic there are indications of congestion, suggesting queue spillback into the EPZ. However, in general, these results show that demand conditions outside of the EPZ are less influential on the ETE than demand generated from inside the EPZ.

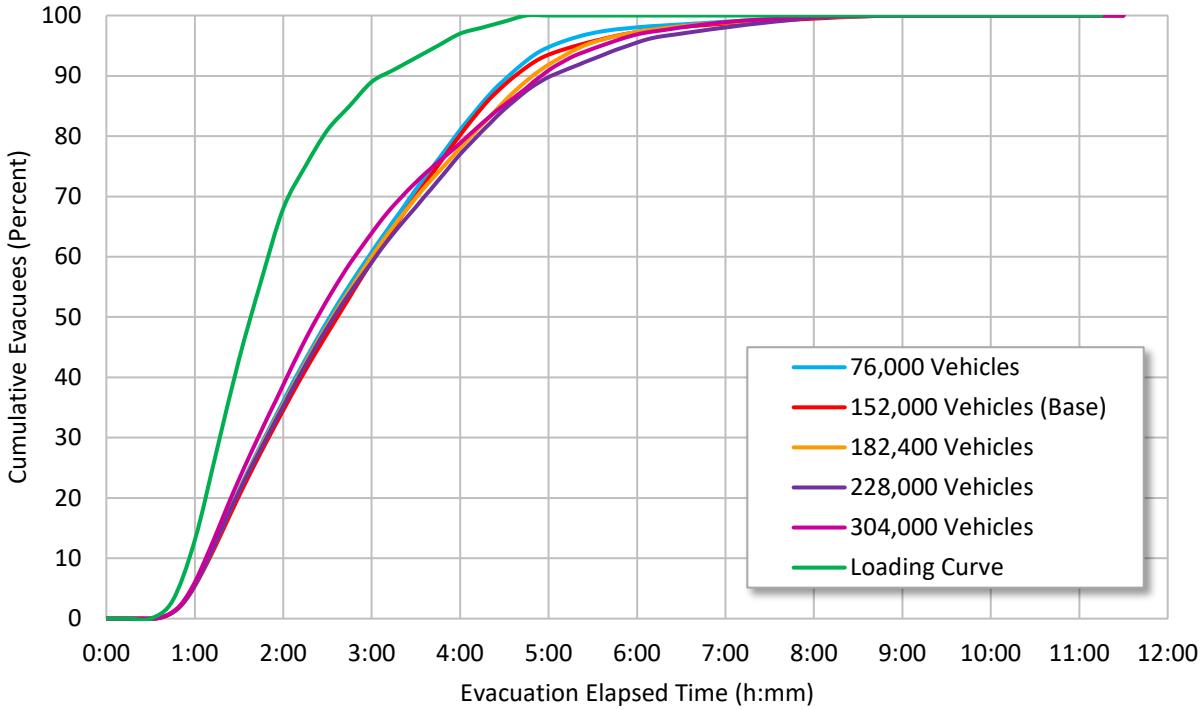

Figure 7-43 Ten Mile ETE Curves, Large Population Site Background Traffic Analysis

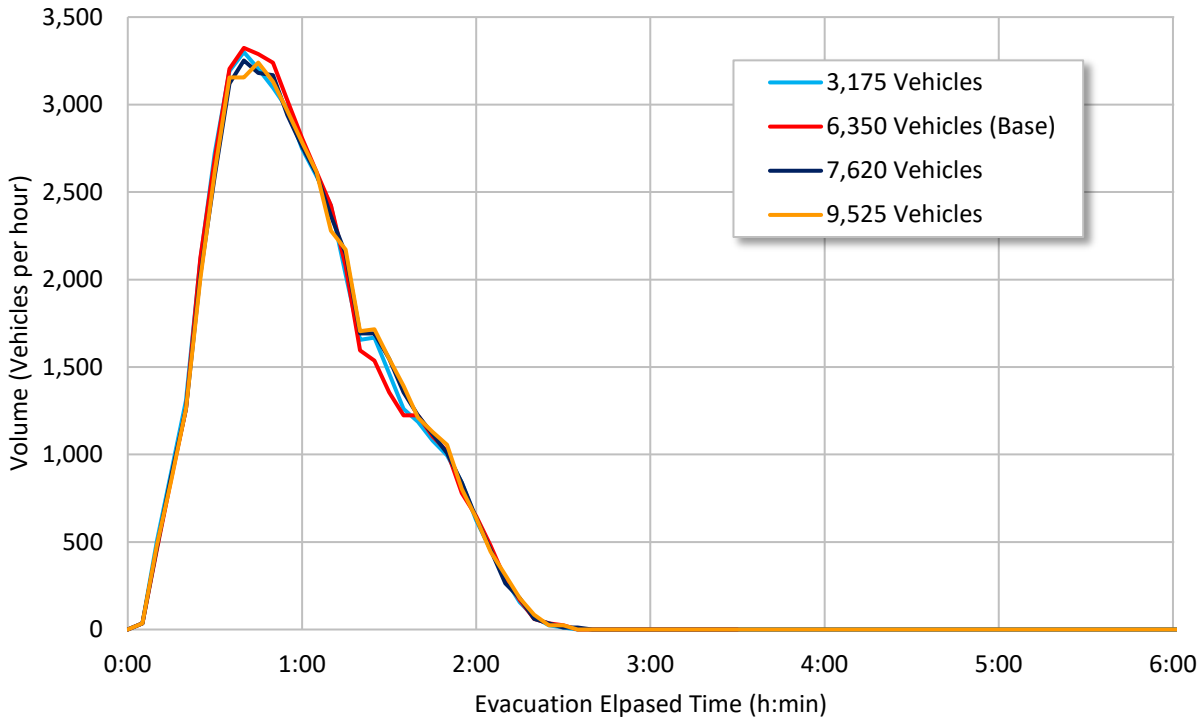

Figure 7-44 EPZ Exit Volumes, Small Population Site Background Traffic Analysis

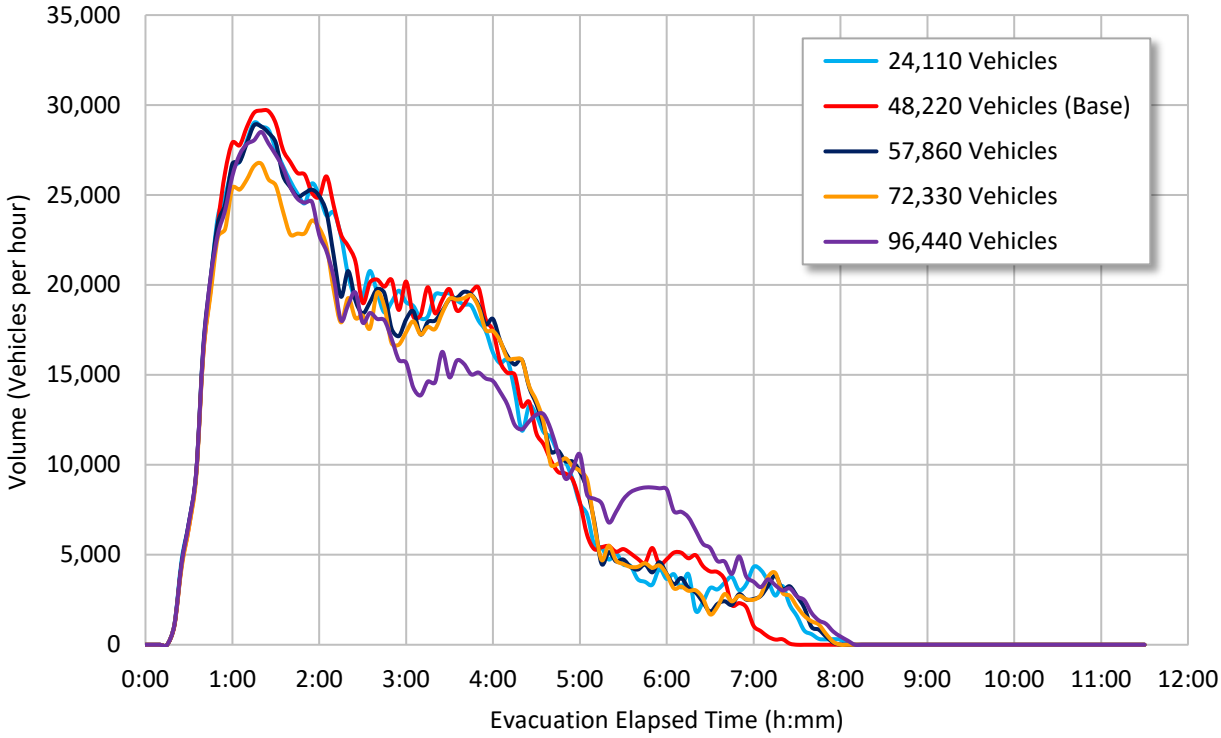

Figure 7-45 EPZ Exit Volumes, Medium Population Site Background Traffic Analysis

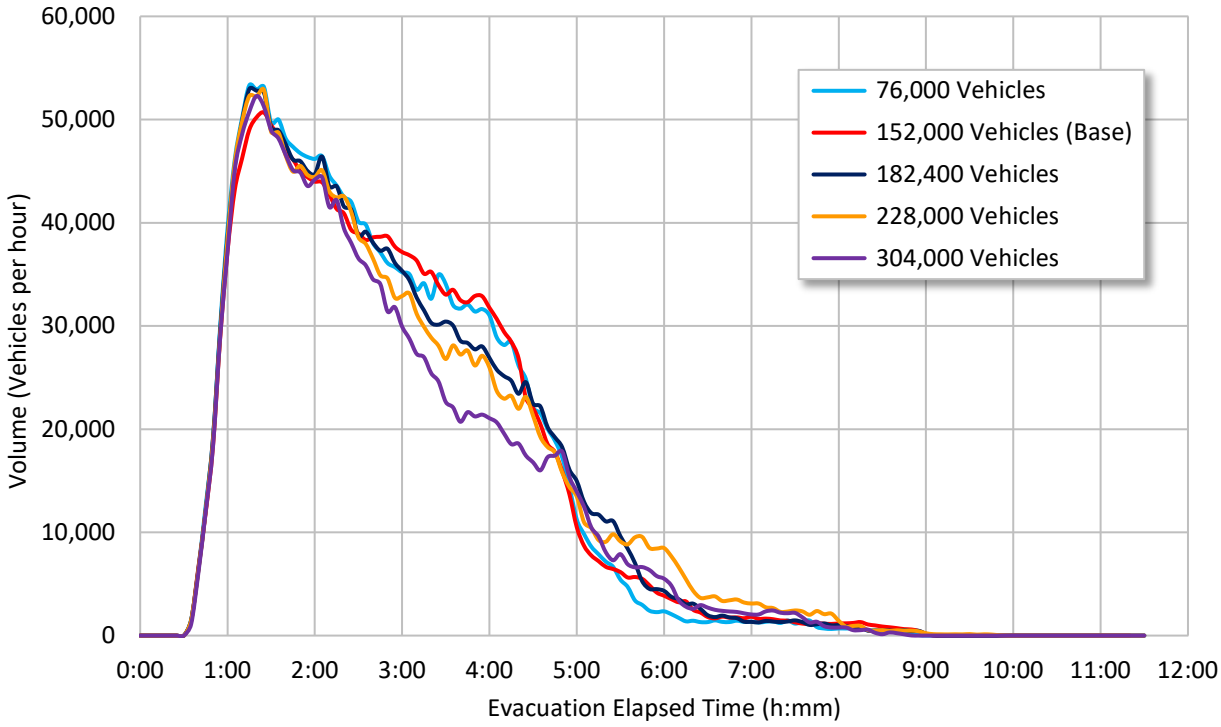

Figure 7-46 EPZ Exit Volumes, Large Population Site Background Traffic Analysis

7.3.3.5 Broader Findings, Background Traffic Analysis Results

Background traffic was not significant enough to alter the travel dynamics in the small population site model and for most of the scenarios in the medium and large population site models. While additional congestion and delay were present in the model, ETEs remained unaffected until background traffic levels nearly doubled. In the medium and large population site models, conditions for evacuees were impacted by the higher background traffic volumes as evidenced by the increase in average evacuee delay. At the highest participation rate in the large population site model, background traffic caused major gridlock and impacted the evacuation process. Although this impact is not evident in the ETE, the impact can be discerned through the other MOEs of average evacuee delay and number of vehicles not exiting the simulation. This finding emphasizes the importance of reviewing other MOEs besides the ETE.

Background traffic did not impact ETEs until unrealistic scenarios were run. This suggests that background traffic is not an important parameter. Background traffic should be included in ETE models, particularly for medium and large population sites, but gathering detailed information on the methods of identifying it will not likely significantly improve ETEs.

7.3.4 Heavy Vehicle Parameter Results

The percentage of heavy vehicles in the network can impact capacity because heavy vehicles are larger and accelerate slower. These characteristics impact surrounding vehicles through a shockwave effect; that is, all vehicles traveling behind the heavy vehicle must subsequently slowdown and speedup as they follow. The extent to which heavy vehicles impact the surrounding traffic depends on how often and by how much trucks are forced to change speeds or stop. There are three primary causes for vehicles to accelerate or decelerate: intersections, congestion and road grade/local topography. This analysis investigated a range of heavy vehicle participation rate on the evacuation process.

It was found that percent heavy vehicles modeled within an EPZ can impact ETEs, but only at high participation rates. The impact of heavy vehicles is likely exacerbated by congestion levels and the density of intersection within the study areas. This analysis investigated a range of heavy vehicle percentages and found that in most cases, the 90 percent ETE was generally insensitive to heavy vehicle percentages between zero and ten percent. However, the 5-mile 90 percent ETE was increased by nearly 1 hour and 20 minutes in the medium population site model. This may suggest that “ball park” estimates of heavy truck percentages may be acceptable in most ETE analysis, so long as it can be reasonably assured the heavy truck percentage would not surpass 10 percent. This study did not investigate the impact of topography and this finding may not be appropriate if roadway grades are in excess of three percent [134].

7.3.4.1 Small Population Site Model Heavy Vehicle Parameter Results

Table 7-29 summarizes the evacuation clearance times for the small population site model at the 2, 5, and 10-mile rings. The results show that 90 percent and 100 percent ETEs were insensitive to the different heavy vehicles scenarios. This was likely due to the low volume of vehicles within the network and relatively few number of intersections. With little congestion and few intersections, trucks were not impacted by “stop-and-go” traffic and therefore did not have to contend with repeated slowing down and accelerating back up to their desired speed. Figure 7-47 shows the cumulative percent evacuated for the small population site model at the 10-mile ring.

The figure shows that the scenario specific evacuation curves are indiscernible. There was no significant effect on the evacuation process by increasing heavy vehicle percentage.

Table 7-29 Small Population Site Heavy Vehicle Analysis

Scenario Number	Heavy Vehicles (Percent)	Average Evacuee Delay (minutes)	2-Mile		5-Mile		10-Mile	
			90% ETE	100% ETE	90% ETE	100% ETE	90% ETE	100% ETE
1	0%	14	1:35	2:18	1:35	2:21	1:44	2:31
2[1]	2%	14	1:35	2:18	1:35	2:21	1:44	2:31
3	10%	15	1:35	2:18	1:35	2:21	1:44	2:31
4	20%	16	1:35	2:18	1:35	2:21	1:44	2:31

[1] Base model.

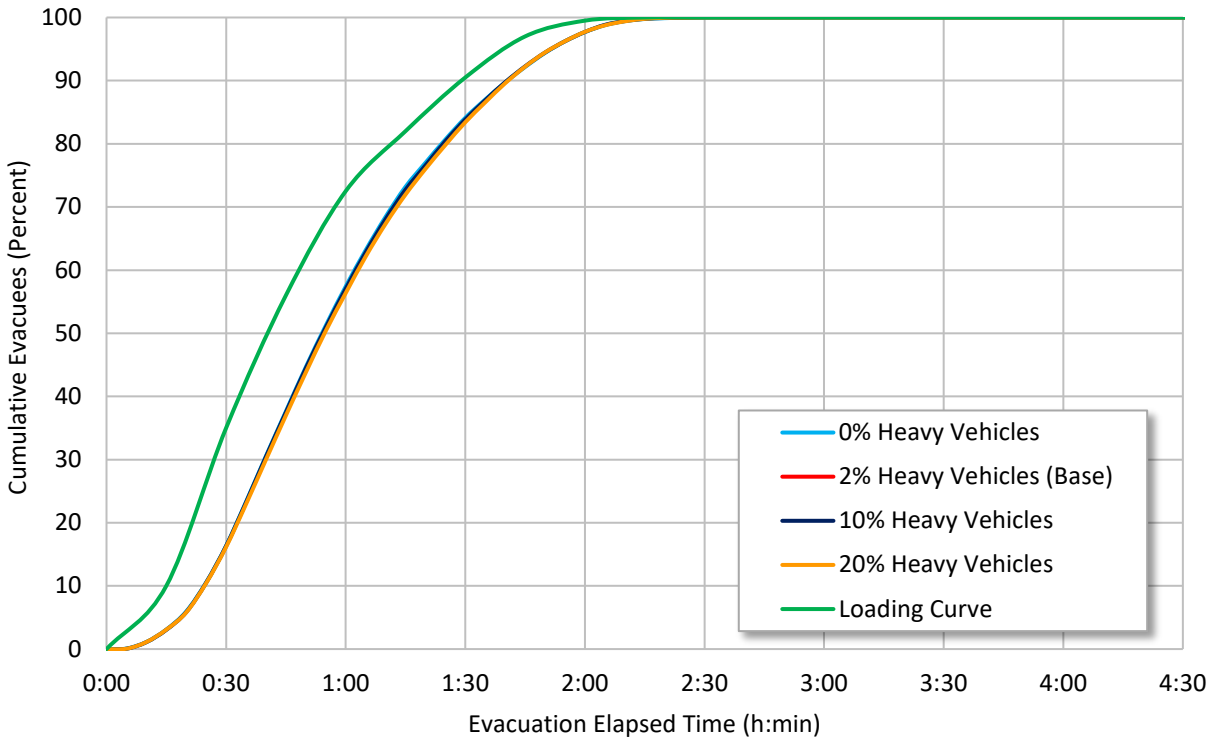

Figure 7-47 Ten Mile ETE Curves, Small Population Site Heavy Vehicle Analysis

7.3.4.2 Medium Population Site Model Heavy Vehicle Parameter Results

Table 7-30 summarizes the evacuation clearance times for the medium population site model at the 2, 5, and 10-mile rings. Within the medium population site model, the 2-mile ring was not impacted. This is because of the rural nature of the southern portion of the medium model. However, at high participation rates for heavy vehicles, a significant effect on the 90 percent and 100 percent ETEs is observed, particularly in the 5-mile ETEs.

The 5-mile 90 percent ETE corresponding to 20 percent heavy vehicles was impacted by over an hour from the base case. However, the 10-mile 90 percent ETE shows only a 20 minute

increase (a non-significant increase). This effect was likely caused by the significant number of residents that live between the 2-mile and 5-mile rings and the limited number of routes to service this demand crossing the 5-mile ring. As the network expands, the population density increases causing an increase in congestion. The density of intersection locations within this area also increases away from the NPP, contributing to the overall impact. At the 10-mile ring the traffic was already hindered by congestion, masking the role played by heavy vehicles. Only when the percentage of heavy vehicles was increased a factor of 10 fold, was the 10-mile 100 percent ETE impacted. In all scenarios, the number of vehicles not exiting the EPZ remained less than 2 percent. These results are shown graphically in Figure 7-48 for the 5-mile ring, and Figure 7-49 for the 10-mile ring.

Table 7-30 Medium Population Site Heavy Vehicle Analysis

Scenario Number	Heavy Vehicles (Percent)	Average Evacuee Delay (minutes)	2-Mile		5-Mile		10-Mile	
			90% ETE	100% ETE	90% ETE	100% ETE	90% ETE	100% ETE
1	0	68	2:40	4:03	2:46	5:11	4:56	7:41
2[1]	2	70	2:40	4:03	2:47	5:05	5:03	7:41
3	10	73	2:40	4:05	3:10	6:23	5:10	7:53
4	20	76	2:40	4:03	4:05	6:58	5:23	8:30

[1] Base model.

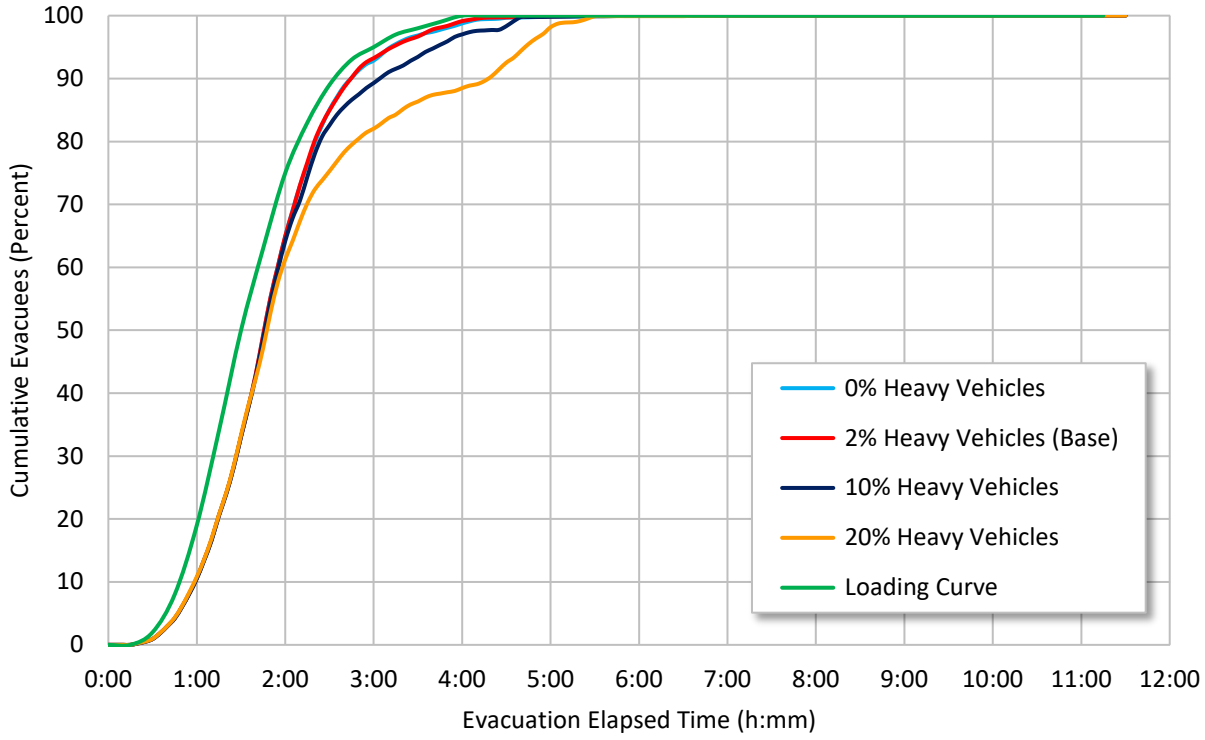

Figure 7-48 Five Mile ETE Curves, Medium Population Site Heavy Vehicle Analysis

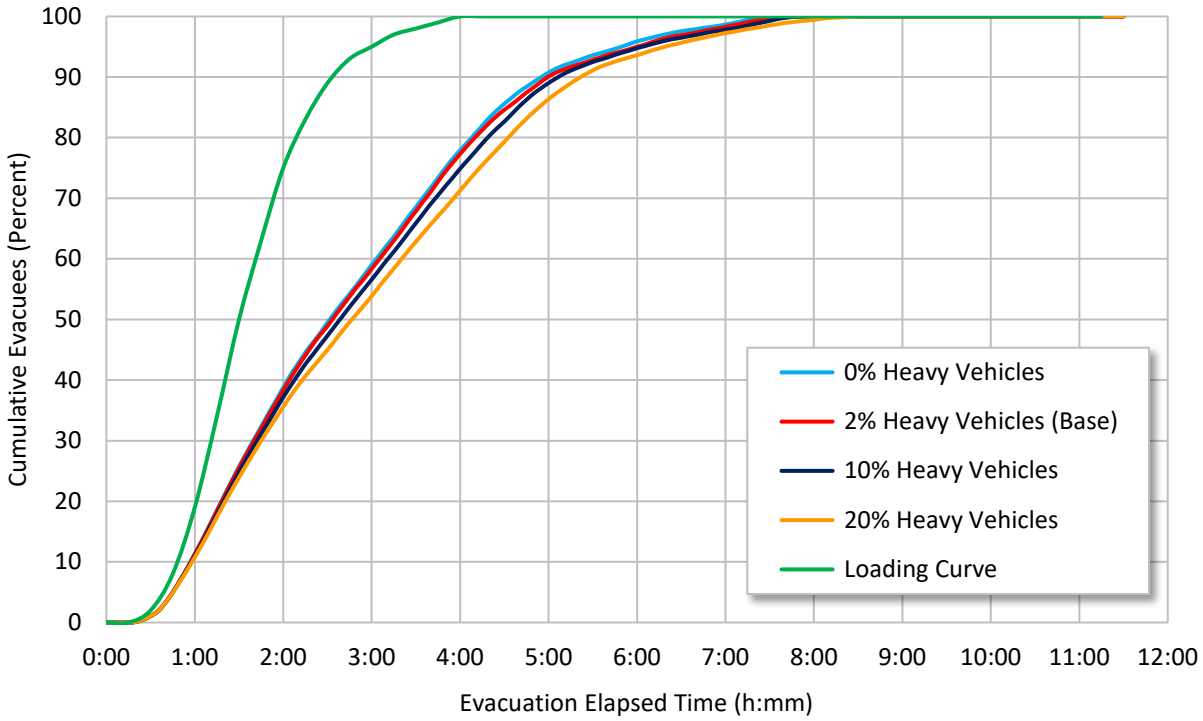

Figure 7-49 Ten Mile ETE Curves, Medium Population Site Heavy Vehicle Analysis

7.3.4.3 Large Population Site Model Heavy Vehicle Parameter Results

Table 7-31 summarizes the evacuation clearance times for the large population site model at the 2, 5, and 10-mile rings. Modeling heavy truck percentages at 0 percent, 2 percent (base model value), and 10 percent showed no meaningful hindrance of the evacuation overall. However, the 5-mile ETE was observed to be impacted significantly with 10 percent heavy vehicles. The high density of intersections within the large population site was likely the key contributing cause to the impact at the 5-mile ring. Figure 7-50 and 7-51 show the cumulative percent evacuated for the large population site model at the 5 and 10-mile rings, respectively. The ETE curves were observed to separate as the percent of heavy vehicles increased, with more relative separation occurring within the EPZ than at the EPZ boundary. Again, this is likely due to the number of intersections within the EPZ, and a masking of the effect of heavy vehicles at the EPZ boundary due to already significant congestion.

Table 7-31 Large Population Site Heavy Vehicle Analysis

Scenario Number	Heavy Vehicles (Percent)	Average Evacuee Delay (minutes)	2-Mile		5-Mile		10-Mile	
			90% ETE	100% ETE	90% ETE	100% ETE	90% ETE	100% ETE
1	0	57	3:40	5:06	3:56	6:31	4:41	8:56
2[1]	2	62	3:40	5:05	3:57	6:35	4:43	9:01
3	10	67	3:48	5:16	4:16	7:08	4:58	9:11
4	20	78	4:18	6:00	4:58	7:56	5:26	9:30

[1] Base model.

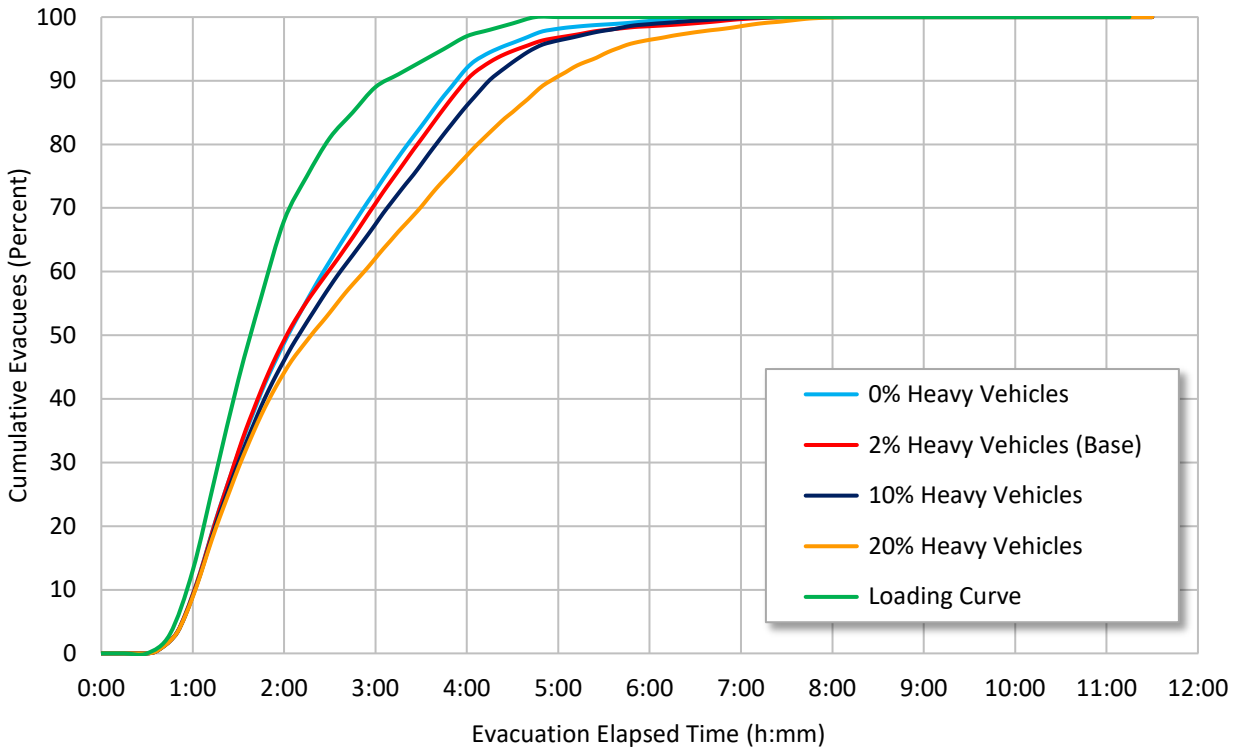

Figure 7-50 Five Mile ETE Curves, Large Population Site Heavy Vehicle Analysis

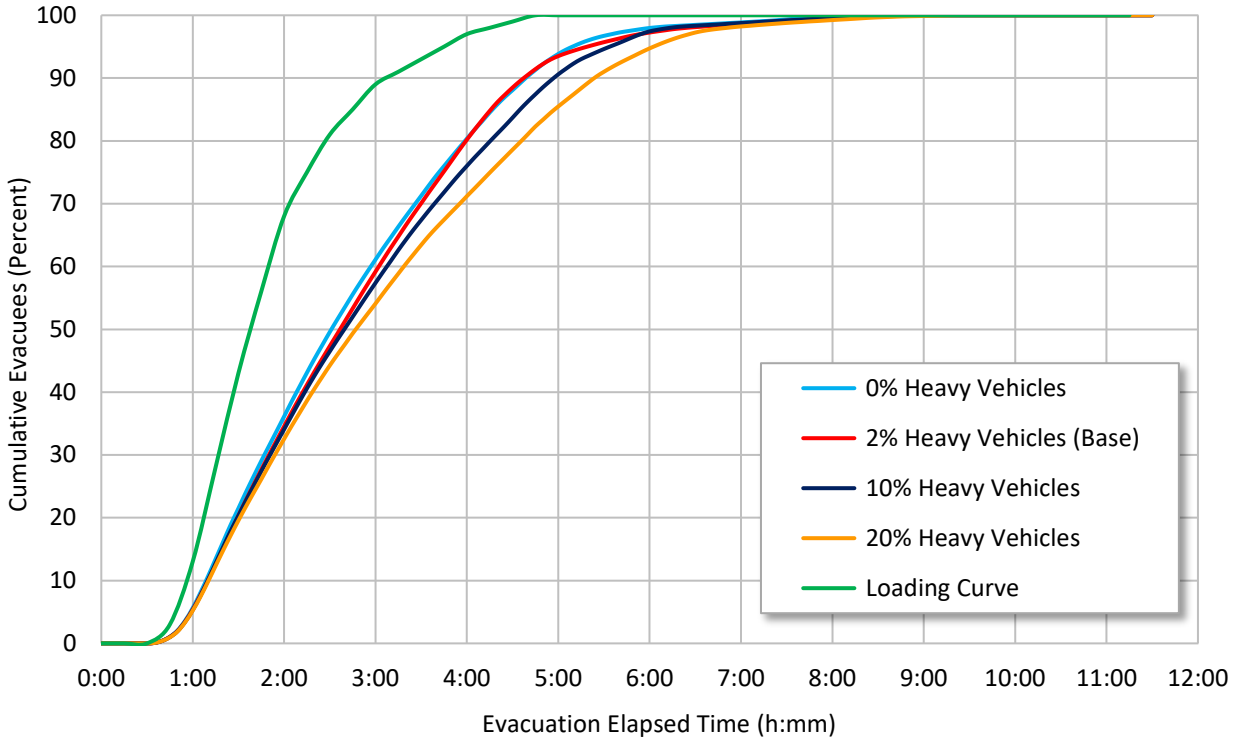

Figure 7-51 Ten Mile ETE Curves, Large Population Site Heavy Vehicle Analysis

7.3.4.4 Exit Volume Results for Heavy Vehicles Parameter

The EPZ exit flow rate was measured as the number of vehicles that exited the 10-mile EPZ over each 5-minute data collection interval. This flow rate was converted into vehicles per hour. Figures 7-52, 7-53, and 7-54 show the rate of vehicles leaving the 10-mile EPZ in the small, medium, and large population site models, respectively. In general, increasing the percent heavy vehicles decreased the peak exit flow rate, and the exit flow rates following the peak, once congestion develops. In all sites, there is a point about half-way through the evacuation where the exit flow rates are sustained at a higher level for increased percent heavy vehicles. This reflects the delayed release of passenger vehicles as the evacuation process catches-up during the evacuation tail.

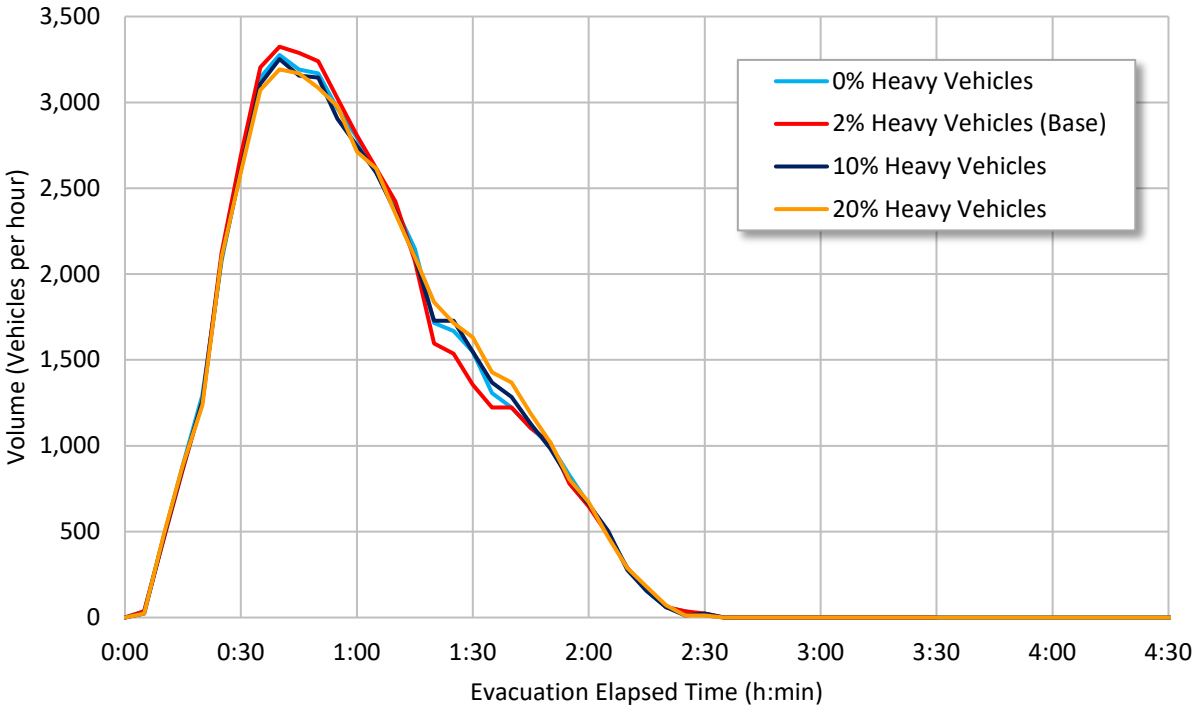

Figure 7-52 EPZ Exit Volumes, Small Population Site Heavy Vehicle Analysis

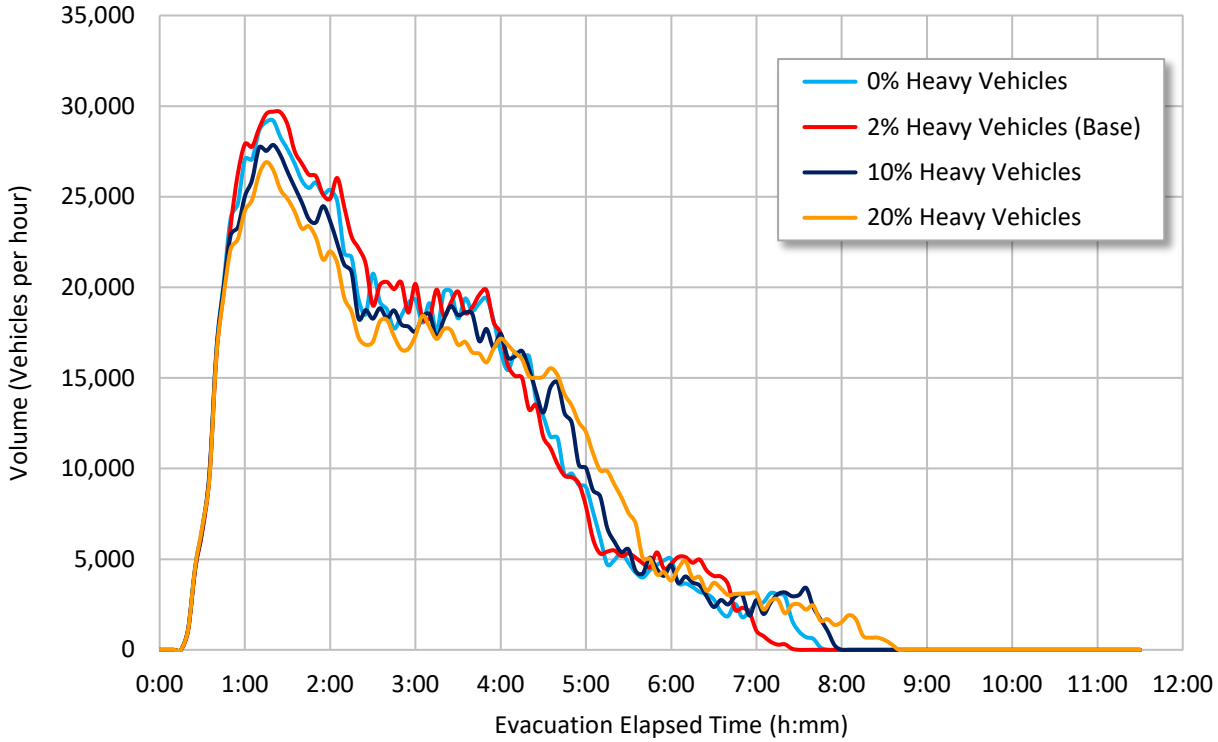

Figure 7-53 EPZ Exit Volumes, Medium Population Site Heavy Vehicle Analysis

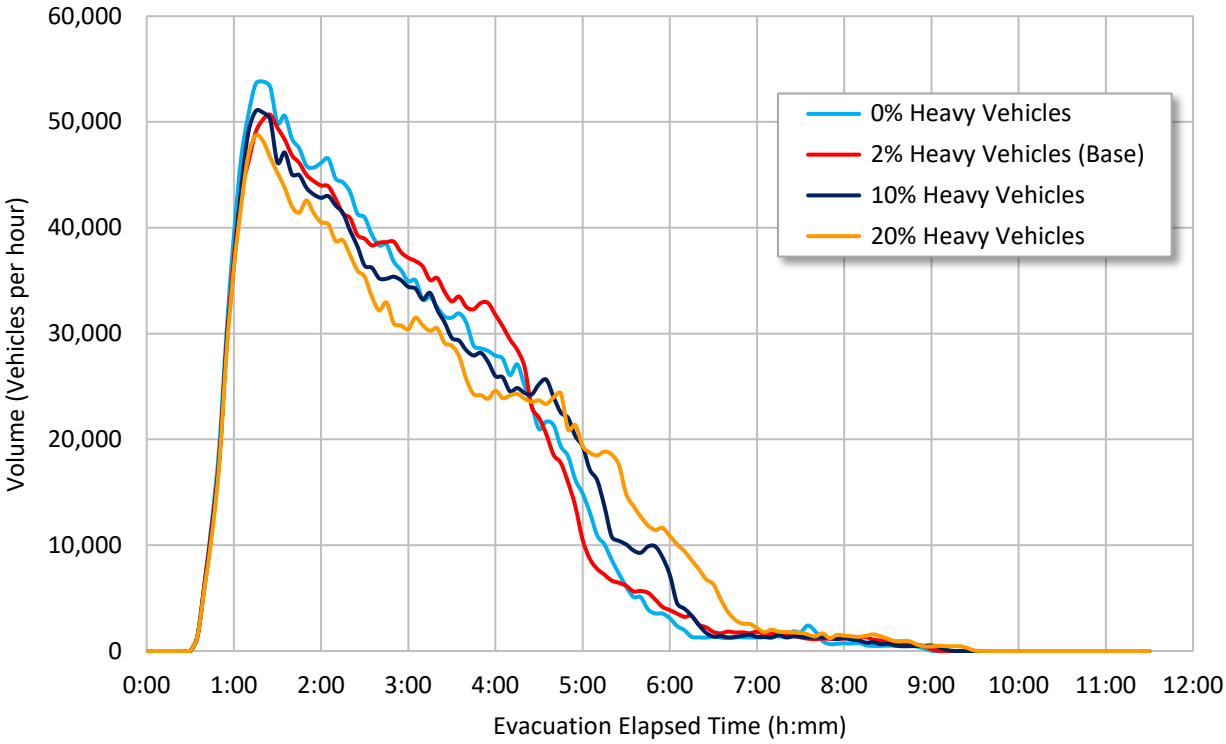

Figure 7-54 EPZ Exit Volumes, Large Population Site Heavy Vehicle Analysis

7.3.4.5 Broader Findings, Heavy Vehicle Parameter Results

Similar to other travel conditions that cause friction and non-uniformity in traffic streams, the presence of large vehicles within passenger car streams, has the potential to slow traffic, reduce available capacity, and increase congestion. The results of this study were consistent with the general assumption that heavy vehicles could lengthen clearance times. However, the specific impact depends on the number of intersections and state of congestion present within the model.

Previous research has shown that heavy vehicles create notable impacts on up-grades. The base models for this study all assumed flat terrain. From a practical perspective the occurrence of higher truck volumes in combination with rolling or mountainous terrain could be more acute. However, these results showed that the mix of heavy vehicles into the evacuation stream is not an important parameter within a reasonable range of values. Additional scrutiny of the methods for estimating heavy vehicle percentages would likely not lead to important information in ETE studies.

7.3.5 Free-Flow Speed Parameter Results

Free-flow travel speed is the maximum speed that drivers want to travel when not impeded by other vehicles. Free-flow speed is not necessarily the speed a vehicle is able to obtain given the limitation of the roadway and surrounding traffic. In general, it can be assumed that if a site experiences little to no congestion, travel time is dependent on free-flow speed. Therefore, it was anticipated that decreases in free-flow speed would increase ETEs in the small population site model. Given the level of congestion in the medium and large population site models, vehicles are expected to travel at or near free-flow speeds only in certain locations or for short durations. As such, the medium and large population site ETEs were expected to be insensitive to changes in free-flow speed and be controlled instead by the outflow rate.

The results suggest that intersections and overall congestion generally govern travel speeds. The presence of uninterrupted roadway facilities such as freeways may also contribute to the role that free-flow speed plays because vehicles are more sensitive to free-flow speed while on such roads. The 90 percent ETEs were not significantly impacted by the free-flow speed reductions investigated in this study. However, it was observed that free-flow speeds had a significant impact on the evacuation tail in the medium population site.

7.3.5.1 Small Population Site Model Free-Flow Speed Parameter Results

Table 7-32 summarizes the average 90 and 100 percent ETEs for the small population site model. No significant impacts resulting from decreases in free-flow speed were observed. In general, ETEs increased slightly as free-flow travel speed decreased, but the impact was less than 10 minutes. Average evacuee delay was not significantly affected. Given the rural and generally uncongested nature of the small population site, vehicles in the small population site have the most opportunity to travel at free-flow speed. However, there exists only a few miles of freeway inside the EPZ and most vehicles stop at intersections. As such, changing the free-flow speeds did not have a major impact. Figure 7-55 shows the cumulative percent evacuated for the small population site model at the 10-mile ring. Only minor variations were evidenced through changes in the free-flow speed parameter.

Table 7-32 Small Population Site Free-flow Speed Analysis

Scenario Number	Free-flow Speed Decrease (Percent)	Average Evacuee Delay (minutes)	2-Mile		5-Mile		10-Mile	
			90% ETE	100% ETE	90% ETE	100% ETE	90% ETE	100% ETE
1[1]	0	14	1:35	2:18	1:35	2:21	1:44	2:31
2	10	15	1:35	2:18	1:37	2:22	1:45	2:34
3	20	15	1:35	2:18	1:39	2:22	1:45	2:36
4	25	15	1:35	2:18	1:39	2:22	1:45	2:37
5	30	15	1:35	2:18	1:40	2:23	1:48	2:39
6	35	16	1:35	2:18	1:40	2:24	1:50	2:41

[1] Base model.

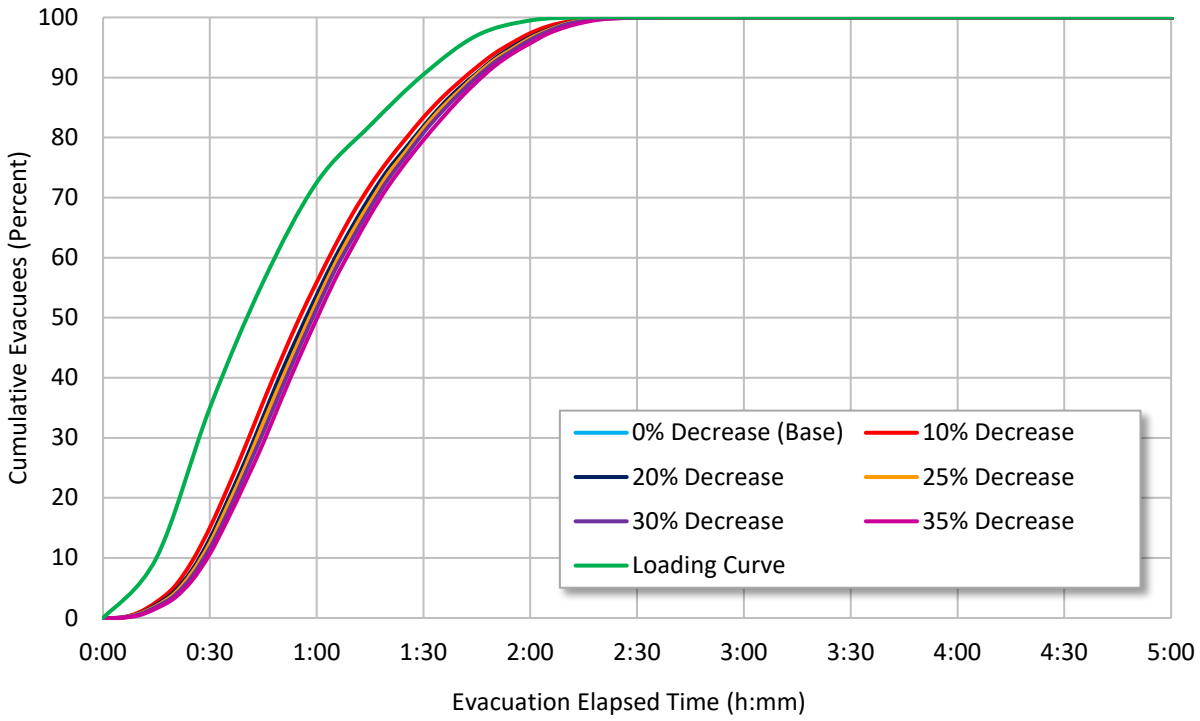

Figure 7-55 Ten Mile ETE Curves, Small Population Site Free-flow Speed Analysis

7.3.5.2 Medium Population Site Model Free-Flow Speed Parameter Results

Table 7-33 summarizes the average 90 and 100 percent ETEs for the medium population site model. Free-flow speed had no significant impact on the 90 percent ETEs. The 100 percent ETEs were longer at the 5 and 10-mile rings; however, average evacuee delay stayed relatively constant. Given the high congestion level in the medium population site model and because most evacuees were traveling in queues, free-flow speeds should not govern the ETE. This was the case for the 90 percent ETE which was observed to be relatively insensitive to free-flow speed. However, the evacuation tail (last 10 percent of evacuees) was consistently inhibited by the free-flow speed reduction. This was likely because vehicles generated during the tail of the traffic-loading curve did not catch up to the bulk of the evacuating traffic, resulting in an

extended evacuation tail and longer 100 percent ETEs. In all scenarios, the number of vehicles not exiting the EPZ remained less than 1.6 percent.

Table 7-33 Medium Population Site Free-flow Speed Analysis

Scenario Number	Free-flow Speed Decrease (Percent)	Average Evacuee Delay (minutes)	2-Mile		5-Mile		10-Mile	
			90% ETE	100% ETE	90% ETE	100% ETE	90% ETE	100% ETE
1[1]	0	70	2:40	4:03	2:47	5:05	5:03	7:41
2	10	71	2:40	4:03	2:47	5:21	5:02	7:50
3	20	70	2:40	4:03	2:50	5:25	5:05	7:53
4	25	70	2:40	4:03	2:57	5:40	5:05	7:48
5	30	70	2:40	4:03	2:53	5:31	5:07	7:50
6	35	72	2:40	4:03	3:08	6:10	5:12	7:52

[1] Base model.

Figure 7-56 and Figure 7-57 show the cumulative percent evacuated for the medium population site model at the 5 and 10-mile rings, respectively. The ETE curves are closely overlapped with the base scenario at the beginning of the evacuation and then start to separate slightly after approximately 80 percent of the vehicles have been loaded into the network. As evidenced in other parts of this study, the 5-mile ring in the medium population site model can be sensitive at the extremes of some variables. However, in general, ETEs are only slightly sensitive to variations in free-flow speed for the majority of the evacuation process.

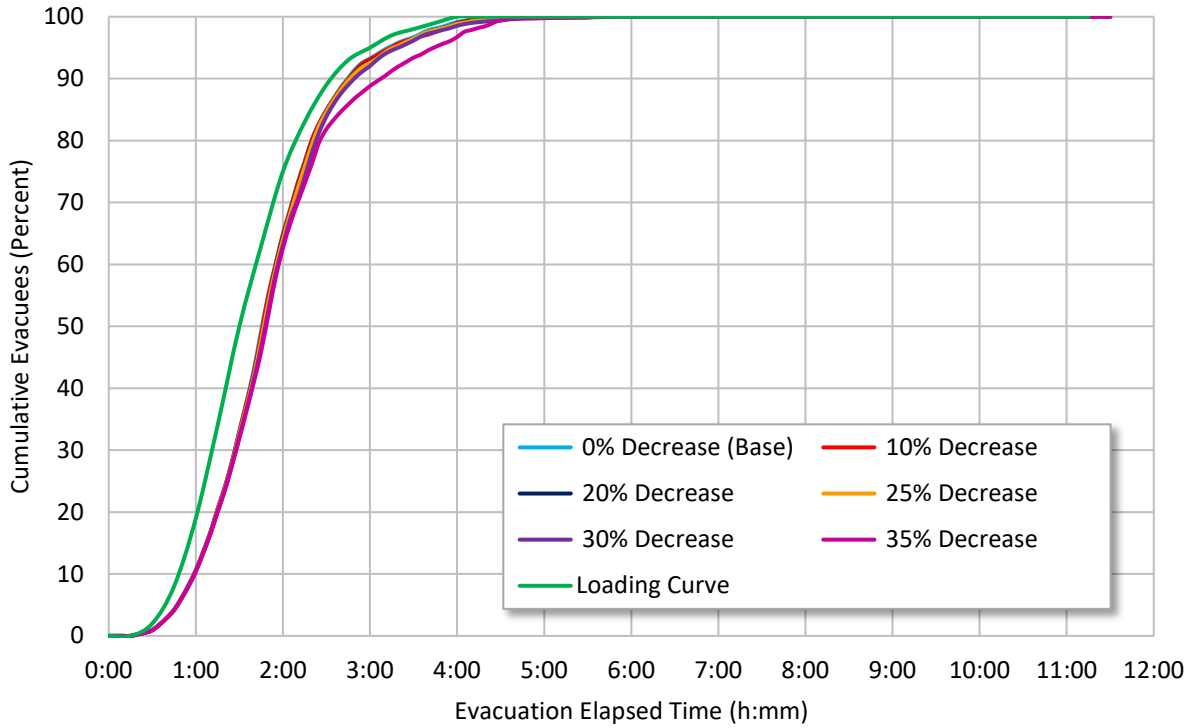

Figure 7-56 Five Mile ETE Curves, Medium Population Site Free-flow Speed Analysis

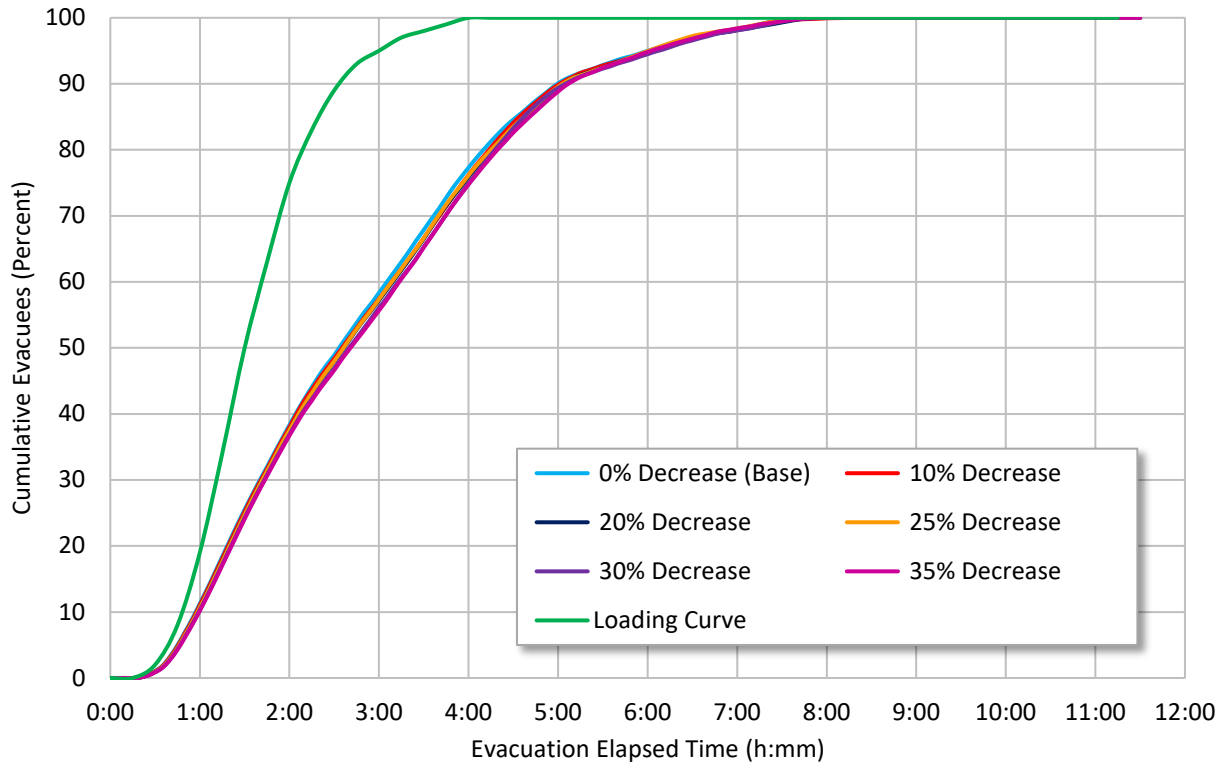

Figure 7-57 Ten Mile ETE Curves, Medium Population Site Free-flow Speed Analysis

7.3.5.3 Large Population Site Model Evacuation, Free-Flow Speed Parameter Results

Table 7-34 summarizes the average 90 and 100 percent ETEs for the large population site model. The 90 percent and 100 percent ETEs were not significantly impacted by decreases in free-flow speed, although in general, ETEs were longer with decreased free-flow speed. The 10-mile 100 percent ETE stayed about the same. This was because congestion and intersections limited the ability to reach or maintain free-flow speeds at some locations in the network. Average evacuee delay in the network was observed to stay relatively constant.

Figure 7-58 shows the ETE curve for the large population site model at the 10-mile ring. The traffic conditions during the evacuation were not significantly impacted by the scenarios tested. Some slight variations in traffic conditions were observed for a short period of time. In all scenarios, the number of vehicles not exiting the EPZ remained less than 0.6 percent.

Table 7-34 Large Population Site Free-flow Speed Analysis

Scenario Number	Free-flow Speed Decrease (Percent)	Average Evacuee Delay (minutes)	2-Mile		5-Mile		10-Mile	
			90% ETE	100% ETE	90% ETE	100% ETE	90% ETE	100% ETE
1[1]	0	62	3:40	5:05	3:57	6:35	4:43	9:01
2	10	60	3:40	5:08	4:00	6:55	4:46	9:02
3	20	59	3:42	5:10	4:01	6:42	4:48	9:02
4	25	59	3:45	5:12	4:00	6:47	4:50	9:05
5	30	60	3:43	5:13	4:03	6:43	4:51	8:58
6	35	61	3:42	5:15	4:07	6:50	4:52	9:02

[1] Base model.

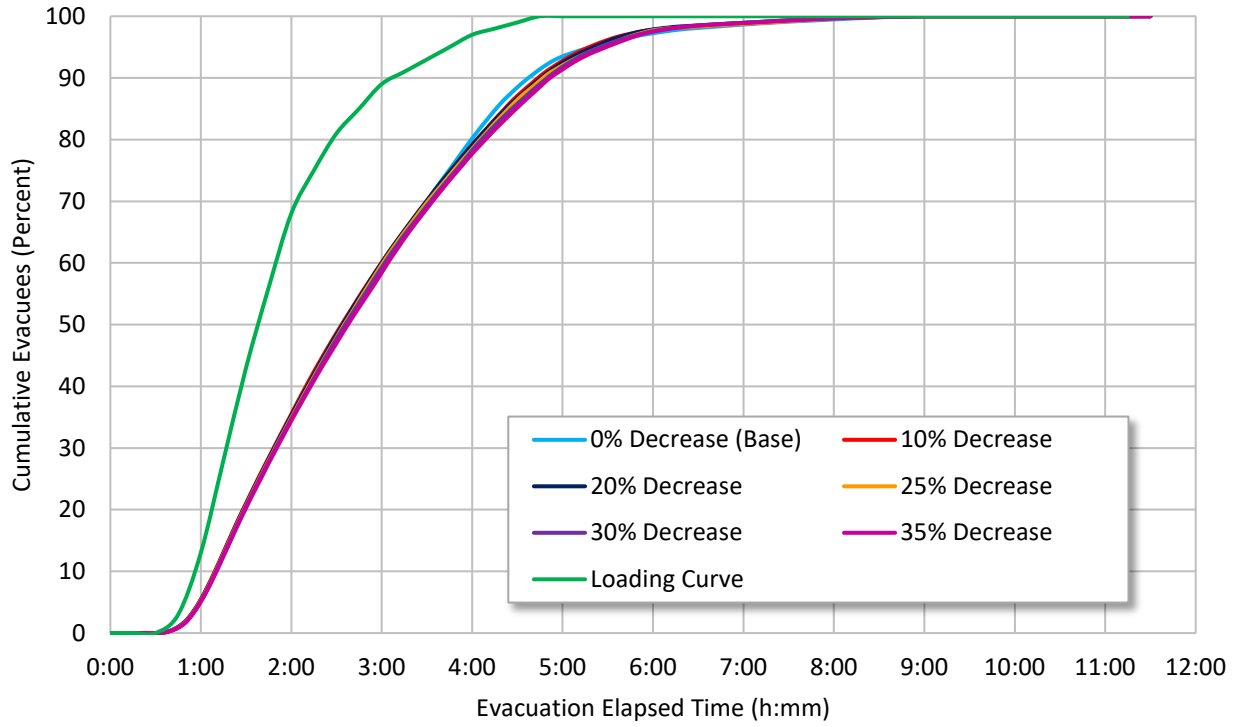

Figure 7-58 Ten Mile ETE Curves, Large Population Site Free-flow Speed Aanalysis

7.3.5.4 Average Travel Speed Results Free-Flow Speed Parameter

The average travel speed of vehicles exiting the EPZ was grouped into 16 compass sectors (N, NNE, NE, ENE, E, etc.). These average speeds are shown at various time periods to illustrate evacuation progression. Figure 7-59 and Figure 7-60 show the average travel speed for each free-flow speed scenario in the small population site model at 0:15 and 1:45 into the evacuation, respectively. Free-flowing conditions were maintained throughout the evacuation because there is little to no congestion within the small population site model. The average travel speeds were observed to decrease in all scenarios as free-flow speed was decreased. Travel speeds were also observed to decrease almost uniformly in all sectors.

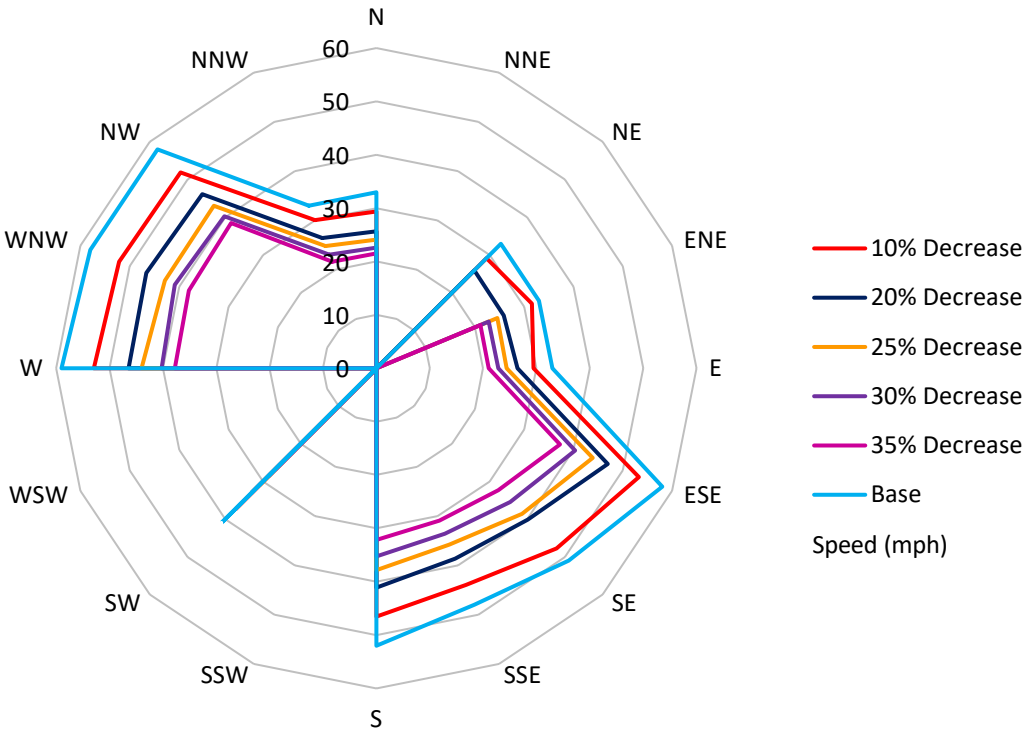

Figure 7-59 Average Exit Speeds at 0:15, Small Population Site Free-flow Speed Analysis

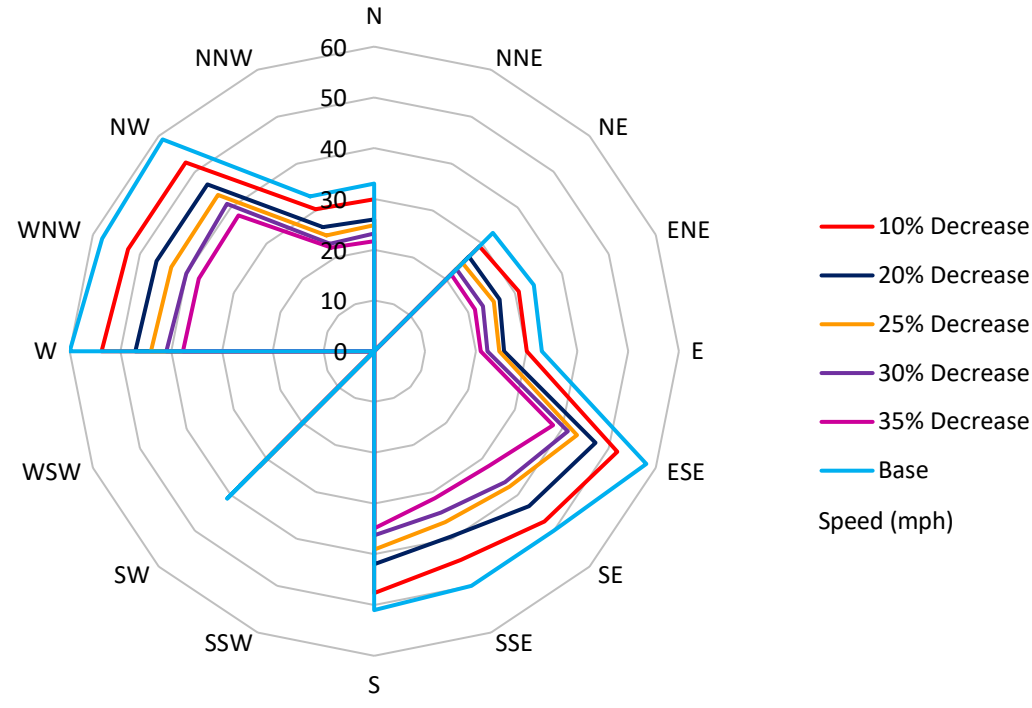

Figure 7-60 Average Exit Speeds at 1:45, Small Population Site Free-flow Speed Analysis

Figures 7-61, 7-62, and 7-63 show the average travel speed in the medium population site model at 2:30, 3:30, and 4:30 into the evacuation, respectively. As expected, the average travel speeds were observed to decrease as free flow speed is decreased and as congestion develops. Earlier in the evacuation, vehicles would most likely be traveling at their free-flow speeds unless impeded by traffic control. In the NNW sector congestion is already evident at 2:30 into the evacuation. At 3:30 into the evacuation average travel speeds in the NNW and SSW sectors for the different free-flow speed scenarios are observed to converge suggesting queues at the EPZ boundary dominate the travel speed. At 4:30, as congestion begins to ease, and average travel speeds are observed to approach free-flow speeds again.

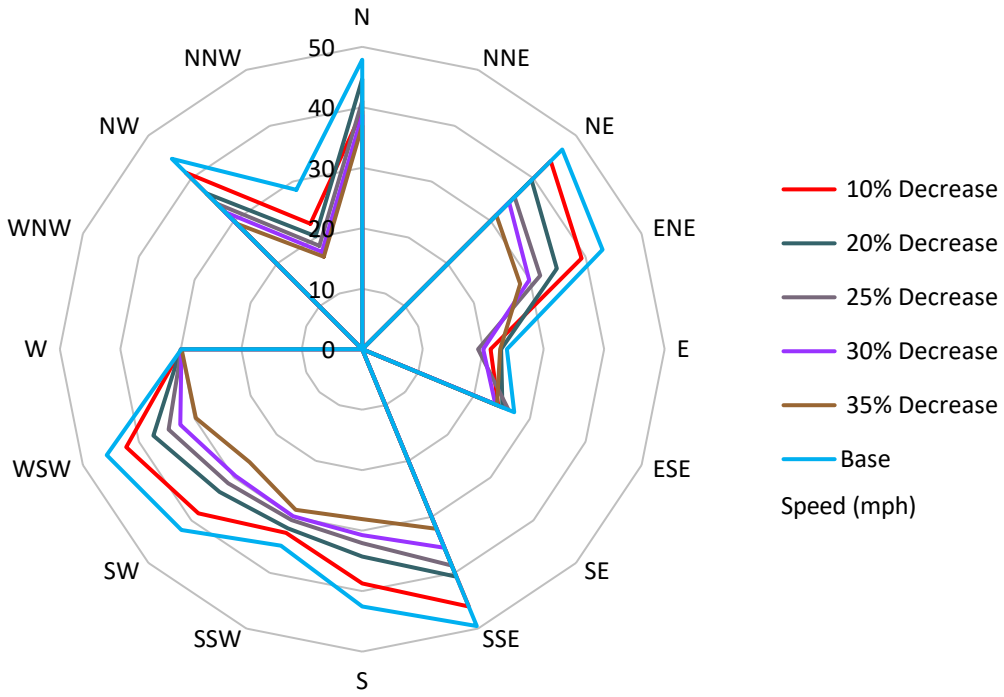

Figure 7-61 Average Exit Speeds at 2:30, Medium Population Site Free-flow Speed Analysis

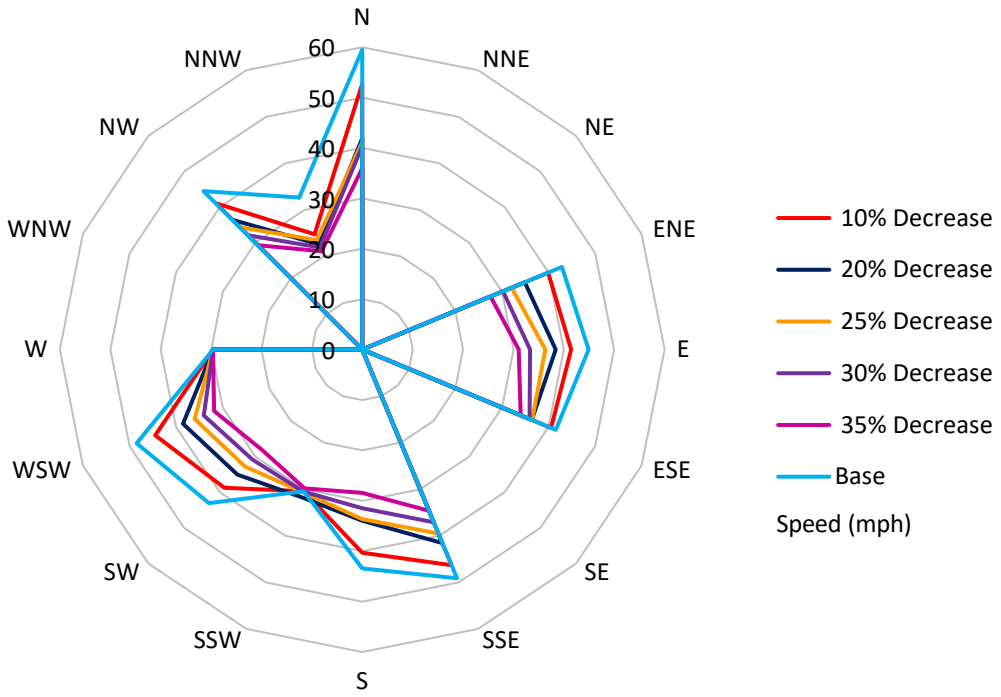

Figure 7-62 Average Exit Speeds at 3:30, Medium Population Site Free-flow Speed Analysis

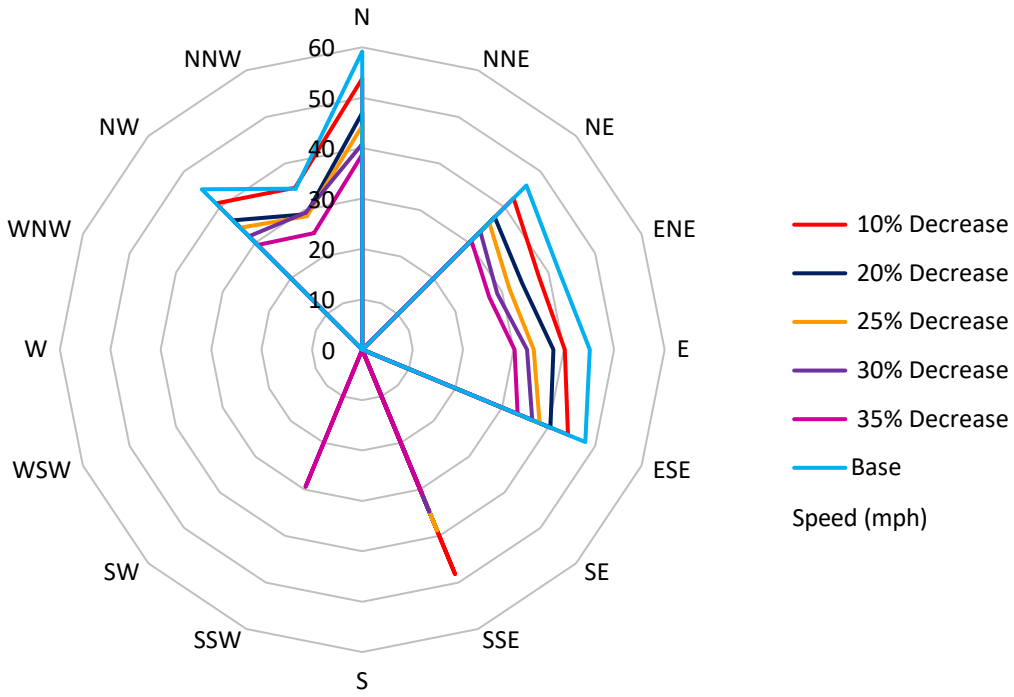

Figure 7-63 Average Exit Speeds at 4:30, Medium Population Site Free-flow Speed Analysis

Figures 7-64 through 7-66 show the average travel speed in the large population site model at 2:30, 3:30, and 4:30 into the evacuation, respectively. As expected, the average travel speeds decreased with lower free-flow speeds and early in the evacuation congestion dominates the overall reduction in average travel speed. As the evacuation continues average travel speeds vary in response either to congestion, or in non-congested regions, the reduction in free flow speed as observed at 3:30 and 4:30 into the simulation shown in Figure 7-67 and Figure 7-68. Additionally, this behavior may be indicative of local queues occurring somewhere within the EPZ and not just at the boundary of the EPZ. The large population site network is most likely internally constrained by these local bottlenecks inside the EPZ.

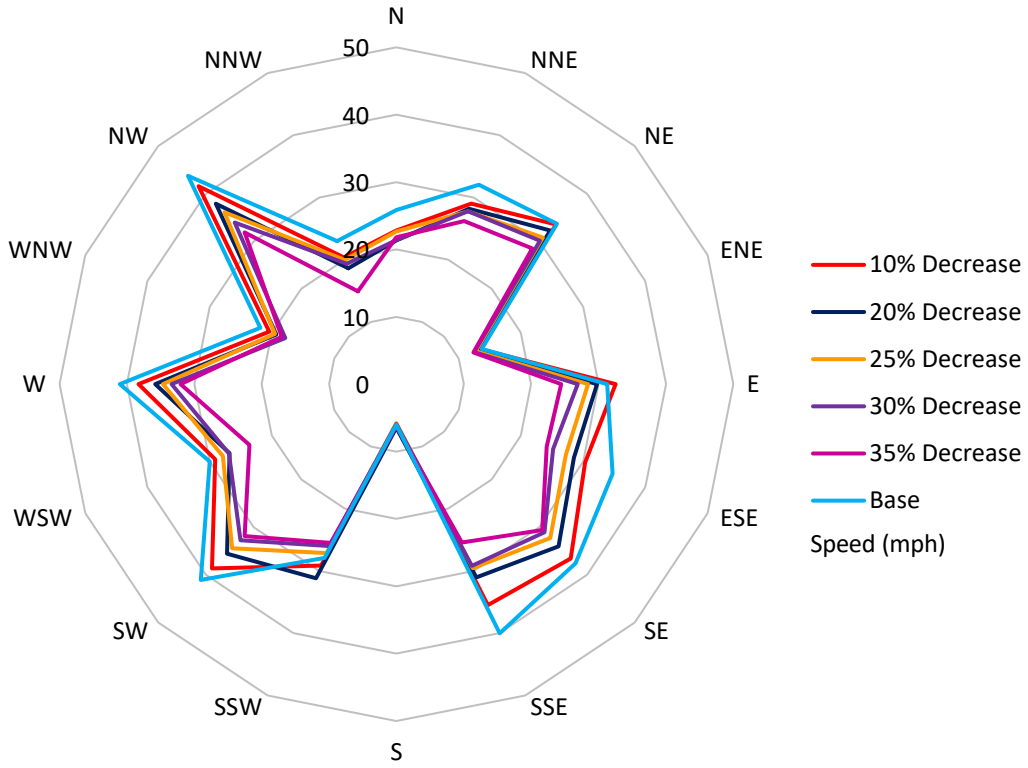

Figure 7-64 Average Exit Speeds at 2:30, Large Population Site Free-flow Speed Analysis

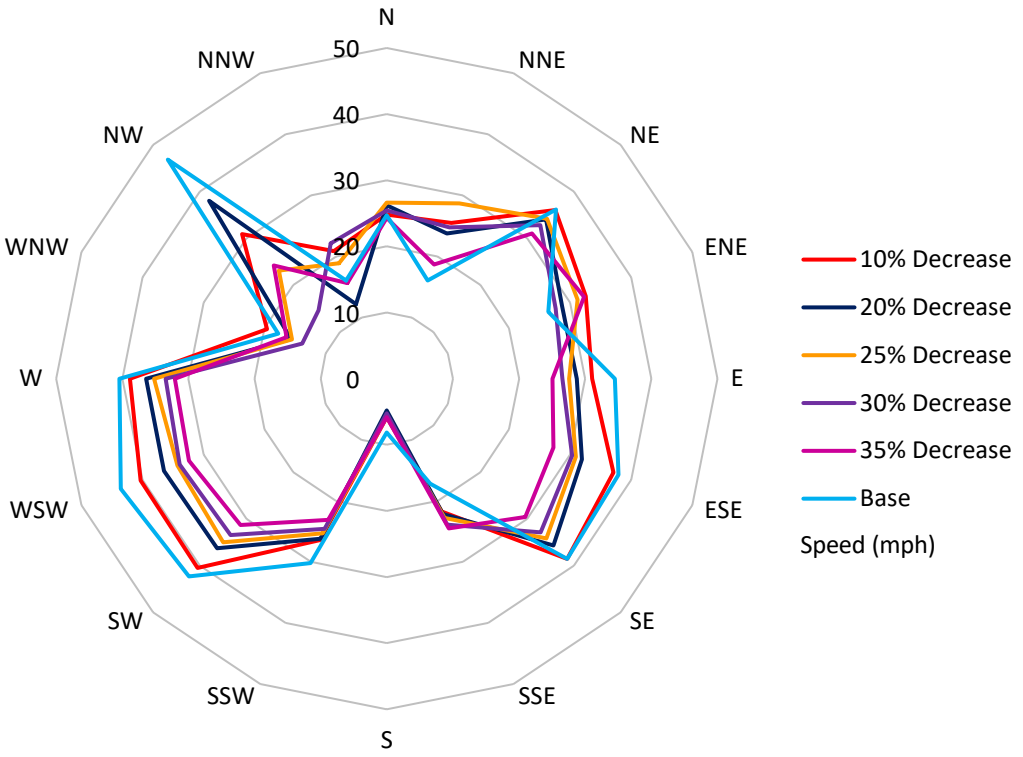

Figure 7-65 Average Exit Speeds at 3:30, Large Population Site Free-flow Speed Analysis

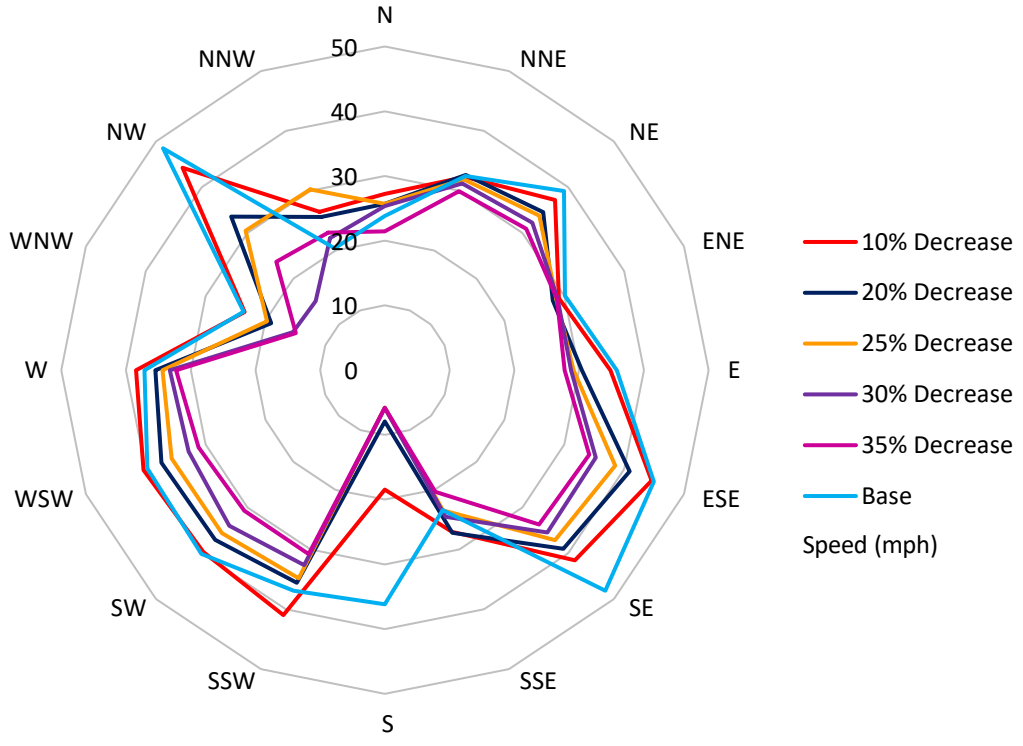

Figure 7-66 Average Exit Speeds at 4:30, Large Population Site Free-flow Speed Analysis

7.3.5.5 Exit Volume Results for Free-Flow Speed Parameter

Figure 7-67 shows the rate of vehicles leaving the 10-mile EPZ in the small population site model. It was observed that the peak rate of egress decreased as free-flow speeds decreased. Additionally, the peak occurs slightly later in successive scenarios. This is because vehicles are arriving at the EPZ boundary at later times since speeds are lower in free-flowing conditions.

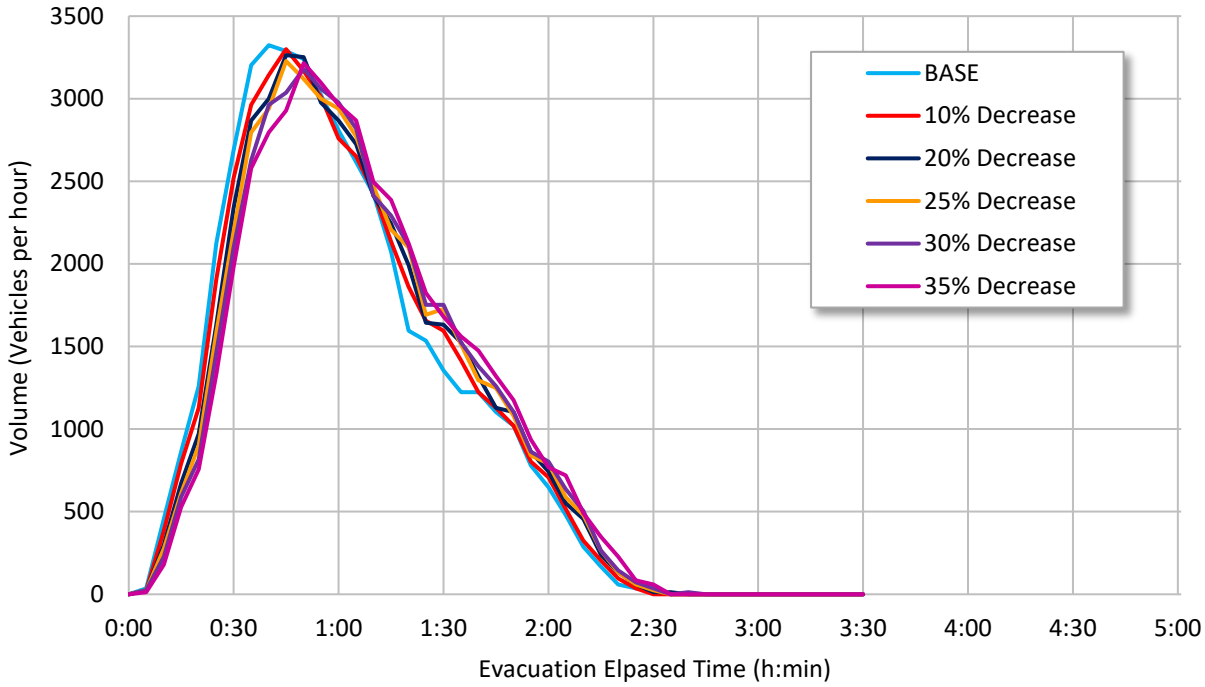

Figure 7-67 EPZ Exit Volumes, Small Population Site Free-flow Speed Analysis

Figure 7-68 and Figure 7-69 show the rate of vehicles leaving the 10-mile EPZ in the medium and large population site models, respectively. Except for small variations from the base scenario, the peak rate of egress is less affected by the reduction in free-flow speed. This indicates that congestion is controlling the rate of egress. As the evacuation progresses, it can be seen that the reduction in free-flow speed is not enough to significantly impact the overall evacuation process.

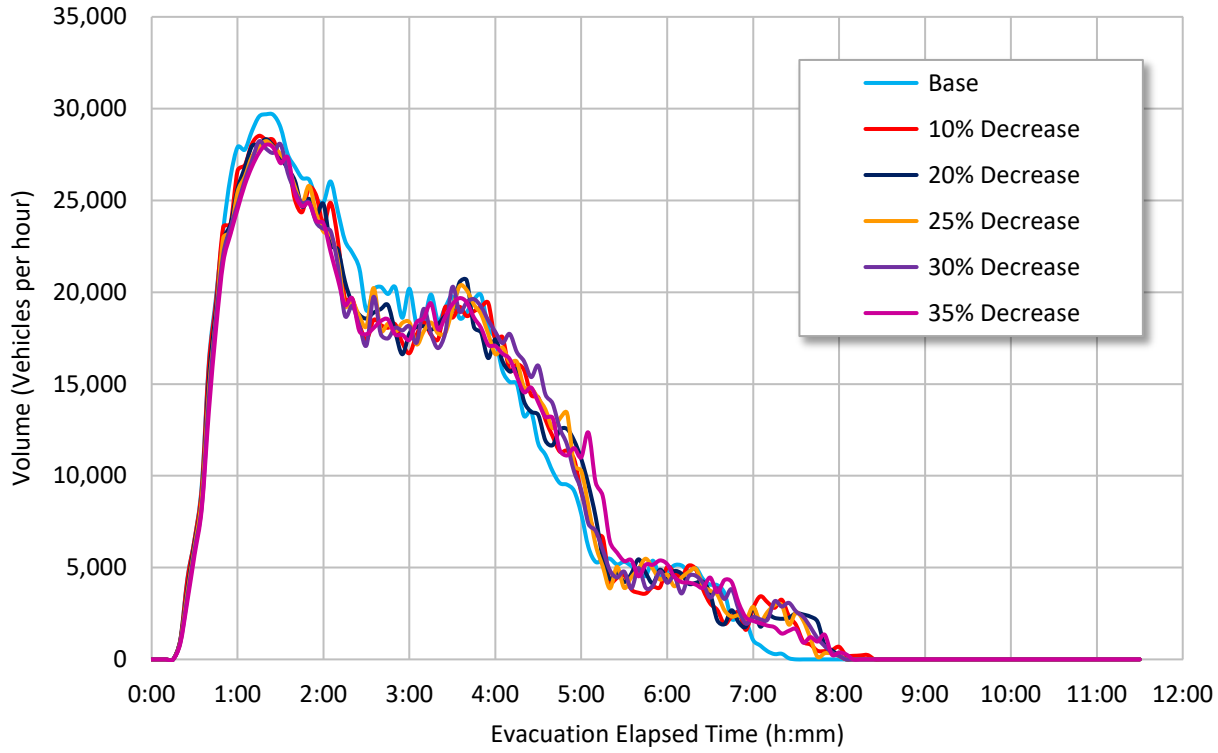

Figure 7-68 EPZ Exit Volumes, Medium Population Site Free-flow Speed Analysis

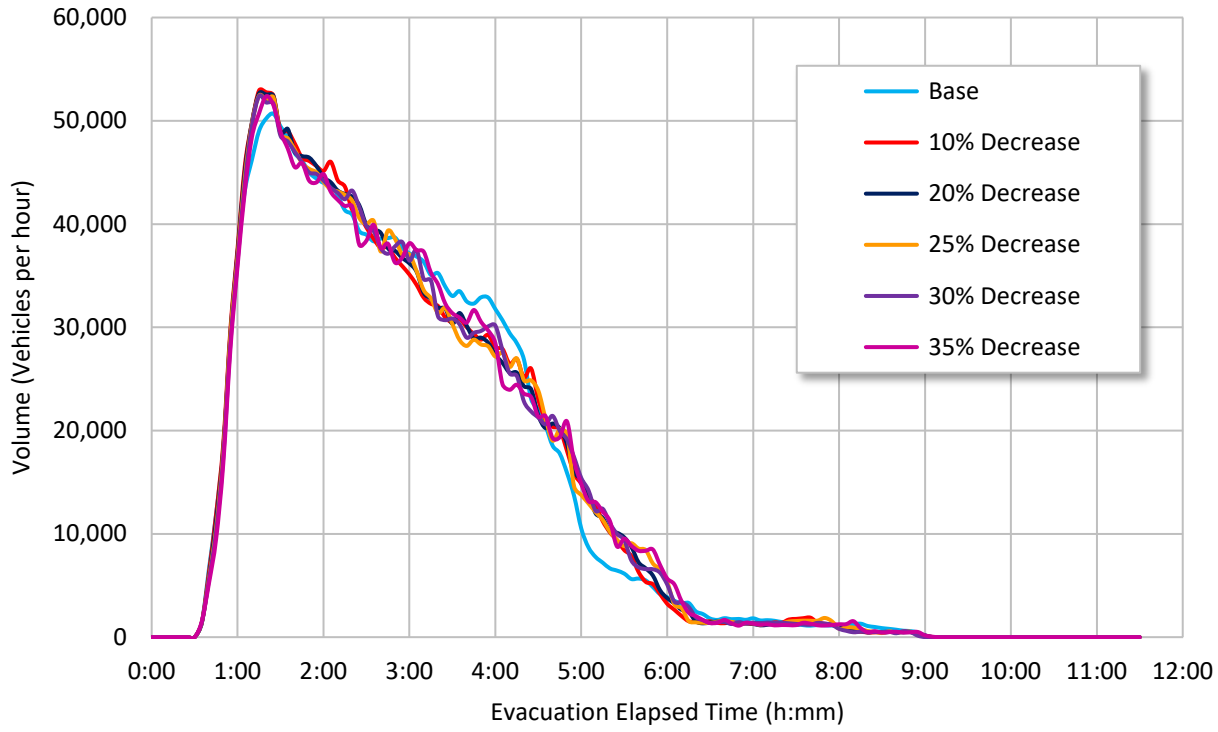

Figure 7-69 EPZ Exit Volumes, Large Population Site Free-flow Speed Analysis

7.3.5.6 Broader Findings, Free-flow Speed Parameter Results

The free-flow parameter analysis showed that ETEs were not significantly impacted by modest reductions in free flow speed. These non-significant findings do not suggest, however, that no differences were observed. There were noticeable variations in average travel speed throughout the evacuation due to the reduction in free-flow speed. At some points this difference could be more than 20 mph. However, these noticeable differences in average speed do not translate into significantly longer evacuation times overall. This is due, in part, to the relatively short distances the average evacuee travels before exiting the EPZ.

When congestion developed, free-flow speed becomes less important because lower speeds result when queues form and demand exceeds capacity regardless of the desired speed of the vehicles. Additionally, free-flow speed is less significant when there are multiple intersections and traffic control measures in place create stop-and-go traffic. In practical terms, the results obtained are consistent with observations of traffic in real-world evacuations such as those observed prior to the landfalls of Hurricanes Katrina and Rita. At the tail end of these evacuations, traffic was recorded traveling at speeds in excess of posted speed limits in the hours preceding landfall because the majority of the evacuation traffic had left the threat area. The lower volume that often exists in the latter stages of an evacuation can provide opportunities to travel at higher speed.

7.3.6 Adverse Weather Parameter Results

Adverse weather negatively impacts roadway capacity and can affect ETEs if severe enough. Data from prior ETE studies show an average increase in the 10-mile 90 percent ETE of 15 minutes in rainy conditions when free-flow speeds and capacity were decreased by 10 percent. For snowy conditions, ETEs increased an average of 41 minutes when free-flow speeds and capacity were decreased by 20 percent and mobilization times lengthened for snow removal. Similarly impacts were observed in the 100 percent ETEs reflecting an overall reduction in capacity and increased mobilization times. This analysis tested the importance of adverse weather in terms of the capacity reduction introduced through modifications to driver behavior resulting in larger headway distances and reduced speeds.

The findings of this analysis confirm that adverse weather can have significant impacts on ETEs. The impact is likely exacerbated by congestion levels and the density of intersections within the study areas. This may suggest that the type of aggregate capacity reductions used in macroscopic simulation models are consistent with these findings and are justified for use. In EPZs with significant variability in network and population density, impacts may be significantly greater in certain locations. Examples of this can be seen throughout the medium population site model and near the 5-mile ring of the large population site model. In the results tables and figures, BX_{add} is the *additive part of safety distance* and BX_{mult} as the *multiplicative part of safety distance* in the Wiedemann 74 car following model as explained in Section 7.1.1.6.

7.3.6.1 Small Population Site Model Adverse Weather Parameter Results

Table 7-35 summarizes the average 90 and 100 percent ETEs for the small population site model. The results show that there was little impact on the ETEs. The 10-mile 90 percent ETEs increased by an average of 1 and 3 minutes in rain and snow, respectively. The 10-mile 100 percent increased an average of 3 and 6 minutes in rain and snow, respectively. Similar to the other parameters evaluated in this task, this is assumed to be due to the overall low traffic demands in the small population site network. With little interaction between vehicles or any

congestion, the larger headway times do not impact output. In addition, as determined in the previous analysis, the lower free-flow speeds do not make a significant impact since most of the roadways in the small population site had some form of traffic control that limited the opportunity to travel at free-flow speeds. Slight variation in network-wide average evacuee delay was evidenced, but these are most likely related to the model randomness.

Table 7-35 Small Population Site Adverse Weather Analysis

Scenario Number	Weather Scenario	Average Evacuee Delay (minutes)	2-Mile		5-Mile		10-Mile	
			90% ETE	100% ETE	90% ETE	100% ETE	90% ETE	100% ETE
1[1]	Fair	14	1:35	2:18	1:35	2:21	1:44	2:31
2	Rain	14	1:35	2:18	1:37	2:22	1:45	2:34
3	Rain	13	1:35	2:18	1:37	2:22	1:45	2:34
4	Snow	14	1:35	2:18	1:37	2:22	1:45	2:34
5	Snow	15	1:35	2:19	1:40	2:24	1:50	2:41

[1] Base model.

Figure 7-70 shows the cumulative percent of evacuees exiting the 10-mile EPZ in the small population site model. Comparison to the free-flow speed analysis and Figure 7-55 show that the changes in ETE are mostly driven by the reduction in free-flow speed. The ETE curve for reduction in free-flow speed of 35 percent and estimated decrease in capacity from 27 to 28 percent departed detectably from the base case, but even this most severe scenario did not significantly affect ETEs.

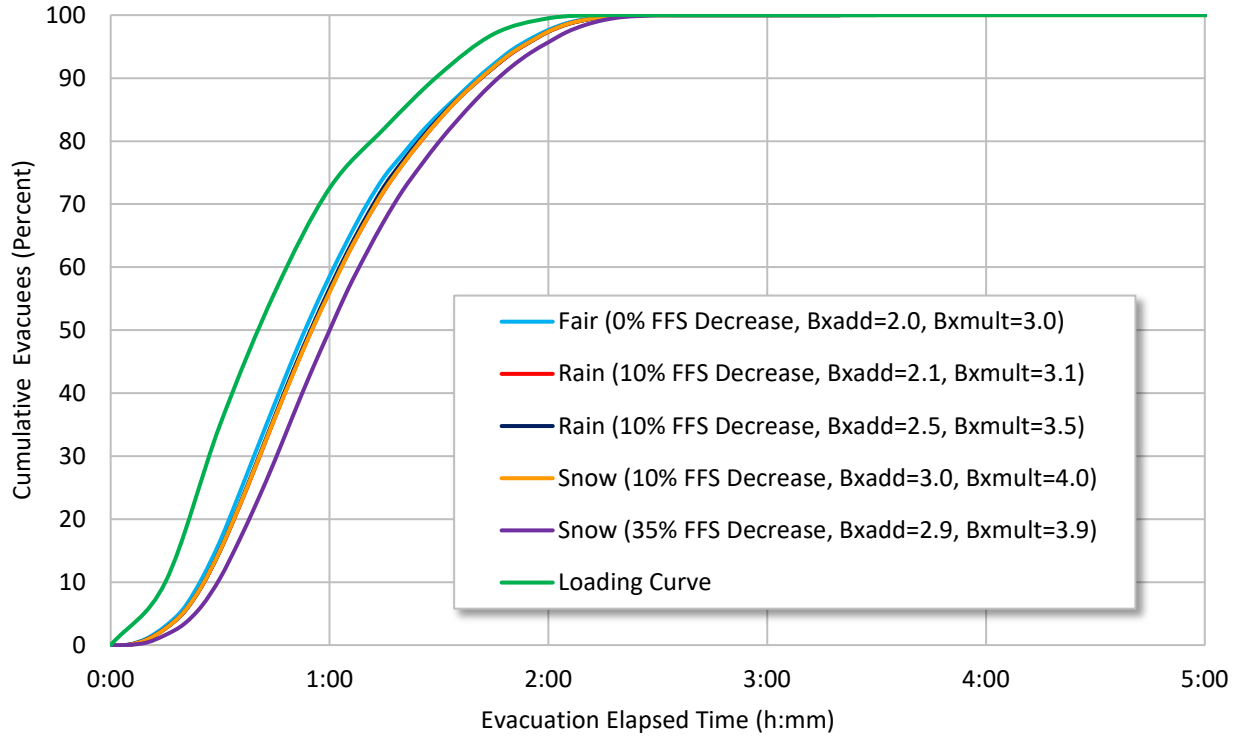

Figure 7-70 Ten Mile ETE Curves, Small Population Site Adverse Weather Analysis

7.3.6.2 Medium Population Site Model Adverse Weather Analysis

Table 7-36 summarizes the average 90 and 100 percent ETEs for the medium population site model. The results showed significant impacts in snowy conditions particularly at the 5 and 10-mile rings. At the 2-mile ring, ETEs remained the same. This is due to the low population density inside the 2-mile ring. At the 5-mile ring, the 100 percent ETEs increased slightly in rain and significantly under snowy conditions. Similar patterns were seen for the 100 percent ETE. The results demonstrate the impact of adverse weather in a congested network. As expected, greater vehicle safety spacing led to longer travel times and increased delay in a more densely travelled network. Network-wide average evacuee delay was observed to increase as headway times and free-flow speeds increased.

The 10-mile 90 percent ETEs increased by an average of 10 and 30 minutes in rain and snow, respectively. The 10-mile 100 percent ETE increased an average of 7 and 23 minutes in rain and snow, respectively. Compared to the free-flow speed analysis and Figure 7-57, the results from the medium population site model clearly show an impact from the capacity reduction introduced by increases in vehicle headway. In all scenarios, the number of vehicles not exiting the EPZ remained less than 1.7 percent.

Table 7-36 Medium Population Site Adverse Weather Analysis

Scenario Number	Weather Scenario	Average Evacuee Delay (minutes)	2-Mile		5-Mile		10-Mile	
			90% ETE	100% ETE	90% ETE	100% ETE	90% ETE	100% ETE
1[1]	Fair	70	2:40	4:03	2:47	5:05	5:03	7:41
2	Rain	72	2:40	4:03	2:47	4:57	5:06	7:43
3	Rain	76	2:40	4:03	2:50	5:16	5:20	7:53
4	Snow	87	2:40	4:03	2:53	6:15	5:31	8:13
5	Snow	86	2:40	4:03	3:10	6:18	5:36	7:56

[1] Base model.

Figure 7-71 shows the cumulative percent of evacuees exiting the 10-mile EPZ in the medium population site model. The ETE curves separate with increasing vehicle headways and decreasing free-flow speeds. The change starts to occur consistently after approximately 30 percent of vehicles have been loaded into the network. The curves get closer together after about 90 percent of the vehicles have exited. In other words, the impact of adverse weather was exacerbated by the presence of congestion.

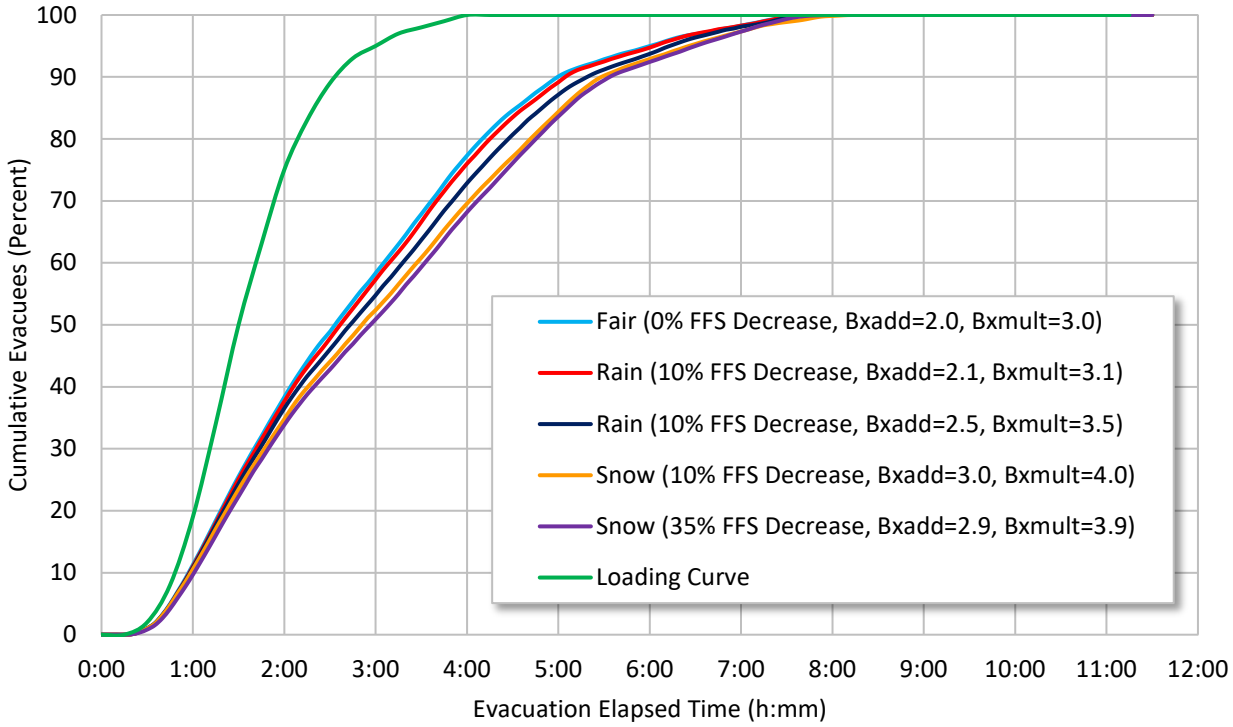

Figure 7-71 Ten Mile ETE Curves, Medium Population Site Adverse Weather Analysis

7.3.6.3 Large Population Site Model Adverse Weather Parameter Results

Table 7-37 summarizes the average 90 and 100 percent ETEs for the large population site model. In general, ETEs were observed to increase with increasing headways and decreasing free-flow speeds. An increase was only observed at the 2-mile ring in the snow scenarios. Both rain and snow increased the ETEs at the 5-mile ring, more so than at the EPZ boundary, but the effect was not significant. These results support the notion that the large population site network is most likely internally constrained by local bottlenecks inside the EPZ. Combined, the large population site model results reinforce the impact of adverse weather, especially in congested networks. Although the heaviest rain and snow scenarios decreased the 10-mile 100 percent ETE, this result is not entirely unexpected. It could be related to the stochasticity of the model; however, it may also be because the increased safety distance and slower speeds opened up capacity (gaps in the traffic flow) for merging and loading of vehicles onto the network. In all scenarios, the number of vehicles not exiting the EPZ remained less than 0.7 percent.

Figure 7-72 shows the cumulative percent of evacuees exiting the 10-mile ring in the large population site model. The separation between the curves widens as vehicle headways increase. The effects start to become apparent after approximately 40 percent of the vehicles have been loaded into the network. But even though the evacuation process slows down due the combined impact of adverse weather and congestion, vehicles catch up toward the end of the evacuation as free-flow speeds can be resumed. A conclusion from the combined results shown in Figures 7-70, 7-71, and 7-72, is that adverse weather is an effect that can potentially impact the entire evacuation, with variation due to the level of congestion.

Table 7-37 Large Population Site Adverse Weather Analysis

Scenario Number	Weather Scenario	Average Evacuee Delay (minutes)	2-Mile		5-Mile		10-Mile	
			90% ETE	100% ETE	90% ETE	100% ETE	90% ETE	100% ETE
1[1]	Fair	62	3:40	5:05	3:57	6:35	4:43	9:01
2	Rain	60	3:40	5:08	4:01	6:38	4:46	8:56
3	Rain	63	3:40	5:08	4:07	6:40	4:52	8:45
4	Snow	68	3:42	5:17	4:25	6:53	5:05	8:55
5	Snow	63	3:45	5:15	4:12	6:50	4:57	8:52

[1] Base model.

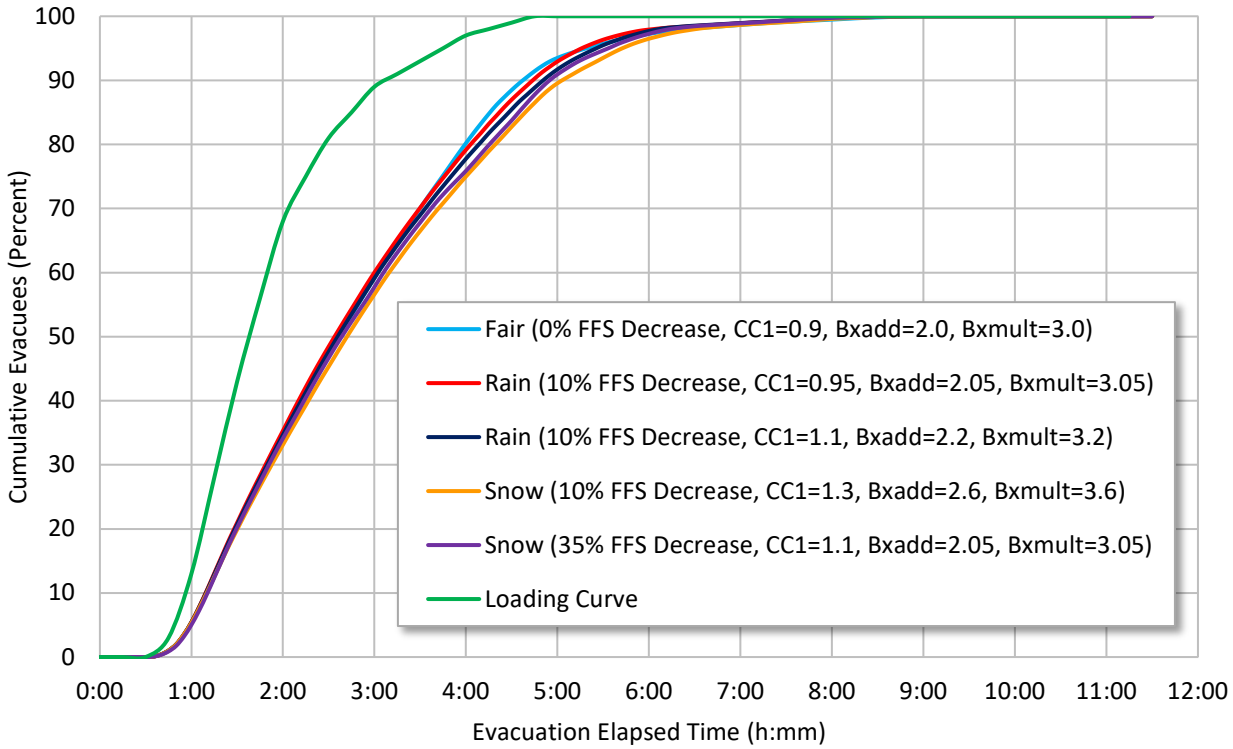

Figure 7-72 Ten Mile ETE Curves, Large Population Site Model Adverse Weather Analysis

7.3.6.4 Exit Volume Results for Adverse Weather Parameter

Figure 7-73 shows the rate of vehicles leaving the 10-mile EPZ in the small population site model. The exit volumes peaked at approximately 3,400 vehicles/hr for all scenarios although the maximum exit volume for a 25 percent decrease in free-flow speed and 30 percent reduction in capacity was observed to be a little lower.

Figure 7-74 shows the rate of vehicles leaving the 10-mile EPZ in the medium population site model. In general, the maximum rate of egress decreases as the capacity reduction increases due to adverse weather conditions. Toward the end of the evacuation, exit volumes go up as congestion subsides.

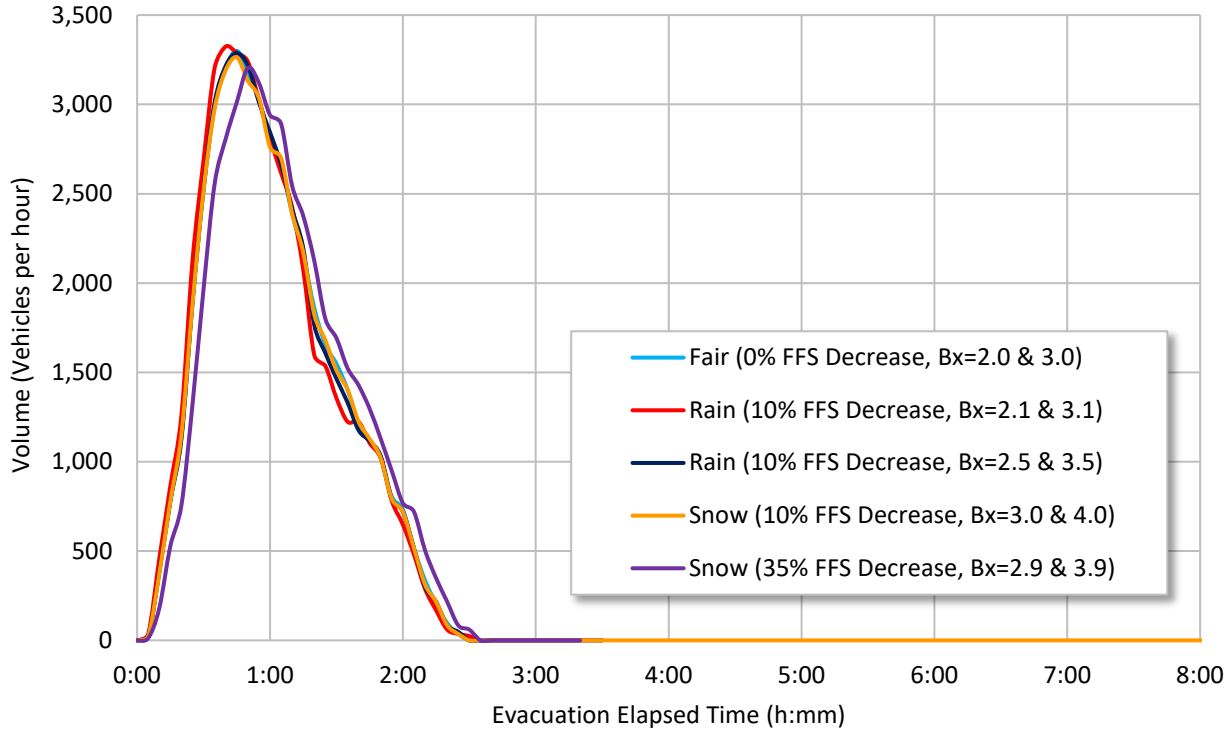

Figure 7-73 EPZ Exit Volumes, Small Population Site Model Adverse Weather Analysis

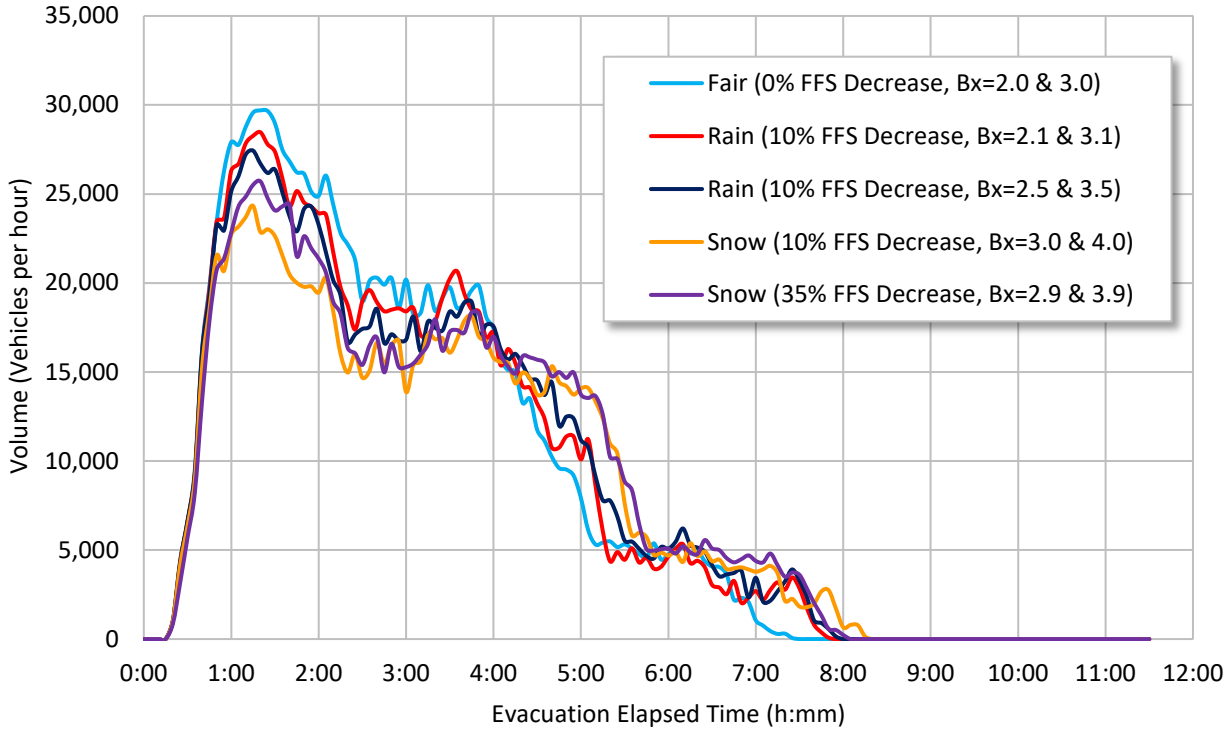

Figure 7-74 EPZ Exit Volumes, Medium Population Site Model Adverse Weather Analysis

Figure 7-75 shows the rate of vehicles leaving the 10-mile EPZ in the large population site model. The maximum rate of egress was slightly higher for some of the adverse weather scenarios compared to the base model. This could be because vehicles are arriving more gradually and therefore, could have delayed the activation of bottlenecks. Even though the demand is greater, the impact of adverse weather in the large model is not as significant as in the medium model due to the more robust transportation network.

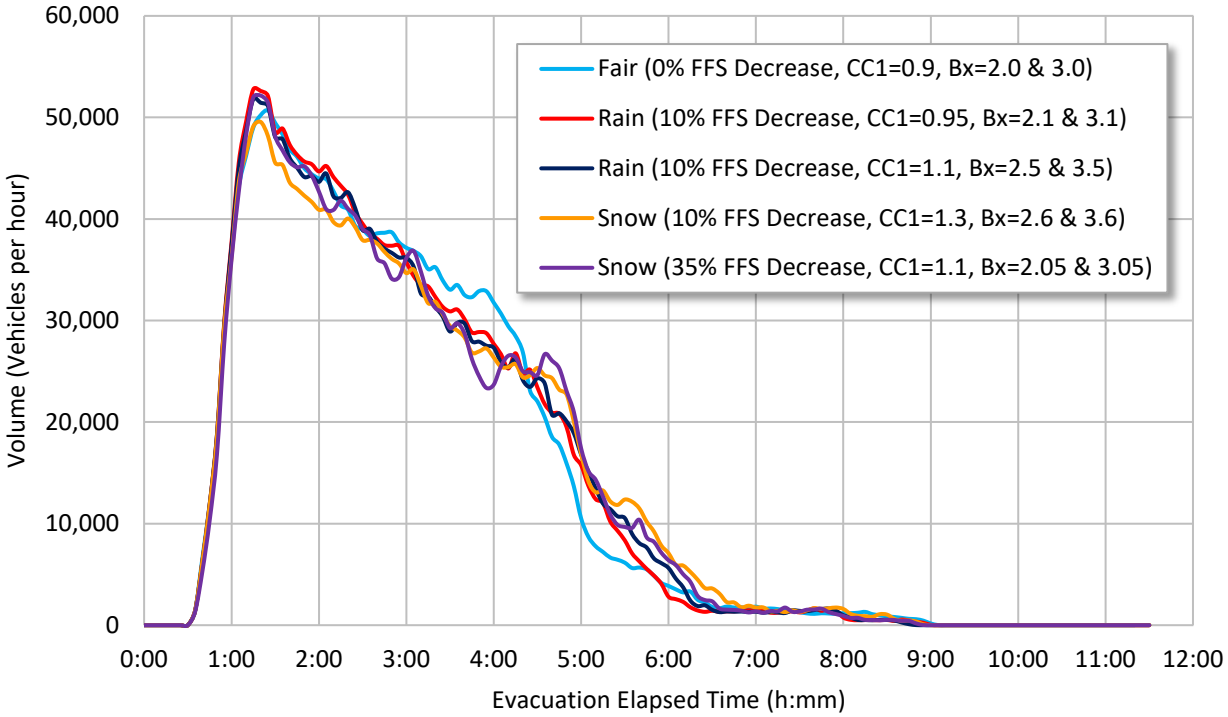

Figure 7-75 EPZ Exit Volumes, Large Population Site Adverse Weather Analysis

7.3.6.5 Broader Findings of Adverse Weather Parameter Results

Adverse weather reduces roadway network capacity. As discussed throughout this report, nearly any set of conditions that appreciably change the relationship between demand and capacity have the potential to result in more congested travel conditions and have an impact on the ETE. Prior study and empirical observation has shown this to be true for conditions of adverse weather like heavy rain and icy road surfaces that require drivers to slow their speed and leave greater spacing between vehicles.

Comparing the findings of this study with prior ETE studies of comparable small, medium, and large population sites, the results for the impact of adverse weather are in fairly good agreement. Although it was noted that the impact of adverse weather on the 10-mile 100 percent ETEs was typically larger when using macroscopic traffic simulation. In small population site ETEs, the average increase in the 10-mile 90 percent ETE was 10 minutes in rainy conditions and 31 minutes in snowy conditions. The average increase in the 10-mile 100 percent ETEs was 20 minutes in rain and 1 hour for snow. For medium population sites, the average increase in the 10-mile 90 percent ETE was 17 minutes in rainy conditions and 29 minutes in snowy conditions. The average increase in 10-mile 100 percent ETE was 45 minutes in rain and 1 hour in snow.

For large population sites, the average increase in the 10-mile 90 percent ETE was 28 minutes in rainy conditions and 36 minutes in snowy conditions. The average increase in the 10-mile 100 percent ETE was 1 hour and 1 hour and 14 minutes for rain and snow, respectively. The difference between the results of this study and typical ETE studies is mobilization time. This study only looked at impact to the ETE based on adverse weather driving conditions. However, as demonstrated in the study of mobilization time, the ETE can also be significantly impacted by mobilization activities. In the case of snow, mobilization times can be increased by well more than an hour. When mobilization time is considered, the results of this study confirm the sensitivity to adverse weather as predicted in site-specific ETE studies.

The nature of VISSIM and its internal DTA could also play a role in these results. A closer inspection of network performance suggested that degraded flow conditions and queue formation were exacerbated on arterial roadways with signalized intersections. This was especially apparent in the medium population site model. It is possible that the DTA function reduced the impact of adverse weather on ETEs by routing vehicles around traffic. However, the adverse weather modeling affects vehicle behavior regardless of route choice, so the effect of DTA is probably minor.

Of significance in this research is that the impacts of adverse weather could be captured through adjustment of only a few variables. Although many other parameters influence driver behavior and are modeled in the Wiedemann models, among other driver behavior models, the free-flow speed and headway were shown to be influential to the same degree as reported in other more comprehensive studies of adverse weather impacts. From a modeling perspective, these results also suggest that the type of aggregate capacity reductions used to represent adverse weather conditions in macroscopic traffic simulation models yield results that are both useful and reasonable.

7.3.7 Roadway Impact Parameter Results

The study of capacity losses resulting from network disruptions due to flooding, work zones or major traffic incidents can significantly impact ETEs. Selected roadway links were partially closed to assess the extent of impact. In general, it was expected that the average 90 and 100 percent ETEs would be affected by the roadway impact scenario.

7.3.7.1 Small Population Site Model Roadway Impact Parameter Results

In the small population site model, the right lane of Link 647 was closed to traffic. Link 647 is a two-lane road located inside the EPZ and near the 10-mile EPZ boundary in the NE sector. Table 7-38 summarizes the 90 and 100 percent ETEs. There was no significant effect on any ETE. This could be because the small demand in the small population site model did not overwhelmed the network to create sufficiently large queues and extend the ETE. Although the link selected for the lane closure was not carrying the largest volume of vehicles, this was the only link with sufficiently high volumes inside the EPZ that had more than one lane to allow modeling the lane closure. In addition, the base model was visually inspected, and queues were observed at this location. However, the lane closure, did not significantly exacerbate the formation of queues. Figure 7-76 shows the cumulative percent of evacuees exiting the 10-mile ring.

Table 7-38 Small Population Site Roadway Impact Analysis

Scenario Number	Link Number Closed	Average Evacuee Delay (minutes)	2-Mile		5-Mile		10-Mile	
			90% ETE	100% ETE	90% ETE	100% ETE	90% ETE	100% ETE
1[1]	-	14	1:35	2:18	1:35	2:21	1:44	2:31
2	647	18	1:35	2:15	1:35	2:20	1:45	2:30

[1] Base model.

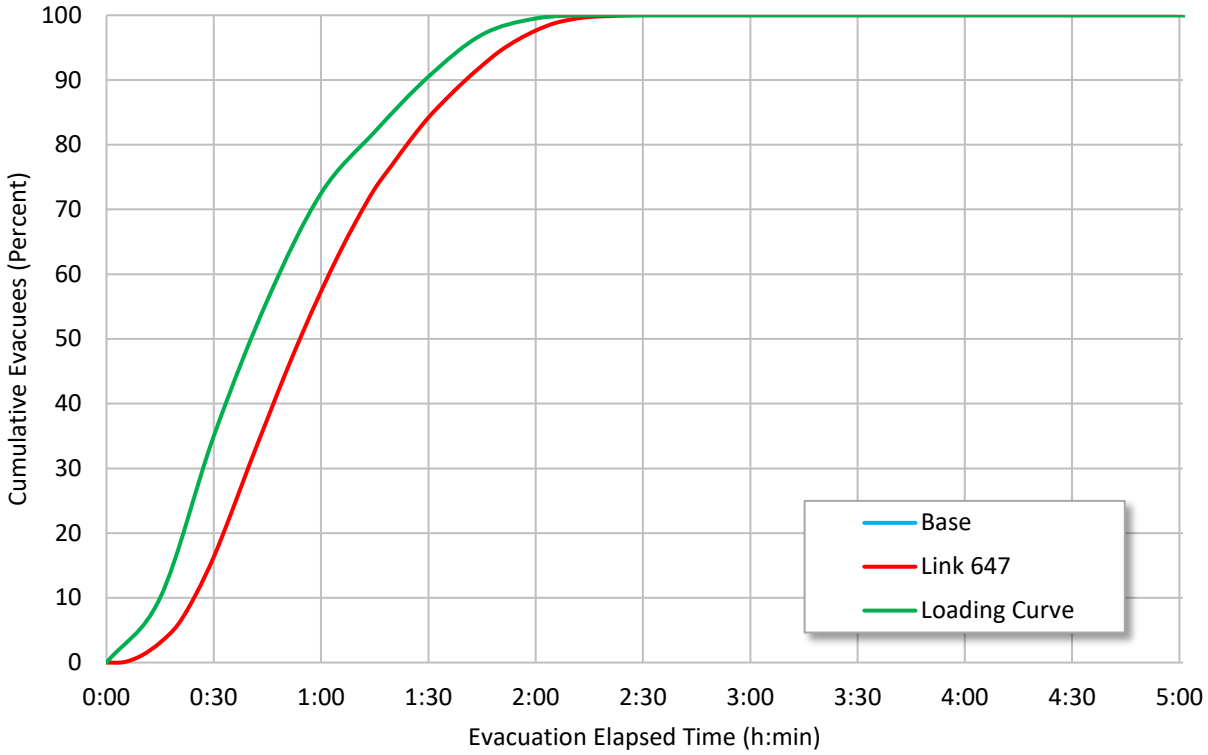

Figure 7-76 Ten Mile ETE Curves, Small Population Site Roadway Impact Analysis

7.3.7.2 Medium Population Site Model Roadway Impact Parameter Results

Table 7-39 summarizes the average 90 and 100 percent ETEs for the medium population site model. Closing the left lane on both segments of a freeway located in the North sector and near the EPZ boundary (Links 133 and 222) had a significant effect on the 90 and 100 percent ETEs at the 5 and 10-mile rings. Since the closures were located near the 10-mile EPZ boundary, it is suggested that queues propagated back to the 5 mile ring. The selected closures were on freeway segments and located close together, as shown in Figure 7-12. These segments were selected for analysis based on the high volume of traffic and the low travel speeds shown in the base model results. In all scenarios, the number of vehicles not exiting the EPZ remained less than 1.7 percent.

Table 7-39 Medium Population Site Roadway Impact Analysis

Scenario Number	Link Number Closed	Average Evacuee Delay (minutes)	2-Mile		5-Mile		10-Mile	
			90% ETE	100% ETE	90% ETE	100% ETE	90% ETE	100% ETE
1[1]	-	70	2:40	4:03	2:47	5:05	5:03	7:41
2	133	86	2:40	4:03	3:22	6:42	6:00	10:52
3	222	82	2:40	4:03	3:28	6:23	5:58	10:17

[1] Base model.

Figure 7-77 and Figure 7-78 show the cumulative percent of evacuees exiting the 5 and 10-mile rings, respectively. In the 5-mile ring, travel conditions in the network are almost the same as in the base model until 2 hours into the evacuation when the ETE curves for the lane closure scenarios and the base start to separate. Because of the proximity to each other, the travel conditions in both lane closure scenarios have very similar impacts; however, some differences are noticeable after 95 percent of the vehicles have left the EPZ. Thus, the evacuation tail experienced longer travel times with the link closure on Link 133 compared to Link 222. From Figure 7-78, it can be seen that the roadway impact scenario affects the ETE for the duration of the evacuation when compared to the base model. This is likely mostly because the lane closures were near the EPZ boundary and traffic conditions downstream of the blockage did not have time to recover prior to exiting the EPZ.

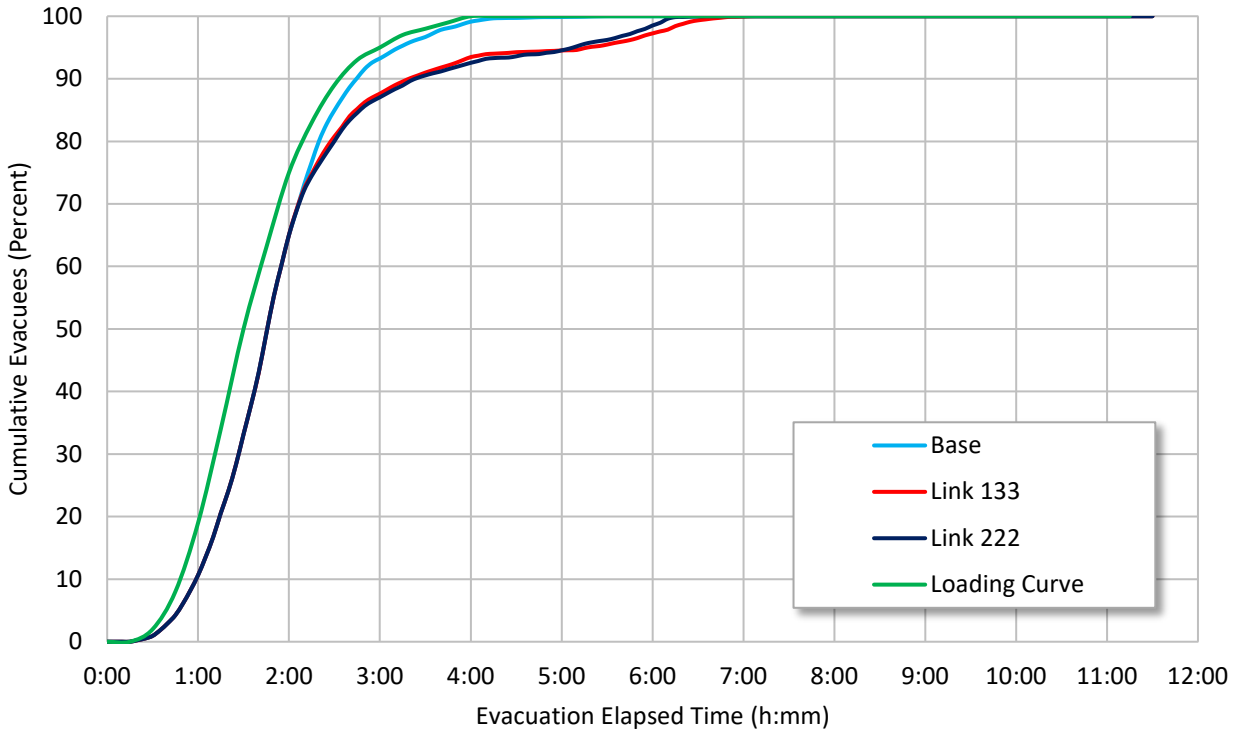

Figure 7-77 Five Mile ETE Curves, Medium Population Site Roadway Impact Analysis

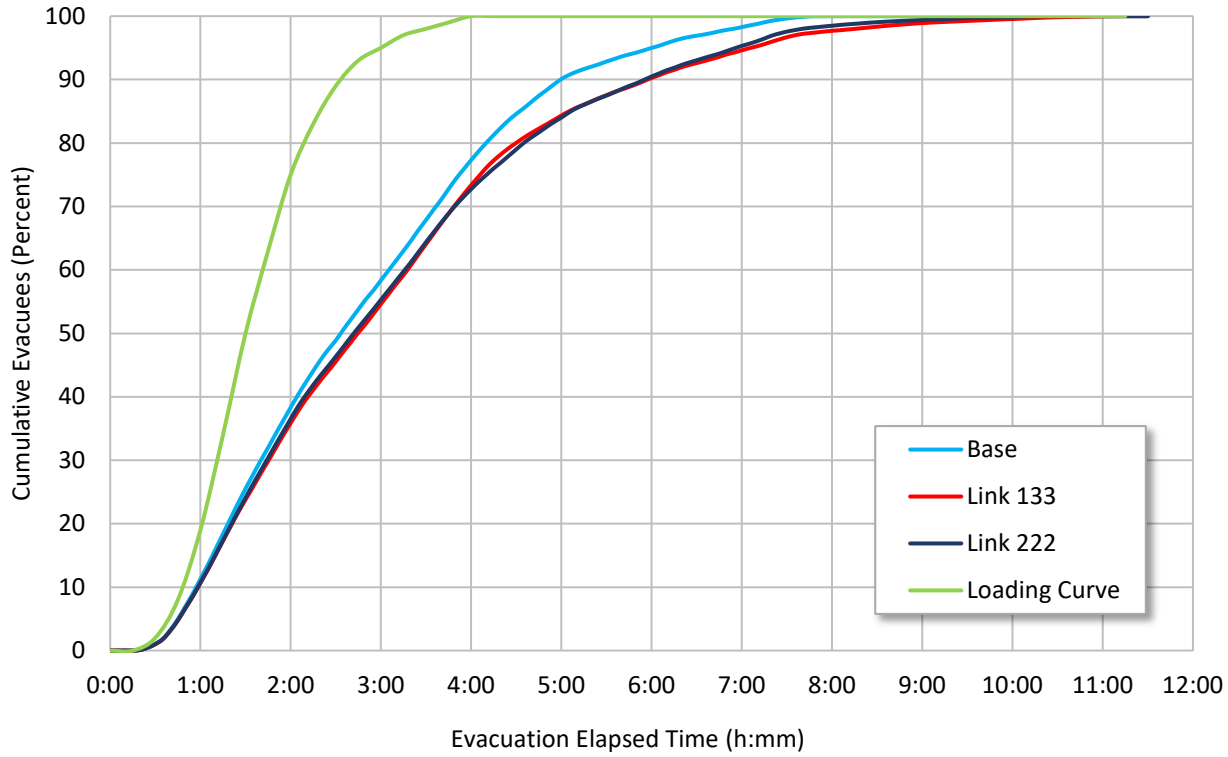

Figure 7-78 Ten Mile ETE Curves, Medium Population Site Roadway Impact Analysis

7.3.7.3 Large Population Site Model Roadway Impact Parameter Results

Table 7-40 summarizes the average 90 and 100 percent ETEs for the large population site model. The lane closure on the freeway segment (link 150) at the EPZ boundary significantly increased the 90 and 100 percent ETEs at the 10-mile ring. The impact was not as significant as the effect in the medium population site; however, the closure of link 150 had a significant impact on the evacuation tail inside the 2 and 5-mile rings. The closure on the interior arterial road in the large population site (link 32909) did not affect the overall clearance process at the EPZ boundary, but was significant at the 5-mile ring. The closure on link 32909 was between miles 7 and 8, so queue formation had more of an impact inside the EPZ. Demand on these links were also different. In all scenarios, the number of vehicles not exiting the EPZ remained less than 1 percent.

Table 7-40 Large Population Site Roadway Impact Analysis

Scenario Number	Link Number Closed	Average Evacuee Delay (minutes)	2-Mile		5-Mile		10-Mile	
			90% ETE	100% ETE	90% ETE	100% ETE	90% ETE	100% ETE
1[1]	-	62	3:39	5:06	4:02	6:35	4:43	9:01
2	150	69	3:41	6:01	4:46	8:35	5:17	9:38
3	32909	60	3:41	5:05	4:25	7:21	4:53	9:05

[1] Base model.

Figure 7-79, Figure 7-80, and Figure 7-81 show the cumulative percent of evacuees exiting the 2, 5, and 10-mile rings, respectively. When Link 150 was partially closed, there was a delay of the last few vehicles exiting the 2-mile area, extending the 100 percent ETE for this ring. The impact was more significant at the 5-mile ring and there is a large separation observed among the ETE curves for both of the lane closure scenarios. The largest impact of the lane closure on the interior Link 32909 was also seen at the 5-mile ring. The ETE curves at the 10-mile ring also differ from the base model, with the lane closure in Link 150 having the greatest impact at the 10-mile ring due to its location near the EPZ boundary.

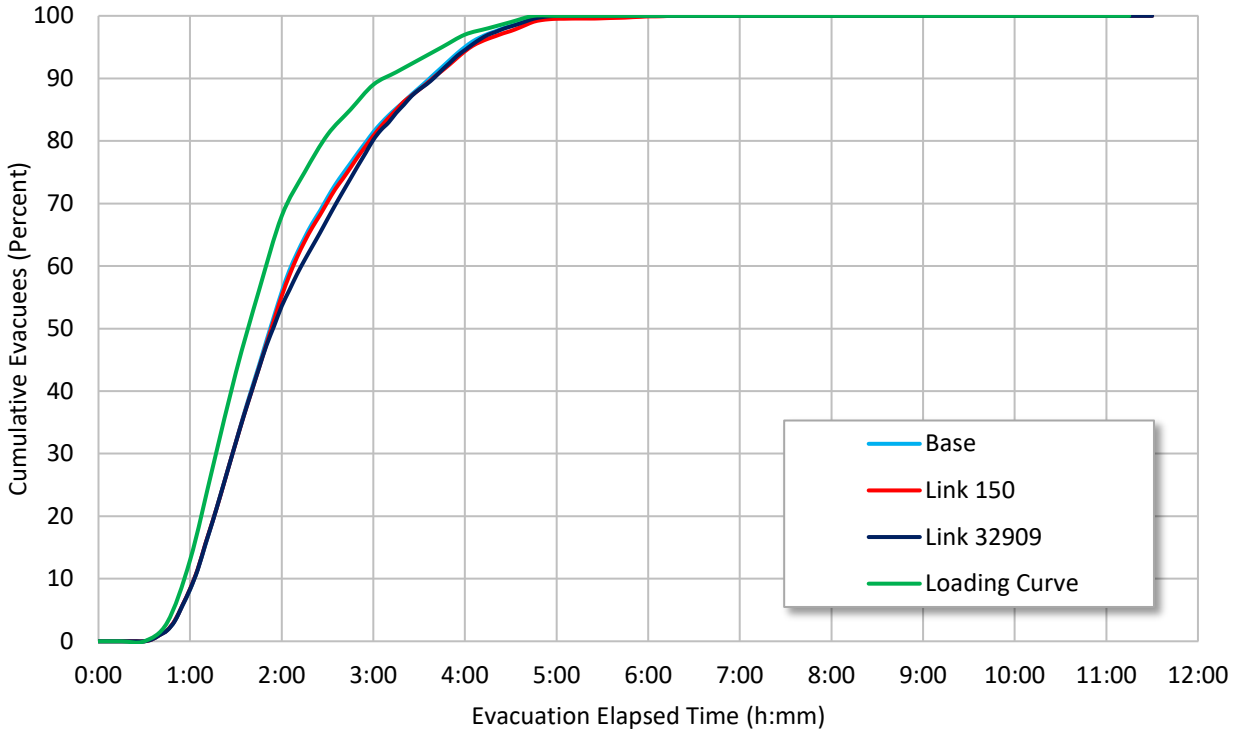

Figure 7-79 Two Mile ETE Curves, Large Population Site Roadway Impact Analysis

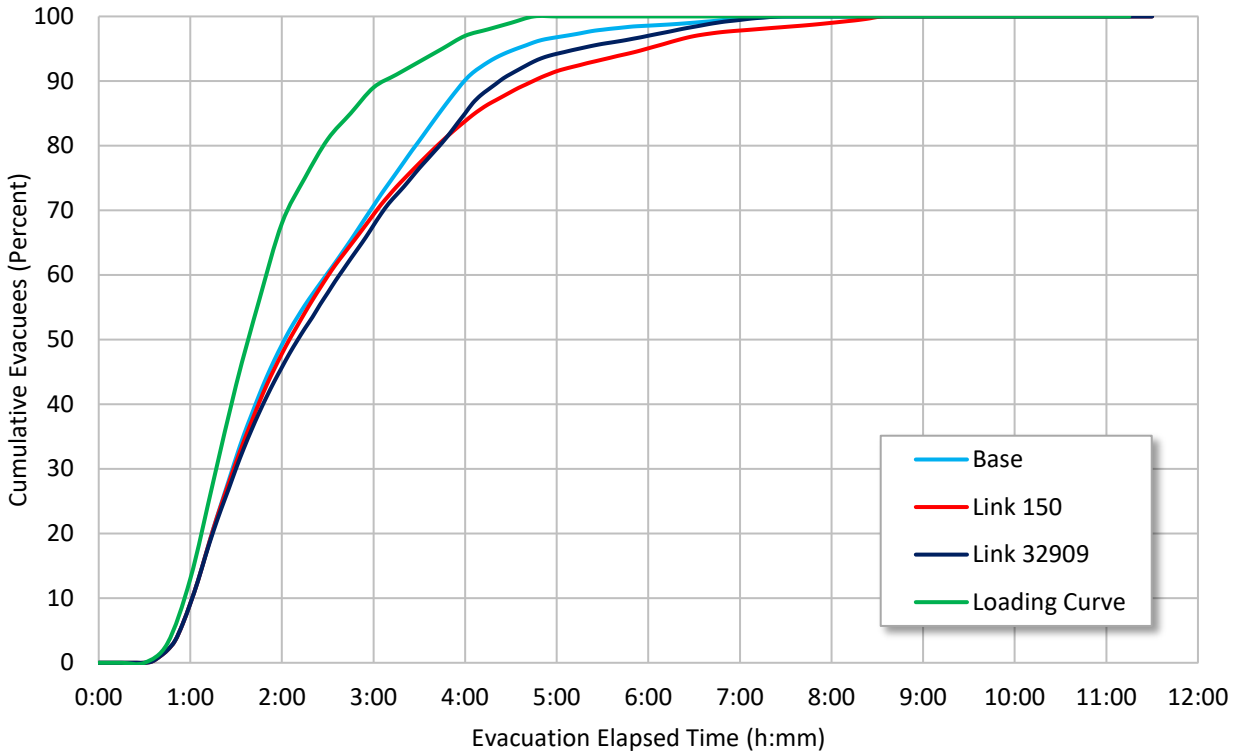

Figure 7-80 Five Mile ETE Curves, Large Population Site Roadway Impact Anaysis

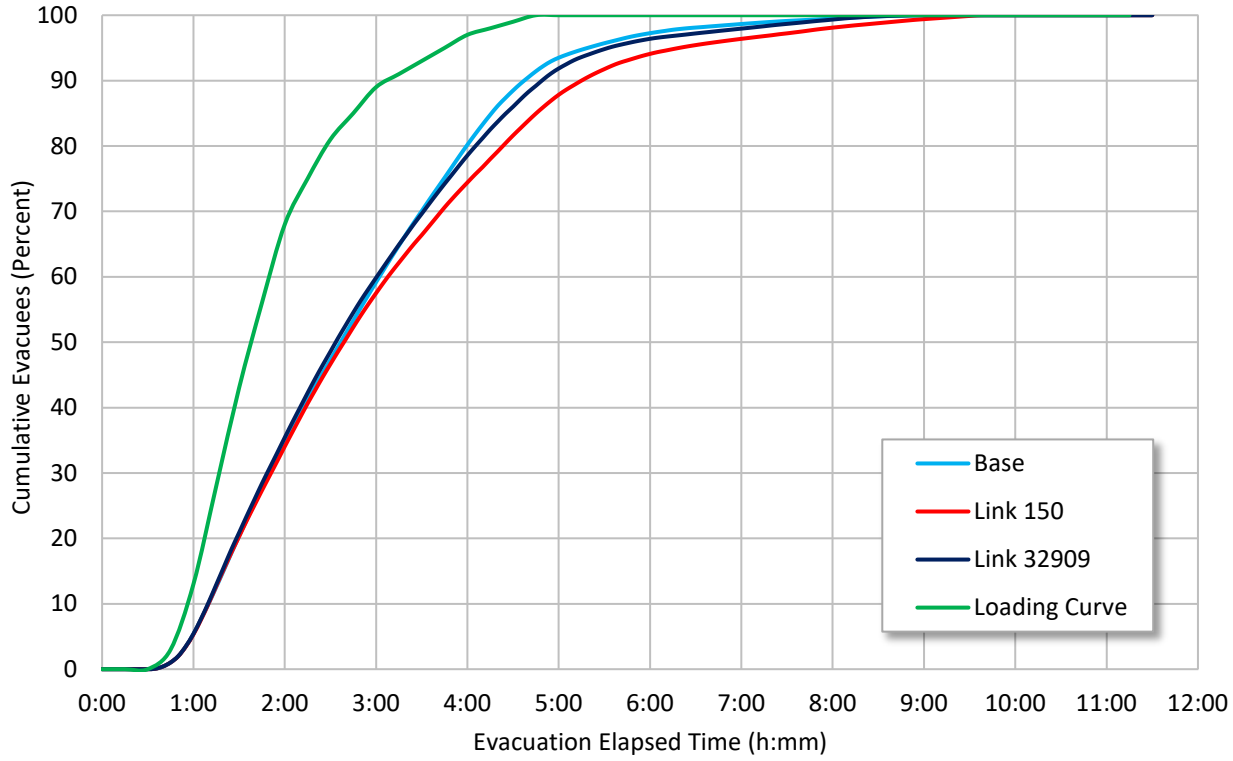

Figure 7-81 Ten Mile ETE Curves, Large Population Site Roadway Impact Analysis

7.3.7.4 Average Travel Time Results Roadway Impact Analysis

Travel times beyond the EPZ were collected and analyzed to determine the effect of the closure on traffic performance in the vicinity of the closure location. Travel time data collectors were placed upstream of the lane closure location in each model. Travel time was also collected at the same location in the base model to draw comparisons. It was expected that the lane closure would incur additional travel time for the drivers around that location, in particular when the demand was higher. Significantly larger average travel times were expected to increase the ETE from the base condition.

Figure 7-82 shows the travel time data for the base and roadway impact scenario in the small population site model. Travel time only increased by one minute, and ETEs were not significantly impacted. Queue length data was also collected which showed no queues formed upstream of the closure. This result is not unexpected since this link was not carrying a large volume of vehicles.

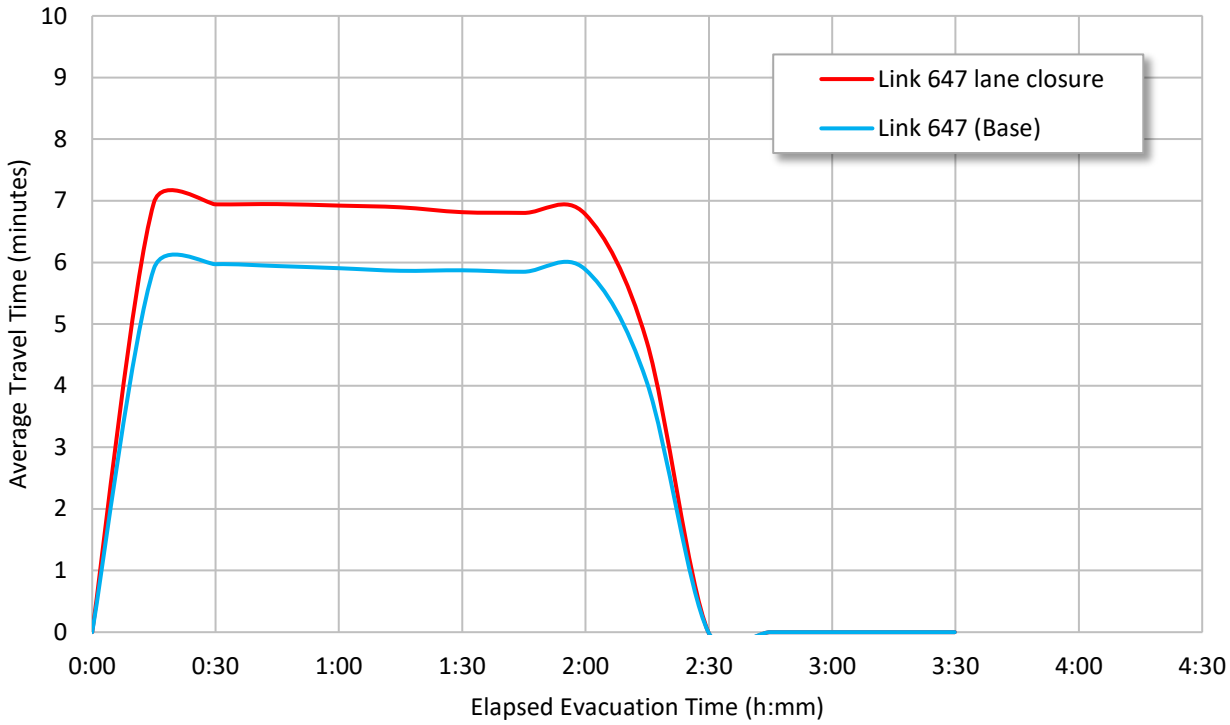

Figure 7-82 Segment (Link 647) Travel Times, Small Population Site Roadway Impact Analysis

Figure 7-83 shows the travel time data for the base scenario and the lane closure on Link 133 in the medium population site. Early on in the evacuation process, travel times for evacuees oscillated around 5 to 10 minutes in the base model upstream of Link 133, indicating slight congestion. Travel times later in the evacuation were only a few minutes. This indicates minimal delay. Closing a lane on Link 133 significantly increased travel time. Slowdowns were observed to start about one hour earlier and queues quickly built up increasing travel times by 30 minutes. Congested conditions remained for about nine hours due to the lane closure. This congestion quickly decreased near the end of the evacuation. The travel conditions on this link affected the ETE .

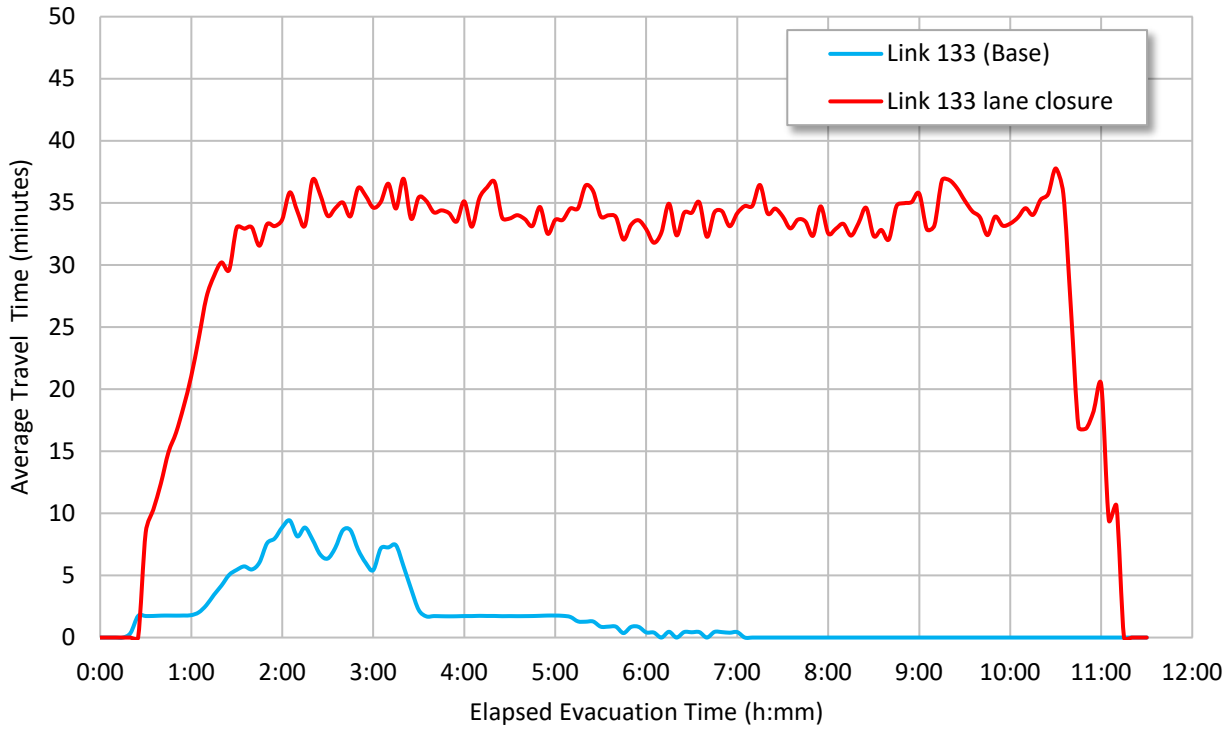

Figure 7-83 Segment (Link 133) Travel Times, Medium Population Site Roadway Impact Analysis

Figure 7-84 shows the travel time data for the base model and lane closure on Link 222 in the medium population site. Base model travel times were approximately the same as on Link 133, since traffic along these links are connected, with Link 222 being upstream inside the EPZ. Closing a lane on Link 222 had a slightly greater impact on average travel time than on Link 133. This may be related to the length of the closure, which was the longest of all the lane closure segments tested in any of the models. Again, longer average travel times were observed to start about one hour earlier than in the base model. The travel time reached a maximum of close to 48 minutes. Average travel time dropped around 4 hours and 30 minutes into the evacuation but persisted at around 30 to 35 minutes until the end of the evacuation. The lane closure on Link 222 acted very similar to Link 133, although overall it had less impact on the ETE. It is possible that the DTA routed vehicles away from this route when travel times significantly increased.

Queue length data was also collected at the roadway impact location to measure the average queue length upstream of the start point of the lane closure. Queue length data was collected in the base model for comparison. Queue lengths were commensurate with the average travel time data. As shown in Figure 7-85, both lane closures showed extensive increases in queue length, with queues extending approximately one-quarter of a mile.

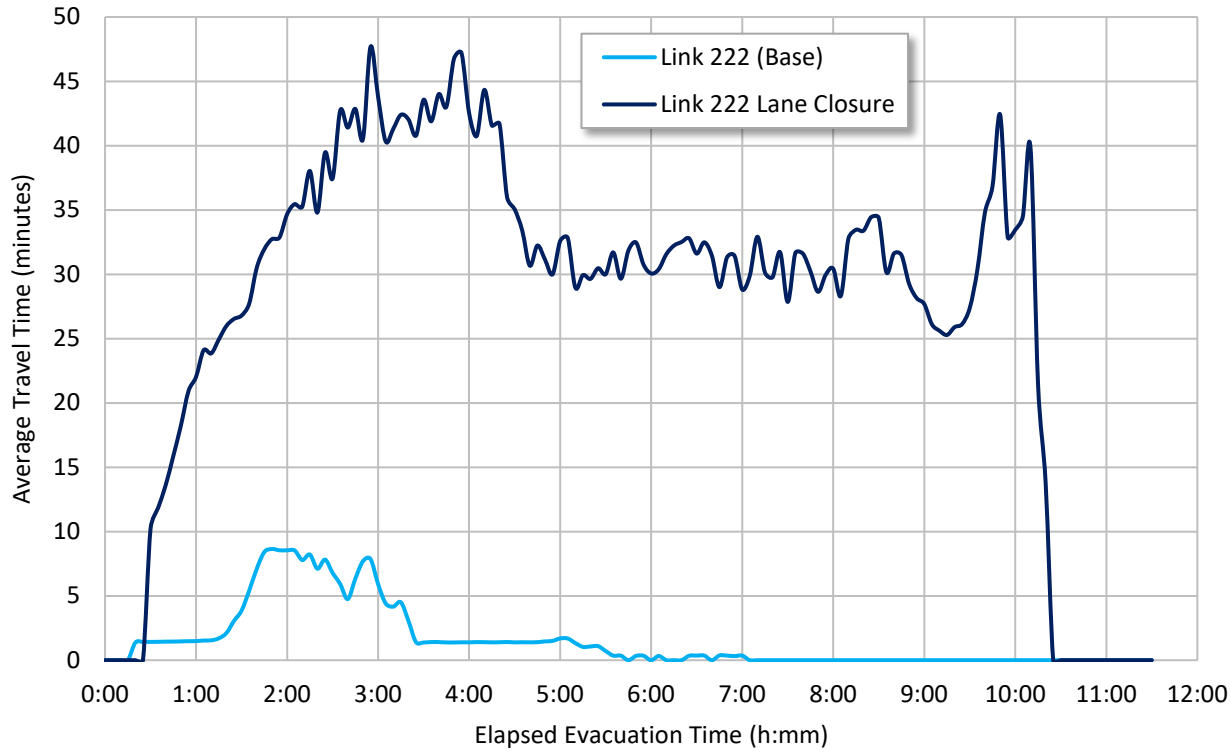

Figure 7-84 Segment (Link 222) Travel Times, Medium Population Site Roadway Impact Analysis

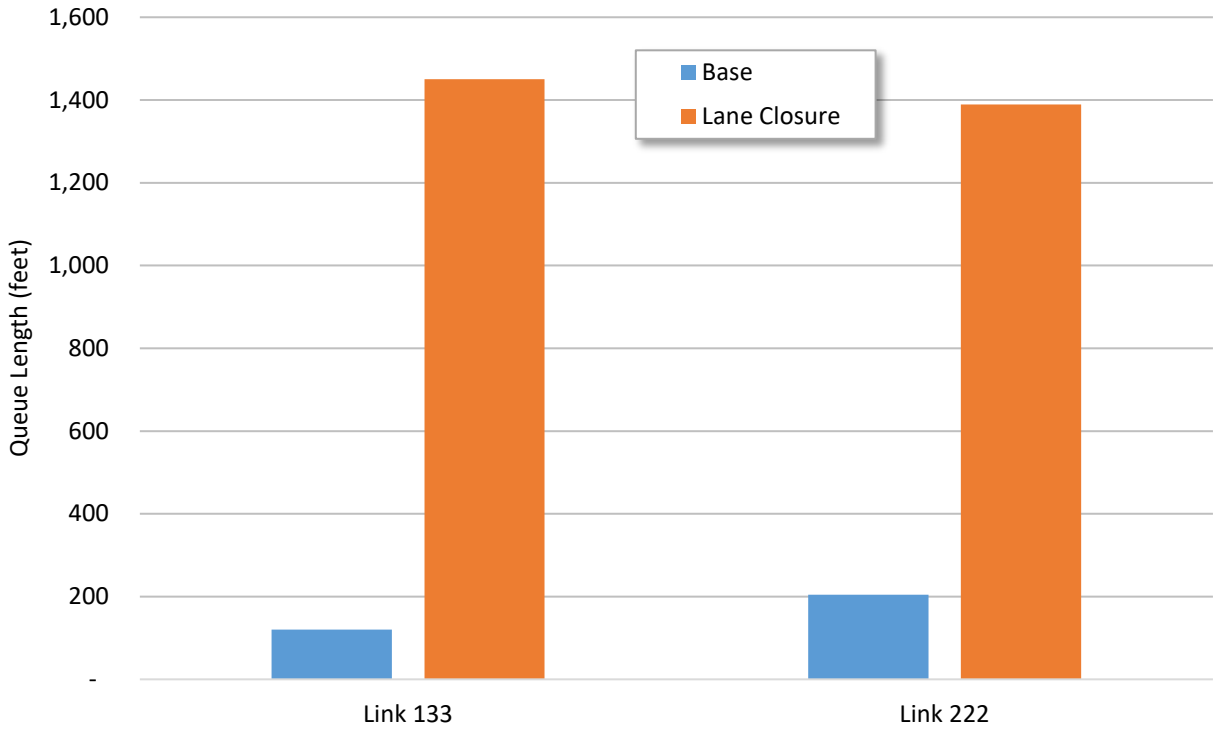

Figure 7-85 Average Queue Length, Medium Population Site Roadway Impact Analysis

Figure 7-86 shows the average evacuee travel time data for the base model and lane closure on Link 150 in the large population site model. Travel times are not long compared to the medium population site model, and the lane closures even appear to improve the average travel time. However, the lane closure had the impact of extending the evacuation process and increasing the average evacuee delay. The steady pace and sudden drop off of travel time suggests that there was a queue and the last vehicle in the queue passed through the segment around 9:30. The base model 10-mile 100 percent ETE was 9:01. Although it contained only a small fraction of the total evacuee vehicle demand, the queue that formed on Link 150, extended the 100 percent ETE by 37 minutes. Thus, even though average travel speed may have increased on the available travel lane, cutting down the average travel time through the segment, the capacity reduction due to the lane closure limited the outflow of vehicles. Since this occurred near the EPZ boundary, it significantly impacted the ETE.

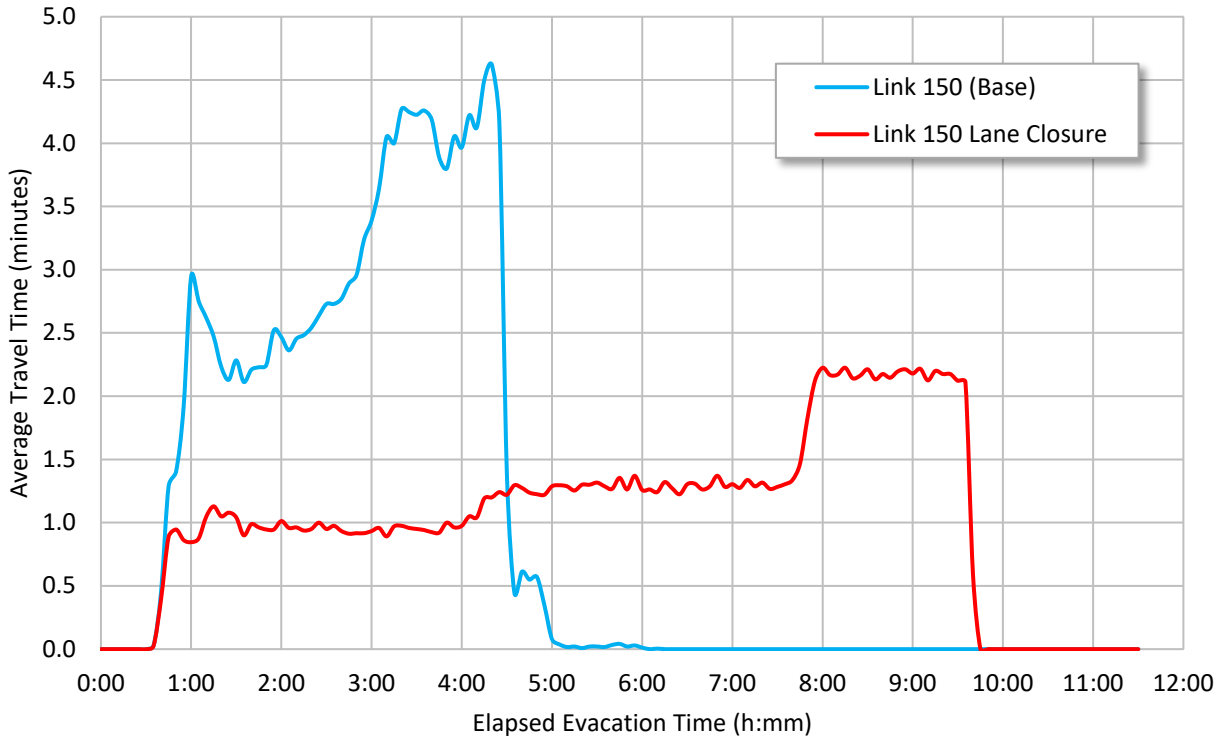

Figure 7-86 Segment (Link 150) Travel Times, Large Population Site Roadway Impact Analysis

Figure 7-87 shows the travel time data for the base and lane closure on Link 32909. The short travel times are related to the length of the lane closure segment which was relatively short. Again, the lane closure was observed to extended evacuation time along this link. The vehicle queue on this link persisted for about 90 minutes longer with the lane closure and this was observed to significantly impact the ETE for the 5-mile ring. However, the queue dissipates a few hours before the last vehicles crosses the EPZ boundary. As a result, the lane closure on Link 32909 had very little impact on the 10-mile ETE.

Queue length data was collected at the roadway disruption location to measure the average queue length upstream of the start point of the lane closure. Queue length data was also collected in the base model to draw comparisons. Figure 7-88 shows that both scenarios extended queues.

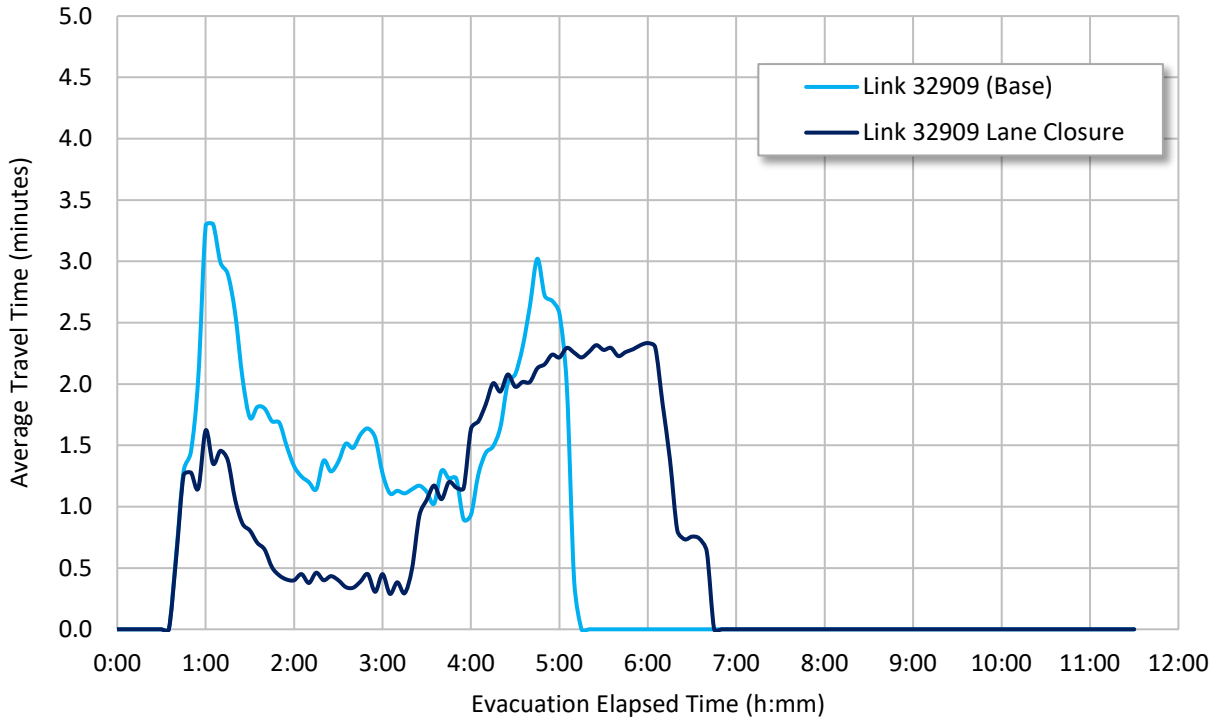

Figure 7-87 Segment (Link 32909) Travel Times, Large Population Site Roadway Impact Analysis

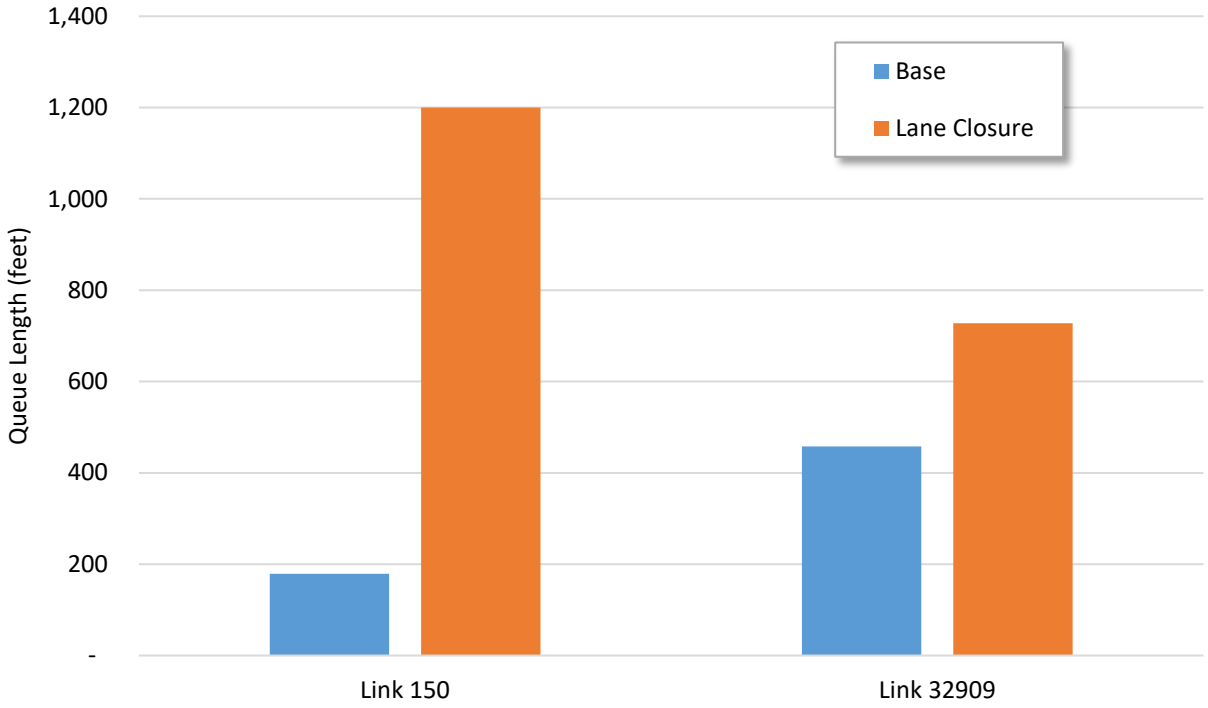

Figure 7-88 Average Queue Length, Large Population Site Roadway Impact Analysis

7.3.7.5 Exit Volume Results for Roadway Impact Parameter

Figure 7-89 shows the rate of vehicles leaving the 10-mile EPZ in the small population site model. The lane closure had no significant impact on the rate of vehicles exiting the EPZ. Figure 7-90 shows the rate of vehicles leaving the 10-mile EPZ in the medium population site model. Both lane closure scenarios impacted the exit flow rate by about 3000 vehicles per hour. The dissipation of the vehicle queues toward the end of the evacuation show how the lane closures significantly impacted the evacuation tail and the resultant ETE.

Figure 7-91 shows the rate of vehicles leaving the 10-mile EPZ in the large population site model. All curves flatten toward the end of the simulation indicative of queue dissipation. Queue dissipation was observed for all three scenarios, because the large population site is heavily congested even in the base model; however, the lane closures extended the duration of the queues, impacting the ETE as previously described.

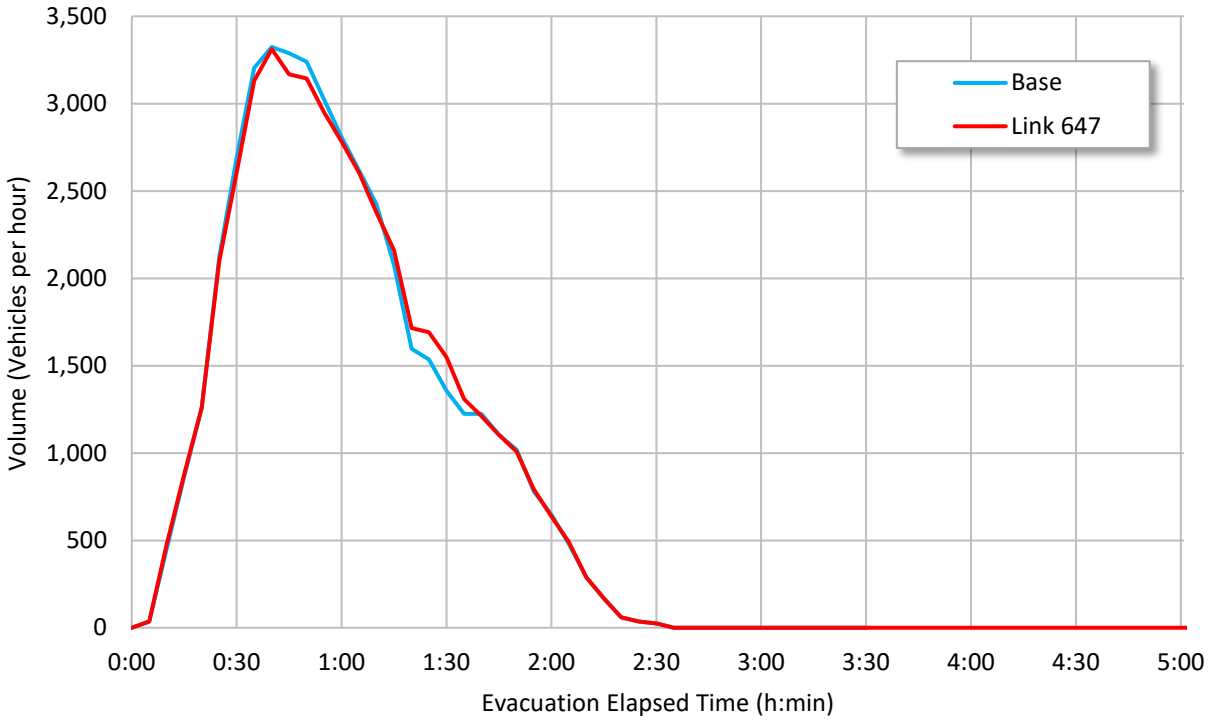

Figure 7-89 EPZ Exit Volumes, Small Population Site Roadway Impact Analysis

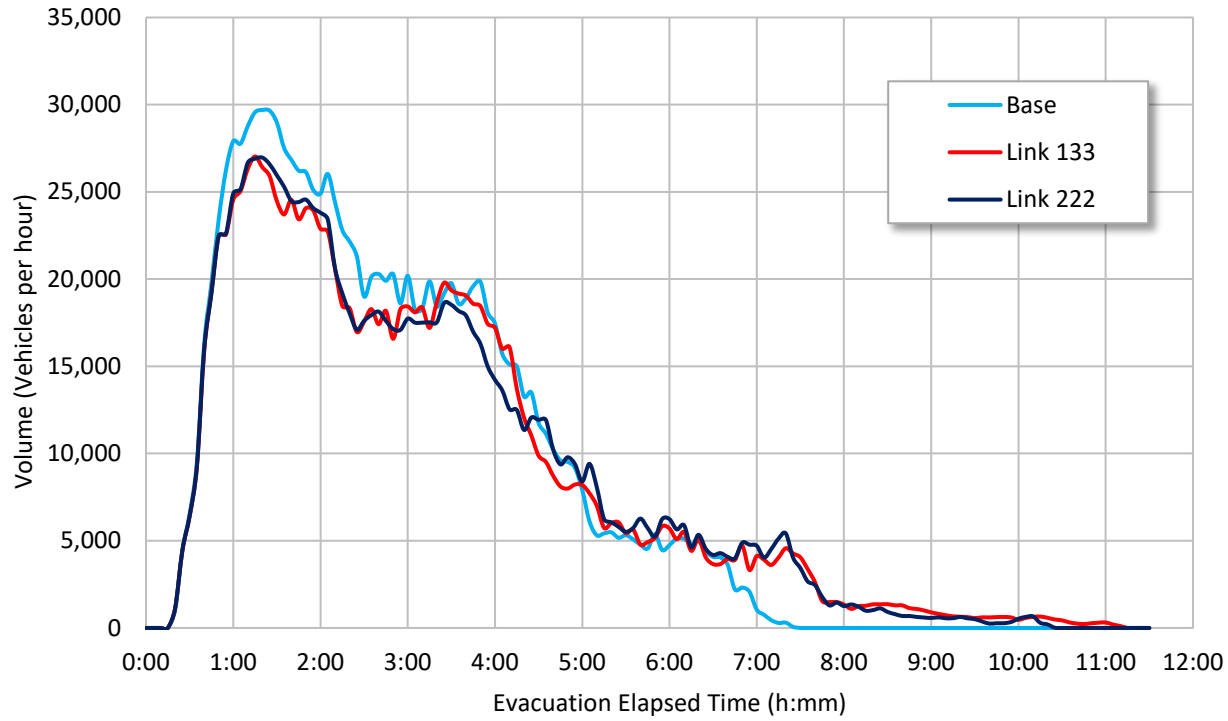

Figure 7-90 EPZ Exit Volumes, Medium Population Site Roadway Impact Analysis

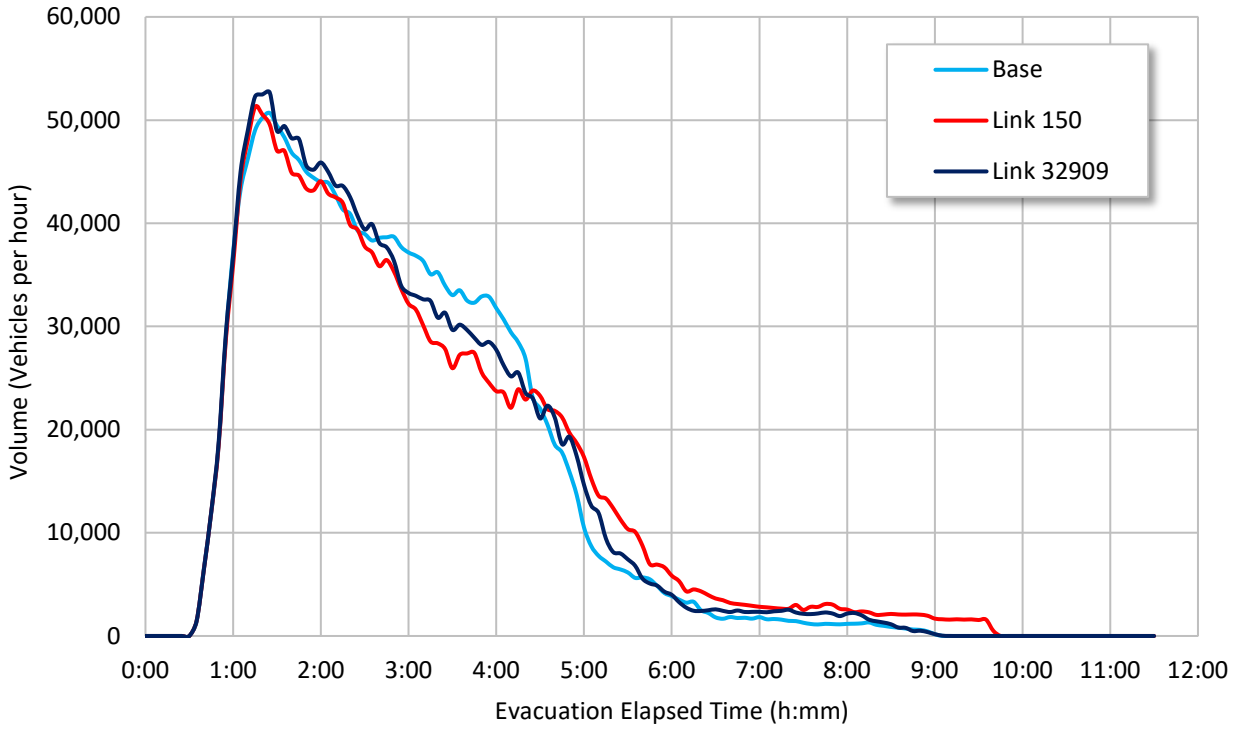

Figure 7-91 EPZ Exit Volumes, Large Population Site Roadway Impact Analysis

7.3.7.6 Broader Findings of Roadway Impact Parameter Results

Incidents and disruptions are known to reduce capacity and cause congestion and delay within roadway networks. The occurrence of such events during an evacuation, when traffic demand is high, can have impacts on the evacuation process in the vicinity of the disruption. This may have significant impacts on the ETE.

The disruptions tested were planned closures of a single lane on important roadway links. Local authorities would be aware of planned closures on evacuation routes or other important roads. They would act to mitigate the planned disruption should it be necessary. Unplanned disruptions are tested in biennial exercises. The Federal Emergency Management Agency often challenges local authorities to cope with a roadway disruption. This is usually ameliorated by dispatching resources to route traffic around the disruption as best as can be accomplished.

From a modeling perspective, these results show the importance of roadway impacts in ETE computation. NRC guidance in NUREG/CR-7002 recommends that a roadway disruption scenario be analyzed. However, disruptions can be highly variable in nature in both time and location of their occurrence. Collection of additional analyses for roadway disruptions in ETEs may provide useful modeling information. Random disruptions cannot be identified in advance and planned disruptions would be addressed by local authorities. However, it may be possible to use ETEs to rank the significance of roadways with respect to percent of network capacity. This would provide local authorities with a sense of the impact disruptions would have should an evacuation be necessary. This information would allow authorities to plan in advance if the disruption is of high significance and not take unnecessary action if it is not.

7.3.8 Processing Time Step Parameter Results

The default processing time step within VISSIM is 10 time steps per second and a parameter value between 5 and 10 time steps per second is recommended to produce more accurate results [21]. The value selected for use throughout this study was 1 time step per second. This was based on the results of initial model testing and to minimize overall processing time. Since the processing time step could impact model performance, the sensitivity of the ETE to this parameter was evaluated in this task.

The results indicate that the representative population site models appeared to be more or less insensitive to the processing time step parameter. In particular, the 90 percent ETE, which is used for protective action recommendations, was not significantly impacted. With regard to computational power and processing time though, the test models used in this research required significantly more time to run than would typically be expected for a site-specific ETE model. The additional time needed to run the models ranged from 2 to 15 hours for just one random seed result.

In general, run time will also depend on the characteristics of the model and the computer capabilities. NPP licensees have historically conducted their ETE analysis using macroscopic and mesoscopic simulation platforms. These platforms require significantly less processing power than a microscopic tool, like the one used in this research. Therefore, there is less need to compromise between processing time/power and model fidelity.

7.3.8.1 Small Population Site Model Processing Time Step Parameter Results

Table 7-41 shows the 90 and 100 percent ETEs for the small population site model at the 2, 5, and 10-mile rings. The 90 percent and 100 percent ETEs remained unchanged with different processing time steps. Similar observations can be made from the cumulative percent evacuees exiting the EPZ boundary shown in Figure 7-92.

Table 7-41 Small Population Site Processing Time Step Analysis

Scenario Number	Processing Time Step (time steps per second)	Average Evacuee Delay (minutes)	2-Mile		5-Mile		10-Mile	
			90% ETE	100% ETE	90% ETE	100% ETE	90% ETE	100% ETE
1[1]	1	14	1:35	2:18	1:35	2:21	1:44	2:31
2	5	11	1:35	2:18	1:35	2:21	1:44	2:31
3	10	10	1:35	2:18	1:35	2:21	1:44	2:31

[1] Base model.

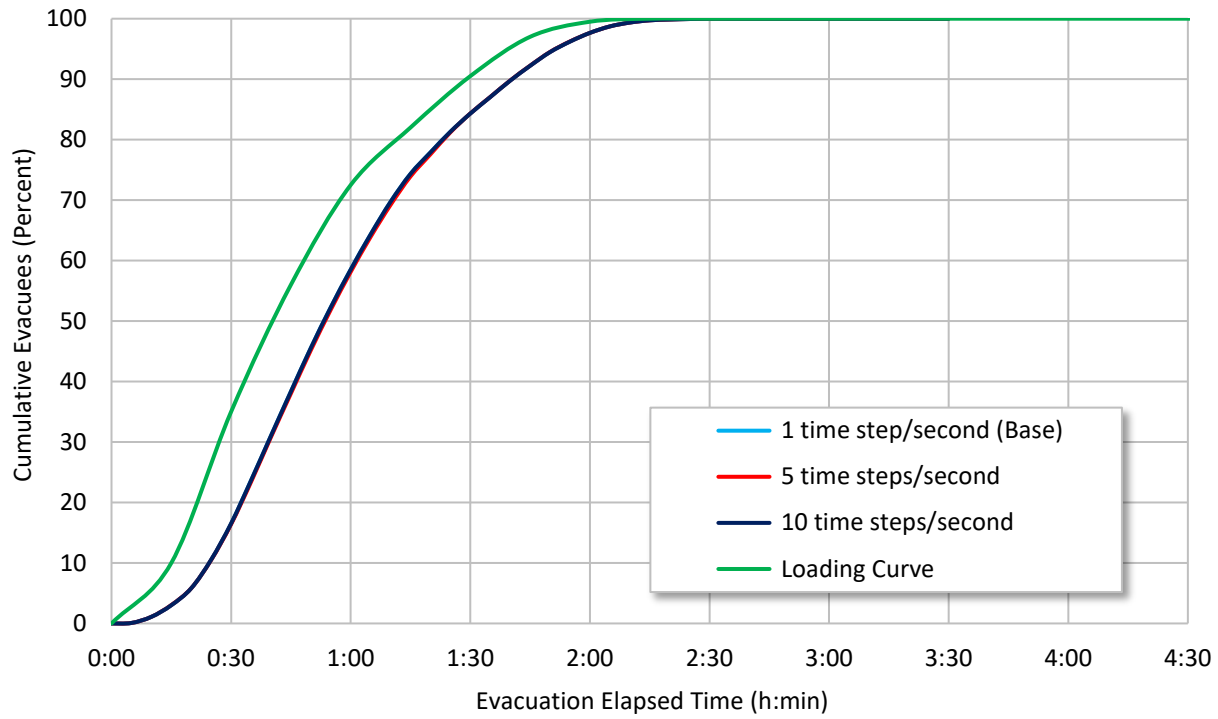

Figure 7-92 Ten Mile ETE Curves, Small Population Site Processing Time Step Analysis

7.3.8.2 Medium Population Site Model Processing Time Step Analysis

Table 7-42 shows the 90 and 100 percent ETEs for the medium population site model at the 2, 5, and 10-mile rings. The 90 percent ETEs were not affected by the higher resolutions. However, the 10-mile 100 percent ETE was observed to decrease significantly with 5 and 10 processing time steps per second. The 5-mile 100 percent ETE was also observed to decrease. In all scenarios, the number of vehicles not exiting the EPZ remained less than 1.5 percent.

Table 7-42 Medium Population Site Processing Time Step Analysis

Scenario Number	Processing Time Step (time steps per second)	Average Evacuee Delay (minutes)	2-Mile		5-Mile		10-Mile	
			90% ETE	100% ETE	90% ETE	100% ETE	90% ETE	100% ETE
1[1]	1	70	2:40	4:03	2:47	5:05	5:03	7:41
2	5	67	2:40	4:03	2:45	4:38	4:45	7:01
3	10	65	2:40	4:03	2:43	4:36	4:42	6:53

[1] Base model.

Figure 7-93, Figure 7-94, and Figure 7-95 show the cumulative ETE for the medium population site model at the 2, 5, and 10-mile rings, respectively. Higher resolutions in time-step were observed to decrease the ETE and show improved evacuation performance.

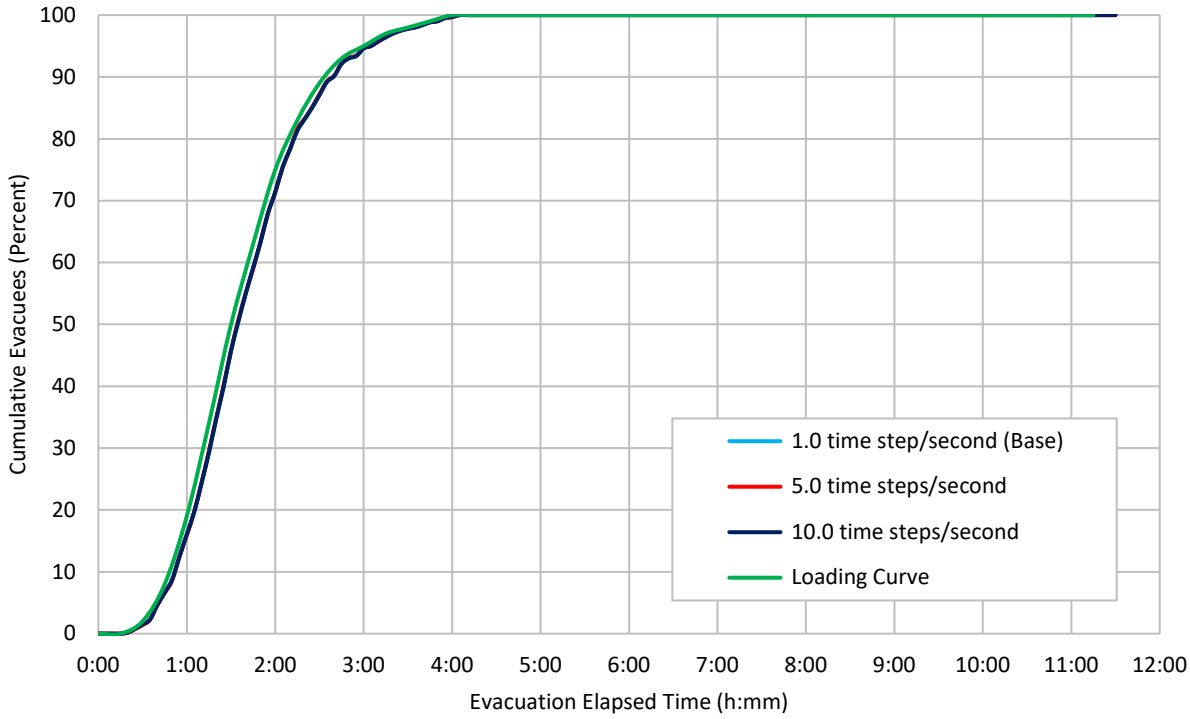

Figure 7-93 Two Mile ETE Curves, Medium Population Site Processing Time Step Analysis

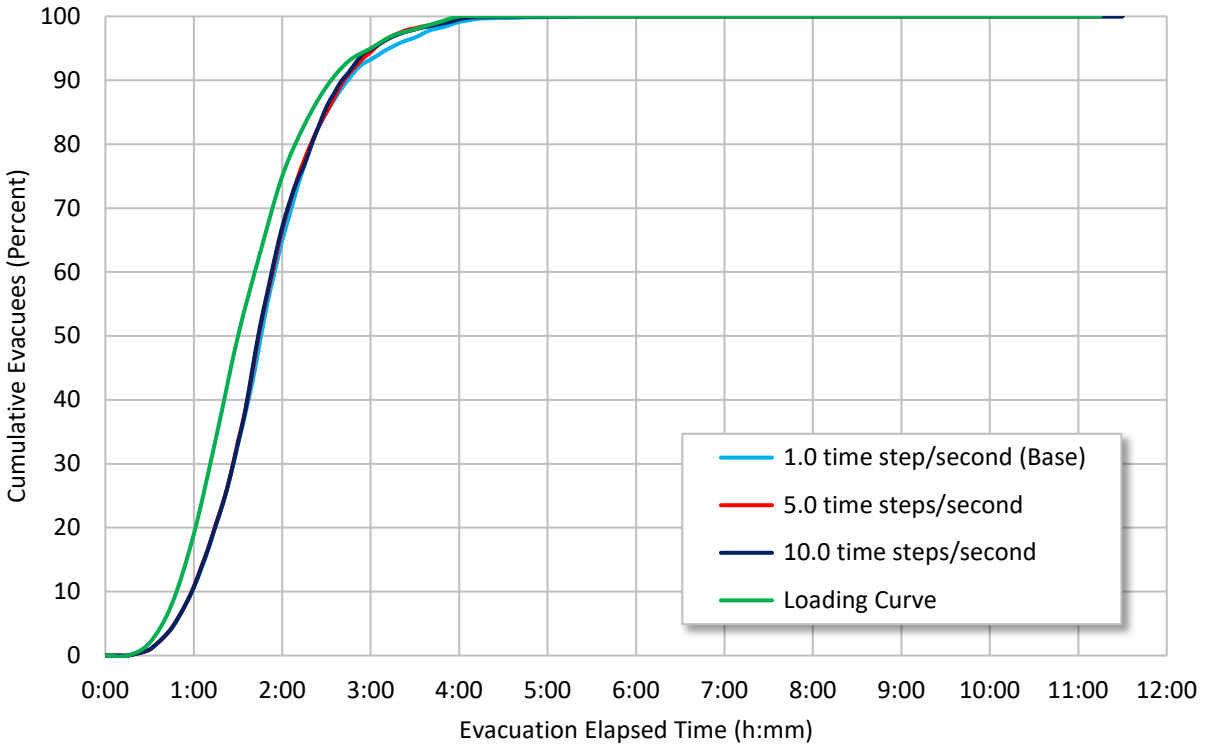

Figure 7-94 Five Mile ETE Curves, Medium Population Site Processing Time Step Analysis

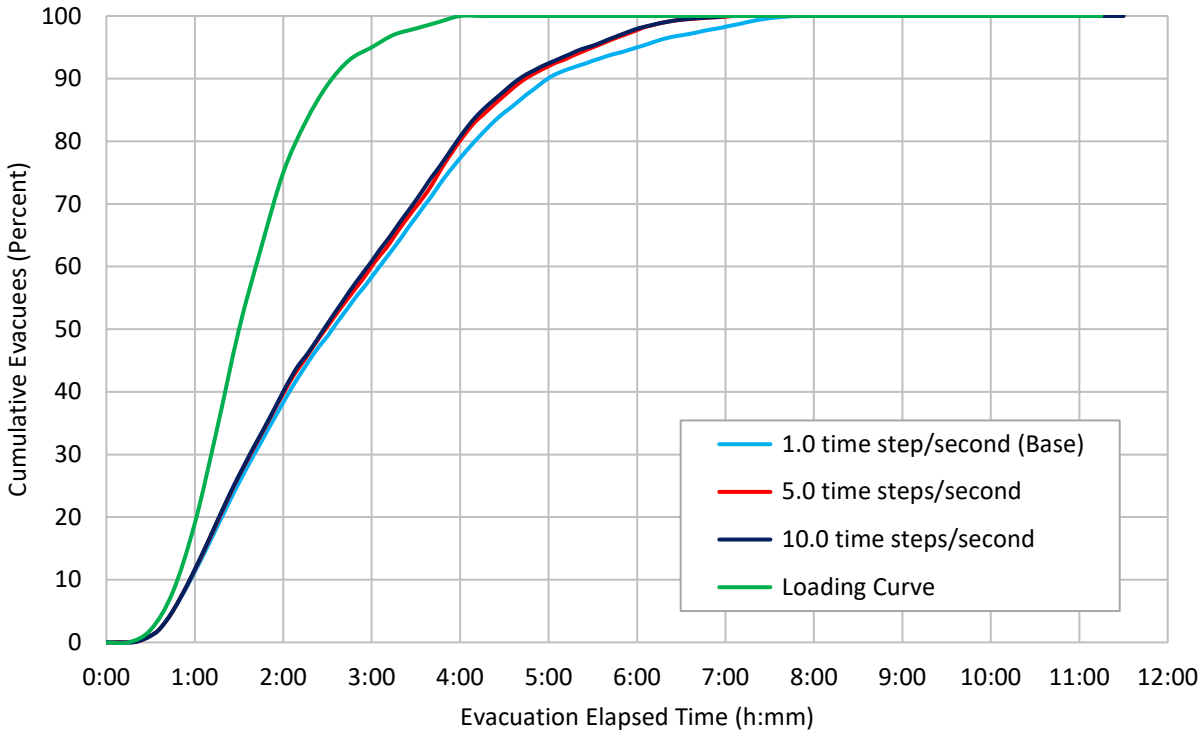

Figure 7-95 Ten Mile ETE Curves, Medium Population Site Processing Time Step Analysis

7.3.8.3 Large Population Site Model Evacuation, Processing Time Step Analysis

Table 7-43 shows the 90 and 100 percent ETEs for the large population site model at the 2, 5, and 10-mile rings. In general, ETEs decreased with increasing processing time steps. ETEs only decreased slightly at the 2-mile ring with higher resolutions and more significantly at the 5 and 10-mile rings. This is likely because of the lower population in the 2-mile area, such that interactions among vehicles was not affected by the frequency of the computation process. Only the 10-mile 100 percent ETE significantly decreased and this was observed at the highest processing time step. In all scenarios, the number of vehicles not exiting the EPZ remained less than 0.6 percent.

Table 7-43 Large Population Site Processing Time Step Analysis

Scenario Number	Processing Time Step (time steps per second)	Average Evacuee Delay (minutes)	2-Mile		5-Mile		10-Mile	
			90% ETE	100% ETE	90% ETE	100% ETE	90% ETE	100% ETE
1[1]	1	62	3:40	5:05	3:57	6:35	4:43	9:01
2	5	58	3:37	5:01	3:58	6:52	4:43	8:35
3	10	57	3:37	5:02	3:56	6:32	4:41	8:17

[1] Base model.

Figure 7-96, Figure 7-97, and Figure 7-98 show the cumulative ETE for the large population site model at the 2, 5, and 10-mile rings, respectively. Higher resolutions in time-step were observed to decrease the ETE and show improved evacuation performance.

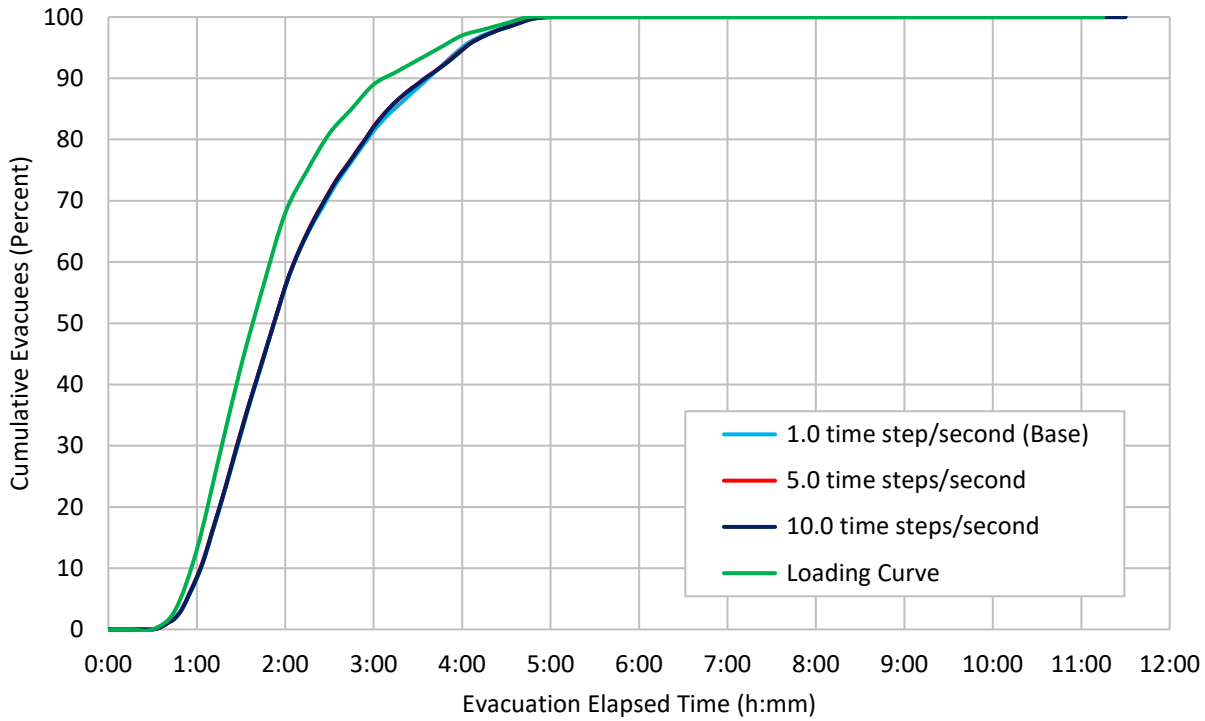

Figure 7-96 Two Mile ETE Curves, Large Population Site Processing Time Step Analysis

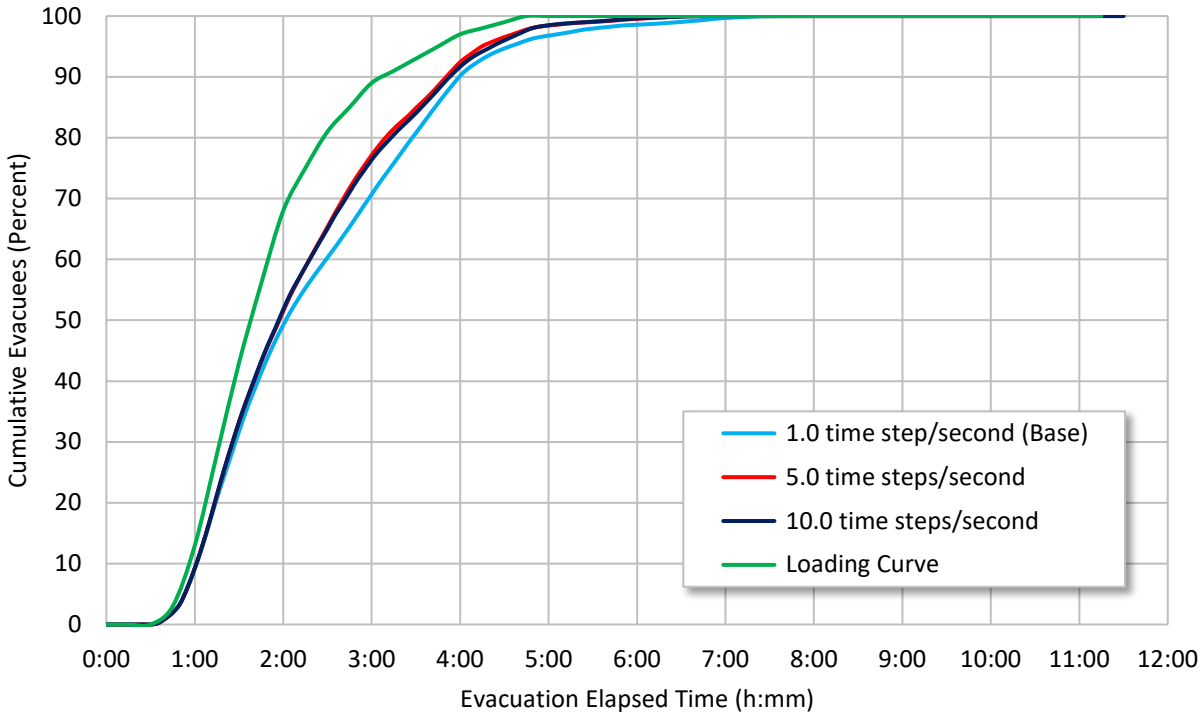

Figure 7-97 Five Mile ETE Curves, Large Population Site Processing Time Step Analysis

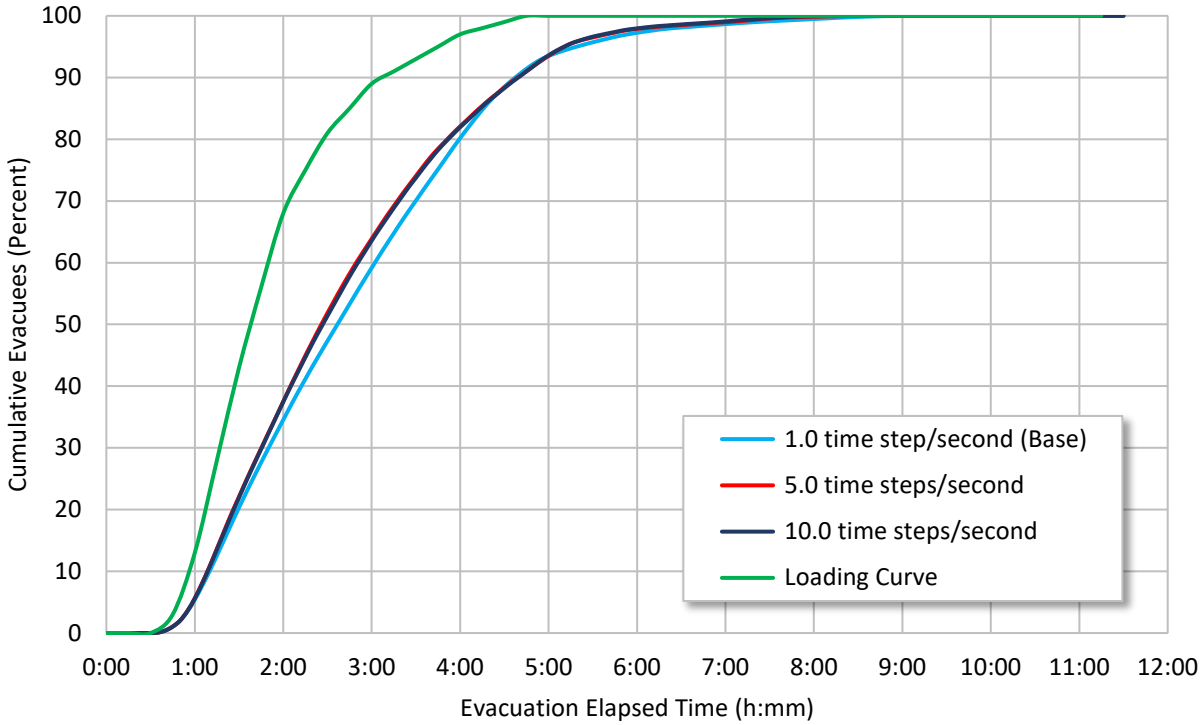

Figure 7-98 Ten Mile ETE Curves, Large Population Site Processing Time Step Analysis

7.3.8.4 Broader Findings, Processing Time Step Parameter Results

Simulation platform computational processing time step was tested because higher fidelity computations would capture vehicle interactions and other subtleties that may be missed in courser simulations. For example, vehicle departures from a signal, or braking actions represented in car following models can change on a sub-second basis and may be missed in a second-by-second simulation.

The results showed that ETEs in uncongested areas are largely insensitive to processing time-step variation. Higher processing time steps decreased some ETEs in the medium and the large population site models. Even though computational power, speed and affordability can be expected to improve in the coming years, the results of this study suggest that the current balance between computational processing time/power and model fidelity is adequate. Additionally, the use of greater time step resolution would not provide important information for the development of protective action strategies nor for improving traffic management plans.

The history of comparison between microscopic and macroscopic-level simulations of evacuations would suggest that these results would apply to macroscopic models as well. More important is that given the time and effort necessary to code and execute models on the micro-level, the findings made here do not support the idea that greater accuracy or model-acceptability would be gained using micro-level models for ETE studies. However, microsimulation models may find more useful application in smaller-sized EPZs and to examine select evacuation routes in detail.

7.3.9 Random Seed Uncertainty Analysis Parameter Results

This task assessed how stochastic variability introduced by the random seeds affected the model output. The summary ETE statistics from multiple runs using different random seeds for all three sites are summarized in Table 7-44 through Table 7-46. The results include the minimum, average and maximum 90 and 100 percent ETEs for the 10 seeds applied in the base models and the additional random seeds applied in the uncertainty analysis. In the small and medium sites, a total of 50 seeds were considered for the uncertainty analysis in each model. These included the 10 seeds used in the base models. In the large site, only 27 additional random seeds were tested and combined with the results from the 10 seeds used in the base model for a total of 37 seeds for the uncertainty analysis.

The average 90 and 100 percent ETEs at the 2, 5, and 10-mile rings from the 10 runs was identical to the average of 50 seeds in the small population site. Similarly, the average 90 and 100 percent ETEs in the large population site were very similar regardless of the number of random seeds; the difference among the average ETEs was approximately one minute. The medium population site was the most sensitive but the average ETEs varied only between two to five minutes. Overall, the results show that the variation of the random seeds did not significantly affect the ETEs in all three representative site models. Given that stochastic parameters introduce variability within a limited range, changing random seeds would not be expected to demonstrate any appreciable effects at a large scale.

Table 7-44 Small Population Site Random Seed Sensitivity Analysis

Number of Random Seeds	ETE Statistic	2-Mile		5-Mile		10-Mile	
		90% ETE	100% ETE	90% ETE	100% ETE	90% ETE	100% ETE
10 seeds[1]	Min	1:35	2:15	1:35	2:15	1:40	2:30
	Mean	1:35	2:17	1:35	2:21	1:44	2:31
	Max	1:35	2:20	1:35	2:25	1:45	2:35
50 seeds	Min	1:35	2:15	1:35	2:15	1:40	2:30
	Mean	1:35	2:17	1:35	2:21	1:44	2:31
	Max	1:35	2:20	1:40	2:25	1:45	2:35

[1] Base model.

Table 7-45 Medium Population Site Random Seed Sensitivity Analysis

Number of Random Seeds	ETE Statistic	2-Mile		5-Mile		10-Mile	
		90% ETE	100% ETE	90% ETE	100% ETE	90% ETE	100% ETE
10 seeds[1]	Min	2:40	4:00	2:40	4:45	4:45	7:05
	Mean	2:41	4:03	2:51	5:18	4:59	7:22
	Max	2:45	4:05	3:50	6:35	5:10	7:40
50 seeds	Min	2:40	4:00	2:40	4:15	4:40	6:55
	Mean	2:41	4:03	2:47	5:23	4:57	7:19
	Max	2:45	4:05	4:00	6:35	5:10	7:55

[1] Base model.

Table 7-46 Large Population Site Random Seed Sensitivity Analysis

Number of Random Seeds	ETE Statistic	2-Mile		5-Mile		10-Mile	
		90% ETE	100% ETE	90% ETE	100% ETE	90% ETE	100% ETE
10 seeds[1]	Min	3:35	5:05	3:55	6:50	4:30	8:55
	Mean	3:39	5:06	4:02	7:16	4:40	9:02
	Max	3:45	5:10	4:15	7:50	4:50	9:10
50 seeds	Min	3:35	5:00	3:55	6:35	4:30	8:55
	Mean	3:39	5:05	4:03	7:15	4:40	9:01
	Max	3:45	5:15	4:15	7:50	4:50	9:10

[1] Base model.

7.4 Conclusion

The results of these task analyses revealed a number of key insights related to parameter assumptions and their representation within and influence upon the simulation of evacuation processes. Variables that spatially or temporally increased the demand or reduced capacity within an evacuation road network were found to have the most significant impacts on clearance time estimations. However, these impacts were not uniform across the representative population sites or necessarily proportional to variation within a parameter of study. The following sections summarize the primary findings and briefly discuss the relevance.

7.4.1 Population

In general, ETEs were sensitive to changes in EPZ population in the small, medium, and large sites when the population was higher than a threshold value. This threshold is related to the interaction of demand and the capacity and the robustness of the transportation network. As suggested in the literature, this relationship means that population alone does not determine the ETE. However, ETEs were more sensitive to an increase in population once population was higher than the threshold. This was observed for both 90 and 100 percent ETEs at the 5 and 10-mile rings. For some sites, significantly large increases in population from the base would be required to reach the threshold. Evaluation of such cases may be unrealistic because the transportation system is typically adjusted with increases in population to service the daily demand, and there are practical limitations to how quickly a population grows.

7.4.2 Mobilization Time

The sensitivity of ETEs to mobilization time strongly depends on the state of congestion. In the congested state, ETEs are governed by the relationship between demand and capacity and may appear to be relatively insensitive to mobilization time. In the non-congested state, ETEs are primarily governed by the mobilization time. Therefore, uncongested sites can clear faster with shorter mobilization times or clear more slowly with longer mobilization times. In terms of the relationship between mobilization time and network performance, the results showed that faster mobilization times in congested sites can increase average evacuee delay. However, slower mobilization times decreased the average evacuee delay significantly. This suggests that there is a trade-off between mobilization time and evacuee delay. This trade-off may be important in considering implementation of protective actions.

7.4.3 Background Traffic

Background traffic has only a minor impact on the evacuation process within the EPZ. In areas beyond the EPZ, where the background traffic remains free to intermix with the evacuation vehicles, average evacuee delay, was observed to increase significantly at the highest level of background traffic. While not a concern for the evacuation of the EPZ, the impact of background traffic beyond the EPZ could be mitigated through planning. As an example of this, in Baton Rouge, there exists a regional phased plan in which major public sector employers, state government offices, and Louisiana State University, may be called to close during an evacuation of New Orleans to keep local traffic to a lower level as evacuees pass through. However, such planning needs would only be necessary for large regional evacuations, which are not representative of an NPP evacuation.

7.4.4 Heavy Vehicles

Within the range of percent heavy vehicles expected to participate in an evacuation, the ETE is not significantly impacted. Only if a very high percentage of the vehicle makeup (about 20 percent) was from heavy vehicles, would there be a noticeable impact on the evacuation. The impact due to heavy vehicles was likely exacerbated by congestion levels and the density of intersections within the study areas. This study did not investigate the impact of topography and this finding may not be appropriate if roadway grades are in excess of three percent.

7.4.5 Free-flow Speed

The analysis of free-flow speed revealed that intersections and congestion generally govern travel speeds. The presence of uninterrupted flow facilities such as freeways contributes to the role that free-flow speed plays because vehicles are more sensitive to free-flow speed on these roads. Given the short travel distance required to evacuate the EPZ, free-flow speed does not typically govern the ETE, even though average travel speeds may vary by 10 to 20 mph. Free-flow speed is a contributor to the impact of adverse weather.

7.4.6 Adverse Weather

Adverse weather can have significant impacts on clearance times within an EPZ when it is likely to be influenced by high traffic volume and density. The impact is likely exacerbated by congestion levels and the density of intersections within the study areas. A key insight is that mobilization times are a strong contributor to the significant increase in ETEs observed in site-specific ETE studies, especially for heavy snow conditions. For microscopic simulation models, the impact of adverse weather can be adequately captured by focusing on the most important driver behavior parameters that impact capacity. The aggregate capacity reductions used in macroscopic models to capture adverse weather impacts are relatively consistent with these findings and are justified for use.

7.4.7 Roadway Impact

Roadway disruptions result in a loss of capacity that may significantly impact ETEs. The analyses revealed queue formation at impact locations that propagated back through routes in the EPZ. The impact on the ETE depends on the location of the roadway disruption. In general, roadway disruptions were a localized effect. If they occur near the evacuation zone boundary, they are likely to have an impact on the clearance time. Downstream of the impact, traffic conditions will recover. It should be understood that such disruptions can be highly variable in both time and space. This potential is thought to be even more pronounced during an event like an evacuation when higher than normal volumes would be using the road network and in locations and times that differ substantially from routine periods. Thus, the type, location, time of occurrence, and level of disruption might need to be based on some additional study of the characteristics of such events.

7.4.8 Processing Time Step

The computational processing time step showed that the models were insensitive to this simulation control parameter. When it comes to computational power and processing time, the test models used in this research required significantly more time to run than would typically be expected for a site-specific ETE model. Computational processing time steps that follow recommended values, should typically yield adequate results.

7.4.9 Random Number Seeding

The random seed number intentionally varies the output of stochastic variables. However, the average ETE values were not significantly impacted by the number of random seed trials. Given that the fundamental basis of stochasticity in simulation is to introduce variance within a distribution range, it was not unexpected that the change in the number of random seeds would demonstrate any appreciable effects.

7.4.10 Overall Findings

Overall, consistent findings emerged to suggest that the configuration of a network renders it susceptible to the influence of evacuation process variables. This finding was best illustrated by the medium population site model which typically experienced more significant impacts than the other two models. This was further demonstrated in the capacity reductions due to the roadway impact parameter. The study findings also lead to the fundamental conclusion that demand—translated into vehicles on the roadway which take up physical space (available capacity)—will likely show significant effects once congested conditions have developed. Any condition or combination of conditions which increase that impact within the EPZ may impact the ETE.

Traffic simulation models require different assumptions and modeling input parameters to represent relevant aspects of traffic movement. In the context of an evacuation, decades of ETE study using traffic simulation modeling has suggested that evacuation traffic simulations can be influenced by the representation of physical processes in modeling and also transportation related aspects as it relates to traffic demand and network supply. As such, a key aspect to ensuring appropriate estimations of clearance times and overall efficacy of ETE studies is to better understand the influence and the importance that simulation modeling parameters have on an evacuation process. Based on this idea, the focus of Task 4 was to perform systematic sensitivity analyses to assess the influence of each study parameter on model results. This analysis also provided an opportunity to analyze elements of traffic flow theory in the context of an evacuation process under a range of different physical and operational characteristics.

The input parameters selected for this research were classified into three main categories of: traffic demand, network supply, and simulation process parameters. In general, traffic demand parameters include variables that describe the temporal and spatial generation, movement, and characteristics of traffic during an evacuation. Conversely, traffic supply parameters are those that are used to influence the overall capacity that exists within a system. Lastly, simulation parameters are not as directly related to the representation of the physical conditions of a system, but rather are those that govern the computational routines of simulation models. Among many others, these would include the duration of system state updating (commonly known as “processing time step” or “simulation resolution”) and random seed uncertainty. Practically, the level of detail that is placed into a model to achieve the desired level of realism may need to be balanced against the computational load of the simulation.

A total of nine input parameters were selected for study. The identification and selection of these parameters were based on a number of sources including those found in a review of relevant literature, guidance documents, prior ETE studies, and the use of expert judgement. These parameters were classified as either traffic demand, traffic supply, or simulation process variables. The traffic demand parameters that were investigated in this study included the size of the evacuating population, its mobilization time, the level of non-evacuation or “background” traffic in the network, and the number of “heavy” vehicles in the system. Traffic supply parameters that were investigated in this study included the free-flow speed of vehicles, the

occurrence of roadway disruptions, and the effect of adverse weather. Finally, the simulation process parameters that were investigated included computation processing time step, and random seed uncertainty.

Overall, the results of the Task 4 analyses revealed a number of key facts related to ETE development, evacuations, and simulation modeling in general. The first of these broad findings was that the results followed well established theories of traffic flow—the most fundamental of these is the basic relationship between network capacity and travel demand. Second, the results were able to illustrate the effect of traffic demand during emergencies. Specifically, the findings showed that the effect of the demand parameters was quite consistent across the three representative population site models, but not necessarily proportional to the variation in population across the representative population sites. The next broad finding was that the effect of network supply parameters was mostly non-uniform across the three representative population sites. The fourth and final major finding was that average evacuee delay captured the state of conditions within the roadway network more effectively than the ETE on its own. From the perspective of NPP evacuation simulation, this is important because, average evacuee delay can be an indicator of exposure duration from a radiological protective action strategy standpoint. Obviously, a longer delay time would result in a higher potential for longer periods of exposure. As a result, there may be no advantage in attempting to get everyone mobilized quickly, because it may actually increase the risk of exposure to evacuees as they drive to their destinations. As such, an ETE, by itself, may not be adequate to determine protective action recommendations and emergency planning and response. Previous traffic/transportation-related research in evacuation modeling has suggested that MOEs other than ETEs could be used to account for traffic conditions (e.g., total travel time) and also radiological or chemical exposure over time and space [28].

8 CONCLUSIONS

The goal of this applied research project was to enhance understanding of the science of evacuation time estimate (ETE) studies and to utilize this knowledge to enhance ETE guidance. Nuclear power plant licensees are required by regulation to develop and periodically update ETE studies. The acceptability of these studies can be assured by adequately addressing elements of the development guidance. However, the adequacy of NRC guidance for ETEs has been questioned in the past and this independent study of current ETE guidance and modeling practices addresses many of the issues raised.

This study contributes to the understanding of ETE development methods and traffic simulation science. Results were as expected in most cases, such as a modest increase in ETEs when shadow populations were substantially increased for the medium and large population sites. Many results added new insights, such as the impact of manual traffic control. The main observations and insights of this applied research are summarized in this section. This study also has broader application in the areas of traffic engineering and traffic simulation, as such the task results are discussed more generally in terms of supply and demand in this section.

8.1 Base Model Development Observations and Insights

The methodology for the development of the three base models and the analyses of the outputs produced insights, observations, and conclusions to achieve the project objective of providing a technical basis for updating NRC ETE guidance contained in NUREG/CR-7002. The results of the study support:

- An enhanced understanding of the impact of shadow evacuations.
- An understanding of the impact of model extent on ETEs and potential travel conditions beyond the EPZ.
- A quantified understanding of the utility of manual traffic control.
- A quantified understanding of select parameters of importance.

The Task 1 effort included the entire process of developing ETE traffic simulation models, acquiring data to populate the models, and conducting analyses to support the specific tasks. The effort employed in the data collection, model development, testing, and application of the traffic simulation models provided insights into the ETE development process and into the importance of inputs, site characteristics, and modeling elements. Throughout the project, models were run, reviewed, modified, and rerun to test, validate, and ensure each model reasonably represented the intended evacuation network. Because these were test models, issues were periodically resolved with simplifying assumptions or alternate modeling approaches necessary to achieve task goals. This was appropriate because the models did not represent any particular site and were used for research purposes only. Some of the modeling assumptions implemented in this analysis would not be appropriate for actual ETE studies (e.g., fixed signal timing).

Task specific analyses compared base model results with the results of scenarios developed to address research objectives. The 90 percent and 100 percent base model ETEs and clearance times produced for the 2, 5, 10, 15, and 20-mile rings are shown in Table 8-1.

Table 8-1 Base Model ETEs and Clearance Times for Each Site

Population Site Model	2-Mile ETE (h:mm)		5-Mile ETE (h:mm)		10-Mile ETE (h:mm)		15-Mile Clearance Time (h:mm)		20-Mile Clearance Time (h:mm)	
	90%	100%	90%	100%	90%	100%	90%	100%	90%	100%
Small	1:35	2:18	1:35	2:21	1:44	2:31	1:55	2:41	2:00	2:45
Medium	2:41	4:03	2:51	5:18	4:59	7:22	5:41	8:04	5:58	8:23
Large	3:39	5:06	4:02	7:16	4:40	9:02	5:14	9:41	5:43	10:07

The following sections summarize observations and insights that were gained during the process of model development. These points document lessons learned regarding key areas that should be explored prior to undertaking model development. Some observations are more relevant for microscopic models, but may have applicability to NPP ETE development efforts.

8.1.1 Model Selection

Microscopic simulation models are useful and powerful tools with many advanced capabilities that yield detailed results. However, as such, they can also require substantial effort to develop. The additional effort to code a microscopic model, select and adjust specific input parameters, and validate the performance to ensure reasonable results for this research was considerable. Significant effort was also required to retrieve model output data for analysis. Consequently, only results that were necessary to complete the task objectives were typically obtained. Microscopic simulation models are best suited for corridors and smaller analyses and are generally not utilized for regional analysis of areas the size of an EPZ [17] [64]. Additionally, macroscopic simulation models have been shown to produce ETEs within a few percent of the microscopic simulation models [23] [28]. While the microscopic model was necessary for this project to achieve task objectives, a microscopic simulation model may not be best suited for a site-specific ETE study, depending on the size of the analysis area. In general, macroscopic, mesoscopic, or microscopic models would all be appropriate to develop an ETE that supports protective action strategies to protect public health and safety.

8.1.2 Static Models and Dynamic Traffic Assignment

Static traffic assignment, where an analyst defines the routes the vehicles will follow, was used for the small population site model. During model development, as the roadway networks expanded outward, determining specific routes from each origin to each destination became more difficult to select. Balancing traffic volumes on the multiple evacuation routes required expert judgment regarding driver decisions at each intersection within the 20-mile analysis area. As such, static models should have a basis for the route decisions. Static route choice was found to be impractical to implement in the medium and large population site models due to the significant number of possible route decisions. As such, dynamic traffic assignment was employed for these models.

8.1.3 Signalized Intersections

Among the significant benefits of microscopic simulation models is their ability to represent signalized intersections with a high degree of representativeness to field conditions. Such detail facilitates accurate modeling of the traffic conditions, provided that sufficient data can be obtained on intersection cycle times. Intersection control was initially built in the medium and

large population models with a high degree of detail representing actuated signals. However, this approach significantly taxed computational processing capabilities and would complicate the task analysis because actuated signal control is not a fixed variable. To facilitate this research, in particular the study of the parameters of importance, all signals were recoded and simulated as fixed time.

For the signalized intersections, additional assumptions on the signal timing needed to be made. To remove unrealistic excessive delays at some locations, alternative intersection designs were implemented to increase intersection throughput in the form of traffic control points. The difficulties associated with attempts to implement actuated signals on a large-scale in the microsimulation model, together with the assumptions that are required with respect to signal timing, suggest that care should be taken when developing the intersection control approach for an ETE study. Review of ETE studies conducted as part of this project found that modeling of actuated signals has not been identified as an issue with macroscopic models, which can be used to readily implement the phasing of intersections.

8.1.4 Boundary Conditions

Boundary conditions define the extent of the network to be modeled. Important changes in infrastructure, beyond the limits of the ETE study analysis area can potentially impact the ETE. Review of ETE studies as a part of this project found that in many instances the modeled network was extended beyond the limits of the shadow region to capture important infrastructure elements in the calculation. There is currently no guidance on including infrastructure elements beyond the shadow region, but the state of the practice is to do so. The shadow region already considers conditions five miles beyond the EPZ which appears to be adequate for most ETE studies. Additional details regarding this topic are discussed in the Task 2 sections of this report.

8.1.5 Background Traffic

Current guidance provides that background traffic be considered in the ETE analysis. In the review of ETE studies, it was observed that this input parameter is not well documented. A finding of the research is that background traffic is not an important parameter to the ETE. This is discussed in Task 4.

8.1.6 Vehicle Loading

In developing the base models, loading at origin nodes varied from as few as 4 vehicles to a maximum number of 3,153 vehicles. During testing, for the origin nodes with large numbers of vehicles assigned the vehicles could not be loaded within the run time of the model, creating file errors. This was corrected by implementing alternative intersection designs at these loading points. Currently, no guidance exists regarding the size of population (e.g., number of vehicles) loaded at a single origin. It may be beneficial to provide guidance for ETE developers on methods to solve this problem should it arise.

8.1.7 Roadway Grade

Current guidance provides that grades greater than about four percent should be included in the analysis [4]. However, review of ETEs identified that the modeling of grade is seldom discussed. The grade of a roadway can influence the acceleration of vehicles, most importantly trucks, with passenger vehicles affected to a lesser degree. Task 4 assessed the effect of various levels of

heavy vehicles on ETE and found the parameter to be unimportant. Significant grades on evacuation routes could increase the important of this parameter and should be assessed in ETE studies if evacuation routes encounter significant grades.

8.1.8 Number of Model Runs

Microscopic models are designed to produce results as an average of a predetermined set of runs. However, the MOEs used in the equation to determine the number of runs is subjective. It may be beneficial to provide guidance regarding the number of microscopic simulation runs to be averaged to produce reasonable averaged results.

8.1.9 Traffic Simulation Model Output

Current guidance [4] specifies selected outputs be included in ETE studies. As a part of this project, the guidance was reviewed to understand whether there is still benefit in documenting the specified model outputs. Generally, model outputs are intended to facilitate the NRC review process, and based on these outputs, confidence is increased in the ETE study. Having studied the outputs and results from the three generic models, the following enhancements should be considered:

Vehicle Queuing: Review of the model results suggest that except for very small population sites, extensive queuing will likely occur at intersections during portions of the evacuation. For medium and high population sites, lengthy queues began early and quickly became indistinguishable from the roadway congestion. Such conditions are normal in large-scale evacuations. Current guidance provides that the longest queue length for the 10 intersections with the highest traffic volume be provided in the ETE. Having observed the queuing in the models developed for this analysis, it is impossible to distinguish the actual length of a queue, particularly when an entire corridor is congested. Requesting queuing data be provided in an ETE study provides little value or benefit to the review. It is suggested queue lengths are not necessary in the review of ETE studies and this item could be removed from current guidance.

Total Vehicles: Realism of the ETE depends, in part, on the vehicle fleet modeled in the study. Current guidance provides that background vehicles, pass-through vehicles, evacuating vehicles, and shadow evacuation vehicles be included. Some simulation platforms, such as VISSIM, remove vehicles from the simulation if they encounter an issue that cannot be resolved within a set time. The loss of a small number of vehicles would not be expected to affect the ETE. However, it may be appropriate to include the total vehicles input and the total exiting and provide an explanation if significant numbers of vehicles are removed from the simulation.

8.2 Supply and Demand

This study reinforced the fundamental relationship between supply and demand in transportation systems. This relationship is the driver of free flow, travel time, congestion and ETEs. In this applied research a range of parameters thought to affect the roadway network capacity and demand on EPZ roadway networks were systematically varied to assess impact on the evacuation process. In Task 1 the impact of shadow evacuee demand and the resultant capacity limitations placed on EPZ evacuees was examined. In Task 2 the impact of increasing the network model extent beyond the shadow region was investigated. In Task 3 the “supply” of road capacity was assessed by varying the characteristics of selected intersections under the

influence of manual traffic control. Finally, in Task 4 a sensitivity analysis was completed for a range of capacity and demand parameters. The findings from this research were consistent with the general principles of traffic engineering in that they showed ETEs increased when demand was increased beyond capacity or when capacity was reduced below the level of demand.

Congestion occurs when the demand exceeds the capacity of the roadway; but the manner in which congestion occurs, is sustained, or is recovered, is based on a number of specific conditions. These conditions may be localized and last for brief periods of time or may be long-lasting and wide-ranging depending on the source of the demand or capacity limitations. As such, it is essential to understand how these conditions—the parameters affecting network demand or capacity—can vary in both time and space. In general, as the population of a region grows, the network capacity also tends to grow. Cities with higher population densities tend to have more roadway network capacity. The results of this research suggest that this equilibrium is a primary driver of congestion formation during evacuations. Realistically, as populations grow, roadway improvements that increase network capacity tend to lag behind. As a result, there is often a delay between the population growth and the ability to effectively provide roadway capacity for that population demand. This can often result in network congestion, which is likely to impact ETEs over time. However, it is not likely that EPZs will experience sudden and drastic changes in population that could significantly alter the ETE within a short period of time. Such trends are important to identify and address in longer-term periodic ETE assessments. Additionally, the scenarios recommended under the guidance in NUREG/CR-7002 are adequate to demonstrate the sensitivity of ETEs to population changes through diurnal, seasonal, and situational (special event) changes in demand.

Demand is only one side of the congestion equation. The capacity of a roadway network can change from day-to-day or even hour-to-hour due to planned and unplanned events such as vehicle crashes, roadway construction or adverse weather. These events can suddenly decrease capacity within a local area, or in the case of adverse weather, affect an entire region. These forms of congestion-related stochastic events are of concern because they can diminish evacuation network capacity, sometimes with little or no-notice. However, while the specific occurrence of such events may be unpredictable, the impact these events may have on ETEs can be assessed and planned for ahead of time. The guidance provided in NUREG/CR-7002 addresses these sudden changes in roadway capacity by incorporating roadway impact and adverse weather scenarios.

Taken together, the results of this study provided a basis for determining the adequacy of current ETE study guidance and key observations and insights to address future guidance development.

9 GLOSSARY

Background Traffic – Traffic generated by residents and transients that is on the roadway within the EPZ when the initial notification occurs.

Base Model – The initial model developed with default parameters and general response characteristics for the small, medium, and large population representative EPZs.

Clearance Time – The time for the last vehicle to exit an analysis area. The analysis area is not necessarily the same as the evacuation area.

Conflict area – Model control measures assigned at signals, stop signs, and yield conditions.

Connector – Link two or more model segments together.

Demand Estimation – The total number of evacuees by population group, including vehicles.

Emergency Response Planning Areas (ERPAs) – EPZ subareas that are typically defined by geographic or political boundaries to support emergency response planning. These may also be referred to as subareas, protective action areas, or other local terminology.

Evacuation Tail – A small portion of the population that takes a longer time to evacuate than the rest of the general public and is the last to leave the evacuation area. The tail generally conforms to about the last 10 percent of the population.

Evacuation Time Estimate – The calculation of an estimated time to evacuate various sectors and distances within the 10-mile plume exposure pathway EPZ.

Heavy Goods Vehicles – These are trucks, buses, and other vehicles with three or more axles.

Keyhole Evacuation – An evacuation of the 2-mile radius around an NPP and the downwind sectors forming a keyhole configuration.

Link – A segment of roadway between two nodes.

Loading Curve – The rate at which vehicles are entered onto the roadway network.

Measure of Effectiveness (MOE) – Output parameters used to describe performance. As applied in this document, these include output data that provide key performance characteristics of the roadway network and evacuation time.

Node – An identification designator used to connect links in a roadway network model or to load modeled vehicles onto the network (e.g., Origin Node). Nodes are at intersections, ramps, etc., and contain characteristics such as traffic control and may be used as input points to assign loading of vehicles.

Origin Node – An identification designator used to load modeled vehicles onto the roadway network.

Pass Through Traffic – Vehicles that enter the EPZ roadway network and 'pass through' prior to the establishment of ACPs at the EPZ boundary. This is also referred to as external to external in the coding of the model. Pass-through vehicles may be expected to travel the freeways and major arterials in the EPZ, because these are the roadways that would facilitate the 'pass through' activity.

Permanent Residents – All people having a residence in the modeled area.

Roadway Capacity – The maximum rate at which vehicles can be reasonably expected to traverse a point or uniform section of roadway during a given time period under prevailing conditions.

Seed – Model seeding is the process of populating a reasonable number of vehicles on the modeled roadway network to represent the scenario being evaluated. This is also known as model equilibration.

Seed Time – The period over which background vehicles are loaded onto the network. This is also known as fill time.

Shadow Evacuation – Evacuation of persons from areas outside any officially declared evacuation zone.

Static Traffic Simulation Model – A model where the analyst defines the routes the vehicles will follow.

Transient Population – Tourists, shoppers, employees, etc., who do not reside within the EPZ, and other people temporarily visiting the EPZ.

Trip Generation Time – Time elapsed for each population group from when the evacuation order was disseminated until the time when the evacuation trip actually begins (e.g., when the car leaves the driveway).

10 REFERENCES

[1] *U.S. Code of Federal Regulations*, "Emergency Planning and Preparedness for Production and Utilization Facilities," Appendix E to Part 50, Chapter I, Title 10, "Energy."

[2] NUREG/CR-4831, "State of the Art in Evacuation Time Estimate Studies for Nuclear Power Plants," U.S. Nuclear Regulatory Commission, Washington DC, March 1992.

[3] NUREG/CR-6863, "Development of Evacuation Time Estimate Studies for Nuclear Power Plants," U.S. Nuclear Regulatory Commission, Washington DC, January 2005.

[4] NUREG/CR-7002, "Criteria for Development of Evacuation Time Estimate Studies," U.S. Nuclear Regulatory Commission, Washington DC, November 2011.

[5] NUREG-0654/FEMA- REP-1, Rev. 1, "Criteria for Preparation and Evaluation of Radiological Emergency Response Plans and Preparedness in Support of Nuclear Power Plants," U.S. Nuclear Regulatory Commission, Washington DC, November 1980.

[6] NUREG/CR-6864, "Identification and Analysis of Factors Affecting Emergency Evacuations," U.S. Nuclear Regulatory Commission, Washington DC, January 2005.

[7] NUREG/CR-6981, "Planning and Implementation for Large Scale Evacuations," U.S. Nuclear Regulatory Commission, Washington DC. October 2008.

[8] NUREG/CR-6953 Volume 2, "Review of NUREG-0654, Supplement 3, Criteria for Protective Action Recommendations for Severe Accidents – Focus Groups and Telephone Survey," U.S. Nuclear Regulatory Commission, Washington DC, October 2008.

[9] NUREG-0800, "Standard Review Plan for the Review of Safety Analysis Reports for Nuclear Power Plants," U.S. Nuclear Regulatory Commission, Washington DC, June 1987.

[10] Weston, R.F., Inc. "Identification and Analysis of Factors Affecting Emergency Evacuations," National Environmental Studies Project, Nuclear Management and Resources Council, 1989.

[11] Zeigler, D.J., S.D. Burn and J. H. Johnson, Jr. "Evacuation from a Nuclear Technological Disaster," Geographical Review, Vol. 71, pp. 1-16, 1981.

[12] NUREG/CR-4873, "Benchmark Study of the I-DYNEV Evacuation Time Estimate Computer Code," U.S. Nuclear Regulatory Commission, Washington DC, June 1988.

[13] NUREG/CR-4874, “The Sensitivity of Evacuation Time Estimates to Changes in Input Parameters for the I-DYNEV Computer Code,” U.S. Nuclear Regulatory Commission, Washington DC, June 1988.

[14] Rogers, G.O., A.P. Watson, J.H. Sorensen, R.D. Sharp, and S.A. Carnes. “Evaluating Protective Actions for Chemical Agent Emergencies,” Oak Ridge National Laboratory. ORNL-6615. Oak Ridge, Tennessee, April 1990.

[15] Ozbay, K., M.A. Yazici. “Analysis of Network-wide Impacts of Behavioral Response Curves for Evacuation Conditions,” IEEE Intelligent Transportation systems Conference. Toronto, Canada, September 2006.

[16] Wolshon, B., J. Jones, F. Walton. “The evacuation tail and its effect on evacuation decision making,” *Journal of Emergency Management*, pp. 37-46, January/February 2010.

[17] Department of Transportation (DOT). “Evacuation Management Operations (EMO) Modeling Assessment: Transportation Modeling Inventory,” Research and Innovative Technology Administration (RITA) Intelligent Transportation System Joint Program Office, October 2007.

[18] Federal Highway Administration (FHWA). “Traffic Analysis Toolbox Volume I: Traffic Analysis Tools Primer,” U.S. Department of Transportation, Washington DC, FHWA Publication Number FHWA-HRT-04-038, July 2004.

[19] Federal Highway Administration (FHWA). “Traffic Analysis Toolbox Volume II: Decision Support Methodology for Selecting Traffic Analysis Tools,” U.S. Department of Transportation, Washington DC, FHWA Publication Number FHWA-HRT-04-039, July 2004.

[20] Federal Highway Administration (FHWA). “Traffic Analysis Toolbox Volume III: Guidelines for Microsimulation Modeling,” U.S. Department of Transportation, Washington DC, FHWA Publication Number FHWA-HRT-04-040, July 2004.

[21] PTV AG. “PTV VISSIM 8 User Manual,” Kalrsruhe, Germany, 2015.

[22] Transportation Research Board. “HCM 2010 Highway Capacity Manual,” National Research Council, Washington DC, 2010.

[23] Goldblatt, R., and K. Weinisch. “Evacuation Planning, Human Factors, and Traffic Engineering,” *Transportation Security Training and Education*. *TR News* 238, pp. 13-17, May-June 2005.

[24] Oregon Department of Transportation (ODOT). “Protocol for VISSIM Simulation,” June 2011.

[25] Washington State Department of Transportation (WSDOT). “Protocol for VISSIM Simulation,” September 2014.

[26] Federal Highway Administration (FHWA). “Guidance on the Level of Effort Required to Conduct Traffic Analysis Using Microsimulation,” U.S. Department of Transportation, Washington DC, FHWA Publication Number FHWA-HRT-13-026, March 2014.

[27] Kentucky Transportation Cabinet. “VISSIM Development and Calibration Report,” CDM Smith, October 2014.

[28] Yuan, F., L. Han. “Improving Evacuation Planning with Sensible Measure of Effectiveness Choices Case Study,” Department of Civil and Environmental Engineering, University of Tennessee. Transportation Research Record 2137, TRB, National Research Council, Washington DC, pp. 54-62, 2009.

[29] Bloomberg, L. and Dale, J. “Comparison of VISSIM and CORSIM Traffic Simulation Models on a Congested Network,” Transportation Research Record 1727, TRB, National Research Council, Washington DC, pp. 52-60, 2000.

[30] Tian, Z. Z., Urbanik, T., Engelbrecht, R., and Balke, K. “Variations in Capacity and Delay Estimates from Microscopic Traffic Simulation Models,” *Transportation Research Record* 1802, TRB, National Research Council, Washington DC, pp. 23-31, 2002.

[31] Murray-Tuite, P.M., B. Wolshon. “Evacuation transportation modeling: An overview of research, development, and practice,” *Transportation Research Part C* 27, pp. 25-45, 2013.

[32] Murray-Tuite, P.M., H.S. Mahmassani. “Model of household trip chain sequencing in an emergency evacuation,” *Transportation Research Record* 1831, pp. 21-29, 2003.

[33] Murray-Tuite, P.M., H.S. Mahmassani. “Transportation network evacuation planning with household activity interactions,” *Transportation Research Record* 1894, pp. 150-159, 2004.

[34] NUREG/CR-7009, “MACCS Best Practices as Applied in the State of the Art Reactor Consequence Analyses Project,” U.S. Nuclear Regulatory Commission, Washington DC, August 2014.

[35] Wheeler, T., G. Wyss, and F. Harper. “Cassini Spacecraft Uncertainty Analysis Data and Methodology Review and Update Volume 1: Updated Parameter Uncertainty Models for the Consequence Analysis,” SAND2000-2719/1, Sandia National Laboratories: Albuquerque, NM, November 2000.

[36] Hallenbeck, M., B. Smith, C. Cornell-Martinez, and J. Wilkinson. “Vehicle Volume Distributions by Classification,” Washington State Transportation Center, July 1997.

[37] National Center for Sustainable Transportation (NCST). “Traffic Flow Models and Impact of Combined Lange Change and Speed Limit Control on Environment in Case of High Truck Traffic Volumes,” University of Southern California, June 2016.

[38] U.S. Department of Transportation Volpe Center. “Dundalk Area Truck Impact Study, Final Project Report,” Baltimore City DOT, Baltimore Maryland, November 2006.

[39] Cutter, S., C. Emrich, G. Bowser, D. Angelo, and J. Mitchell. “2011 South Carolina Hurricane Evacuation Behavioral Study—Final Report,” Hazards and Vulnerability Research Institute. University of South Carolina, August 2011.

[40] Dixit, V., B. Wolshon. “Evacuation traffic dynamics,” *Transportation Research Part C* 49, pp. 114-125, 2014.

[41] Agnello, P., J. Jones, W. Allen Jr. “An Innovative Approach to Truck Modeling,” 9th TRB Conference on Application of Transportation Planning Methods. Baltimore Metropolitan Council, 2004.

[42] Federal Highway Administration (FHWA). “Signalized Intersections: Informational Guide,” U.S. Department of Transportation, Washington DC, FHWA Publication No. FHWA-HRT-04-091, August 2004.

[43] Deardoff, M., B. Wiesner, J. Fazio. “Estimating Free-flow Speed from Posted Speed Limit Signs,” Procedia Social Behavior Sciences, Vol. 16, pp. 306-316, 2011.

[44] Lindell, M., C. Prater, H. Wu, L. Siebeneck. “Household Evacuation Decision-Making in Response to Hurricane Ike,” *Natural Hazards Review*, pp. 283-296, 2012.

[45] Fellendorf, M. and Vortisch P. “Validation of the Microscopic Traffic Flow model VISSIM in different Real-World Situations,” 80th Annual Meeting Preprint CD-ROM, Transportation Research Board of the National Academies, Washington DC, 2001.

[46] Chiu, Y., J. Bottom, M. Mahut, A. Paz, R. Balakrishna, T. Waller, J. Hicks. “Dynamic Traffic Assignment – A Primer,” Transportation Research Circular E-C153. *Transportation Research Board,* Washington DC, June 2011.

[47] Mineta Transportation Institute (MTI). “A Framework for Developing and Integrating Effective Routing Strategies within the Emergency Management Decision Support System,” MTI Report 11-12, Sacramento CA, May 2012.

[48] Chin, S., O. Franzese, D. Greene, H. Hwang, R. Gibson. “Temporary Losses of Highway Capacity and Impacts on Performance: Phase 2,” Oak Ridge National Laboratory. ORNL/TM-2004/2009. November 2009.

[49] Mississippi Department of Transportation (MDOT). “Emergency Evacuation Study for the Greater Jackson Area: Evacuation Traffic from New Orleans,” *Jackson State University*, Jackson Mississippi, May 21, 2011.

[50] Leyn, U. and P. Vortisch. “Calibrating VISSIM for the German Highway Capacity Manual,” *Transportation Research Record: Journal of the Transportation Research Board*, Transportation Research Board of the National Academies, Washington DC, Vol. 2483, pp. 74-79, 2015.

[51] Park, B. and Qi, H. “Development and Evaluation of a Procedure for the Calibration of Simulation Models,” *Transportation Research Record: Journal of the Transportation Research Board*, Transportation Research Board of the National Academies, Washington DC, Vol. 1934, 2005.

[52] Lindell, M., R. Perry. “The protective action decision model: theoretical modifications and additional evidence,” *Risk Analysis,* 32 (4), pp. 616-632, June 2012.

[53] Federal Emergency Management Agency (FEMA). “FEMA Program Manual for Radiological Emergency Preparedness,” FEMA P-1028. Washington DC, January 2016.

[54] NUREG-0654/FEMA-REP-1, Rev. 1, Supplement 3, “Criteria for Preparation and Evaluation of Radiological Emergency Response Plans and Preparedness in Support of Nuclear Power Plants, Guidance for Protective Action Strategies,” U.S. Nuclear Regulatory Commission, Washington DC, November 2011.

[55] U.S. Government Accountability Office (GAO). “Emergency Preparedness—NRC Needs to Better Understand Likely Public Response to Radiological Incidents and Nuclear Power Plants,” GAO-13-243, March 2013.

[56] Mitchell, J.T., S.L. Cutter, and A.S. Edmonds. “Improving shadow evacuation management: Case study of the Graniteville, South Carolina, chlorine spill,” *Journal of Emergency Management*, 5(1): pp. 28-34, 2007.

[57] Lindell, M., C. Prater. “Critical Behavior Assumptions in Evacuation Time Estimate Analysis for Private Vehicles: Examples from Hurricane Research and Planning,” *Journal of Urban Planning and Development*, March 2007.

[58] Zeigler, D.J., and J.H. Johnson, Jr. “Evacuation Behavior in Response to Nuclear Power Plant Accidents,” *Professional Geographer*, 36(2), pp. 207-215, 1984.

[59] Baker, E.J. “Hurricane Evacuation Behavior,” *International Journal of Mass Emergencies and Disasters.* Vol. 9, No. 2, pp. 287-310, August 1991.

[60] Texas House of Representatives: House Research Organization (HRO). “Evacuation Planning in Texas: Before and After Hurricane Rita,” Interim News. Number 79-2. February 14, 2006.

[61] Central Florida Regional Planning Council (CFRPC). “The 2010 Statewide Regional Evacuation Study for the Central Florida Region.” Florida, 2010.

[62] Weinisch, K., P. Brueckner. “The impact of shadow evacuation on evacuation time estimates for nuclear power plants,” *Journal of Emergency Management*. Vol. 13, Issue 2, pp. 145-158, March 2015.

[63] Morales, L., “Gov’t Employment Ranges from 38% in DC to 12% in Ohio,” Gallup Poll, Economy, August 6, 2010. (http://www.gallup.com/poll/141785/gov-employment-ranges-ohio.aspx).

[64] U.S. Department of Transportation (DOT). “Structuring Modeling and Simulation Analyses for Evacuation Planning and Operations,” U.S. DOT Research and Innovative Technology Administration. FHWA-JPO-10-033; FHWA-HOP-10-025. Washington DC, June 2009.

[65] Hall, F.L., and K. Agyemang-Duah. “Freeway capacity drop and the definition of capacity,” *Transportation Research Record: Journal of the Transportation Research Board*, No. 1320, pp. 20-28, 1991.

[66] Banks, J.H. “Flow processes at a freeway bottleneck,” *Transportation Research Record: Journal of the Transportation Research Board,* No. 1278, pp.20-28, 1991.

[67] Lorenz, M., and L. Elefteriadou. “A Probabilistic Approach to Defining Freeway Capacity and Breakdown,” Proceedings of the 4th International Symposium on Highway Capacity, TRB-Circular E-C018, Transportation Research Board, Washington DC, pp. 84-95, 2000.

[68] Brilon, W., J. Geistefeldt, and M. Regler. “Reliability of Freeway Traffic Flow: A Stochastic Concept of Capacity. In: Transportation and Traffic Theory: Flow, Dynamics and Human Interaction,” Proceedings of the 16th International Symposium on Transportation and Traffic Theory, Elsevier Ltd., Oxford, pp. 125-144, 2005.

[69] Modi, V., A. Kondyli, S. Washburn, and D.S. McLeod. “Freeway Capacity Estimation Method for Planning Applications,” *Journal of Transportation Engineering (ASCE)*, No. 140, 2014.

[70] Shojaat, S., J. Geistefeldt, S.A. Parr, C.G. Wilmot, and B. Wolshon. “Sustained Flow Index: A Stochastic Measure of Freeway Performance,” *Transportation Research Record: Journal of the Transportation Research Board*, No. 2554, 2016.

[71] Chiu, Y., J. Bottom, M. Mahut, A. Paz, R. Balakrishna, T. Waller, J. Hicks. “Dynamic Traffic Assignment – A Primer,” *Transportation Research Circular E-C153*. Transportation Research Board, Washington DC, June 2011.

[72] Wolshon, B., J. Jones, F. Walton. “The Evacuation Tail and Its Effect on Evacuation Decision Making,” *Journal of Emergency Management*, Vol. 8, No. 1, pp. 37-46, 2010.

[73] Mannering, F., Washburn, S., and Kilareski, W. *Principles of Highway Engineering and Traffic Analysis*, Fourth Edition, pp. 139-226, 2009.

[74] Nie, Y., Zhang, H.M. “Oscillatory Traffic Flow Patterns Induced by Queue Spillback in a Simple Road Network,” *Transportation Science*. Vol. 42, No.2, May 2008.

[75] Daganzo, C.F. “The cell transmission model: A dynamic representation of highway traffic consistent with the hydrodynamic theory,” *Transportation Research Part B: Methodological,* Vol. 28, Issue 4, pp. 269-287, 1994.

[76] Daganzo, C.F. “Queue Spillovers in Transportation Networks with a Route Choice,” *Transportation Science*, No. 1, p. 3, 1998.

[77] *Traffic Analysis Handbook A Reference for Planning and Operations,* Florida Department of Transportation, March 2014.

[78] Knoop, V., Hoogendoorn, S., and Zuylen, H. “Importance of spillback modeling in assessing ITS,” IEEE Conference on Intelligent Transportation Systems, pp. 909-914, 2006.

[79] Wolshon B., A. Catarella-Michel, and L. Lambert. “Louisiana Highway Evacuation Plan for Hurricane Katrina: Proactive Management of Regional Evacuations,” *ASCE Journal of Transportation Engineering*, Vol. 132, Issue 1, pp. 1-10, January 2006.

[80] *Traffic Management Plan for US 1 at Palm Drive in Florida City – for Implementation during Florida Keys Hurricane Evacuation,* Draft Report, Florida Department of Transportation, Miami, Florida, 2009. (FDOT, 2009a).

[81] *State of Florida One-Way Evacuation Plan Major Turnpike – South Dixie Hwy/US 1 to Ocoee (MP 0 to MP 270)*, Draft Plans, Florida Department of Transportation, August 2009 (FDOT, 2009b).

[82] *State of Florida One-Way Evacuation Plan Northern Turnpike – Lantana to Ocoee (MP 88 to MP 270)*, Draft Plans, Florida Department of Transportation, August 2009 (FDOT, 2009c).

[83] Weston, P.B. “The police traffic control function,” Springfield: C.C. Thomas Publisher, 1996.

[84] Carson, J., and R. Bylsma. “NCHRP SYNTHESIS 309: Transportation Planning and Management for Special Events,” (1st edition.), *Transportation Research Board*, Washington DC, pp. 1-19, 2003. Web. http://onlinepubs.trb.org/onlinepubs/nchrp/nchrp_syn_309a.pdf

[85] Marsh, B. “Traffic signals, when and where?” National Safety Council Transactions (3), p. 157, 1930.

[86] U.S. Department of Homeland Security. Overview: ESF and support annexes coordinating federal assistance in support of the national response framework, January 2008.

[87] Parr, S., and Kaisar, E. “Critical intersection signal optimization during urban evacuation utilizing dynamic programming,” *Journal of Transportation Safety and Security*, Vol. 3(1), pp. 59-76, 2011.

[88] Hawkins, H.G. “Evolution of the MUTCD: Early standards for traffic control devices,” *ITE Journal*, pp. 23-26, 1992.

[89] American Association of State Highway Officials. Manual and specifications for the manufacture display and erection of U.S. standard road markers and signs (2nd Ed). Washington DC, AASHO, 1929.

[90] American Engineering Council for the National Conference on Street and Highway Safety (1930a). Manual on street traffic signs, signals and markings. Washington DC, AEC, NCSHS, 1930.

[91] American Engineering Council for the National Conference on Street and Highway Safety (1930b). *Model municipal traffic ordinance.* Washington DC, AEC, NCSHS, 1930.

[92] Hoover, J.E. “Police training for traffic control,” *Traffic Quarterly*, Vol. 1(4), pp. 301-311, 1947.

[93] Hoover, J.E. “FBI provides a varied program for traffic instruction,” *Traffic Quarterly*, 4(3), pp. 310-319, 1950.

[94] Bradford, D. “A Brief History of NUCPS,” Northwestern University, 2013. Web. http://www.scs.northwestern.edu/program-areas/public-safety/about-nucps.asp

[95] Woods, J. *Directing traffic, what it is and what it does*. Evanston: Northwestern University Traffic Institute, 1952.

[96] Northwestern University Traffic Institute. *Directing traffic: Signals and gestures*. Evanston, IL: Northwestern University, pp. 1-9, 1986.

[97] Northwestern University Traffic Institute. *Directing vehicle movements,* Evanston, IL: Northwestern University, pp. 1-14, 1961.

[98] Hale, A., and Hamilton, J.A. *Police traffic services basic training program,* Washington DC: Superintendent of Documents, U.S. Government Printing Office, 1973.

[99] *A manual of model police traffic services: Policies and procedures*. Washington DC: U.S. Dept. of Transportation, National Highway Traffic Safety Administration, 1986.

[100] Leonard, V.A. *Police traffic control*. Springfield: Thomas, 1971.

[101] *Federal Highway Administration, Florida Highway Patrol (FHP)*. Traffic Direction and Control (17.17), 1996.

[102] Traffic Control, City of Houston – Office of the Chief of Police, October 2004.

[103] Shults, J.F. *The Fine, Fading Art of Directing Traffic*. Adams State College, 2005. Web. http://www.santacruzcountycert.org/Local_Downloads/Traffic_Control/fadingarttraffic.pdf

[104] Epperson, C. *Traffic direction and control number 40.25*. Rockford Police Department, 2006.

[105] Jones, J.C. "Developing Traffic Control Assistant Training Programs," Emergency Responder Safety Institute Cumberland Valley, 2008.

[106] *Traffic Management and Control 1907*, Anne Arundel County Police Department, 2009.

[107] Lincoln Police Department Traffic Control Guide. Report GO8.5, Lincoln, NA, 2011.

[108] Lundborn, J. Truro Police Department. Policy and Procedure: Traffic Enforcement, Investigation Direction and Control. 2011. Web. May 2013.

[109] Techniques of Traffic Law Enforcement, Burlington Police Department. Web. May 2013.

[110] Traffic Officer Task List, City of Los Angeles Personnel Department, *n.d.* Web. 2013 http://per.lacity.org/eeo/TrafficOfficer-Tasks.pdf

[111] Johnston, B. Snohomish County Online Government Information and Services. Manual Traffic Control for CERT Operations, *n.d*. Web. 2013. http://www1.co.snohomish.wa.us/Departments/Emergency_Management/Services/Volunteers/CERT/

[112] *DHS senior leadership: The first five years: 2003-2008*. U.S. Department of Homeland Security, November 2009. Web. http://www.dhs.gov/xabout/history/

[113] Sessions, G. M. *Traffic devices: Historical aspects thereof*. Washington DC: Institute of Traffic Engineers, 1971.

[114] Sutermeister, O. "Capacity of narrow streets with manual control and signal control," *Highway Research Board Bulletin*, 112, pp. 1-15, 1956.

[115] Pretty, R. "Police control of traffic: A study at a Brisban intersection," *Australian Road Research Board (ARRB) Conference*, 7, pp. 83-95, 1974.

[116] May, A.D., and Montgomery, F. O. "Control of congestion at highly congested junctions," *Transportation Research Record*, 1057, pp. 42-48, 1986.

[117] Mahalel, D., Gur, Y., and Shiftan, Y. "Manual versus automatic operation of traffic signals," *Transportation Research Part A: Policy and Practices*, Vol. 25A, pp. 121-127, 1991.

[118] Al-Madani, H.M.N. “Dynamic vehicular delay comparison between a police-controlled roundabout and a traffic signal,” *Transportation Research Part A: Policy and Practice*, 37 (8), pp. 681-688, 2003.

[119] Ye, Z., Veneziano, D., and Lassacher, S. “Analysis of manual traffic control at all-way stop-controlled intersections during special events,” Transportation Research Board 88th Annual Meeting Compendium of Papers, Washington DC: Transportation Research Board. Print, 2009.

[120] Eno, W. P. *The science of highway traffic regulation*. New York: Press of Byron Adams, 1927.

[121] Schad, B.T. *Traffic control at signalized street Intersection*. (Doctoral Dissertation). University of Michigan, MI, 1935.

[122] Marsh, B. “Traffic control,” *Annals of the American Academy of Political and Social Sciences*, Vol. 133, p. 91, September 1927.

[123] Hosmer D.W. and Lemeshow, S. “A goodness-of-fit test for the multiple logistic regression model,” *Communications in Statistics,* A10, pp. 1043-1069, 1980.

[124] Ben-Akiva, M., and Lerman, S. *Discrete choice analysis: Theory and application to travel demand*. Cambridge: The MIT Press, 1985.

[125] Wilson, W. *Statistical methods*. San Diego, CA: Academic, 2009.

[126] Parr, S.A. “Analysis and Modeling of Manual Traffic Control for Signalized Intersections,” *Louisiana State University*, 2014.

[127] Federal Highway Administration (FHWA). “Traffic Analysis Toolbox Volume XI: Weather and Traffic Analysis, Modeling and Simulation,” U.S. Department of Transportation, Washington DC, FHWA Publication No. FHWA-JPO-11-019, December 2010.

[128] Federal Highway Administration (FHWA). “Empirical Studies on Traffic Flow in Inclement Weather,” U.S. Department of Transportation, Washington DC, FHWA Publication No. FHWA-HOP-07-073, October 2006.

[129] CDM Smith, “VISSIM Development and Calibration Report,” Prepared for Kentucky Transportation Cabinet, 2014.

[130] Mannering, F., Washburn, S., and Kilareski, W. *Principles of Highway Engineering and Traffic Analysis*, Fourth Edition. pp. 139-226, 2009.

[131] Federal Highway Administration (FHWA). National Household Travel Survey (NHTS). Summary of Travel Trends, 2011.

[132] National Cooperative Highway Research Program (NCHRP) 365: Travel Estimation Techniques for Urban Planning. Washington DC, 1998.

[133] Sullivan, J.L., Novak, D.C., Aultman-Hall, L., Scott, D.M. “Identifying critical road segments and measuring system-wide robustness in transportation networks with isolating links: A link-based capacity-reduction approach,” *Transportation Research Part A*, 2010.

[134] American Association of State Highway Officials. “A policy on geometric design of highways and streets,” Washington DC, AASHO, 2011.

[135] Tamminga, G., Daamen, W., and Hoogendoorn, S. “Influence of Departure Time Spans and Corresponding Network Performance on Evacuation Time,” Transportation Research Board of the National Academies, Washington DC, pp. 89–96, 2011.

[136] McGhee, C.C., Grimes, M.C. “An operational analysis of the Hampton roads hurricane evacuation traffic control plan,” Virginia Department of Transportation (Ed.). Virginia Transportation Research Council, Richmond, 2006.

[137] Paz de Araujo, M., Casper, C.T., Lupa, M.R., Hershkowitz, P., Waters, B. “Adapting a Four-Step MPO Travel Model for Wildfire Evacuation Planning: A Practical Application from Colorado Springs,” Transportation Research Board 90th Annual Meeting, 2011.

[138] Brown, C., White, W., van Slyke, C., Benson, J.D. “Development of a strategic hurricane evacuation–dynamic traffic assignment model for the Houston, Texas, Region,” *Transportation Research Record: Journal of the Transportation Research Board*, 2137, pp. 46-53, 2009.

[139] Collins, A.J., Foytik, P., Frydenlund, E., Robinson, R. M., & Jordan, C. A. “Generic Incident Model for Investigating Traffic Incident Impacts on Evacuation Times in Large-Scale Emergencies,” *Transportation Research Record: Journal of the Transportation Research Board*, Vol., 2459, pp. 11-17, 2014.

[140] Zheng, H.; Chiu, Y.C.; Mirchandani, P.; Hickman, M. “Modeling of evacuation and background traffic for optimal zone-based vehicle evacuation strategy,” *Transportation Research Record: Journal of the Transportation Research Board*, Vol. 2196, pp. 65–74, 2010.

[141] Pel, A., Hoogendoorn S, Bliemer M. “Impact of Variations in Travel Demand and Network Supply Factors for Evacuation Studies,” *Transportation Research Record*, Vol. 2196, pp. 45-55, 2010.

[142] Ozbay, K., and M. A. Yazici. “Analysis of Network-Wide Impacts of Behavioral Response Curves for Evacuation Conditions,” *IEEE Intelligent Transportation Systems Conference, Intelligent Transportation Systems Conference*, Vol. 157, 2006.

[143] McGhee, C.C., Grimes, M.C. “An Operational Analysis of the Hampton Roads Hurricane Evacuation Traffic Control Plan,” Virginia Department of Transportation (Ed.). Virginia Transportation Research Council, Richmond, 2006.

[144] Tanaboriboon, Y., and Aryal, R. “Effect of Vehicle Size on Highway Capacity in Thailand,” *Journal of Transportation Engineering*, Vol. 116, No. 5, pp. 658–666, 1990.

[145] Krammes, R.A., and K.W. Crowley. “Passenger Car Equivalents for Trucks on Level Freeway Segments,” *Transportation Research Record,* Vol. 1091, pp. 10–17, 1986.

[146] Ahmed, U., Ng, M., and Drakopoulos, A. “Impact of Heavy Vehicles on Freeway Operating Characteristics Under Congested Conditions,” *Transportation Research Record*, Vol. 2396, pp. 28-37, 2013.

[147] NUREG/CR-6864, “Identification and Analysis of Factors Affecting Emergency Evacuations,” Division of Preparedness and Response, Office of Nuclear Security and Incident Response, U.S. Nuclear Regulatory Commission, 2005.

[148] Bahaaldin, K., Fries, R., Williamson, M., and Chowdhury M.A. “The Impact of Traffic Incident Locations on a Metropolitan Evacuation,” *SIUE Faculty Research*, Scholarship, and Creative Activity, 2016.

[149] Fonseca, D.J. Lou, Y., Moynihan, G.P., and Gurupackiam, S. “Incident Occurrence Modeling during Hurricane Evacuation Events: The Case of Alabama's I-65 Corridor,” *Modelling and Simulation in Engineering*, 2013.

[150] Robinson, M., Khattak, A., Sokolowski, J.A., Foytik, P. and Wang, X. “What is the role of traffic incidents in Hampton Roads Hurricane Evacuation,” Presented at the Transportation Research Board Annual Meeting Washington, 2009.

[151] U.S. Department of Transportation. n.d., accessed from: https://www.its.dot.gov/research_archives/clarus/index.htm, on August 2018.

[152] Ibrahim, A.T., and F.L. Hall. “Effect of Adverse Weather Conditions on Speed- Flow Occupancy Relationships,” *Transportation Research Record*, Vol. 1457, 1994.

[153] Lamm, R., E. M. Choueiri, and T. Mailaender. “Comparison of Operating Speeds on Dry and Wet Pavements of Two-Lane Rural Highways,*” Transportation Research Record*, Vol. 1280, 1990.

[154] Liang, W.L., M. Kyte, F. Kitchener, and P. Shannon. “The Effect of Environmental Factors on Driver Speed: A Case Study,” *Transportation Research Record*, Vol. 1635, 1998.

[155] Federal Highway Administration. “Identifying and Assessing Key Weather-Related Parameters and Their Impacts on Traffic Operations Using Simulation,” U.S. Department of Transportation, Federal Highway Administration, Research, Development, and Technology, Turner-Fairbank Highway Research Center. Publication Number FHWA-HRT-04-131, 2004.

[156] Federal Highway Administration. “Microscopic Analysis of Traffic Flow in Inclement Weather - Part 2,” U.S. Department of Transportation, Washington DC, FHWA Publication No. FHWA-JPO-11-020, December 2010.

[157] Jung S, Qin X, Noyce D. “Modeling Highway Safety and Simulation in Rainy Weather,” *Transportation Research Record.* Vol. 2237, pp. 134-143, 2011.

[158] Asamer, J., van Zuylen, H.G, and Hailmann, B. “Calibrating car-following parameters for snowy road conditions in the microscopic traffic simulator VISSIM,” *IET Intelligent Transport Systems,* 2012.

APPENDIX A LITERATURE REVIEW

Traffic simulation models represent the framework of the analyses conducted under this effort. Every ETE submitted after the 2010 census was developed using a traffic simulation model with dynamic traffic assignment capabilities. Developing the models for the project analyses required in-depth knowledge of traffic simulation, evacuations, ETEs, and shadow evacuations. Each of these topics has been studied in great detail and a summary of the literature reviewed in the conduct of this effort is provided below.

A.1 Traffic Simulation Modeling

As computational resources have increased in capacity and decreased in cost, advanced features of traffic analysis have been developed for traffic simulation. The FHWA published a multi-volume traffic analysis toolbox providing guidance on appropriate application of traffic simulation models and listing more than 50 macroscopic, mesoscopic, and microscopic models [1] [2] [3]. Many of the models identified in the toolbox are appropriate for use in calculating evacuation times. Volume III of the toolbox provides a methodology for development and application of microscopic simulation models [3].

The VISSIM traffic simulation model was developed in Germany [4] and is widely used in the US. VISSIM has been compared to CORSIM, which is a benchmarked traffic simulation tool developed by the FHWA [5]. Specific measures, like throughput and level of service, have compared well, and relative travel times were also consistent between the two models [5]. Differences were identified in vehicle and driver behavior, including the car following and gap logic [5].

Tian and Urbanik et al., [6], compared VISSIM to CORSIM and Sim Traffic which are also microscopic traffic simulation models. The authors investigated the variations in the performance measures generated, focusing on capacity and delay estimates at a signalized intersection. The effects of link length, speed, and vehicle headway generation distribution were also investigated. Regarding variations in performance measures, the study found that CORSIM yields the lowest variations, and SimTraffic yielded the highest. The highest variation in each simulation model normally occurred when the traffic demand approached capacity. Delays were found to be affected by the link length and speed, where shorter links and higher link speeds generally resulted in lower delays. The study identified that a large number of runs may be necessary to accurately estimate delay at, near, or over capacity. When the average values were considered from multiple runs, the throughput flow rates from all three models matched the input demand closely for under-capacity conditions. Tian and Urbanik, found that different results were produced when the default traffic flow parameters from each simulation model were used. In general, VISSIM produced the highest capacity and lowest delay estimates, and SimTraffic produces the lowest capacity and highest delay estimates.

Fellendorf and Vortisch, [7] published an approach to validation of the VISSIM microscopic model, noting the VISSIM car following model was originally designed to model driver behavior on German freeways [7]. There is no general speed limit on German freeways, but many parts of the network are limited to 75 mph (120 km/h). As a result of German driving behavior, the maximum flow on a single lane is about 1,800 vehicles per hour. Fellendorf discussed that driving behavior on US freeways is different than driving on German highways because there is a speed limit and lane usage is not as strictly regulated resulting in higher capacities on US freeways [7]. To model the American driving style for high traffic volumes, the car following

parameters should be timed to provide a tighter following process (smaller safety distances and less random oscillations). Combined with a time step of 0.2 seconds, lane capacities of up to 2,700 vehicles per hour could be achieved in the model [7], though this may not represent reality. Fellendorf discusses that simulation tools based on the Wiedemann psycho-physical car following model can reproduce traffic flow very realistically under different real-world conditions, but the model was built for 1974 European roadway travel conditions; therefore, it is necessary to adapt the model to the local traffic situation [7]. The need to adapt VISSIM parameters to local conditions is further emphasized in the VISSIM User Manual which states that all functions should be adapted to local conditions, if they are substantially different than Western European driving [4]. Leyn and Vortisch [8] changed many of the default parameters to reflect local conditions in their calibration of VISSIM for the Germany Highway Capacity Manual.

Numerous applied studies have been conducted using traffic simulation models. A Mineta Transportation Institute study assessed the effectiveness of evacuation strategies including modeling, calibration, and validation of a VISSIM traffic flow simulation of downtown San Jose, California [9]. The study suggests that the 'real world' is represented more practically in micromodels. Gomes [10] studied calibration of a congested freeway in northern California and determined the look back default distance was too small for large numbers of vehicles. Gomes adjusted the wait line before diffusion default from 15 to over 600 seconds and found that modest adjustments to the Wiedemann parameters were necessary [10]. A study of the Greater Jackson Area [11] provided detailed aspects of the benefit and impact from contra-flow and phased evacuation with respect to various performance measures such as travel time, cumulative safe arrival, and space-time speed profile. A large DYNASMART-P traffic simulation model which included 4,607 nodes, 10,288 links, and 691 traffic analysis zones was used to determine beneficial evacuation strategies. The largest dynamic traffic assignment model identified in this research was developed in Sydney, Australia, with a focus on understanding model output [14]. The network consisted of 58,583 links, 20,730 nodes, 2,282 zones, 1,262,930 vehicle demand, 490 signalized intersections, and 1,059 bus routes. DTA was applied because it was able to more realistically capture time-dependent phenomena of queue spill back and congestion. A finding of the study was that microscopic models result in more accurate estimations of measures of performance than other models [14].

Lownes and Machemehl [12] considered link capacity as a measure of effectiveness and conducted experiments with six different combinations of car following parameters of the Wiedemann 99 model in VISSIM. The authors conducted a two-way Analysis of Variance (ANOVA) to find the individual parameters producing significant effect on the value of the capacity, and the interaction among the parameters. The impact on capacity for CC8 and CC4/CC5 were dependent on the values of CC0 and CC1, respectively [12]. The authors explain that capacity of a roadway is so heavily dependent upon headway, that when calibrating a simulation for capacity it would be simple to alter the capacity of the roadway using CC0 and CC1. The results of their study indicate that the value of CC0 or CC1 can have a joint impact with other driver behavior parameters on capacity [12]. Rrecaj et al., [13] summarized the approach and findings of 14 calibration studies that included arterials, freeways, and intersections. In one case study on coordinated actuated signal systems, Latin Hypercube sampling was used to produce 200 parameter sets with 5 random seeds for a total of 1,000 runs. The most influential parameters were found to be the additive part of safety distance and desired speed distribution [13].

The application of traffic simulation models as standard engineering tools in municipal infrastructure design has resulted in transportation departments developing standard guidance to meet local conditions. This literature review identified the FHWA, Caltrans, Wisconsin DOT,

Oregon DOT, Washington State DOT, Kentucky, and the Virginia Transportation Research Council as agencies that have established validation standards and targets for microscopic simulation models [15] [16] [17] [18]. It is expected many more state and local agencies have developed standards in this area. The Oregon Protocol [15] identifies standstill distance, headway time, and following variation as having the greatest influence on car following behavior in VISSIM. These are the most intuitive in terms of their impact on following behavior because they are key parameters used to determine desired safety distance. The standstill distance, which is the desired rear bumper to front bumper distance between stopped cars, has a greater impact to maximum flow rate when traffic is congested.

Park, et al., developed the "Microscopic Simulation Model Calibration and Validation Handbook," [18] and identified calibration, described as the fine-tuning of inputs related to driving behavior and vehicle characteristics, as the most important element of traffic simulation modeling. The handbook, sponsored by the Virginia Transportation Research Council, provides a process for calibration of CORSIM and VISSIM microscopic simulation models [18]. The importance of properly calibrating traffic simulations is evidenced by the adoption of microsimulation calibration standards by several state and federal transportation authorities, most of which parallel standards adopted by the FHWA [3]. Calibration has been identified as critical in many studies and publications [3] [38].

A.2 Evacuations

Evacuations have been studied for over a century. Reports in the U.S. identify people evacuating in response to the Great Chicago Fire of 1871 and from fires resulting from the San Francisco Earthquake of 1906. Of greater relevance to emergency planning and preparedness for NPPs are incidents that have occurred in the NPP era, which began in the 1960s. The EPA conducted a study to determine the risk associated with evacuations and collected data on more than 450 evacuations of at least 20 people covering a 13-year period from 1960 to 1973 [19]. The EPA concluded, among other things, that most evacuees use their own personal transportation during an evacuation, most assume responsibility for acquiring their own food and shelter, and no panic was observed [19]. Evacuations were orderly, and traffic traveled at low speeds [19].

From 1980 to 1984, an international study of chemical accidents identified 293 evacuations. No injuries were identified due to the evacuations, although injuries were identified due to the hazards [20]. Additional studies focused on large-scale evacuations, defined as more than 1,000 people from more than one building [21] [24], found that such evacuations are implemented in the United States about once every two to three weeks in response to technological hazards, train derailments, wildfires, hurricanes, and other hazards. This rate has been found to be consistent over a period of more than 20 years, from 1980 to 1987 in a Nuclear Management and Resource Council (NUMARC) sponsored study [21] and in an NRC study of evacuations over the period of January 1990 through June of 2003 [24]. The NUMARC study identified training and drills, cooperation among government agencies, use of an Emergency Operations Center, and route alerting (a common backup notification in EPZs) as factors that significantly affect the positive outcome of evacuations [21]. All these factors are integral to current radiological emergency response planning provided in NRC guidance [25]. NRC studies on large-scale evacuations [24] [26] profiled almost 250 evacuations and found similar factors to those identified in the NUMARC study also contributed to the positive outcome of evacuations.

Traffic intersections are designed and built to accommodate vehicle interactions in a roadway network. They are designed to facilitate improved throughput but are not necessarily designed to perform optimally. Because intersection control is placed on major and minor roadways, it inherently reduces the capacity and contributes to delay. Research has confirmed that evacuation traffic can be significantly impacted by signalized intersections, particularly for evacuations in urban areas [22]. Capacity reduction and delay are both observed at sub-optimally performing intersections, which make up the majority of intersections in the U.S. [23]. Oak Ridge National Laboratory (ORNL) studied capacity reduction and found that the majority of capacity loss was due to less than optimal intersection performance on major arterials. Although the authors were able to attribute the loss to intersections, they noted that most delay is unavoidable. Non-signalized intersections can also be inefficient in evacuations.

A.3 Evacuation Time Estimates

The EPA has been studying evacuations since the early 1970s with citations in the EPA work referencing development of ETEs dating back to the 1950s [19]. Guidance on development of ETEs was first published in Appendix 4 of NUREG-0654/FEMA-REP-1, Rev.1, establishing the concepts of population groups, trip generation times, and probabilistic analyses based on combining distributions for various evacuation time components [25].

One of the early models used to develop ETEs for nuclear power plants was the I-DYNEV model. The I-DYNEV model was developed for FEMA to simulate evacuation conditions. The NRC sponsored a benchmark of the model, which is documented in NUREG/CR-4873, "Benchmark Study of the I-DYNEV Evacuation Time Estimate Computer Code," [27]. One of the most critical input parameters for the model was identified as the mean queue discharge headway, which is the time spacing between vehicles [27]. A corresponding document, also sponsored by the NRC, was NUREG/CR-4874, "The Sensitivity of Evacuation Time Estimates to Changes in Input Parameters for the I-DYNEV Computer Code" [28], which investigated the relationship of changes in parameters to evacuation time. Some conclusions to the study include:

- The rate of increase in ETEs is dependent upon the characteristics of the transportation network.
- Changes in the network capacity affected evacuation time in a linear manner, reflecting the direct relationship between vehicle demand and capacity.
- The ETE can be sensitive to the loading time of vehicles onto the network.
- The loading time is most likely to affect evacuation time at low population sites.

In 1992, NRC published NUREG/CR-4831, “State of the Art in Evacuation Time Estimate Studies for Nuclear Power Plants” [29], which expanded on the guidance in NUREG-0654/FEMA-REP-1, Rev. 1, adding discussion regarding the use of traffic models in the development of ETEs, providing additional detail in developing trip generation times, and describing in greater detail the data necessary for estimating evacuation times for special facilities and special needs residents. NUREG/CR-6863 [30] added guidance regarding the use of the ETE in Early Site Permits and expanded guidance on the use of traffic simulation models and assessment of shadow evacuations. The most recent ETE guidance, NUREG/CR-7002 [31], addresses selecting traffic simulation models, characteristics of the model that should be described in the ETE study, inputs to the model that support the analysis, and outputs which provide the MOEs used in review of the ETE studies.

ETEs require assumptions regarding the trip generation time, which encompasses all activities in the mobilization of the public as they prepare to evacuate [31]. Generally, ETE studies include a telephone survey of the EPZ to gather much of the trip generation time data. Research of response expectations of residents of EPZs was conducted in NUREG/CR-6953 Volume 2, "Review of NUREG-0654, Supplement 3, 'Criteria for Protective Action Recommendations for Severe Accidents – Focus Groups and Telephone Survey," [32]. The nationwide research of EPZ residents concluded that residents within the EPZ have a good understanding of what to do in the event of an emergency and are largely prepared to respond to the directions received [32]. These results provide a level of confidence in the time elements developed for the trip generation times.

Regarding ETE results, macroscopic and microscopic analyses of the same EPZ have been shown to provide similar results [33] [34]. A study of the Nine Mile Point NPP compared macroscopic and microscopic models for the same network of 964 links and showed less than a 5 percent difference in ETEs; however, the microsimulation model took 300 times longer to run [33]. An independent microscopic study of portions of the Sequoyah EPZ produced an ETE of 8:00 [34] which was also within 5 percent of the macroscopic developed ETE for the site at the time of the analysis.

A.4 Shadow Evacuations

Defined by Zeigler et al., in 1981, a shadow evacuation is the tendency of an official evacuation advisory to cause departure from a much larger area than intended [35]. The first shadow evacuations were observed in the response to TMI accident [35]. After the TMI emergency, shadow evacuations have since been observed, researched, and documented for many large-scale evacuations [24] [36] [37] [38]. Baker [36] described the shadow in terms of risk stating it is when evacuation from high and risk areas influence response in areas that do not need to evacuate. Baker's definition is effectively the same as Zeigler, because risk areas must be defined, an advisory must be issued before the shadow begins. Murray-Tuite et al., [38] chose to simply cite Zeigler's definition in work on transportation modeling. Some research has also been attempted to quantify the shadow [37], but accuracy in quantification has proven to be difficult. One reason is that in discussions with emergency responders, counting people who leave areas that are beyond the evacuation zone is not a priority, because the focus of these emergencies is on the residents at risk. Thus, there is limited first-hand knowledge available and data must be developed at some time after the incident. Another problem with quantifying the shadow is a disparity in the application of the shadow definition. Researchers have been found to use the terms shadow, spontaneous, and early evacuation interchangeably. Even people who have been ordered to evacuate have been counted as shadow evacuees [40].

Quantifying the shadow has been attempted in research, but the results are difficult to interpret because published reports seldom adhere to the specific criteria of the shadow definition. The inconsistent application of the formal definition often limits the use of the data and conclusions of shadow evacuation studies [29] [37] [41] [42]. Although the shadow evacuation was defined quite explicitly from the very beginning [35], even Zeigler and Johnson [43] interchanged spontaneous evacuation with shadow evacuation, and this may have contributed to the misuse of the term. Shadow evacuations are spontaneous, but the term spontaneous evacuation is more appropriately applied to residents who leave before the official evacuation advisory or order is issued. Some research and emergency management guidance were found to cite the Zeigler definition precisely or otherwise define shadow appropriately [24] [36] [38] [39] [45]. Baker, [36] recognized inconsistencies of this nature, though not specifically with the shadow, and suggested caution in developing general evacuation behavior models, noting that such generalizations must be qualified in terms of the known specifics of the situations which could restrict the findings.

In post-evacuation research of the 2005 Graniteville train accident, which had a one-mile radius declared evacuation area, Mitchell, et al., [40] determined through a post evacuation telephone survey, that 59 percent of the residents from one to two miles had evacuated as a shadow. However, the study identifies that more than half of those residents were instructed to evacuate via Reverse 911 or fire/police officials knocking on their door [40]. The difficulties in quantifying the shadow evacuation were obvious in post evacuation assessments of the Hurricane Rita evacuation. In response to the hurricane, a local official suggested that all residents who had previously experienced flooding should evacuate [26] [44]. The response was overwhelming, and some researchers have included all of those residents in multi-million person shadow estimates. Hurricane Rita was very much an anomaly, although there is much that can be learned. The hurricane occurred only a few weeks after Hurricane Katrina had devastated New Orleans and the Gulf Coast along Louisiana, Mississippi, and Alabama. Many evacuees from Louisiana had gone to Houston. The Hurricane Katrina catastrophe was fresh in the minds of the entire nation, so when the evacuation order was issued for those who had experienced flooding in the past, residents took the warning literally. Many residents believed they had been ordered to evacuate. The biggest failure of the Hurricane Rita evacuation was communication to the public [44], which makes quantifying the shadow for this hazard virtually impossible.

There is a subtle, though important, difference in the responses to Hurricane Rita and Graniteville from a shadow evacuation. In these evacuations, the advisory didn't cause residents to leave. The advisory clearly ordered the residents to leave; although in post evacuation reviews, the areas from which these residents evacuated from was not intended to be evacuated. By definition, a shadow occurs when the advisory causes residents to leave from a much larger area than intended. In both evacuations, residents were ordered to evacuate, thus they were in the evacuation area. It was the officials or the responders who expanded the evacuation area, whether or not they realized what they were doing. Any resident that was ordered to evacuate, even inadvertently, should not have been included in the shadow contribution. Such estimates do not accurately reflect the shadow contribution.

Weinisch and Bruekner [46], reviewed 48 ETE studies prepared for nuclear power plants to determine impacts from shadow evacuations. Each of the ETE reports used in the study included a sensitivity analysis that increased the size of the shadow to 60 percent of the public residing in the area 5 miles beyond the EPZ. The shadow response curve and EPZ evacuee response curve were the same, reflecting an early shadow evacuation. Of the 48 ETEs reviewed, only 7 showed a clearance time increase of 30 minutes or more for the 100^{th} percentile ETE. More than 70 percent of the sites showed little to no change in the ETE [46]. Based on their research, an early response of the shadow area that begins coincident with the EPZ evacuation, has little impact on the EPZ evacuation.

A.5 References

[1] Federal Highway Administration (FHWA). "Traffic Analysis Toolbox Volume I: Traffic Analysis Tools Primer," U.S. Department of Transportation, Washington DC, FHWA Publication Number FHWA-HRT-04-131, September 2004.

[2] Federal Highway Administration (FHWA). "Traffic Analysis Toolbox Volume II: Decision Support Methodology for Selecting Traffic Analysis Tools," U.S. Department of Transportation, Washington DC, FHWA Publication Number FHWA-HRT-04-131, September 2004.

[3] Federal Highway Administration (FHWA). “Traffic Analysis Toolbox Volume III: Guidelines for Microsimulation Modeling,” U.S. Department of Transportation, Washington DC, FHWA Publication Number FHWA-HRT-04-040, 2004.

[4] PTV AG. “PTV VISSIM 7 User Manual,” Kalrsruhe, Germany, 2015.

[5] Bloomberg, L. and Dale, J. “Comparison of VISSIM and CORSIM Traffic Simulation Models on a Congested Network,” Transportation Research Record 1727, TRB, National Research Council, Washington DC, pp. 52-60, 2000.

[6] Tian, Z.Z., Urbanik, T., Engelbrecht, R., and Balke, K. “Variations in Capacity and Delay Estimates from Microscopic Traffic Simulation Models,” Transportation Research Record 1802, TRB, National Research Council, Washington DC, pp. 23-31, 2002.

[7] Fellendorf, M. and P. Vortisch. “Validation of the Microscopic Traffic Flow model VISSIM in different Real-World Situations,” 80th Annual Meeting Preprint CD-ROM, Transportation Research Board of the National Academies, Washington DC, 2001.

[8] Leyn, U. and P. Vortisch. “Calibrating VISSIM for the German Highway Capacity Manual,” Transportation Research Record: Journal of the Transportation Research Board, Vol. 2483, pp. 74-79, Transportation Research Board of the National Academies Washington DC, 2015.

[9] Mineta Transportation Institute (MTI). “A Framework for Developing and Integrating Effective Routing Strategies within the Emergency Management Decision Support System,” MTI Report 11-12, Sacramento CA, May 2012.

[10] Gomes, B., A. May, R. Horowitz. “Calibration of VISSIM for a Congested Freeway,” California PATH Program Institute of Transportation Studies, University of California, Berkeley, UCB-ITS-PRR-2004-4. 2004.

[11] Mississippi Department of Transportation (MDOT). “Emergency Evacuation Study for the Greater Jackson Area: Evacuation Traffic from New Orleans,” Jackson State University, Jackson Mississippi, May 21, 2011.

[12] Lownes, E., and Machemehl, R. “VISSIM. A Multi-Parameter Sensitivity Analysis,” Proceedings of the 2006 Winter Simulation Conference, Institute of Electrical and Electronics Engineers (IEEE), January 2006.

[13] Rrecaj, A., and K. Bombol. “Calibration and Validation of VISSIM Parameters – State of the Art,” *TEM Journal*, Vol. 4, No. 3, pp. 255-269, 2015.

[14] Duell, M., N. Saxena, S Chand, N. Amini, H. Grzybowska, and S.T. Waller. “Deployment and Calibration Considerations for Large Scale Regionally Dynamic Traffic Assignment: A Case Study for Sydney, Australia,” Transportation Research Record Journal of the Transportation Research Board, 2567: pp. 78-86. January 2016.

[15] Oregon Department of Transportation (ODOT). “Protocol for VISSIM Simulation,” June 2011.

[16] Washington State Department of Transportation (WSDOT). “Protocol for VISSIM Simulation,” September 2014.

[17] Kentucky Transportation Cabinet. “VISSIM Development and Calibration Report,” October 2014.

[18] Park, B. and Jongsun, W. “Microscopic Simulation Model Calibration and Validation Handbook,” Virginia Transportation Research Council, Charlottesville Virginia, October 2006.

[19] EPA-520/6-74-002, “Evacuation Risks – An Evaluation,” U.S. Environmental Protection Agency, Washington DC, June 1974.

[20] Sorensen, J.H. “Evacuations Due to Off-Site Releases from Chemical Accidents from 1980 to 1984,” *Journal of Hazardous Materials,* Vol. 14, 1987.

[21] Weston, R.F., Inc. “Identification and Analysis of Factors Affecting Emergency Evacuations,” National Environmental Studies Project, Nuclear Management and Resources Council. 1989.

[22] Murray- Tuite, P.M., B. Wolshon. “Evacuation transportation modeling: An overview of research, development, and practice,” Transportation Research Part C 27, pp. 25-45, 2013.

[23] Chin, S., O. Franzese, D. Greene, H. Hwang, R. Gibson. “Temporary Losses of Highway Capacity and Impacts on Performance: Phase 2,” Oak Ridge National Laboratory, ORNL/TM-2004/2009, November 2009.

[24] NUREG/CR-6864, “Identification and Analysis of Factors Affecting Emergency Evacuations,” U. S. Nuclear Regulatory Commission, Washington DC, January 2005.

[25] NUREG-0654/FEMA-REP-1, Rev. 1. “Criteria for Preparation and Evaluation of Radiological Emergency Response Plans and Preparedness in Support of Nuclear Power Plants,” U.S. Nuclear Regulatory Commission, Washington DC, November 1980.

[26] NUREG/CR-6981, “Planning and Implementation for Large Scale Evacuations,” U. S. Nuclear Regulatory Commission, Washington DC, October 2008.

[27] NUREG/CR-4873, “Benchmark Study of the I-DYNEV Evacuation Time Estimate Computer Code,” U.S. Nuclear Regulatory Commission, Washington DC, June 1988.

[28] NUREG/CR-4874, “The Sensitivity of Evacuation Time Estimates to Changes in Input Parameters for the I-DYNEV Computer Code,” U.S. Nuclear Regulatory Commission, Washington DC, June 1988.

[29] NUREG/CR-4831, “State of the Art in Evacuation Time Estimate Studies for Nuclear Power Plants,” Washington DC, 1992.

[30] NUREG/CR-6863, “Development of Evacuation Time Estimate Studies for Nuclear Power Plants,” U.S. Nuclear Regulatory Commission, Washington DC, January 2005.

[31] NUREG/CR-7002, “Criteria for Development of Evacuation Time Estimate Studies,” U.S. Nuclear Regulatory Commission, Washington DC, November 2011.

[32] NUREG/CR-6953 Volume 2, “Review of NUREG-0654, Supplement 3, Criteria for Protective Action Recommendations for Severe Accidents – Focus Groups and Telephone Survey,” NRC Washington DC, October 2008.

[33] Goldblatt, R., and K. Weinisch. “Evacuation Planning, Human Factors, and Traffic Engineering,” Transportation Security Training and Education, TR News 238, pp. 13-17. May-June 2005.

[34] Yuan, F., L. Han, “Improving Evacuation Planning with Sensible Measure of Effectiveness Choices – A Case Study,” Department of Civil and Environmental Engineering, University of Tennessee, Paper No 09-2899, November 15, 2008.

[35] Zeigler, D.J., S.D. Brunn and J.H. Johnson, Jr. “Evacuation from a Nuclear Technological Disaster,” *Geographical Review*, 71, pp. 1-16, 1981.

[36] Baker, E.J. “Hurricane Evacuation Behavior,” *International Journal of Mass Emergencies and Disasters,* Vol. 9, No. 2, pp. 287-310, August 1991.

[37] Mitchell, Jerry T., Andrew S. Edmonds, Susan L. Cutter, Mathew Schmidtlein, Reggie McCarn, Michael E. Hodgson, and Sonya Duhé. “Evacuation behavior in response to the Graniteville, South Carolina, Chlorine Spill,” Quick Response Research Report 178, Boulder, CO, Natural Hazards Center, University of Colorado, 2005.

[38] Murray-Tuite, P.M., B. Wolshon. “Evacuation transportation modeling: An overview of research, development, and practice,” Transportation Research Part C 27, pp. 25-45, 2013.

[39] Yin, Weihao, P. Murray-Tuite, S. Ukkusuri, and H. Gladwin. “An agent-based modeling system for travel demand simulation for hurricane evacuation,” Transportation Research Part C, 42, pp. 44-59, 2014.

[40] Mitchell, J.T., S.L. Cutter, and A.S. Edmonds. “Improving shadow evacuation management: Case study of the Graniteville, South Carolina, chlorine spill,” *Journal of Emergency Management*, Vol. 5(1), pp. 28-34, 2007.

[41] Ozbay, K., M.A. Yazici. “Analysis of Network-wide Impacts of Behavioral Response Curves for Evacuation Conditions,” *2006 IEEE Intelligent Transportation Systems Conference*, Toronto, Canada, September 2006.

[42] Lindell, M., C. Prater. “Critical Behavior Assumptions in Evacuation Time Estimate Analysis for Private Vehicles: Examples from Hurricane Research and Planning,” *Journal of Urban Planning and Development*, March 2007.

[43] Zeigler, D.J., and J.H. Johnson, Jr. “Evacuation Behavior in Response to Nuclear Power Plant Accidents,” *Professional Geographer*, 36(2), pp. 207-215, 1984.

[44] Texas House of Representatives: House Research Organization (HRO). “Evacuation Planning in Texas: Before and After Hurricane Rita,” Interim News. Number 79-2, February 14, 2006.

[45] Central Florida Regional Planning Council (CFRPC). “The 2010 Statewide Regional Evacuation Study for the Central Florida Region,” Florida, 2010.

[46] Weinisch, K., P. Brueckner. “The impact of shadow evacuation on evacuation time estimates for nuclear power plants,” *Journal of Emergency Management*, Vol. 13, Issue 2, pp. 145-158, March 2015.

APPENDIX B INPUT PARAMETERS

Three base models were developed for representative small, medium, and large population sites. The VISSIM microscopic simulation program was used for all three models. This appendix includes a comprehensive list of input parameters and additional detail on selected modeling processes.

B.1 Driving Behavior Parameters

The traffic flow model in VISSIM is a discrete, stochastic model that contains a psycho-physical car following model for all interactions along the same lane. VISSIM utilizes the following Wiedemann car following models:

- Wiedemann 74: Model suitable for urban traffic and merging areas
- Wiedemann 99: Model for freeway traffic with no merging areas

The VISSIM default Wiedemann 74 and 99 model settings used in all three representative site models are provided in Table B-1 and Table B-2, respectively. Some default values are identified in the User Manual while others are prepopulated within the VISSIM model.

Table B-1 Driver Behavior Parameters for Non-Freeways (Wiedemann 74)

Parameter	Description	Modeled Value	Default Value
Observed vehicles	The number of observed vehicles affects how well vehicles in the link can predict other vehicle movements and react accordingly.	4	4
Maximum look ahead distance	Maximum distance that a vehicle can see forward in order to react to other vehicles either in front or to the side.	820.21 ft	820.21 ft
Minimum look ahead distance		0 ft	0 ft
Maximum look back distance	Maximum distance that a vehicle can see backwards in order to react to other vehicles.	492.13 ft	492.13 ft
Minimum look back distance		0 ft	0 ft
Temporary lack of attention: Duration and probability		0 seconds; 0 percent	0 seconds; 0 percent
Average standstill distance		6.56 ft	6.56 ft
Additive part of desired safety distance	Value used for the computation of the desired safety distance.	6.56 ft	6.56 ft
Multiplicative part of desired safety distance	Value used for the computation of the desired safety distance.	9.84 ft	9.84 ft

Table B-2 Driver Behavior Parameters for Freeways (Wiedemann 99)

Parameter	Description	Modeled Value	Default Value
CC0 Standstill Distance	The average desired standstill distance between 2 vehicles	4.92 ft	4.92 ft
CC1 Headway Time	The distance in seconds which a driver wants to maintain while following another car	0.9 s	0.9 s
CC2 'Following' Variation	How much more distance than the desired distance a driver allows before intentionally moving closer to the car in front. (longitudinal oscillation)	13.12 ft	13.12 ft
CC3 Threshold for Entering 'Following'	Controls the start of the deceleration process. The number of seconds before reaching the safety distance.	-8 s	-8 s
CC4 Negative "Following' Threshold	Defines negative speed difference during the following process. Low values result in more sensitive driver reaction to the acceleration or deceleration of the preceding vehicle.	-0.35	-0.35
CC5 Positive 'Following Threshold	Defines positive speed difference during the following process.	0.35	0.35
CC6 Speed Dependency of Oscillation	Influence of distance on speed oscillation while in the following process.	11.44	11.44
CC7 Oscillation Acceleration	Oscillation during acceleration.	0.82 ft/s2	0.82 ft/s2
CC8 Standstill Acceleration	Desired acceleration when starting from standstill.	11.48 ft/s2	11.48 ft/s2
CC9 Acceleration at 50 mph	Desired acceleration at 50 mph.	4.92 ft/s2	4.92 ft/s2
Maximum look ahead distance	Maximum distance that a vehicle can see forward in order to react to other vehicles either in front or to the side.	820.21 ft	820.21 ft
Minimum look ahead distance		0 ft	0 ft
Maximum look back distance	Maximum distance that a vehicle can see backwards in order to react to other vehicles.	492.13 ft	492.13 ft
Minimum look back distance		0 ft	0 ft
Temporary lack of attention: Duration and probability		0 seconds; 0 percent	0 seconds; 0 percent

Table B-3 Lane Changing Parameters

Parameter	Description	Modeled Value	Default Value
Maximum deceleration	Maximum deceleration technically possible.	-13.12 ft/s2	-13.12 ft/s2
Accepted deceleration	Used as the upper bound of deceleration in prescribed cases.	-3.28 ft/s2	-3.28 ft/s2
Maximum deceleration – trailing vehicle	Maximum deceleration technically possible.	-9.84 ft/s2	-9.84 ft/s2
Accepted deceleration – trailing vehicle	Used as the upper bound of deceleration in prescribed cases.	-3.28 ft/s2	-3.28 ft/s2
Wait time before diffusion		900 s (medium and large site) 9,999 s (small site)	60 s
Minimum Headway front/rear	The minimum distance between 2 vehicles that must be available after a lane change, so that the change can take place.	1.64 ft	1.64 ft
Safety distance reduction factor		0.6	0.6
Maximum deceleration for cooperative braking		-9.84 ft/s2	-9.84 ft/s2
Cooperative lane change – max speed difference		6.71 mph	6.71 mph
Cooperative lane change – max collision time		10 s	10 s

B.2 Population Distribution

The base populations modeled in the small, medium, and large population site models are shown in Table B-4, Table B-5, and Table B-6, respectively. The populations are shown by radial distance from the NPP by sector.

Table B-4 Small Population Site Population Distribution

Sector	0-2 mile	2-5 mile	5-10 mile	10-15 mile	15-20 mile
N	2,300	0	300	4,000	5,000
NNE		0	300	700	500
NE		0	200	400	200
ENE		0	100	300	400
E		0	50	50	300
ESE		50	200	50	150
SE		100	150	100	400
SSE		100	550	100	200
S		50	300	1,000	3,700
SSW		50	200	300	450
SW		50	150	400	850
WSW		100	750	2,500	9,300
W		100	350	1,700	4,700
WNW		150	200	1,200	3,300
NW		100	250	2,000	5,200
NNW		100	200	200	800
Sum	2,300	950	4,250	15,000	35,450
Cumulative	2,300	3,250	7,500	22,500	57,950

Table B-5 Medium Population Site Population Distribution

Sector	0-2 mile	2-5 mile	5-10 mile	10-15 mile	15-20 mile
N	0	1,472	25,349	3,429	4,000
NNE	0	1,413	13,479	1,839	6,000
NE	0	226	4,787	7,462	5,500
ENE	0	0	10,742	8,409	5,000
E	0	7	41,403	26,913	31,500
ESE	0	0	38,563	69,623	82,000
SE	0	0	0	3,491	18,000
SSE	0	178	641	12,197	6,500
S	61	748	1,770	1,589	2,000
SSW	0	144	289	513	1,000
SW	0	175	907	559	500
WSW	0	307	1,363	375	1,000
W	0	296	886	338	1,000
WNW	0	25	192	308	1,000
NW	0	707	18,101	22	4,000
NNW	0	550	35,219	12,931	6,000
Sum	61	6,249	193,690	150,000	175,000
Cumulative	61	6,310	200,000	350,000	525,000

Table B-6 Large Population Site Population Distribution

Sector	0-2 mile	2-5 mile	5-10 mile	10-15 mile	15-20 mile
N	2,044	9,141	6,798	5,712	10,000
NNE	756	3,590	4,239	17,423	10,000
NE	62	1,407	7,617	5,534	26,500
ENE	46	5,005	12,113	31,762	66,500
E	750	6,838	25,610	29,527	85,500
ESE	1,033	5,972	27,855	51,643	88,000
SE	757	13,473	21,420	34,828	62,500
SSE	325	6,866	31,575	27,202	36,500
S	467	2,818	5,316	31,630	43,500
SSW	651	1,788	6,545	24,033	44,000
SW	943	2,138	4,597	4,706	30,000
WSW	1,593	2,861	3,456	4,099	15,000
W	230	5,847	3,499	6,843	50,000
WNW	569	20,749	17,232	15,867	60,000
NW	1,064	11,286	6,778	4,204	13,000
NNW	1,521	7,610	20,151	4,988	9,000
Sum	12,811	107,389	204,800	300,000	650,000
Cumulative	12,811	120,200	325,000	625,000	1,275,000

Figure B-1, Figure B-2, and Figure B-3 illustrate the distribution of the base populations and road network for the small, medium, and large population sites, respectively.

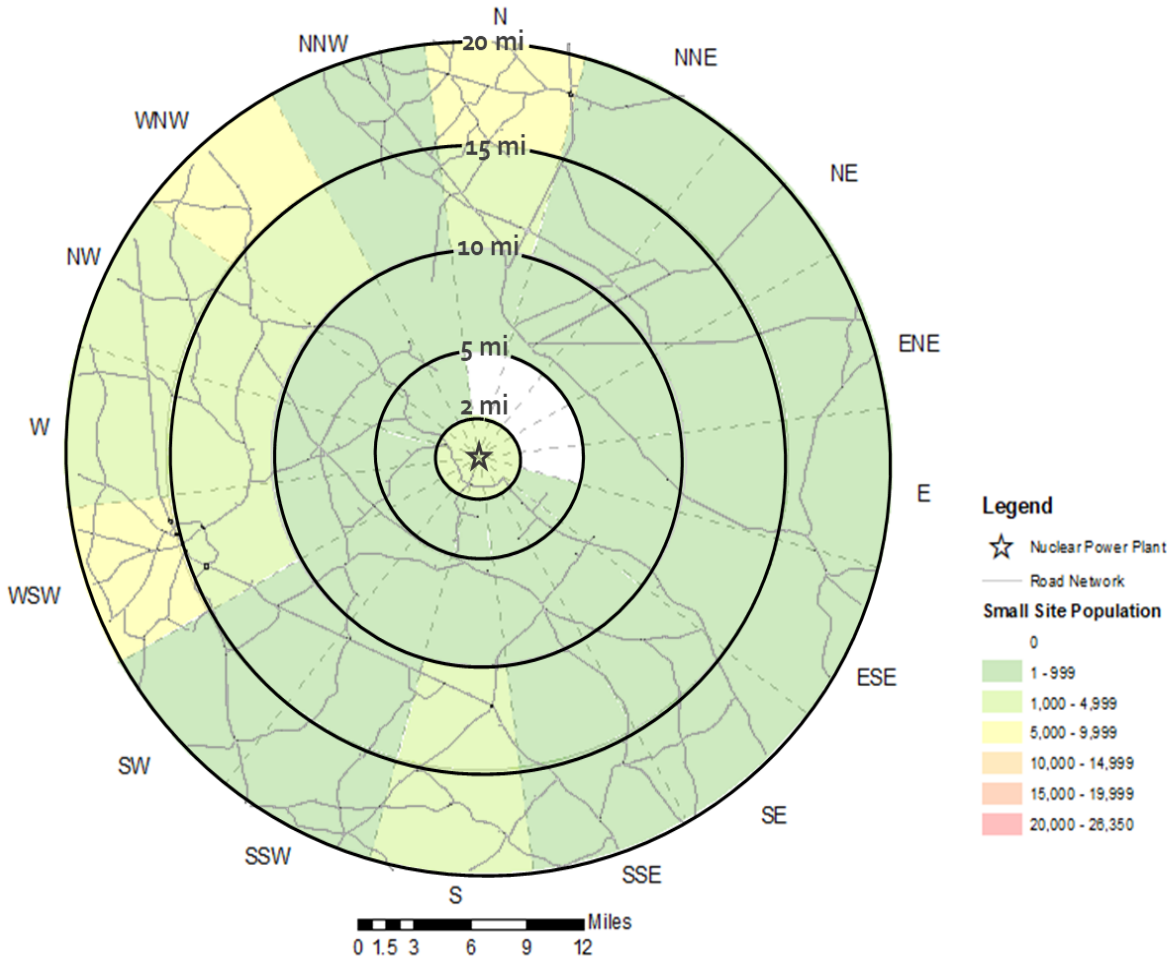

Figure B-1 Population and Road Network in the Small Population Site Base Model

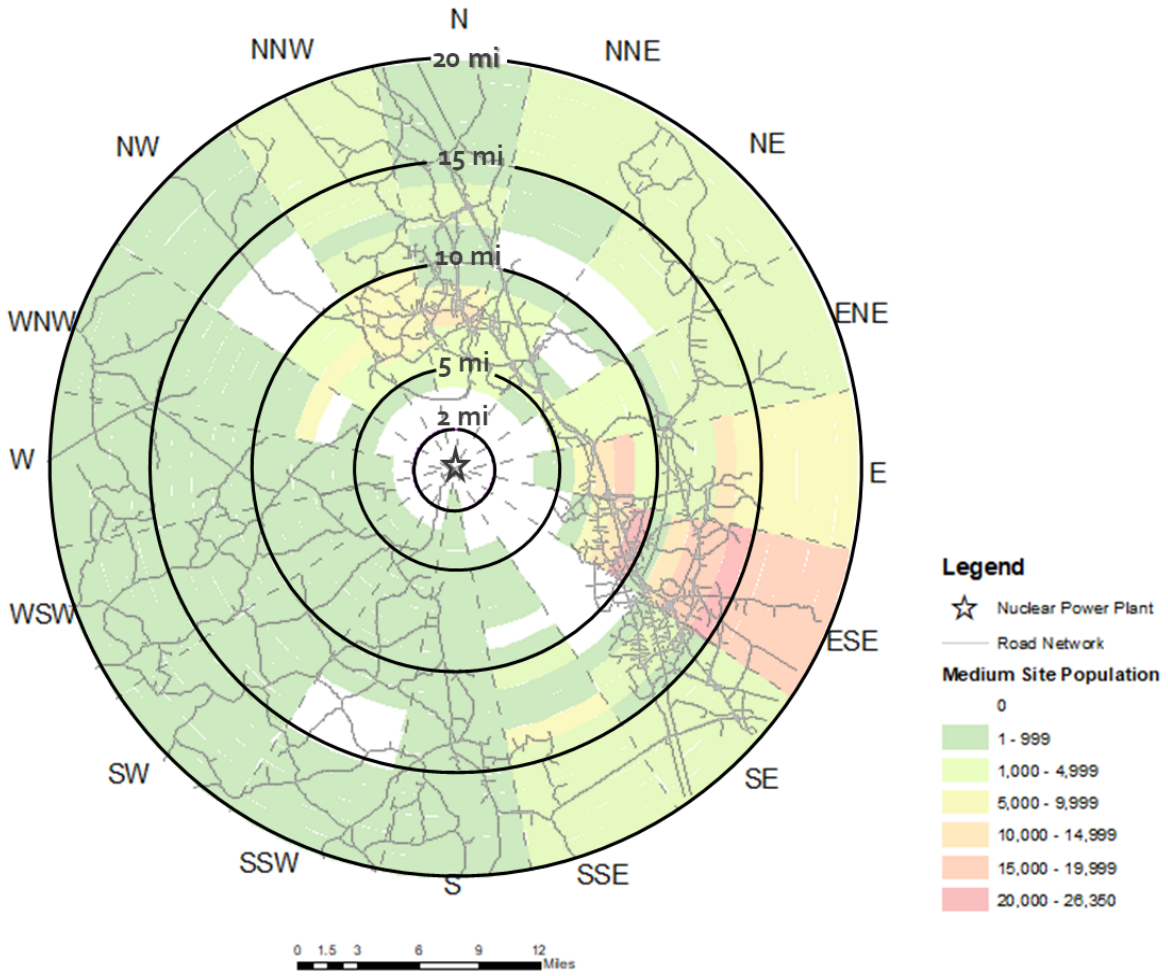

Figure B-2 Population and Road Network in the Medium Population Site Base Model

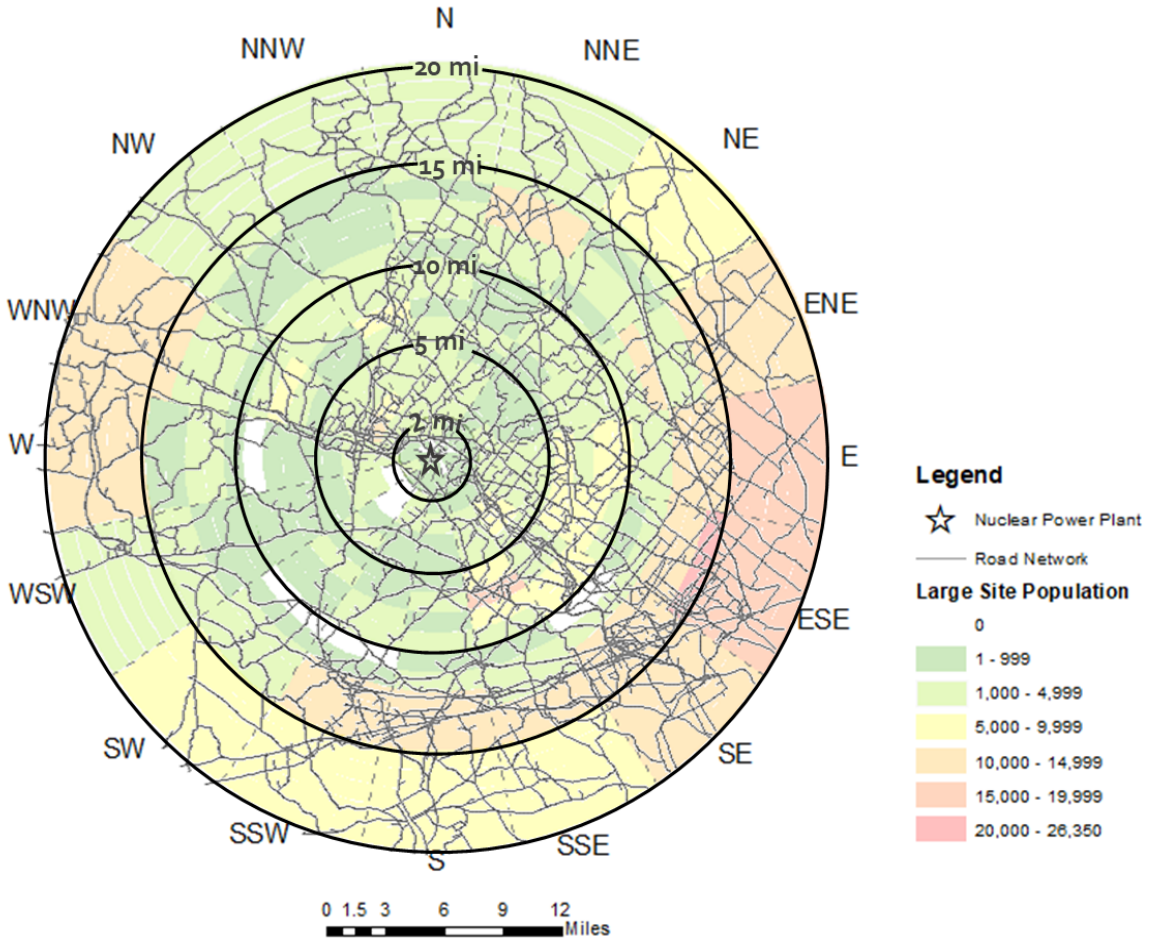

Figure B-3 Population and Road Network in the Large Population Site Base Model

Information supporting the development of the mobilization time is typically obtained through site-specific telephone surveys conducted during the development of an ETE study. The loading curves for the medium and large population sites were developed from an average of multiple ETEs representative of the respective populations. The average loading curves used for the medium and large population sites incorporate average trip generation times. Following current guidance in NUREG/CR-7002, the shadow evacuees were loaded consistent with the loading of the EPZ population.

Table B-7 Loading Curve

Traffic simulation model time[1] (h:mm)	Evacuation interval number	Evacuation time (h:mm)	Evacuation period (minutes)	Small site EPZ loading	Medium site EPZ loading	Large site EPZ loading
Traffic simulation initialization period — 30 minutes[2]						
0:30	1	0:00	15	10%	0%	0%
0:45	2	0:15	15	25%	2%	0%
1:00	3	0:30	15	21%	6%	3%
1:15	4	0:45	15	16.5%	11%	10%
1:30	5	1:00	15	9.5%	15%	15%
1:45	6	1:15	15	8.5%	16%	15%
2:00	7	1:30	15	6.5%	13%	13%
2:15	8	1:45	15	2.5%	12%	12%
2:30	9	2:00	15	0.5%	8%	7%
2:45	10	2:15	15		6%	6%
3:00	11	2:30	15		4%	4%
3:15	12	2:45	15		2%	4%
3:30	13	3:00	15		2%	2%
3:45	14	3:15	15		1%	2%
4:00	15	3:30	15		1%	2%
4:15	16	3:45	15		1%	2%
4:30	17	4:00	15			1%
4:45	18	4:15	15			1%
5:00	19	4:30	15			1%
5:15	20	4:45	15			
5:30	21	5:00	15			
5:45	22	5:15	15			
6:00	23	5:30	15			
6:15	24	5:45	15			
6:30	25	6:00	15			
Total				100%	100%	100%

[1] Evacuation order is given at simulation clock time 0:30.

[2] A 30 minute initialization period is used to load background traffic onto the network prior to the evacuation.

B.3 Speeds

Speeds were implemented using the VISSIM desired speed decision function. For posted speeds below 40 mph, desired speeds were set with a range of 5 mph above and below the posted speed. For posted speeds above 45 mph, a range of 10 mph above and below the posted speed was set. In all cases, the 85th percentile was set at the posted speed. Figure B-4 presents an illustration of the desired speed distribution profiles applied in the modeling.

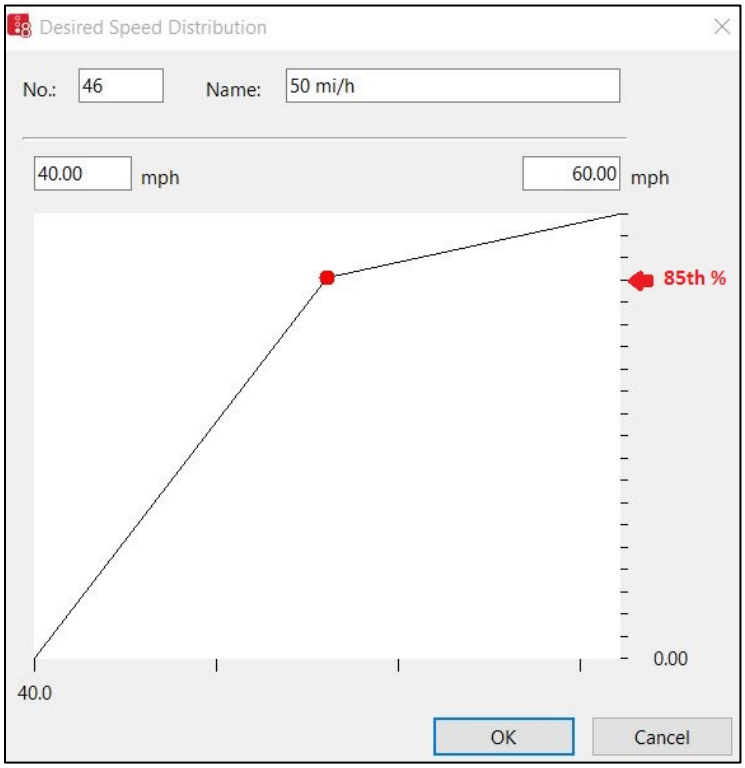

Figure B-4 Speed Distribution Profile with Posted Speed at 85th Percentile

B.4 Collector Points

Simulation output data was primarily gathered from predetermined collector points. Collector points were placed at the locations where routes used in the analysis crossed the specified distances of 2, 5, 10, 15, and 20 miles from the center. Collector points reported data on vehicle counts, speed, travel distance, and other factors in 5 minute intervals and stratified by vehicle type. Figure B-5, Figure B-6, and Figure B-7 illustrate the data collector locations for the small, medium and large population site models, respectively.

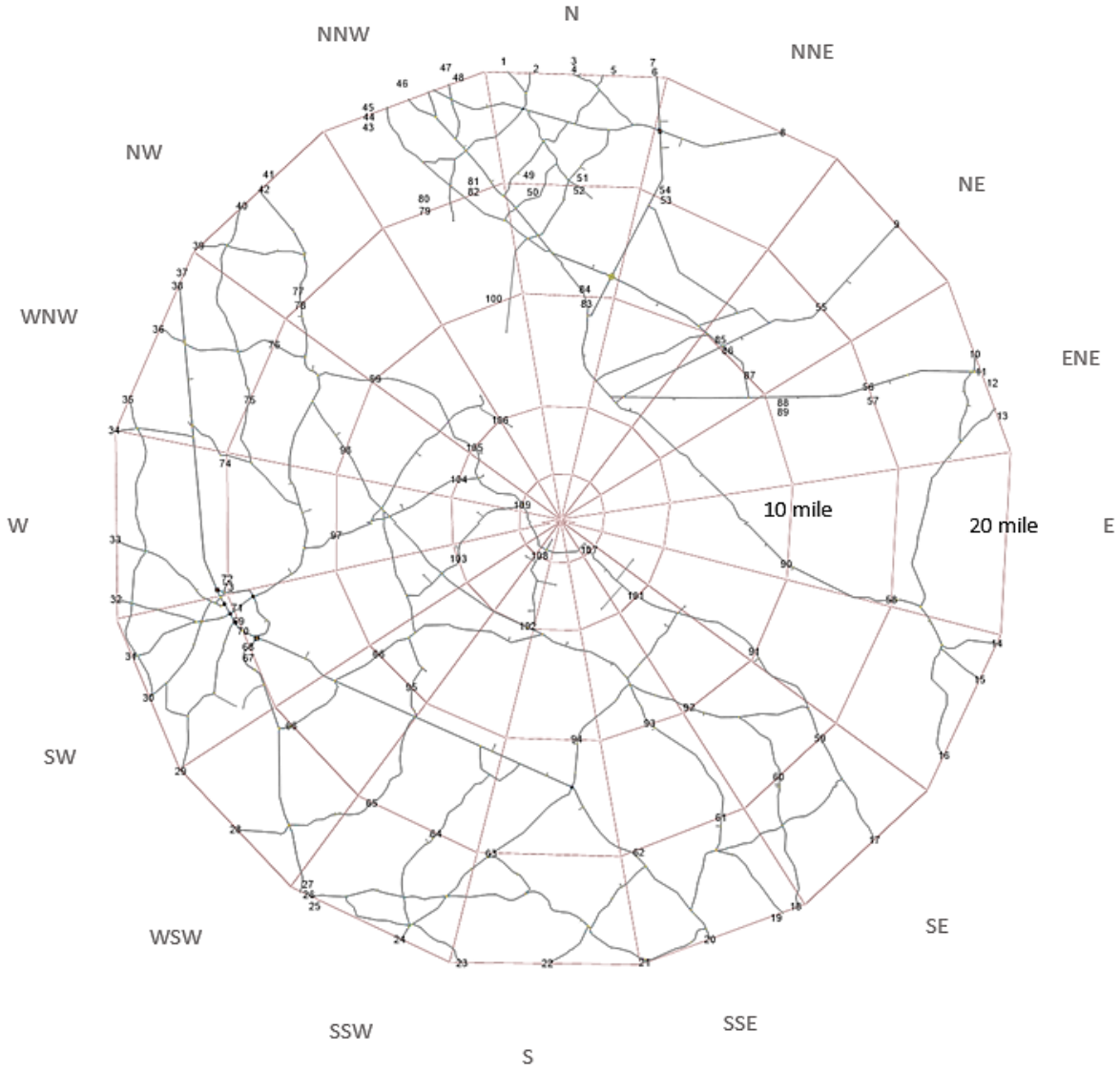

Figure B-5 Small Population Site Model Data Collection Points

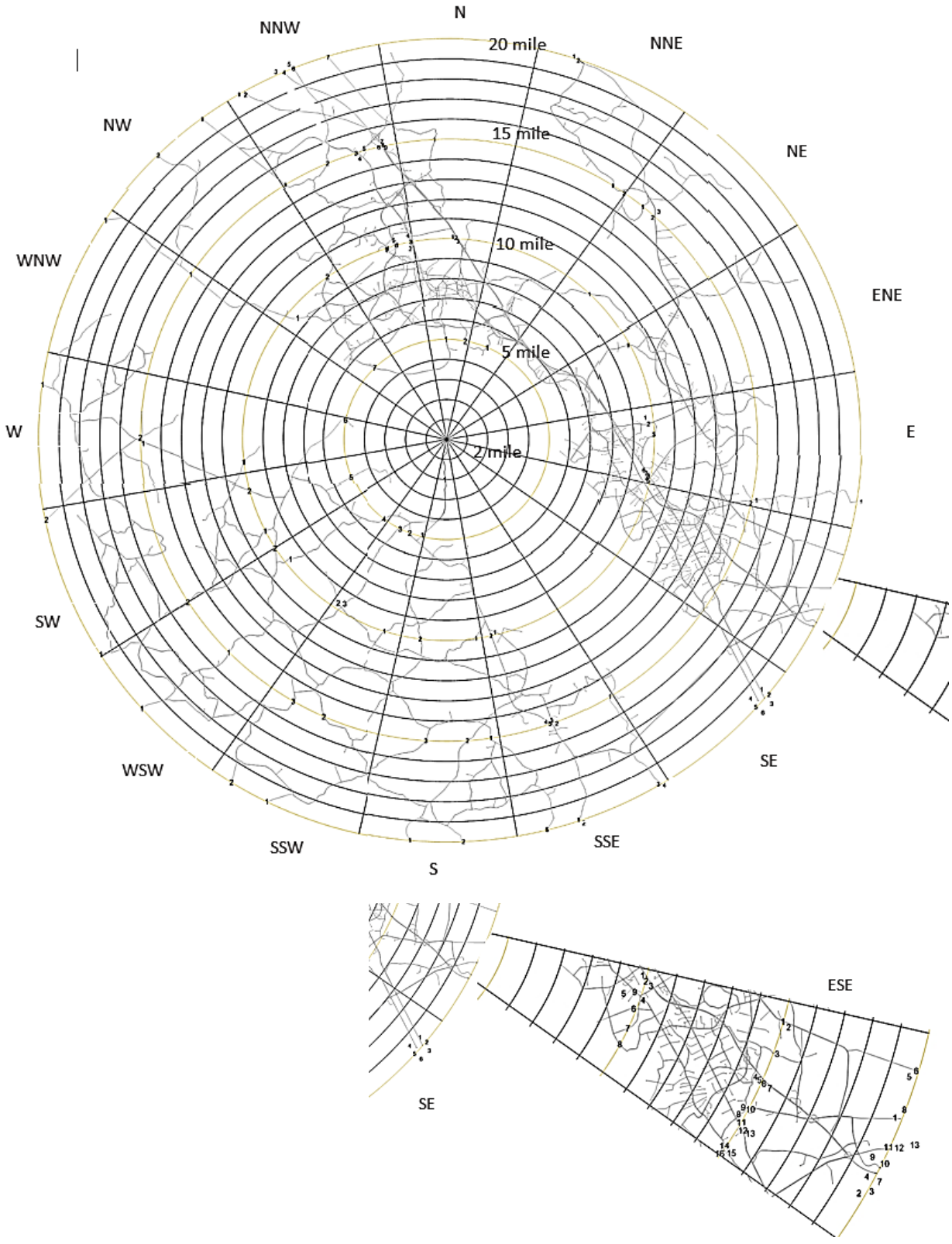

Figure B-6 Medium Population Site Model Data Collection Points

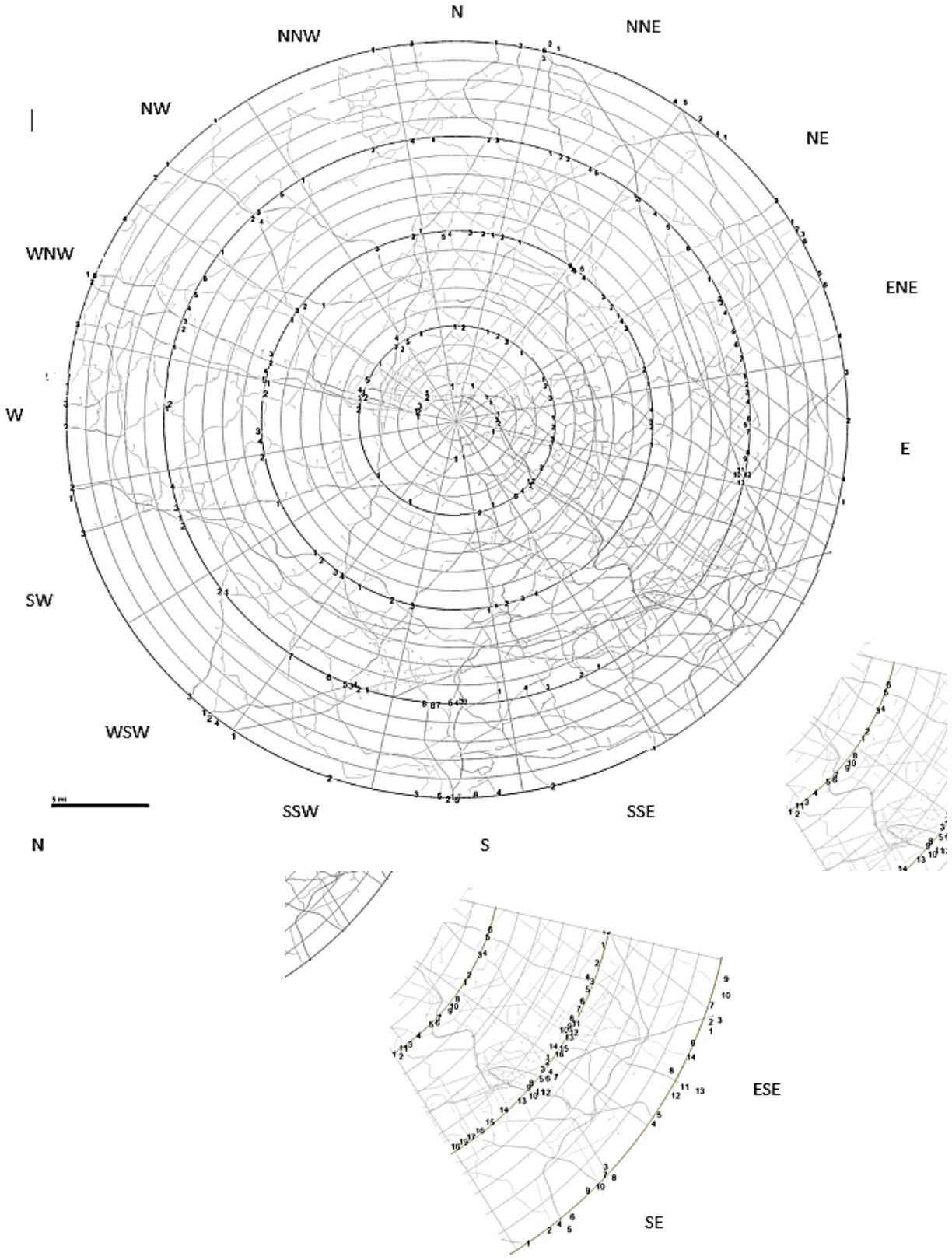

Figure B-7 Large Population Site Model Data Collection Points

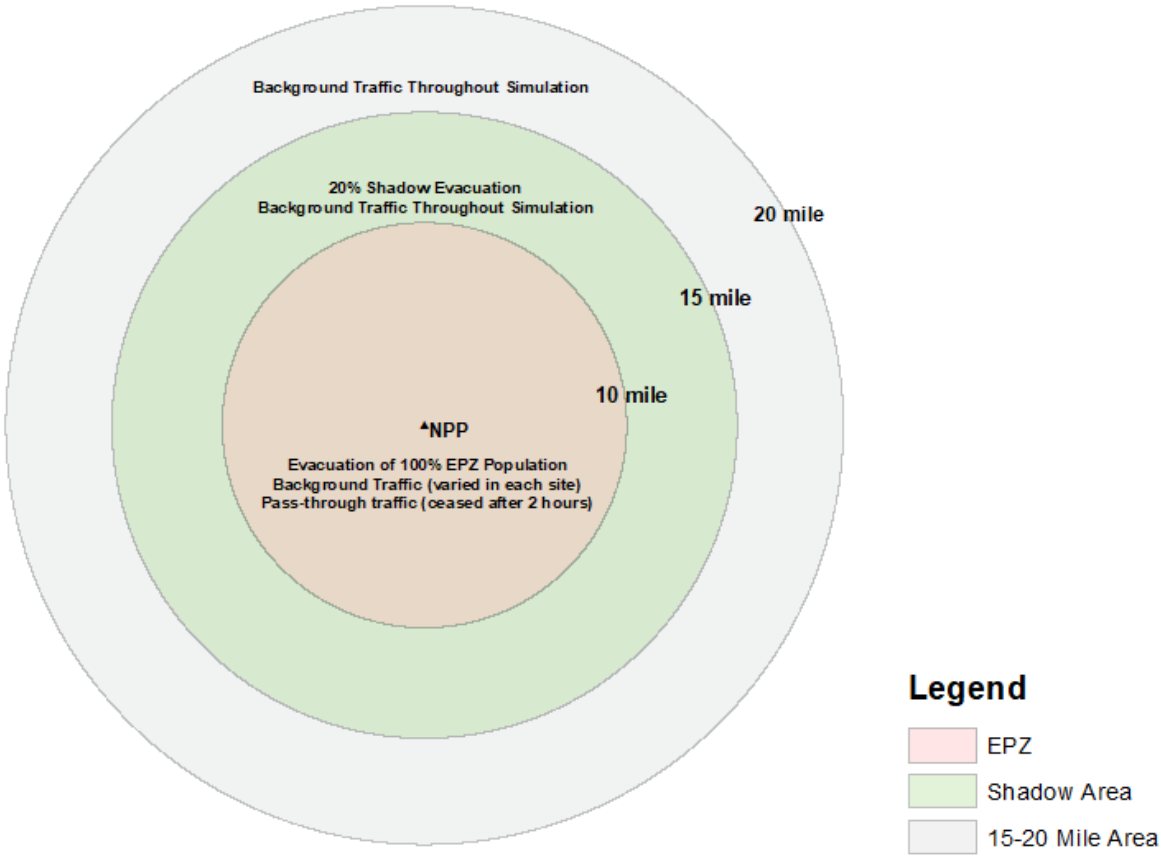

Figure B-8 Radial Distances Used in the Base Models

APPENDIX C SELECTION OF REPRESENTATIVE SITES

The selection of representative sites was a necessary first step in the performance of this research. However, with nuclear reactors in operation at more than 60 unique locations across the U.S., choosing a few sites to model to represent a diverse set of site-specific populations and transportation networks was a significant challenge. A clear basis for selection was needed that would ensure the representativeness of the research results across the entire fleet of operating reactors sites.

Fundamentally, evacuation processes can be described within a construct of capacity and demand relationships. As such, population (demand) and roadway characteristics (capacity) should provide a useful bases for assessing the similarity and differences among ETE studies. Each operating reactor licensee submitted updated evacuation time estimate (ETE) reports to the NRC based on population data from the 2010 Census in accordance with the requirements in Appendix E to 10 CFR Part 50. The data from the ETE reports was extracted and analyzed in a number of ways to search for useful relationships among the various demand and capacity parameters that would reveal broader levels of classification.

C.1 Demand Basis

Evacuation time estimate studies provide estimates of many segments of the evacuating population including permanent residents, transients, special facility residents, and schools. The majority of evacuees are permanent residents within the 10-mile emergency planning zone (EPZ). As such, the relationship between the ETE and the permanent resident population was examined graphically to look for identifying features. Figure C-1 shows the site-specific permanent resident population plotted against the 90 percent ETE for evacuation of the entire EPZ. The 90 percent ETE was chosen since this value is used in the development of protective action strategies [1]. It was expected that ETEs would typically increase with increases in population. This is generally true, as illustrated in Figure C-1. Figure C-1 also reveals other discernible features in the relationship between population and ETE:

- **Resident Population < 50,000:** Below a population of about 50,000 permanent residents there is a tight grouping of site-specific 90 percent ETEs with values that are generally less than 200 minutes and bounded between 100 and 300 minutes. Generally, this grouping shows a narrow range of ETEs within a narrow range of population. About 30 sites fit in this category.

- **50,000 < Resident Population < 200,000:** Between 50,000 and 200,000 permanent residents there is a broad grouping of sites with some that contain longer 90 percent ETEs than for sites with < 50,000 people. The ETEs are bounded between 100 and 400 minutes and can be seen to gradually increase with population up to about 200,000 permanent residents. Generally, this grouping shows a moderate range of ETEs in a broad range of population. About 20 sites fit in this category.

- **Resident Population > 200,000:** Above 200,000 permanent residents, there is a grouping with wide variation in both population and ETE. The 90 percent ETE varies anywhere between 200 and 600 minutes even for sites with similar populations. Generally, this grouping shows a broad range of ETEs in a broad range of large populations. About 10 sites fit in this category.

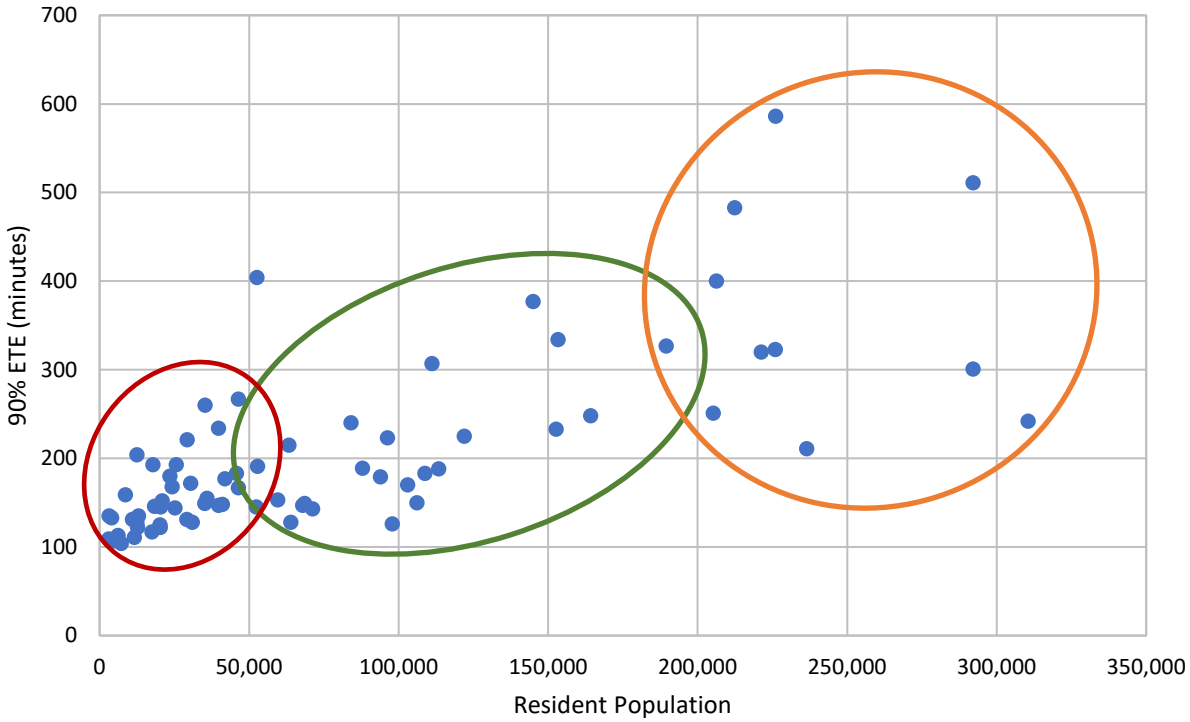

Figure C-1 Relationship Between Resident Population and 90 Percent ETE for the EPZ

Based on the groupings observed, population thresholds of 50,000 and 200,000 were chosen as the demarcation between small, medium, and large population groups. From this, it was expected that at least three representative models would be necessary.

C.2 Capacity Basis

The capacity of a road network is a complex function of the arrangement of the roadways (i.e., network topology), traffic controls (signals, lane regulations, etc.), driver behavior, and mix of vehicles in the traffic stream, among other variables. The capacity of a network is not static and can change frequently in both space and time during emergencies. For example, bottlenecks, adverse weather, and traffic incidents can decrease outflow capacity while use of contraflow can increase it. Microscopic and macroscopic simulation models calculate roadway capacity differently, with microscopic models estimating saturated flow and macroscopic models implementing the equations of the Highway Capacity Manual [2]. While some ETE reports provide detailed data on the capacity assumed for each roadway segment in the model, it is difficult to reduce this data to a simple measure of overall network capacity.

A simple representation of network capacity was needed. To provide this, an examination was first performed on the roadways within the 10-mile plume exposure pathway emergency planning zone surrounding each operating nuclear power plant. Figure C-2 shows the agglomeration of network topologies in the 10-mile by 10-mile area surrounding 63 specific power plant locations. These figures were extracted from ArcGIS datafiles and include primary roads (freeways and highways) and secondary roads (major and arterial roads); local roads (collectors and local streets) were generally not resolved at the scale of these figures and were omitted.

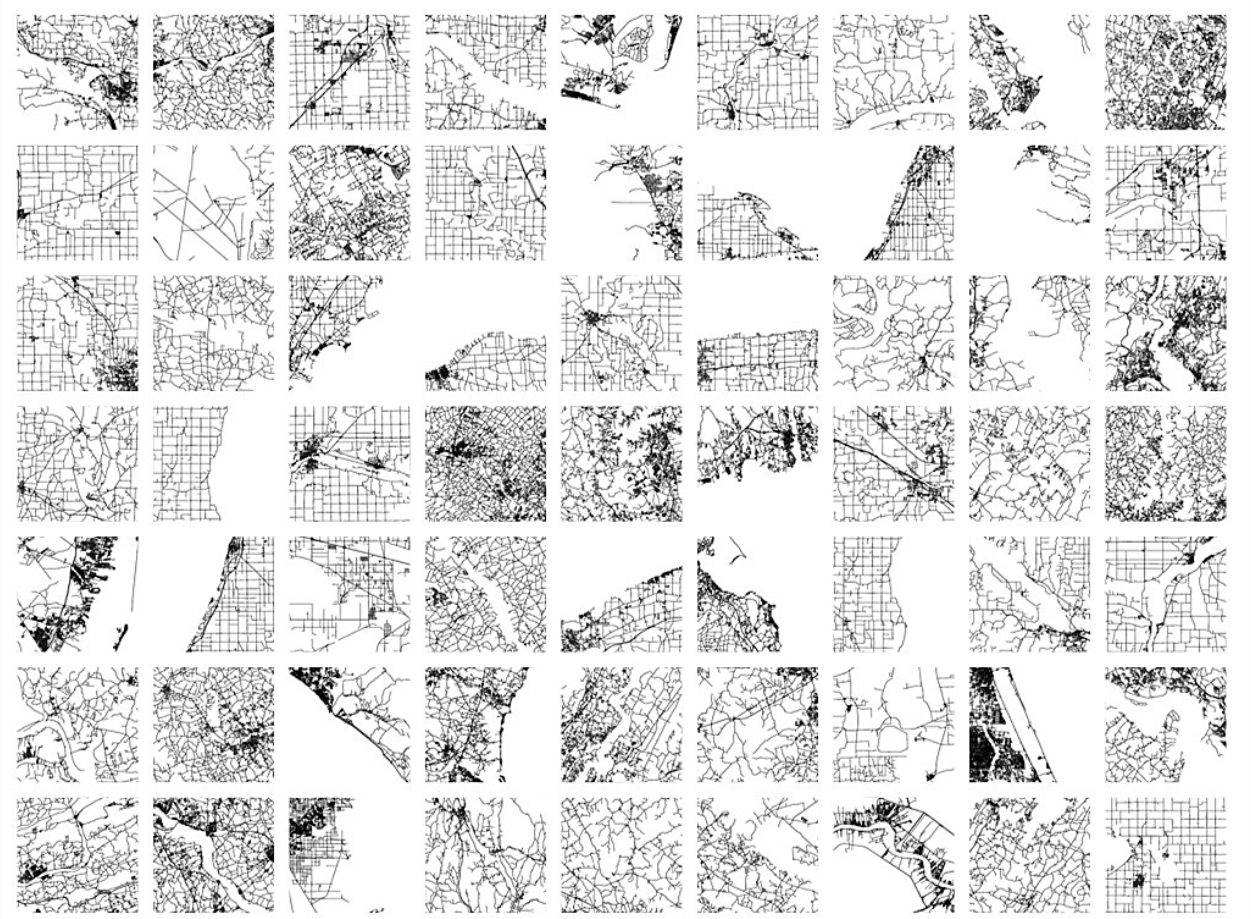

Figure C-2 Road Network Topology in the 10-mile Region Around 63 Nuclear Plant Sites

A closer look at these road networks reveals characteristics of fractal behavior. A fractal is a geometric structure that appears the same at different levels of scale. In geometry, fractals represent dimensions between Euclidean space dimensions of 0 (point), 1 (line), 2 (plane), etc. A road network lies somewhere between a line and a plane, and therefore has a fractal dimension between 1 and 2. The fractal nature of roadways has been widely studied, particularly in relation to how cities grow [3] [4]. Fractal theory has also been applied successfully in many fields of science, including traffic flow and traffic management [5] [6]. The branching structure of a transportation network suggests that it can be characterized by a recurrent, scale invariant geometry, at least over some limited range [7]. More importantly, the fractal dimension is a number that can provide insight into the complexity of roadways which exhibit self-similarity at multiple scales [7].

The fractal dimension of the road network within 10 miles of each nuclear power plant site was found by analyzing the images using the box-count method in MATLAB. A validation was performed using the box-count method in Fractalyse, an independent software tool for computing fractal dimensions. The fractal dimension for each road network is shown in Figure C-3. This figure also shows a comparison between the MATLAB and Fractalyse results, which showed good agreement.

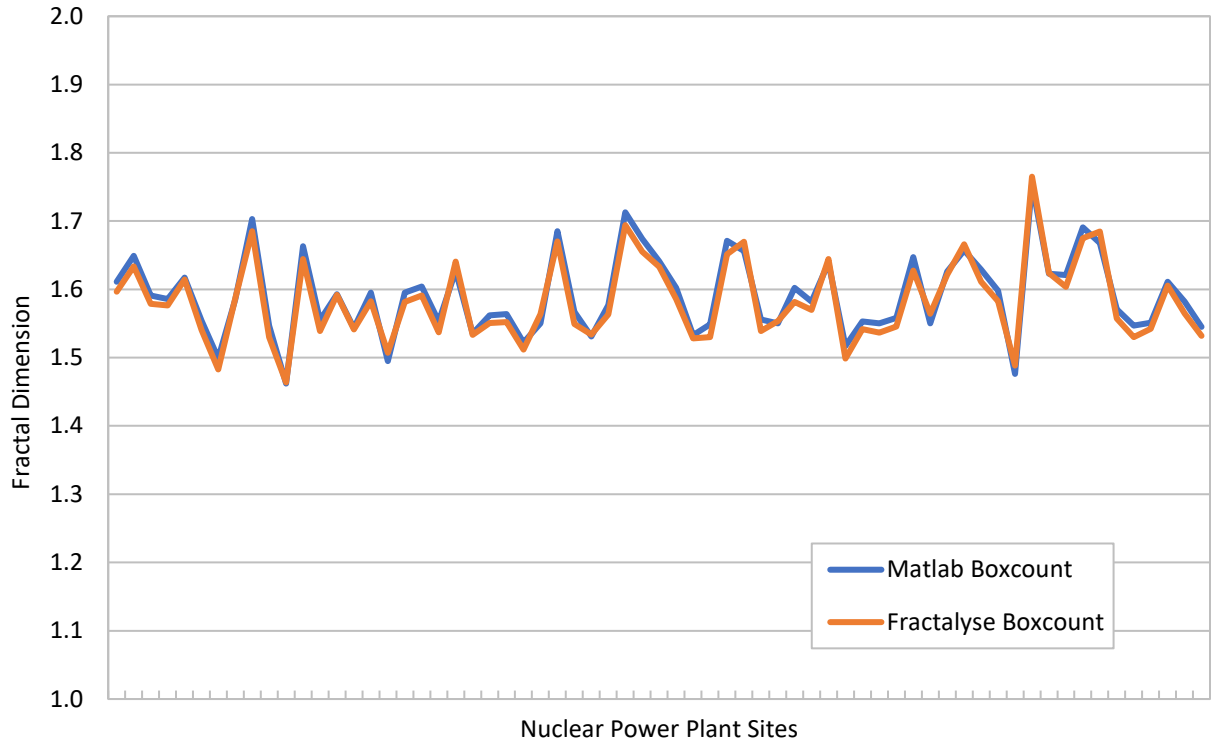

Figure C-3 Comparison of Road Network Fractal Dimensions Using MATLAB and Fractalyse Box-counting Methods

The fractal dimension, d_f, of the 63 unique nuclear power plant sites varies from about 1.45 to 1.75. The fractal dimension is a measure of the space-filling capacity of the pattern, so this number represents the extent of the road network. Lower fractal numbers represent less dense road networks, such as are found in rural locations. An urban location will have a high degree of space-filling roads, and a fractal dimension closer to 2. Because permanent resident population is closely related to infrastructure development, it seems intuitive that there should be some relation between the fractal dimension and population. This is generally the case, as illustrated in Figure C-4 which is a plot of fractal dimension verses resident population. While characteristics of the fractal dimension can be observed that correspond to the population groupings observed in Figure C-1, this analysis provides limited information to aid in selection of a representative site because it lacks detail on topological features that may distinguish groupings of sites from each other. To search for such details, additional characteristics of the fractal nature of road networks were examined.

Unlike a true mathematical fractal, road networks are not likely to be self-similar at each length scale. For a fractal structure, it may not be sufficient to characterize its form and structure with only one fractional dimension [8]. A set of fractal patterns, ratios of fractal dimensions, or other fractal data may be needed to describe the scaling behavior. An example of scaling behavior is provided in Figure C-5 which shows the fractal dimensional computed at each scale of the 2D box-count method in MATLAB for the site roadway shown, which has an overall fractal dimension (d_f) of 1.6. This scaling behavior is unique to each site and offers additional information on the structure of the road network which lends itself to analysis.

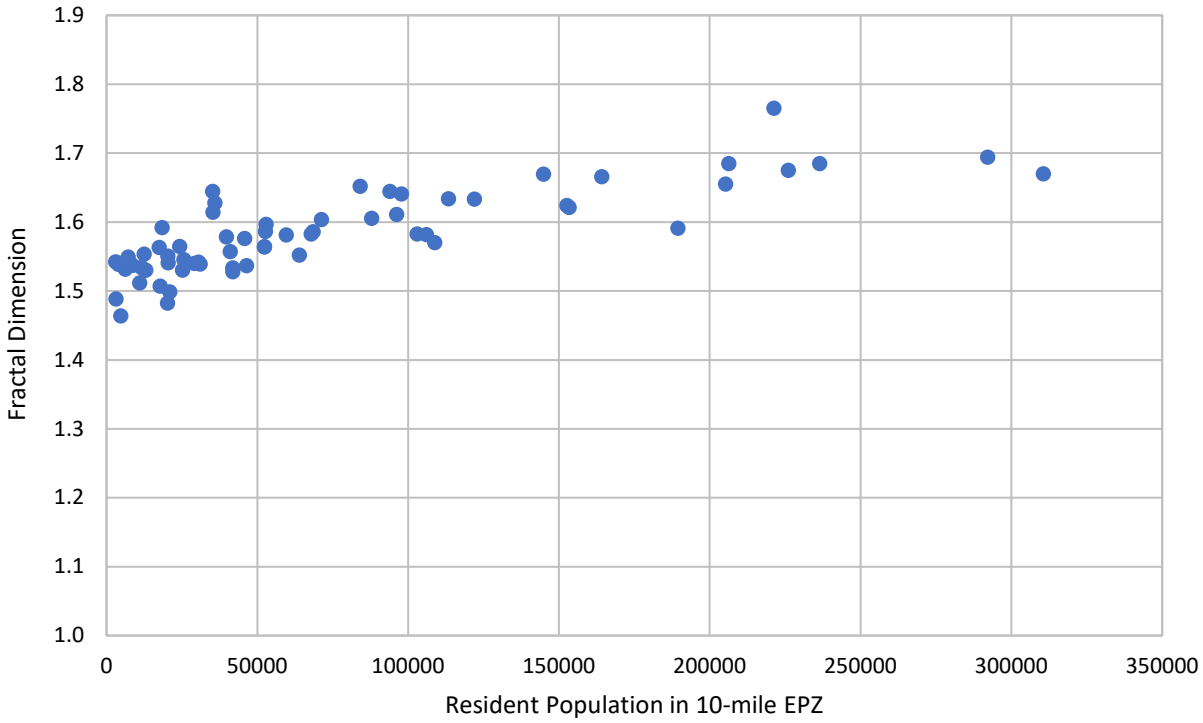

Figure C-4 Road Network Fractal Dimension vs. Resident Population in the 10-mile EPZ

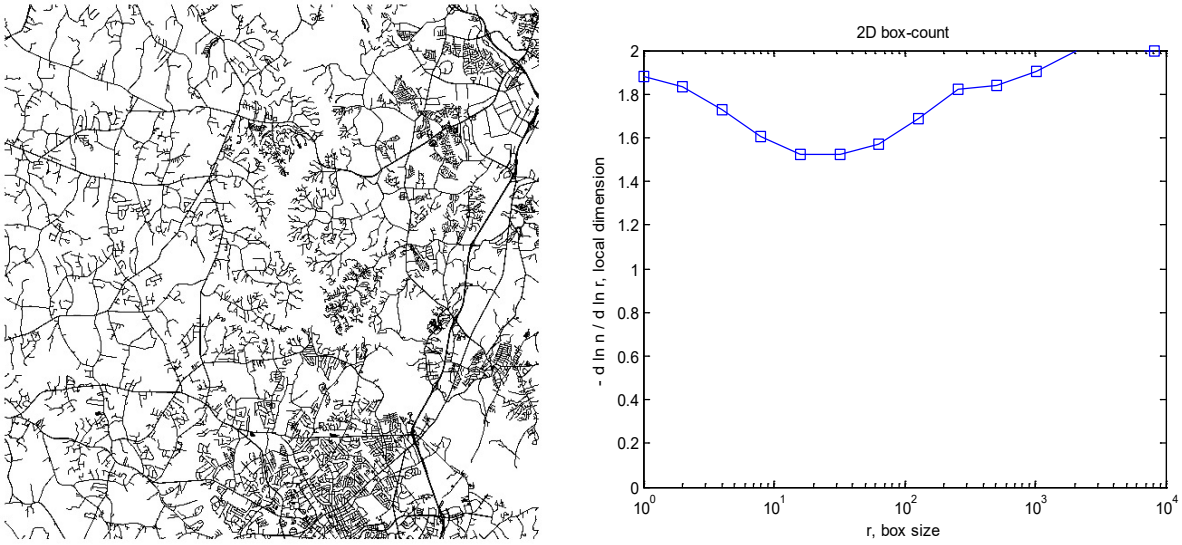

Figure C-5 Example Fractal Dimension Curve of Scaling Behavior for a Site with d_f = 1.6

A self-organizing neural network was used to search for patterns in the fractal behavior of the transportation networks and to categorize the topologies. A neural network is a data processing system consisting of a large number of simple, highly interconnected processing elements (artificial neurons) in an architecture inspired by the structure of the brain [9]. Neural networks are widely used in pattern recognition applications and are an appropriate tool to search for patterns in the fractal scaling behavior. The neural network toolbox in MATLAB was setup to organize the 63 unique power plant site topologies into distinct categories. The input to the network was a 63 x 13 matrix of fractal numbers corresponding to each of the 13 length scales (box sizes) utilized in the box-count method for each of the 63 unique sites (as shown in the example in Figure C-5). The inputs were organized by the neural network into three output categories. The results of the categorization are shown in Figure C-6.

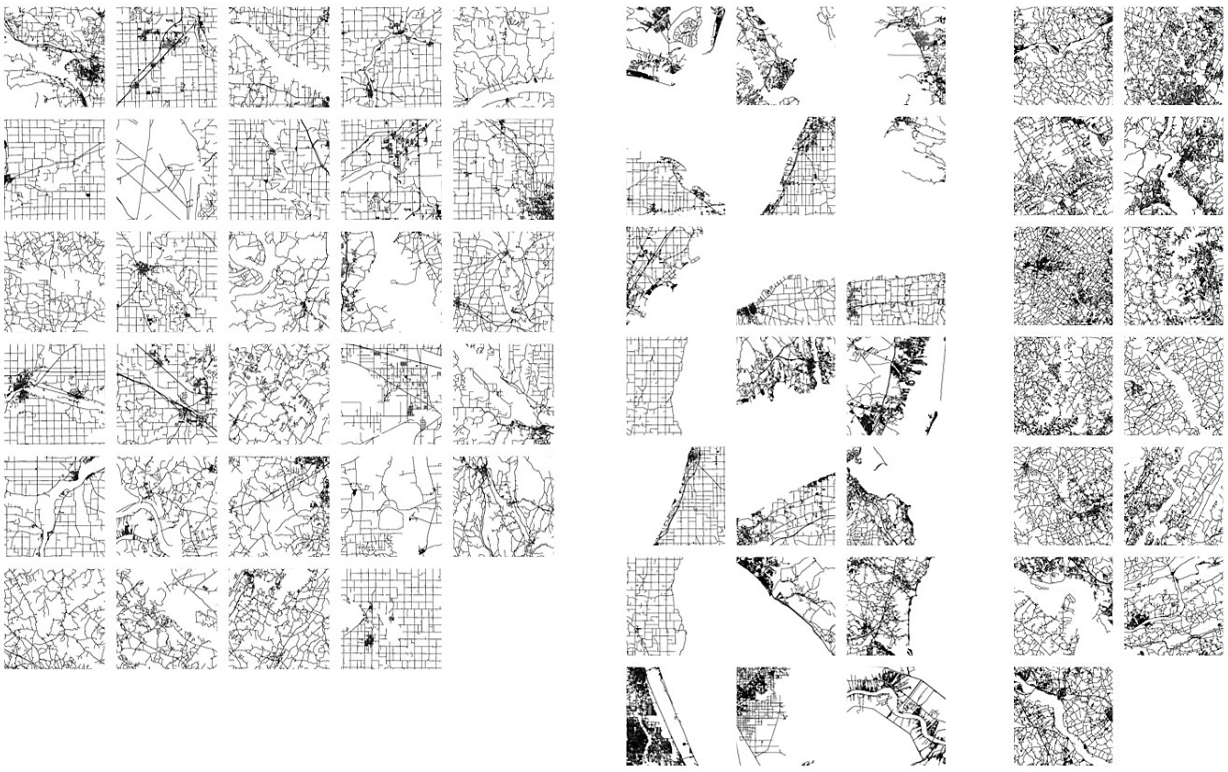

Figure C-6 Neural Network Classification of Road Networks: Rural, Coastal, Urban

The neural network classification revealed distinct topological details that were not apparent from examination of the fractal dimension alone. From this classification analysis it can be seen that nuclear power plant sites can be broadly classified into rural, coastal, and urban locations. The distinguishing feature of coastal locations is that there is approximately half as much road network within the 10-mile EPZ as in the rural or urban sites, even though the roads within these areas show a wide variation in complexity. Clearly this has implications for evacuation planning along coastal locations and locations sited on the Great Lakes where approximately half of the EPZ is water and choice of evacuation route may be limited. As such, these classifications (rural, coastal, urban) are likely to be important in ETE studies and formed the basis for selecting representative sites based on road network topology.

C.3 Combined Capacity and Demand Basis

With each of the 63 unique nuclear power plant sites categorized by demand and capacity, a plot of road network classification verses resident population was arranged to aid in selecting suitable representative sites to model for this research. Based on the population categories of small (< 50,000), medium (50,000-200,000), and large (> 200,000) it was apparent that the small population site should be representative of a rural road network, the medium population site should be a coastal site, and the large population site should be an urban site in order to cover the representative populations and topologies.

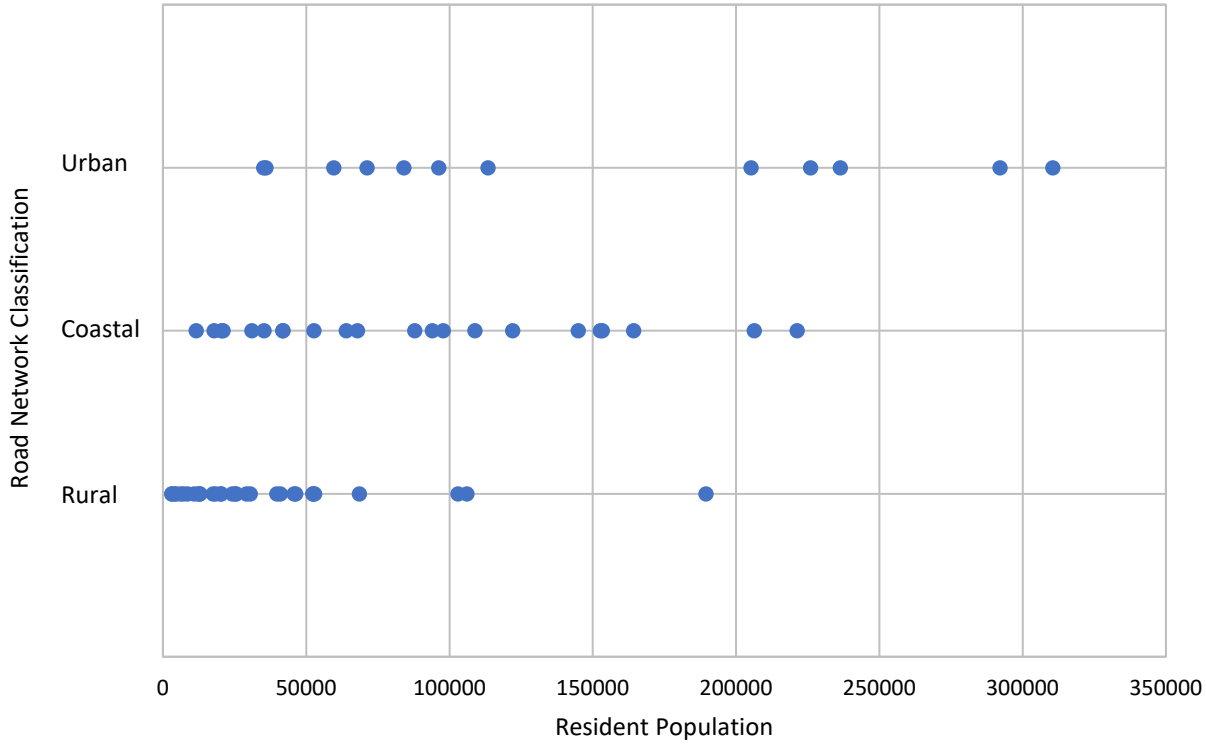

Figure C-7 Road Network Classification vs. Resident Population

Of note, the medium population site ultimately selected for modeling provided essentially two dynamic models in one. As shown in Figure C-8, the road network of the medium site is essentially two independent road networks. The northern half of the site has a very urban road structure with a major evacuation route running from the northwest to the southeast. The southern half of the site is very rural and sparsely populated. Although the neural network classified this site as urban based on the curve of scaling behavior of the fractal dimension, during other classification trials this site was often classified as coastal because of the expansive river running through the site. The urban and rural characteristics of this site, the lack of connectivity between the upper and lower portions of the road network, and the base resident population made this site useful for study as a representative coastal location with medium population.

Figure C-8 Medium Population Site Road Network

The selection of representative sites was further refined by giving consideration to the specific ETE study research objectives, availability of microsimulation model data, and familiarity with specific site data from other research studies. It is important to note that the selection of representative sites was not based on any particular site-specific ETE report, nor are the models a replication of any site-specific ETE study. During the contract kickoff meeting, researchers from LSU presented a list of five candidate representative sites based on their expert judgment that matched the sites the NRC had independently selected as suitable candidates. This agreement in representative sites from both an un-biased scientific analysis of population and network topologies and informed judgment by evacuation experts provided assurance that the selected sites would serve as representative small, medium, and large population site models.

C.4 References

[1] NUREG-0654/FEMA-REP-1, Rev. 1, Supplement 3, “Criteria for Preparation and Evaluation of Radiological Emergency Response Plans and Preparedness in Support of Nuclear Power Plants, Guidance for Protective Action Strategies,” U.S. Nuclear Regulatory Commission, Washington DC, November 2011.

[2] Transportation Research Board. “HCM 2010 Highway Capacity Manual,” National Research Council, Washington DC, 2010.

[3] Frankhauser, P., “The Fractal Approach: A New Tool for the Spatial Analysis of Urban Agglomeration,” Population: An English Selection, Vol. 10, No. 1, pp. 205-240, 1998.

[4] Thomas, I., Frankhauser, P., Frenay, B., Verleysen, M., “Clustering Patterns of Urban Built-Up Areas With Curves of Fractal Scaling Behavior,” *Environment and Planning B: Planning and Design*, Vol. 27, pp. 942-954, 2010.

[5] Haleem, K., Alluri, P., Gan, A., Hongtai, Li, and Li, T., “Synthesis of the Advance in and Application of Fractal Characteristics of Traffic Flow,” Prepared for State of Florida Department of Transportation Research Center, Contract No. BDK80 977-25, Final Report, July 2013.

[6] Vojak, R., Vehel, J., Danech-Pahouh, M., “Multifractal Description of Road Traffic Structure,” IFAC Proceedings Volumes, Vol. 27, Issue 12, pp.877-882, 1994.

[7] Abundo, C, Bodnar, T., Driscoll, J., Hatton, I., and Wright, J., “City Population Dynamics and Fractal Transport Networks,” *Proceedings of the Santa Fe Institute’s CSSS2013*, September 16, 2013.

[8] Chen, Y., “Characterizing Growth and Form of Fractal Cities with Allometric Scaling Exponents, Discrete Dynamics in Nature and Society, Vol. 2010, Article ID 194715, 2010.

[9] Tsoukalas, L., Uhrig, R., “Fuzzy and Neural Approaches in Engineering,” John Wiley & Sons, Inc., NY, 1996.

NRC FORM 335
(12-2010)
NRCMD 3.7

U.S. NUCLEAR REGULATORY COMMISSION

BIBLIOGRAPHIC DATA SHEET

(See instructions on the reverse)

1. REPORT NUMBER
(Assigned by NRC, Add Vol., Supp., Rev., and Addendum Numbers, if any.)

NUREG/CR-7269

2. TITLE AND SUBTITLE

Enhancing Guidance for Evacuation Time Estimate Studies

3. DATE REPORT PUBLISHED

MONTH	YEAR
March	2020

4. FIN OR GRANT NUMBER

5. AUTHOR(S)

Brian Wolshon, Scott Parr, Todd Smith, Joseph Jones, Nelida Herrera, Efe Tuncer

6. TYPE OF REPORT

Technical

7. PERIOD COVERED (Inclusive Dates)

8. PERFORMING ORGANIZATION - NAME AND ADDRESS (If NRC, provide Division, Office or Region, U. S. Nuclear Regulatory Commission, and mailing address; if contractor, provide name and mailing address.)

Louisiana State University
156 Thomas Boyd Hall
Baton Rouge, LA 70803

9. SPONSORING ORGANIZATION - NAME AND ADDRESS (If NRC, type "Same as above", if contractor, provide NRC Division, Office or Region, U. S. Nuclear Regulatory Commission, and mailing address.)

Office of Nuclear Regulatory Research *and*
Office of Nuclear Security and Incident Response
U.S. Nuclear Regulatory Commission
Washington, D.C. 20555-0001

10. SUPPLEMENTARY NOTES

T. Smith, NRC Technical Monitor

11. ABSTRACT (200 words or less)

Evacuation time estimates (ETEs) are an analysis of the time required to evacuate various sectors and distances within the plume exposure pathway emergency planning zone (EPZ) for permanent and transient populations. All nuclear power plant licensees are required to submit an updated ETE study after each decennial census. The objective of this study was to develop a technical basis for revision of NUREG/CR-7002, “Criteria for Development of Evacuation Time Estimate Studies,” in support of the next required ETE update. This applied research examines various aspects of ETE studies. Evacuation models were built for representative small, medium, and large population EPZs. Parametric analyses were conducted to examine modeling of traffic movement during evacuations, including: the impact of shadow evacuations; the effect of model extent; effectiveness of manual traffic control; and significance of parameter values. This report describes the model development and summarizes insights and observations to inform NRC staff efforts to enhance ETE guidance.

12. KEY WORDS/DESCRIPTORS (List words or phrases that will assist researchers in locating the report.)

Evacuation Time Estimate
Evacuation
ETE
Shadow Evacuation
Traffic Simulation
Emergency Preparedness
Protective Actions

13. AVAILABILITY STATEMENT

unlimited

14. SECURITY CLASSIFICATION

(This Page)
unclassified

(This Report)
unclassified

15. NUMBER OF PAGES

16. PRICE

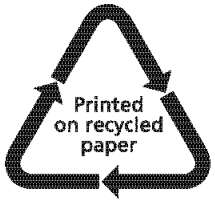

Federal Recycling Program

UNITED STATES
NUCLEAR REGULATORY COMMISSION
WASHINGTON, DC 20555-0001

OFFICIAL BUSINESS